Characterising the role of the Cajal Body during a productive adenovirus infection

Laura White

Submitted in accordance with the requirements for the degree of Doctor of Philosophy

The University of Leeds

Faculty of Biological Sciences

December 2012

The candidate confirms that the work submitted is their own and that appropriate credit has been given where reference has been made to the work of others.

This copy has been supplied in the understanding that it is copyright material and that no quotation from the thesis may be published without proper acknowledgement.

Acknowledgements

Abstract

Human adenoviruses (Ads) are DNA viruses believed to hold potential as gene therapy vectors. However, Ad vectors often express residual late structural proteins, which stimulate immune responses resulting in rapid clearance of the vector. Therefore a greater understanding of the mechanisms controlling Ad late gene expression is required. During the late phase of adenovirus 5 (Ad5) infection it was previously shown that a nuclear compartment involved in RNA metabolism known as the Cajal body (CB) is disassembled from 1-6 punctate domains per cell into numerous microfoci. Furthermore, the marker protein of CBs, p80 coilin, was suggested to play a role in the expression of Ad late phase proteins. However, the exact function of coilin in Ad late protein expression is unknown. The aim of this investigation was to determine the roles of coilin and additional CB proteins during Ad infection.

Immunofluorescence microscopy was utilised to investigate the redistribution of key CB proteins following Ad5 infection of A549 cells. Whilst coilin was redistributed from CBs into microfoci, another CB protein, termed survival of motor neuron (SMN), was redistributed from CBs into the nucleoplasm. To assess the roles of coilin and SMN during Ad5 infection, coilin was depleted in A549 cells by RNA interference (RNAi). Cells were infected with Ad5 and the virus yield, Ad proteins levels and Ad mRNA levels were assessed. Depletion of coilin reduced the virus yield and decreased the synthesis of Ad early, intermediate and late phase proteins. Although Ad mRNA expression was mostly unaffected, nuclear export of Ad mRNAs was abrogated in coilin-depleted cells. This indicated that coilin plays a role in Ad mRNA transport. Similar to coilin, SMN depletion significantly reduced the virus yield. However, in contrast to coilin, SMN depletion resulted in significant decreases in the levels of Ad capsid proteins, whilst non-structural proteins were either increased or unaffected. SMN depletion was found to reduce early gene transcription and altered alternative splicing patterns of Ad mRNAs. This suggested that SMN plays a role in Ad transcription and mRNA splicing.

This investigation uncovered the involvement of two CB proteins in two very distinct roles during Ad infection. This is the first report suggesting a role for CBs in mRNA export. Further study is now required to identify the exact function of coilin in Ad mRNA export. Furthermore, investigation of a role for coilin in cellular mRNA export and mRNA export during infection with other viruses is also warranted. Although SMN was known to play a role in cellular mRNA splicing, this is the first report indicating that SMN may be involved in splicing of virus mRNAs. Additional work is required to define the precise function of SMN in transcription and mRNA splicing during Ad infection and during infection with other virus species.

Table of Contents

List of Figures

xii

List of Tables

Abbreviations

AAV	Adeno-Associated Virus
Ad	Adenovirus
ADAR	Adenosine Deaminase, RNA-specific
ADP	Adenovirus Death Protein
Ad-pol	Adenovirus DNA polymerase
AEBSF.HCl	4-(2-Aminoethyl) benzenesulfonylfluoride, HCl
AIDA	Advanced Image Data Analyser
AIDS	Acquired Immunodeficiency Syndrome
ALT	Alternative Lengthening of Telomeres
APC	Anaphase-promoting complex
APS	Ammonium Persulphate
AraC	Cytosine Arabinoside
ASF	Anti-Silencing Factor
ATM	Ataxia Telangiectasia Mutated
ATP	Adenosine Triphosphate
ATR	Ataxia Telangiectasia and Rad3-related
BAK	BCL-2 homologous Antagonist Killer
BAX	BCL-2-associated-X protein
BCL-2	B-cell lymphoma 2
BPV	Bovine Papillomavirus
BSA	Bovine Serum Albumin
CAR	Coxsackievirus and Adenovirus Receptor
CB	Cajal Body
CBP	CREB-binding protein
CD46	Cluster of Differentiation 46
CDK	Cyclin-Dependent Kinase
cDNA	Complementary DNA
CHK2	Checkpoint Kinase 2
CHX	Cycloheximide
CPE	Cytopathic Effect
CREB	cAMP-Response Element Binding protein
CRM1	Chromosome Region Maintenance 1
CuMV	Cucumber Mosaic Virus
DAPI	4',6-diamidino-2-phenylindole

DAPK1	Death-Associated Protein Kinase 1
Daxx	Death domain-associated protein
DBP	DNA Binding Protein
DEPC	Diethylpyrocarbonate
DFC	Dense Fibrillar Centre
DMEM	Dulbecco's Modified Eagles Medium
DMSO	Dimethyl Sulfoxide
dNTPs	Deoxynucleoside Triphosphate
DOC	Sodium Deoxycholate
dsDNA	Double-Stranded DNA
DSG-2	Desmoglein 2
DTT	Dithiothreitol
EBV	Epstein Barr Virus
ECL	Enhanced Chemiluminescence
EDTA	Ethylenediaminetetraacetic Acid
eIF	Eukaryotic Initiation Factor
FBI-1	Factor Binding Inducer of short transcripts protein 1
FC	Fibrillar Centre
FCS	Foetal Calf Serum
FCV	Feline Calcivirus
FFU	Fluorescent Focus-forming Units
FIP	14.K-Interacting Protein
FITC	Flourescein Isothyocyanate
FIX	Factor IX
FLASH	FLICE-Associated Huge Protein
FMDV	Foot and Mouth Disease Virus
FVIII	Factor VIII
FX	Factor X
GAPDH	Glyceraldehyde 3-Phosphate Dehydrogenase
GAR1	H/ACA ribonucleoproteins complex subunit 1
GC	Granular Centre
GON	Groups Of Nine
GRV	Groundnut Rosette Virus
h.p.i	Hours post-infection
HAUSP	Herpes virus-Associated Ubiquitin-Specific Peptidase
HCMV	Human Cytomegalovirus

HCV	Hepatitis C Virus
HDAC	Histone Deacetylase
HDM2	Human Double Minute 2
HEPES	4-(2-hydroxyethyl)-1-piperazineethanesulfonic acid
HiNF-P	Histone H4 Transcription Factor
HIPK2	Homeodomain Interacting Protein Kinase 2
HIRA	Histone cell cycle Regulation defective homolog A
HIV-1	Human Immunodeficiency Virus 1
HLB	Histone Locus Body
hPOP1	Human Processing of Precursor 1
HPV	Human Papillomavirus
HRP	Horseradish Peroxidise
HRR	Homologous Recombination Repair
HSPG	Heparan Sulphate Proteoglycan
HSV-1	Herpes Simplex Virus 1
hTERT	Human Telomerase Reverse Transcriptase
HTLV-1	Human T-cell Lymphotrophic Virus 1
hTR	Human Telomerase RNA
HVS	Herpesvirus Saimiri
IBV	Influenza B Virus
ICG	Interchromatin Granule
IFN	Interferon
IgG	Immunoglobulin G
IRES	Internal Ribosome Entry Site
ITR	Inverted Terminal Repeat
IV	Intravenous
kDa	Kilodaltons
L4P	L4 Promoter
Lsm	U7 snRNA-associated Sm-like protein
m7G	7-methylguanosine
MALAT1	Metastasis associated lung adenocarcinoma transcript 1
MAPK	Mitogen-Activated Protein Kinase
MED23	Mediator of RNA polymerase II transcription subunit 23
MHC	Major Histocompatibility Complex
miRNA	Micro-RNA
MLB	Membrane Lysis Buffer

MLP	Major Late Promoter
MNK1	MAP kinase serine/threonine interacting kinase 1
MOI	Multiplicity of infection
MRN	Mre11, Rad50 and Nbs1
mRNA	Messenger RNA
MTOC	Microtubule Organising Centre
mTOR	Mammalian Target Of Rapamycin
MTT	3-(4,5-Dimethylthiazol-2-yl)-2,5-diphenyltetrazolium bromide
MU	Map Unit
MVM	Minute Virus of Mouse
Na^+/H^+	Sodium/proton Exchanger
NEAT	Nuclear Enriched Abundant Transcript
NF	Nuclear Factor
NGS	Normal Goat Serum
NHP2	H/ACA ribonucleoprotein complex subunit 2
NONO	Non-POU domain containing Octamer binding protein
NOP	Nucleolar Protein
Nopp140	140 kDa Nucleolar Phosphoprotein
NP40	Nonidet P-40
NPAT	Nuclear Protein Ataxia Telangiectasia locus
NPC	Nuclear Pore Complex
nSB	Nuclear Stress Body
Nxf1	Nuclear RNA export Factor 1
Oct-1	Octamer Transcription Factor 1
OD	Optical Density
OPT	Oct-1/PTF/Transcription
ORF	Open Reading Frame
p14-ARF	14 kDa Alternative Reading Frame protein
P-body	Processing body
PBS	Phosphate Buffered Saline
PcG	Polycomb Group
PCR	Polymerase Chain Reaction
PFU	Plaque Forming Unit
PI3K	Phosphoinositide 3 Kinase
PIAS	Protein Inhibitor of Activated Stat
PIKA	Polymorphic Interphase Karyosomal Association

PK	Protein Kinase
PML	Promyelocytic Leukaemia
PML-NB	Promyelocytic Leukaemia Nuclear Body
Pol	Polymerase
Poly(A)	Polyadenylated
PP	Protein Phosphatase
pRb	Retinoblastoma protein
PSLV	Poa Semilatent Virus
PSP	Paraspeckle protein
P-TEFb	Positive Transcription Elongation Factor b
PTEN	Phosphatase and Tensin
PV	Poliovirus
PVDF	Polyvinylidene Fluoride
qPCR	Quantitative PCR
Rbx1	RING box protein 1
rDNA	Ribosomal DNA
RGD	Arginine-Glycine-Aspartic acid
RID	Receptor Internalisation and degradation complex
RIPA	Radioimmunoprecipitation assay
RISC	RNA-Induced Silencing Complex
rRNA	Ribosomal RNA
RT	Reverse Transcription
SAE	SUMO-Activating Enzyme
SAHF	Senescence-Associated Heterochromatin Foci
scaRNA	Small Cajal body-specific RNA
SDS	Sodium Dodecyl Sulphate
SDS-PAGE	SDS Polyacrylamide Gel Electrophoresis
SEM	Standard Error of the Mean
SENP5	SUMO-1/Sentrin-specific Peptidase 5
SFPQ	Splicing Factor Proline/Glutamine-rich
siCoilin	Coilin siRNA
siControl	Scrambled control siRNA
siRNA	Small interfering RNA
siSMN	SMN siRNA
Sm	Smith antigen
SMA	Spinal Muscular Atrophy

SMN	Survival Motor Neuron
snoRNA	Small Nucleolar RNA
snoRNP	Small Nucleolar Ribonucleoprotein
snRNA	Small Nuclear RNA
snRNP	Small Nuclear Ribonucleoprotein
SP1	Specificity protein 1
SP100	Speckled 100 kDa nuclear antigen
SRSF	serine/arginine-rich splicing factor
ssDNA	Single-Stranded DNA
Stat1	Signal transducer and activator of transcription 1
SUMO1	Small Ubiquitin-like Modifier 1
TAF	Template Activating Factor
TAP	Tip-Associated Protein
TBE	Tris/Borate/EDTA
TE	Tris/EDTA
TEMED	N,N,N',N'-Tetramethylethylenediamine
TIF-1	Transcriptional intermediary family 1
T_m	Salt-adjusted melting temperature
TNF-α	Tumour Necrosis Factor α
TP	Terminal Protein
TPL	Tripartite Leader
TRAIL	TNF-α-Related Apoptosis-Inducing Ligand
tRNA	Transfer RNA
TRT	Telomerase Reverse Transcriptase
U2AF	U2 small nuclear RNA Auxiliary Factor
UBC9	Ubiquitin Carrier Protein 9
UBF	Upstream Binding Factor
UbL	Ubiquitin Ligase
UTR	Untranslated Region
VA-RNA	Virus-Associated RNA
VP	Virus Particle
VZV	Varicella Zoster Virus
w/v	Weight/volume
WNV	West Nile Virus
WRAP53	WD-Repeat-containing Antisense to P53

Chapter 1 - Introduction

1.1 Introduction

Viruses are infectious agents able to replicate only within the cells of a host organism. Following entry to the host cell, there is a stepwise dismantling of the virus capsid in order to release the viral genome for replication and gene transcription. Following protein translation, virus genomes are packaged into newly-assembled capsids to form progeny virions which are then released to infect neighbouring cells. However, due to their limited genome coding capacity, viruses are not able to encode all the proteins required for their replication. As a result, viruses have developed mechanisms of hijacking host cellular proteins in order to complete their life cycles.

A prime cellular target of many viruses is the host cell nucleus, as it contains proteins required for RNA and DNA polymerisation and processing as well as factors required for the maturation and release of new virus particles (reviewed in Greco, 2009; Zakaryan and Stamminger, 2011). The nucleus is the site for numerous cellular processes including DNA replication, RNA transcription and ribosome assembly. In order to efficiently co-ordinate its many functions, the nucleus is subdivided into specialised domains which include the nucleolus, promyelocytic leukaemia nuclear bodies (PML-NBs) and Cajal Bodies (CBs). The nucleolus is primarily involved in the biogenesis and assembly of ribosomes, CBs are involved in RNA metabolism whilst PML-NBs have been implicated in diverse roles including transcriptional regulation, apoptosis and immune surveillance. During virus infection, nuclear substructures are disrupted and rearranged in order to facilitate virus replication (reviewed in Tavalai and Stamminger, 2008; Greco, 2009; Boulon *et al.*, 2010). Most DNA viruses (with the exception of poxviruses) replicate within the host cell nucleus, with key life cycle stages including DNA replication, mRNA transcription and virus assembly occurring in this compartment. Although RNA viruses replicate in the cytoplasm, they can also interact with the nucleus in order to promote genome replication and mRNA transport (reviewed in Hiscox, 2007; Hiscox *et al.*, 2010).

Considering their role in immune surveillance, it is unsurprising that multiple viruses including adenovirus (Ad), herpes simplex virus 1 (HSV-1) and varicella zoster virus (VZV) reorganise and/or degrade PML-NB components in order to subvert immune responses (Ullman and Hearing, 2008; El Mchichi *et al.*, 2010; Boutell *et al.*, 2011; Cuchet *et al.*, 2011; Jiang *et al.*, 2011a; Wang *et al.*, 2011). Some viruses also interfere with the transcriptional regulatory functions of PML-NBs; abrogation of the PML-NB transcriptional repressor proteins Daxx and SP100 appears to enhance viral transcription during infection with Epstein-Barr virus (EBV), Ad and human cytomegalovirus (HCMV) (Adler *et al.*, 2011; Kim *et al.*, 2011; Tsai *et al.*, 2011; Schreiner *et al.*, 2012).

The nucleolus appears to play a key role in viral genome replication. The RNA virus West Nile virus (WNV) and the DNA viruses HSV-1, Ad and HCMV redistribute certain nucleolar proteins to viral genome replication centres, which appears to be necessary for replication (Lawrence *et al.*, 2006; Calle *et al.*, 2008a; Stow *et al.*, 2009; Lymberopoulos and Pearson, 2010; Strang *et al.*, 2010; Strang *et al.*, 2012; Xu *et al.*, 2011). The nucleolus is also required for RNA trafficking during infection with certain RNA viruses. Human immunodeficiency virus (HIV-1) and herpes virus Saimiri (HVS) both hijack the nucleolus in order to traffic viral mRNA from the nucleus to the cytoplasm (Michienzi *et al.*, 2000; Michienzi *et al.*, 2002; Boyne and Whitehouse, 2006; Michienzi *et al.*, 2006). The mRNA from these viruses is unsuitable for trafficking alongside normal cellular RNA; HIV-1 mRNA is incompletely spliced, making it prone to nonsense-mediated decay (Feinberg *et al.*, 1986; Terwilliger *et al.*, 1986) whilst HVS mRNAs are intronless thus cannot enter the usual mRNA export route that is intrinsically linked to splicing (Albrecht *et al.*, 1992; Boyne and Whitehouse, 2006).

In addition to the nucleolus, CBs also appear to play a role in viral RNA trafficking. During infection with the RNA plant virus Groundnut Rosette virus (GRV), CBs are fragmented from 1-6 punctate domains per cell into smaller, more numerous microfoci. This was shown to promote the trafficking of the GRV movement protein ORF3 to the nucleolus, facilitating the assembly of viral RNA-protein complexes required for viral spread (Kim *et al.*, 2007a; Kim *et al.*, 2007b; Canetta *et al.*, 2008). Interestingly, similar CB microfoci have also been observed during infection with the highly unrelated human DNA virus, Ad (Rebelo *et al.*, 1996; Rodrigues *et al.*, 1996). Although it has been suggested that CBs are required for the expression of Ad late proteins (James *et al.*, 2010), the role of the CB during Ad infection is still unclear.

A thorough understanding of viral life cycles is not only crucial for development of new anti-viral agents, but also for the safe use of viruses as vectors for gene therapy, vaccine and oncolytic (cancer-killing) regimens. To date, Ads account for the highest proportion of viral vectors in clinical trials worldwide. As these Ad vectors are intended for use in the clinical setting, it is imperative that the Ad lifecycle is fully understood in order to ensure vector safety and efficacy. Unfortunately, although Ad early gene expression and DNA replication are well characterised, the later stages of Ad infection, in particular the mechanisms controlling Ad late gene expression, are less well defined. As CBs have been suggested to play a role in Ad late protein expression, characterising the interaction of Ads with CBs may expand our knowledge of the late phase of the Ad lifecycle.

1.2 Adenoviruses

1.2.1 Adenovirus classification

In 1953, an infectious agent was extracted from human adenoids and was later termed 'adenovirus' (Ad) (Rowe *et al.*, 1955; Enders *et al.*, 1956). By the late 1960s, over 30 related isolates had been isolated and classified according to neutralisation properties (Stevens *et al.*, 1967). Members of the *Adenoviridae* family are non-enveloped icosahedral viruses with double-stranded DNA genomes ranging from 26-45 kbp in size. Ads infect a broad range of vertebrate species and have been classified into five clades based on genome sequencing and bioinformatic analysis; the *Mastadenoviruses* (isolates originating from mammals), *Aviadenoviruses* (isolates from birds), *Atadenoviruses* (isolates from birds, mammals and reptiles that share high AT genome content) (Benko and Harrach, 1998; Both, 2002), *Siadenoviruses* (several bird isolates, one amphibian and one reptilian isolate) (Davison *et al.*, 2003; Zsivanovits *et al.*, 2006; Rivera *et al.*, 2009) and the *Ichtadenoviruses*, consisting of a single isolate from a sturgeon (Kovacs *et al.*, 2003).

Human Ads originate from the *Mastadenoviridae*, and to date there are over 55 different serotypes of human Ads divided into seven species (A to G) (Table 1-1). Classification of Ads is based on multiple parameters including neutralisation by specific antisera, haemagglutination properties and genome sequence homology (reviewed in Berk, 2007). The species B Ads are further subdivided into groups B1 (serotypes 3, 7, 16, 21 and 50) and B2 (serotypes 11, 14, 34 and 35) based on conservation of restriction endonuclease sites (Wadell *et al.*, 1986; Segerman *et al.*, 2003). This classification of the species B viruses also broadly correlates with tissue tropism; B1 viruses generally cause upper respiratory tract infection whilst the B2 viruses cause kidney and urinary tract infections (Wadell, 1984). The species B viruses have also been re-classified according to receptor usage (Tuve *et al.*, 2006). More recently, it has been proposed that Ads should be completely re-classified according to whole genome sequence similarity as opposed to serological approaches (Seto *et al.*, 2011; Singh *et al.*, 2012).

1.2.2 Pathology and disease associated with human adenovirus infection

Ads are known to cause acute respiratory, gastrointestinal and ocular infections in a serotype-specific manner (Table 1-1). Species A, F and G are most commonly associated with gastroenteritis, species B:1, C and E with respiratory disease, B:2 can cause urinary tract disease and species D can cause keratoconjunctivitis (reviewed in Zhang and Bergelson, 2005; Berk, 2007). Some Ads are responsible for a variety of clinical manifestations, such as the species B:2 virus Ad3 which in addition to respiratory infection can also cause conjunctivitis (O'Donnell *et al.*, 1986; Guo *et al.*, 1988). A more severe and highly contagious form of conjunctivitis termed

epidemic keratoconjuctivitis is caused by the species D serotypes 8, 19 and 37 and by an Ad chimera composed of elements from Ads 8, 22 and 37 (Aoki *et al.*, 2008; Ford *et al.*, 1987). Ad4 can cause considerable morbidity as the causative agent of acute respiratory disease which has been reported in military recruits (Hilleman *et al.*, 1956; Gray *et al.*, 2000). Recently, a novel Ad termed titi monkey adenovirus was identified as capable of infecting both monkeys and humans, resulting in respiratory disease (Chen *et al.*, 2011).

However, in the majority of cases, Ad infections in immunocompetent individuals are mild and self-limiting. In contrast, Ad infections in immunocompromised individuals can cause more serious infection (Hale *et al.*, 1999). Those at risk include young people due to lack of previous exposure, transplant patients on immunosuppressive drugs and AIDS patients. Indeed, certain Ad serotypes that are rarely isolated from the immunocompetent population, such as Ad35, are more frequently isolated from immunocompromised individuals (Flomenberg *et al.*, 1987; Hierholzer, 1992). Although there is currently no definitive treatment for Ad infection, the nucleoside phosphonate analogue cidofovir is used in most transplant centres albeit with substantial adverse side effects (reviewed in De Clercq, 2003). However, a lipid conjugate of cidofovir known as CMX001 was recently shown to exhibit substantial efficacy against Ad infections in immunocompromised patients with negligible side effects, indicating a promising new treatment for Ad infection (Florescu *et al.*, 2012).

1.2.3   Adenoviruses as gene therapy and oncolytic vectors

Gene therapy is the transfer of therapeutic genes into cells with the aim of correcting a defective gene. In order to achieve this, the DNA must be transported into the cell and delivered to the nucleus for gene expression. Transfer of the therapeutic gene into the target cell requires a vector, and these can be broadly classified as viral or non-viral vectors. Non-viral vectors include liposomes, polypeptides and nanoparticles (reviewed in Mintzer and Simanek, 2009). To date, Ad vectors have been utilised in 428 clinical trials and account for the largest proportion (23.2%) of all gene therapy clinical trials worldwide, inclusive of both viral and non-viral vectors (Wiley.co.uk/genemedicine, as of June 2012). Ads possess many characteristics ideal for a virus vector: their genome can be easily manipulated, they are able to infect a wide range of dividing and non-dividing cells and they can be easily and inexpensively grown to high titres (reviewed in Shen and Post, 2007). Ads are believed to hold promise for oncolytic (cancer-killing) regimens, vaccination regimens and gene-addition for inherited diseases.

The first-generation Ad vectors had the E1 region of the genome deleted, which both prevented virus replication and provided coding capacity for insertion of a therapeutic transgene (Yang *et al.*, 1995). However these vectors were rapidly cleared by the host immune system (Yang *et al.*, 1995). The E1 deletions were combined with additional deletions in E2, E3 and E4 gene regions

5

Table 1-1. The adenovirus serotypes and the associated clinical manifestation following infection by each species.

Adapted from Jones *et al.*, 2007; Ishiko *et al.*, 2008; Walsh *et al.*, 2009; Hall *et al.*, 2010; Walsh *et al.*, 2010; Kaneko *et al.*, 2011a; Kaneko *et al.*, 2011b; Kaneko *et al.*, 2011c; Robinson *et al.*, 2011

Species	Serotype(s)	Associated disease	GC content of genome (%)	Oncogenic potential (in rodents)
A	12, 18, 31	Gastroenteritis	48-49	High
B1	3, 7, 16, 21, 50	Respiratory disease	50-52	Moderate
B2	11, 14, 34, 35, 55	Urinary tract disease	50-52	Low
C	1, 2, 5, 6	Respiratory disease	57-59	Low
D	8, 9, 10, 13, 15, 17, 19, 20, 22-30, 32, 33, 36-39, 42-49, 51, 53, 54, 56	Keratoconjunctivitis	57-61	Low
E	4	Respiratory disease, conjunctivitis	57-59	Low
F	40, 41	Gastroenteritis	Unknown	Unknown
G	52	Gastroenteritis	Unknown	Unknown

to reduce toxicity and further increase coding capacity (Engelhardt *et al.*, 1994; Armentano *et al.*, 1995). Unfortunately, there was still stimulation of the inflammatory response following administration of these vectors and rapid antibody neutralisation was elicited upon subsequent inoculation. This lead to the development of helper-dependent ("gutless") vectors, which have all the coding genes deleted (Schiedner *et al.*, 1998). Despite improved toxicity and immunogenic profiles due to lack of immunogenic peptide expression, immune responses were still generated to the virus capsid (reviewed in Brunetti-Pierri and Ng, 2008).

Indeed, most Ad vectors to date have exhibited a sub-optimal capacity to produce beneficial therapeutic effect (efficacy) and often induce potent host immune responses. The high prevalence of species C Ads within the general population means that most humans have been exposed to these Ads, therefore upon administration there is rapid clearance of these vectors by pre-existing antibodies (reviewed in Bessis *et al.*, 2004). Interestingly, although the E1 region is believed to be essential for Ad replication, E1-deleted Ad vectors still express residual late proteins, leading to inflammatory responses and reduced vector efficacy (Yang *et al.*, 1994b; Yang *et al.*, 1994c; Yang *et al.*, 1995). The presence of Ad DNA or transgene DNA in host cells also stimulates innate inflammatory responses (Everett *et al.*, 2003; Zhu *et al.,* 2007). In addition, intravenous (IV)-administered vectors become sequestered by the liver, resulting in low levels of vector transduction at the target site and local toxicity in the liver (Engelhardt *et al.*, 1994; Lieber *et al.*, 1997; Everett *et al.*, 2003). High doses of Ad vectors can lead to exaggerated responses, which have been shown to be lethal in mouse studies (reviewed in Varnavski *et al.*, 2005) and also one case in a human clinical trial (Raper *et al.*, 2003).

Whilst immune stimulation has served as a major drawback in Ad gene therapy regimens, it can serve as an advantageous property for oncolytic (cancer killing) and vaccine vectors by enhancing immune responses to tumour cells or vaccine antigens, respectively. Oncolytic Ads are intended to specifically target, invade and replicate within tumour cells resulting in tumour cell lysis, releasing progeny virions able to infect and kill surrounding tumour cells. The most well-studied oncolytic Ad has been ONYX-015, which contains a mutation in the E1B-55K region of the Ad genome (Bischoff *et al.*, 1996). This mutation abolished the ability of the E1B-55K protein to bind and inhibit p53, thus restricting virus replication to cells in which the p53 pathway is already inhibited, which occurs in a high proportion of human cancers. Although the efficacy of ONYX-015 was found to be inadequate in Phase I and II trials when used as a single agent (Mulvihlll *et al.*, 2001; Nemunaitis *et al.*, 2001), utilising ONYX-15 in combination with chemotherapy or radiotherapy resulted in complete tumour regression (Khuri *et al.*, 2000; Geoerger *et al.*, 2003). A similar E1B-deleted virus, termed H101, has been certified for use against head and neck cancer in China (Garber, 2006). An immunostimulatory Ad expressing

CD40L was recently found to substantially boost anti-tumour immune responses in clinical trials for bladder cancer (Malmstrom *et al.*, 2010; Pesonen *et al.*, 2012).

Both replication-deficient and replication-competent Ads have also shown promise in vaccine regimens. These Ads are engineered to express antigens from microbial sources in order to trigger immune responses to the antigen, resulting in adaptive immunity against the pathogen. Expression of polyvalent HIV-1 antigens by a recombinant Ad26 vector resulted in induction of potent anti-HIV-1 immune responses in rhesus macaque monkeys (Barouch *et al.*, 2010). Additionally, combining the Ad vaccine with protein adjuvants and other viral or DNA vaccines appeared to enhance immune responses to malaria and HIV-1 (Koup *et al.*, 2010). This indicates that as with oncolytic regimens, combination therapies using Ad vectors may hold promise for boosting immune responses in vaccine regimens.

1.2.4   Adenovirus structure

The adenovirus capsid comprises a non-enveloped icosahedron of approximately 90 nm in diameter. The proteins comprising the capsid act to promote entry into the host cell, facilitate disassembly of the capsid and deliver the genome to the nucleus for replication. The virus particle has been visualised by cryo-electron microscopy at 10 Å resolution (Silvestry *et al.*, 2009) and the crystal structure has been solved at 3.5 Å resolution (Reddy *et al.*, 2010). The Ad particle comprises 13 structural proteins. The capsid shell is formed of 252 capsomeres of which 240 are trimeric hexon protein (polypeptide II) and the remaining 12 are penton protein (polypeptide III) (reviewed in Hall *et al.*, 2010). Pentons are located at each of the 12 vertices of the capsid, and comprise a pentamer of penton base protein with a trimeric fibre protein (polypeptide IV) projection. The other minor capsid components are proteins IIIa, VI, VIII and IX (reviewed in Vellinga *et al.*, 2005) (Figure 1-1).

Within the capsid core, the remaining structural polypeptides V, VII, Mu (polypeptide X) and terminal protein (TP) are associated with the double-stranded DNA genome. Located at either end of the DNA genome are inverted terminal repeats (ITRs) which range in size from 36-200 bp. Each 5′ terminus of the DNA is covalently linked to a TP and is non-covalently associated with the basic Ad proteins pV, pVII and Mu to form the viral chromatin (Black and Center 1979; Chatterjee *et al.,* 1985; Anderson *et al.,* 1989) (Figure 1-1).
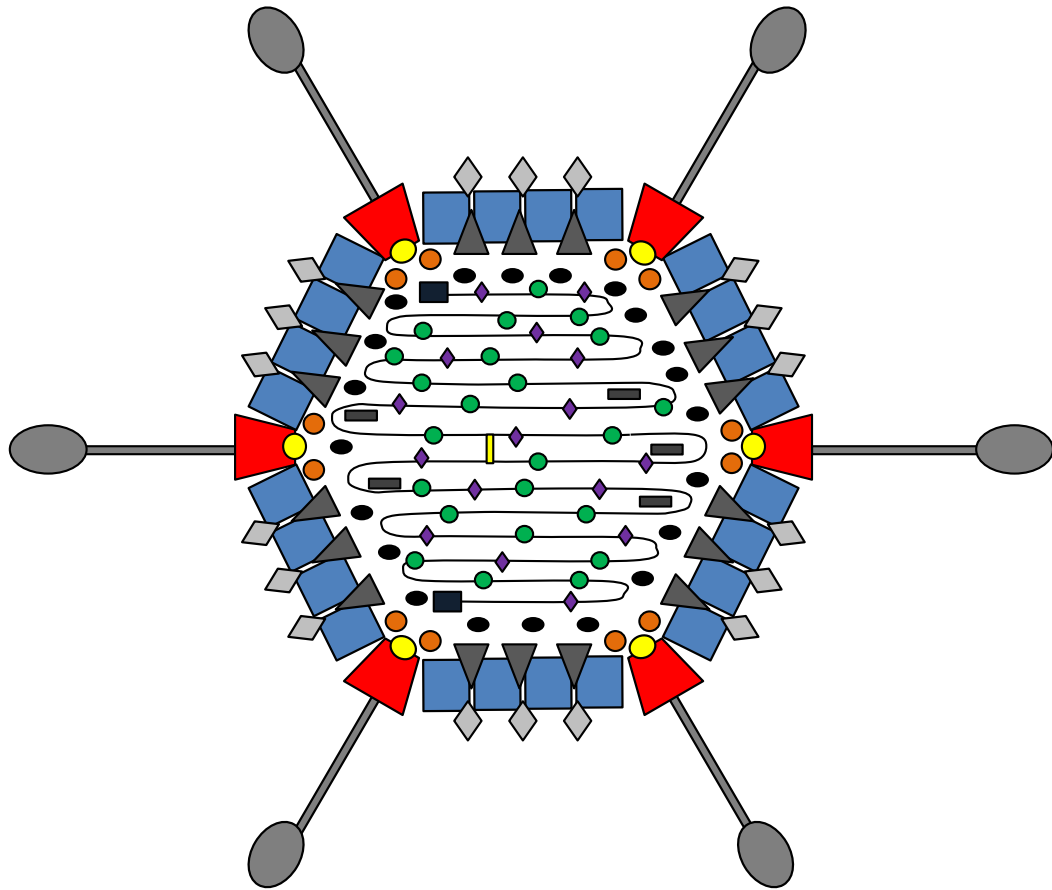
Capsid proteins

Hexon (II)	■ (blue square)
Penton base (III)	▰ (red trapezoid)
Fibre (IV)	●— (grey oval with stalk)
IIIa	● (yellow circle)
VI	● (orange circle)
VIII	▲ (dark grey triangle)
IX	◆ (light grey diamond)

Core proteins

V	● (black oval)
VII	● (green circle)
Mu (X)	◆ (purple diamond)
TP	■ (dark square)
IVa2	▮ (yellow bar)
Protease	▬ (grey rectangle)

Figure 1-1. The structure of the adenovirus capsid.

A schematic diagram of the structural proteins associated with the adenovirus capsid. The major capsid components are hexon, penton base and fibre. The minor capsid components are IIIa, VI, VIII and IX. Proteins V, VII, Mu, TP, IVa2 and protease are associated with the DNA genome within the capsid core. Figure is taken from White and Blair, 2012, with permission. White and Blair, (2012

1.2.1.1 Major capsid components

1.2.1.1.1 Hexon (polypeptide II)

Hexon is the major structural protein of the Ad capsid and forms the facets of the icosahedron (Van Oostrum and Burnett, 1985). As determined by crystallography studies of the Ad2 hexon, each hexon capsomere is composed of three identical subunits producing a pseudo-hexagonal structure (Roberts *et al.*, 1986; Athappilly *et al.*, 1994). Hexon capsomeres are found associated with proteins IX and VI (Furcinitti *et al.*, 1989; Matthews and Russell, 1994; Fabry *et al.*, 2009). Hexons associated with pentons are termed 'peripentonal hexons' or H1, whereas the remainder on the faces of the icosahedron are termed 'groups of nine' (GON) (Van Oostrum *et al.*, 1987). Depending on their orientation, the GON hexons are further subdivided into H2 and H3. Hexons that are not GONs or peripentonal hexons are classed as H4 (Van Oostrum *et al.*, 1987). The protein-protein interaction networks between the GONs and the other capsid proteins was recently characterised by cryo-electron microscopy at 3.6 Å resolution (Liu *et al.*, 2010).

1.2.1.1.2 Penton base (polypeptide III)

Penton base are found at each of the 12 vertices of the capsid and play an important role in the stability of the Ad capsid (Ensinger and Ginsberg, 1972). Penton monomers form pentamers which are known as penton base. Penton base is found associated with a trimer of fibre protein (polypeptide IV), and this complex is known as penton (Pettersson and Hoglund, 1969; Wadell and Norrby, 1969). Penton is important in facilitating uptake of the virus into host cells, with fibre promoting initial attachment and interactions of the penton base with cellular integrins promoting internalisation (Wickham *et al.*, 1993; Wickham *et al.*, 1994). During infection with certain Ad serotypes, it has been shown that some penton and penton base structures are also able to form large particles known as dodecahedra, which comprise 12 copies of penton or penton base (Fender *et al.*, 1997; Fuschiotti *et al.*, 2006). Although the exact function of dodecahedra during Ad infection is currently undefined, they have been shown to interact with cellular junctions and induce cell remodelling, therefore may play a role in dissemination of the virus (Fender *et al.*, 2012).

1.2.1.1.3 Fibre (polypeptide IV)

Fibre is found projecting from each of the 12 vertices of the capsid and plays an important role in the initial attachment of the particle to host cells (Philipson *et al.*, 1968). Whilst the majority of Ad serotypes express only one form of fibre protein, the species F serotypes express both long and short fibres (Kidd *et al.*, 1993; Seiradake and Cusack, 2005). Fibre consists of an N-terminal tail, a variable length shaft and a C-terminal knob domain, and it is the knob domain that facilitates interaction with host cell-surface molecules (Louis *et al.*, 1994; Xia *et al.*, 1994).

Although there are five potential fibre binding sites on the penton base, only three fibre molecules are able to bind due to steric hindrance, resulting in a trimeric fibre molecule (Van Oostrum and Burnett, 1985; Hong and Engler, 1996).

1.2.1.2 Minor capsid components

1.2.1.2.1   Polypeptide IIIa

Protein IIIa is believed to play a role in capsid assembly and stabilisation of the capsid vertices (Bourdin *et al.*, 1980; Lemay *et al.*, 1980; Chroboczek *et al.*, 1986; Silvestry *et al.*, 2009; Ma and Hearing, 2011). There are 60 copies of IIIa per capsid, with five copies of IIIa arranged symmetrically on the underside of each penton base (Saban *et al.*, 2006). It appears that IIIa may be located in-between penton base and peripentonal hexons (San Martin *et al.*, 2008). In addition to its structural functions, IIIa is also believed to be involved in viral genome packaging (Ma and Hearing, 2011). IIIa is processed from a precursor form (pre-IIIa) to mature IIIa by the Ad protease (Boudin *et al.*, 1980).

1.2.1.2.2   Polypeptide VI

Polypeptide VI (pVI) associates with hexon and there are approximately 1.5 pVI per hexon trimer (Saban *et al.*, 2006). The protein also appears to associate with IIIa, penton base and viral DNA (Stewart *et al.*, 1993; Saban *et al.*, 2006). The precursor form of pVI, pre-VI, is cleaved by the Ad protease, adenain, to yield the mature pVI (Anderson *et al.*, 1973; Weber, 1976; Sung *et al.*, 1983b; Tremblay *et al.*, 1983). The cleavage peptide of pre-VI is thought to function as a co-factor for adenain (Mangel *et al.*, 1993). Roles attributed to pVI include disruption of the host cell endosome following capsid internalisation, nuclear import of hexon, capsid assembly and transcriptional activation of early viral genes (Matthews and Russell, 1995; Wodrich *et al.*,2003; Wiethoff *et al.*,2005; Wodrich *et al.*, 2010; Schreiner *et al.*, 2012).

1.2.1.2.3   Polypeptide VIII

There are 120 copies of pVIII per capsid, with groups of three located along the icosahedral threefold symmetry axis of the capsid, acting in cohesion with pIX for stabilisation of the GONs. In addition, single copies of pVIII are also found linking each peripentonal hexon to the GONs in co-operation with IIIa (Saban *et al.*, 2006). Similar to pVI, pVIII is synthesised in a precursor form (pre-VIII) which is subsequently cleaved to the mature protein by the activity of adenain (Weber, 1976; Tremblay *et al.*, 1983). Although the function of pVIII is currently undefined, mutations in pVIII appear to result in heat instability of the capsid, suggesting a role in capsid stability (Liu *et al.*, 1985).

1.2.1.2.4   Polypeptide IX

This protein is only found in Ads of the *Mastadenovirus* clade. There are 240 copies of pIX per capsid arranged as trimers on the outer face of each facet (Saban *et al.*, 2006; Fabry *et al.*, 2009; Boulanger *et al.*, 1979). Ad mutants lacking pIX display increased heat sensitivity, indicating that pIX contributes to stability of the capsid (Colby and Shenk, 1981; Ghoshchoudhury *et al.*, 1987). Interestingly, IX-deleted Ad vectors display enhanced tropism for cell lines which do not express the Cocksackie B and Adenovirus Receptor (CAR), the primary attachment receptor for Ad species A, C, D, E and F (de Vrij *et al.*, 2011). This suggests that pIX may play a role in the cell tropism of Ads. Polypeptide IX is expressed during the delayed early phase before any of the other structural proteins and may function in activation of late gene transcription (Lutz *et al.*, 1997; Rosa-Calatrava *et al.*, 2001). Polypeptide IX has also been shown to play a role in nuclear reorganisation by sequestering the PML protein, the major structural component of PML-NBs, resulting in increased virus replication (Rosa-Calatrava *et al.*, 2001; Rosa-Calatrava *et al.*, 2003).

1.2.1.3 Core proteins

1.2.1.3.1   Polypeptide V

Within the core of the Ad particle, pV is found associated with pVI, pVII and the viral DNA (Chatterjee *et al.*, 1985, 1986) and functions to link the core of the virion to the outer capsid (Matthews and Russell, 1998b). Polypeptide V contains numerous nuclear localisation signals and appears to associate with the cellular protein p32 to promote the transport of Ad DNA into the host cell nucleus (Matthews and Russell, 1998a). It is also responsible for redistribution of the nucleolar proteins C23 (nucleolin) and B23 (nucleophosmin) during infection. The reason for the redistribution of these two proteins is currently unclear; redistribution of C23 was suggested to antagonise the transcriptional repressor function of C23 (Matthews, 2001). Although the redistribution of B23 was suggested to facilitate the assembly of viral chromatin (Matthews, 2001; Samad *et al.*, 2007; Samad *et al.,* 2012), some data indicates that B23 redistribution promotes virion assembly (Ugai *et al.*, 2012).

1.2.1.3.2   Polypeptide VII

Polypeptide VII is the most abundant core protein with around 800 copies found per capsid. Although the arrangement of the Ad genome with the core proteins is not well defined, it is thought that pVII is most tightly associated with the Ad genome (Sung *et al.*, 1983a; Chatterjee *et al.,* 1986). Polypeptide VII is synthesised as a precursor (pre-VII) and is cleaved by adenain into mature form (Anderson *et al.*, 1973; Weber, 1976; Tremblay *et al.*, 1983). Polypeptide VII contains multiple nuclear localisation signals and interacts with DNA to facilitate nuclear import of the Ad genome (Lee *et al.*, 2003; Wodrich *et al.*, 2006). The nuclear import of Ad

DNA appears to involve an interaction of pVII with transportin, a subunit of nucleoporins (Hindley *et al.*, 2007). The binding of pVII to incoming Ad DNA may facilitate subversion of the host Mre11, Rad50 and Nbs1 (MRN)-dependent DNA damage response (Karen and Hearing, 2011). Polypeptide VII is thought to interact with Ad E1A following DNA replication, facilitating the release of pVII from DNA to allow transcription of late-phase genes (Chen *et al.*, 2007). Polypeptide VII also plays a role in condensing the viral DNA prior to packaging into newly-assembled capsids (Vayda *et al.*, 1983; Vayda and Flint, 1987).

1.2.1.3.3   Mu (polypeptide X)

Mu is a very small (19 amino acid), highly basic polypeptide and is present in around 100 copies per virion. Pre-Mu is cleaved by adenain to produce the mature polypeptide (Weber, 1976; Tremblay *et al.*, 1983). Mu contains a nucleolar localisation signal and has been shown to play a role in the condensation of Ad DNA (Anderson *et al,.* 1989). Pre-Mu appears to regulate E2 protein expression; pre-Mu was shown to inhibit the expression of pre-TP without altering the expression of DNA-Binding Protein (DBP) (Lee *et al.,* 2004).

1.2.1.3.4   Terminal protein (TP)

TP is found attached to the 5′ ends of Ad DNA (Rekosh *et al.*, 1977). Pre-TP was found to associate in a functional complex with Ad DNA polymerase (Ad-pol) and the cellular protein nuclear factor 1 (NF-I) to prime Ad DNA replication (Enomoto *et al.*, 1981; Chen *et al.*, 1990; Gounari *et al.*, 1990; Mul *et al.*, 1990). Pre-TP may also be anchored to the nuclear matrix via an interaction with the enzyme carbamyl phosphate I synthetase, aspartate transcarbamylase and dihydroototase (CAD) (Angeletti and Engler, 1998). During the late phase of infection, pre-TP is cleaved by adenain to produce mature TP (Weber, 1976; Tremblay *et al.*, 1983).

1.2.1.3.5   IVa2

IVa2 is an ATP-binding protein and appears to bind specific viral DNA sequences near the left terminal end of the Ad genome, facilitating packaging of the genome into capsid precursors (Zhang and Imperiale, 2000; Zhang *et al.*, 2001; Ostapchuk and Hearing, 2003; Ostapchuk *et al.*, 2005; Ostapchuk and Hearing, 2008). IVa2 is present in six to eight copies per capsid and is required for genome packaging. IVa2 binds to specific sequences on Ad DNA known as the 'A repeats' which are located at the far left of the genome (Ostapchuk *et al.*, 2005; Tyler *et al.*, 2007). To facilitate genome packaging, IVa2 forms a complex on the packaging sequence with Ad L4-22K (Ewing *et al.*, 2007; Tyler *et al.*, 2007; Ostapchuk *et al.*, 2011; Yang and Maluf, 2012). IVa2 is also thought to function as a transcriptional enhancer at the late region 4 promoter (L4P) (Morris *et al.*, 2010) and the major late promoter (MLP) (Tribouley *et al.*, 1994; Lutz and Kedinger, 1996). IVa2 may also interact with pVII (Zhang and Arcos, 2005).

1.2.1.3.6   Protease (adenain)

The Ad protease, adenain, is synthesised in an inactive form and becomes partially activated following interaction with Ad DNA (Mangel *et al.*, 2003; Gupta *et al.*, 2004). Partially active adenain is able to cleave pre-VI, producing mature VI and an 11 amino acid cleavage product (Wodrich *et al.*, 2003). The 11 amino acid cleavage peptide binds to adenain resulting in full activation of the protease (McGrath *et al.*, 2003). Activated adenain is then able to cleave the precursor forms of late proteins IIIa, VI, VII, VIII, TP and Mu to yield an infectious virus particle (Tremblay *et al.*, 1983; Anderson, 1990; Webster *et al.*, 1993). Adenain may also facilitate cell lysis and the subsequent release of virus progeny by cleaving the cellular protein cytokeratin (Brown *et al.*, 2002; Brown and Mangel, 2004).

1.2.5   Life cycle of human adenoviruses

1.2.5.1   Cell entry

The classical pathway of Ad infection has been investigated in species C Ads (i.e. Ad2 and 5) in great detail. However, there are differences in recognition of cell surface molecules by species B Ads which leads to alternate cellular trafficking compared to species C Ads. The classical infection pathway is utilised by Ad species A, C, D, E, and F. Initial attachment to host cells *in vitro* is mediated by fibre binding to the Coxsackie and Adenovirus Receptor (CAR) (Bergelson *et al.*, 1997; Roelvink *et al.*, 1998) (Figure 1-2). CAR is a cellular attachment molecule and generally located in close proximity to tight junctions in polarised epithelial cells (reviewed in Philipson and Pettersson, 2004). As CAR expression is generally restricted to tight junctions and the basolateral membrane *in vivo*, there has been some debate as to whether CAR functions as the cellular attachment protein for Ads *in vivo* when it is located in seemingly inaccessible sites at the cell surface. Indeed, an alternative hypothesis for the interaction of the fibre with CAR is to facilitate escape of the virus following replication. Excess fibre protein produced during infection may facilitate disruption of CAR tight junction interactions, allowing release of the virus into the airway lumen (Walters *et al.*, 2002). However, a splice variant of CAR known as CAR Ex[8] has been detected on the apical surface of polarised airway epithelial cells (Excoffon *et al.*, 2010), therefore it is plausible that this variant of CAR may allow initial adhesion of the virus *in vivo*. In addition, it was recently found that Ad transduction of polarised epithelial cells is enhanced by a cytokine response from macrophages; production of chemokine 8 enhanced the apical localisation of CAR and $a_v\beta_3$ integrin, facilitating Ad transduction of target cells (Lutschg *et al.*, 2011).

In contrast to other Ad species, the species B Ads do not utilise CAR as the primary cell surface attachment receptor (Roelvink *et al.*, 1998). The species B Ads were classified into three groups by Tuve *et al* (2006) according to conserved restriction endonuclease cleavage sites, which also
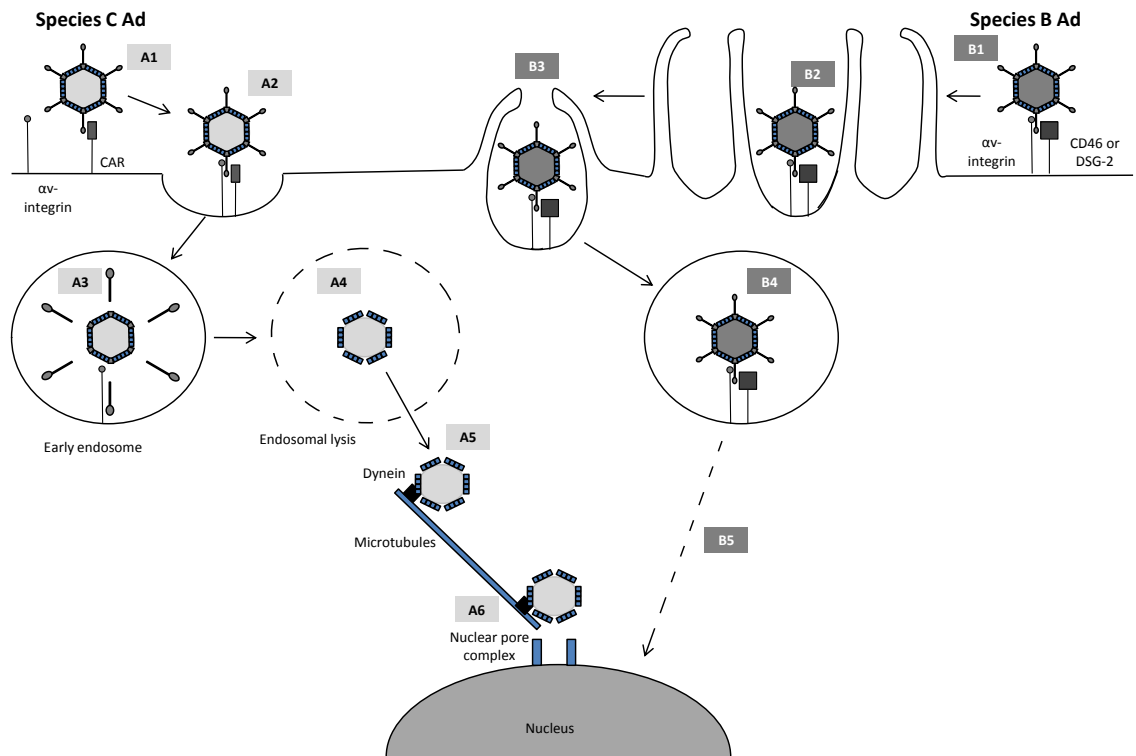
Figure 1-2. The cellular entry pathways of species C and species B adenoviruses.

The entry pathway of species C Ads appears to include the following stages. A1. Attachment of the virus fibre protein to the primary receptor, CAR, on the host cell surface. A2. Subsequent interaction of cellular $\alpha_v\beta_{3/5}$ integrins with the RGD motif of penton base. This results in clathrin-mediated endocytosis of the virus into early endosomes. A3. Within the acidic environment of the endosome, the virus capsid begins to dismantle leading to release of vertex proteins. A4. Protein VI promotes lysis of the endosomal membrane, allowing escape of the partially dissembled virus capsid into the cytoplasm. A5. The Ad capsid associates with microtubules in the cytoplasm and is trafficked via dynein to the microtubule organising centres (MTOCs) located adjacent to the nucleus. A6. At the nuclear pore, the viral genome is imported into the nucleus.

In contrast to species C Ads, the entry pathway of species B Ads appears to involve the following stages. B1. The virus fibre protein attaches to the primary receptor, CD46 or DSG-2. B2. Subsequent interaction of the RGD motif in the penton base protein with cellular $\alpha_v\beta_{3/5}$ integrins. This interaction stimulates membrane ruffling (B2) and macropinocytic uptake of the virus into the cell (B3). The subsequent escape of the virus from the endosome (B4) and trafficking of the capsid to the nucleus (B5) is currently undefined. Taken from White and Blair, 2012, with permission.

correlates with receptor usage; the Species B Group I Ads (Ad16, -21, -35, and -50) nearly exclusively use CD46, Group II (Ad3, -7p, and -14) appear to utilise desmoglein 2 (DSG-2) whilst Group III (Ad11p) can use both CD46 and DSG-2 (Segerman *et al.*, 2003; Marttila *et al.*, 2005; Tuve *et al.*, 2006; Wang *et al.*, 2010).

Following adhesion of Ads to the host cell surface, there is a secondary low-affinity interaction between the arginine-glycine-aspartate (RGD) motif (conserved among all human Ads except species F) within one of the exterior loops of the Ad penton base protein and α_v integrins (primarily $\alpha_v\beta_3$ and $\alpha_v\beta_5$) on the host cell surface (Wickham *et al.*, 1993; Mathias *et al.*, 1994; Wickham *et al.*, 1994; Nemerow and Stewart, 1999). As each penton base is a pentamer, the penton base is able to bind five integrin molecules, which promotes integrin clustering and triggers various cell signalling pathways. In species C Ads, the initial interaction of penton base with the integrin molecule is believed to induce a conformational change in the integrin which stimulates phosphoinositide 3-kinase (PI3K). The stimulation of PI3K leads to activation of Rac GTPase and cell division control protein 42 (CDC42), resulting in the polymerisation of actin monomers and cytoskeletal rearrangement within the cell (Li *et al.*, 1998a; Li *et al.*, 1998b). This facilitates the internalisation of species C Ads by endocytosis into clathrin-coated vesicles in a dynamin-dependent manner (Wickham *et al.*, 1994; Wang *et al.*, 1998) (Figure 1-2).

In contrast to species C Ads, the species B2 Ad3 appears to utilise an alternate entry mechanism (Figure 1-2). Entry of Ad3 into various cell types was shown to be minimally affected by dynamin mutation, indicating Ad3 does not utilise dynamin-dependent endocytosis as the primary cell entry mechanism (Wang *et al.*, 1998; Meier *et al.*, 2002). Instead, Ad3 uptake appears to be mainly by macropinocytosis, as Ad3 interaction with CD46 and cell surface integrins has been observed to induce membrane ruffling and fluid phase uptake (Amstutz *et al.*, 2008) (Figure 1-2). The species B2 Ad35 has also been reported to utilise macropinocytosis for entry into epithelial cells, suggesting this may be a common entry pathway in species B Ads (Kaelin *et al.*, 2010). Cellular factors required for macropinocytic uptake of Ad3 and Ad35 include the sodium-proton (Na^+/H^+) exchanger, actin, p21-activated kinase 1 (PAK1), Rac, protein kinase C (PKC) and C-terminal binding protein 1 of E1A (CtBP1) (Amstutz *et al.*, 2008; Kaelin *et al.*, 2010).

Additional factors appear to influence the cell transduction of Ads *in vivo*. Despite the evidence that interactions with CAR facilitate attachment of Ad5 *in vitro,* the biodistribution of Ads in mouse models does not correlate with *in vivo* CAR expression. Although liver hepatocytes generally have low CAR expression, intravenously (IV)-administered Ad5 vectors exhibit high liver transduction (Lieber *et al.*, 1997; Fechner *et al.*, 1999; Shayakhmetov *et al.*, 2004).

Furthermore, mutation of fibre residues necessary for CAR binding was shown to have no effect on the biodistribution of Ads following systemic delivery, suggesting the liver transduction of Ads is independent of CAR (Alemany and Curiel, 2001; Martin *et al.*, 2003). Later studies revealed the role of blood factors such as protein C, complement family member 4b binding protein (C4BP), Factor VII (FVII), Factor IX (FIX) and Factor X (FX) in Ad5 biodistribution *in vivo,* with FX demonstrating the greatest contribution to liver transduction (Shayakhmetov *et al.*, 2004; Parker *et al.*, 2006). These blood factors were shown to interact with Ad5 and facilitate binding of the Ad5 capsid protein hexon to heparan sulphate proteoglycans (HSPGs) and low density lipoprotein receptor (LDLR)-related proteins on the cell surface of liver hepatocytes (Kalyuzhniy *et al.*, 2008; Waddington *et al.*, 2008). A secondary interaction with α_v integrins is then required for internalisation (Bradshaw *et al.*, 2010). Recent *in vivo* studies have confirmed the role of FX in Ad5 liver transduction in a non-human primate model (Alba *et al.*, 2012). FX was also shown to facilitate hepatocyte transduction with Ad5 vectors with fibre proteins of species D Ads, indicating the role of FX in hepatocyte transduction may extend to serotypes other than Ad5 (Parker *et al.*, 2007; Waddington *et al.*, 2007). However, studies using species B fibre-pseudotyped or chimeric-fibre Ad5 vectors revealed greatly reduced liver tropism compared to wildtype Ad5 (Sakurai *et al.*, 2008; Ganesh *et al.*, 2009; Greig *et al.*, 2009; Rogee *et al.*, 2010). As these vectors all contain Ad5 hexon, this indicates that additional factors than hexon, FX and HSPGs contribute to liver tropism. A recent study into the role of other capsid proteins in Ad5 liver tropism revealed that whilst the binding of both wildtype Ad5 and Ad5 containing pseudotyped Ad35 fibre (Ad5F35) was enhanced by FX, the transduction of Ad5F35 was reduced compared to Ad5 (Corjon *et al.*, 2011). It was found that Ad5F35 vectors accumulated in the late endosome resulting in fewer virus particles reaching the cell nucleus. Entry into this trafficking pathway appeared to be dictated by the fibre protein (Corjon *et al.*, 2011). In contrast to species B and C Ads, certain species A Ads were shown to have enhanced affinity for respiratory or intestinal epithelial cells and this appeared to be mediated by FIX binding to cell surface heparan sulphate-containing glycosaminoglycans (Lenman *et al.*, 2011).

Taken together, it appears that CAR may only play a small role in the cell surface attachment of Ads administered intravenously; it seems that blood factors such as FX and FIX may have a greater influence on biodistribution. Following cell entry, it appears that fibre protein may then dictate the intracellular fate of the virus. It should be noted that although Ad dissemination in the bloodstream is unlikely during infection, Ad vectors are frequently administered intravenously in gene therapy regimens.

1.2.5.2 Transit of adenovirus to the nucleus

With regards to species C Ads, recent data indicates that capsid disassembly may commence at the cellular attachment stage (Burckhardt *et al.*, 2011). The lumen of the early endosome following internalisation rapidly becomes more acidic due to the activity of the H+ ATPase, which may induce conformational changes in certain viral capsid components, facilitating capsid disassembly (Greber *et al.*, 1993; Wiethoff *et al.*, 2005). It is thought the fibre proteins dissociate first, followed by penton base, pIIIa, pV, pVI and finally pIX. It appears that species C Ads do not traffic through the late endosome or lysosome (Gastaldelli *et al.*, 2008). Protein VI plays an important role in lysis of the endosome by disrupting the endosomal membrane, allowing the partially uncoated virus particle to be released into the cytoplasm (Wiethoff *et al.*, 2005; Maier *et al.*, 2010; Moyer *et al.*, 2011) (Figure 1-2).

The pathway of Ad3 from macropinosomes into the cytoplasm is less well defined, however it appears to be a much slower process than the escape of species C Ad2 from endosomes (30-40 minutes [Ad3] vs. 15 minutes [Ad2]) (Amstutz *et al.*, 2008). Furthermore, Ad5 viruses carrying species B fibre proteins appear to remain within endosomes for longer than wildtype Ad5 (Miyazawa *et al.*, 2001; Shayakhmetov *et al.*, 2003), indicating a lower pH may be required for species B capsid disassembly compared to species C.

Once species C Ads escape from the endosome, the partially uncoated virus particle associates with microtubules in the cytoplasm (Dales and Chardonnet, 1973; Mabit *et al.*, 2002; Kelkar *et al.*, 2006) (Figure 1-2). Transport of the species C Ads along microtubules is dependent on integrin signalling upon infection; the activation of p38 mitogen-activated protein kinase (MAPK) (Suomalainen *et al.*, 1999; Suomalainen *et al.*, 2001) facilitates trafficking of the virus particle by hexon-dynein interaction to the microtubule organising centres (MTOCs) located adjacent to the nucleus (Leopold *et al.*, 2000; Bremner *et al.*, 2009). The dynein co-factor dynactin appears to enhance the speed and efficiency of Ad particle transport to the nucleus (Engelke *et al.*, 2011). Ad pVI appears to play an integral role in movement of the virus particle to the nucleus; a PPXY motif exposed on pVI during capsid disassembly recruits Nedd4 E3 ubiquitin ligases, leading to ubiquitination of pVI which facilitates trafficking of the particle along microtubules (Wodrich *et al.*, 2010). Once the virus particle arrives at the MTOC, the nuclear export factor chromosome region maintenance 1 (CRM1) or an associated factor is thought to facilitate detachment of the virus from microtubules and promote association of the virus with the nuclear pore complex (NPC) (Strunze *et al.*, 2005).

1.2.5.3 Import of species C adenoviruses into the nucleus

As the Ad capsid is too large to diffuse through the nuclear pore, the particle undergoes further disassembly resulting in release of the Ad genome into the nucleus (Greber *et al.*, 1997). Docking of the capsid with the NPC is mediated by interactions between hexon and a cytoplasmic filament component of the NPC known as Nup214 (Trotman *et al.*, 2001) as well as kinesin-1 light chain (Strunze *et al.*, 2011). Soluble histone H1 appears to interact with a conserved hexon sequence in species C Ads, which recruits binding of the H1 importin 7/importin β import factor. However, this sequence is not conserved in species B Ads, indicating they may undergo a different import pathway (Trotman *et al.*, 2001). The chaperone heat-shock cognate 70 stress protein (Hsc70) is also required for nuclear import of Ad DNA (Saphire *et al.*, 2000). A nucleoporin associated with Nup214 known as Nup358 interacts with the kinesin-1 heavy chain, resulting in an indirect association between the capsid and the kinesin motor (Strunze *et al.*, 2011). Action of kinesin-1 then disrupts the Nup214-docked capsid resulting in release of capsid proteins and associated nucleoporins into the cytoplasm. The action of kinesin-1 simultaneously increases the nuclear envelope permeability (Strunze *et al.*, 2011) allowing the interaction of pVII with multiple nuclear import pathways, leading to import of the DNA-protein VII complex into the nucleus (Trotman *et al.*, 2001; Wodrich *et al.*, 2006; Hindley *et al.*, 2007). Once the complexes are inside the nucleus, pVII binds the transcription factors template activating factor (TAF)-1β and TAF-II (Kawase *et al.*, 1996; Haruki *et al.*, 2006). This leads to remodelling of chromatin on the virus genome, resulting in transcription of Ad genes.

1.2.6 The genome of species C adenoviruses

The genome organisation of species C Ads is highly conserved and encodes the five early transcription units E1A, E1B, E2A, E2B, E3 and E4, intermediate genes IX and IVa2 and late genes L1-5 (Figure 1-3) (Galibert *et al.*, 1979; Herisse *et al.*, 1980; Akusjarvi *et al.*, 1981; Herisse *et al.*, 1981; Gingeras *et al.*, 1982; Kruijer *et al.*, 1982; Sung *et al.*, 1983a; Akusjarvi *et al.*, 1984; Alestrom *et al.*, 1984; Roberts *et al.*, 1984). The late transcription units are expressed from the MLP whilst the intermediate genes L4-33K and L4-22K are initially expressed from a novel promoter located in the L4 region, the L4P (Morris *et al.*, 2010). Additional minor transcriptional units include the virus-associated (VA) RNAs I and II (Mathews, 1975). At either end of the genome are the ITRs, which are important for genome replication. The Ad genome is traditionally divided into 100 map units (mu) and the Ad E1A gene is conventionally placed at the far left of the genome.

The expression of the Ad genes during infection is regulated on a temporal basis consisting of four stages; immediate early, delayed early, intermediate and late, depending upon the time
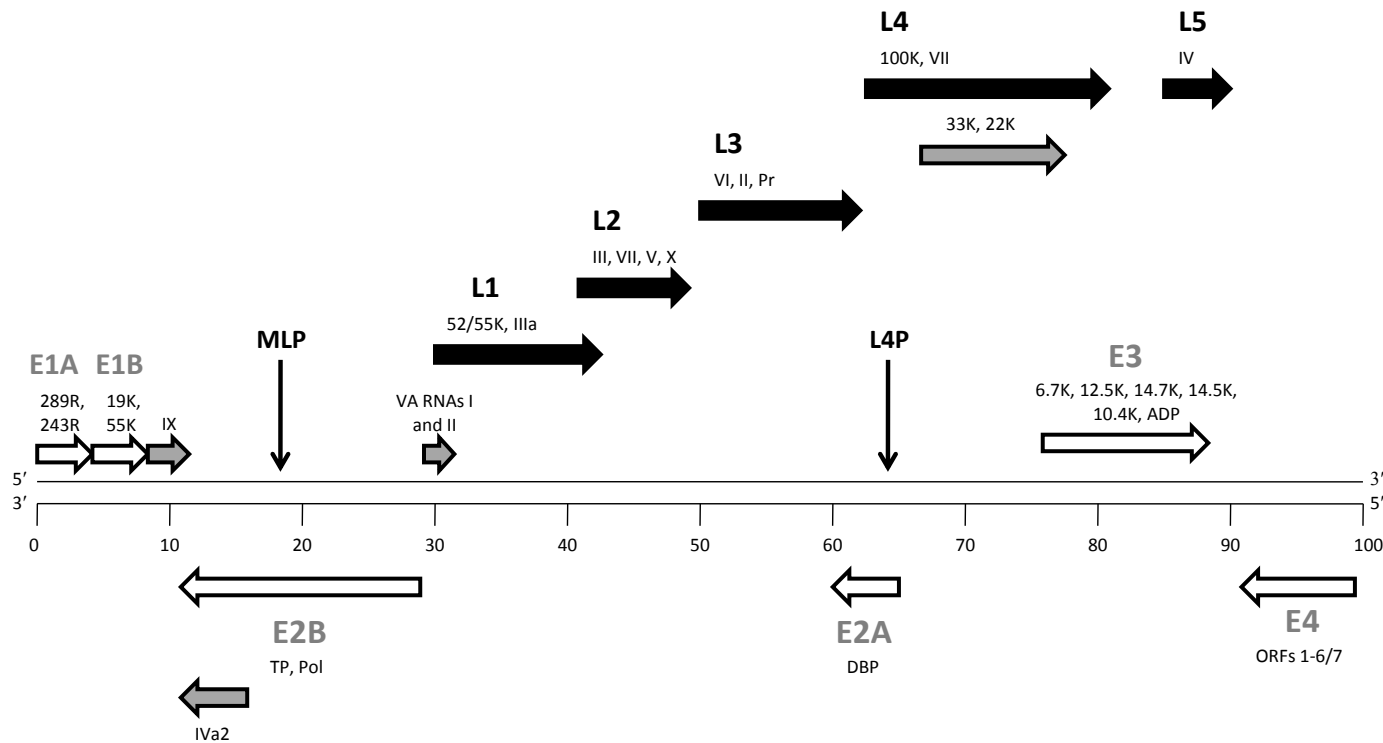
Figure 1-3. The genome of species C adenovirus.

The genome is represented as map units (mu) from the 5′ end of the rightward strand. The rightward strand encodes the E1A, E1B, IX, L1 – L5, VA RNA and E3 transcription units. The leftward strand encodes the E2A, E2B, E4 and IVa2 transcriptional units. Early expressed units are represented by white arrows, intermediate units by grey arrows and late expressed units are represented by the black arrows. The expression of the intermediate genes L4-33K and L4-22K is under the control of the L4 promoter (L4P). The expression of the L1-L5 units is under the control of the major late promoter (MLP). Pol – Polymerase. DBP – DNA Binding Protein. VA-RNA – Virus-Associated RNA. Pr – Protease. ADP – Adenovirus Death Protein. ORF – Open Reading Frame. Taken from White *et al* (2012), with permission.

point at which the gene product can be detected (Akusjarvi, 2008; Morris *et al.*, 2010). The immediate early gene E1A is expressed shortly after the viral genome enters the host cell nucleus. The expression of other early units E1B, E2A, E3 and E4 is driven by the activity of E1A alongside a variety of cellular factors (reviewed in Berk, 2007). The MLP is also active at this stage at low level, producing only the L1-52/55K proteins. Proteins encoded in the early gene regions act to promote cell cycle progression, genome replication and suppression of host cell anti-viral mechanisms. At the onset of DNA replication, the intermediate transcription units E2B, IVa2 and IX become activated (Berk, 2007). Gene transcription from the L4P is also activated at this time point (Morris and Leppard, 2009; Morris *et al.*, 2010). The intermediate genes act to up-regulate expression from the MLP. Following genome replication, transcription from the MLP proceeds to the full length of the unit resulting in expression of the late genes. Late proteins function mainly to co-ordinate virus capsid assembly and the subsequent release of progeny virions from the host cell.

1.2.6.1 Early gene expression in species C adenoviruses

1.2.6.1.1 E1A

E1A is the immediate early unit and is the first gene to be expressed upon entry of the virus to the host cell nucleus (Berk and Sharp, 1978; Chow *et al.*, 1979; Nevins *et al.*, 1979). The expression of E1A was recently shown to be facilitated by the Ad capsid protein pVI (Schreiner *et al.*, 2012). The primary E1A transcript is processed by alternative splicing to yield five mRNAs which in Ad5 have sedimentation coefficients of 13S, 12S, 11S, 10S and 9S (Stephens and Harlow, 1987; Ulfendahl *et al.*, 1987). Alternative splicing of the E1A transcript is regulated in a temporal manner, such that during the early stages of infection the two major E1A mRNA species are the 13S and 12S mRNAs (Perricaudet *et al.*, 1979; Hearing and Shenk, 1983; Boulanger and Blair, 1991). The 9S mRNA product is the most abundant protein at late times, whilst the 11S and 10S are minor mRNA species at late stages of infection (Stephens and Harlow, 1987; Ulfendahl *et al.*, 1987). The 13S, 12S, 11S, 10S and 9S mRNAs encode the 289 residue (R), 243R, 217R, 171R and 55R proteins respectively. The E1A proteins drive numerous cellular processes during infection including transcriptional activation, transcriptional repression, immune subversion, immortalisation of primary rodent cells and transformation in cooperation with Ad E1B-55K or activated cellular RAS (reviewed in Berk, 2005).

The 9S E1A mRNA is expressed during the late stage of infection due to temporal changes in splice site usage (Ulfendahl *et al.*, 1987). The encoded 55R E1A protein appears to stimulate transcriptional activation and promote viral replication (Miller *et al.*, 2012). The 10S and 11S E1As are also expressed at late time points, however the roles of the 217R and 171R E1As during infection is less clear. Deletion mutants for the 217R and 171R proteins do not exhibit

defective growth and they appear dispensable for transformation activities (Ulfendahl *et al.*, 1987). Although the 217R E1A was shown to have transcriptional activation properties in transient transfection assays, this activity appeared negligible in the context of virus infection (Ulfendahl *et al.*, 1987).

Ad 289R and 243R E1As are expressed immediately following entry of the viral genome into the host cell nucleus. Ad 289R E1A is required for stimulating transcription from the four early Ad transcription units by associating with cellular transcription factors that bind to the early Ad promoters (Berk *et al.*, 1979; Jones and Shenk, 1979; Webster and Ricciardi, 1991; Liu and Green, 1994). E1A was found to bind the transcriptional co-activators p300/CBP (Eckner *et al.*, 1994; Arany *et al.*, 1995; Lundblad *et al.*, 1995; Avantaggiati *et al.*, 1996; Yang *et al.*, 1996; Somasundaram and El-Deiry, 1997) as well as a subunit of the Mediator complex known as MED23 (Boyer *et al.*, 1999b; Stevens *et al.*, 2002) to activate transcription *in vitro*. E1A alongside IVa2, E4orf3 and viral DNA replication was also found to promote transcription of the intermediate genes L4-33K and L4-22K from the L4P (Morris *et al.*, 2010).

Both the 289 and 243R E1As are responsible for driving progression of the cell cycle from G1 to S-phase in infected cells (Braithwaite *et al.*, 1983; Spindler *et al.*, 1985; Zerler *et al.*, 1987). This function of E1A alongside the activity of E1B or activated RAS is sufficient to induce transformation of primary rodent cells (Spindler *et al.,*1984; Howe *et al.*, 1990; Stein *et al.*, 1990, Yew and Berk, 1992). E1A binds to the cellular retinoblastoma protein (pRb) and the Rb-related proteins p107 and p130 (Barbeau *et al.*, 1992; Dyson *et al.*, 1992). The Rb proteins are a family of tumour suppressors which directly bind and inhibit the activity of the E2F family of transcription factors. The Rb-E2F complex also recruits transcriptional repressors such as histone deacetylase complexes (HDACs) and Polycomb (PcG) histone methyltransferases to chromatin (Chellappan *et al.*, 1991; Nevins, 1992; Kato *et al.*, 1993; Brehm *et al.*, 1998). Under normal circumstances, cell signalling leads to phosphorylation and inactivation of Rb by CDK-cyclin complexes, relieving E2F repression and allowing progression of the cell cycle. Binding of E1A to Rb displaces Rb from E2F thus facilitates transcription from E2 promoters (Nevins *et al.*, 1997; Dyson, 1998; Nevins, 2001; Trimarchi *et al.*, 2001; Ghosh and Harter, 2003; Frolov and Dyson, 2004). The activation of E2Fs results in enhanced transcription of cell cycle regulatory proteins including CDK2 and cyclins E and A, resulting in progression to S-phase of the cell cycle.

E1A has been implicated in innate immune subversion by abrogating interferon (IFN) signalling (Ackrill *et al.*, 1991; Gutch and Reich, 1991). This was shown to be facilitated by direct interaction of E1A with Stat1 (Look *et al.*, 1998) and IFN regulatory factor 9 (IRF9) (Leonard

and Sen, 1997), components of the IFN signalling pathway. E1A of Ad12, but not Ad5, was also shown to facilitate immune evasion by down-regulating the expression of MHC class I from the surface of rodent cells (Ackrill and Blair, 1988).

E1A is also involved in attenuation of p53 function by two separate mechanisms; preventing acetylation and subsequent activation of p53 and preventing up-regulation of p21 by impairing binding of the transcription factor SP1 to the p21 promoter (Savelyeva and Dobbelstein, 2011). However, expression of E1A alone induces apoptosis in host cells (Rao *et al.*, 1992; Debbas and White, 1993; Yageta *et al.*, 1999). E1A interferes with proteasome function resulting in the stabilisation of p53 (Lowe and Ruley, 1993; Zhang *et al.*, 2004). E1A can also trigger apoptosis in a p53-independent mechanism by inducing proteasomal degradation of the anti-apoptotic BCL-2 family member myeloid leukaemia sequence 1 (MCL-1), which results in the release of pro-apoptotic BAK and initiation of apoptosis (Cuconati *et al.*, 2003). However, during infection a multitude of Ad proteins act to prevent p53-dependent and independent apoptosis, including products of the E1B transcriptional unit.

1.2.6.1.2   E1B

The major gene products of the E1B region are the E1B-55K and E1B-19K proteins. Both proteins act to suppress p53-dependent and independent cell cycle arrest and apoptosis triggered by the activity of E1A (Debbas and White, 1993). E1B-19K is a homologue of the cellular anti-apoptotic protein BCL-2 (Rao *et al.*, 1992), and acts to prevent initiation of the apoptotic cascade by binding BAK and also another pro-apoptotic cellular protein, BAX (Cuconati *et al.*, 2002; Cuconati and White, 2002). E1B-19K can also prevent p53-mediated apoptosis induced by TNF-α and Fas ligand by the same mechanism (Debbas and White, 1993).

E1B-55K was observed to sequester p53 in peri-nuclear bodies, termed aggresomes (Sarnow *et al.*, 1982; Zantema *et al.*, 1985; Liu *et al.*, 2005), a subcellular structure that forms at the MTOC in response to misfolded proteins (Kopito, 2000; Garcia-Mata *et al.*, 2002). E1B-55K was also found to bind p53 in the nucleus preventing p53-mediated transcriptional activation (Yew and Berk, 1992; Querido *et al.*, 1997; Teodoro and Branton, 1997; Martin and Berk, 1998, 1999). In addition, E1B-55K can function as an E3 small ubiquitin-like modifier 1 (SUMO1)-p53 ligase; the SUMOylation and subsequent sequestration of p53 in nuclear PML-NBs may facilitate export of p53 from the nucleus (Pennella *et al.*, 2010). E1B-55K also suppresses p53 activity by preventing p53 acetylation by p300/CBP-associated factor (PCAF) (Liu *et al.*, 2000). Acetylation of p53 promotes high-affinity DNA binding, promoting transcription at p53 promoters. The interaction of E1B-55K with HDAC complexes may also suppress p53-dependent transcription (Punga and Akusjarvi, 2000).

E1B-55K is able to form a ubiquitin ligase complex with the Ad E4 open reading frame 6 (E4orf6) protein (Sarnow *et al.*, 1984) alongside the cellular proteins elongins B and C, cullin 5 and Rbx-1 (Yew *et al.*, 1994). In this complex, E1B-55K acts as the substrate recognition domain whilst E4orf6 binds elongin C (Blanchette *et al.*, 2004). This complex promotes the ubiquitination and proteasomal degradation of proteins involved in the DNA damage response, including p53 (Querido *et al.*, 2001; Harada *et al.*, 2002), the MRN complex (Stracker *et al.*, 2002) which is involved in DNA double-strand break repair (D'Amours and Jackson, 2002; Stracker *et al.*, 2002; Carson *et al.*, 2003; Petrini and Stracker, 2003; van den Bosch *et al.*, 2003) and DNA ligase IV (Baker *et al.*, 2007). In cells infected with E4 deletion mutants, the MRN complex promotes concatemerisation of viral DNA by non-homologous end joining (Weiden and Ginsberg, 1994; Boyer *et al.*, 1999a; Evans and Hearing, 2003). Following reorganisation of PML-NBs into nuclear tracks by Ad E4orf3, E4orf6 interacts with MRN within the modified PML-NBs (Carvalho *et al.*, 1995; Doucas *et al.*, 1996; Evans and Hearing, 2005). A complex of E1B-55K, E4orf6, E4orf3 and MRN is then exported to cytoplasmic aggresomes, where accelerated degradation of ubiquitinated MRN complex proteins occurs (Liu *et al.*, 2005).

E1B-55K also plays a role in the export of late viral mRNAs from the nucleus into the cytoplasm whilst simultaneously inhibiting the export of cellular mRNAs (Beltz and Flint, 1979). It is also believed that E1B-55K may stimulate translation of late viral mRNAs (Harada and Berk, 1999). Although the exact mechanism by which E1B-55K enhances late viral mRNA export and/or protein synthesis is currently unknown, it has been proposed that the E1B-55K/E4orf6 complex may interact with a cellular factor involved in both mRNA export and mRNA translation (Berk, 2007). Ubiquitin ligase activity of the E1B-55K/E4orf6 complex appears to be required for mRNA export, indicating that ubiquitination of cellular target proteins may be required for Ad late mRNA export (Woo and Berk, 2007; Blanchette *et al.*, 2008). In addition, the accumulation of late mRNAs in the cytoplasm appears to require the Nxf1/TAP exporter (Yatherajam *et al.*, 2011) and is dependent on the nuclear export signal of E4orf6 (Weigel and Dobbelstein, 2000).

1.2.6.1.3 E2

Proteins encoded by the E2 region of Ads are indispensible for viral replication (De Jong *et al.*, 2003b) (see Chapter 1.2.6.2). The three proteins encoded in this region are Ad-pol, DBP and pTP. Cellular proteins including octamer transcription factor 1 (Oct-1) and NF-I are also required for efficient replication (de Jong and van der Vliet, 1999).

1.2.6.1.4 E3

The E3 region encodes a number of proteins with roles in host immune subversion. The E3-19K protein binds to MHC class 1 molecules, preventing their trafficking to the cell surface (Fessler *et al.*, 2004). This abrogates the presentation of viral peptides by MHC class I to circulating cytotoxic T cells. E3-19K also reduces cell surface levels of the NK cell-activating ligand NKG2D, preventing NK cell recognition of infected cells (McSharry *et al.*, 2008). The E3-10.4K and 14.5K proteins also affect cell surface receptor expression by forming the Receptor Internalisation and Degradation (RID) complex (Gooding *et al.*, 1991). The RID complex acts to down-regulate cell surface expression of the Fas and TRAIL ligands, preventing circulating NK and T cells from killing the infected cell (Shisler *et al.*, 1997). E3 14.7K plays a role in preventing host cell death by blocking TNF-α and TRAIL-induced apoptosis (Gooding *et al.*, 1991; Tollefson *et al.*, 2001; Schneider-Brachert *et al.*, 2006). In addition, E3 14.7K interacts with four cellular proteins designated the 14.7K-interacting proteins (FIPs) (reviewed in Horwitz, 2004). The FIPs have diverse roles within the cell, including NF-κB signal transduction and mitochondrial-induced apoptosis.

1.2.6.1.5 E4

The E4 region encodes a multitude of proteins with a variety of functions. E4orf3 is a highly multifunctional protein with roles in immune evasion, suppression of p53 activity, mRNA transport and inhibition of the MRN complex. E4orf3 suppresses induction of the host IFN response by re-organising nuclear PML-NBs (Ullman *et al.*, 2007, 2008) (see Chapter 1.4.2). E4orf3 targets the transcriptional co-repressor TIF-1 to the rearranged PML-NBs for proteasome-mediated degradation (Yondola and Hearing, 2007; Forrester *et al.*, 2012). E4orf3 was also implicated in reorganisation of several protein components of the cytoplasmic mRNA processing bodies (p-bodies), a structure involved in mRNA degradation (Greer *et al.*, 2011). P-body proteins appear to be targeted to cytoplasmic aggresomes, the site of protein inactivation/degradation. The targeting of proteins involved in mRNA degradation to sites of protein degradation may facilitate the accumulation of late Ad mRNAs (Greer *et al.*, 2011). E4orf3 is also able to suppress p53 function by forming a nuclear complex capable of inducing formation of heterochromatin at p53 target promoters, preventing p53 binding to DNA (Soria *et al.*, 2010).

E4orf3 shares some activities with another E4 protein, E4orf6. Both E4orf3 and E4orf6 influence alternative splicing of late Ad mRNAs, resulting in accumulation of late mRNA transcripts in the nucleus (Bridge *et al.*, 1991; Nilsson *et al.*, 2001). E4orf3 and E4orf6 are also able to inhibit MRN complex function independently of the E1B-55K/E4orf6 ubiquitin ligase activity (Boyer *et al.*, 1999a; Shepard and Ornelles, 2004). In addition to shared functions with

E4orf3, E4orf6 forms a complex with E1B-55K; the ubiquitin ligase activity of the E1B-55K/E4orf6 complex is required for the nuclear export of Ad late mRNAs (Bridge and Ketner, 1990; Woo *et al.,* 2007; Blanchette *et al.,* 2008). E4orf6 is also responsible for SUMO-1 modification of E1B-55K (Lethbridge *et al.*, 2003).

E4orf4, E4orf6 and E4orf6/7 play roles in transcription. E4orf4 functions as a transcriptional co-repressor; it appears to regulate early gene transcription by associating with the key cellular phosphatase, protein phosphatase 2A (PP2A) (Bondesson *et al.*, 1996; Mannervik *et al.*, 1999). This complex negatively regulates the transcription of early viral genes by down-regulating transcription of *JunB*, a component of the transcription factor AP-1 (Kleinberger and Shenk, 1993). E4orf6 was recently shown to associate with the cellular transcription factor homeobox B7 (HoxB7), facilitating transcription from Ad promoters (Muller *et al.*, 2012). E4orf6/7 appears to act as a transcriptional enhancer by promoting the dimerisation of a heteromeric E2F complex at the E2 promoter (Obert *et al.*, 1994). In addition, E4orf6/7 induces transactivation of E2F by recruitment of the E2F complex to the E2F-1 promoter (Schaley *et al.*, 2000).

1.2.6.2 DNA replication in species C adenoviruses

Species C Ads have been shown to undergo an infectious cycle of around 36 hours, with virus replication being initiated at approximately 8 hours post-infection (h.p.i) (Wigand and Kumel, 1977; Bodnar and Pearson, 1980; Rowe *et al.*, 1984; Glenn and Ricciardi, 1988). During the early phase of infection the early region genes are expressed, some of which (the E2 proteins DBP, Ad-pol and pTP) are required for the initiation of DNA replication (Lichy *et al.*, 1981; Lichy *et al.*, 1982). Ad-pol and pTP form a heterodimer (Lichy *et al.*, 1982) and the cellular transcription factors NFI and NFIII promote the assembly of the pre-initiation complex at the binding site of the pTP-Ad-pol complex (Mul *et al.*, 1990). Both Oct-1 and NFI was shown to bend the replication origin into a favourable structural conformation for pre-initiation complex assembly (Mysiak *et al.*, 2004a; Mysiak *et al.*, 2004c). In addition to E2 and cellular proteins, the ITRs located at either end of the genome contain the origin of replication as defined by *cis*-acting sequences (Leegwater *et al.*, 1985; Nowock *et al.*, 1985).

Following formation of the pre-initiation complex, pTP functions as a primer for replication and replication is carried out by Ad-pol (King *et al.*, 1997; Webster *et al.*, 1997). DBP is thought to act as a helicase, unwinding DNA to allow access of the polymerase to a single-stranded template (Dekker *et al.*, 1997). DNA synthesis is initiated by Ad-pol catalysing a covalent reaction between pTP and a deoxycytidine triphosphate (dCTP), forming the dCTP-pTP complex (Nagata *et al.*, 1982; de Jong *et al.*, 2003a; Mysiak *et al.*, 2004b). Two further nucleotides (AT) are then added to the complex to form the intermediary pTP-CAT complex (de

Jong *et al.*, 2003a). This complex is then able to bind the GTA sequence at position 1 of the genome and initiate elongation. Elongation occurs by a strand-displacement mechanism which involves Ad-pol, pTP, DBP and cellular protein NF-II (Nagata *et al.*, 1983; de Jong and van der Vliet, 1999; de Jong *et al.*, 2003a). This process results in the production of a DNA duplex which contains one parental and one daughter strand. A complementary strand to the displaced parental strand is then synthesised. The mechanism of this is still unclear; the displaced strand may anneal to other displaced strands, or annealing of the ITRs may result in a pan handle structure from which DNA replication can be initiated (reviewed in Liu *et al.*, 2003).

1.2.6.3 Intermediate gene expression in species C adenoviruses

Upon initiation of DNA replication, the intermediate genes IVa2 and IX are expressed (Natarajan *et al.*, 1984; Matsui *et al.*, 1986; Vales and Darnell, 1989; Winter and Dhalluin, 1991). The expression of IVa2 is regulated by a currently undefined cellular repressor which is titrated out upon genome replication (Huang *et al.*, 2003; Iftode and Flint, 2004). IX and IVa2 alongside viral DNA replication play roles in up-regulating transcriptional activity of the MLP (Tribouley *et al.*, 1994; Lutz and Kedinger, 1996; Lutz *et al.*, 1997). Transcription from the L4P is stimulated by a combination of DNA replication, IVa2, E1A and E4orf3 and results in production of the MLP-positive regulators L4-22K and L4-33K (Morris *et al.*, 2010).

1.2.6.4 Late gene expression in species C adenoviruses

Following the initiation of DNA replication, there is a large increase in late gene expression and mRNA synthesis due to activation of the MLP (Manley *et al.*, 1980). The MLP directs transcription from the major late transcriptional unit (MLTU) regions L1 to L5. The primary transcript is differentially spliced and polyadenylated to produce an array of late proteins (reviewed in Akusjarvi, 2008). Each mRNA has an identical tripartite leader sequence of non-coding RNA at the 5′ end formed from the removal of three introns during splicing (Akusjarvi and Pettersson, 1978; Chow and Broker, 1978; Dunn *et al.*, 1978; Ziff and Evans, 1978; Berget and Sharp, 1979). Transcription from the MLP reaches a maximum at 18 h.p.i and stays constant for the remainder of infection, resulting in high yields of virus structural and non structural proteins required for formation of the Ad capsid or for packaging of the Ad genome into the capsid.

The temporal regulation of MLP expression is both transcriptional and post-transcriptional and these effects require the activity of L4-22K and L4-33K. Early phase transcripts from the MLP are not alternately spliced or elongated beyond the L3 poly(A) sequence (Shaw and Ziff, 1980; Iwamoto *et al.*, 1986), with the L1-poly(A) site being preferentially used, leading to an accumulation of large amounts of L1-52/55K protein (Nevins and Wilson, 1981). In the L1

region the 52/55K splice-acceptor site is exclusively utilised during the early phase. However the action of the splicing factor L4-33K changes the preference to the distal IIIa acceptor site during the late stage of infection (Larsson *et al.*, 1992; Farley *et al.*, 2004; Tormanen *et al.*, 2006; Akusjarvi, 2008).

Both L4-22K and L4-33K, in the presence of L4-100K, are able to induce production of late phase proteins (Morris and Leppard, 2009). The L4-22K and L4-33K proteins act post-transcriptionally to produce the full complement of major late transcriptional unit mRNAs (Farley *et al.*, 2004; Tormanen *et al.*, 2006; Morris and Leppard, 2009) and also up-regulate IVa2, which acts in conjunction with L4-22K and/or L4-33K to up-regulate MLP activity (Tribouley *et al.*, 1994; Lutz and Kedinger, 1996; Ostapchuk *et al.*, 2006; Ali *et al.*, 2007; Morris and Leppard, 2009). It was recently shown that L4-33K activity is controlled in a phosphorylation-dependent manner by cellular kinases; DNA-protein kinase appears to act as an inhibitory factor whereas phosphorylation by PKA appears to enhance L4-33K function (Persson *et al.*, 2012).

Alternative late pre-mRNA splicing is also controlled by the reversible phosphorylation of cellular splicing factors known as serine/arginine-rich splicing factors (SRSFs). During the early stages of infection, SRSFs bind to the intronic IIIa-repressor element within the L1 transcript which prevents recruitment of the U2 subunit of the spliceosome at the distal IIIa 3′ site (Kanopka *et al.*, 1996). E4orf4 dephosphorylates SRSFs by activating PP2A, allowing splicing to commence at the distal site resulting in expression of late-phase transcripts (Kanopka *et al.*, 1998).

Following transcription and processing, mature late viral mRNAs are selectively exported to the cytoplasm whilst cellular mRNA export is inhibited. Although not well defined, this process appears to require the ubiquitin ligase activity of the Ad E1B-55K/E4orf6 complex and is dependent upon the cellular mRNA export receptor known as Nxf1/TAP (Woo and Berk, 2007; Blanchette *et al.*, 2008; Yatherajam *et al.*, 2011). Once in the cytoplasm, late viral mRNAs are selectively translated whilst the translation of cellular mRNAs is inhibited. The L4-100K protein is responsible for the inhibition of cellular protein synthesis by binding the elongation initiation factor 4G (eIF4G), displacing the kinase Mnk1 (Cuesta *et al.*, 2000; Xi *et al.*, 2004). Displacement of Mnk1 from the cap initiation complex prevents Mnk1-mediated phosphorylation and activation of the cap binding protein eIF4E, resulting in inhibition of cap-dependent translation (Cuesta *et al.*, 2000; Xi *et al.*, 2004). However, the presence of the common tripartite leader in the 5′ UTR of Ad late mRNAs allows selective translation of these mRNAs (Logan and Shenk, 1984; Dolph *et al.*, 1988; Dolph *et al.*, 1990; Huang and Flint,

1998). L4-100K binds Ad mRNAs with a preference for tripartite leader-containing mRNAs (Adam and Dreyfuss, 1987; Xi *et al.*, 2004). This results in enhanced association of late mRNAs with eIF4G and poly(A) binding protein, facilitating translation of viral late mRNAs by an alternative mechanism known as 'ribosome shunting' (Yueh and Schneider, 1996, 2000). This translation mechanism involves initial assembly of the 40S ribosome subunits onto the 5′ end of the capped mRNA followed by minimal scanning. 'Shunting elements' in the tripartite leader then direct the translocation of the 40S ribosome to the initiation site of the mRNA.

1.2.6.5 Capsid assembly in species C adenoviruses

Following transcription of Ad genes and translation of Ad mRNA transcripts, the resulting Ad proteins are transported from the cytoplasm into the nucleus for particle assembly. With regards to hexon, the L4-100K protein acts as a protein scaffold to aid assembly of hexon monomers into trimers (Hong *et al.*, 2005). The hexon trimers then associate with pVI to be targeted to the nucleus (Kauffman and Ginsberg, 1976). Penton base monomers appear to independently assemble into pentamers in the cytoplasm. Likewise, fibre proteins autonomously assemble into trimers in the cytoplasm. Both penton base and fibre contain nuclear localisation signals (NLS), allowing import of assembled multimers into the nucleus. Subsequent assembly of penton capsomers is thought to occur spontaneously in the nucleus (Karayan *et al.*, 1994; Franqueville *et al.*, 2008).

Once all capsid components are located inside the nucleus, L4-33K functions as a scaffold for the assembly of virus particles (Fessler and Young, 1999). In Ad5-infected cells, distinct nuclear penton aggregates are visible at 48 h.p.i which may correspond to capsid assembly platforms (Franqueville *et al.*, 2008). In contrast, Ad3-infected cells display smaller, more punctuate aggregates of pentons, which may indicate differences in capsid assembly between these two serotypes (Hall *et al.*, 2010).

Once the procapsid has been assembled, the Ad genome is packaged into the virus particle at a precise vertex. A packaging sequence containing several AT-rich regions is located at the far left of the genome and is believed to direct insertion of the genome into the capsid (Ostapchuk and Hearing, 2005). The subsequent uptake of DNA into the capsid is then thought to be provided by the ATPase activity of IVa2 (Ostapchuk and Hearing, 2008). Once the DNA is packaged, sealing of the pro-capsid is promoted by binding of L4-22K, L1-52/55K and IVa2 to the DNA packaging sequence (Perez-Romero *et al.*, 2005; Ewing *et al.*, 2007). IIIa also associates with L1-52/55K and with the viral DNA packaging domain (Ma and Hearing, 2011). The L3-23K cysteine protease (adenain) then promotes maturation of the particle to a mature capsid. Adenain is activated by Ad DNA and the cleavage peptide of pre-VI; the activated

protease cleaves the protein precursors of VI, VII, VII, Mu and TP resulting in formation of the mature infectious virion. However, some studies have shown that the packaging of the Ad genome may be intrinsically linked to capsid assembly (Zhang and Imperiale, 2003), therefore it may be that the capsid is assembled around a DNA complex, rather than the Ad genome being imported into a pre-assembled capsid.

1.2.6.6   Virus release from host cells

During infection with species C Ads, the accumulation of Ad death protein (ADP) leads to lysis of host cells (Tollefson *et al.*, 1996a; Tollefson *et al.*, 1996b). ADP localises to intracellular membranes and may interact with the anaphase-promoting complex (APC) inhibitor MAD2B to promote cell lysis by an as yet undefined mechanism (Ying and Wold, 2003). However, species B Ads do not encode ADP so cannot release progeny virions by this route; it is yet to be seen if they possess an alternative lysis mechanism. Ads also promote cell lysis by the activity of the Ad protease cleaving the cytoskeletal component cytokeratin (Chen *et al.*, 1993). Ads may also induce autophagy in infected cells to promote release of infectious virions (Jiang *et al.*, 2008). The dynein co-factor dynactin appears to enhance trafficking of species C Ad particles to the cell periphery (Engelke *et al.*, 2011).

1.3 The eukaryotic nucleus

1.3.1   Sub-compartmentalisation of the nucleus

The nucleus is a highly heterogeneous structure containing multiple subdomains. Development of protein tagging and immunofluorescence techniques has allowed the identification of a number of nuclear domains which display dynamic behaviour both in regard to their location within the cell and their protein constituents. Unlike cytoplasmic organelles, nuclear domains do not have outer membranes and are divided into distinct sub-compartments defined by location of chromosomes (Lichter *et al.*, 1988) or excess replication (Wei *et al.*, 1998), transcription (Jackson *et al.*, 1993) or splicing components (Spector *et al.*, 1991).

Functionally specialised nuclear bodies include the nucleolus, PML-NBs, Cajal Bodies (CBs), splicing speckles and paraspeckles (Figure 1-4). Less well-characterised nuclear bodies include cleavage bodies (Schul *et al.*, 1996; Schul *et al.*, 1999b; Gall, 2000; Bleoo *et al.*, 2001; Li *et al.*, 2006b), PcG domains (reviewed in Margueron and Reinberg, 2011), nuclear stress bodies (nSBs) (reviewed in Biamonti, 2004; Gabriela Thomas *et al.*, 2011), Oct1/PTF/Transcription (OPT) domains (Pombo *et al.*, 1998; Harrigan *et al.*, 2011) and polymorphic interphase karyosomal associations (PIKAs) (Saunders *et al.*, 1991; Pombo *et al.*, 1998). DNA replication, RNA transcription and DNA repair have also been observed to occur in defined nuclear foci of around 100 nm in diameter. Transcription and replication foci appear to contain all the
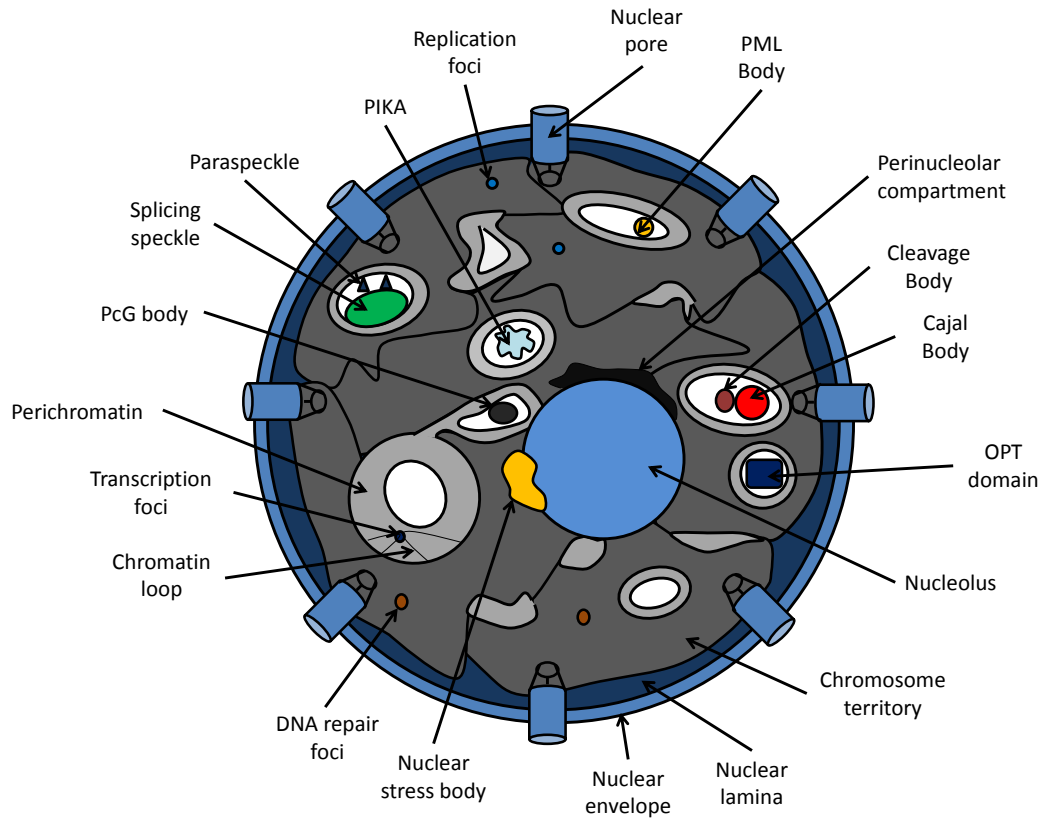
Figure 1-4. The sub-compartmentalisation of the mammalian cell nucleus.

The nucleus is enclosed by the nuclear membrane and a meshwork of intermediate filaments known as the nuclear lamina. The membrane is penetrated by nuclear pores allowing the exchange of factors between the nucleus and the cytoplasm. Chromatin domains originating from the same chromosome form the chromosome territories (dark grey regions), which may overlap or create interchromatin spaces (white regions). Perichromatin domains (light grey regions) are regions of less dense, transcriptionally active chromatin. Proteinaceous sub-nuclear bodies including the Cajal body, PML body, nucleolus, splicing speckles, paraspeckles, Polycomb group (PcG) bodies, Oct-1/PTF/Transcription (OPT) domains, nuclear stress bodies, Polymorphic Interphase Karyosomal Associations (PIKAs) and cleavage bodies are located in the interchromatin space. The perinucleolar compartment is located at the periphery of the nucleolus. DNA replication, RNA transcription and DNA repair occur in small foci ('factories') of around 100nm. Adapted from Lanctot *et al.*, 2007; Hemmerich *et al.*, 2011.

necessary enzymatic activity for their reactions therefore have been termed 'factories'. It has been proposed that RNA polymerase II (RNA pol II) is bound to a transcription factory that subsequently attracts chromatin templates to the site (Cook, 1999; Cook, 2010). DNA replication also appears to occur at sites where necessary factors are already concentrated (Leonhardt *et al.*, 2000). In contrast to transcription and replication foci, repair of damaged DNA may to require orchestrated recruitment of necessary repair factors (Lukas *et al.*, 2005).

1.3.2 Nucleolus

The nucleolus is a highly multifunctional unit with its best-characterised role being ribosome subunit biogenesis. At the end of mitosis, nucleoli form around the tandem repeat clusters of ribosomal DNA (rDNA) genes, resulting in a sub-nuclear domain concentrated in proteins required for rDNA transcription and processing (reviewed in Boisvert *et al.*, 2007). The genes encoding the initial 45S ribosomal RNA (rRNA) are found on nucleolar organising regions (NORs) located on specific chromosomes and these NORs decondense following mitosis, facilitating the formation of the nucleolus containing transcription factories (Roussel *et al.*, 1996). Transcription of the 45S rRNA is carried out by RNA pol I and the transcript is cleaved to produce the mature 28S, 18S and 5.8S s rRNAs (reviewed in Boisvert *et al.*, 2007). These RNAs are post-transcriptionally modified by nucleolar-RNA containing protein complexes known as the small nucleolar ribonucleoproteins (snoRNPs). The rRNAs are then assembled with the ribosomal subunits and exported to the cytoplasm (Boisvert *et al.*, 2007).

In order to carry out this complex set of reactions, the nucleolus is organised into regions which have different functions. Electron microscopic analysis of the nucleolus has identified that it consists of three main sub-compartments; the fibrillar centres (FC; regions containing rDNA), the surrounding dense fibrillar component (DFC; regions involved in rRNA transcription and initial processing) and the granular component (GC; regions involved in initial ribosome assembly) (Scheer and Hock, 1999). In addition to rRNA synthesis and ribosome assembly, the nucleolus is also implicated in sensing stress (Rubbi and Milner, 2003), inducing p53 activation (Itahana *et al.*, 2003; Korgaonkar *et al.*, 2005; Gjerset, 2006), cell cycle control (Cockell and Gasser, 1999; Diaz-Cuervo and Bueno, 2008; Hwang and Madhani, 2009), DNA repair (Lee *et al.*, 2005; Kotoglou *et al.*, 2009; Mastrocola and Heinen, 2010) and RNA processing (reviewed in Gerbi *et al.*, 2003).

Cell cycle regulation by the nucleolus is mediated by post-translational modification of cell cycle proteins. The SUMO-specific protease termed SUMO1/sentrin-specific peptide 5 (SENP5) is found concentrated within nucleoli (Gong and Yeh, 2006) and depletion of SENP5 caused defects in cell cycle regulation and nucleolar morphology (Di Bacco *et al.*, 2006).

Protein phosphatase 1γ (PP1γ) is found concentrated in nucleoli during interphase and relocates to the cytoplasm and kinetochores during mitosis (Trinkle-Mulcahy *et al.*, 2006). At the onset of anaphase, a PP1γ-specific binding protein termed cell division cycle-associated 2 (CDCA2) induces the redistributed of PP1γ from the cytoplasm to chromosomes (Vagnarelli *et al.*, 2006). PP1γ appears to remain associated with chromosomes during interphase and accumulates in nucleoli (Trinkle-Mulcahy *et al.*, 2006), indicating a role for the nucleolus in chromosome segregation.

In addition to protein modifications, protein sequestration in the nucleolus also appears to facilitate cell cycle regulation. Telomerase reverse transcriptase (TRT) is sequestered into nucleoli by interaction with the nucleolar protein C23 (Khurts *et al.*, 2004) and is released at the end of mitosis to facilitate telomere replication at the end of G2 phase (Wong *et al.*, 2002). This indicates that the nucleolus may regulate the activity of telomerase during the cell cycle. This is supported by evidence that the nucleolar sequestration of TRT is lost in transformed or DNA-damaged cells, indicating loss of this activity may contribute to tumorigenesis (Wong *et al.*, 2002).

The nucleolus also appears to regulate stress responses. p14^{ARF} is a positive regulator of p53 stabilisation and activation by sequestering the p53-ubiquitin ligase HDM2 in the nucleolus (Wsierska-Gadek and Horky, 2003). This results in an increase in levels of p53, facilitating transcription of p21 and cell cycle arrest. Ribosome subunit biogenesis in the nucleolus is also tightly regulated following cellular stress. Following stress, c-Jun N terminal kinase 2 (JNK2) phosphorylates the transcription factor TIF-1A, which can no longer interact with RNA pol I thus inhibiting transcription (Mayer *et al.*, 2005). Ribosome subunit transcription is also thought to be negatively regulated by a mTor-PI3K-MAPK pathway following various stress stimuli (James and Zomerdijk, 2004). DNA damage has also been shown to reduce RNA pol I synthesis in an ATR-dependent manner by abrogating assembly of the transcription initiation complex (Kruhlak *et al.*, 2007). Epigenetic modifications also appear to play a role in the regulation of rRNA synthesis following stress. Post-translational modification of histone proteins resulted in transcriptionally silent chromatin in the nucleolus (Tanaka *et al.*, 2010; Xie *et al.*, 2012).

The nucleolus is also involved in RNA modification. The most prevalent post-transcriptional modifications of rRNA are 2′-0-ribose methylation and pseudouridylation, which are carried out on the pre-rRNA template by snoRNPs in the nucleolus (reviewed in Kiss, 2002; Matera *et al.*, 2007). The snoRNAs have complementary sequences to the target RNAs and thus act as a guide for modification. SnoRNAs responsible for 2′-0-methylation have a conserved motif known as a C/D box, which is thought to determine the site of modification which is then carried out by a

snoRNP (KissLaszlo *et al.*, 1996; Omer *et al.*, 2002). The C/D box snoRNAs interact with a specific set of proteins to form the C/D RNPs; fibrillarin, NOP56, NOP58 and 15.5K (Omer *et al.*, 2002; Aittaleb *et al.*, 2003; Bortolin *et al.*, 2003; Rashid *et al.*, 2003; Tran *et al.*, 2003). The snoRNAs which catalyse pseudouridylation of target RNAs typically exhibit short consensus sequences known as H/ACA boxes and a characteristic hairpin loop structure (Ganot *et al.*, 1997b). Akin to C/D box snoRNAs, H/ACA box snoRNAs dictate the site of pseudouridylation (Ganot *et al.*, 1997a). These RNAs interact with proteins dyskerin, NHP2, GAR1 and NOP10 to form the H/ACA snoRNP (Baker *et al.*, 2005; Charpentier *et al.*, 2005).

Nucleoli have also been implicated in the production and modification of RNP classes other than rRNPs. Post-translational modification and assembly of spliceosomal small nuclear ribonucleoprotein (snRNPs), telomerase and microRNAs (miRNAs) were found to involve the nucleolus (reviewed in Gerbi *et al.*, 2003). Numerous RNA pol III-transcribed RNAs appear to required modification or maturation in the nucleolus, including the 7S RNA of the signal recognition particle (SRP) (Jacobson and Pederson, 1998), a tRNA processing enzyme known as RNase P (Jacobson *et al.*, 1997) and spliceosomal snRNP U6 (Ganot *et al.*, 1999). This indicates that RNA pol III-transcribed RNAs may follow a specific nucleolar import pathway for modification. In addition to RNA modifications, the nucleolus has also been implicated in RNA editing. Photobleaching experiments revealed that the RNA editing enzymes RNA specific RNA deaminase 1 (ADAR1) and ADAR2 are in constant flux into and out of the nucleolus (Desterro *et al.*, 2003), with ADAR2-mediated RNA editing occurring within the nucleolus (Vitali *et al.*, 2005).

Finally, the nucleolus also appears to be involved in the production of small interfering RNA (siRNA). An miRNA known as *miR206* was shown to colocalise with the 28S rRNA in the GC of the nucleolus (Politz *et al.*, 2006). This indicates that miRNAs may be able to associate both with nascent ribosomes in the nucleolus and with mature ribosomes in the cytoplasm. In plant cells, multiple siRNA processing enzymes were found to localise in the nucleolus alongside siRNAs, indicating that processing of siRNAs may occur in this compartment (Li *et al.*, 2006a). It was also suggested that storage or sequestration of the RNA-induced silencing (RISC) complex may also occur in the nucleolus (Pontes *et al.*, 2006).

1.3.3   Promyelocytic leukaemia nuclear bodies (PML-NBs)

PML-NBs are defined by the localisation of marker proteins to form ring-shaped structures within the nucleus, and generally do not contain nucleic acid (Boisvert *et al.*, 2000). Despite being devoid of DNA, PML-NBs can associate via chromatin with transcriptionally active gene regions including the MHC class 1 gene locus and the p53 gene locus (Shiels *et al.*, 2001; Sun

et al., 2003; Wang *et al.*, 2004; Kumar *et al.*, 2007). PML-NBs are often found in close proximity to other nuclear bodies, such as CBs, splicing speckles and nucleoli (Grande *et al.*, 1996). They are dynamic structures and can change in terms of size, number and position within the nucleus as the cell cycle progresses (Chang *et al.*, 1995; Kurki *et al.*, 2003). PML-NBs appear to be stress responsive; they have been noted to disperse in response to cellular shock induced by heat, heavy metal exposure (Maul *et al.*, 1995), DNA damage (Carbone *et al.*, 2002; Bernardi *et al.*, 2004; Conlan *et al.*, 2004; Salomoni *et al.*, 2005) and viral infection (Doucas *et al.*, 1996; Ahn and Hayward, 1997; Leppard and Everett, 1999; Adamson and Kenney, 2001; Burkham *et al.*, 2001). Moreover, there is transcriptional up-regulation of PML-NB constituents following stress; PML is up-regulated at the transcriptional level by p53 (de Stanchina *et al.*, 2004) and both PML and SP100 are transcriptionally up-regulated by IFN-γ treatment (Grotzinger *et al.*, 1996), resulting in an increase in the number and size of PML-NBs.

PML is a tumour suppressor protein which becomes fused to the retinoic acid receptor α (RARα) in acute promyelocytic leukaemia, leading to inactivation of the PML protein (Dethe *et al.*, 1991; Kakizuka *et al.*, 1991). PML is essential for the formation of PML-NBs (Ishov *et al.*, 1999). Multiple proteins have been associated with PML-NBs either partially or temporally, including the transcriptional repressor Daxx and the transcriptional regulator SP100 (Ishov *et al.*, 1999). Formation of PML-NBs appears to require protein modification by SUMOs, which are conjugated to target proteins by the activity of three proteins; the E1 SUMO-activating enzyme (SAE1/SAE2 heterodimer), the E2 SUMO-conjugating enzyme UBC9 and E3 SUMO protein ligases (Johnson and Blobel, 1997; Johnson *et al.*, 1997; Schwarz *et al.*, 1998). Multiple PML-NB proteins are covalently modified by conjugation to SUMOs (Sternsdorf *et al.*, 1997; Zhong *et al.*, 2000a; Van Damme *et al.*, 2010). This modification is reversible and appears to be crucial for the recruitment of proteins to PML-NBs, as it enables non-covalent interactions between SUMOylated proteins with proteins containing SUMO-interacting motifs (Shen *et al.*, 2006). SUMO-1 modification of PML appears to induce formation of PML-NBs (Muller *et al.*, 1998) and is essential for the recruitment of Daxx (Ishov *et al.*, 1999). The current model for the formation of PML-NBs suggests that disassembly (e.g. during mitosis) is due to deSUMOylation of PML, whilst SUMOylation of PML (e.g. during interphase) facilitates interaction of PML with other SUMOylated proteins, resulting in formation of PML-NBs (Shen *et al.*, 2006).

The function of PML-NBs appears to be a site for protein recruitment and modification including phosphorylation, acetylation, ubiquitination and SUMOylation. These modifications can have varied outcomes including protein activation, inactivation, sequestration or degradation. As a result, PML-NBs have been implicated in a diverse array of cellular functions

35

including senescence, apoptosis, immune signalling and transcriptional regulation (reviewed in Bernardi and Pandolfi, 2007; Bernardi *et al.*, 2008; Tavalai and Stamminger, 2008). The implication of PML-NBs in such an array of cellular functions may also be a reflection of the heterogeneous nature of PML-NBs. Alternative PML isoforms can result in formation of different PML-NBs (Muratani *et al.*, 2002). Indeed, subsets of PML-NBs within a cell appear to have diverse protein compositions and can also be associated with different chromosomal regions (Shiels *et al.*, 2001).

In addition to their formation being dependent on SUMOylation, PML-NBs have been proposed to act as a key cellular site for protein SUMOylation (Van Damme *et al.*, 2010; Saitoh *et al.*, 2006). Indeed, protein SUMOylation appears to be induced by PML in yeast (Quimby *et al.*, 2006) and the SUMOylation of PML itself and target proteins appears to depend on PML (Shen *et al.*, 2006). Although PML has been proposed to act as a U3 SUMO ligase, this is yet to be proven in a mammalian system. However, other U3 SUMO ligases have been shown to locate in PML-NBs (reviewed in Seeler and Dejean, 2003), indicating they are a key site for protein SUMOylation. SUMOylated proteins can also be recruited to PML-NBs for further modifications including acetylation and phosphorylation (Georges *et al.*, 2011). SUMOylation of target proteins may also trigger their release from PML-NBs (Park *et al.*, 2007).

PML-NBs also appear to have roles in transcriptional regulation. Transcriptional activators, repressors and histone modifiers are all present in PML-NBs (Ishov *et al.*, 1999; Zhong *et al.*, 2000a; Kiesslich *et al.*, 2002; Seeler *et al.*, 1998; Wu *et al.*, 2001). PML-NBs are frequently found in close proximity to highly acetylated chromatin (Boisvert *et al.*, 2000) and nascent RNA has been detected at the periphery of PML-NBs, particularly at the G1 phase of the cell cycle (Kiesslich *et al.*, 2002). PML-NBs have been suggested to modulate transcription at the MHC class I gene locus by modifying chromatin architecture (Shiels *et al.*, 2001; Wang *et al.*, 2004; Kumar *et al.*, 2007). PML-NBs have also been implicated in heterochromatin remodelling at the G2 phase of the cell cycle (Luciani *et al.*, 2006) and chromatin condensation by PML-NBs is suggested to induce transcriptional suppression during cellular senescence (Zhang *et al.*, 2005; Ye *et al.*, 2007; Vernier *et al.*, 2011).

Another key role for PML-NBs is DNA damage control. PML-NBs colocalise with sites of DNA repair and single-stranded DNA (ssDNA) (Bischof *et al.*, 2001; Boe *et al.*, 2006) and also contain numerous proteins involved in DNA repair and cell cycle checkpoint control (reviewed in Dellaire and Bazett-Jones, 2004, 2007). Moreover, PML is phosphorylated and activated by several DNA damage-activated kinases including ATM, ATR, homeodomain-interacting protein kinase 2 (HIPK2) and checkpoint kinase 2 (CHK2) (Dellaire *et al.*, 2006). Some studies

have also indicated a role for PML-NBs in DNA repair. However, the association of DNA repair proteins with PML-NBs generally occurs at late time points following DNA damage (Carbone *et al.*, 2002; Dellaire *et al.*, 2006) and the association of PML-NBs with ssDNA is more proficient in cells defective in certain DNA repair functions (Boe *et al.*, 2006). Nevertheless, there is accumulating evidence of a role for PML-NBs in homologous recombination repair (HRR). PML-knockout cells exhibit a high level of sister chromatid exchange, which occurs when there is defective HRR pathway (Zhong *et al.*, 1999). PML-NBs were also shown to interact with telomeres in certain cancer cells which maintain telomere length in a telomerase-independent manner by a mechanism known as alternative lengthening of telomeres (ALT) (Bernardi and Pandolfi, 2003). Although the process is not well understood, it is thought to involve HR of telomeric DNA (Muntoni and Reddel, 2005; Draskovic *et al.*, 2009). However, ALT can occur in telomerase-negative cell lines in the absence of PML-NBs, indicating that PML-NBs are not essential for HR (Jeyapalan *et al.*, 2008).

Although the role of PML-NBs in active DNA repair remains inconclusive, the role of PML in induction of cell cycle arrest and apoptosis following DNA damage is well clarified. PML knockout mouse cell lines exhibit marked defects in apoptosis induction following activation by a panel of pro-apoptotic stimuli (Bernardi and Pandolfi, 2003; Takahashi *et al.*, 2004). Following DNA damage, ATR activation results in phosphorylation and activation of PML. By association with the nucleolar protein L11, PML sequesters the p53 ubiquitin ligase HDM2 in the nucleolus resulting in an increased stability of p53 (Bernardi *et al.*, 2004). PML also promotes the phosphorylation of p53, which enhances the acetylation and activation of p53 by CBP (Hofmann *et al.*, 2002b). Additional p53 regulators have also been shown to accumulate in PML-NBs, including protein inhibitor of activated STAT (PIAS), herpes virus-associated ubiquitin-specific protease (HAUSP) and the deacetylase sirtuin 1 (SIRT1) (Campagna *et al.*, 2011). This indicates that a fine balance between p53-suppressors (e.g. SIRT1) and p53 activators (e.g. CBP) within the PML-NB may dictate the activation or suppression of p53.

PML can also stimulate apoptosis by p53-independent pathways. Following DNA damage, PML induces the autophosphorylation and activation of CHK2, which is then released from PML-NBs to exert apoptotic effect (Yang *et al.*, 2002; Yang *et al.*, 2006). PML also interacts with a positive regulator of Fas-induced apoptosis known as FLICE-associated huge protein (FLASH) (Milovic-Holm *et al.*, 2007). Under steady state conditions, FLASH is located at the PML-NB. Following Fas activation, FLASH is released from PML-NBs and targets to the mitochondria where it stimulates the cleavage and activation of caspase 8 (Milovic-Holm *et al.*, 2007). In contrast to PML which appears primarily pro-apoptotic, Daxx has been reported to

both stimulate and suppress apoptosis (Torii *et al.*, 1999; Zhong *et al.*, 2000b; Chen and Chen, 2003; Meinecke *et al.*, 2007).

PML, Daxx and SP100 have all been implicated in the anti-viral functions of PML-NBs. Daxx induces transcriptional silencing at viral promoters following viral infection by interaction with a histone deacetylase (Saffert and Kalejta, 2006; Huang *et al.*, 2008). SP100 has also been implicated in suppression of early viral gene expression (Negorev *et al.*, 2009). In addition, PML can stimulate IFN-γ-mediated apoptosis by interfering with ubiquitination. Under steady state conditions, an E3-ubiquitin ligase (E3-UbL) complex targets and ubiquitinates Death-associated protein kinase 1 (DAPK1), a positive stimulator for IFN-γ-mediated cell death. Upon IFN-γ treatment, the E3-UbL complex is sequestered by PML into PML-NBs, preventing DAPK1 ubiquitination and degradation, thus stimulating apoptosis (Lee *et al.*, 2010).

Another key cellular function of PML-NB appears to be senescence. As mentioned previously, PML is able to induce p53 activation by a number of mechanisms, resulting in stimulation of senescence pathways (Hofmann *et al.*, 2002b; Bernardi and Pandolfi, 2003; de Stanchina *et al.*, 2004). PML-NBs also appear important for formation of heterochromatin domains known as senescence-associated heterochromatin foci (SAHFs) which are believed to suppress activity of growth-inducing genes (Narita *et al.*, 2003). The formation of these domains appears to depend on the histone chaperones HIRA and anti-silencing factor 1 (ASF1) which stimulates the incorporation of histone protein 1 (HP1) and the transcriptional silencing histone macro2A on to target chromatin (Zhang *et al.*, 2005; Ye *et al.*, 2007; Jiang *et al.*, 2011b). Prior to its association at SAHFs, HIRA traffics via PML-NBs and this appears to be critical for SAHF formation and induction of senescence (Zhang *et al.*, 2005).

PML appears to control the activity of various cellular phosphatases and kinases in order to exert tumour suppressor functions. PML abrogates PP1A-mediated pRb phosphorylation by dephosphorylating pRb, facilitating suppression of proliferation and increased differentiation in neuronal progenitor cells (Regad *et al.*, 2009). PML can also exert anti-neoangiogenic activities by abrogating the pro-angiogenic mTOR-PKB pathway at two different levels. PML firstly enhances PP2A phosphorylation of the proto-oncogene PKB by sequestering both proteins into PML-NBs, resulting in dephosphorylation and inactivation of PKB (Trotman *et al.*, 2006). Secondly, PML can promote nuclear retention of the suppressor protein phosphatase and tensin homologue (PTEN) by abrogating its ubiquitination by HAUSP (Song *et al.*, 2008). Ubiquitination of PTEN appears to correlate with nuclear retention and tumour suppressor activity (Song *et al.*, 2008).

1.3.4 Splicing speckles

Nuclear speckles (interchromatin granule clusters [ICGs]), are sub-nuclear domains containing high levels of factors required for pre-mRNA processing, transcriptional elongation and chromatin remodelling complexes (reviewed in Lamond and Spector, 2003). Nuclear speckles range in size from one to several micrometers in diameter and are composed of granules connected by thin fibrils (Thiry, 1995). Splicing speckles, like many nuclear bodies, are highly dynamic structures; fluorescence microscopy studies revealed dynamic change in the shape and fluorescence intensity of speckles over time (Misteli *et al.*, 1997) whilst photobleaching experiments revealed that there is a rapid flux of speckle components between speckles and the surrounding nucleoplasm (Kruhlak *et al.*, 2000; Phair and Misteli, 2000). Splicing speckles vary in number and size according to levels of splicing and transcription factors (Spector *et al.*, 1991; Spector, 1993; Melcak *et al.*, 2000; Huang and Spector, 1996; Misteli *et al.*, 1997), cell cycle stage (Reuter *et al.*, 1985; Spector and Smith, 1986; Ferreira *et al.*, 1994; Thiry, 1995; Verheijen *et al.*, 1986; Leser *et al.*, 1989; Ferreira *et al.*, 1994; Prasanth *et al.*, 2003; Brown *et al.*, 2008) and following virus infection (Jimenez-Garcia and Spector, 1993; Bridge *et al.*, 1995).

The exchange rate of factors between speckles and the nucleoplasm appears be dictated by phosphorylation. Phosphorylation of the serine/arginine-rich domain of SRSFs appears necessary for translocation of SRSFs from speckles to sites of transcription and pre-mRNA processing (Misteli *et al.*, 1998) and is also required for their association with the spliceosome (Mermoud *et al.*, 1994). Kinases involved in regulation of SRSFs and RNA pol II are also present in speckles (Colwill *et al.*, 1996; Ko *et al.*, 2001; Kojima *et al.*, 2001; Sacco-Bubulya and Spector, 2002). Increased exit of proteins from speckles can be induced by introduction of genes (Jimenez-Garcia and Spector, 1993; Bridge *et al.*, 1995) or over-expression of kinases (Colwill *et al.*, 1996; Sacco-Bubulya and Spector, 2002).

The structural proteins of nuclear speckles are not well defined. Recent studies revealed that depletion of the large SRSF protein Son abrogated the recruitment of RNA-processing factors to nuclear speckles, indicating a role for Son in speckle assembly (Sharma *et al.*, 2010). Speckles also contain abundant long-lived polyadenylated pre-mRNAs which are thought to play a role in the structure of speckles (Huang and Spector, 1996; Hutchinson *et al.*, 2007). Furthermore, it was recently shown that a tethered, spliced RNA pol II mRNA transcript recruited pre-mRNA splicing factors resulting in formation of speckles, indicating that ongoing transcription is necessary for speckle formation (Shevtsov and Dundr, 2011).

Nuclear speckles contain a plethora of proteins involved in gene expression, including pre-mRNA splicing and 3′ end-processing factors, transcription factors, RNA pol II, mRNA export

and translation factors (Larsson *et al.*, 1995; Mortillaro *et al.*, 1996; Zeng *et al.*, 1997; Schul *et al.*, 1998b; Saitoh *et al.*, 2004; Dostie *et al.*, 2000). Splicing speckles are believed to act as a local store of splicing factors whilst splicing itself occurs primarily in the surrounding perichromatin fibrils (reviewed in Spector and Lamond, 2011). Furthermore, numerous kinases and phosphatases responsible for regulation of splicing components are enriched in speckles, indicating a role for splicing speckles in the regulation and storage of splicing factors (Colwill *et al.*, 1996; Trinkle-Mulcahy *et al.*, 1999; Ko *et al.*, 2001; Kojima *et al.*, 2001; Trinkle-Mulcahy *et al.*, 2001; Brede *et al.*, 2002; Sacco-Bubulya and Spector, 2002). Splicing speckles contain high concentrations of spliceosome components such as snRNPs and SRSFs (Perraud *et al.*, 1979; Spector *et al.*, 1983; Fu and Maniatis, 1990; Fu, 1995; Saitoh *et al.*, 2004). SRSFs appear to be involved in both constitutive and alternative pre-mRNA splicing (Caceres *et al.*, 1997; Xiao and Manley, 1997; Lai *et al.*, 2001; Lin *et al.*, 2005). SRSFs are required to commit the pre-mRNA to the splicing pathway (Fu, 1993) and have been shown to be co-transcriptionally recruited alongside other splicing factors to the RNA pol II complex to facilitate co-transcriptional splicing (Gornemann *et al.*, 2005; Lacadie and Rosbash, 2005; Listerman *et al.*, 2006). Splicing speckles have also been shown to contain a long, nuclear retained non-coding mRNA termed metastasis-associated lung adenocarcinoma transcript 1 (MALAT1) (reviewed in Wilusz *et al.*, 2009). MALAT1 appears to be involved in the recruitment of SRSFs from nuclear speckles to sites of active transcription (Bernard *et al.*, 2010).

Despite often being close to sites of active transcription, speckles are generally found in nucleoplasmic regions containing little to no DNA (Thiry, 1995). Their close association with sites of active transcription indicates a close association with gene expression. Indeed, chromosomal regions rich in gene-coding regions (R bands) appear to associate with speckles at much higher frequency than chromosomal regions encoding lower numbers of genes (G bands) (Shopland *et al.*, 2003). Moreover, certain genes have been shown to preferentially locate in close proximity to splicing speckles, although this appears to be independent of transcription or pre-mRNA splicing at these loci (Huang and Schneider, 1991; Xing *et al.*, 1993; Xing *et al.*, 1995; Smith *et al.*, 1999; Johnson *et al.*, 2000; Moen *et al.*, 2004; Brown *et al.*, 2008). Several components of the RNA pol II complex have been shown to be enriched in speckles (Bregman *et al.*, 1995; Mortillaro *et al.*, 1996; Mintz *et al.*, 1999; Saitoh *et al.*, 2004). A regulator of the RNA pol II complex, the CDK9/cyclin T1 complex, also partially colocalises with speckles (Herrmann and Mancini, 2001). This complex is responsible for phosphorylation of RNA pol II, stimulating transcriptional elongation (reviewed in Price, 2000). Furthermore, the cellular protein termed factor that binds to inducer of short transcripts protein 1(FBI-1) was found to colocalise in speckles with its cellular co-factor positive transcription elongation factor b (P-

TEFb) and the HIV-1 transcriptional activator Tat (Pendergrast *et al.*, 2002; Pessler *et al.*, 1997). A chromatin remodelling factor known as high mobility group (HMG)-17 has also been shown to localise in a similar nuclear distribution to FBI-1 (Hock *et al.*, 1998). Therefore although transcription is not believed to occur within splicing speckles, a subset of transcription-associated proteins appears to be present in speckles. This indicates a strong link between splicing and transcription, which may facilitate formation of splicing complexes once transcription is initiated or regulation of transcription by modification of specific factors.

In addition to acting as a store for splicing factors, recent data indicates splicing speckles may also have a direct role in splicing. Pre-mRNA splicing is an essential mechanism for gene expression in mammals where protein coding regions in genes are separated by non-coding regions (introns). Splicing is conducted by the spliceosome, a multimeric complex composed of the U1, U2, U4, U5 and U6 snRNPs alongside an assortment of protein factors (reviewed in Wahl *et al.*, 2009). In addition, some transcripts are spliced by an alternative spliceosome (the U12 spliceosome) in which U1, U2, U4 and U6 snRNPs are replaced by the U11, U12, U4atac and U6atac snRNPs (Will and Luhrmann, 2005). RNA splicing can occur either co- or post-transcriptionally. The distinction between co- and post-transcriptional splicing appears to be important for regulation of splicing; co-transcriptional splicing may allow regulation by transcription-dependent factors, whereas post-transcriptional splicing may allow regulation by more diverse mechanisms (reviewed in Han *et al.*, 2011; Razin *et al.*, 2011). The ratio of co-transcriptional versus post-transcriptional splicing is currently unknown, as are the factors governing the selection. It seems that whilst constitutive introns are co-transcriptionally processed, alternative splicing can occur after transcription, when the mRNA is released into the nucleoplasm (Vargas *et al.*, 2011). Co-transcriptional splicing appears to occur for the majority of constitutively expressed transcripts; in-situ hybridisation revealed the location of spliced mRNAs at their corresponding gene loci (Zhang *et al.*, 1994) and spliced mRNA was shown to locate at sites of disrupted chromatin (Bauren and Wieslander, 1994; Pandya-Jones and Black, 2009). In transcriptionally-synchronised cells, introns were removed from nascent RNA prior to completion of transcription (Singh and Padgett, 2009). Splicing factors also appear to be recruited to nascent transcripts in a co-transcriptional manner (Gornemann *et al.*, 2005; Lacadie and Rosbash, 2005; Listerman *et al.*, 2006; Pandit *et al.*, 2008). It has been proposed that as most eukaryotic cells contain short exons and long introns, this allows sufficient time for the splicing machinery to recognise the 5′ and 3′ splice sites associated with the exon, facilitating co-transcriptional splicing of exons located at the 5′ end of genes. In contrast, pre-mRNA introns located at the 3′ end of multiple-intron transcripts more frequently undergo post-transcriptional splicing, presumably because termination of transcription and cleavage of the

transcripts occurs before the splicing machinery is able to remove the introns (Bauren and Wieslander, 1994; Pandya-Jones and Black, 2009).

Although the majority of nascent pre-mRNA appears to locate to adjacent perichromatin fibrils (Monneron and Bernhard, 1969; Fakan and Bernhard, 1971; Fakan and Nobis, 1978; Cmarko *et al.*, 1999), nucleoplasmic pre-mRNAs were found to accumulate at nuclear speckles (Dias *et al.*, 2010; Vargas *et al.*, 2011; Girard *et al.*, 2012). This indicates that whilst co-transcriptional splicing occurs primarily in the surrounding perichromatin fibrils, post-transcriptional splicing may occur at the splicing speckles (Vargas *et al.*, 2011; Girard *et al.*, 2012). As multiple splicing factors contain signals for speckle retention, it is possible that spliceosomes along with their RNA substrate may have an enhanced affinity for speckles (Spector and Lamond, 2011; Girard *et al.*, 2012). The subsequent release of spliced mRNA from speckles may then depend on interactions with the mRNA nuclear export pathway (Dias *et al.*, 2010; Girard *et al.*, 2012).

Nuclear speckles have also been implicated in alternative splicing. Most eukaryotic genes are subject to alternative splicing, whereby different mRNA spliceoforms are produced from the same pre-mRNA transcript (reviewed in Luco and Misteli, 2011). Alternative splicing allows for increased regulation of gene expression and increased variety in the resulting proteome. The transcription elongation regulator 1 (TCERG1) functions as an integrator between transcription and splicing and appears to be enriched in nuclear speckles (Sanchez-Alvarez *et al.*, 2006). This protein was found to dictate alternative splicing of pre-mRNA, implying that splicing speckles may play a role in alternative splicing (Montes *et al.*, 2012). In addition, MALAT1 appears to play a role in alternative splicing by modulating the phosphorylation status of the essential splicing factor SRSF2 (Tripathi *et al.*, 2010).

1.3.5 Paraspeckles

Paraspeckles are nuclear subdomains defined by location of several paraspeckle marker proteins; paraspeckle protein 1 (PSP1), PSP2, non-POU domain-containing, octamer binding protein (NONO) and splicing factor proline/glutamine-rich (SFPQ) (Dundr and Misteli, 2002; Fox *et al.*, 2002). Paraspeckles appear in the nucleus as foci in close proximity to, but distinct from, splicing speckles. Recent bioinformatic data found that a long non-coding mRNA known as NEAT1 was specifically localised to paraspeckles, whilst NEAT2 localised exclusively to splicing speckles (Hutchinson *et al.*, 2007; Chen and Carmichael, 2009; Clemson *et al.*, 2009; Sasaki *et al.*, 2009; Sunwoo *et al.*, 2009). Depletion of NEAT1 was shown to disrupt paraspeckle morphology, indicating it is a necessary structural component (Chen and Carmichael, 2009; Clemson *et al.*, 2009; Sasaki *et al.*, 2009; Sunwoo *et al.*, 2009). The NEAT1 locus encodes two forms of NEAT1, a short transcript (NEAT1_1) and a long transcript

(NEAT1_2) (Guru *et al.*, 1997). Depletion of NEAT1_2 was shown to disrupt paraspeckle morphology, indicating it that it is a necessary structural factor (Sasaki *et al.*, 2009). Although NEAT1_1 cannot induce paraspeckle formation alone, its over-expression increased the number of paraspeckles in NEAT1_2-expressing cells (Clemson *et al.*, 2009), indicating it may regulate paraspeckle formation under certain conditions. The formation of speckles is proposed to occur via a recruitment mechanism; NEAT1_2 interacts with SFPQ and NONO, leading to recruitment of additional factors PSP1 and NEAT1_1 to form paraspeckles (Sasaki *et al.*, 2009; Souquere *et al.*, 2010).

The function of paraspeckles appears to be regulation of the expression of highly-edited transcripts by associating these transcripts with other nuclear bodies (Bond and Fox, 2009; Chen and Carmichael, 2010). An alternatively spliced form of the cationic amino acid transporter mRNA termed CTN-RNA was shown to localise to paraspeckles (Prasanth *et al.*, 2005). The 3′ untranslated region (UTR) of this transcript contains inverted retrotransposon sequences which form intra-strand double-stranded RNAs (Prasanth *et al.*, 2005). This structure is recognised by ADAR, which catalyses the conversion of adenosines to inosines (Bass and Weintraub, 1988; Wagner *et al.*, 1989). ADAR-mediated modification of the 3′ UTR of CTN-RNA appears to lead to its accumulation in paraspeckles and retention in the nucleus, thereby inhibiting its expression (Prasanth *et al.*, 2005). Inverted retrotransposon sequences are found in the 3′ UTR of a number of mammalian mRNAs, therefore the expression of these transcripts may also be regulated by paraspeckle retention (Faulkner *et al.*, 2009).

Paraspeckles have been found to be absent in human embryonic stem cells (Chen and Carmichael, 2009), indicating the regulation of certain mRNA expression by these structures may be developmentally regulated. In addition, NEAT1-knockout mice appear viable and fertile (Nakagawa *et al.*, 2011), indicating paraspeckles are not an essential structure and therefore may be required for mRNA regulation under certain stress conditions.

1.3.6 Cajal Bodies

Cajal bodies are highly conserved, intranuclear subdomains that function in RNA metabolism (reviewed in Cioce and Lamond, 2005; Morris, 2008). There are normally between one and ten CBs per cell and typically appear in transmission electron micrographs (TEMs) as a tangled ball of fibrillar threads (Cajal, 1903; Hardin *et al.*, 1969; Monneron and Bernhard, 1969; Lafarga *et al.*, 1983). Their number and size can vary in response to cell cycle stage, transcriptional activity, snRNP level and cellular stresses such as virus infection (Andrade *et al.*, 1993; Carmo-Fonseca *et al.*, 1993; Sleeman *et al.*, 2001; Fernandez *et al.*, 2002). The number of CBs in a cell may be dictated by the ability of the CB to fuse into larger structures or divide into smaller ones

(Boudonck *et al.*, 1999; Platani *et al.*, 2002). In addition, *de novo* formation of CBs may also occur; this appears to be closely correlated with the snRNP cycle (Navascues *et al.*, 2004).

CBs are able to move throughout the nucleoplasm mostly by diffusion, although active processes may be employed in some instances (Platani *et al.*, 2000; Gorisch *et al.*, 2004). It seems that not all CBs within a cell are dynamic at the same time and can be either mobile or tethered to specific regions of chromatin (Platani *et al.*, 2000; Sleeman *et al.*, 2003; Dundr *et al.*, 2004). The structural integrity of CBs appears to depend on the CB proteins coilin, WD Repeat-containing Antisense to p53 (WRAP53) and FLASH (Barcaroli *et al.*, 2006b; Mahmoudi *et al.*, 2010). Genes encoding U1 and U2 snRNAs as well as histone gene loci associate with CBs (Frey and Matera, 1995; Smith *et al.*, 1995; Gao *et al.*, 1997; Schul *et al.*, 1998a; Jacobs *et al.*, 1999; Schul *et al.*, 1999a; Frey and Matera, 2001; Shopland *et al.*, 2001). In addition to their close association with specific gene loci, CBs can also associate with other nuclear bodies including PML-NBs, cleavage bodies and nucleoli (Carmo-Fonseca *et al.*, 1993; Bohmann *et al.*, 1995; Malatesta *et al.*, 1994; Grande *et al.*, 1996; Schul *et al.*, 1999b; Li *et al.*, 2006b), indicating a role for CBs in intranuclear trafficking.

Although CBs can be surrounded by transcription sites (Jordan *et al.*, 1997), they contain inactive RNA pol II (Xie and Pombo, 2006), indicating that they are not sites of active transcription. In addition, they do not contain poly(A) RNA or the essential splicing factors U2 Auxiliary Factor (U2AF) and SRSF2 and are therefore unlikely to function in splicing (Raska, 1995; Cmarko *et al.*, 1999; Gall, 2000). However, poly(A) RNA was recently shown to be present in the CBs of European larch microsporocytes (Kolowerzo *et al.*, 2009; Smolinski and Kolowerzo, 2012). Larch microsporocyte CBs did not contain nascent RNA or splicing factors, indicating the CB is not a site of transcription or splicing; instead it was suggested that CBs may act as a storage site for certain mRNAs prior to nuclear export. However, the presence of mRNA in CBs is yet to be observed in animal cells (Visa *et al.*, 1993; Huang *et al.*, 1994).

The well-characterised functions of CBs are the assembly and recycling of the spliceosomal machinery (reviewed in Cioce and Lamond, 2005; Morris, 2008). CBs have been shown to be enriched in many snRNP and snoRNP components, including the U snRNPs that form part of the spliceosome for pre-mRNA splicing (Carmo-Fonseca *et al.*, 1992; Matera and Ward, 1993). CBs also contain nonspliceosomal RNAs including the U7 snRNP necessary for histone 3′-end processing and the human telomerase RNA (hTR) component of telomerase (Bachand *et al.*, 2002; Jady *et al.*, 2004; Zhu *et al.*, 2004). In contrast to the U7 snRNP of amphibian (Wu and Gall, 1993) and HeLa cells (Frey and Matera, 1995), the U7 snRNP of *Drosophila*

melanogaster is found within separate sub-nuclear structures known as histone locus bodies (HLBs) rather than CBs (Liu *et al.*, 2006).

The snRNP assembly functions attributed to CBs are U2 snRNP assembly (Nesic *et al.*, 2004), reformation of the 'tri-snRNP' post-splicing (Schaffert *et al.*, 2004; Stanek and Neugebauer, 2004) and U snRNA modification (Jady *et al.*, 2003). The biogenesis of snRNPs involved a series of reactions in both the cytoplasm and the nucleus. Small nuclear RNA (snRNA) molecules U1, U2, U4 and U5 are synthesised in the nucleus by RNA pol II (Murphy *et al.*, 1982). Following transcription, there is addition of a 7-methylguanosine (m^7G) cap at the 5′ end of the RNA molecule and additional nucleotides are added at the 3′ end (Mattaj, 1986; Jacobson *et al.*, 1993). The m^7G cap is bound by the cap-binding complex (CBC) to promote transport of snRNAs into the cytoplasm, alongside the phosphorylated adaptor protein for RNA export (PHAX) (Ohno *et al.*, 2000). Interestingly, recent data also suggests that trafficking of snRNAs via the CB may be required for snRNA export (Suzuki *et al.*, 2010). Once in the cytoplasm, the RNA undergoes maturation of the 3′ end and this facilitates binding of Smith (Sm) proteins to form the snRNP, which is facilitated by the multimeric survival motor neuron (SMN) complex (reviewed in Kolb *et al.*, 2007; Chari *et al.*, 2009). The 5′ end of the RNA molecule is processed to form a 2,2,7-methylguanosine (m_3G) cap (Mattaj, 1986) which is then recognised by snurportin 1 (Huber *et al.*, 1998). The SMN protein complex functions to import snRNPs from the cytoplasm into the nucleus via importin β (Narayanan *et al.*, 2004). Recently, the RNA chaperone protein WRAP53 was also identified as an essential factor for cytoplasmic snRNP assembly and subsequent trafficking into the nucleus (Mahmoudi *et al.*, 2010).

Once inside the nucleus, SMN interacts with coilin (Hebert *et al.*, 2001) and phosphorylation of coilin appears to dictate the interaction of coilin with SMN and the Sm protein B′ (SmB′) (Toyota *et al.*, 2010). At the CB, snRNAs undergo post-transcriptional modifications including 2′-*O*-methylation and pseudouridylation, which are guided by the CB-specific guide RNAs (scaRNAs) (Darzacq *et al.*, 2002; Jady *et al.*, 2004). Akin to the nucleolar snoRNPs, the scaRNAs guide complementary base-pairing between RNAs and target sequences in order to synchronise RNA modification. U2 snRNP assembly is also believed to occur within the CB (Nesic *et al.*, 2004) and the reformation of the tri-snRNP after each round of splicing (Schaffert *et al.*, 2004; Stanek and Neugebauer, 2004). Following modification at the CB, mature snRNPs acquire additional accessory proteins from splicing speckles (Misteli and Spector, 1997) and undergo further maturation before the mature spliceosome complex is assembled at transcription sites on pre-mRNAs (reviewed in Nilsen, 2003; Patel and Bellini, 2008). U snRNPs can then be recycled back to CBs from other regions of the nucleus by the SMN complex (Stanek *et al.*, 2008).

In addition to snRNP biogenesis, CBs are involved in the recruitment of telomerase to telomeres. Telomeres are regions of repetitive DNA sequence located at the end of linear chromosomes, and function to protect the DNA from degradation. However, limitations in the cellular DNA replication machinery result in telomere shortening over time, leading to cellular senescence (Harley *et al.*, 1990; Bodnar *et al.*, 1998). Cancer cells act to prevent telomere shortening and cellular senescence by activating telomerase, a ribonucleoprotein complex which acts to extend telomere length (Counter *et al.*, 1992; Kim *et al.*, 1994; Shay and Bacchetti, 1997). Active telomerase consists of three subunits known as hTERT, hTR and dyskerin; hTERT functions as the reverse transcriptase catalytic subunit, hTR is the RNA subunit which functions as a template for telomere extension whilst dyskerin is required for telomerase stability (Feng *et al.*, 1995; Nakamura *et al.*, 1997; Mitchell *et al.*, 1999; Cohen *et al.*, 2007). CBs were shown to accumulate telomerase and transiently associate with telomeres (Zhu *et al.*, 2004; Jady *et al.*, 2006). The accumulation of telomerase within CBs was found to be due to the activity of WRAP53, which was shown to play a role in hTR trafficking (Tycowski *et al.*, 2009; Jady *et al.*, 2004; Venteicher *et al.*, 2009). The association of telomerase or telomeres with CBs appears to occur during S phase of the cell cycle (Jady *et al.*, 2006; Li *et al.*, 2010). Studies of mouse, *Xenopus* and human TR indicates that CBs may be necessary for telomerase recruitment to telomeres under steady-state conditions, whilst WRAP53 activity appears to be essential for telomerase recruitment under both steady state conditions and when telomerase is over-expressed (Li *et al.*, 2010; Tomlinson *et al.*, 2010; Stern *et al.*, 2012). Indeed, disruption of WRAP53 function leads to ablation of telomerase trafficking in dyskeritosis congenita, a genetic disorder characterised by defective tissue maintenance and cancer predisposition (Zhong *et al.*, 2011).

CBs, or the related HLBs in *Drosophila*, are responsible for expression of replication-dependent histone mRNAs. Histone expression is activated during S-phase to ensure sufficient histone levels for packaging of newly replicated DNA before the onset of cell division. Histone expression commences at the G1/S transition and is controlled by the cyclin E/CDK2-mediated phosphorylation and activation of Nuclear Protein Ataxia Telangiectasia (NPAT) (Zhao *et al.*, 1998; Ma *et al.*, 2000). Phosphorylated NPAT activates a histone H4 transcription factor known as HiNF-P, stimulating histone gene transcription (Miele *et al.*, 2005). Metazoan replication-dependent histone mRNAs are intronless so do not require splicing and are also the only mRNAs which do not undergo polyadenylation (reviewed in Marzluff *et al.*, 2008). Instead, production of mature histone mRNA requires cleavage of a conserved 3′ stem-loop structure. The stem loop binds Stem Loop Binding Protein (SLBP) whilst a conserved downstream sequence known as the histone downstream element binds the U7 snRNP (Mowry and Steitz,

1987). Cleavage between these two elements is then conducted by recruitment of cleavage factor and currently undefined elements (Dominski *et al.*, 2005, Kolev and Steitz, 2005, Wagner *et al.*, 2007; Kolev *et al.*, 2008; Sullivan *et al.*, 2009). Another protein shown appears to be required for both histone gene transcription and histone mRNA 3′ end processing is FLASH (Barcaroli *et al.*, 2006a; Yang *et al.*, 2009), which appears to associate with the transcription factor p73 (a homologue of p53) to promote histone gene transcription (De Cola *et al.*, 2012). MYC has also been implicated in histone gene transcription by HLBs (Daneshvar *et al.*, 2011). The association of FLASH with Lsm10 and Lsm11 to form the U7 snRNP is required for histone 3′ end-processing (Burch *et al.*, 2011). Depletion of HLB proteins involved in histone expression impacts progression of the cell cycle (Ma *et al.*, 2000; Zhao *et al.*, 2000; Miele *et al.*, 2005; Barcaroli *et al.*, 2006a; Bongiorno-Borbone *et al.*, 2010).

As the coilin knockout mouse model is still viable, this indicates that neither coilin nor CBs are required for the essential steps of spliceosome assembly (Tucker *et al.*, 2001). However, coilin knockout mice exhibit decreased fertility, fecundity and viability (Walker *et al.*, 2009). The general consensus for CBs function is to enhance processes that would normally occur at slower rates in the nucleoplasm, possibly by bringing together essential factors (Stanek and Neugebauer, 2006). Indeed, a recent model proposed that tri-snRNP assembly occurs approximately 10 times faster in CBs than in the surrounding nucleoplasm (Novotny *et al.*, 2011). In contrast to coilin, SMN knockout is embryonic lethal, as it is an essential factor in snRNP biogenesis and delivery to the nucleus (Schrank *et al.*, 1997). Mutations in SMN is the causative agent of the autosomal recessive disorder spinal muscular atrophy (SMA), which results in progressive atrophy of motor neurons and muscle wasting (Lefebvre *et al.*, 1995). However, it is currently unclear how mutation in a ubiquitously-expressed protein can cause damage in only a subset of cell types. SMN-deficient mice were found to have altered stoichiometry of snRNAs, resulting in widespread and tissue-specific splicing defects (Gabanella *et al.*, 2007; Zhang *et al.*, 2008). The formation of the minor spliceosome was also found to be severely abrogated in SMN-depleted cells, resulting in inhibition of splicing at some U12-type introns (Boulisfane *et al.*, 2011). This indicates that defects in splicing of a subset of U12-type introns may contribute to the pathogenesis of SMA. However, SMN depletion does not appear to impact post-transcriptional modification of snRNAs, indicating that affects on differential splicing in SMN-deficient cells are not due to deficient snRNP maturation (Deryusheva *et al.*, 2012). In addition to SMN, NPAT, FLASH and HinF-P homozygous knockouts are also embryonic lethal, highlighting their essential roles in histone gene transcription and processing (Di Fruscio *et al.*, 1997; Xie *et al.*, 2009; De Cola *et al.*, 2012).

1.3.7 Other nuclear bodies

In recent years a number of additional nuclear bodies have been discovered, although their functions are not well characterised. Cleavage bodies have been shown to associate with CBs in a cell-cycle dependent manner (Schul *et al.*, 1996; Schul *et al.*, 1999b; Li *et al.*, 2006b). PcG bodies are believed to be involved in transcriptional silencing; PcG proteins form transcriptional repressive complexes which silence target genes by inducing post-translational modification of histones (Margueron and Reinberg, 2011). The nSB (also known as the Sam68 nuclear body) forms in response to cellular stresses including heat shock, heavy metal exposure, protease inhibition or translation inhibition and is often found in close proximity to the nucleolus (Biamonti, 2004). During stress, general transcription is suppressed in cells and there is hyperactivation of transcription of repetitive non-coding satellite III (sat III) repeats on chromosome 9q11-12 (Valgardsdottir *et al.*, 2005). The sat III transcripts remain associated with the chromosome locus and recruit various heat-shock specific transcription factors such as ASF/SF2, resulting in nSB formation (Shevtsov and Dundr, 2011). PIKAs were first observed as a nuclear substructure consisting of a group of small related auto-antigens. They appear to be variable in both size and number particularly during the cell cycle (Saunders *et al.*, 1991). Although the PIKA proteins may associate with chromatin (Saunders *et al.*, 1991), the function of PIKAs is still undefined. OPT domains are small nuclear foci that are present in the cell at the G1 phase but are absent by the S phase (Pombo *et al.*, 1998). They often colocalise with large PIKA domains and contain high concentrations of the transcription factors PTF and Oct1 as well as TATA-binding protein (TBP), SP1 and RNA pol II (Pombo *et al.*, 1998). These domains appear to act as sites of transcription and certain chromosomes preferentially associate with this domain, indicating OPT domains may facilitate expression of certain genes (Pombo *et al.*, 1998). OPT domains may play a role in DNA damage signalling; incomplete DNA synthesis during S phase was shown to stimulate the formation of OPT domains at sites of damaged DNA in the following G1 phase (Harrigan *et al.*, 2011).

1.3.8 Transcription and DNA replication foci

In recent years it has become apparent that RNA transcription, DNA replication and DNA repair occur in small foci within the nucleus of around 100 nm. Pulse-labelling of mammalian cells during S-phase with nucleoside analogues such as bromodeoxyuridine (BrdU) resulted in the appearance of DNA replication at several discrete sites within the nucleus, termed 'replication foci' (Nakamura *et al.*, 1986; Nakayasu and Berezney, 1989). Immunolabelling of replisome components including DNA pol A revealed that these components also exhibit punctate nuclear staining in S-phase nuclei of mammalian and yeast cells (Meister *et al.*, 2005; Meister *et al.*, 2007; Natsume *et al.*, 2008). These were termed 'replication factories' as they were shown to

colocalise with replication foci thus indicating ongoing DNA synthesis at this site (Hiraga *et al.*, 2005; Kitamura *et al.*, 2006). Although the dynamics of DNA replication factories are not well understood, it is believed that factories form after the initiation of DNA replication (Cardoso *et al.*, 1993; Jackson, 1995; Yan and Newport, 1995; Kitamura *et al.*, 2006). Akin to numerous other nuclear bodies, replication factories show dynamic assembly and disassembly kinetics dependent on cell cycle stage (Leonhardt *et al.*, 2000; Somanathan *et al.*, 2001). Each replication focus is believed to contain multiple replicons that initiate replication in synchrony during S phase (Berezney *et al.*, 2000). Interestingly, as S phase proceeds, an early firing replication factory becomes in close proximity to a later firing factory indicating that a change in local chromatin state may trigger replication from the adjacent factory in a temporal manner (Sporbert *et al.*, 2002; Sadoni *et al.*, 2004).

In recent years, accumulating evidence indicates that transcription occurs in designated regions within the nucleus, termed 'transcription factories'. There are three types of transcription factory; containing RNA pol I, II or III alongside a specific set of co-factors (Melnik *et al.*, 2011). Transcription by RNA pol I synthesises rRNAs (with the exception of the 5S rRNA), RNA pol II is responsible for mRNA synthesis whilst RNA pol III is required for transcription of 5S rRNA, tRNA and other small nuclear RNAs. The nucleolus is an example of a transcription factory as it is the site of rDNA transcription by RNA pol I (reviewed in Boisvert *et al.*, 2007; Sirri *et al.*, 2008). Ribosomal DNA was shown to slide over these centres and nascent RNAs were released into the surrounding DFC (Hozak *et al.*, 1994). RNA pol II and III transcripts also arise in a limited number of nuclear foci which are enriched in phosphorylated, active RNA pol II or RNA pol III, respectively (Iborra *et al.*, 1996; Jackson *et al.*, 1998; Kimura *et al.*, 1999; Pombo *et al.*, 1999).

Transcription factories can be highly variable in size depending on tissue-specific demands (reviewed in Sexton *et al.*, 2007). A single transcription factory can co-ordinate transcription from several different loci, either on the same chromosome or from different chromosomes Osborne *et al.*, 2004; Osborne *et al.*, 2007; Papantonis *et al.*, 2010; Schoenfelder *et al.*, 2010). Genes sharing transcription factories are commonly genes which are under the control of the same regulatory factors (Schoenfelder *et al.*, 2010), indicating that different transcription factories may be highly specialised for transcription of a specific subset of genes. Co-expressed genes are often found *in-cis* on the chromosome, which may facilitate co-ordinated expression from one transcription factory (Caron *et al.*, 2001; Boutanaev *et al.*, 2002; Spellman and Rubin, 2002; Zhou *et al.*, 2006). In contrast, the vast majority of tissue-specific genes are found scattered throughout the genome (Yager *et al.*, 2004). Instead, these genes appear to be directed to specific transcription factories alongside distal functionally-related genes (Fraser and

Bickmore, 2007; Xu and Cook, 2008) and this may also be the case for stress-responsive genes (Papantonis *et al.*, 2010; Larkin *et al.*, 2012). Although not well defined, it is thought that movement of these genes to common transcription foci may be mediated by actin-myosin motor movement (Chuang *et al.*, 2006). Transcription factories are also often located in close proximity to splicing speckles and perichromatin fibrils and to sites of mRNA export components (reviewed in Maniatis and Reed, 2002; Hagiwara and Nojima, 2007), facilitating efficient processing and export of an mRNA once transcribed.

1.4 Impact of adenovirus infection on nuclear substructures

In order to facilitate infection, multiple viruses have been shown to redistribute components of nuclear bodies. A comprehensive summary of known virus interactions with the nucleolus, PML bodies, splicing speckles and CBs is provided in Tables 1-2, 1-3, 1-4 and 1-5 respectively. The redistribution of nuclear substructures during Ad infection is discussed below.

1.4.1   The nucleolus

Nucleoli are disrupted during the late stages of Ad infection, with several nucleolar proteins being redistributed to novel new compartments within the nucleus (Walton *et al.*, 1989; Puvion-Dutilleul and Christensen, 1993; Rodrigues *et al.*, 1996; Lam *et al.*, 2010). B23 and Upstream Binding Factor (UBF) are sequestered into viral replication centres and appear to be crucial for Ad DNA replication (Okuwaki *et al.*, 2001; Lawrence *et al.*, 2006; Samad *et al.*, 2007). When complexed with Ad core proteins, B23 may act as a stimulator for DNA replication (Okuwaki *et al.*, 2001). However, recent data indicates a role for B23 in the assembly of viral chromatin rather than DNA replication (Samad *et al.*, 2012). A role for B23 in capsid assembly has also been suggested (Ugai *et al.*, 2012). The role of UBF during Ad replication is currently not well defined; although UBF is known to directly inhibit RNA pol I activity (Copenhaver *et al.*, 1994; Voit and Grummt, 2001; Mais *et al.*, 2005; Prieto and McStay, 2007), the sequestration of UBF during Ad5 infection does not appear to affect RNA pol I distribution or prevent rRNA synthesis (Lawrence *et al.*, 2006).

Akin to UBF and B23, the nucleolar proteins processing of precursor 1 (hPOP1) and Nopp140 were also found to be depleted from the nucleolus during Ad5 infection (Lam *et al.*, 2010). Following Ad infection, hPOP1 was shown to be redistributed into a nucleoplasmic speckle pattern separate from viral DNA replication centres, whilst Nopp140 displayed some colocalisation with DBP but was mainly enriched in centres adjacent to DBP (Lam *et al.*, 2010; Lawrence *et al.*, 2006). Although hPOP1 is normally involved in rRNA processing (Lygerou *et al.*, 1996; Welting *et al.*, 2006) and Nopp140 normally functions an snRNA chaperone

Table 1-2. Nucleolar targeting by viruses.

Whilst numerous virus proteins are known to locate to the nucleolus, only virus proteins with a known effect on the nucleolus are listed. Ad – Adenovirus. HSV-1 – herpes simplex virus 1. HCMV – human cytomegalovirus. GRV – Groundnut rosette virus. PSLV – Poa semilatent virus. WNV – West Nile virus. CuMV – Cucumber mosaic virus. FCV – feline calcivirus. AAV2 – adeno-associated virus 2. HVS – herpesvirus saimiri. HIV-1 – human immunodeficiency virus 1. *suggested not proven.

Virus	Protein	Effect on domain	Function	Reference
Ad	pV	Nuclear export and degradation of C23	Subversion of C23-mediated transcriptional repression*	Matthews, 2001
		B23 and UBF redistributed to DNA replication centres	Ad DNA replication*/ assembly of virus chromatin/ virion assembly*	Okuwaki *et al.*, 2001; Samad *et al.*, 2007; Lam *et al.*, 2010; Ugai *et al.*, 2012
	Not known	UBF redistributed to DNA replication centres	Unknown	Lawrence *et al.*, 2006
HSV-1	ICP4	Redistribution of C23 to DNA replication centres	Viral DNA replication*	Calle *et al.*, 2008b
	Not known	Redistribution of fibrillarin	Unknown	Lymberopoulos and Pearson, 2007
	UL24	Dispersal of B23 by UL24	Nuclear egress	Lymberopoulos and Pearson, 2007; Bertrand and Pearson, 2008; Lymberopoulos *et al.*, 2011
	UL12	US12 interacts with C23	Nucleocapsid egress	Sagou *et al.*, 2010
	US11	US11 interacts with C23	Trafficking of US11 to the cytoplasm	Greco *et al.*, 2012
	Not known	Sequestration of UBF into DNA replication centres	Viral DNA replication	Stow *et al.*, 2009
HCMV	UL44	C23 is redistributed to viral replication centres	Maintenance of replication centre architecture	Strang *et al.*, 2010; Strang *et al.*, 2012
	Pp65	Pp65 locates to the nucleolus	Cell cycle progression to G1/S phase*	Arcangeletti *et al.*, 2011
GRV	ORF3	ORF3 interacts with fibrillarin	Formation of viral snRNPs and viral spread	Kim *et al.*, 2007a; Canetta *et al.*, 2008
PSLV	TGBp1	TGBp1 interacts with fibrillarin	Viral spread*	Semashko *et al.*, 2012a
WNV	WNV capsid	Dead box helicase 56 (DX56) redistributed to the cytoplasm	Particle assembly	Xu *et al.*, 2011
CuMV	2b	2b interacts with the RNA silencing machinery	Abrogates RNA silencing machinery	Zhang *et al.*, 2006; Goto *et al.*, 2007
FCV	NS6, NS7	C23 interacts with NS6/7and 3'UTR	Viral DNA replication	Cancio-Lonches *et al.*, 2011
AAV2	AAP	AAP targets capsid proteins to the nucleolus	Capsid assembly	Sonntag *et al.*, 2010
HVS	ORF57	ORF57 traffics via the nucleolus	Viral mRNA export	Boyne and Whitehouse, 2006
HIV-1	Rev	Rev localises to the nucleolus	Viral mRNA export	Cochrane *et al.*, 1990; Fankhauser *et al.*, 1991; Michienzi *et al.*, 2000

(Meier and Blobel, 1992; Isaac *et al.*, 1998), their colocalisation with DBP and UBF implicates roles for these proteins in viral DNA replication.

In contrast to the proteins described above, C23 is exported from the nucleolus to the cytoplasm following Ad2 infection (Matthews, 2001). This redistribution of C23 may be a mechanism by Ad2 to subvert the transcriptional repressive abilities of C23 (Yang *et al.*, 1994a). Indeed, it was suggested that the Ad genome contains potential C23 binding sites (Matthews, 2001).

Multiple Ad proteins localise to the nucleolus during infection; pV (Matthews and Russell, 1998b; Matthews, 2001), Mu (Lee *et al.*, 2004), pVII (Lee *et al.*, 2003), IVa2 (Lutz *et al.*, 1996) and E4orf4 (Miron *et al.*, 2004). Ad2 pV was shown to redistribute C23 and B23 from the nucleolus into the cytoplasm in transfected cells (Matthews, 2001). Although the inhibition of rRNA synthesis using actinomycin D relocates multiple nucleolar proteins to the nucleoplasm, including B23 and C23 (Yung *et al.*, 1985; Perlaky *et al.*, 1997), it does not affect the localisation of transfected pV, indicating pV is not dependent on B23 or C23 for its nucleolar association (Matthews, 2001). However, findings in Ad5-infected cells appear to contrast with findings in pV-transfected cells described above. In Ad2-infected cells, C23 is degraded whilst B23 is redistributed from the nucleoli to a speckled pattern within the nucleus (Matthews, 2001). This indicates that other viral proteins may impact on the activity of pV and the localisation of nucleolar proteins during infection.

The role of other Ad proteins localising to the nucleolus is less well defined. Pre-Mu locates to the nucleolus and appears to modulates E2 expression (Lee *et al.*, 2004). IVa2 colocalises with nucleoli in Ad-infected cells but was not found to impact either the location of specific nucleolar proteins or indeed rRNA synthesis (Lutz *et al.*, 1996). Polypeptide VII contains both nuclear and nucleolar targeting sequences and appears to colocalise with human chromosomes (Lee *et al.*, 2003). The nucleolar localisation of E4orf4 was shown to correlate with cell death (Miron *et al.*, 2004). The toxicity of E4orf4 appears to be due to an interaction of E4orf4 with a subunit of PP2A, leading to inactivation of PP2A and the unscheduled activation of the APC. This results in mitotic defects and apoptosis of host cells (Mui *et al.*, 2010).

1.4.2 PML-NBs

Ad infection was shown to induce the rearrangement of PML protein from punctate PML-NBs into nuclear tracks and this was found to be caused by the Ad E4orf3 protein (Carvalho *et al.*, 1995; Puvion-Dutilleul *et al.*, 1995). E4orf3 targets and disrupts PML-NBs via its interaction with PML isoform II (Evans and Hearing, 2003; Hoppe *et al.*, 2006; Leppard *et al.*, 2009) and the rearrangement of PML-NBs was found to correspond to efficient viral replication (Doucas *et al.*, 1996). PML disruption by E4orf3 appears to be a mechanism to subvert antiviral responses

Table 1-3. Viruses targeting promyelocytic leukaemia bodies (PML-NBs).

Ad – adenovirus. HCMV – human cytomegalovirus. HSV-1 – herpes simplex virus 1. EBV – Epstein Barr virus. VZV – varicella zoster virus. * suggested not proven.

Virus	Protein(s)	Effect on domain	Functional significance	Reference
Ad	E4orf3	Redistribution of PML	Immune subversion*	Leppard and Everett, 1999; Hoppe *et al.*, 2006; Ullman *et al.*, 2007; Ullman and Hearing, 2008; Leppard *et al.*, 2009
	E1B-55K	E1B-55K binds and degrades Daxx	Inhibits Daxx-dependent p53 transcription	Zhao *et al.*, 2003; Schreiner *et al.*, 2010; Schreiner *et al.*, 2011
		E1B-55K binds PML	Immune subversion*	Wimmer *et al.*, 2010
		Sequestration of p53 in PML-NBs	Inactivation and nuclear export of p53	Pennella *et al.*, 2010
	pIX	Sequestration of PML by pIX	Immune subversion*	Rosa-Calatrava *et al.*, 2001; Rosa-Calatrava *et al.*, 2003
HCMV	IE1/IE2	Disruption of PML	Alleviates PML-mediated transcriptional repression	Ahn and Hayward, 1997; Wilkinson *et al.*, 1998; Ahn *et al.*, 1999; Ahn and Hayward, 2000; Xu *et al.*, 2001
	Various	Disruption/decreased number of PML-NBs	Unknown	Salsman *et al.*, 2008
	UL35	SP100 and Daxx recruited to novel UL35 bodies	Manipulation of cell cycle and DNA damage responses	Salsman *et al.*, 2008; Salsman *et al.*, 2011
	UL82	Daxx degradation	Relieves transcriptional repression by Daxx	Hofmann *et al.*, 2002a; Cantrell and Bresnahan, 2006
HSV-1	ICP0	Redistributes PML	Immune subversion	Maul *et al.*, 1993; Everett *et al.*, 2006; Everett *et al.*, 2008
	Not known	PML redistributed to replication compartments	Genome replication*	Burkham *et al.*, 1998; Burkham *et al.*, 2001; Sourvinos and Everett, 2002; Everett and Murray, 2005; Everett *et al.*, 2007
	Vmw110	Degradation of PML	Immune subversion	Everett and Maul, 1994; Everett *et al.*, 1998; Chee *et al.*, 2003; Cuchet *et al.*, 2011
	ICP4 and ICP27	Interact with Daxx	Viral transcriptional activation	Tang *et al.*, 2003
	UL8.5, UL14, US10	Disruption of PML-NBs	Suppression of PML-NB-mediated apoptosis*	Salsman *et al.*, 2008
EBV	BZLF1	Redistribution of PML-NB proteins	Activation of gene expression and the lytic cycle	Bell *et al.*, 2000; Sivachandran *et al.*, 2010; Tsai *et al.*, 2011;Salsman *et al.*, 2008
VZV	ORF61	PML-NB disruption	Prevents capsid entrapment in PML-NBs	Reichelt *et al.*, 2011; Wang *et al.*, 2011

mediated by Daxx and PML (Ullman *et al.*, 2007; Ullman and Hearing, 2008). In addition to independent function, E4orf3 can associate in a complex with E1B-55K to disrupt PML distribution (Leppard and Everett, 1999). Following Ad infection, SP100 is also redistributed into tracks alongside PML. However, as infection progresses SP100 appears to segregate into DNA replication centres separate from the PML tracks (Doucas *et al.*, 1996).

E1B-55K can also act independently to affect PML-NB function. E1B-55K sequesters p53 in PML-NBs prior to facilitating the nuclear export of p53 (Pennella *et al.*, 2010). Following SUMO-1 conjugation, E1B-55K interacts with and targets Daxx for degradation in a proteasome-dependent manner (Schreiner *et al.,* 2010, 2011). This abrogates the transcriptional repressive and anti-viral activities of Daxx and also inhibits Daxx-dependent p53 transcription (Zhao *et al.*, 2003). SUMO1 modification of E1B-55K also appears to facilitate its binding to PML isoforms IV and V (Wimmer *et al.*, 2010).

In addition to E1B-55K and E4orf3, E1A and pIX have been shown to interact with PML-NBs. E1A was found to concentrate in PML tracks; this was dependent on the LXCXE motif of E1A responsible for pRb binding (Carvalho *et al.*, 1995). It was also found that the interaction of E1A with the SUMO-conjugating enzyme UBC9 interferes with PML-NB SUMOylation (Yousef *et al.*, 2010). Ad pIX sequesters PML within nuclear inclusions and this was shown to be necessary for efficient viral replication (Rosa-Calatrava *et al.*, 2001; Rosa-Calatrava *et al.*, 2003).

1.4.3 Splicing speckles

Whilst expression of early Ad proteins does not appear to alter mRNA biogenesis, the onset of late phase infection results in reorganisation of splicing factors within the nucleus. Ads hijack the transcriptional and splicing factors of the cell to facilitate viral replication (Pombo *et al.,* 1994; Bridge *et al.,* 1995, 1996; Gama-Carvalho *et al.,* 2003b). U2AF and the pre-mRNA and alternative splicing factor ASF/SF2 were shown to be redistributed to sites of active transcription and splicing during adenovirus infection (Gama-Carvalho *et al.,* 1997, 2003b; Lindberg *et al.,* 2004). There is a dynamic change in splicing factor distribution following the switch to late phase infection (Puvion-Dutilleul *et al.*, 1994; Aspegren *et al.*, 1998). During the intermediate phase, ASF/SF2 is redistributed into ring-like structures surrounding DNA replication centres and colocalises with snRNPs (Bridge *et al.*, 1993a; Gama-Carvalho *et al.*, 2003b). At later stages, both ASF/SF2 and snRNPs are found at enlarged interchromatin granules at the nuclear periphery (Bridge *et al.*, 1993b). Viral late RNA also accumulates in these late stage structures, and interestingly E4-deletion mutants have significantly reduced late mRNAs in these structures (Bridge *et al.*, 1996; Bridge *et al.*, 2003). The clusters of ICGs at late

Table 1-4. Viruses targeting splicing speckles.

Ad – adenovirus. IBV – influenza B virus. HTLV-1 – human T-cell lymphotrophic virus 1. HCMV – human cytomegalovirus. HSV-1 – herpes simplex virus 1. HPV-5 – human papillomavirus 5. SRPK1 – SR Protein Kinase 1. CSF-64 – Cleavage Stimulatory Factor 64 kDa. PTB – Polypyrimidine-tract Binding protein. *suggested but not proven.

Virus	Protein	Effect on domain	Function	Reference
Ad	E4 region	Late mRNAs accumulate in enlarged ICGs	Late mRNA export*	Bridge *et al.*, 1993a
	Not known	Movement of splicing factors to transcription sites	Activation of late phase alternative splicing*	Gama-Carvalho *et al.*, 2003b; Lindberg *et al.*, 2004
IBV	NS1	Redistribution of SRSF2 to novel sub-nuclear structures	Gene expression/ inhibition of cellular splicing?	Fortes *et al.*, 1995; Schneider *et al.*, 2009
HTLV-1	Tax	Tax localises with snRNPs, and SRSF2 in nuclear foci	Activation of viral gene expression*	Semmes and Jeang, 1996; Bex *et al.*, 1997
HCMV	Not known	SRPK1 redistributed to the cytoplasm, up-regulation of CSF-64, temporal regulation of PTB	Temporal control of HCMV pre-mRNA processing*	Gaddy *et al.*, 2010
HSV-1	ICP22	Remodelling of speckles into punctate foci	Enhanced viral gene expression*	Salsman *et al.*, 2008
	Not known	Replication compartments coalesce with splicing speckles	Viral mRNA export	Chang *et al.*, 2011
	ICP27	Redistribution of snRNPs and SRSF2, inactivation of SRPK1, inhibition of spliceosome assembly	Impairment of host cell and HSV-1 splicing	Sandrigoldin *et al.*, 1995; SandriGoldin and Hibbard, 1996; Bryant *et al.*, 2001; Sciabica *et al.*, 2003
	IE63	Redistribution of snRNPs, interacts with p32 to disrupt cellular splicing	Host cell splicing shutoff and export of splicing independent transcripts	Phelan *et al.*, 1993; Wadd *et al.*, 1999; Bryant *et al.*, 2000
	Not known	Splicing factors recruited to transcription sites, nascent mRNA trafficked to SRSF2 domains	Transcription and splicing of viral mRNAs	Melcak *et al.*, 2000
HVS	ORF57	ORF57 associates with Sm proteins in splicing speckles, redistributes SRSF2	Enhance intronless viral RNA splicing	Majerciak *et al.*, 2008
HIV-1	Vpr	Binds SF3b subunit of the spliceosome	Checkpoint mediated G2 cell cycle arrest	Terada and Yasuda, 2006
	Tat	Associates with FBI-1 in splicing speckles	Stimulation of viral gene transcription	Pendergrast *et al.*, 2002
HPV-5	E2	Interacts with ASF/SF2, SRSF2 and snRNPs U1 and U5 in splicing speckles	Facilitates splicing of viral transcripts	Lai *et al.*, 1999

stages are thought to reflect an intranuclear mRNA trafficking route for late Ad mRNAs from the nucleus to the cytoplasm (Besse and Puvion-Dutilleul, 1995).

1.4.4 Cajal Bodies

During Ad5 infection, the nucleolar proteins fibrillarin, UBF and RNA pol I associate in punctate nuclear microfoci alongside the CB marker protein, coilin (Rebelo *et al.*, 1996; Rodrigues *et al.*, 1996). These microfoci do not contain snRNPs or Ad mRNA, indicating they are not involved in Ad gene transcription (Rebelo *et al.*, 1996; Rodrigues *et al.*, 1996). Although it was initially suggested that the disassembly of CBs during Ad infection is secondary to the block of host protein synthesis during Ad infection (Rebelo *et al.*, 1996), recent work indicates that coilin plays a role in Ad late protein expression (James *et al.*, 2010). However, the exact function of CBs during the later stages of Ad infection is still undefined. Intriguingly, the redistribution of CBs into microfoci has also been shown to occur during infection with the RNA plant virus GRV. The rearrangement of CBs during GRV infection was shown to facilitate the transport of the GRV ORF3 protein to the nucleolus, whereby viral RNA was packaged into a viral snRNP with fibrillarin (Kim *et al.*, 2007a; Kim *et al.*, 2007b).

In contrast to the redistribution of coilin, CB-associated actin was found to be relocated to the nuclear periphery following Ad5 infection (Gedge *et al.*, 2005). It has been proposed that the actin content of CBs is related to the disassembly of CBs (Gedge *et al.*, 2005; James *et al.*, 2010). Although a functional significance for this has not yet been elucidated, it is possible that actin is redistributed to late transcription sites, as the assembly of transcription complexes is dependent on actin (Hofmann *et al.*, 2004). Alternatively, redistributed actin was also found to locate in close proximity to sites of Ad capsid assembly (Gedge *et al.*, 2005), suggesting a possible role for nuclear actin in capsid assembly.

Table 1-5. Viruses targeting Cajal bodies (CBs).

Ad – adenovirus. GRV – Groundnut rosette virus. MVM – minute virus of mouse. EBV – Epstein Barr virus. HVS – herpesvirus saimiri. CuMV – cucumber mosaic virus. HIV-1 – human immunodeficiency virus, PV – poliovirus. FMDV − foot and mouth disease virus. HCV − hepatitis C virus. BPV − bovine papillomavirus. IRES - internal ribosome entry site. *suggested not proven

Virus	Viral protein(s)	Effect on domain	Function	Reference
Ad	Not known	Redistribution of coilin and fibrillarin into nuclear microfoci	Facilitates late protein expression	Rebelo *et al.*, 1996; Rodrigues *et al.*, 1996; James *et al.*, 2010
	Not known	CB-associated actin is redistributed to the nuclear periphery	Unknown	Gedge *et al.*, 2005
GRV	ORF3	CB proteins coilin and fibrillarin redistributed to nuclear microfoci	Trafficking of ORF3 to the nucleolus for viral RNP assembly	Kim *et al.*, 2007a; Kim *et al.*, 2007b; Canetta *et al.*, 2008
MVM	NS1, NS2	Interacts with SMN in novel viral replication compartments	Viral replication or capsid assembly*	Young *et al.*, 2002a, b; Young *et al.*, 2005
Herpesvirus	UL3, UL30	Disruption of CBs	Unknown	Salsman *et al.*, 2008
Hordeivirus	Movement protein	Interacts with coilin	Unknown	Semashko *et al.*, 2012b
EBV	EBNA2	Interacts with SMN	Transactivation of the LMP1 promoter	Barth *et al.*, 2003 Voss *et al.*, 2001
	EBNA3, EBNA6	Colocalise with SMN	Unknown	Krauer *et al.*, 2004
	EBNA3C	Stabilises Gemin3	Blockage of p53-mediated apoptosis	Cai *et al.*, 2011
Influenza	Not known	Redistribution of CBs into microfoci	Unknown	Fortes *et al.*, 1995
	NS1	Redistribution of snRNPs	Inhibition of host cell splicing	
HVS	HSURs	Use SMN complex to assemble viral snRNPs	Replication	Golembe *et al.*, 2005
CuMV	2b	Localises to CBs, binds siRNAs and miRNAs	Abrogates gene silencing machinery	Duan *et al.*, 2012; Hamera *et al.*, 2012
HIV-1	Integrase	Binds Gemin 2	Viral cDNA synthesis	Hamamoto *et al.*, 2006
PV	2A	Cleavage of Gemin 3	Reduced snRNP assembly	Almstead and Sarnow, 2007
FMDV	Not known	Gemin5 binds IRES	Enhanced viral protein translation	Pacheco *et al.*, 2009
HCV	Not known	Gemin5 binds IRES	Enhanced viral protein translation	
BPV	E2	Binds SMN	Transcriptional activation at E2 promoters	Strasswimmer *et al.*, 1999

1.5 Project Aims

Although the early phase and DNA replication stages of Ad infection are well characterised, the mechanism controlling Ad late gene expression are not well understood. Understanding late gene expression is crucial for Ad vector development, since E1-deleted Ad vectors retaining late coding regions still express residual late proteins, resulting in induction of immune responses to the vector (Yang *et al.*, 1994b; Yang *et al.*, 1994c; Yang *et al.*, 1995). Interestingly, it was shown that during the late phase of Ad infection, CBs are redistributed from 1-6 punctate domains per cell into numerous microfoci (Rebelo *et al.*, 1996; Rodrigues *et al.*, 1996). Moreover, the CB marker protein coilin appears to be required for Ad late protein expression (James *et al.*, 2010). However, the mechanism by which CBs contribute to Ad late protein expression is unknown. Therefore characterising the role of the CB during Ad5 infection may facilitate the understanding of the control of Ad late phase protein expression.

The main aims of this investigation were as follows;

- Characterise the subcellular redistribution of key CB proteins during Ad5 infection

- Determine the time point at which CB proteins are redistributed from CBs

- Determine the function of key CB proteins during Ad5 infection.

Chapter 2 – Materials and Methods

2.1 Materials

2.1.1 Chemicals and reagents

Unless otherwise stated, all chemicals were obtained from Sigma Aldrich (Dorset, UK). The standard cell culture medium Dulbecco's modified Eagles medium (DMEM), L-glutamine and trypsin were all purchased from Sigma-Aldrich (Dorset, UK). Keratinocyte 2 Medium was purchased from PromoCell (Heidelberg, Germany). Foetal calf serum (FCS) was purchased from Biosera (Sussex, UK). Optimem-1 and Lipofectamine-2000 were obtained from Invitrogen (Paisley, UK). The Biorad DC Assay Kit and thick filter paper were purchased from Bio-Rad Inc (Hertfordshire, UK). Polyvinylidine fluoride (PVDF) membrane was purchased from Millipore (Watford, UK). The enhanced chemiluminescence (ECL) detection kit was purchased from GE Healthcare (Little Chalfont, UK). Normal goat serum (NGS) and Vectashield mounting medium were obtained from Vector Laboratories (Peterborough, UK). EDTA-free protease inhibitor cocktail and Slide-a-Lyser mini dialysis units were purchased from Pierce (Cramlington, UK). Caesium chloride was purchased from Invitrogen (Paisley, UK). Phosphate buffered saline (PBS) tablets were purchased from Oxoid (Hampshire, UK).

2.1.2 Custom primers

Table 2-1 describes all PCR primers used in this study. All primers were purchased from Invitrogen. Salt-adjusted melting temperatures (T_m) were calculated using Oligocalc (www.basic.northwestern.edu/biotools/oligocalc.html). The design strategy for all primers is described in Appendix Figures 1-6.

2.1.3 siRNA

Table 2-2 describes all siRNAs used in this study.

2.1.4 Antibodies

All primary antibodies raised against Ad proteins are described in Table 2-3. All primary antibodies directed against cellular proteins are described in Table 2-4. Secondary antibodies were used in Western blotting, indirect immunofluorescence and flow cytometry and are described in Table 2-5.

Table 2-1. PCR primers.

T_m – melting temperature. GC – guanine/cytosine content. F – forward primer. R- reverse primer.

Target mRNA	Primer name	Sequence (5′ to 3′)	T_m (°C)	% GC
Ad5 IIIa	IIIa (F)	ACAGTCGCAAGATGATGCAAGA	60.1	45
	IIIa (R)	GCCAGCGCGTTTACGATCG	61.6	63
Ad5 Hexon	Hexon (F)	ACAGTCGCAAGATGGCTACC	60.5	55
	Hexon (R)	GCAGTACGCAGTATCCTCAC	60.5	55
Ad5 Fibre	Fibre (F)	CAGTCGCAAGATGAAGCGC	59.5	58
	Fibre (R)	ACAGTGGTTACATTTTGGGAGG	60.1	45
Ad5 L4-100K	L4-100K (F)	AGATGGAGTCAGTCGAGAAGA	59.5	48
	L4-100K (R)	ACTTGTTCCTCGTTTGCCTCT	59.5	48
Ad5 DBP (RT1)	Early DBP (F)	ACC AGC GCG TCT TGT GAT GA	60.5	55
	DBP (R)	CAG CTG CGG GAG AAG GAA A	59.5	58
Ad5 DBP (RT2)	Late DBP (F)	ACC AGC GCG TCT TGT GAT GA	60.5	55
	DBP (R)	GGC GAT ATC AGG AGA AGG AAA	59.5	48
Ad5 13S E1A	E1A 13S/11S (F)	CCT TTC CCG GCA GCC CGA	62.9	72
	E1A 13S (R)	CAG ACA CAG GAG TAG ACA AAC	59.5	48
Ad5 12S E1A	E1A 12S (F)	GAT CGA AGA GGT ACT GGC TGA	61.2	52
	E1A 12S/10S (R)	ACA GGA CCT CTT CAT CCT CG	60.5	55
Ad5 11S E1A	E1A 11S/10S (F)	TGA TCG AAG AGC CGA GCA G	59.5	58
	E1A 13S/11S (R)	CAG ACA CAG GAG TAG ACA AAC	59.5	48
Ad5 10S E1A	E1A 11S/10S (F)	TGA TCG AAG AGC CGA GCA G	59.5	58
	E1A 10S (R)	ACA GGA CCT CTT CAT CCT CG	60.5	55
Ad5 9S E1A	E1A 9S (F)	CTG ATC GAA GAG TCC TGT GTC	61.2	52
	E1A 9S (R)	TCT CAC GGC AAC TGG TTT AAT G	60.1	45
Ad5 IVa2	IVa2 (F)	GAA ACC AGA GGG CGA AGA C	59.5	58
	IVa2 (R)	CAT CTC GAT CCA GCA TAT CTC	59.5	48
Ad5 IX	IX (F)	CTC GTT TGA TGG AAG CAT TGT GA	60.9	43
	IX (R)	GTC AAC TTG TCA TCG CGG G	59.5	58
Human GAPDH	GAPDH (F)	CTCAACTACATGGTTTACATGTTC	60.3	38
	GAPDH (R)	GCAAATGAGCCCCAGCCTT	59.5	58
Ad5 pre-IVa2	pre-IVa2 (F)	GGA AAC CAG AGG TAA GAA ACG	59.5	48
	pre-IVa2 (R)	GAC TTT TGA GGG CGT AGA GC	60.5	55
Ad5 pre-DBP	pre-DBP (F)	CTG TCC TTC TTC TCG ACT GAC	61.2	52
	DBP (R)	ACC AGC GCG TCT TGT GAT GA	60.5	55
Ad5 pre-E1A	pre-E1A (F)	TTA AAA GGT CCT GTG TCT GAA CC	60.9	43
	E1A 9S (R)	TCT CAC GGC AAC TGG TTT AAT G	60.1	45
Ad5 pre-tripartite leader (TPL)	pre-TPL (F)	ATC GCT GTC TGC GAG GGC	60.8	67
	pre-TPL (R)	CTG TCC AAC GCC CTC TAC G	61.6	63
pre-GAPDH	pre-GAPDH (F)	TAT CGT GGA AGG ACT CAT GGT AT	60.9	43
	pre-GAPDH (R)	GCA TGG ACT GTG GTC TGC AA	60.5	55

Table 2-2. siRNAs.

GC – Guanine/cytosine content.

Target	Name	Sequence (5' to 3')	GC (%)	Source
Human coilin	Coilin siRNA 2a	GAG AGG AGU UGC UGA GAA UTT	47	Eurogentec
	Coilin siRNA 2b	AUU CUC AGC AAC UCC UCU CTT	42	
Human SMN	Human SMN siRNA (sc-36510)	Sequence not provided. Supplied as a pool of three target-specific 19-25 nucleotide siRNAs	-	Santa Cruz
None	AllStars negative control siRNA (SI03650318)	Sequence not provided	-	Qiagen

Table 2-3. Primary antibodies specific for adenovirus proteins.

IgG – immunoglobulin. GST- Glutathione S-transferase.

Antibody	Specificity	Species and isotype	Source
2Hx2	Ad hexon	Mouse monoclonal IgG	In house as described previously (Cepko *et al.*, 1981). Hybridoma cells HB-117 were obtained from the American Type Culture Collection (ATCC)
Ad5PB	Ad5 penton base	Rabbit polyclonal sera	In house (unpublished results)
B6-8	Ad E2A-72K	Mouse monoclonal IgG	K Leppard, Warwick University, UK (Reich *et al.*, 1983)
DBP	Ad E2A-72K	Rabbit polyclonal sera	K Leppard, Warwick University, UK (Made in house; raised to bacterially expressed GST-DBP)
Ad5F	Ad5 fibre	Rabbit polyclonal sera	In house (Caygill *et al.*, 2012)
TB5	Ad5 fibre	Mouse monoclonal IgG	In house as previously described (Franqueville *et al.*, 2008)
Ad3F	Ad3 fibre	Rabbit polyclonal sera	P. Fender, le Centre National de la Recherche Scientifique (CNRS), France
sc-430	Ad 2/5 E1A	Rabbit polyclonal IgG	Santa Cruz
IIIa	Ad2/5 IIIa	Rabbit polyclonal IgG	G. Akusjarvi, Uppsala University, Sweden (Everitt *et al.*, 1992)
IX	Ad IX	Rabbit polyclonal sera	In house as described previously (Boulanger *et al.*, 1979)
Pn	Ad IVa2	Rabbit polyclonal IgG	M. Imperiale, University of Michigan, USA (Tribouley *et al.*, 1994)
L4-33K	Ad2 L4-33K	Rabbit polyclonal sera	W. Deppert, Hamburg University, Germany (Gambke and Deppert, 1981)
L4-100K	Ad2 L4-100K	Rabbit polyclonal IgG	W. Deppert, Hamburg University, Germany (Gambke and Deppert, 1981)
ab36851	Capsid proteins from Ad serotypes 2, 3, 4, 5 and 6	Goat polyclonal IgG	Abcam

Table 2-4. Primary antibodies specific for cellular proteins.

IgG – immunoglobulin.

Antibody	Specificity	Species and isotype	Source
ab5821-100	Human fibrillarin	Rabbit polyclonal IgG	Abcam
PG-M3	Human PML	Mouse monoclonal IgG$_1$	Santa Cruz
11G5	Human Aly	Mouse monoclonal IgG$_1$	Abcam
D6	Human C23	Mouse monoclonal IgG$_1$	Santa Cruz
0412	Human B23	Mouse monoclonal IgG$_1$	Santa Cruz
H-300	Human coilin	Rabbit polyclonal IgG	Santa Cruz
F-7	Human coilin	Mouse monoclonal IgG$_1$	Santa Cruz
8	Human SMN	Mouse monoclonal IgG$_1$	BD Biosciences
H-195	Human SMN	Rabbit polyclonal IgG	Santa Cruz
A301-442A	Human WRAP53	Rabbit polyclonal IgG	Bethyl Laboratories
C65	Human GAPDH	Mouse monoclonal IgG$_1$	Calbiochem
Y12	Human Smith (Sm) antigen	Mouse monoclonal IgG$_3$	Abcam
M5409	None	Mouse monoclonal IgG$_{2a}$	Sigma Aldrich
UNLB	None	Rabbit polyclonal IgG	BioLegend

Table 2-5. Secondary antibodies.

IgG – immunoglobulin. HRP - horseradish peroxidise.

Antibody	Specificity	Species	Label	Source
A-21447	Goat IgG	Donkey	Alexa Fluor-647	Invitrogen
A-11029	Mouse IgG	Goat	Alexa Fluor-488	Invitrogen
A-21202	Mouse IgG	Donkey	Alexa Fluor-488	Invitrogen
A-11070	Rabbit IgG	Goat	Alexa Fluor-488	Invitrogen
A-21206	Rabbit IgG	Donkey	Alexa Fluor-488	Invitrogen
A-11020	Mouse IgG	Goat	Alexa Fluor-594	Invitrogen
A-21203	Mouse IgG	Donkey	Alexa Fluor-594	Invitrogen
A-11037	Rabbit IgG	Goat	Alexa Fluor-594	Invitrogen
A-21207	Rabbit IgG	Donkey	Alexa Fluor-594	Invitrogen
A-6782	Mouse IgG	Sheep	HRP	Sigma Aldrich
A-6154	Rabbit IgG	Goat	HRP	Sigma Aldrich

2.1.5 Cells and cell lines

Primary human keratinocytes were kindly provided by Miriam Whittmann (University of Leeds, UK). All cell lines were purchased from the European Collection of Animal Cell Cultures (Salisbury, UK).

A549	Human lung adenocarcinoma cell line (Giard *et al.*, 1973).
HeLa	Human cervical carcinoma cell line isolated from the cervical tumour of Henrietta Lacks (Gey *et al.*, 1952).

2.1.6 Viruses

Ad5	Wild type Ad5 virus was kindly provided by W.C Russell (University of St. Andrews, UK).
Ad3	Wild type Ad3 virus was kindly provided by W.C Russell (University of St. Andrews, UK).
Ad12	Wild type Ad12 virus was kindly provided by Bela Tarodi (University of Szeged, Hungary).

2.1.7 Buffers and solutions

2.1.7.1 Agarose gel electrophoresis

10x Tris-Borate (TBE) Buffer (1 l)

108 g Tris, 55 g Boric acid, 40 ml 0.5 M EDTA (pH 8.0)

10x Orange Gel Loading Buffer (20 ml)

5 g Ficoll 400, 2 ml 1 M Tris-HCl (pH 7.4), 4 ml 1 M EDTA (pH 8.0), 0.04 g Orange G

2.1.7.2 SDS-PAGE

5x Resolving Gel Buffer (RGB) pH 8.5

1.875 M Tris-HCl (227.06 g/l), 0.5% (w/v) SDS

10x Stacking Gel Buffer (SGB) pH 6.5

1.25 M Tris-HCl (151.37 g/l), 1% (w/v) SDS

12% Resolving Acrylamide Gel (20 ml)

30% Acrylamide (8 ml), dH_2O (8 ml), 5x RGB (4 ml), 10% (w/v) APS (200 μl), 1% TEMED (20 μl)

5% Stacking Gel (12 ml)

30% Acrylamide (2 ml), dH$_2$O (8.8 ml), 10x SGB (1.2 ml), 10% (w/v) APS (100 μl), TEMED (20 μl)

5x SDS-PAGE loading buffer (50 ml)

5 g (10% w/v) SDS, 12.5 ml 1 M Tris-HCl (pH 6.8), 50 mg Bromophenol Blue, 25 ml glycerol, 1.75 ml mercaptoethanol

SDS-PAGE 10x running buffer (1 l) pH 8.3

30.3 g Tris, 144.2 g glycine, 10 g SDS

2.1.7.3   Western blotting

Western blotting (Towbin) transfer buffer pH 8.3

25 mM Tris, 92 mM Glycine, 20% methanol

Western blotting blocking buffer

10% (w/v) Marvel, 0.1% Tween-20 in PBS

2.1.7.4   Lysis buffers

RIPA Buffer

50 mM Tris-HCl (pH 8.0), 150 mM NaCl, 1% NP40 substitute, 0.5% DOC, 0.1% SDS

Membrane Lysis Buffer (MLB)

50 mM HEPES-KOH (pH 7.5), 150 mM NaCl, 2 mM mgCl$_2$, 2 mM CaCl$_2$, 1% Triton X-100, 10% glycerol

2.1.7.5   Spectophotometry

TE Buffer

10 mM Tris-HCl (pH 8.0), 1 mM EDTA

2.1.7.6   Virus purification

DNase solution

20 mM Tris-HCl (pH 7.4), 50 mM NaCl, 1 mM DTT, 0.1 mg/ml BSA, 10 mg/ml bovine pancreatic DNase 1, 50% glycerol

CsCl solutions

1.5d – 90.8 g CsCl, 109.2 g 10 mM Tris-HCl pH 8.0
1.35d – 70.4 g CsCl, 129.6 g 10 mM Tris-HCl pH 8.0
1.25d – 54.0 g CsCl, 146.0 g 10 mM Tris-HCl pH 8.0

2.2 General Methods

2.2.1 Cell culture

Unless otherwise stated, cell lines were grown in DMEM supplemented with 10% (v/v) heat-inactivated FCS and 20 mM L-glutamine (referred to hereon in as 'complete DMEM'). Primary human keratinocytes were grown in Keratinocyte Media 2. Cells were grown in CellBIND® culture flasks (Corning) and maintained at 37 °C in a humidified atmosphere containing 5% CO_2.

2.2.2 SDS-PAGE and Western Blotting

2.2.2.1 Preparation of whole cell lysates

Ice-cold RIPA buffer was supplemented with 1% protease inhibitor cocktail (100 mM AEBSF.HCl, 80 μm aprotinin, 5 mM bestatin, 1.5 mM E-64, 2 mM leupeptin, 1 mM pepstatin A) and 200 μl was added to each well of a 6-well plate. Cells were incubated on ice at 4 °C for 15 minutes. Cells were scraped in the buffer using a cell scraper and were transferred to a microcentrifuge tube. Cells were centrifuged at 15,000 g for 10 minutes at 4 °C. Supernatant (whole cell lysate) was transferred to a fresh microcentrifuge tube and stored at -80 °C.

2.2.2.2 Preparation of nuclear and cytoplasmic fractions

Cells were detached from 6-well plates by trypsin treatment (0.5 ml). Once cells had detached, they were neutralised with 0.5 ml complete DMEM. Following a PBS wash, cells were resuspended in 1 ml of ice-cold MLB supplemented with 1% protease inhibitor cocktail and incubated on ice for 30 minutes. Nuclei were pelleted at 10,000 g for 20 minutes at 4 °C. The supernatant (cytoplasmic fraction) was transferred to a new tube on ice. Nuclei were lysed in 200 μl RIPA buffer on ice for 15 minutes. Samples were centrifuged at 15,000 g for 10 minutes at 4 °C to remove cellular debris. The supernatant (nuclear fraction) was removed and transferred to a fresh tube. Samples were either stored at -80 °C or analysed by SDS-PAGE.

2.2.2.3 Protein quantification

The concentration of protein in whole cell lysates was determined using the BioRad DC assay system which is based on the Lowry assay (Bio-Rad Inc.). In brief, Reagent A′ was prepared by adding 20 μl of Reagent S to 1 ml of Reagent A. 125 μl Reagent A′ was then added to 25 μl standards of bovine serum albumin (BSA) (concentrations 0-5 mg/ml) in sterile quotient (SQ) water or to 25 μl whole cell lysate. Each tube was vortexed. Reagent B (1 ml) was added to each tube and the tube was immediately vortexed. After 15 minutes the absorbance was measured at 750 nm using a spectrophotometer (Genova), calibrating between each reading using the 0 mg/ml BSA standard. The BSA standards were used to plot a calibration curve and the protein concentration of the samples was subsequently determined.

2.2.2.4   SDS-PAGE

Protein extracts analysed by SDS-PAGE were separated on a 10, 12% or 15% resolving gel and a 5% stacking gel. SDS loading buffer (5x) was added to each sample to give a final concentration of 1x buffer. The sample was loaded directly onto the gel and electrophoresis was conducted in SDS-PAGE running buffer at 100 V for approximately 15 minutes or until the bromophenol blue had passed into the stacking gel. Electrophoresis was then conducted at 150 V for 1.5 hours or until the bromophenol blue band had reached the bottom of the gel.

2.2.2.5   Western Blotting

Two sheets of BioRad blotting paper were soaked in Towbin transfer buffer. PVDF membrane was soaked in methanol followed by transfer buffer. One sheet of blotting paper was placed on the conductance plate of a transfer chamber (Biometra) and the PVDF membrane was placed on top. The SDS-PAGE gel was rinsed in transfer buffer before being placed directly onto the PVDF membrane. The second sheet of blotting paper was placed on top before the lid of the transfer chamber was closed. Electrophoretic transfer was conducted for 1 hour at 15 V. Bound antibody was detected using the ECL detection system (GE Healthcare) and images were captured on a Las 3000 Imager (Fujifilm). Densitometric analysis was carried out using Advanced Image Data Analyser (AIDA) software.

2.2.3   Nucleic acid extraction and purification

2.2.3.1   Total RNA extraction (Trizol-chloroform extraction)

Cell monolayers at approximately 90% confluency in 6-well dishes were washed in PBS before addition of 500 μl Trizol (Invitrogen) per well. Cells were incubated for 5 minutes at room temperature before being transferred to a microcentrifuge tube. Chloroform (200 μl) was added to the sample, vigorously mixed then centrifuged at 13,000 g for 15 minutes at 4 °C. The upper aqueous layer of the supernatant was transferred to a new microcentrifuge tube, 200 μl chloroform was added and the sample was centrifuged at 13,000 g for 10 minutes at 4 °C. The upper layer of the supernatant was transferred to a new microcentrifuge tube and 200 μl isopropanol was added. Following vigorous mixing the tube was incubated at room temperature for 10 minutes. The sample was centrifuged at 13,000 g for 10 minutes at 4 °C to pellet the RNA. Ethanol (70%) in diethyl pyrocarbonate-treated H_2O (DEPC-H_2O) (Invitrogen) was added without resuspending the pellet. The solution was centrifuged at 7,500 g for 10 minutes at 4 °C and the supernatant was removed. The sample was pulse-centrifuged to remove the remaining ethanol then the pellet was left to air dry for 20 minutes. The pellet was resuspended in 25 μl DEPC-H_2O. In order to remove contaminant DNA, five units of RNAse-free DNAse (Promega) were added to the sample along with 5x DNAse buffer in a total reaction volume of 50 μl. The

sample was incubated with the DNAse at 37 °C for 30 minutes before inactivation of the enzyme by incubation at 65 °C for 10 minutes. The RNA sample was stored at -80 °C.

2.2.3.2 Extraction of nuclear and cytoplasmic RNA

Cells were detached from 6-well plates by trypsin treatment (0.5 ml). Once cells had detached, they were neutralised with 0.5 ml complete DMEM. Following a PBS wash, cells were resuspended in 1 ml of ice-cold MLB supplemented with 1% protease inhibitor cocktail and incubated on ice for 30 minutes. Nuclei were pelleted at 10,000 g for 20 minutes at 4 °C. The supernatant (cytoplasmic fraction) was transferred to a new tube on ice and 800 µl Trizol was added. The nuclear pellet was resuspended in 500 µl Trizol. Samples were incubated at room temperature for 5 minutes. Samples were subject to Trizol-chloroform RNA extraction as detailed in Chapter 2.2.3.1.

2.2.4 Nucleic acid analysis

2.2.4.1 Quantification by spectrophotometry

Purified RNA was analysed using a Nanodrop 1000 spectrophotometer, with OD_{260}: OD_{280} ratios higher than 1.7 indicative of good quality RNA and lower values indicating protein contamination. OD_{260}: OD_{230} ratios were also taken, with 2.0 signifying pure RNA and lower values indicating contamination by phenol or other organic compounds.

2.2.4.2 Reverse-transcription (RT)

Reverse-transcription (RT) of RNA was conducted as detailed in the Roche Transcriptor First Strand cDNA Synthesis Kit manual (version April 2007) using random hexamer primers (Roche). In brief, random hexamer primers were added to 1 µg total RNA in a total reaction mix of 13 µl. The template primer mixture was subject to initial denaturation at 65 °C for 10 minutes in a thermal block cycler with a heated lid. The samples were cooled on ice before addition of the following components to a total reaction volume of 20 µl; 4 µl 5x Transcriptor Reverse Transcriptase Reaction Buffer, 0.5 µl Protector RNAse Inhibitor, 2 µl Deoxynucleoside Triphosphate (dNTPs) Mix (10 µm) and 0.5 µl Transcriptor Reverse Transcriptase (Roche). The tubes were placed in a thermal block cycler and incubated for 10 minutes at 25 °C followed by 1 hour at 50 °C to synthesise cDNA from mRNA.

2.2.4.3 Semi-quantitative PCR

Semi-quantitative PCR amplification of cDNA was performed using 1 µl cDNA in a reaction mix containing 2.5 µl of 1 µM custom-made primers (see Table 1), 0.5 µl dNTPs (10 µm), 0.125 µl Phusion DNA polymerase and 5x Standard High Fidelity (HF) buffer (Invitrogen) in a total

reaction volume of 25 μl. PCR reaction conditions were chosen according to the manufacturer's recommendations for Phusion polymerase with an annealing temperature of 60 °C.

2.2.4.4 Quantitative PCR (qPCR)

Quantitative PCR of cDNA was carried out using 1 μl cDNA in a reaction mix containing 2.5 μl of 1 μM custom primers, 7.5 μl SYBR Green PCR Master Mix (Qiagen) and 4 μl DEPC-H_2O. An initial 5 minute incubation at 95 °C was carried out to activate the HotStarTaq Plus DNA polymerase. Two-step cycling procedure was then performed on a Rotorgene 6000 cycler (Corbett) according to instructions in the Rotor-Gene SYBR Green Handbook (version July 2011) with an annealing temperature of 60 °C. Data was analysed using Rotorgene 6000 software (Corbett). Standard curves were produced for each set of primers. The average Ct value was determined from duplicate reactions and was normalised against the average Ct value obtained for the 'housekeeping' control transcript, GAPDH. The identities of the products obtained were confirmed by melting curve analysis.

2.2.4.5 Agarose gel electrophoresis

Agarose was dissolved in 1x TBE buffer to a final concentration of 0.8-2% (w/v) depending on the size of the DNA to be identified. Samples were loaded in Orange G loading buffer and 1/10,000 dilution of stock SYBR Green I (concentration not provided) (Sigma Aldrich), with a 1Kb$^+$ DNA ladder (Invitrogen) to determine approximate size. Electrophoresis was conducted at 100 V for approximately 1 hour in 1x TBE buffer.

2.2.5 Transfection using siRNA
2.2.5.1 Standard siRNA transfection

Cells were seeded in 6 well plates and grown to ~50% confluence in complete DMEM. Tubes A and B were made up; tube A containing the optimised amount of stock siRNA in 250 μl Optimem-1 and tube B containing 3 μl Lipofectamine-2000 in 250 μl Optimem-1. The tubes were left to stand at room temperature for 10 minutes before addition of tube B to tube A, producing tube AB. Tube AB was incubated at room temperature for 30 minutes before addition to the wells. After 4 hours the media was replaced with complete DMEM. Cells were incubated at 37 °C for 24 hours.

2.2.5.2 Reverse siRNA transfection

Stock siRNA was diluted to 1 μM in Optimem-1 and 5 μl was added to each well of a 96-well tissue culture plate. An eppendorf tube containing 0.2 μl Lipofectamine 2000 and 15 μl Optimem-1 was prepared and incubated at room temperature for 5 minutes. The contents of the tube were then added to the well and the plate was incubated for 30 minutes at room

temperature with occasional agitation. Cells (80 μl of 2.5 x 10^4 cells/ml) were then added to each well. Cells were incubated for 6 hours to allow adherence to the well. The medium was then exchanged for complete DMEM and cells were incubated for a further 18 hours.

2.2.6   Virus infection

2.2.6.1   Standard infection

Cells were seeded in 6-well plates and grown to approximately 80% confluence in complete DMEM. Adenovirus was diluted in 1 ml DMEM and, unless otherwise stated, was adsorbed to the cells at a multiplicity of infection (MOI) of 5 FFU/cell. After 1 hour, 1 ml of complete DMEM was added to each well. The cells were incubated at 37 °C in a humidified atmosphere containing 5% CO_2.

For treatment with cytosine arabinoside (AraC), 20 μg/ml was added at the same time as virus infection. Cells were then incubated for 24 hours before harvesting. For treatment with cycloheximide (CHX), 30 μg/ml was added at 12 h.p.i with Ad5 and cells were incubated with the CHX-containing medium for 6 hours. Cells were harvested at 24 h.p.i.

2.2.6.2   Second-round infection (virus yield assay)

Ad5-infected cells were treated with trypsin and once detached were neutralised in complete DMEM. Cells were pelleted at 350 g for 5 minutes at 4 °C. The supernatant was removed and cell pellets were frozen in liquid nitrogen, thawed in warm water and sonicated in a bath-type sonicator. The freeze-thaw-sonicate process was repeated twice. The cell suspension was made up to 250 μl with DMEM. A ten-fold dilution series was constructed to a final dilution of 10^{-5}. A set of positive controls comprising ten-fold dilutions of Ad5 virus stock was also prepared. A 100 μl aliquot of each dilution was then added to 1 ml DMEM before addition to the cells.

2.2.7   Indirect immunofluorescence

Cells were grown to sub-confluence on coverslips in 6 well plates prior to infection or transfection and then incubated at 37 °C for 24 or 48 hours. Cells were washed three times in PBS prior to fixation for 10 minutes in 10% formalin. Cells were washed three times in PBS before permeabilisation with 0.1% (v/v) Triton X-100 in PBS for 10 minutes at room temperature. Cells were washed three times in PBS before blocking in 10% (v/v) NGS in PBS for 20 minutes. Cells were washed three times in PBS before being incubated with 200 μl of primary antibody (diluted in 0.1% Triton X-100, 1% NGS in PBS) for 1 hour at room temperature. Cells were washed three times in PBS before being incubated with the appropriate secondary Alexa-Fluor conjugate antibody for 30 minutes in the dark. Cells were washed three times in PBS. Cell nuclei were stained by incubating with 4', 6-diamidino-2-phenylindole

(DAPI) (Sigma Aldrich) in PBS for 2 minutes before washing three times with PBS. Coverslips were mounted on slides using Vectashield mounting medium. Confocal microscopy was performed using an inverted LSM510 confocal microscope (Zeiss) coupled to LSM Image Browser (Zeiss). All images are single confocal sections of 0.8 μm. The same exposures were used throughout any one experiment. Different exposures were used between different experiments.

2.2.8 Flow cytometry

Cells were detached from 6-well plates by trypsin treatment (0.5 ml). Once detached, cells were neutralised with 0.5 ml complete DMEM. The samples were transferred to an eppendorf tube and cells were pelleted by centrifugation (all centrifugation steps were conducted at 350 g for 4 minutes at 4 °C. Supernatant was removed and the cells were resuspended in 200 μl of 10% formalin. The samples were incubated at room temperature for 10 minutes then cells were pelleted by centrifugation. The supernatant was removed and the cells resuspended in 200 μl 1% Triton X-100 in PBS and incubated at room temperature for 5 minutes. Cells were pelleted by centrifugation before resuspension in 10% NGS in PBS. The sample was subsequently divided into two eppendorf tubes, each containing 100 μl and labelled tube 1 and tube 2. Samples were incubated at room temperature for 10 minutes. Samples were pelleted and the supernatant removed. Tube 1 cells were resuspended in 50 μl of primary antibody diluted in 1% NGS, 0.1% Triton X-100 in PBS while tube 2 cells were resuspended in 50 μl of isotype-matched control antibody in 1% NGS, 0.1% Triton X-100 in PBS. Cells were incubated for one hour at room temperature. Cells were then pelleted by centrifugation and the supernatant was removed. Cells were resuspended in 50 μl of the appropriate Alexa Fluor-488-labelled secondary fluorescent conjugate antibody in 1% NGS, 0.1% Triton-X-100 in PBS and incubated for 30 minutes at room temperature in the dark. Cells were pelleted by centrifugation and the supernatant was removed. The cells were resuspended in 200 μl PBS and kept on ice in the dark until running on a Fortessa flow cytometer (BD Biosciences). A total of 10,000 cells were analysed in each sample and the geometric mean fluorescence of the whole cell population was calculated using FlowJo software (TreeStar Inc.).

2.2.9 MTT assay

Stock (5 mg/ml in PBS) 3-(4, 5-Dimethylthiazol-2-yl)-2, 5-diphenyltetrazolium bromide (MTT) (Sigma Aldrich) was diluted to 2.5 mg/ml in complete DMEM and 40 μl was added to each well of a 96-well plate. Cells were incubated for 4 hours at 37 °C. The medium was removed and cells were washed in PBS. In living cells, the yellow tetrazole MTT was reduced to insoluble purple formazan dye which was subsequently solubilised using 200 μl stock DMSO (Sigma Aldrich) (Carmichael *et al.*, 1987). Cells were incubated at room temperature in the dark with

agitation for 10 minutes. The coloured solution was quantified using a spectrophotometer reading at 570 nm. A reading was also taken at 620 nm to account for background.

2.2.10 Plaque assay

Virus dilutions were prepared from infected cell lysate as described in Chapter 2.2.6.2. At 4 h.p.i, carboxylmethylcellulose (CMC) (1.6% in PBS) was diluted 1:2 in complete DMEM and 2 ml was added to each well of a 6-well plate. Cells were then incubated for 6 days at 37 °C and 5% CO_2. Wells were washed in PBS before fixation in 1% gluteraldehyde in PBS for 10 minutes. Cells were washed in PBS before addition of crystal violet (0.05% (w/v) crystal violet, 20% ethanol, 80% SQ water) and incubated at room temperature for 10 minutes. The crystal violet was then washed off and the plaques were counted.

2.2.11 Production of wild type viruses

2.2.11.1 Propagation of wild type viruses

Wild type Ad12 virus was propagated in the A549 cell line. Wild type Ad5 virus was propagated in the HeLa cell line. Wildtype Ad3 virus was a kind gift from Kathryn Hall (Leeds Institute of Molecular Medicine, Leeds).

To propagate adenovirus, a T175 cell culture flask containing monolayer cells at approximately 90% confluency was infected with Ad5 or Ad12 virus at an MOI of 1 as described in Chapter 2.2.6.1. Infected cells were incubated at 37 °C and 5% CO_2 for three days or until cytopathic effect was evident. Cells were pelleted at 1,500 g for 5 minutes at room temperature and the supernatant was discarded. Pellets were frozen in liquid nitrogen, thawed in warm water then sonicated for 45 seconds in a bath type sonicator and this process was repeated twice. The cell pellet was split between five T175 cell culture flasks each containing cell monolayers of approximately 90% confluency. This process was repeated until pellets from 30 T175 flasks were obtained. Pellets were stored at -80 °C.

2.2.11.2 Virus purification

Viruses were purified using the caesium chloride (CsCl) density centrifugation method as previously described (Tollefson *et al.*, 1999). Infected cell pellets from 30 T175 flasks were frozen in liquid nitrogen, thawed in warm water and sonicated for 45 seconds in a bath type sonicator; this process was repeated twice. Pellets were combined and resuspended in 10 ml of sterile 0.1 M Tris-HCl (pH 8.0). To this, 1 ml of 5% (w/v) sodium deoxycholate (DOC) was added, mixed and incubated at room temperature for 30 minutes or until viscous. Aliquots of 100 μl of 2 M $mgCl_2$ and 50 μl of DNase 1 (10 mg/ml) solutions were added and the solution was incubated at 37 °C for 30 minutes with mixing every 10 minutes until the viscosity

decreased. The virus lysate was centrifuged at 3,000 rpm for 15 minutes at 4 °C. The supernatant was transferred to a clean tube and stored on ice. CsCl gradients for each 5 ml of clarified virus lysate were set up in SW40 ultraclear Beckman tubes using a kwill (NHS Supplies) to layer the lower density CsCl above the higher density CsCl as follows: 1 ml of 1.5 d CsCl (bottom), 2.5 ml 1.35 d CsCl, 2.5 ml 1.25 d CsCl (top). Virus lysate (5 ml) was layered on top of the gradients and 0.1 M Tris-HCl (pH 8.0) was used to balance. The gradients were centrifuged in a SW40 rotor in a Beckman (L5-50B) centrifuge at 35,000 rpm for 1 hour at 10 °C at the slowest acceleration and deceleration settings. The virus band located at the 1.35/1.25 d interface was collected by aspiration from the two tubes. The virus band was layered on top of 2 ml 1.35 d CsCl in a SW55 centrifuge tube, diluting with 0.1 M Tris-HCl (pH 8.0) to achieve layering if required. Samples were centrifuged in a Beckman (L5-50B) centrifuge in a SW40 rotor at 35,000 rpm for 15 hours at 4 °C at minimum acceleration without braking. Infectious whole virus particles were present as the lower of two visible bands; both bands were collected. The CsCl was then removed from the purified virus by extensive dialysis against 3 changes of 10 mM HEPES-KOH buffer (pH 8.0) using a Slide-a-Lyser dialysis cassette 3500MWCO over the course of a day at 4 °C. Sterile glycerol was added to the virus preparation at a 10% (v/v) ratio. The virus preparation was divided into 10 μl aliquots and stored at -80 °C.

2.2.11.3 Virus quantification

2.2.11.3.1 Virus particles per ml (vp/ml)

Virus stocks were diluted 1:10 in TE buffer containing 0.1% (v/v) SDS. The solution was incubated for 5 minutes at 50 °C before determination of the OD_{260}. Virus particles per ml (vp/ml) were calculated according to the following equation (Maizel *et al.*, 1968):

$$1 \text{ unit } A_{260} = 1.1 \times 10^{12} \text{ vp/ml} \times \text{dilution factor}$$

2.2.11.3.2 Focus-forming units per ml (FFU/ml)

A549 cells were grown to confluency in 6 well plates. Virus preparations were serially diluted 10^{-2} to 10^{-6} in 1 ml DMEM. The dilutions were then added to the wells and incubated for 1 hour at 37 °C. Complete DMEM (1 ml) was then added to each well and the samples were incubated for 24 hours. Samples were then subject to flow cytometry (see Chapter 2.2.8) using mouse anti-hexon or mouse isotype control antibodies. The dilution that gave around 50% FITC-positive cells is then used to calculate the FFU/ml using the following equation:

$$\text{FFU/ml} = \% \text{ positive (as a fraction)} \times \text{dilution factor} \times \text{number of cells in sample } (6 \times 10^{5}).$$

Chapter 3 – Defining the redistribution of Cajal body proteins during Ad5 infection

3.1 Introduction

Cajal bodies (CBs) are highly multifunctional nuclear subdomains which contain numerous proteins including coilin, fibrillarin, snRNPs, SMN and WRAP53 (Raska *et al.*, 1990; Carvalho *et al.*, 1999; Mahmoudi *et al.*, 2010). During Ad5 infection, coilin and fibrillarin are redistributed into numerous microfoci termed 'rosettes' (Rebelo *et al.*, 1996; Rodrigues *et al.*, 1996; James *et al.*, 2010). In contrast, snRNPs are redistributed into ring-shaped structures in the nucleoplasm (demarking regions of active splicing and transcription), before accumulating in enlarged interchromatin granules at late stages of infection (Rebelo *et al.*, 1996; Rodrigues *et al.*, 1996; Bridge *et al.*, 2003). As snRNPs no longer locate to CBs following Ad5 infection, this indicates that snRNP trafficking and/or assembly in CBs may be abrogated during Ad5 infection. It has been previously shown that the location of snRNPs in CBs is dependent on the snRNP trafficking proteins, WRAP53 and SMN (Girard *et al.*, 2006; Mahmoudi *et al.*, 2010). However, the subcellular location of WRAP53 and SMN following Ad5 infection is currently unknown. To further define the impact of Ad5 infection on CB proteins, this chapter will address the subcellular distribution of SMN and WRAP53 following Ad5 infection. To address the potential function of CB proteins during infection, their redistribution will be defined by immunofluorescence microscopy relative to markers of other nuclear substructures including PML-NBs, nucleoli, splicing factors, viral DNA replication centres and sites of virus assembly.

Defining the time point at which a cellular protein is redistributed can aid with identification of potential viral proteins responsible for redistribution of the cellular protein. In addition, defining the time point at which a cellular protein is redistributed may also aid in characterising the role of the protein during infection. The time point at which CB proteins are redistributed from CBs will also be addressed by confocal microscopy utilising inhibitors of DNA replication and protein translation as well as virus marker proteins for certain stages of infection.

The redistribution of CBs during Ad5 infection has previously been characterised only in the HPV-18 transformed cervical cancer cell line, HeLa (James *et al.*, 2010; Rebelo *et al.*, 1996; Rodrigues *et al.*, 1996). Considering the natural infection by Species C Ads is respiratory tract epithelium (Schmitz *et al.*, 1983), this chapter will investigate the redistribution of CBs in the respiratory epithelial cell line, A549, before extending the study to primary cells. Finally, the disassembly of CBs has to date only been characterised in terms of species C Ad5 infection (James *et al.*, 2010; Rebelo *et al.*, 1996; Rodrigues *et al.*, 1996). To establish whether the redistribution of CBs is specific to species C Ad infection or conserved across Ad species, CB redistribution will also be investigated following infection with species B virus Ad3 and species A virus Ad12.

3.2 Impact of Ad5 infection on the cellular levels of CB proteins

In order to study the redistribution of CBs during Ad5 infection, the time between initial infection and host cell lysis in the cell line of choice must firstly be established. Marker proteins of early and late phase infection can also allow identification of the time points at which early and late phase infection commence. A549 cells were chosen as the cell line in which to study Ad5 infection as they are derived from respiratory epithelial cells, which are the cellular target for natural species C Ad infection *in vivo* (Schmitz *et al.*, 1983). From extensive review of the literature, the general consensus for virus titre when studying Ad infection of cell lines appears to be an MOI of 1-10 FFU/cell. Therefore an intermediate MOI of 5 was chosen for this study.

For western blotting analysis of Ad protein levels across a time course of infection, A549 cells were mock or Ad5 infected (Chapter 2.2.6.1) and cells were harvested at 0, 4, 8, 12, 16, 24 and 48 h.p.i. The final time point to be harvested was 48 h.p.i, as by this time there was evidence of cytopathic effect (CPE) in a substantial proportion of the Ad5-infected cells indicating that the cells were beginning to lyse (Hilleman and Werner, 1954; Rowe *et al.*, 1955). Protein from whole cell lysates were analysed by SDS-PAGE and Western blotting (Chapter 2.2.2), using an anti-E1A and an anti-penton base antibody as markers for early and late phase infection, respectively. Membranes were also incubated with an antibody raised against the cellular 'housekeeping' protein GAPDH as an internal loading control.

As shown in Figure 3-1, the level of GAPDH remained constant across the time course, indicating that Ad5 infection does not alter the levels of housekeeping proteins during infection. E1A 293R and 249R proteins were first detectable at 8 h.p.i, consistent with their known immediate early expression (Berk and Sharp, 1978; Nevins *et al.*, 1979). At 24 h.p.i, penton base was first detected, with increased expression at 48 h.p.i. This indicates that in A549 cells at an MOI of 5, the immediate early protein E1A and late protein penton base are first detectable at 4-8 h.p.i and 16-24 h.p.i, respectively.

The levels of CB proteins coilin, SMN, WRAP53, Sm (a component of all spliceosomal snRNPs) and fibrillarin were investigated over the time course. As shown in Figure 3-1, the protein levels of SMN, Sm and fibrillarin remained constant across the time course. Although the cellular levels of coilin and WRAP53 appeared to stay stable up until 24 h.p.i, there was an apparent decrease in coilin and WRAP53 levels by 48 h.p.i (Figure 3-1). Quantification of changes in CB protein levels was carried out by densitometric analyses of the protein band signal intensities (Figure 3-2). No significant alterations in protein levels were observed across the time course for SMN, Sm or fibrillarin, indicating that the levels of these proteins are not altered during the course of Ad5 infection. In contrast, the protein levels of both coilin and
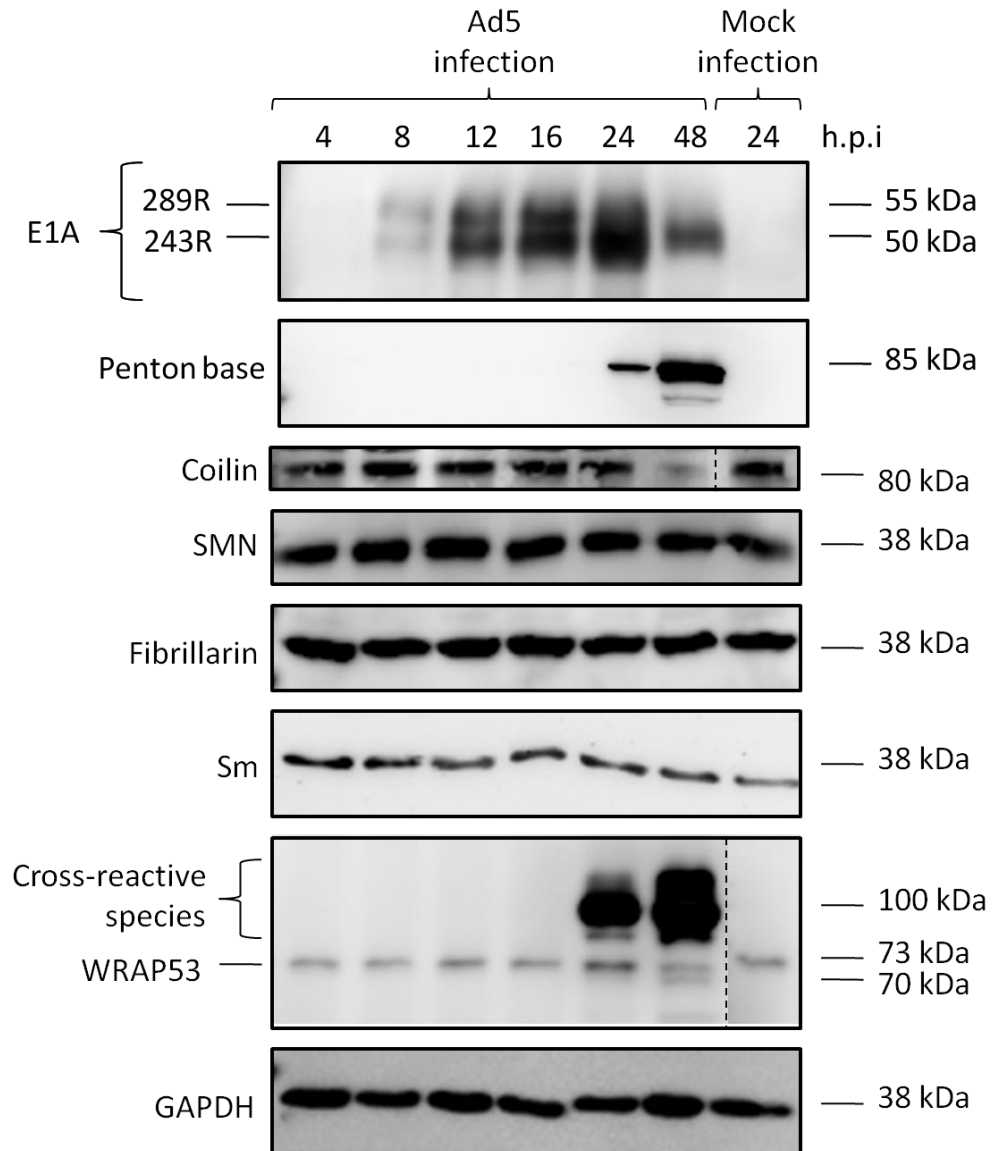
Figure 3-1. Ad5 and CB protein levels over a time course of Ad5 infection in A549 cells.
A549 cells were mock or Ad5 infected and incubated for 4, 8, 12, 16, 24 or 48 hours. Cell lysates were prepared and equal masses of protein from each sample (20 μg) were separated by SDS-PAGE and analysed by Western blotting. Bound antibody was detected using the ECL system and images were captured using a LAS 3000 imager. GAPDH was used as a loading control. During the time course of Ad5 infection, Ad5 E1A proteins 289R and 243R were first detected at 8 h.p.i and penton base was first detected at 24 h.p.i. Levels of SMN, Sm and fibrillarin stayed constant during the time course whilst levels of coilin and WRAP53 were decreased at 48 h.p.i. The lanes corresponding to the mock-infected samples for WRAP53 and coilin were moved from the same exposure on the same gel in order to align with the other panels (as indicated by the dashed lines). The anti-WRAP53 antibody exhibited cross-reactivity with an unidentified protein of approximately 100 kDa. The anti-coilin antibody cross-reacted with an unidentified protein of approximately 65 kDa, which was cropped from the image in this instance. h.p.i – hours post-infection. R – residue. kDa – kilodaltons.
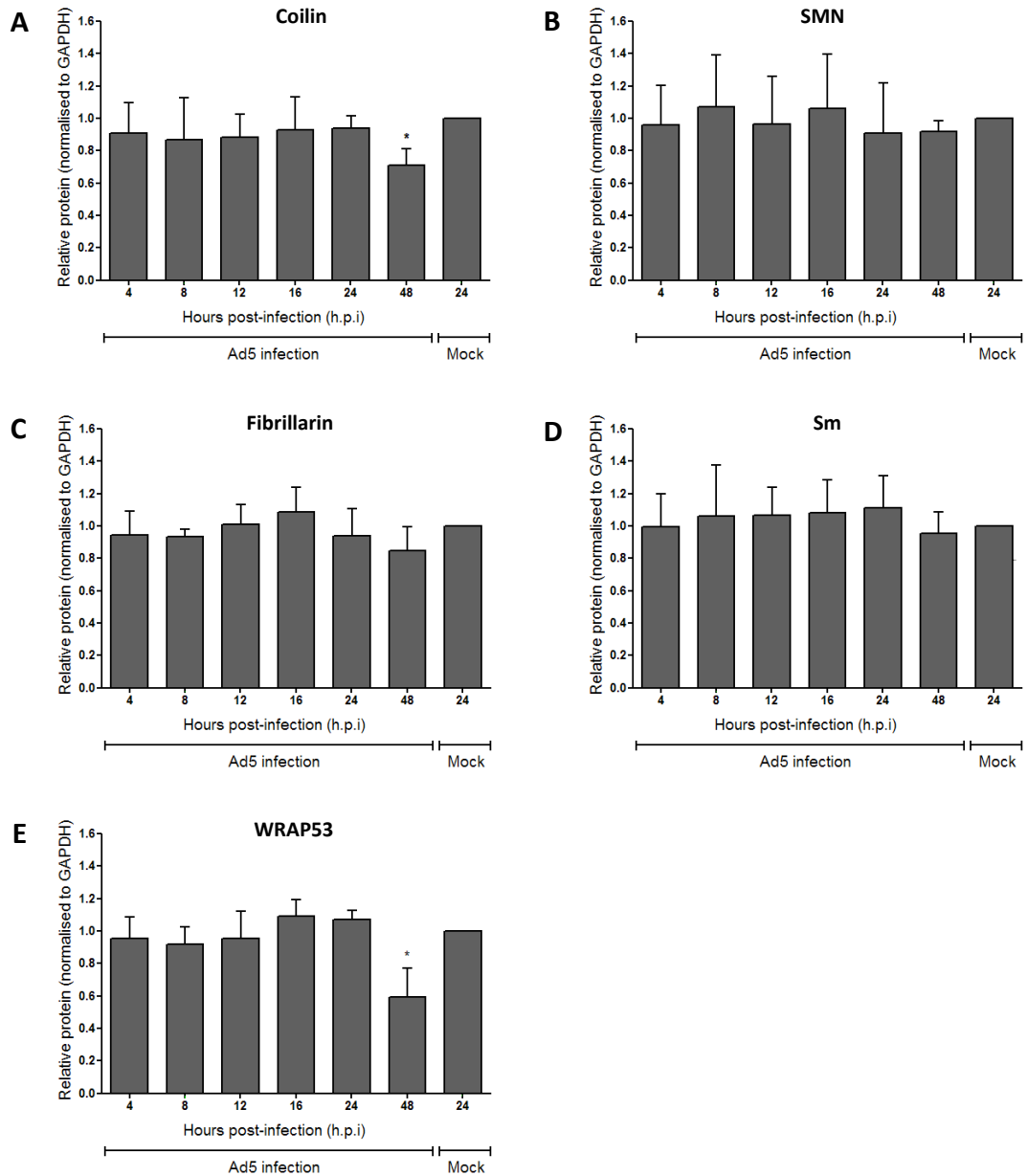
Figure 3-2. Densitometric analysis of CB protein levels over a time course of Ad5 infection.
Signal intensities from Western blots were calculated by densitometric analysis and were normalised to the signal intensity of the loading control, GAPDH. (i) coilin (ii) SMN (iii) fibrillarin (iv) Sm (v) WRAP53. Results are shown as the mean fold change in protein level ($\pm$ standard error of the mean [SEM]) from three independent experiments. Results are relative to 24 hours post-mock infection, which was set to a value of 1. All statistics were calculated using the paired 1-sample t-test. Protein levels of SMN, fibrillarin and Sm remained constant during the Ad5 infection time course, whereas WRAP53 and coilin were reduced at 48 h.p.i. * $p < 0.05$.

WRAP53 were significantly reduced by 48 h.p.i (p < 0.05) (Figure 3-2, A and E). This indicated that coilin and WRAP53 may be degraded at a late stage of Ad5 infection.

As shown in Figure 3-1, there was a strong cross reaction of the WRAP53 antibody with an unidentified protein of around 100 kDa. As this cross-reacting protein appeared to be absent from cell lysates until 24 h.p.i, this indicated that it is likely to be a late-expressed Ad protein. Therefore an Ad protein in its denatured form may share some structural homology with denatured WRAP53. Alternatively, the non-specific band may correspond to a cellular protein that is normally not expressed in A549 cells but whose expression is greatly induced upon Ad infection.

3.3 Analysis of CB redistribution in Ad5-infected A549 cells by immunofluorescence microscopy

3.3.1   A time course of coilin redistribution in Ad5-infected A549 cells

Having established the kinetics of Ad5 infection in A549 cells, the most appropriate time point to study the redistribution of CBs during Ad5 infection was investigated by indirect immunofluorescence microscopy. Previous work showed that the redistribution of coilin from CBs occurred after Ad DNA replication (James *et al.*, 2010). Ad DNA replication has been estimated to commence at around 8 h.p.i, with late phase protein expression reaching a peak at 18 h.p.i (Akusjarvi, 2008). Therefore in order to span the intermediate and late phases of infection, the following time points were chosen for immunofluorescence analysis of CB redistribution; 0, 12, 18, 24 and 48 h.p.i. A549 cells were mock or Ad5 infected (Chapter 2.2.6.1) before fixation at the appropriate time post-infection. Cells were subject to indirect immunofluorescence (Chapter 2.2.7), using an anti-coilin antibody as a marker of CBs and an anti-E1A antibody as a marker of Ad5-infected cells.

As shown in Figure 3-3, there were three distinct distributions of coilin during the infection time course. At 12 h.p.i, the prominent CB distribution evident in Ad5-infected cells (as depicted by positive E1A staining [green]) was indistinguishable from the CB distribution found in mock-infected cells; 1-6 punctate domains per cell (image g, arrow). By 24 h.p.i with Ad5, approximately 90% of cells exhibited positive E1A staining. In addition, at this time point the majority of Ad5-infected cells exhibited CBs which had been disassembled into rosettes (image k, arrow) as previously described (James *et al.*, 2010). By 48 h.p.i, the majority of Ad5-infected cells exhibited microfoci that were distributed evenly throughout the nucleoplasm rather than the discrete ring structures characteristic of rosettes; this distribution was termed 'speckled' (image o, arrow). Importantly, all cells exhibiting CB redistribution, either rosette or speckled,

	Nucleus	E1A	Coilin	Overlay
Mock 24 h.p.i	a	b	c	d
Ad5 12 h.p.i	e	f	g	h
Ad5 24 h.p.i	i	j	k	l
Ad5 48 h.p.i	m	n	o	p
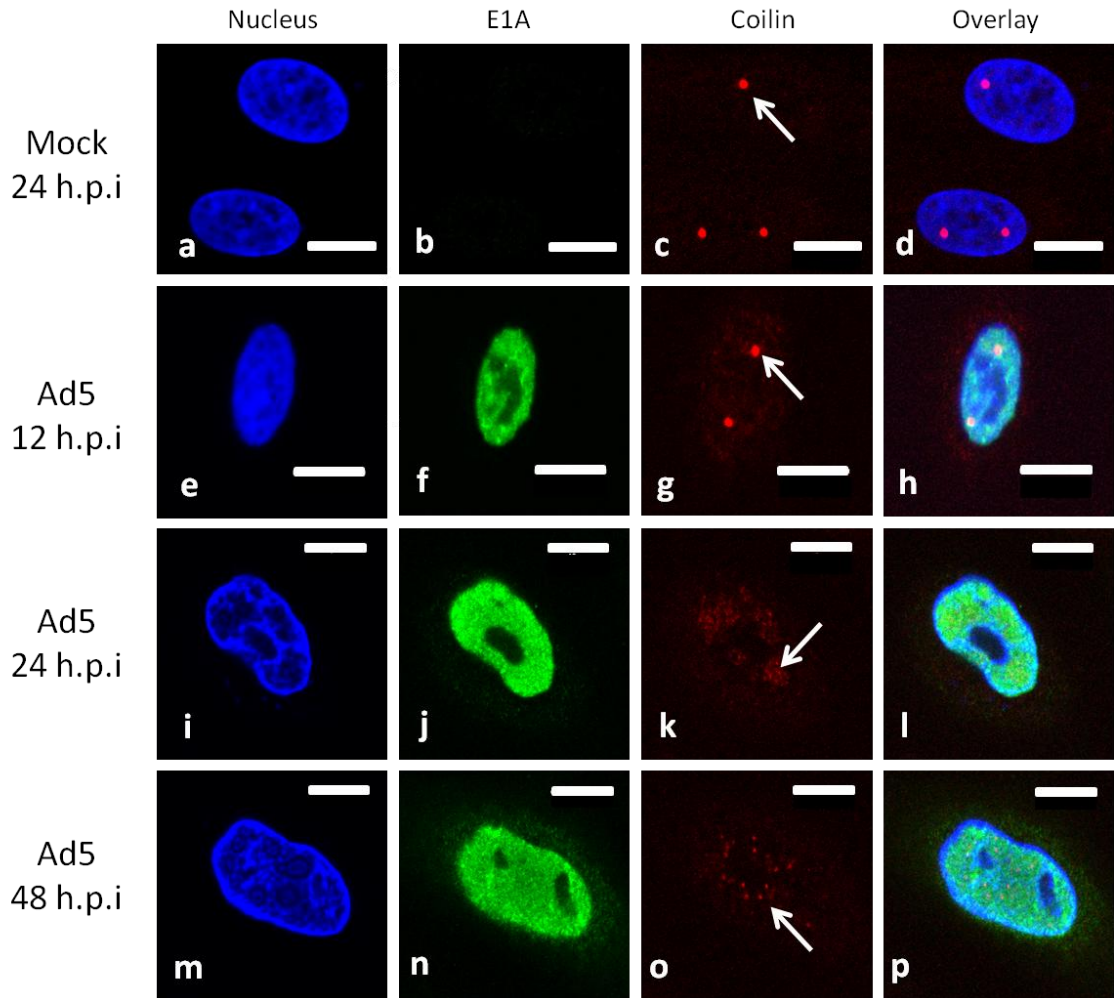
Figure 3-3. The redistribution of coilin during Ad5 infection of A549 cells.

A549 cells were mock or Ad5 infected at an MOI of 5 FFU/cell and incubated for 0, 12, 18, 24 or 48 hours. Cells were fixed and subjected to indirect immunofluorescence using a mouse anti-coilin and a rabbit anti-E1A antibody followed by incubation with the appropriate fluorescent-labelled secondary antibodies. Nuclei were stained using DAPI. Confocal microscopy was performed using an inverted LSM510 confocal microscope coupled to LSM Image Browser. In mock-infected cells, coilin remained within large punctate Cajal bodies (CBs) for the duration of the time course (image c, arrow). By 12 h.p.i with Ad5, the majority of cells were positive for the Ad5 early marker protein E1A (image f) indicating that they were infected. At this time the cells exhibited a punctate distribution of coilin (image g, white arrow) that was indistinguishable from that seen in mock-infected cells (image c, arrow). By 24 h.p.i, the majority of Ad5-infected cells exhibited a redistribution of coilin into microfoci arranged into clusters (image k, arrow). By 48 h.p.i, the majority of Ad5-infected cells exhibited coilin microfoci that were distributed evenly throughout the nucleoplasm (image o, arrow). These data indicated that CBs undergo a stepwise dismantling during Ad5 infection. Bars = 10 μm.
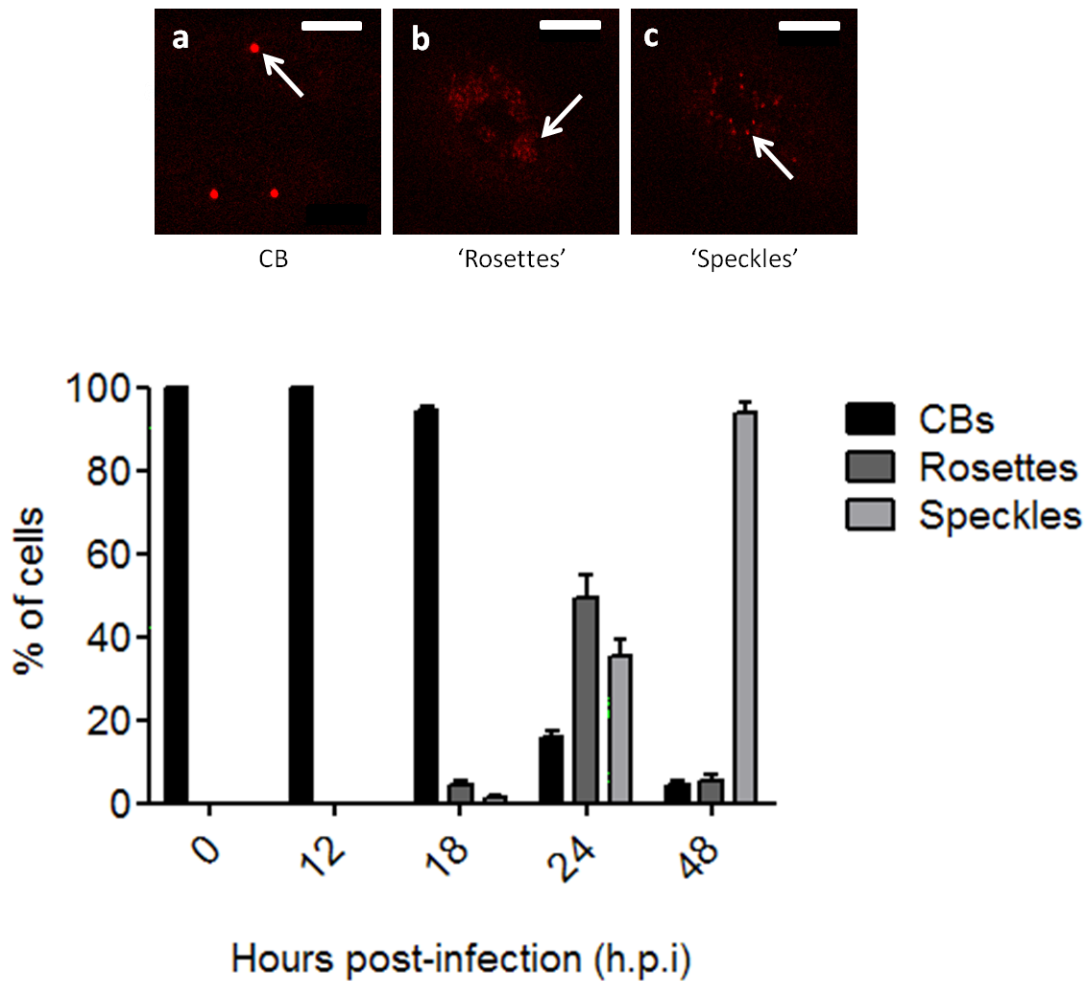
Figure 3-4. The temporal appearance of Cajal body (CB), rosette and speckle distributions of coilin during Ad5 infection of A549 cells.

A549 cells were mock or Ad5 infected at an MOI of 5 FFU/cell and incubated for 0, 12, 18, 24 or 48 hours. Cells were fixed and subjected to indirect immunofluorescence using a mouse anti-coilin and a rabbit anti-E1A antibody followed by incubation with the appropriate fluorescent-labelled secondary antibodies. Nuclei were stained using DAPI. Confocal microscopy was performed using an inverted LSM510 confocal microscope coupled to LSM Image Browser. At early stages of infection, large punctate CBs were evident in Ad5-infected cells (image a, arrow) that were indistinguishable from CBs in uninfected cells. As infection progressed from 18-24 h.p.i, coilin was redistributed into microfoci arranged into clusters (image b, white arrow), termed 'rosettes'. At late stages of infection (24-48 h.p.i) the coilin microfoci were distributed evenly throughout the nucleoplasm (image c, arrow), termed 'speckles'. Over the time course of Ad5 infection, three fields of 100 cells from each coverslip were analysed for their coilin distribution and categorised as CB, 'rosette' or 'speckles'. Results are shown as the mean percentage of cells (± SEM) from three independent experiments. These data indicated that during Ad5 infection, CBs are disassembled into rosettes at a late stage of infection (18-24 h.p.i) prior to further disassembly into speckles at very late time points (24-48 h.p.i). Bars = 10 μm.

were positive for E1A. This indicated that CB redistribution occurred only in the Ad5-infected cells and was not simply a reaction by the cell to the presence of virus in the vicinity.

To quantify the redistribution of CBs during the infection time course, three fields of 100 cells from each coverslip were analysed for their coilin distribution (Figure 3-4). Cells were categorised as either CB (image a), 'rosettes' (image b) or 'speckles' (image c) and this experiment was repeated twice. Throughout the time course, the mock-infected cells retained 100% CB distribution. At 12 h.p.i, 100% of the Ad5-infected cells still exhibited intact CBs. However, at 18 h.p.i a small proportion (4.5%) of Ad5-infected cells exhibited CBs which had been reorganised into rosettes. As infection progressed to 24 h.p.i, the proportion of Ad5-infected cells positive for rosettes increased to 49.1%. By 48 h.p.i, the percentage of Ad5-infected cells exhibiting rosettes had decreased to 5.5% whilst 93.7% of cells were positive for coilin speckles. The peak in percentage of Ad5-infected cells positive for rosettes occurs at 24 h.p.i, whereas the peak for cells positive for speckles occurs much later in infection, at 48 h.p.i. This indicated that rosette structures are formed transiently during Ad infection and are disassembled into speckles late in infection. There was evidence of rosettes that had already disassembled into speckles at earlier times than 48 h.p.i, an observation consistent with the asynchrony of virus infection (Gama-Carvalho *et al.*, 2003a). As the peak in percentage of cells positive for CBs redistribution into rosettes was at 24 h.p.i, this was the time point chosen to study the redistribution of additional CB components.

3.3.2   Analysis of CB trafficking proteins SMN and WRAP53 during Ad5 infection by immunofluorescence microscopy

As snRNPs no longer locate to residual CB structures containing coilin in Ad5-infected cells (Bridge *et al.*, 1993a), this indicates that snRNP trafficking to CBs is impaired during Ad5-infection. The transport of snRNPs to CBs was recently shown to depend on the trafficking proteins WRAP53 and SMN (Mahmoudi *et al.*, 2010). However, the subcellular location of the snRNP trafficking proteins WRAP53 and SMN following Ad5 infection is unknown. To establish the impact of Ad5 infection on the subcellular distribution of WRAP53 and SMN, A549 cells were mock or Ad5 infected (Chapter 2.2.6.1). At 24 h.p.i, cells were fixed and subject to indirect immunofluorescence (Chapter 2.2.7).

As show in Figure 3-5, in mock-infected cells, coilin was located in punctate CBs (image b, arrow). WRAP53 was also concentrated in CBs (image c, arrow), as described previously (Mahmoudi *et al.*, 2010). WRAP53 and coilin colocalised in CBs as shown by the yellow regions in the overlay (image i, arrow). In Ad5-infected cells, WRAP53 was redistributed into microfoci (image g, arrow) and colocalised with coilin in rosettes as shown by the yellow
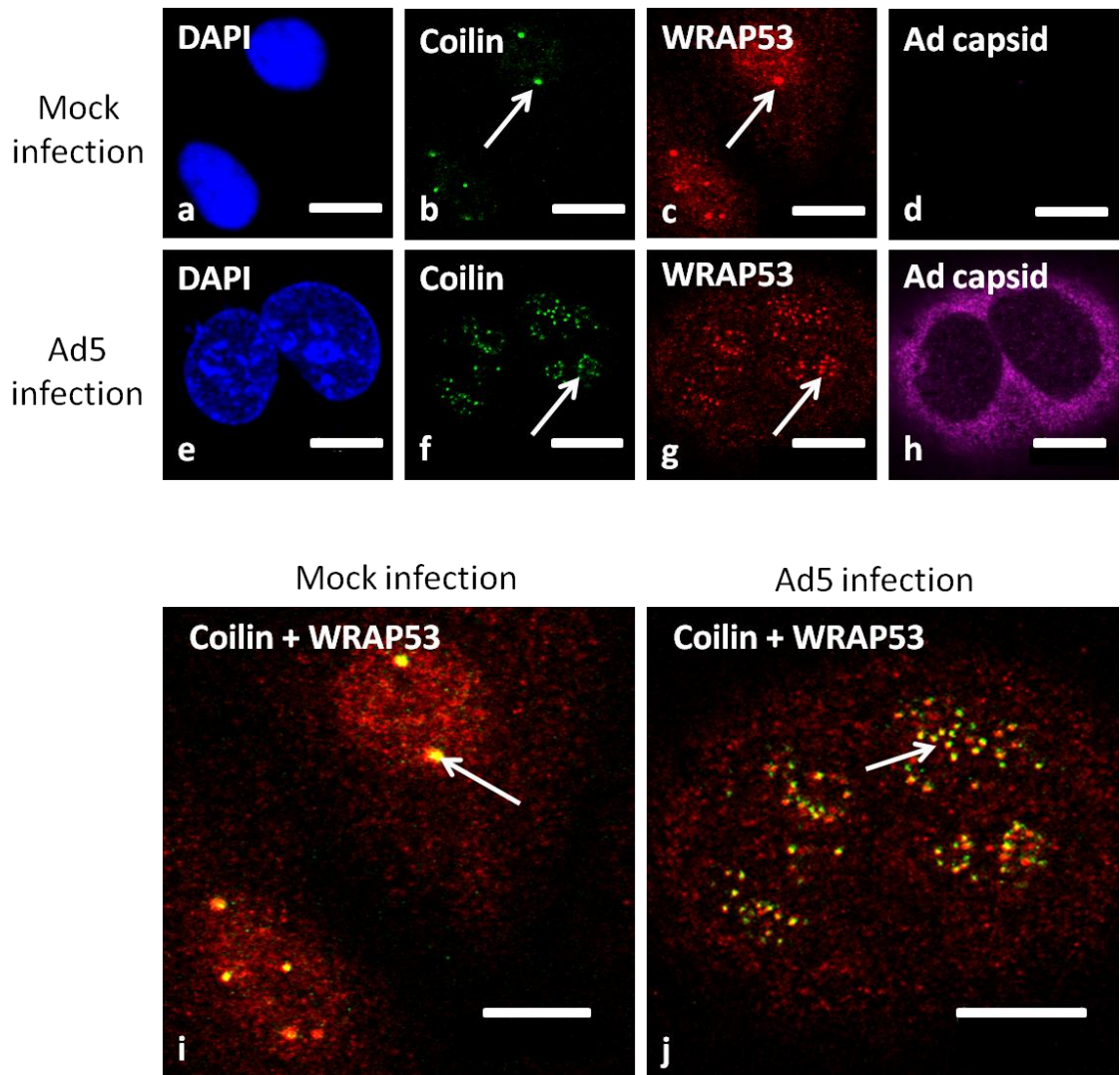
Figure 3-5. The redistribution of WRAP53 relative to coilin following Ad5 infection of A549 cells.
A549 cells were mock or Ad5 infected at an MOI of 5 FFU/cell and incubated for 24 hours. Cells were fixed and subjected to indirect immunofluorescence. Cells were incubated with a mouse anti-coilin, a rabbit anti-WRAP53 and a goat anti-Ad capsid antibody followed by incubation with the appropriate fluorescent-labelled secondary antibodies. Nuclei were stained using DAPI. Confocal microscopy was performed using an inverted LSM510 confocal microscope coupled to LSM Image Browser. In mock-infected cells, coilin (image b, arrow) and WRAP53 (image c, arrow) were found in punctate CBs and colocalised in these structures as shown by the yellow regions in the overlay (image i, arrow). In Ad5-infected cells, coilin (image f, arrow) and WRAP53 (image g, arrow) were both redistributed into microfoci arranged into clusters, The microfoci of coilin and WRAP53 partially colocalised, as shown by the yellow regions in the overlay (image j, arrow). Bars = 10 µm.
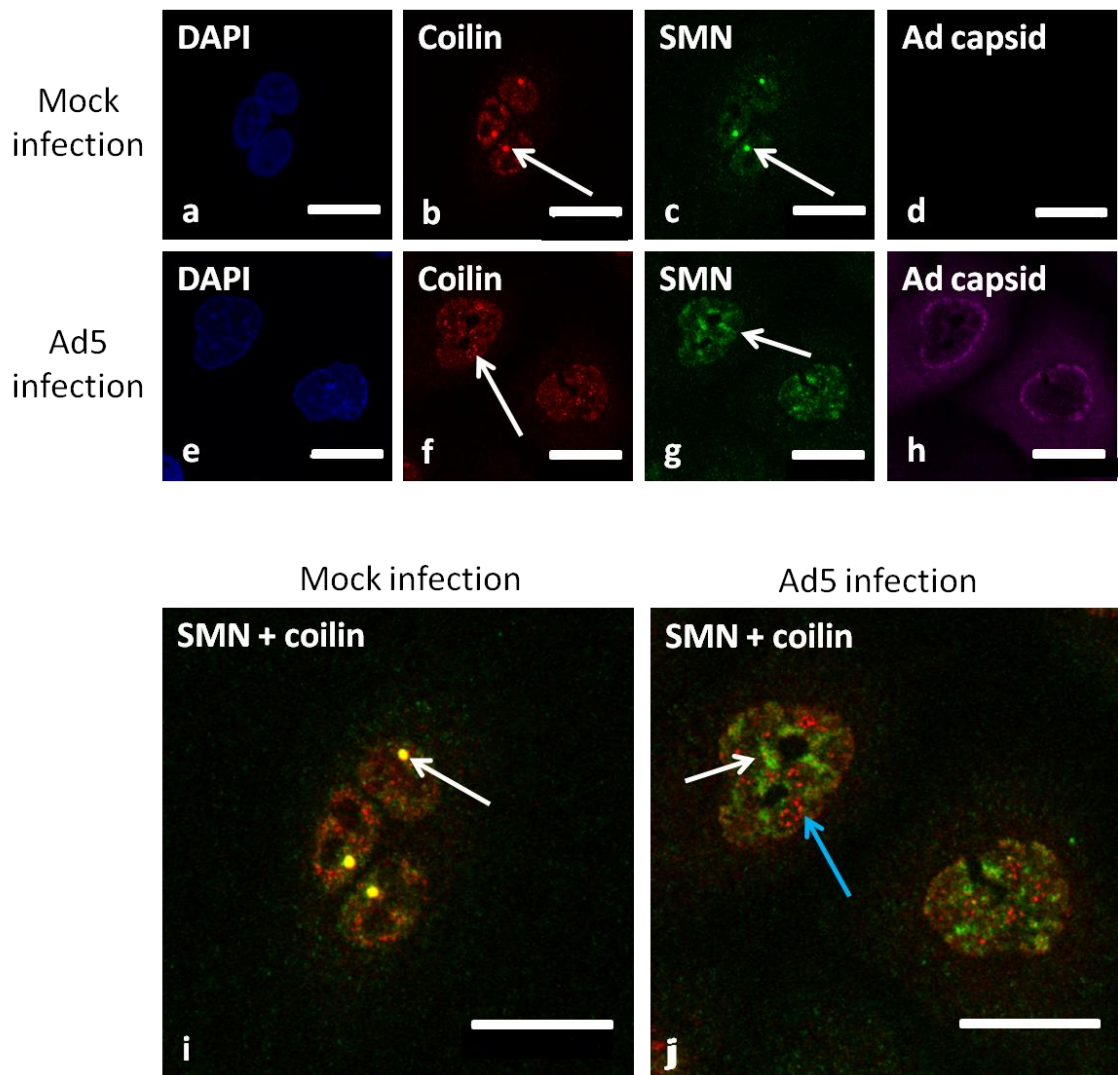
Figure 3-6. The redistribution of SMN relative to coilin following Ad5 infection of A549 cells.

A549 cells were mock or Ad5 infected at an MOI of 5 FFU/cell and incubated for 24 hours. Cells were fixed and subjected to indirect immunofluorescence. Cells were incubated with a mouse anti-SMN, a rabbit anti-coilin and a goat anti-Ad capsid antibody followed by incubation with the appropriate fluorescent-labelled secondary antibodies. Nuclei were stained using DAPI. Confocal microscopy was performed using an inverted LSM510 confocal microscope coupled to LSM Image Browser. In mock-infected cells, coilin (image b, arrow) and SMN (image c, arrow) were found in punctate CBs and colocalised in these structures as shown by the yellow regions in the overlay (image i, arrow). In Ad5-infected cells, coilin was redistributed into microfoci (image f, arrow) whilst SMN was redistributed into rod-shaped structures within the nucleus (image g, arrow). As shown in the overlay (image j), the rod-shaped structures of SMN (white arrow) did not colocalise with the coilin microfoci (blue arrow). Bars = 20 μm.

regions in the overlay (image j, arrow). This suggested that WRAP53 is a component of rosettes in Ad5-infected cells. It should be noted that the WRAP53 antibody exhibited a high degree of cross-reactivity in Western blotting analysis (Figure 3-1), therefore it is possible that some of the staining seen in immunofluorescence analysis may be due to recognition of the unidentified 100 kDa cross-reactive species by this antibody.

The subcellular distribution of SMN following Ad5 infection was also assessed. As shown in Figure 3-6, in mock-infected cells coilin was concentrated in CBs (image b, arrow) where it colocalised with SMN (image i, arrow), as previously documented (Hebert *et al.*, 2001; Mahmoudi *et al.*, 2010). In Ad5-infected cells, coilin was redistributed into microfoci (image f, arrow). Strikingly, in Ad5-infected cells, SMN was localised diffusely in the nucleoplasm and, in some cells, was concentrated in nucleoplasmic rod-shaped structures (image g, white arrow). There was no colocalisation between redistributed SMN (image j, white arrow) and coilin rosettes (image j, blue arrow). This indicated that SMN was redistributed to a domain separate from coilin, fibrillarin and WRAP53 during Ad5 infection.

3.3.3 The redistribution of SMN during Ad5 infection

To assess the disassembly of SMN from CBs over a time course of Ad5 infection, cells were mock or Ad5 infected (Chapter 2.2.6.1). At 0, 12, 18, 24 and 48 h.p.i, cells were fixed and subjected to indirect immunofluorescence (Chapter 2.2.7) using a mouse anti-SMN antibody along with a rabbit anti-E1A antibody as a marker of Ad5-infected cells.

As shown in Figure 3-7, Ad5-infected cells (as defined by positive E1A staining; image f) at 12 h.p.i exhibited a CB distribution of SMN (image g, arrow) were indistinguishable from CBs in uninfected cells (compare image c and image g). As infection progressed to 24 h.p.i, SMN was present diffusely in the nucleoplasm and in some stronger-staining nuclear structures in the majority of cells (image k, white arrow). This distribution of SMN was termed 'nucleoplasmic'. At 48 h.p.i, SMN staining appeared fainter than at earlier time points and SMN appeared to be distributed diffusely throughout the cell (image o, arrow); this distribution was termed 'diffuse/undetectable'. As Western blotting analysis indicated that the total cellular level of SMN was unchanged by 48 h.p.i (Chapter 3.2), this suggested that the reduced SMN staining at 48 h.p.i by immunofluorescence was not due to reduced levels of SMN protein. The reduced SMN staining at 48 h.p.i may be due to decreased accessibility of the antibody to its epitope; it is possible that there is an increased association of SMN with another protein during the late phase of Ad5 infection, causing masking of the antigenic site. Further investigation would be required to investigate these possibilities.
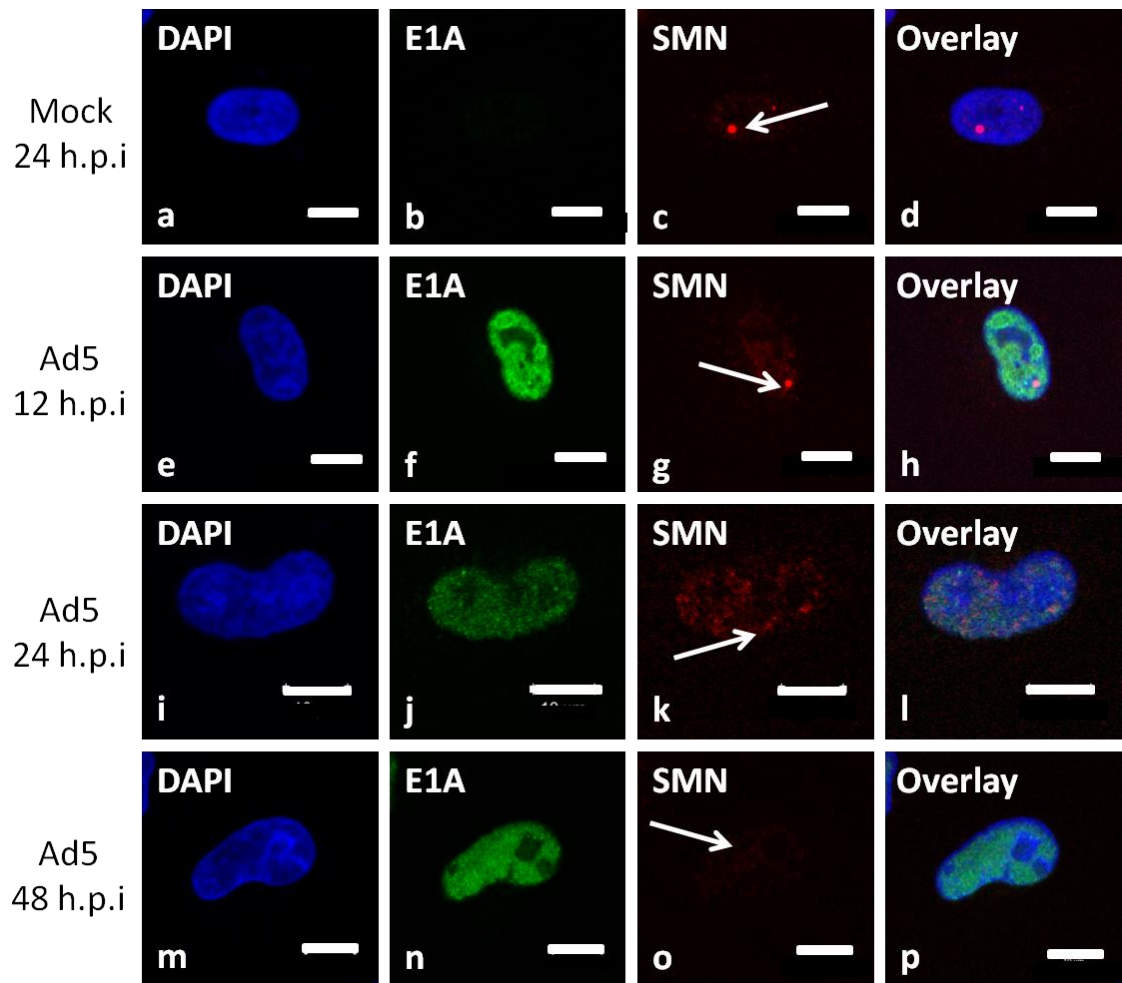
Figure 3-7. The redistribution of SMN during a time course of Ad5 infection in A549 cells.

A549 cells were mock or Ad5 infected at an MOI of 5 FFU/cell and incubated for 12, 24 or 48 hours. Cells were fixed and subjected to indirect immunofluorescence using a mouse anti-SMN and a rabbit anti-E1A antibody followed by incubation with the appropriate fluorescent-labelled secondary antibodies. Nuclei were stained using DAPI. Confocal microscopy was performed using an inverted LSM510 confocal microscope coupled to LSM Image Browser. In mock-infected cells, SMN remained within large punctate Cajal bodies (CBs) for the duration of the time course (image c, arrow). By 12 h.p.i with Ad5, the majority of cells were positive for the Ad5 early marker protein E1A (image f) indicating that they were infected. At this time the cells exhibited a punctate distribution of SMN (image g, white arrow) that was indistinguishable from that seen in mock-infected cells (image c, arrow). By 24 h.p.i, the majority of Ad5-infected cells exhibited a redistribution of SMN into the nucleoplasm and into stronger-staining structures within the nucleus (image k, arrow). By 48 h.p.i, the majority of Ad5-infected cells exhibited low-level SMN staining (image o, arrow). Bars = 10 μm.
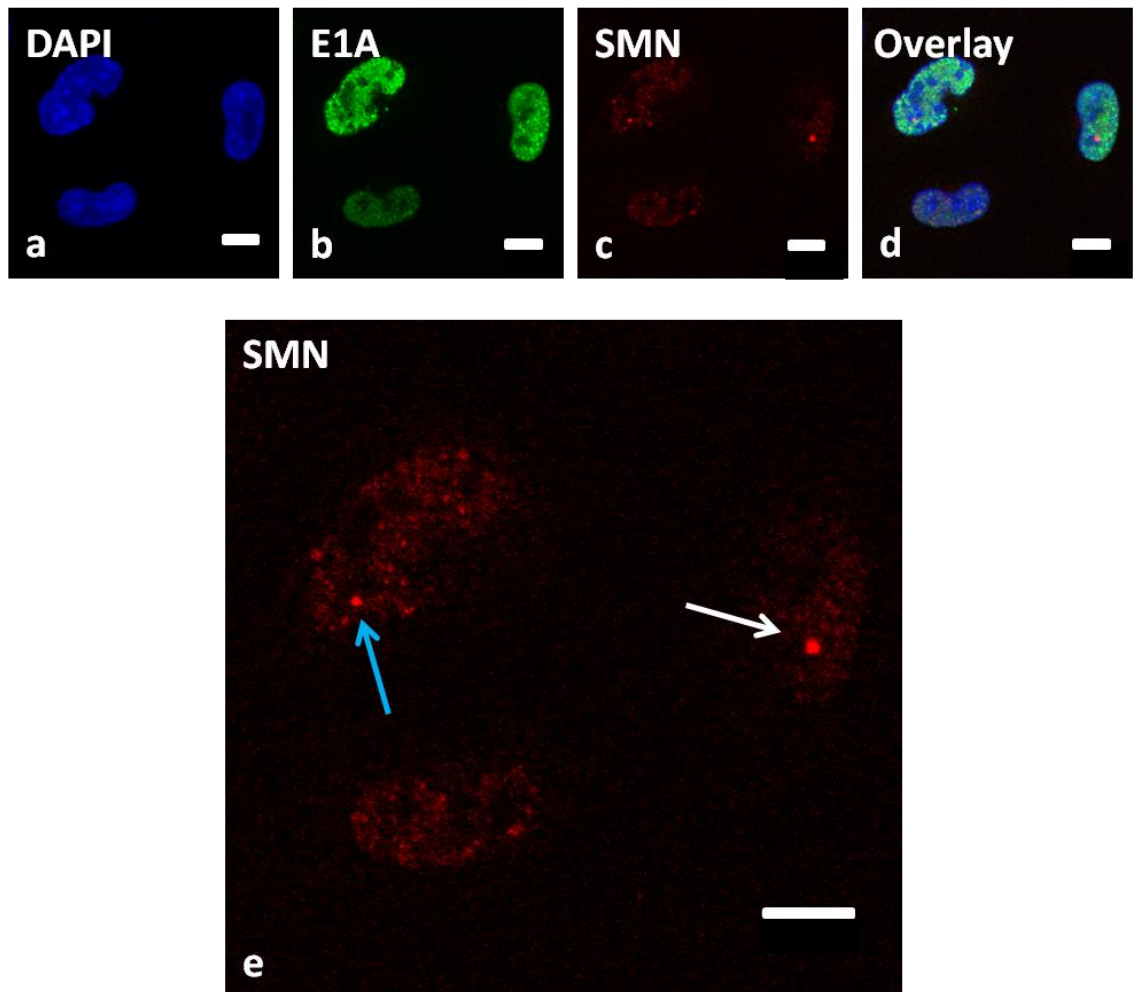
Figure 3-8. The temporal reduction in size of SMN foci during Ad5 infection of A549 cells.

A549 cells were mock or Ad5 infected at an MOI of 5 FFU/cell and incubated for 24 hours. Cells were fixed and subjected to indirect immunofluorescence using a mouse anti-SMN and a rabbit anti-E1A antibody followed by incubation with the appropriate fluorescent-labelled secondary antibodies. Nuclei were stained using DAPI. Confocal microscopy was performed using an inverted LSM510 confocal microscope coupled to LSM Image Browser. At 24 h.p.i, the majority of cells were positive for the Ad5 early marker protein E1A (image b) indicating that they were infected. In some Ad5-infected cells, CBs containing SMN were noticeably smaller (image e, blue arrow) than conventional CBs (image e, white arrow). Bars = 10 μm.

Interestingly, it was noted that CBs in some Ad5-infected cells were noticeably smaller than conventional CBs (Figure 3-8, image e; compare regular CB [white arrow] with small CB [blue arrow]). These 'small CBs' were only observed in the Ad5-infected cells and were not found in the mock infected cells, indicating that the reduction in CB size was a result of Ad5 infection. Furthermore, the occurrence of small CBs in Ad5-infected cells appeared to increase as the infection time course progressed. It is possible that as Ad5 infection progressed, SMN was released from CBs into the nucleoplasm, resulting in a gradual reduction in CB size. Further studies measuring CB diameters following Ad5 infection would be required to address this.

In order to quantify the disassembly of SMN from CBs over the time course of Ad5 infection, three fields of 100 cells from each time point were analysed for their SMN distribution (Figure 3-9). The distribution of SMN in cells was categorised as either 'CB' (image a, arrow), 'nucleoplasmic' (image b, arrow) or 'diffuse/undetectable' (image c, arrow). At 18 h.p.i, 19% of Ad5-infected cells exhibited nucleoplasmic SMN and this increased to a peak of 39% of cells by 24 h.p.i. At 48 h.p.i, only 5% of cells exhibited a nucleoplasmic distribution of SMN, indicating this was a transient SMN distribution during Ad5 infection. The diffuse/undetectable distribution of SMN appeared to be a late phase occurrence; the first appearance of this distribution was at 24 h.p.i (18% of cells) with increased prevalence at 48 h.p.i (95% of cells). This indicated that following Ad5 infection, SMN was released from CBs into the nucleoplasm prior to locating diffusely throughout the cell at very late stages of infection.

3.4 The rearrangement of CB proteins relative to other nuclear bodies and host factors

From the previous section it was shown that, following Ad5 infection, the CB proteins coilin and WRAP53 are redistributed to rosettes whilst SMN is redistributed to separate structures within the nucleoplasm. However, it is not known whether these CB proteins are redistributed to known sub-nuclear structures or to novel domains. Indeed, both coilin and SMN have previously been shown to interact with protein components of other nuclear bodies. SMN can form an RNAse-sensitive complex with the nucleolar proteins B23 and C23, and can directly interact with fibrillarin (Pellizzoni *et al.*, 2001a; Lefebvre *et al.*, 2002). Coilin is known to interact with the nucleolar protein Nopp140 (Isaac *et al.*, 1998) and PML-NB protein PIASγ (Sun *et al.*, 2005). Therefore it is possible that during Ad5 infection these proteins may become associated with other nuclear substructures. If so, identifying these associated nuclear bodies may give clues to the function of CB proteins during Ad5 infection. To this end, the redistribution of coilin and SMN was assessed relative to splicing factors, nucleoli, PML-NBs, Ad DNA replication centres and Ad virus assembly platforms.

CBs   Nucleoplasmic   Diffuse/undetectable
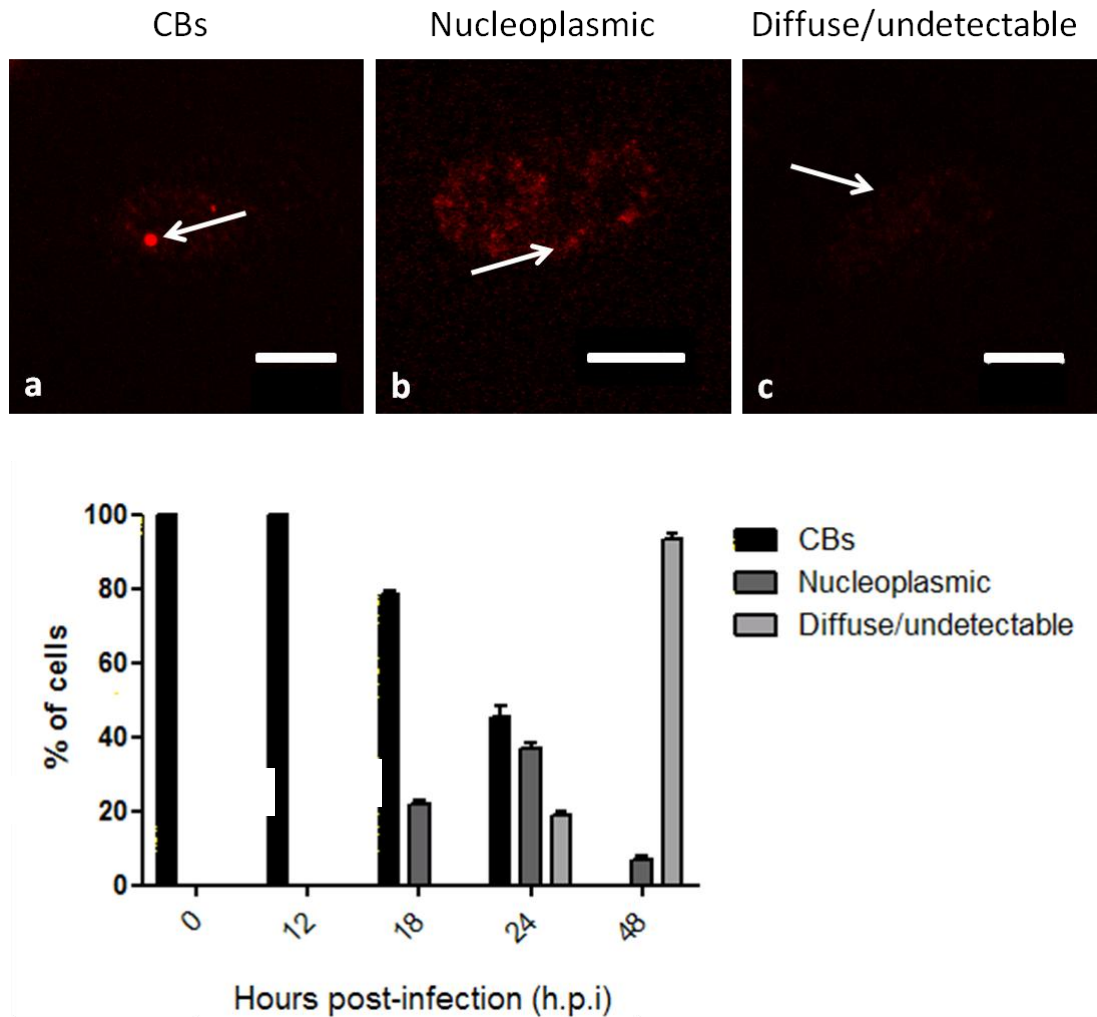
Figure 3-9. The temporal appearance of Cajal body (CB), nucleoplasmic and diffuse/undetectable distributions of SMN during Ad5 infection of A549 cells.

A549 cells were mock or Ad5 infected at an MOI of 5 FFU/cell and incubated for 0, 12, 18, 24 or 48 hours. Cells were fixed and subjected to indirect immunofluorescence. Images show the three major SMN distributions identified during the Ad5 infection time course. Three fields of 100 cells from each sample were counted and the SMN distribution was categorised as either 'CB', 'nucleoplasmic' or 'diffuse/undetectable'. Results are displayed in the graph as the mean percentage of cells (± SEM) from three independent experiments. These data indicated that during Ad5 infection, SMN is redistributed from CBs into novel nuclear structures at a late stage of infection (18-24 h.p.i) prior to further disassembly into diffuse/undetectable staining at very late time points (24-48 h.p.i). Bars = 10 μM.

3.4.1　Cellular splicing factors

During Ad infection, spliceosomal snRNPs are found surrounding ssDNA sites in a diffuse nucleoplasmic distribution (Bridge *et al.*, 1993a). Cells at this stage are known as 'ring cells' and this snRNP pattern is indicative of active transcription and splicing (Aspegren *et al.*, 1998; Gama-Carvalho *et al.*, 2003a). At later stages of infection, snRNPs accumulate in enlarged ICGs at the nuclear periphery (Bridge *et al.*, 1993a). In order to stain areas of active splicing, mock- and Ad5-infected cells were subjected to indirect immunofluorescence microscopy using a mouse anti-Sm antibody along with a rabbit anti-coilin or a rabbit anti-SMN antibody. An anti-Ad capsid antibody was used to identify Ad5-infected cells.

As shown in Figure 3-10 and previously (Bridge *et al.*, 1993a; Rebelo *et al.*, 1996), in mock-infected cells, Sm was located diffusely in the nucleoplasm and also concentrated in CBs (image b, arrow) and coilin was also found in CBs (image c, arrow). Sm and coilin colocalised in CBs, as shown by the yellow regions in the overlay (image i, arrow). In Ad5-infected cells, Sm was located diffusely in the nucleoplasm and was concentrated in enlarged nuclear ICGs (image f, arrow). As shown in the overlay (image j), Sm in enlarged ICGs (white arrow) did not colocalise with coilin in rosettes (image j, blue arrow). This indicated that rosettes are closely associated, but do not colocalise with, regions of active splicing.

The redistribution of SMN relative to snRNPs was also investigated (Figure 3-11). In mock-infected cells, Sm was located diffusely in the nucleoplasm and was concentrated in CBs (image b, arrow). SMN was also located in CBs (image d, arrow) and colocalised with Sm in these structures (image i, arrow). A rabbit anti-SMN antibody was used in this experiment, which appeared to give greater cytoplasmic SMN staining than that observed when using the mouse anti-SMN antibody (see Figure 3-6). In Ad5-infected cells, Sm was redistributed into diffusely in the nucleoplasm and within enlarged nuclear ICGs (image f, arrow). SMN was also redistributed into the nucleoplasm (image g, arrow). The rabbit anti-SMN antibody appeared to give a more diffuse staining of SMN in the nucleus of Ad5-infected cells than the mouse anti-SMN antibody, which was found to stain rod-shaped structures of SMN in the nucleus of Ad5-infected cells (Figure 3-6). Due to the diffuse nucleoplasmic distributions of SMN and Sm following Ad5 infection, a specific association of redistributed SMN with Sm was difficult to establish. Both proteins localised in the nucleoplasm and were excluded from nucleoli. However, SMN did not specifically accumulate in enlarged ICGs (image j, white arrow). This indicated that following Ad5 infection, snRNPs partially colocalised with SMN in the nucleoplasm, but SMN did not localise to enlarged snRNP-containing ICGs.
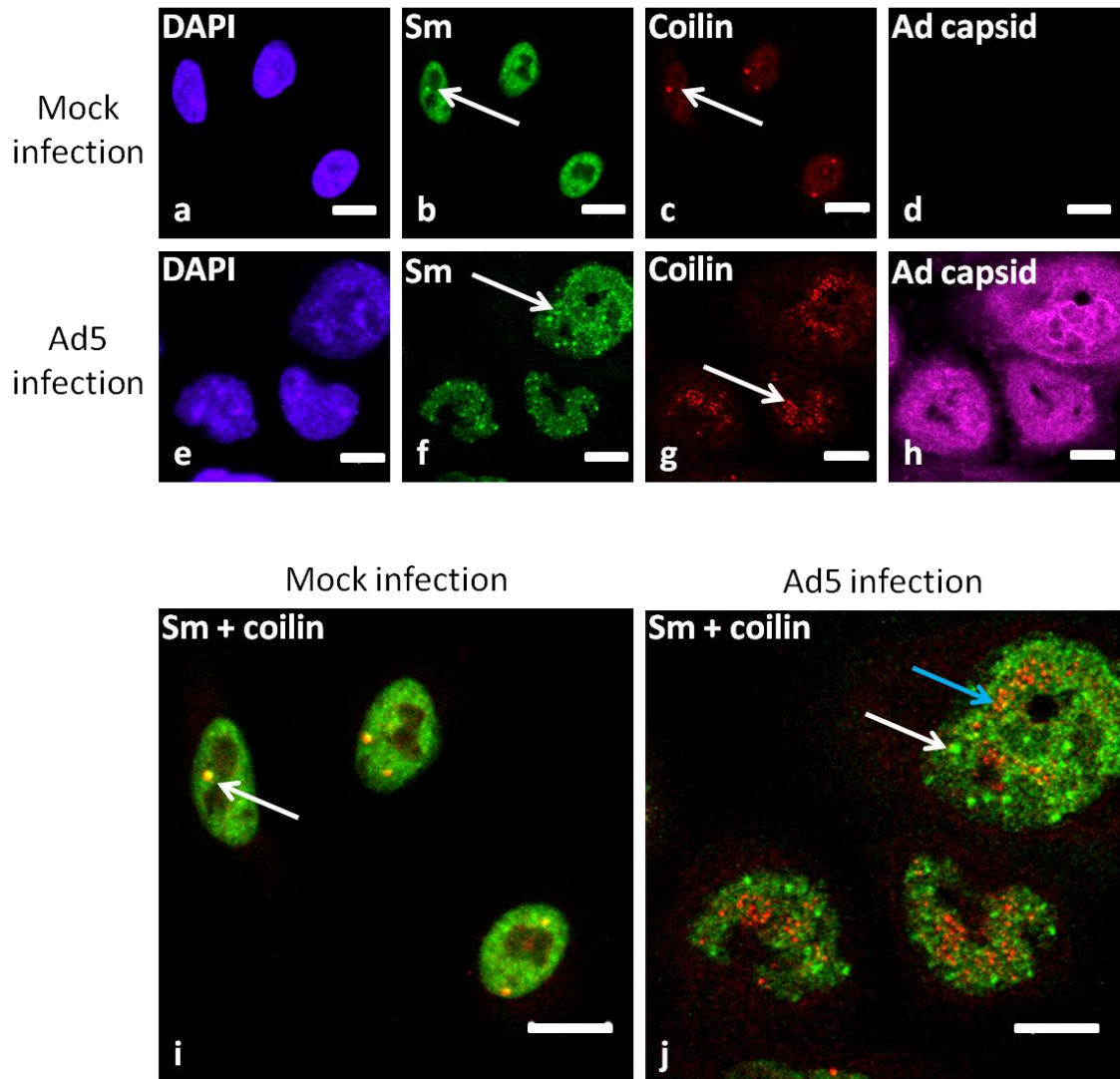
Figure 3-10. The redistribution of coilin relative to spliceosomal snRNPs in Ad5-infected A549 cells. A549 cells were mock or Ad5 infected at an MOI of 5 FFU/cell and incubated for 24 hours. Cells were fixed and subjected to indirect immunofluorescence using a mouse anti-Sm, a rabbit anti-coilin and a goat anti-Ad capsid antibody followed by incubation with the appropriate fluorescent-labelled secondary antibodies. Nuclei were stained using DAPI. Confocal microscopy was performed using an inverted LSM510 confocal microscope coupled to LSM Image Browser. In mock-infected cells, Sm was located diffusely within the nucleoplasm, with increased concentration in punctate CBs (image b, arrow). Coilin was found primarily within punctate CBs (image c, arrow). As shown by the yellow regions in the overlay, coilin and Sm colocalised in CBs (image i, arrow). In Ad5-infected cells, Sm was redistributed from CBs into numerous foci within the nucleus (image f, arrow). Coilin was redistributed from CBs into microfoci (image g, arrow). As shown in the overlay (image j), there was no colocalisation between the foci of Sm (white arrow) and the foci of coilin (blue arrow) in Ad5-infected cells. Bars = 10 μm.
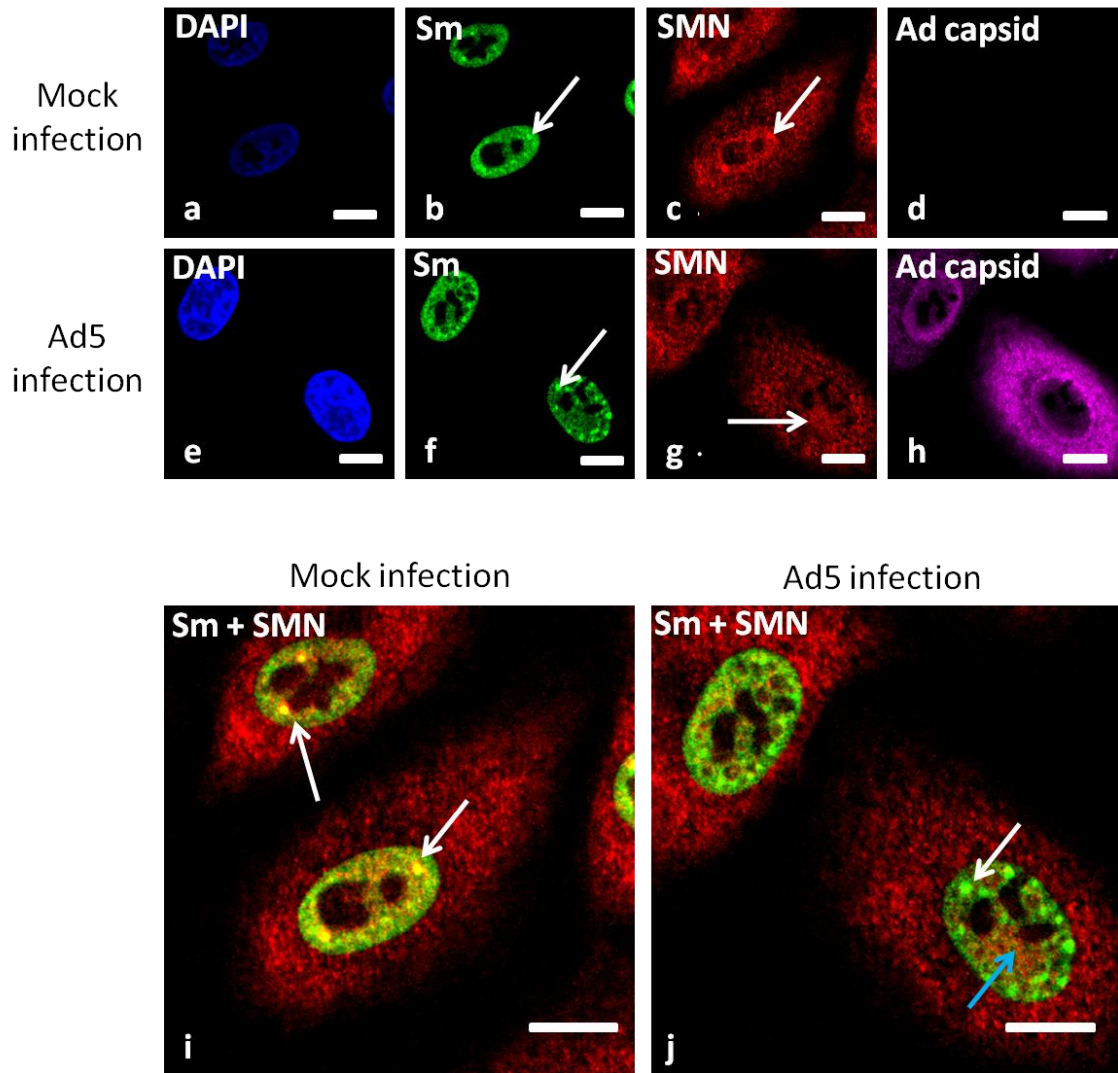
Figure 3-11. The redistribution of SMN relative to spliceosomal snRNPs in Ad5-infected A549 cells. A549 cells were mock or Ad5 infected at an MOI of 5 FFU/cell and incubated for 24 hours. Cells were fixed and subjected to indirect immunofluorescence using a mouse anti-Sm, a rabbit anti-SMN and a goat anti-Ad capsid antibody followed by incubation with the appropriate fluorescent-labelled secondary antibodies. Nuclei were stained using DAPI. Confocal microscopy was performed using an inverted LSM510 confocal microscope coupled to LSM Image Browser. In mock-infected cells, Sm was located diffusely within the nucleoplasm, with increased concentration in punctate CBs (image b, arrow). SMN was found primarily within punctate CBs (image c, arrow). As shown by the yellow regions in the overlay, SMN and Sm colocalised in CBs (image i, arrow). In Ad5-infected cells, Sm was redistributed from CBs into numerous foci within the nucleus (image f, arrow). SMN was redistributed from CBs into the nucleoplasm (image g, arrow). As shown in the overlay (image j), there was no colocalisation between the foci of Sm (white arrow) and nucleoplasmic SMN (blue arrow) in Ad5-infected cells. Bars = 10 μm.

3.4.2   Nucleoli

Similar to CBs, nucleolar proteins have been shown to be redistributed during Ad5 infection; B23 is redistributed to viral DNA replication centres (Hindley *et al.,* 2007), C23 (nucleolin) is exported to the cytoplasm (Matthews, 2001) and fibrillarin is redistributed into rosettes along with coilin (Rebelo *et al.*, 1996; Rodrigues *et al.*, 1996). CBs have long been known to have a close association with the nucleolus, with both coilin and SMN previously shown to interact with nucleolar proteins (Isaac *et al.*, 1998; Pellizzoni *et al.*, 2001a; Lefebvre *et al.*, 2002; Sun *et al.*, 2005). Therefore it is possible that during Ad5 infection, CB proteins and nucleolar proteins may become associated in novel domains. To this end, the distribution of coilin and SMN relative to the nucleolar marker proteins B23, C23 and fibrillarin was investigated in mock and Ad5-infected A549 cells (Chapter 2.2.6.1) at 24 h.p.i by indirect immunofluorescence microscopy (Chapter 2.2.7).

As shown in Figure 3-12, mock-infected cells exhibited a primarily nucleolar distribution of fibrillarin (image b, blue arrow) and were also found within CBs (image b, white arrow). Coilin was located in punctate CBs (image c, arrow). Fibrillarin in CBs colocolised with coilin, as shown by the yellow regions in the overlay (image i, white arrow) whilst fibrillarin in nucleoli did not colocolise with coilin (image i, blue arrow). In Ad5-infected cells, there was partial colocalisation of these two proteins in rosettes (image j, white arrow), as shown previously (Rebelo *et al.*, 1996; Rodrigues *et al.*, 1996). Fibrillarin within nucleoli of Ad5-infected cells did not colocalise with coilin (image j, blue arrow). This indicated that a proportion of fibrillarin was associated with rosettes whilst the bulk remained associated with the nucleolus.

As shown in Figure 3-13, in mock-infected A549 cells, B23 was concentrated in the nucleolus (image b, arrow) whilst coilin was localised in CBs (image c, arrow). CBs were closely associated, but did not colocalise with, nucleoli (image i; CBs [white arrow] are separate to nucleoli [blue arrow]). Following Ad5 infection, coilin was redistributed into rosettes (image g, arrow). Interestingly, B23 was not redistributed from the nucleolus in Ad5-infected cells (image f, arrow), contrasting with previously published data (Hindley *et al.,* 2007). There was no colocalisation between coilin rosettes (image j, white arrow) and B23 in nucleoli (image j, blue arrow). This indicated that there was no association of coilin with B23 during Ad5 infection.

Finally, the redistribution of coilin relative to C23 was assessed (Figure 3-14). In mock-infected cells, coilin was localised in CBs (image c, arrow) whereas C23 was concentrated in the nucleolus (image b, white arrow) and was also found diffusely in the nucleoplasm (image c, blue arrow). In Ad5-infected cells at 24 h.p.i, coilin was redistributed into rosettes (image g, arrow) whilst C23 staining was reduced in the nucleolus (image f, white arrow) with some
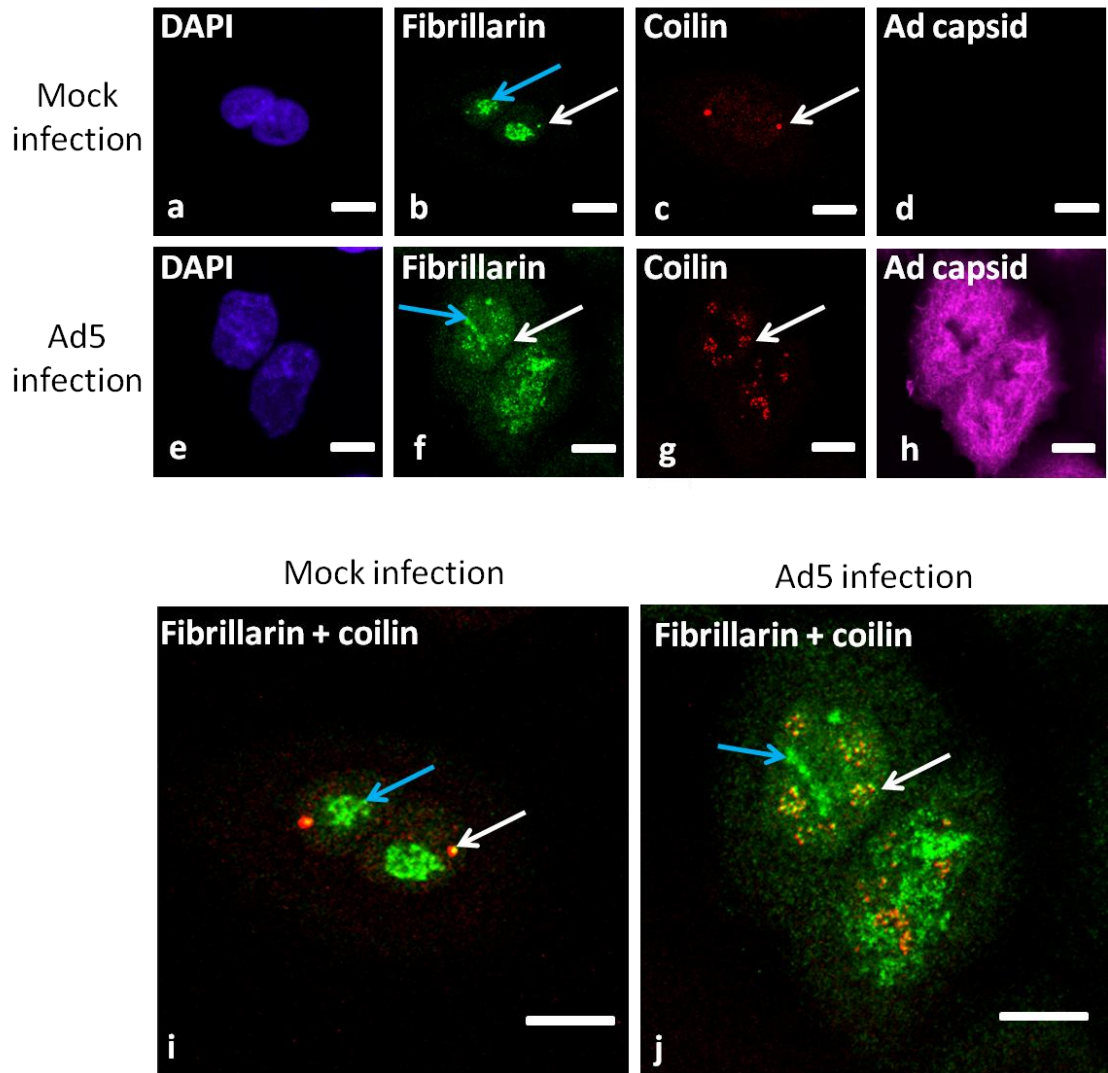
Figure 3-12. The redistribution of coilin relative to fibrillarin in Ad5-infected of A549 cells.

A549 cells were mock or Ad5 infected at an MOI of 5 FFU/cell and incubated for 24 hours. Cells were fixed and subjected to indirect immunofluorescence using a mouse anti-coilin, a rabbit anti-fibrillarin and a goat anti-Ad capsid antibody followed by incubation with the appropriate fluorescent-labelled secondary antibodies. DAPI was used to stain nuclei. Confocal microscopy was performed using an inverted LSM510 confocal microscope coupled to LSM Image Browser. In mock-infected cells, fibrillarin (image b) was found in the nucleolus (blue arrow) and in CBs (white arrow). Coilin was also located in CBs (image c, arrow) and colocalised with fibrillarin in these structures, as shown by the yellow regions in the overlay (image i, arrow). In Ad5-infected cells, a proportion of fibrillarin remained associated with the nucleolus (image f, blue arrow) whilst CB-associated fibrillarin was redistributed into microfoci (image f, white arrow). Coilin was also reorganised into microfoci (image g, arrow); coilin and fibrillarin partially colocalised in these microfoci, as shown by the yellow regions in the overlay (image j, white arrow). Nucleolar fibrillarin did not colocalise with coilin (image j, blue arrow). Bars = 10 µm.
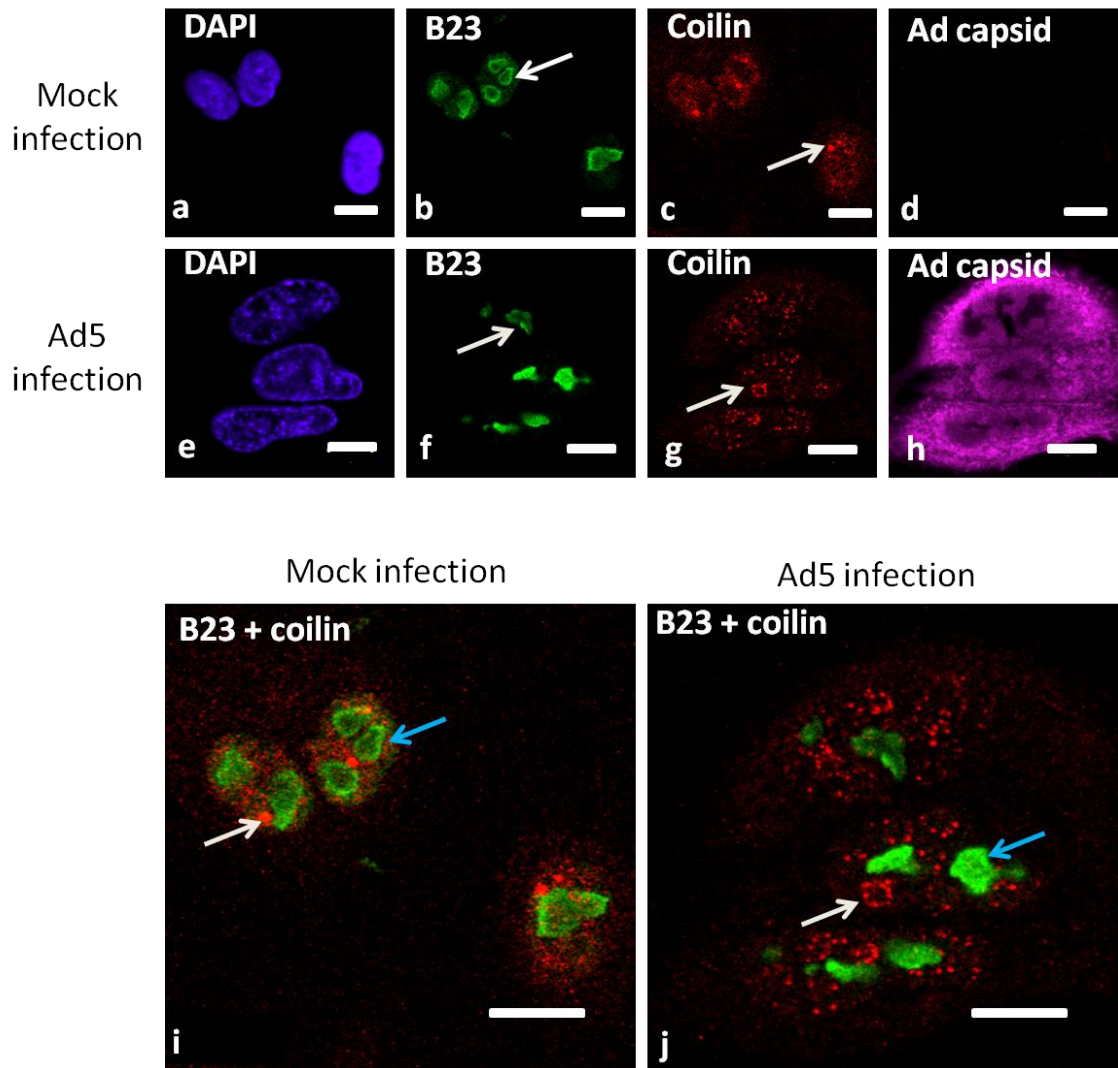
Figure 3-13. The redistribution of coilin relative to B23 in Ad5-infected of A549 cells.

A549 cells were mock or Ad5 infected at an MOI of 5 FFU/cell and incubated for 24 hours. Cells were fixed and subjected to indirect immunofluorescence using a mouse anti-B23, a rabbit anti-coilin and a goat anti-Ad capsid antibody followed by incubation with the appropriate fluorescent-labelled secondary antibodies. DAPI was used to stain nuclei. Confocal microscopy was performed using an inverted LSM510 confocal microscope coupled to LSM Image Browser. In mock-infected cells, B23 (image b) was found in the nucleolus (image b, arrow) whilst coilin was located in CBs (image c, arrow). As shown in the overlay (image i), there was no colocalisation of B23 (blue arrow) with coilin (white arrow). In Ad5-infected cells, B23 remained associated with the nucleolus (image f, arrow), whereas coilin was reorganised into microfoci (image g, arrow). As shown in the overlay (image j), there was no colocalisation of B23 (blue arrow) with coilin (white arrow) in Ad5-infected cells. Bars = 10 μm.
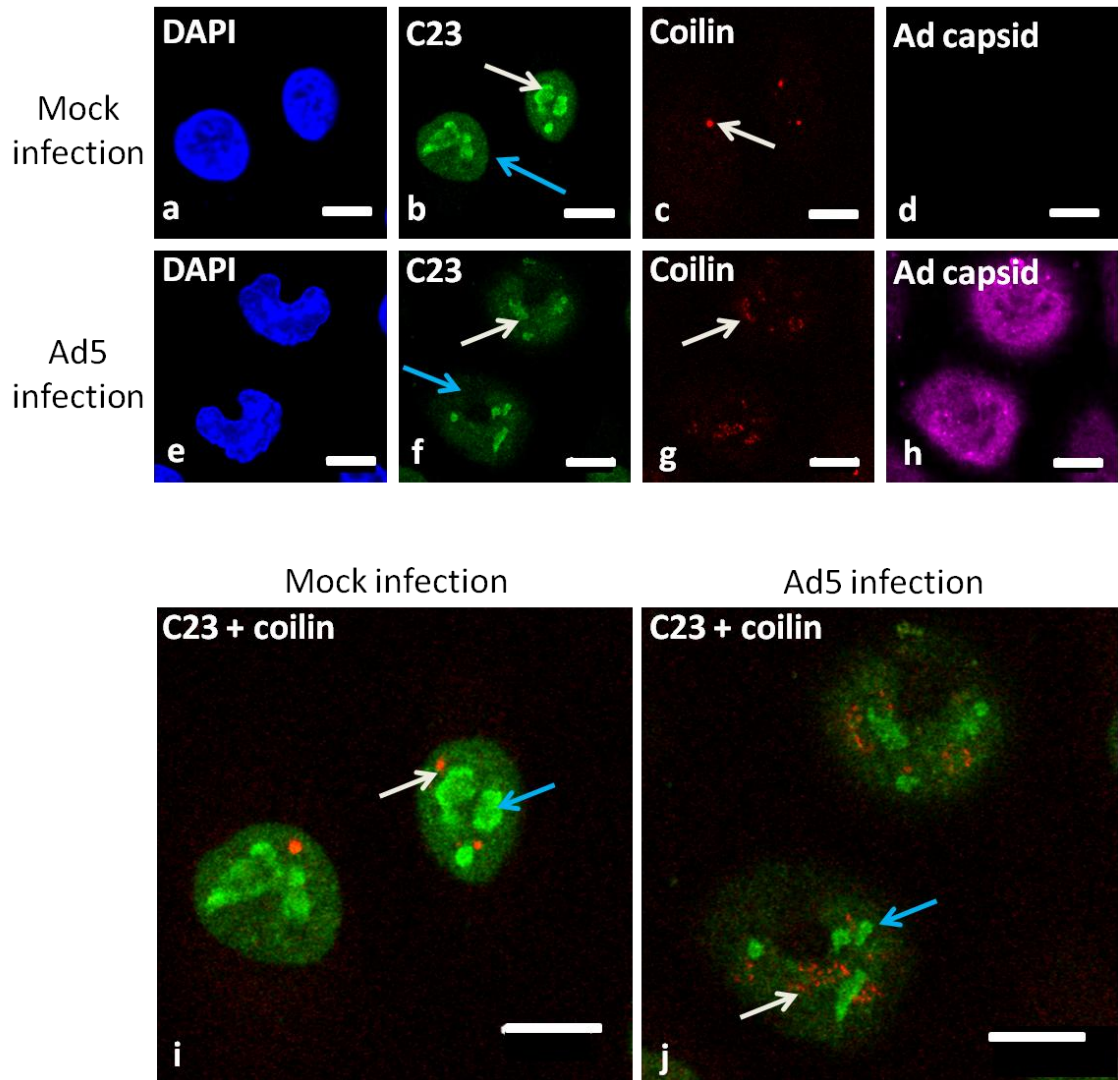
Figure 3-14. The redistribution of coilin relative to the C23 in Ad5-infected of A549 cells.

A549 cells were mock or Ad5 infected at an MOI of 5 FFU/cell and incubated for 24 hours. Cells were fixed and subjected to indirect immunofluorescence using a mouse anti-C23, a rabbit anti-coilin and a goat anti-Ad capsid antibody followed by incubation with the appropriate fluorescent-labelled secondary antibodies. DAPI was used to stain nuclei. Confocal microscopy was performed using an inverted LSM510 confocal microscope coupled to LSM Image Browser. In mock-infected cells, C23 (image b) was found in the nucleolus (white arrow) and the nucleoplasm (blue arrow), whilst coilin was located in CBs (image c, arrow). As shown in the overlay (image i), there was no colocalisation of nucleolar C23 (blue arrow) with coilin in CBs (white arrow). In Ad5-infected cells, C23 staining was reduced in the nucleolus (image f, white arrow) with increased staining in the cytoplasm (image f, blue arrow). Coilin was redistributed into microfoci (image g, arrow). As shown in the overlay (image j), there was no colocalisation of nucleolar C23 (blue arrow) with coilin microfoci (white arrow) in Ad5-infected cells. Bars = 10 μm.

cytoplasm staining (image f, blue arrow) consistent with previous observations (Matthews, 2001) (Figure 3-14). There was no colocalisation between coilin rosettes (image j, white arrow) with C23 in nucleoli (blue arrow). This indicated that during Ad5 infection, C23 is not associated with rosettes.

The redistribution of SMN relative to nucleolar markers was also assessed. As shown in Figure 3-15, in mock-infected cells, fibrillarin was concentrated in nucleoli (image b, blue arrow) and was also found in CBs (image b, white arrow). SMN was concentrated in CBs (image c, arrow). Fibrillarin and SMN colocalised in CBs, as shown by the yellow regions in the overlay (image i, blue arrow). SMN did not colocalise with fibrillarin in nucleoli (image i, white arrow). In Ad5-infected cells, fibrillarin remained in nucleoli (image f, blue arrow) with partial redistribution into rosettes (image f, white arrow). In contrast, SMN was redistributed into the nucleoplasm (image g, arrow). As shown in the overlay (image j), there was no colocalisation of SMN (white arrow) with fibrillarin in nucleoli (blue arrow) or with fibrillarin microfoci (yellow arrow).

The localisation of SMN relative to B23 was also investigated (Figure 3-16). In mock-infected cells, B23 was located in the nucleolus (image b, arrow) whilst SMN was concentrated in CBs (image c, arrow). As shown in the overlay (image i), there was no colocalisation between B23 in nucleoli (blue arrow) and SMN in CBs (white arrow). In Ad5-infected cells, SMN was redistributed into the nucleoplasm (image g, arrow) whilst B23 remained within nucleoli (image f, arrow). There was no colocalisation between redistributed SMN (image j, white arrow) and nucleoli containing B23 (image j, blue arrow).

The redistribution of SMN relative to C23 was determined (Figure 3-17). In mock-infected cells, C23 was concentrated in the nucleolus (image b, white arrow) with diffuse staining in the nucleoplasm (image b, blue arrow). SMN was concentrated in CBs (image c, white arrow) and, as previously mentioned (Section 3.4.1), the rabbit anti-SMN antibody also exhibited strong cytoplasmic staining (image c, blue arrow), in contrast to findings with the mouse anti-SMN antibody (Figure 3-3). In Ad5-infected cells, SMN became increasingly nucleoplasmic as infection proceeded (image g, white arrow) and there was increased cytoplasmic staining of SMN in some cells (image g, blue arrow). In Ad5-infected cells, C23 staining was reduced in the nucleus (image f, white arrow) and in the nucleoplasm (image f, blue arrow), and increased in the cytoplasm (image f, yellow arrow), consistent with previous observations (Matthews, 2001). As shown in the overlay (image j), C23 and SMN colocalised in the cytoplasm in some Ad5-infected cells (blue arrow) whilst SMN in the nucleoplasm did not colocalise with nucleoplasmic C23 (white arrow). These data indicated that during Ad5 infection there was colocalisation of SMN and C23 in the cytoplasm.
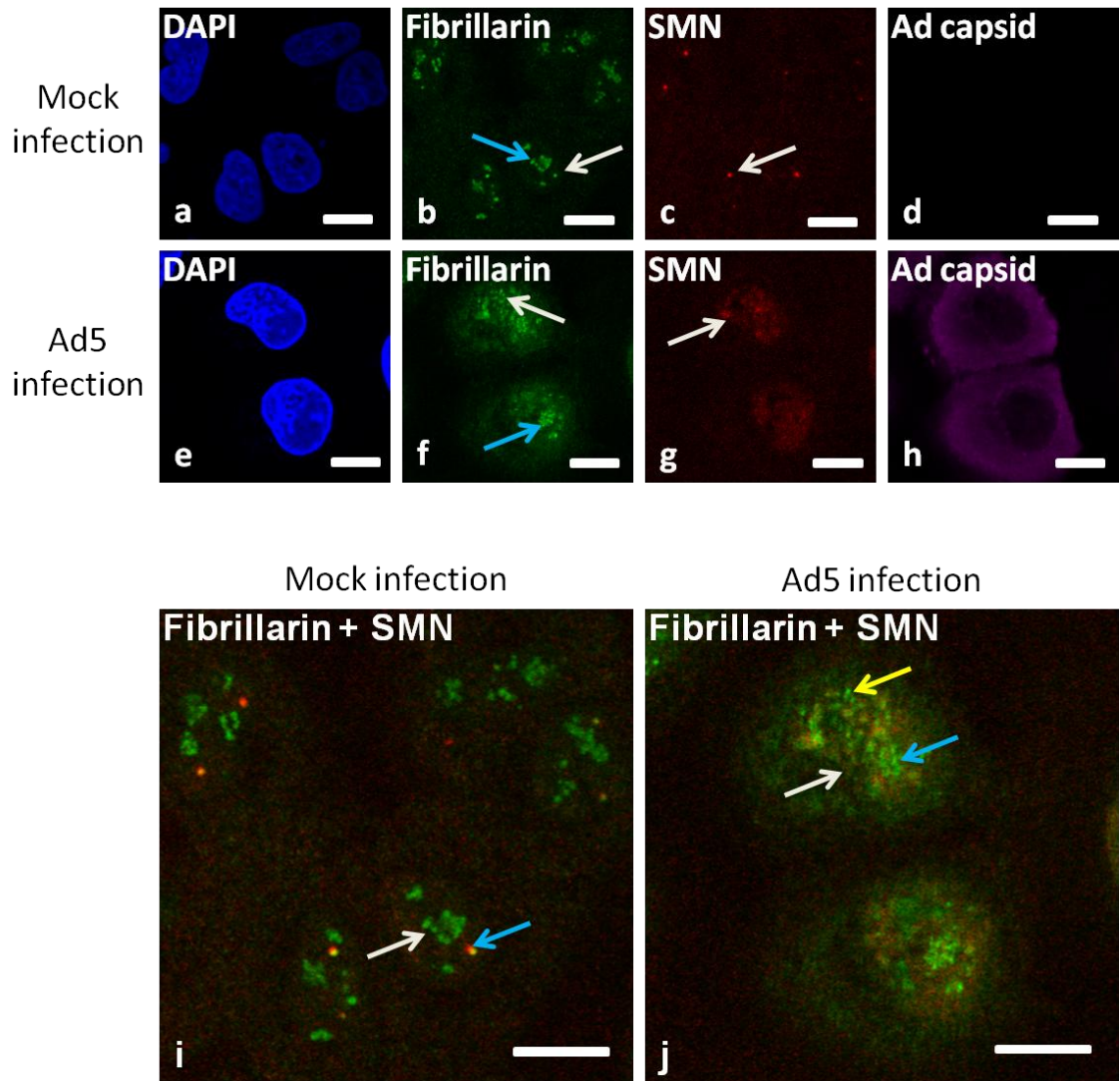
Figure 3-15. The redistribution of SMN relative to fibrillarin in Ad5-infected A549 cells.

A549 cells were mock or Ad5 infected at an MOI of 5 FFU/cell and incubated for 24 hours. Cells were fixed and subjected to indirect immunofluorescence using a mouse anti-SMN, a rabbit anti-fibrillarin and a goat anti-Ad capsid antibody followed by incubation with the appropriate fluorescent-labelled secondary antibodies. DAPI was used to stain nuclei. Confocal microscopy was performed using an inverted LSM510 confocal microscope coupled to LSM Image Browser. In mock-infected cells, fibrillarin (image b) was found in the nucleolus (blue arrow) and in CBs (white arrow). SMN was also located in CBs (image c, arrow) and colocalised with fibrillarin in these structures, as shown by the yellow regions in the overlay (image i, arrow). In Ad5-infected cells, a proportion of fibrillarin remained associated with the nucleolus (image f, blue arrow) whilst CB-associated fibrillarin was redistributed into microfoci (image f, white arrow). SMN was reorganised into separate structures within the nucleoplasm (image g, arrow). As shown in the overlay (image j), redistributed SMN (white arrow) did not colocalise with nucleolar fibrillarin (blue arrow) or fibrillarin microfoci (yellow arrow). Bars = 10 μm.
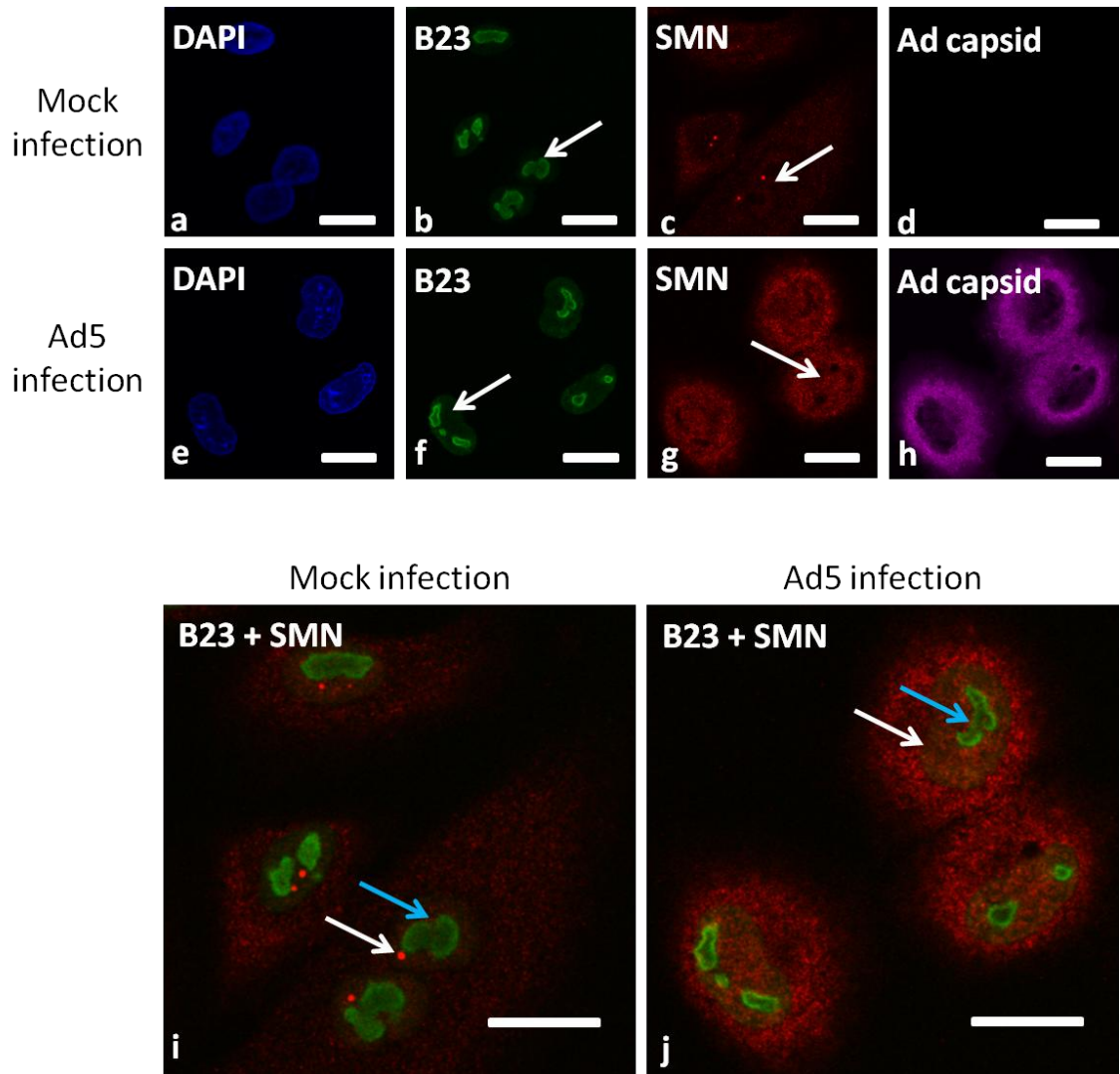
Figure 3-16. The redistribution of SMN relative to B23 in Ad5-infected of A549 cells.
A549 cells were mock or Ad5 infected at an MOI of 5 FFU/cell and incubated for 24 hours. Cells were fixed and subjected to indirect immunofluorescence using a mouse anti-B23, a rabbit anti-SMN and a goat anti-Ad capsid antibody followed by incubation with the appropriate fluorescent-labelled secondary antibodies. DAPI was used to stain nuclei. Confocal microscopy was performed using an inverted LSM510 confocal microscope coupled to LSM Image Browser. In mock-infected cells, B23 (image b) was found in the nucleolus (image b, arrow) whilst SMN was located in CBs (image c, arrow). As shown in the overlay (image i), there was no colocalisation of B23 (blue arrow) with SMN (white arrow). In Ad5-infected cells, B23 remained associated with the nucleolus (image f, arrow), whereas SMN was reorganised from CBS into the nucleoplasm (image g, arrow). As shown in the overlay (image j), there was no colocalisation of B23 (blue arrow) with nucleoplasmic SMN (white arrow) in Ad5-infected cells. Bars = 10 μm.
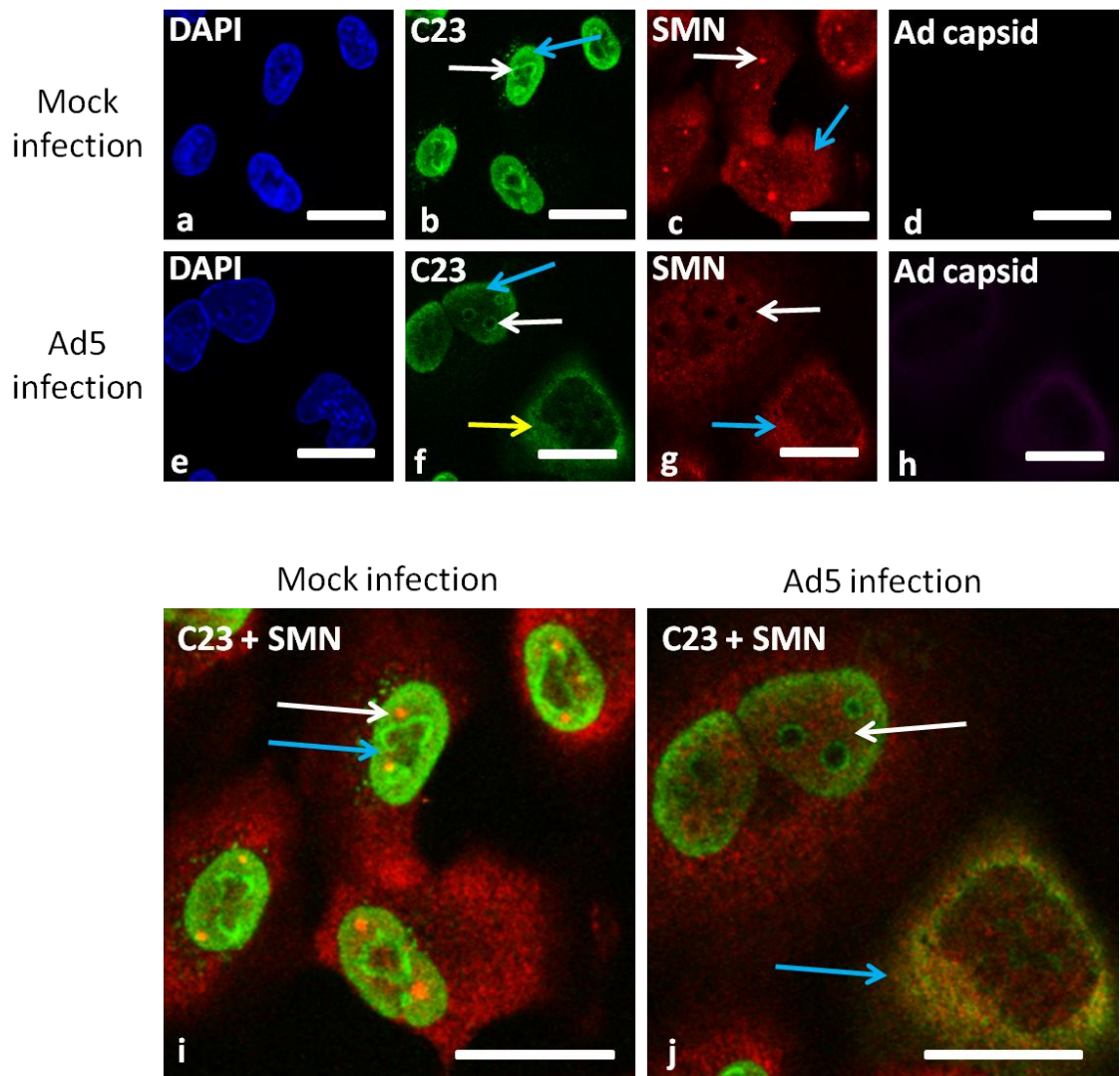
Figure 3-17. The redistribution of SMN relative to the C23 in Ad5-infected of A549 cells.

A549 cells were mock or Ad5 infected at an MOI of 5 FFU/cell and incubated for 24 hours. Cells were fixed and subjected to indirect immunofluorescence using a mouse anti-C23, a rabbit anti-SMN and a goat anti-Ad capsid antibody followed by incubation with the appropriate fluorescent-labelled secondary antibodies. DAPI was used to stain nuclei. Confocal microscopy was performed using an inverted LSM510 confocal microscope coupled to LSM Image Browser. In mock-infected cells, C23 (image b) was found in the nucleolus (white arrow) and the nucleoplasm (blue arrow), and SMN was located in CBs (image c, arrow). Cytoplasmic SMN was also observed when using the rabbit anti-SMN antibody (image c, blue arrow). As shown in the overlay (image i), there was no colocalisation of nucleolar C23 (blue arrow) with SMN in CBs (white arrow). In Ad5-infected cells, C23 (image f) staining was reduced in the nucleolus (white arrow) and in the nucleoplasm (blue arrow), with increased staining in the cytoplasm (yellow arrow). SMN (image g) was redistributed into the nucleoplasm (white arrow), and, in some cells, also exhibited increased cytoplasmic staining (blue arrow). As shown by the yellow regions in the overlay (image j, blue arrow), C23 colocalised with SMN in the cytoplasm of Ad5-infected cells. No such colocalisation was observed for C23 and SMN in the nucleoplasm (image j, white arrow). Bars = 10 μm.
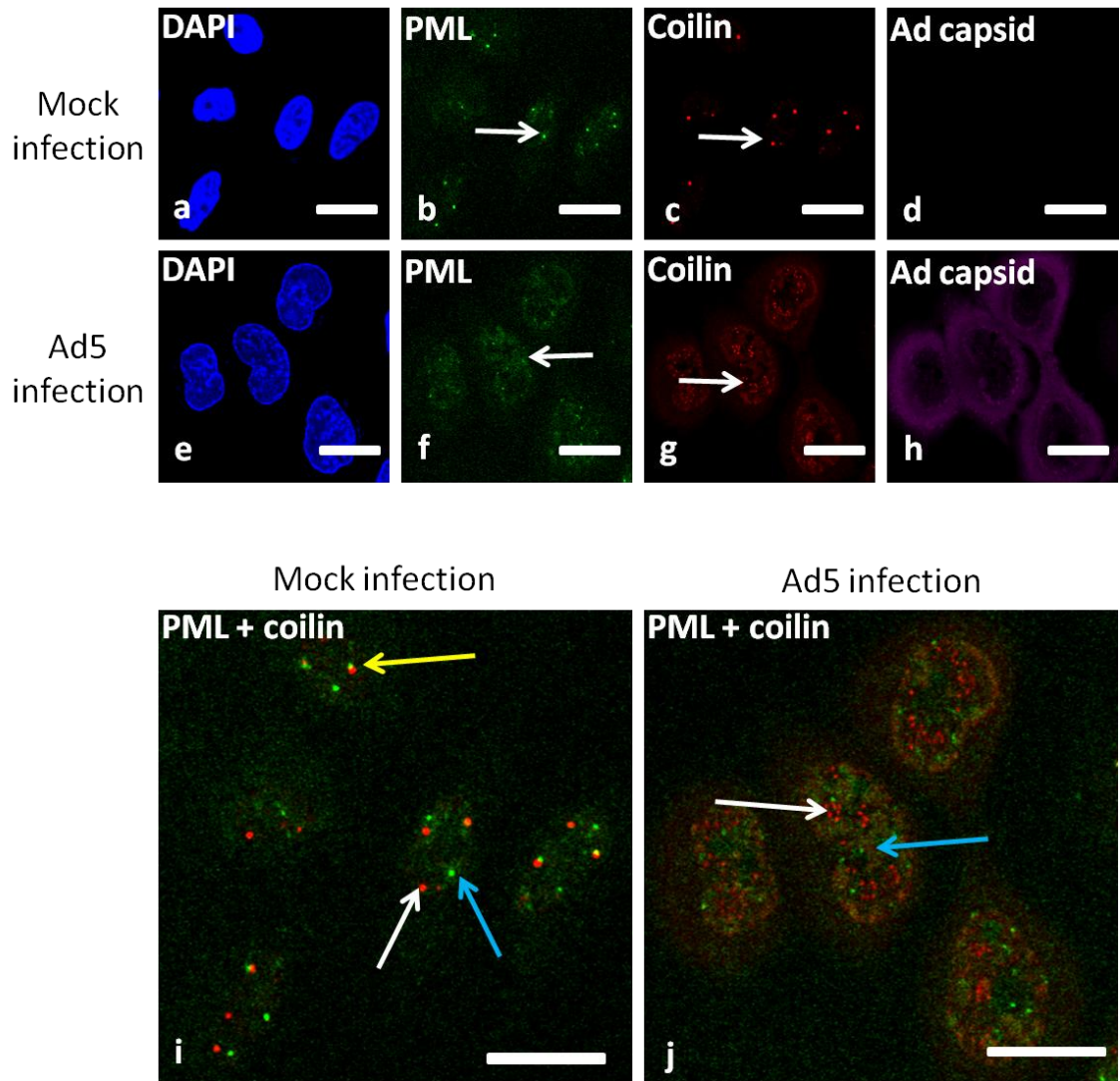
Figure 3-18. The redistribution of coilin relative to PML-NBs in Ad5-infected A549 cells.

A549 cells were mock or Ad5 infected at an MOI of 5 FFU/cell and incubated for 24 hours. Cells were fixed and subjected to indirect immunofluorescence. Cells were incubated with a mouse anti-PML, a rabbit anti-coilin and a goat anti-Ad capsid antibody followed by incubation with the appropriate fluorescent-labelled secondary antibodies. Nuclei were stained using DAPI. Confocal microscopy was performed using an inverted LSM510 confocal microscope coupled to LSM Image Browser. In mock-infected cells, PML was found in discrete foci within the nucleus (image b, arrow). Coilin was also found within punctate nuclear foci (image c, arrow). As shown in the overlay (image i), the majority of PML foci (blue arrow) and coilin foci (white arrow) did not colocalise. However, a subset of PML and coilin foci did partially overlap (image i, yellow arrow). In Ad5-infected cells, PML was redistributed within the nucleus and exhibited a decrease in staining intensity (image f, arrow). Coilin was redistributed from CBs into microfoci (image g, arrow). As shown in the overlay (image j), redistributed PML (blue arrow) did not colocolise with coilin microfoci (white arrow). Bars = 20 μm.

3.4.3 PML-NBs

During Ad5 infection, PML-NB components are redistributed and/or degraded in order to subvert immune responses and transcriptional repression (Puvion-Dutilleul *et al.*, 1995; Doucas *et al.*, 1996; Leppard and Everett, 1999; Zhao *et al.*, 2003; Hoppe *et al.*, 2006; Ullman *et al.*, 2007; Ullman and Hearing, 2008; Schreiner *et al.*, 2010). As PML-NB components are redistributed and/or degraded at an early stage of Ad infection (Doucas *et al.*, 1996), it appears unlikely that CB proteins, which are not redistributed until a much later stage, would be associated with the novel PML tracks (James *et al.*, 2010). However, the observed redistribution of coilin into novel nuclear microfoci warranted investigation of colocalisation with redistributed PML-NBs during Ad infection. As SMN was redistributed diffusely within the nucleoplasm and into larger nucleoplasmic accumulations rather than discrete foci, potential colocalisation of SMN with PML-NBs was not investigated. As shown in Figure 3-18, and previously (Grande *et al.*, 1996), in mock-infected cells, both PML (image b, arrow) and coilin (image c, arrow) were located in punctate nuclear foci. As shown in the overlay (image i), PML foci (blue arrow) and coilin foci (white arrow) were generally not associated in mock-infected cells. However, some coilin and PML foci partially overlapped, as shown by the yellow regions in the overlay (image i, yellow arrow). In Ad5-infected cells, PML staining was greatly reduced (image f, arrow) and coilin was redistributed into rosettes (image g, arrow). There was no colocalisation between coilin rosettes (image j, white arrow) and residual PML foci (image j, blue arrow). This indicated that rosettes are not associated with PML-NBs during Ad5 infection.

3.4.4 Viral DNA replication centres

Large, globular DNA replication centres containing DBP can be used as a marker of the onset of viral DNA replication (Pombo *et al.*, 1994, Puvion-Dutilleul 1990a,b). Dual staining of DBP with SMN or coilin was performed to determine whether CB proteins are associated with DNA replication centres.

As shown in Figure 3-19A, in mock-infected cells there was no detectable DBP staining (image b) and coilin was found in CBs (image c, arrow). In Ad5-infected cells, DBP was present in large globular structures within the nucleus (image f, arrow) and coilin was redistributed into rosettes (image g, arrow). Coilin rosettes located at the periphery of, but did not colocalise with, DBP-containing DNA replication centres (image h, white arrow). This indicated that rosettes were located in close proximity to regions of Ad DNA replication.

Dual staining of SMN and DBP was also performed (Figure 3-19B). Mock-infected cells were negative for DBP (image b) and SMN was located in CBs (image c, arrow). In Ad5-infected cells, DBP formed large globular structures within the nucleus (image f, arrow) whilst SMN
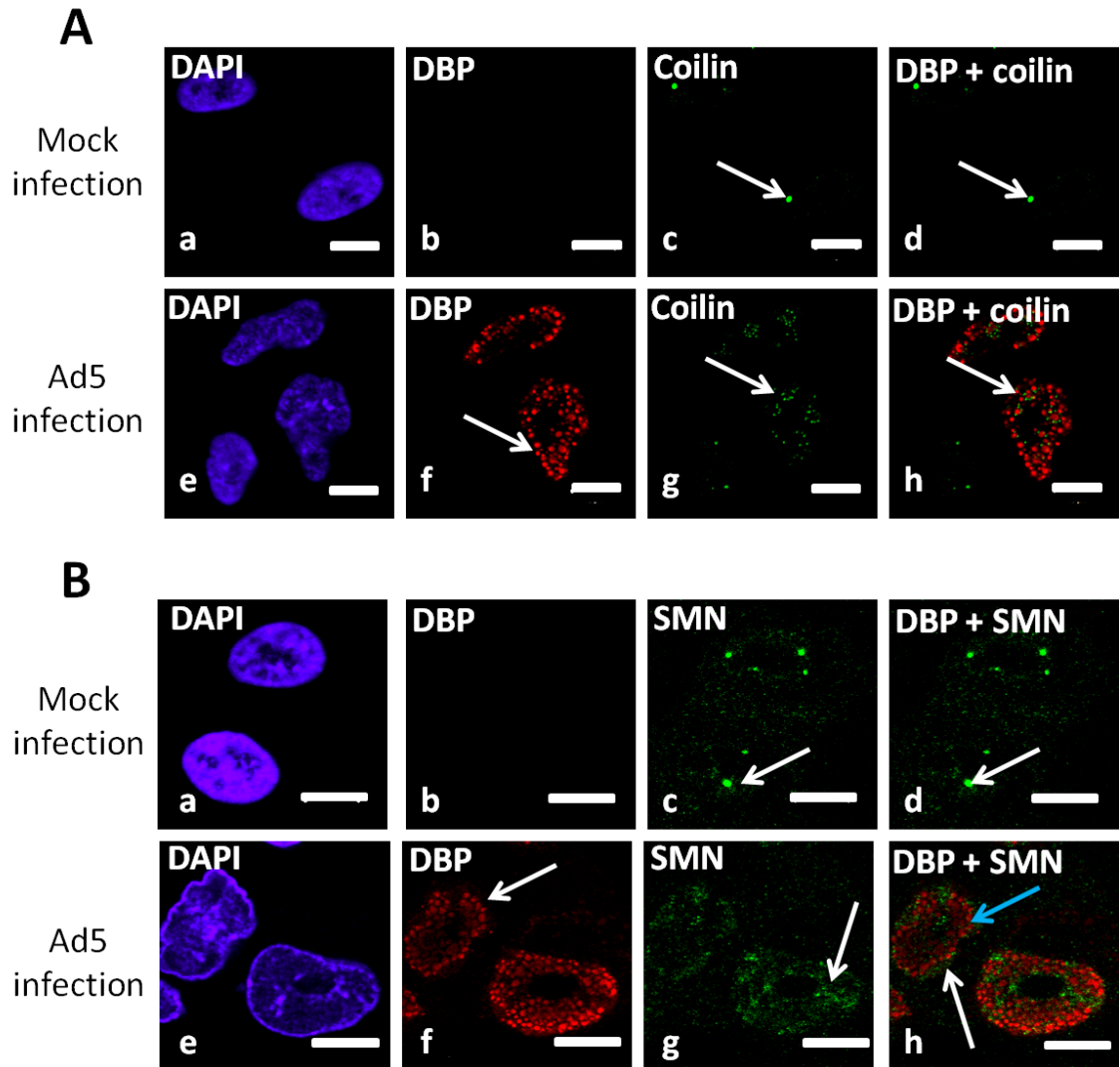
Figure 3-19. The redistribution of coilin and SMN relative to viral DNA replication centres in Ad5-infected A549 cells.

A549 cells were mock or Ad5 infected at an MOI of 5 FFU/cell and incubated for 24 hours. Cells were fixed and subjected to indirect immunofluorescence. Cells were incubated with a rabbit anti-DBP antibody along with a mouse anti-coilin or a mouse anti-SMN antibody followed by incubation with the appropriate fluorescent-labelled secondary antibodies. Nuclei were stained using DAPI. Confocal microscopy was performed using an inverted LSM510 confocal microscope coupled to LSM Image Browser. As shown in A, mock-infected cells were negative for Ad5 DBP (image b) and coilin was found in CBs (image c, arrow). In Ad5-infected cells, DBP was present in large nuclear globular foci (image f, arrow) and coilin was redistributed into microfoci (image g, arrow). As shown in the overlay, coilin microfoci surrounded, but did not colocalise with, DBP-positive foci (image h, arrow). As shown in B, mock-infected cells were negative for Ad5 DBP (image b) and SMN was found in CBs (image c). In Ad5-infected cells, DBP was located in large nuclear foci (image f, arrow) and SMN was redistributed into rod-shaped structures within the nucleus (image g, arrow). As shown in the overlay (image h), DBP (blue arrow) did not colocolise with redistributed SMN (white arrow) in Ad5-infected cells. Bars = 10 μm.
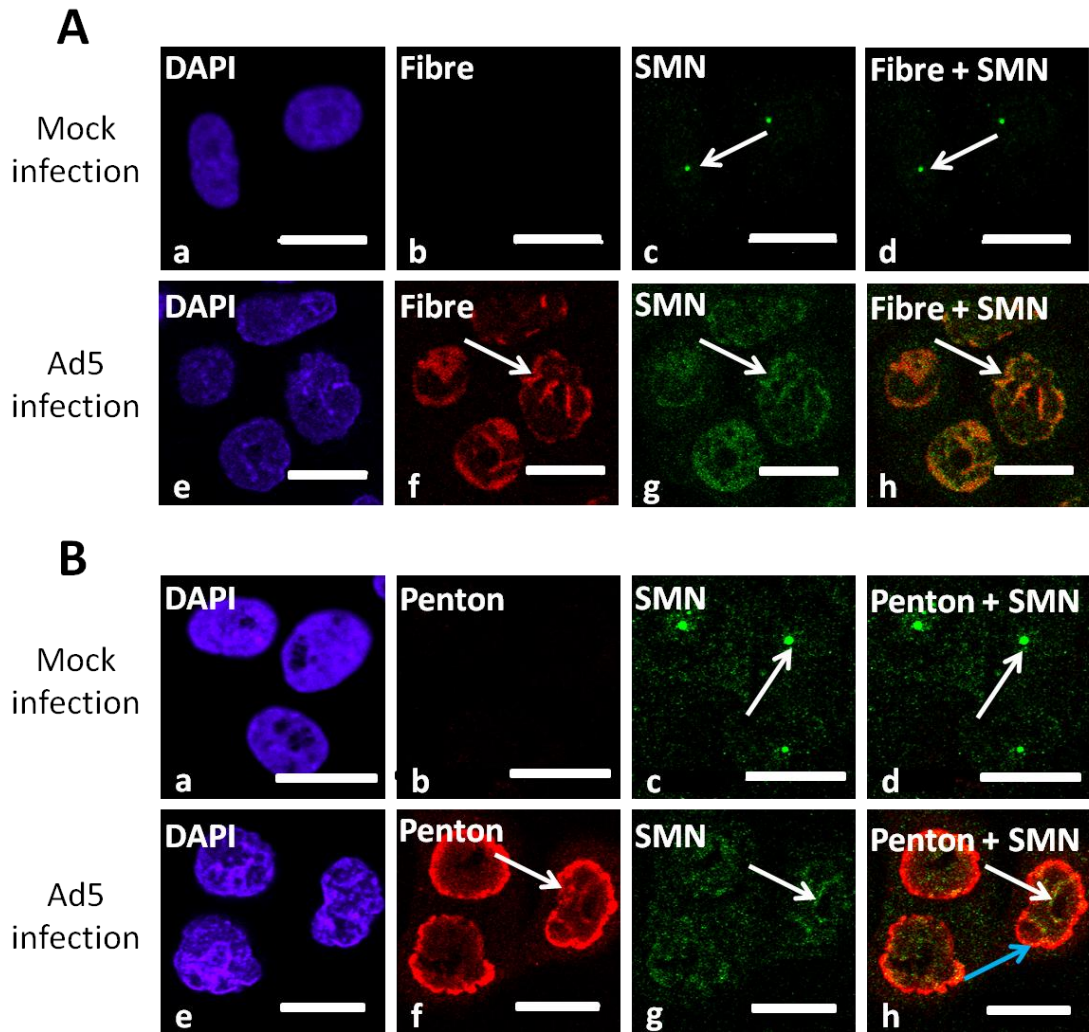
Figure 3-20. Redistribution of SMN relative to virus assembly platforms in Ad5-infected A549 cells.
A549 cells were mock or Ad5 infected at an MOI of 5 FFU/cell and were incubated for 24 hours. Cells
were fixed and subjected to indirect immunofluorescence using a rabbit anti-SMN and a mouse anti-fibre
antibody or a mouse anti-SMN and a rabbit anti-penton base antibody followed by incubation with the
appropriate fluorescent-labelled secondary antibodies. Nuclei were stained using DAPI. Confocal
microscopy was performed using an inverted LSM510 confocal microscope coupled to LSM Image
Browser. A. Redistribution of SMN relative to fibre during Ad5 infection. Mock-infected cells were
negative for Ad5 fibre (image b) and SMN was found in CBs (image c, arrow). In Ad5-infected cells,
fibre formed large nuclear aggregates (image f, arrow). SMN was redistributed from CBs into rod-shaped
nuclear structures (image g, arrow). As shown by the yellow regions in the overlay, fibre protein
colocalised with SMN in the nuclei of Ad5-infected cells (image h, arrow). B. Redistribution of SMN
relative to penton base during Ad5 infection. Mock-infected cells were negative for Ad5 penton base
(image b) and SMN was present in CBs (image c, arrow). In Ad5-infected cells, penton base formed large
nuclear aggregates, with intense staining at the nuclear periphery (image f, arrow). SMN was redistributed
into rod-shaped nuclear structures (image g, arrow). As shown by the yellow regions in the overlay
(image h), penton base and SMN partially colocalised in the nuclei of Ad5-infected cells (white arrow).
Penton base located at the nuclear periphery did not colocalise with SMN (blue arrow). Bars = 20 μm.

was located diffusely in the nucleoplasm and in nuclear rod-shaped structures (image g, arrow). SMN rod-shaped structures (image h, white arrow) were excluded from DBP-positive replication centres (image h, blue arrow). This suggested that SMN was not associated with DNA replication domains during Ad5 infection.

3.4.5 Virus assembly platforms

During the latter stages of Ad5 infection, large crystalline structures form within the nucleus and around the nuclear periphery, composed of large aggregations of late viral proteins (Franqueville *et al.*, 2008). These structures are thought to correspond to regions of virus capsid assembly. As SMN was found to locate in nuclear rod-shaped structures in Ad5-infected cells, the colocalisation of SMN with regions of virus assembly was investigated. As shown in Figure 3-20A, Mock-infected cells were negative for Ad5 fibre (image b, arrow) and SMN was located in punctate CBs in these cells (image c, arrow). In Ad5-infected cells, Ad5 fibre was located in nuclear aggregates (image f, arrow) and SMN was redistributed from CBs into nuclear rod-shaped structures (image g, arrow). Redistributed SMN partially colocalised with regions of fibre staining, as shown by the yellow regions in the overlay (image h, arrow). To confirm the colocalisation of SMN with viral assembly platforms, the experiment was repeated using a different SMN antibody and an antibody raised against a different Ad late protein, the penton base. As shown in Figure 3-20B, in Ad5-infected cells penton base was found in nuclear aggregates (image b, arrow) and SMN was redistributed into nuclear rod-shaped structures (image g, arrow). Redistributed SMN colocalised with penton base within the nucleus, as shown by the yellow regions in the overlay (image h, white arrow). However, accumulations of penton base at the nuclear periphery did not co-localise with SMN (image h, blue arrow). This indicated that during Ad5-infection, SMN partially associated with regions of virus assembly.

3.5 Defining the stage of infection during which CBs are rearranged

Considering the relatively large coding capacity of Ads and the expression of over 30 virus proteins, identifying potential Ad proteins responsible for the redistribution and/or degradation of a cellular protein is somewhat daunting. It would be logical to assume that expression of the causative viral protein would shortly be followed by the cellular effect in question. Therefore the time point during infection at which a cellular protein is redistributed may correlate with the initial expression of the causative viral protein. It is not currently known which, if any, Ad protein is responsible for CB redistribution during Ad5 infection, and the stage of infection at which CB redistribution occurs has not been precisely defined. Although CB rearrangement in Ad5-infected cells is known to be inhibited upon treatment with the DNA replication inhibitor cytosine arabinoside (AraC) (Rebelo *et al.*, 1996; Rodrigues *et al.*, 1996; James *et al.*, 2010), it

is not known whether the rearrangement is dependent on DNA replication itself or the expression of late proteins. The time point at which SMN is redistributed from CBs is also unknown. It cannot be assumed that SMN is redistributed at the same time as coilin, since SMN is non-essential for maintenance of CB architecture (Lemm *et al.*, 2006), and depletion of coilin results in accumulation of SMN in Gems, which appear as punctate nuclear structures similar to CBs (Tucker *et al.*, 2001). Therefore SMN could be redistributed from CBs at a different time point in infection to coilin, without any obvious impact on CB architecture. In this section, the stage of infection during which CB proteins are redistributed from CBs was investigated.

3.5.1 Treatment of Ad5-infected cells with cytosine arabinoside (AraC) to determine the time point of CB rearrangement relative to Ad DNA replication

Cytosine arabinoside (AraC) has long been used as a DNA replication inhibitor during virus infection (Gaynor *et al.*, 1982). As the Ad late phase occurs after the onset of DNA replication (Green *et al.*, 1970; Sharp *et al.*, 1974; Tibbetts *et al.*, 1974), the inhibition of DNA replication prevents progression to the later stages of infection. Therefore inhibiting DNA replication is a useful tool for determining whether a cellular process occurs during the early or late stages of Ad infection.

3.5.1.1 Inhibition of Ad5 DNA replication using AraC

In order to confirm that late protein expression was inhibited following AraC treatment, AraC at the optimised concentration (25 µg/ml) was added to mock- or Ad5-infected A549 cells at the same time as the Ad5 innoculum (Chapter 2.2.6.1) and incubated for 24 hours. Protein from whole cell lysates was separated by SDS-PAGE and analysed by Western blotting (Chapter 2.2.2). Membranes were incubated with an anti-DBP and an anti-penton base antibody as markers of early phase and late phase protein expression, respectively. An anti-GAPDH antibody was used as an internal loading control.

As shown in Figure 3-21, in the absence of AraC, there is expression of both DBP and penton base at 24 h.p.i. In the presence of AraC, penton base protein was not detected in Ad5-infected cells, whereas expression of DBP was unaffected. AraC treatment did not alter the levels of cellular proteins, as shown by the loading control GAPDH. This indicated that at the concentration used (25 µg/ml), AraC prevented the progression of the Ad5 lifecycle to the late phase without affecting the expression of early phase proteins or host cell proteins.

3.5.1.2 Immunofluorescence microscopy of Ad5-infected cells treated with AraC

To assess the impact of inhibition of DNA replication on the redistribution of CB components during Ad5 infection, A549 cells were treated with AraC at the same time as mock or Ad5
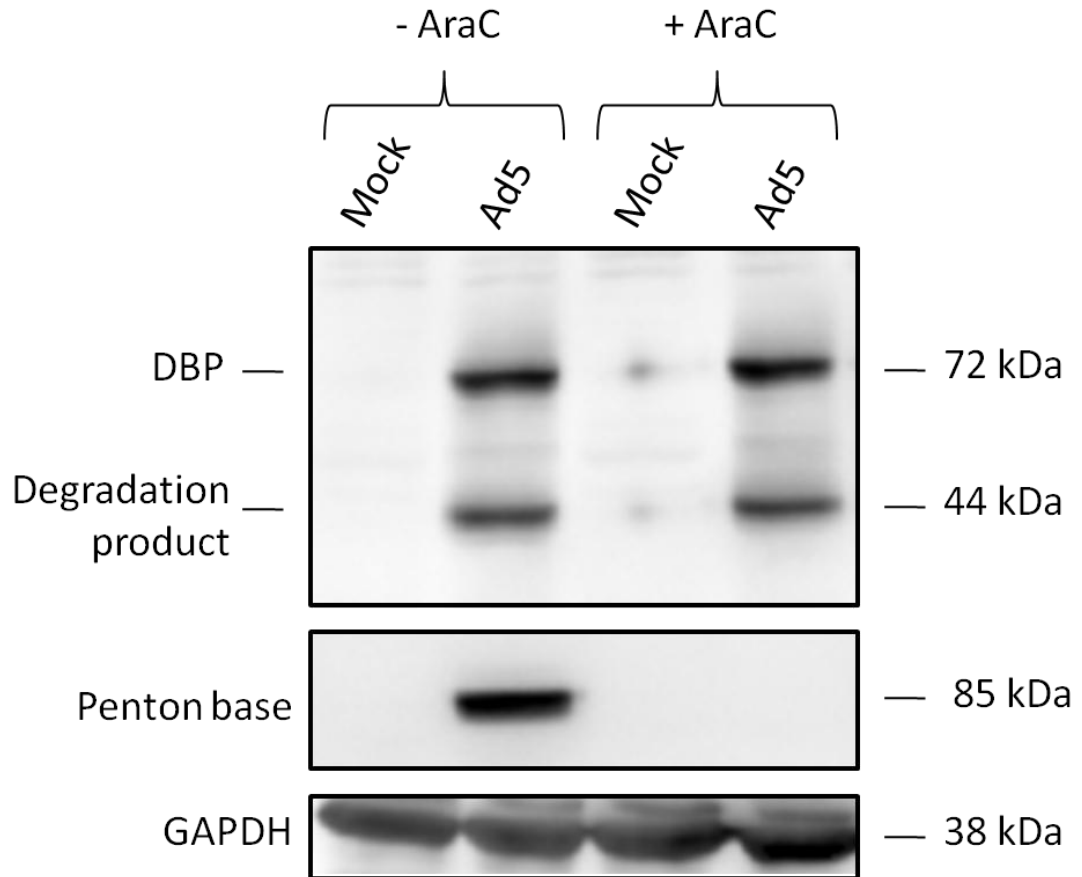
Figure 3-21. Inhibition of late phase protein expression in Ad5-infected A549 cells following treatment with the DNA replication inhibitor, cytosine arabinoside (AraC).

A549 cells were mock or Ad5 infected at an MOI of 5 FFU/cell in DMEM ('- AraC') or DMEM supplemented with 25 μg/ml AraC ('+ AraC'). At 24 h.p.i, whole cell lysates were prepared and equal masses of protein from each sample (20 μg) were separated by SDS-PAGE and analysed by Western blotting using a mouse anti-DBP, a rabbit anti-penton base or a mouse anti-GAPDH antibody followed by the appropriate secondary HRP-conjugate antibody. Bound antibody was detected using the ECL system and images were captured using a LAS 3000 imaging system. Mock-infected cells (in the presence or absence of AraC) were negative for Ad5 DBP and penton base expression. Ad5-infected cells in the absence of AraC were positive for both DBP and penton base expression at 24 h.p.i. Ad5-infected cells treated with AraC were positive for DBP expression, but were negative for penton base expression. These data showed that AraC treatment inhibited late but not early phase protein expression in Ad5-infected cells. AraC did not alter the protein levels of the internal loading control, GAPDH, in mock- or Ad5-infected cells.
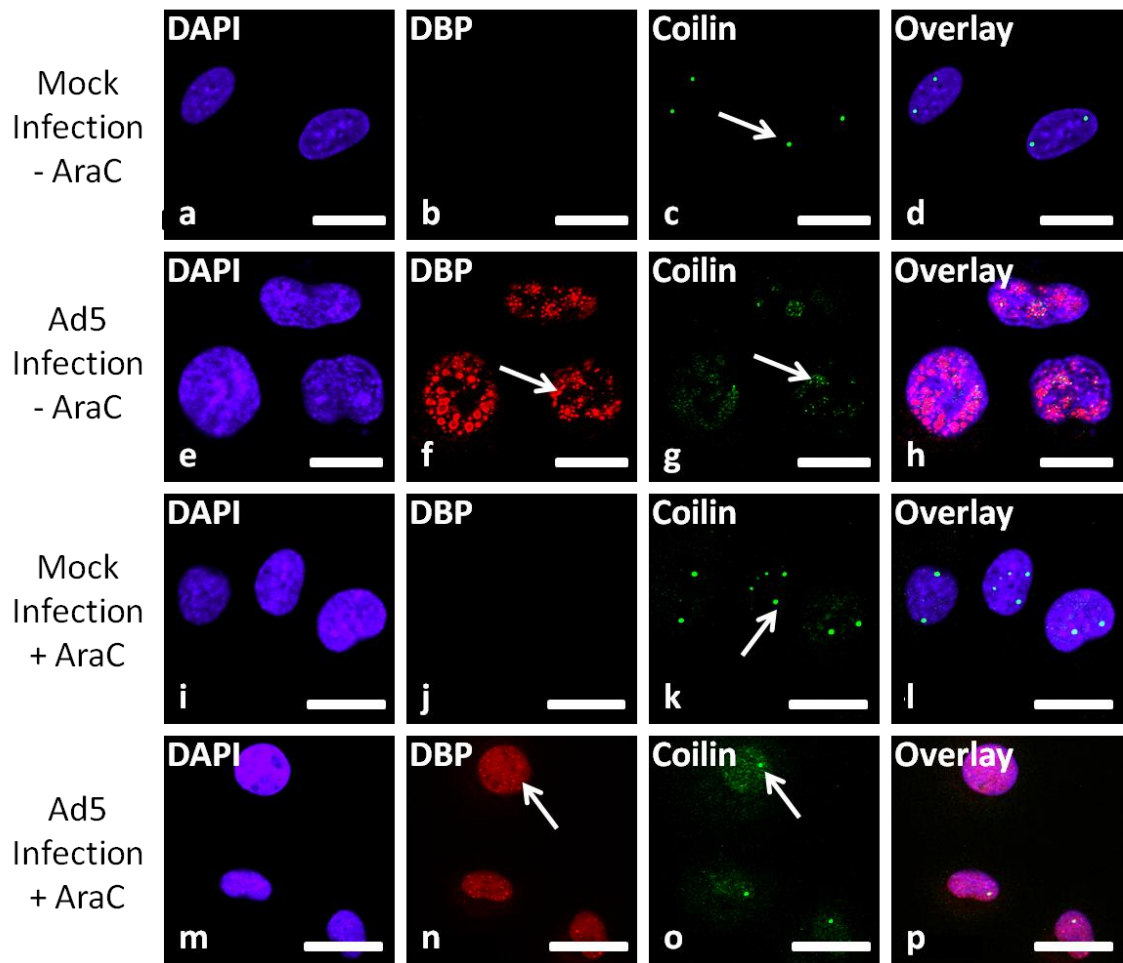
Figure 3-22. Prevention of coilin redistribution from CBs following treatment of Ad5-infected A549 cells with the DNA replication inhibitor, cytosine arabinoside (AraC).

A549 cells were mock or Ad5 infected at an MOI of 5 FFU/cell in DMEM ('- AraC') or DMEM supplemented with 25 µg/ml AraC ('+ AraC') and incubated for 24 hours. Cells were fixed and subjected to indirect immunofluorescence. Cells were incubated with a rabbit anti-DBP and a mouse anti-coilin antibody followed by incubation with the appropriate fluorescent-labelled secondary antibodies. Nuclei were stained using DAPI. Confocal microscopy was performed using an inverted LSM510 confocal microscope coupled to LSM Image Browser. In the absence of AraC, mock-infected cells were negative for DBP expression (image b) and coilin was located in punctate CBs (image c, arrow). In Ad5-infected cells in the absence of AraC, DBP was present in nuclear foci (image f, arrow) and coilin was redistributed into microfoci (image g arrow). In the presence of AraC, mock-infected cells were negative for DBP expression (image j) and coilin was found in punctate CBs (image k, arrow) which appeared indistinguishable from CBs seen in untreated, mock-infected cells (image c, arrow). Ad5-infected cells treated with AraC exhibited a diffuse nuclear localisation of DBP (image n, arrow) and coilin were retained in punctate CBs (image o, arrow). These data indicated that AraC treatment prevented the redistribution of coilin from CBs into microfoci in Ad5-infected cells. Bars = 20 µm.
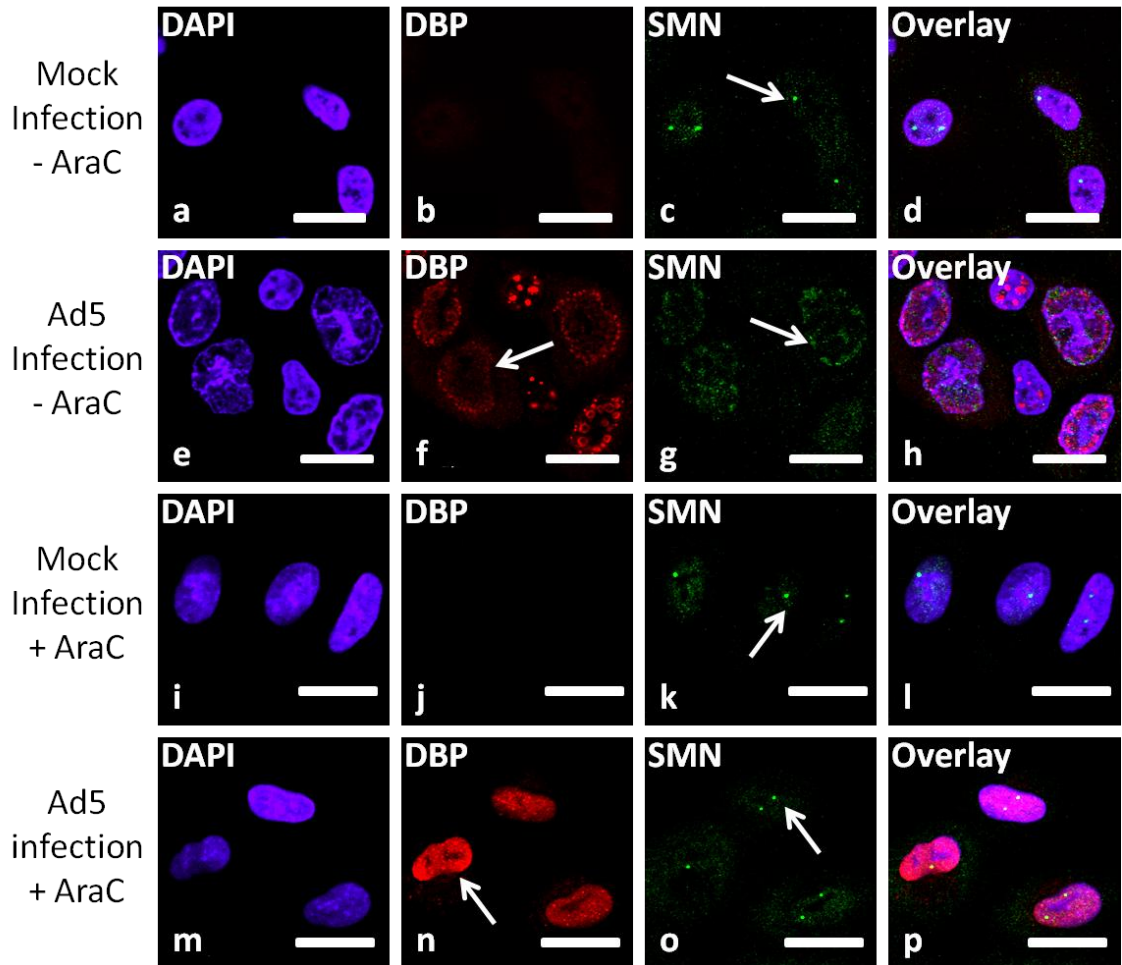
Figure 3-23. Prevention of SMN redistribution from CBs following treatment of Ad5-infected A549 cells with the DNA replication inhibitor, cytosine arabinoside (AraC).

A549 cells were mock or Ad5 infected at an MOI of 5 FFU/cell in DMEM ('- AraC') or DMEM supplemented with 25 µg/ml AraC ('+ AraC') and incubated for 24 hours. Cells were fixed and subjected to indirect immunofluorescence. Cells were incubated with a rabbit anti-DBP and a mouse anti-SMN antibody followed by incubation with the appropriate fluorescent-labelled secondary antibodies. Nuclei were stained using DAPI. Confocal microscopy was performed using an inverted LSM510 confocal microscope coupled to LSM Image Browser. In the absence of AraC, mock-infected cells were negative for DBP expression (image b) and SMN was located in punctate CBs (image c, arrow). In Ad5-infected cells in the absence of AraC, DBP was present in nuclear foci (image f, arrow) and SMN was redistributed into rod-shaped structures in the nucleus (image g, arrow). In the presence of AraC, mock-infected cells were negative for DBP expression (image j) and SMN was found in punctate CBs (image k, arrow) which appeared indistinguishable from CBs seen in untreated, mock-infected cells (image c, arrow). Ad5-infected cells treated with AraC exhibited a diffuse nuclear localisation of DBP (image n, arrow) and SMN was found in punctate CBs (image o, arrow). These data indicated that AraC treatment prevented the redistribution of SMN from CBs into rod-shaped nucleoplasmic structures in Ad5-infected cells. Bars = 20 µm.

infection (Chapter 2.2.6.1). At 24 h.p.i, cells were subjected to indirect immunofluorescence (Chapter 2.2.7) using an antibody raised against the CB protein in question (coilin or SMN) along with an anti-DBP antibody as a marker of Ad5-infected cells. DBP was chosen as the marker of Ad5-infected cells as this protein has a very different sub-nuclear distribution depending on the stage of infection. Prior to DNA replication, DBP appears diffusely in the nucleoplasm (Puvion-Dutilleul 1990a, 1990b). Upon DNA replication and transition into the intermediate/late phase, DBP was present in distinct, globular structures within the nucleus containing ssDNA intermediates (Puvion-Dutilleul 1990a, 1990b). As a result, DBP can be used to distinguish between Ad5-infected cells in the early phase of infection (diffuse DBP) from cells which are undergoing viral DNA replication (punctate, globular DBP).

As shown in Figure 3-22 and previously (James *et al.*, 2010), In mock-infected cells in the absence of AraC, there was no detectable DBP (image b) and coilin was located in CBs (image c, arrow). In Ad5-infected cells in the absence of AraC, DBP formed characteristic globular foci (image f, arrow) known to demark virus DNA replication centres (Puvion-Dutilleul 1990a, 1990b) and coilin was redistributed into rosettes (image g, arrow). In the presence of AraC, the mock-infected cells exhibited punctate CBs (image k, arrow) similar to those seen in untreated cells (image c, arrow). This suggested that AraC treatment did not have any effect on normal CB morphology in terms of alteration to the CB diameter. In Ad5-infected cells, the redistribution of coilin into rosettes was prevented in the presence of AraC; coilin remained in CBs (image o, arrow). This suggested that coilin redistribution from CBs is dependent on Ad DNA replication, as previously reported (Rebelo *et al.,* 1996; Rodrigues *et al.,* 1996; James *et al.,* 2010). As DNA replication was inhibited in these cells, the redistribution of DBP into the characteristic globular domains associated with viral DNA replication was also prevented; DBP was located diffusely in the nucleoplasm (image n, arrow), characteristic of its distribution in the early phase (Puvion-Dutilleul 1990a, 1990b).

The redistribution of SMN during Ad5 infection was also assessed in AraC-treated A549 cells (Figure 3-23). In untreated, mock-infected cells, there was no detectable DBP (image b) and SMN was located in punctate CBs (image c, arrow). In untreated, Ad5-infected cells, DBP formed large globular foci (image f, arrow) and SMN was redistributed into rod-shaped structures in the nucleus (image g, arrow). CBs in mock-infected cells treated with AraC displayed CBs analogous to those seen in untreated cells (compare image k [arrow] with image c [arrow]). In AraC-treated, Ad5-infected cells, the redistribution of SMN into nuclear rod-shaped structures was prevented; SMN remained within intact CBs (image o, arrow). This indicated that, as with coilin, the redistribution of SMN occurs after Ad DNA replication.

3.5.2 Treatment of Ad5-infected cells with cycloheximide (CHX) to determine dependence of CB rearrangement on late phase protein expression

Cycloheximide (CHX) is an inhibitor of protein biosynthesis and was previously used to inhibit the expression of late proteins during Ad infection when cells are treated during the intermediate phase (Horwitz *et al.*, 1973; Sohn and Hearing, 2011). Therefore, CHX treatment during the intermediate/late phase of infection can be used to distinguish whether a process is reliant upon Ad DNA replication or the expression of Ad late proteins.

3.5.2.1 Inhibition of Ad5 late phase protein expression using CHX

To verify the inhibition of late protein synthesis using CHX, A549 cells were mock or Ad5 infected and incubated for 12 hours (Chapter 2.2.6.1). At 12 h.p.i, the medium was exchanged for DMEM or DMEM supplemented with the optimised concentration of CHX (30 µg/ml) and cells were incubated for 6 hours (Sohn and Hearing, 2011). It was decided to remove the CHX media after 6 hours, as a similar level of protein inhibition was observed as for incubation with CHX for 12 hours, without the concomitant deleterious effects on cell morphology. The medium was exchanged for complete DMEM and incubated for a further 6 hours. Whole cell lysates were prepared and protein was separated by SDS-PAGE and analysed by Western blotting (Chapter 2.2.2). A mouse anti-DBP and a rabbit anti-penton base antibody were used as markers of early and late phase protein expression, respectively.

As shown in Figure 3-24, treatment of Ad5-infected cells with CHX prevented expression of the late phase penton base protein. There was also a substantial decrease in the level of early DBP protein; this was probably due to the fact that continued DBP expression would be prevented during the intermediate/late phase by treatment with CHX and, as the half life of DBP is around 5-7 hours (Neale and Kitchingman, 1989), this would result in a reduction in DBP levels by 24 h.p.i. As DBP is a necessary factor for Ad DNA replication (Lindenbaum *et al.*, 1986; Cleat and Hay, 1989), this reduction in DBP levels following CHX treatment may negatively impact DNA replication. This should be taken into account when analysing the impact of CHX treatment on the redistribution of CB proteins during Ad5 infection.

3.5.2.2 Immunofluorescence microscopy of Ad5-infected cells following CHX treatment

The impact of CHX treatment on the redistribution of CB proteins during Ad5 infection was assessed. A549 cells were mock or Ad5 infected (Chapter 2.2.6.1) and incubated for 12 hours. Cells were incubated with either complete DMEM or complete DMEM supplemented with CHX for 6 hours. The medium was replaced with complete DMEM and incubated for a further 6 hours before harvesting. Cells were subjected to indirect immunofluorescence (Chapter 2.2.2)
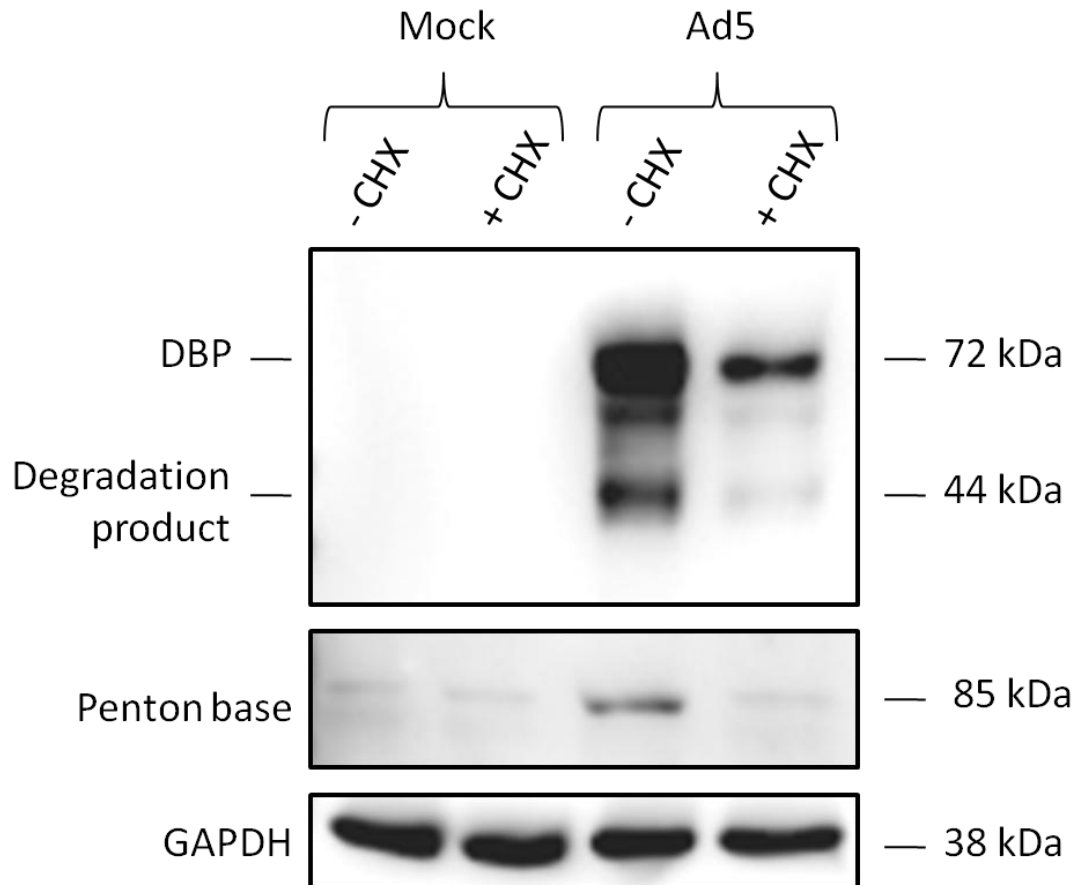
Figure 3-24. Inhibition of Ad5 late protein expression following treatment with the protein translation inhibitor, cycloheximide (CHX) from 12-18 h.p.i.

A549 cells were mock or Ad5 infected at an MOI of 5 FFU/cell and incubated for 12 hours. Cells were incubated with complete DMEM ('- CHX') or complete DMEM supplemented with 30 µg/ml CHX ('+ CHX') from 12 to 18 h.p.i. At 24 h.p.i, whole cell lysates were prepared and equal masses of protein (20 µg) were separated by SDS-PAGE and analysed by Western blotting. Bound antibody was detected using the ECL system and images were captured using a LAS 3000 imaging system. Mock-infected cells in the absence or presence of CHX did not express DBP or penton base. Ad5-infected cells that were not treated with CHX were positive for DBP and penton base expression at 24 h.p.i. Ad5-infected cells treated with CHX had reduced DBP expression at 24 h.p.i and were negative for penton base expression at this time point. CHX treatment did not alter the protein levels of the internal loading control, GAPDH, in mock- or Ad5-infected cells. These data indicated that CHX treatment of Ad5-infected cells reduced the level of early phase proteins and prevented expression of late phase proteins.
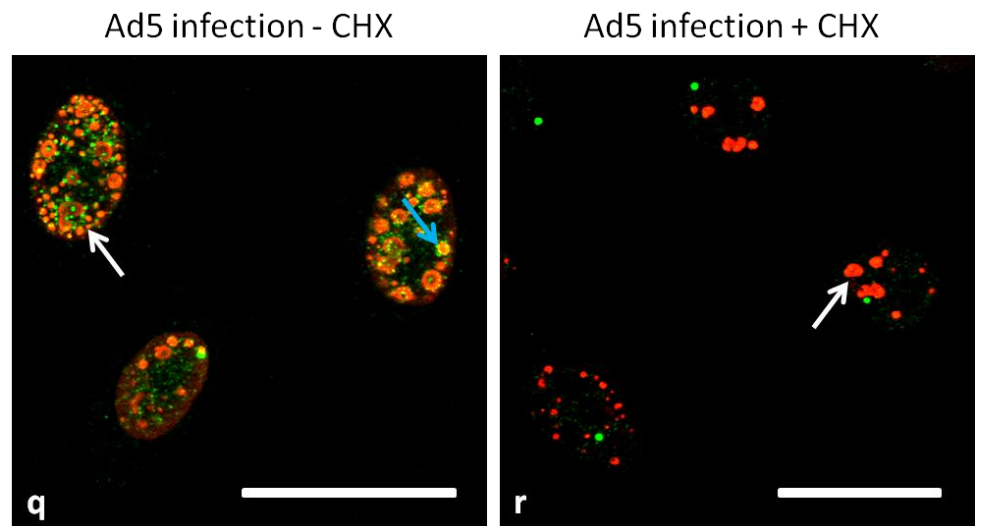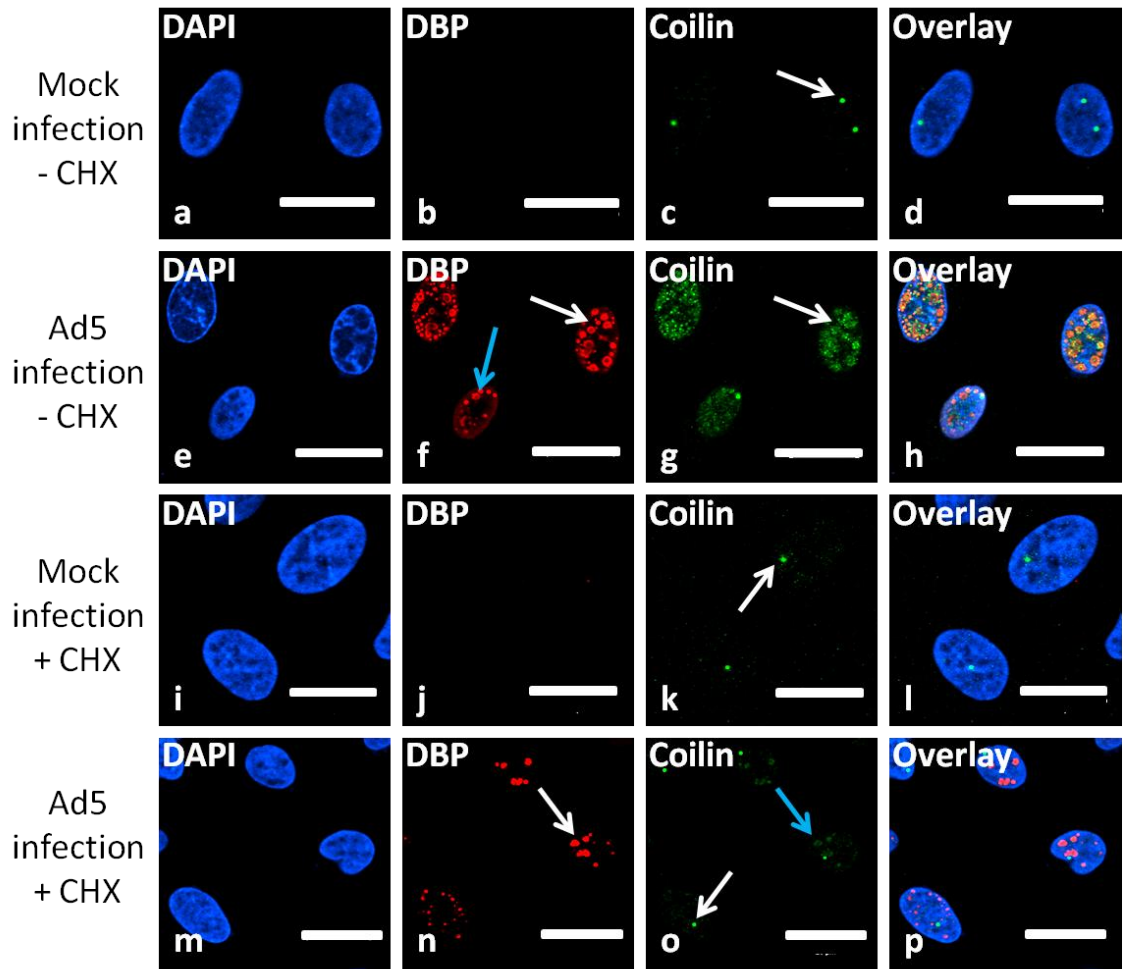
Figure 3-25. Prevention of coilin redistribution from CBs following treatment of Ad5-infected A549 cells with the protein translation inhibitor, cycloheximide (CHX) from 12-18 h.p.i

A549 cells were mock or Ad5 infected at an MOI of 5 FFU/cell. At 12 h.p.i, complete DMEM ('- CHX') or complete DMEM supplemented with 30 µg/ml CHX ('+ CHX') was added to the cells. Following a 6 hour incubation period, medium was replaced with fresh complete DMEM. Cells were fixed at 24 h.p.i and subjected to indirect immunofluorescence using a rabbit anti-DBP and a mouse anti-coilin antibody followed by incubation with the appropriate fluorescent-labelled secondary antibodies. Nuclei were stained using DAPI. Confocal microscopy was performed using an inverted LSM510 confocal microscope coupled to LSM Image Browser. In the absence of CHX, mock-infected cells were negative for DBP expression (image b) and coilin was located in CBs (image c, arrow). In Ad5-infected cells in the absence of CHX, DBP was present in the nucleus (image f), either in a limited number of large, bright foci (blue arrow; a distribution of DBP seen at earlier time points post-infection) or in numerous, smaller foci (white arrow; a distribution of DBP usually seen at later time points post-infection). In Ad5-infected cells, coilin was redistributed into microfoci (image g, arrow). As shown in the overlay, coilin microfoci typically surrounded DBP foci but did not colocalise with these structures (image q, white arrow); however, in some cells there was partial colocalisation of coilin foci around the periphery of DBP centres (image q, blue arrow). In the presence of CHX, mock-infected cells were negative for DBP expression (image j) and coilin was found in CBs (image k, arrow) which appeared indistinguishable from CBs seen in untreated, mock-infected cells (image c, arrow). In Ad5-infected cells treated with CHX, only the large, bright foci of DBP were seen (image n, arrow); there was no evidence of the numerous, smaller DBP foci usually seen at late time points post-infection. In Ad5-infected cells treated with CHX, coilin was retained in CBs (image o, white arrow) and was also present at low-level in adjacent, larger foci (image o, blue arrow). As shown in the overlay, coilin in these larger foci colocalised with DBP foci (image r, arrow). These data indicated that CHX treatment during the intermediate phase of Ad5-infection prevented redistribution of coilin from CBs into microfoci, and resulted in a partial accumulation of coilin in DBP-positive foci. Bars = 20 µm.
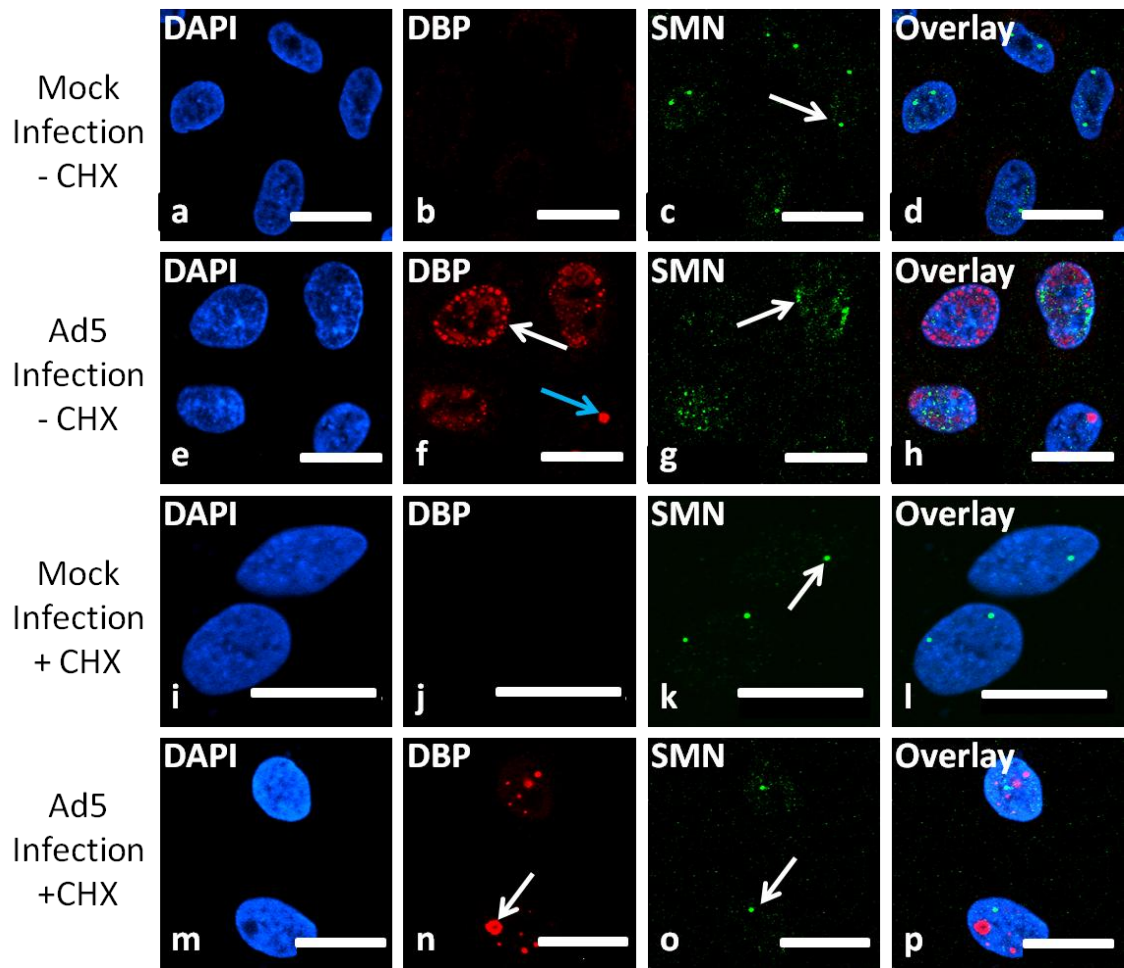
Figure 3-26. Prevention of SMN redistribution from CBs following treatment of Ad5-infected A549 cells with the protein translation inhibitor, cycloheximide (CHX) from 12-18 h.p.i.

A549 cells were mock or Ad5 infected at an MOI of 5 FFU/cell. At 12 h.p.i, complete DMEM ('- CHX') or complete DMEM supplemented with 30 µg/ml CHX ('+ CHX') was added to the cells; cells were incubated for 6 hours. Medium was replaced with fresh complete DMEM. Cells were fixed at 24 h.p.i and subjected to indirect immunofluorescence using a rabbit anti-DBP and a mouse anti-SMN antibody followed by incubation with the appropriate fluorescent-labelled secondary antibodies. Nuclei were stained using DAPI. Confocal microscopy was performed using an inverted LSM510 confocal microscope coupled to LSM Image Browser. In the absence of CHX, mock-infected cells were negative for DBP (image b) and SMN was located in CBs (image c, arrow). In Ad5-infected, untreated cells, DBP was present in the nucleus (image f), either in a limited number of large, bright foci (blue arrow; a distribution of DBP seen at early time points post-infection) or in numerous, smaller foci (white arrow; a distribution of DBP usually seen at late time points post-infection). In Ad5-infected, untreated cells, SMN was redistributed into nuclear rod-shaped structures (image g, arrow). Mock-infected, CHX-treated cells were negative for DBP (image j) and SMN was found in CBs (image k, arrow) which appeared indistinguishable from CBs seen in mock-infected, untreated cells (image c, arrow). In Ad5-infected, CHX-treated cells CHX, only the large, bright foci of DBP were seen (image n, arrow). SMN was retained in CBs in these cells (image o, arrow). These data indicated that CHX treatment during the intermediate phase of Ad5 infection prevented the redistribution of SMN from CBs. Bars = 20 µm.

115

using an anti-DBP antibody to identify Ad5-infected cells along with an antibody raised against the CB protein in question (coilin or SMN).

As shown in Figure 3-25, in mock-infected, untreated cells there was no detectable DBP (image b) and coilin was found in CBs (image c, arrow) and. In Ad5-infected, untreated cells, DBP formed large globular foci in the nuclei (image f, arrow) and coilin was redistributed into rosettes (image g, arrow). Treatment of mock-infected cells with CHX did not appear to affect the integrity of CBs in terms of CB diameter (compare image k [arrow] with image c [arrow]). Treatment of Ad5-infected cells with CHX prevented the formation of coilin rosettes (image o, arrow). This indicated that the redistribution of coilin from CBs to rosettes required protein synthesis in the late phase. Interestingly, coilin in the Ad5-infected, CHX-treated cells, coilin partially localised in Ad DNA replication centres with DBP (image r, arrow). This was in contrast to Ad5-infection of CHX-untreated cells, where coilin rosettes generally surrounded DBP-positive DNA replication centres (image q, white arrow) with some colocalisation of rosettes with DBP at the periphery of these domains (image q, blue arrow). This indicated that upon inhibition of intermediate/late phase protein expression in Ad5-infected cells, coilin is not redistributed into rosettes; instead, coilin remains within CBs and a subset of coilin becomes partially associated with Ad DNA replication domains.

The impact of CHX treatment on SMN redistribution during the late phase of Ad5 infection was also assessed (Figure 3-26). Mock-infected, untreated cells were negative for DBP (image b) and SMN was present in punctate CBs (image c, arrow). In Ad5-infected, untreated cells, DBP formed globular nuclear foci (image f, arrow) and SMN was redistributed into the nucleoplasm and into nuclear rod-shaped structures (image g, arrow). In mock-infected cells, CHX treatment did not alter the morphology of CBs in terms of CB diameter (image k, arrow). In Ad5-infected, CHX-treated cells, SMN remained within intact CBs (image o, arrow). This indicated that, as with coilin, protein synthesis in the late phase is required for the redistribution of SMN during Ad5 infection.

The formation of nuclear spot and ring structures by DBP is indicative of the onset of viral DNA replication and this was evident in untreated Ad5-infected cells (Figure 3-25 and Figure 3-26, image f) and CHX-treated, Ad5-infected cells (Figure 3-25 and Figure 3-26, image n). This indicated that viral DNA replication was still occurring in Ad5-infected cells treated with CHX. In the Ad5-infected, untreated cells, the globular accumulations of DBP exhibited two distinct structures. Early in the infectious cycle, DBP located in a small number of large, bright foci (Figure 3-25 and Figure 3-26, image f, blue arrow), whilst at a later stage DBP is predominantly found in more numerous, weaker staining accumulations (Figure 3-25 and Figure 3-26, image f,

white arrow). In the Ad5-infected, CHX-treated cells, only the large, bright, less numerous foci of DBP were present (Figure 3-25 and Figure 3-26, image n, white arrow) i.e. the morphology present at an early stage of infection. This suggested that the temporal shift in DBP morphology was slowed in CHX-treated cells. The altered morphology of DNA replication centres could also be due to the reduced protein levels of DBP following CHX treatment (Figure 3-24). In addition, CHX has been previously shown to inhibit Ad DNA replication (Sohn and Hearing, 2011), which could account for disrupted distribution of DBP, a protein required for Ad DNA replication. Further work is required to address these suggestions.

3.5.3 Rearrangement of CBs in relation to L4-33K expression

Ad5 L4-33K is expressed immediately following the initiation of Ad DNA replication (Akusjarvi, 2008; Morris *et al.*, 2010) and therefore represents the onset of intermediate gene expression. By co-staining Ad5-infected cells with an anti-L4-33K antibody alongside an antibody raised against a CB protein (coilin or SMN) CB re-arrangement relative to the expression of L4-33K can be determined. The presence or absence of L4-33K expression in Ad5-infected cells along with the sub-nuclear distribution of the CB protein can establish whether CB disassembly occurs prior to, or following, expression of L4-33K.

As shown in Figure 3-27A, mock-infected cells were negative for L4-33K (image b) and coilin was located in punctate CBs (image c, arrow) in these cells. At 24 h.p.i, the majority of Ad5-infected cells expressed L4-33K (image b, arrow) and exhibited a rosette distribution of coilin (image c, white arrow). Ad5-infected cells expressing L4-33K either exhibited intact CBs (image h, white arrow) or rosettes (image h, blue arrow). Interestingly, no cells were found to exhibit rosettes in the absence of L4-33K expression, indicating that coilin is redistributed after L4-33K expression. To quantify the redistribution of coilin relative to L4-33K expression, the following parameters were used: the presence or absence of L4-33K and the distribution of coilin ('CB' or 'rosette/speckled'). Three fields of 100 cells were counted from each sample and the experiment was repeated twice. As shown in Figure 3-27B, 53% of Ad5-infected cells were negative for L4-33K expression and exhibited CBs, indicating they are either uninfected cells or cells at an early stage of infection prior to L4-33K expression. The proportion of cells positive for L4-33K and rosettes was 39%. No cells were found to exhibit rosettes in the absence of L4-33K expression, whilst 7% of L4-33K-positive cells exhibited intact CBs. This suggested that during Ad5 infection, the expression of L4-33K preceded the redistribution of coilin into rosettes. Interestingly, coilin and L4-33K exhibited partial co-localisation in rosettes in the Ad5-infected cells (Figure 3-27A, image h, blue arrow), suggesting that L4-33K may be a component of rosettes in Ad5-infected cells.
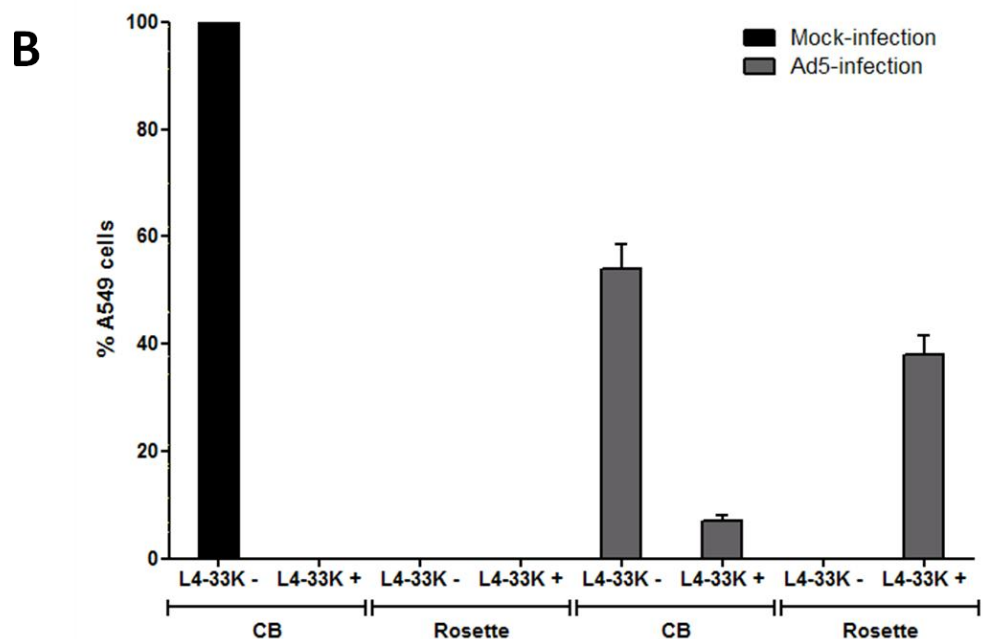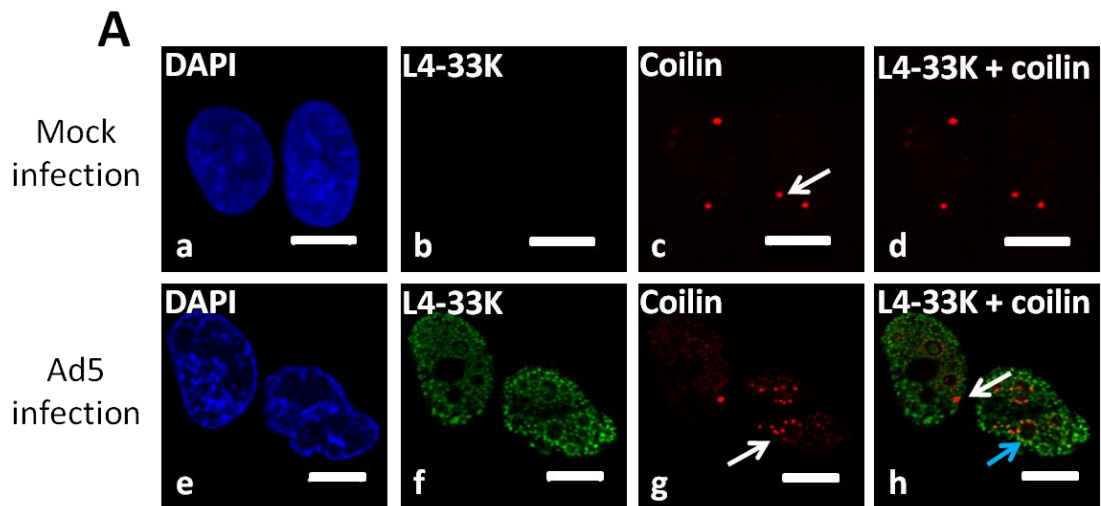
Figure 3-27. The redistribution of coilin during Ad5 infection relative to expression of Ad5 L4-33K.
Cells were mock or Ad5 infected at an MOI of 5 FFU/cell. At 24 h.p.i, cells were fixed and subjected to indirect immunofluorescence using a rabbit anti-L4-33K and a mouse anti-coilin antibody followed by incubation with the appropriate fluorescent-labelled secondary antibodies. Nuclei were stained using DAPI. Confocal microscopy was performed using an inverted LSM510 confocal microscope coupled to LSM Image Browser. A. Representative confocal microscopy images of coilin and L4-33K at 24 h.p.i. Mock-infected cells were negative for L4-33K (image b) and coilin was located in CBs (image c, arrow). In Ad5-infected cells, L4-33K (image f, arrow) and coilin (image g, arrow) were found in nuclear microfoci. As shown in the overlay (image h), cells expressing L4-33K exhibited coilin in CBs (white arrow) or in microfoci (blue arrow). No Ad5-infected cells contained coilin microfoci in the absence of L4-33K expression. Bars = 10 μm. B. Quantification of coilin and L4-33K distributions in Ad5-infected cells at 24 h.p.i. Cells were quantified using the following parameters: presence (+) or absence (-) of L4-33K and coilin distribution (CB or rosette). Three fields of 100 cells were counted from each coverslip. Results are the mean percentage of cells (± SEM) from three independent experiments.
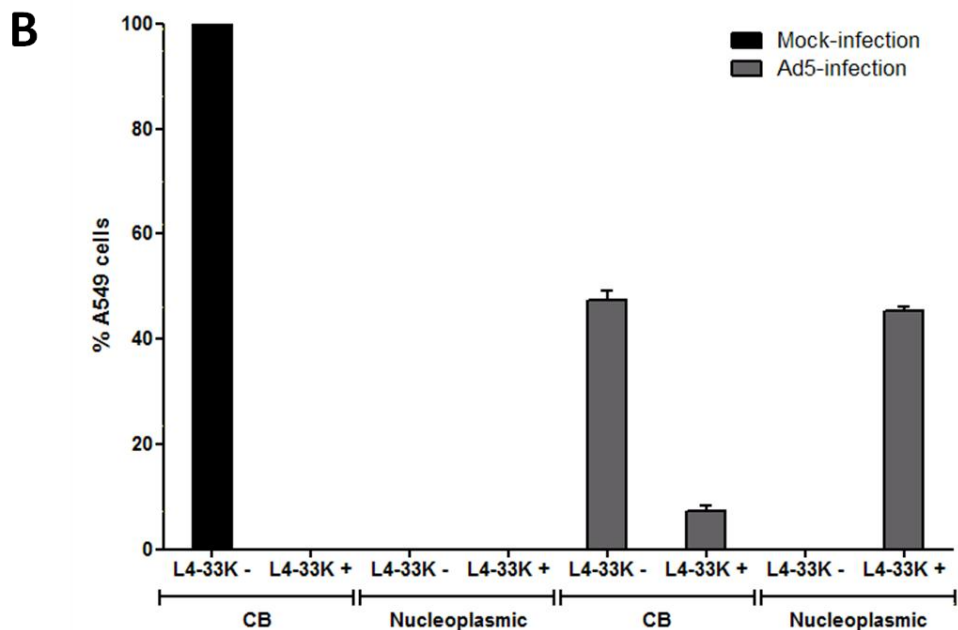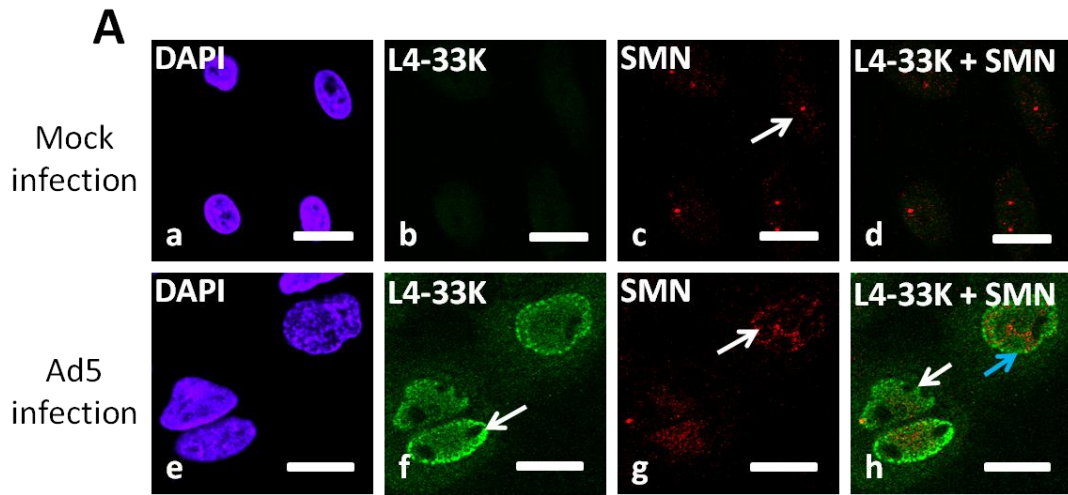
Figure 3-28. The redistribution of SMN during Ad5 infection relative to expression of Ad5 L4-33K.
Cells were mock or Ad5 infected at an MOI of 5 FFU/cell and incubated for 24 hours. Cells were fixed and subjected to indirect immunofluorescence. Cells were incubated with a rabbit anti-L4-33K and a mouse anti-SMN antibody followed by incubation with the appropriate fluorescent-labelled secondary antibodies. Nuclei were stained using DAPI. Confocal microscopy was performed using an inverted LSM510 confocal microscope coupled to LSM Image Browser. A. Representative confocal microscopy images of SMN and L4-33K at 24 h.p.i. Mock-infected cells were negative for L4-33K (image b) and SMN was located in CBs (image c, arrow). In Ad5-infected cells, L4-33K (image f, arrow) was found in nuclear microfoci and SMN was redistributed in the nucleoplasm (image g, arrow). As shown in the overlay (image h), cells expressing L4-33K exhibited SMN in CBs (white arrow) or nucleoplasmic SMN (blue arrow). No Ad5-infected cells contained redistributed SMN in the absence of L4-33K expression. Bars = 20 μm. B. Quantification of SMN and L4-33K distributions in Ad5-infected cells at 24 h.p.i. Cells were quantified using the following parameters: presence (+) or absence (-) of L4-33K and SMN distribution (CB or nucleoplasmic). Three fields of 100 cells were counted from each coverslip. Results are the mean percentage of cells (± SEM) from three independent experiments.

119

The redistribution of SMN in relation to L4-33K expression was also investigated. As shown in Figure 3-28A, Mock-infected cells did not express L4-33K (image b) and SMN was found in punctate CBs (image c, arrow). In Ad5-infected cells, there was a punctate distribution of L4-33K (image f, arrow) and SMN was redistributed within the nucleoplasm and into rod-shaped structures in the nucleus (image g, arrow). Ad5-infected cells expressing L4-33K either contain intact CBs (image h, white arrow) or redistributed SMN (image h, blue arrow). No cells exhibited redistributed SMN in the absence of L4-33K expression. The cells were quantified using the following parameters; the presence or absence of L4-33K and the distribution of SMN (CB or nucleoplasmic/diffuse SMN). Three fields of 100 cells were counted from each coverslip and this experiment was repeated three times. As shown in Figure 3-28B, 47% of Ad5-infected cells were negative for L4-33K expression and exhibited intact CBs, indicating they are either uninfected or at an earlier stage of the infectious cycle. The proportion of cells exhibiting L4-33K and redistributed SMN was 45%. Interestingly, no cells exhibited redistributed SMN in the absence of L4-33K expression, whilst 8% of cells exhibited intact CBs in L4-33K-positive cells. This suggested that, similar to the results obtained with coilin, the expression of L4-33K precedes the redistribution of SMN during Ad5 infection.

3.5.4 Ad5-induced CB redistribution in primary human keratinocytes

To date, the redistribution of CBs following species C Ad infection has only been reported in the cervical cancer cell line HeLa (Rebelo *et al.*, 1996; Rodrigues *et al.*, 1996; James *et al.*, 2010). Although cell lines are often good models for virus infection, the interaction of Ads with primary cells may be different to that of transformed cell lines. To address this question, CB distribution in Ad5-infected primary human keratinocytes was investigated.

To establish an infection time course of Ad5 in primary human keratinocytes, cells were mock or Ad5 infected (Chapter 2.2.6.1), whole cell lysates were prepared at 0, 4, 8, 12, 16, 24 and 48 h.p.i and protein was subjected to analysis by SDS-PAGE and Western blotting (Chapter 2.2.2). As found with A549 cells (Chapter 3.2), the first signs of CPE in the primary human keratinocytes were at 48 h.p.i, therefore this was the final time point at which cells were harvested. A mouse anti-DBP and a rabbit anti-penton base antibody were used to detect early and late phase protein expression, respectively. A mouse anti-GAPDH antibody was used as an internal loading control.

As shown in Figure 3-29, DBP was first detected at 12 h.p.i. Penton base was first detected at 24 h.p.i, with increased expression by 48 h.p.i. These results are similar to penton base expression in Ad5-infected A549 cells (Figure 3-1). These data indicated that the time course of
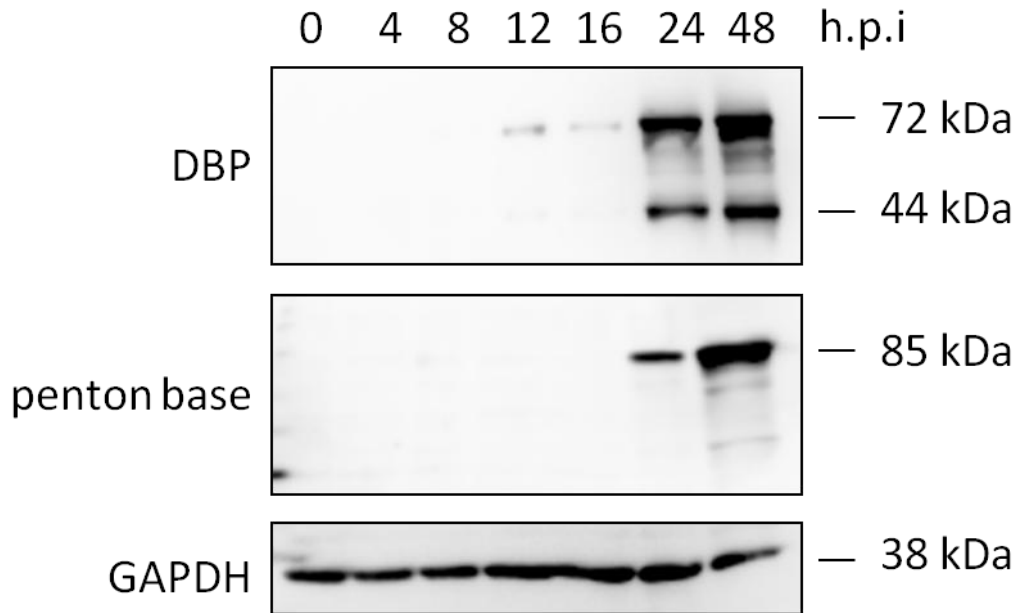
Figure 3-29. Ad5 infection of primary human keratinocytes.

A. A time course of Ad5 infection in primary human keratinocytes. Cells were mock or Ad5 infected at an MOI of 5 FFU/cell and incubated for 0, 4, 8, 12, 16, 24 or 48 hours. Whole cell lysates were prepared and equal masses of protein (20 μg) were separated by SDS-PAGE and analysed by Western blotting. Bound antibody was detected using the ECL system and images were visualised using a Las 3000 imaging system. DBP was first detected in the Ad5-infected cells at 12 h.p.i, with increased expression at 48 h.p.i. Penton base was first detected at 24 h.p.i, with increased expression at 48 h.p.i. Mock-infected cells at 24 h.p.i were negative for both DBP and penton base expression. Levels of the internal loading control, GAPDH, remained constant during the time course of Ad5 infection.
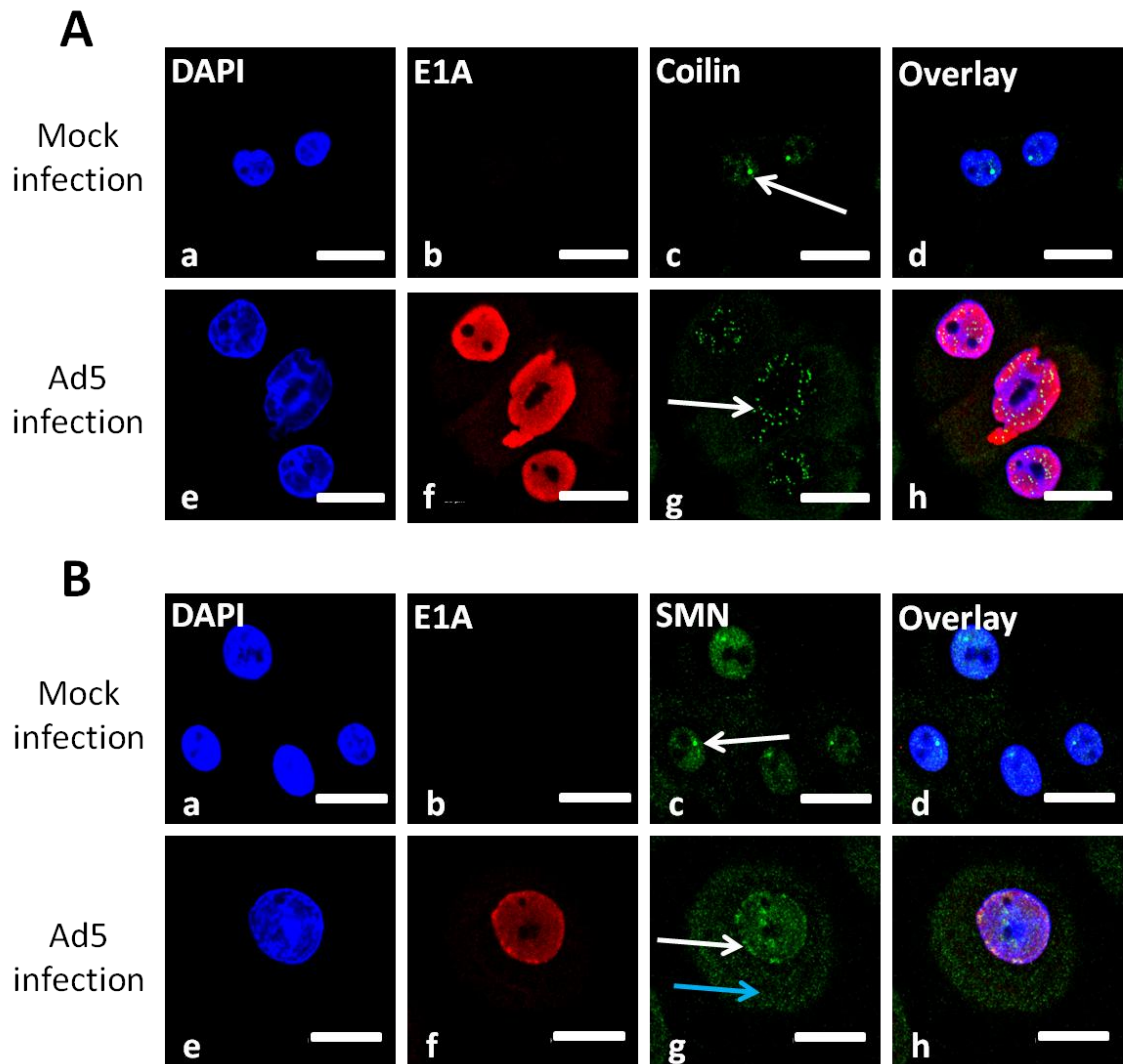
Figure 3-30. B. The redistribution of coilin and SMN following Ad5 infection of primary human keratinocytes.

Cells were mock or Ad5 infected at an MOI of 5 FFU/cell and incubated for 24 hours. Cells were fixed and subjected to indirect immunofluorescence using a rabbit anti-E1A antibody along with a mouse anti-coilin or a mouse anti-SMN antibody followed by incubation with the appropriate fluorescent-labelled secondary antibodies. Nuclei were stained using DAPI. Confocal microscopy was performed using an inverted LSM510 confocal microscope coupled to LSM Image Browser. A. The redistribution of coilin following Ad5-infection of primary human keratinocytes. Mock-infected cells were negative for E1A (image b) and coilin was found in CBs (image c, arrow). Ad5-infected cells were positive for E1A (image f, red cells) and coilin was redistributed from CBs into microfoci in these cells (image g, arrow). B. The redistribution of SMN following Ad5-infection of primary human keratinocytes. Mock-infected cells were negative for E1A (image b) and SMN was located in CBs (image c, arrow). Ad5-infected cells were positive for E1A (image f, red cells); SMN was redistributed into nuclear rod-shaped structures (image g, white arrow) and also exhibited increased cytoplasmic staining (image g, blue arrow). Bars = 20 μm.

Ad5 infection time course in primary human keratinocytes was similar to that observed in A549 cells. As the abundance of cells exhibiting rosette distribution of coilin in Ad5-infected A549 cells reached a peak at 24 h.p.i (Figure 3-1), it was reasoned that this would be an appropriate time point to study the redistribution of CBs in the primary human keratinocytes.

Primary human keratinocytes were mock or Ad5 infected (Chapter 2.2.6.1) and subjected to indirect immunofluorescence at 24 h.p.i (Chapter 2.2.7). Cells were stained using either a mouse anti-coilin or a mouse anti-SMN antibody along with a rabbit anti-E1A antibody to identify Ad5-infected cells. As shown in Figure 3-30A, mock-infected primary human keratinocytes were negative for E1A expression (image b) and coilin was located in large, punctate CBs in these cells (image c, arrow). Ad5-infected cells were positive for E1A expression (image f, red cells) and coilin was redistributed from CBs into rosettes in these cells (image g, arrow). These data are similar to results obtained with A549 cells (Figure 3-3) and previous data in HeLa cells (Rebelo *et al.*, 1996; Rodrigues *et al.*, 1996; James *et al.*, 2010). Therefore, in addition to the transformed cell lines HeLa and A549, the redistribution of coilin from CBs into rosettes also occurs during Ad5 infection of primary human keratinocytes.

The redistribution of SMN following Ad5 infection of primary human keratinocytes was also investigated (Figure 3-30B). Mock-infected primary human keratinocytes were negative for E1A expression (image b) and exhibited a punctate CB distribution of SMN (image c, arrow), with some nucleoplasmic and cytoplasmic staining. Ad5-infected primary human keratinocytes were positive for E1A staining (image f) and SMN was located in the nucleoplasm and in stronger-staining nucleoplasmic structures (image g, arrow), similar to that observed in Ad5-infected A549 cells when using the mouse anti-SMN antibody (Figure 3-6). However, there also appeared to be increased cytoplasmic staining of SMN in Ad5-infected primary human keratinocytes (image g, blue arrow); this was not observed in studies in Ad5-infected A549 cells using the mouse anti-SMN antibody (Figure 3-6). This indicated that whilst the Ad5-induced redistribution of SMN from CBs into stronger-staining structures in the nucleoplasm occurred in both primary human keratinocytes and A549 cells, the location of SMN in the cytoplasm may differ between these two cell lines. Further studies in these two cell lines with additional SMN antibodies would be required to confirm this. Taken together, these data obtained with primary human keratinocytes validate the CB redistribution data found in A549 cells. Furthermore, these data also validate A549 cells as an appropriate host-cell model for the study of Ad5 infection.
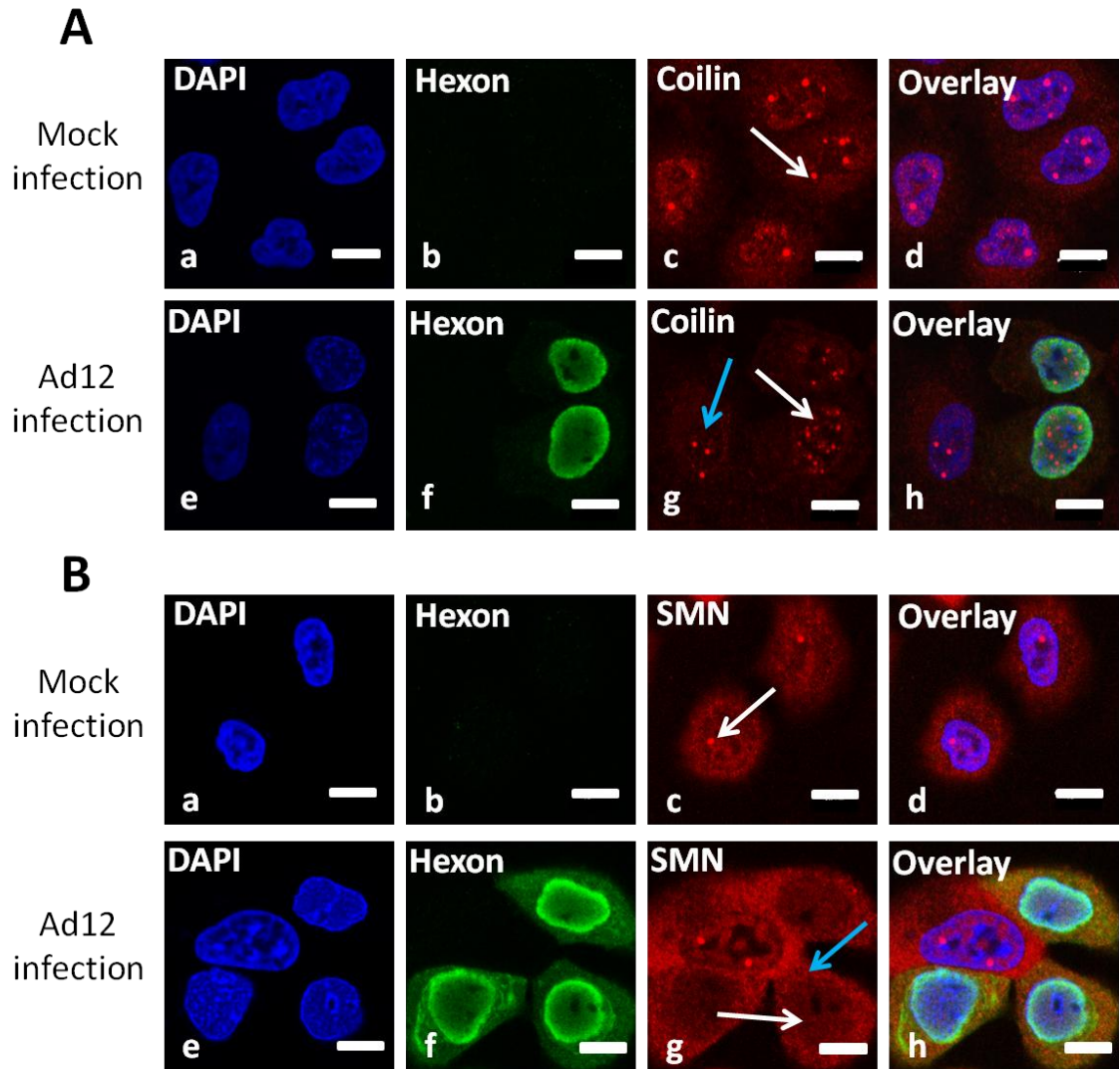
Figure 3-31. The redistribution of coilin and SMN following Ad12 infection of A549 cells.

A549 cells were mock or Ad12 infected at an MOI of 5 FFU/cell and incubated for 24 hours. Cells were fixed and subjected to indirect immunofluorescence. Cells were incubated with a mouse anti-hexon antibody along with a rabbit anti-coilin or a rabbit anti-SMN antibody followed by incubation with the appropriate fluorescent-labelled secondary antibodies. Nuclei were stained using DAPI. Confocal microscopy was performed using an inverted LSM510 confocal microscope coupled to LSM Image Browser. A. Redistribution of coilin following Ad12-infection of A549 cells. Mock-infected cells were negative for hexon expression (image b) and coilin was found in CBs (image c, arrow). Ad12-infected cells were positive for hexon (image f, green cells); these cells exhibited smaller, more numerous coilin foci in the nucleus (image g, white arrow) compared with CBs seen in uninfected cells (image g, blue arrow). B. Redistribution of SMN following Ad12-infection of A549 cells. Mock-infected cells were negative for hexon expression (image b) and SMN was found in CBs (image c, arrow). Ad12-infected cells were positive for hexon (image f, green cells); these cells exhibited nucleoplasmic SMN (image g, white arrow) and cytoplasmic SMN levels were increased (image g, blue arrow). Bars = 10 μm.
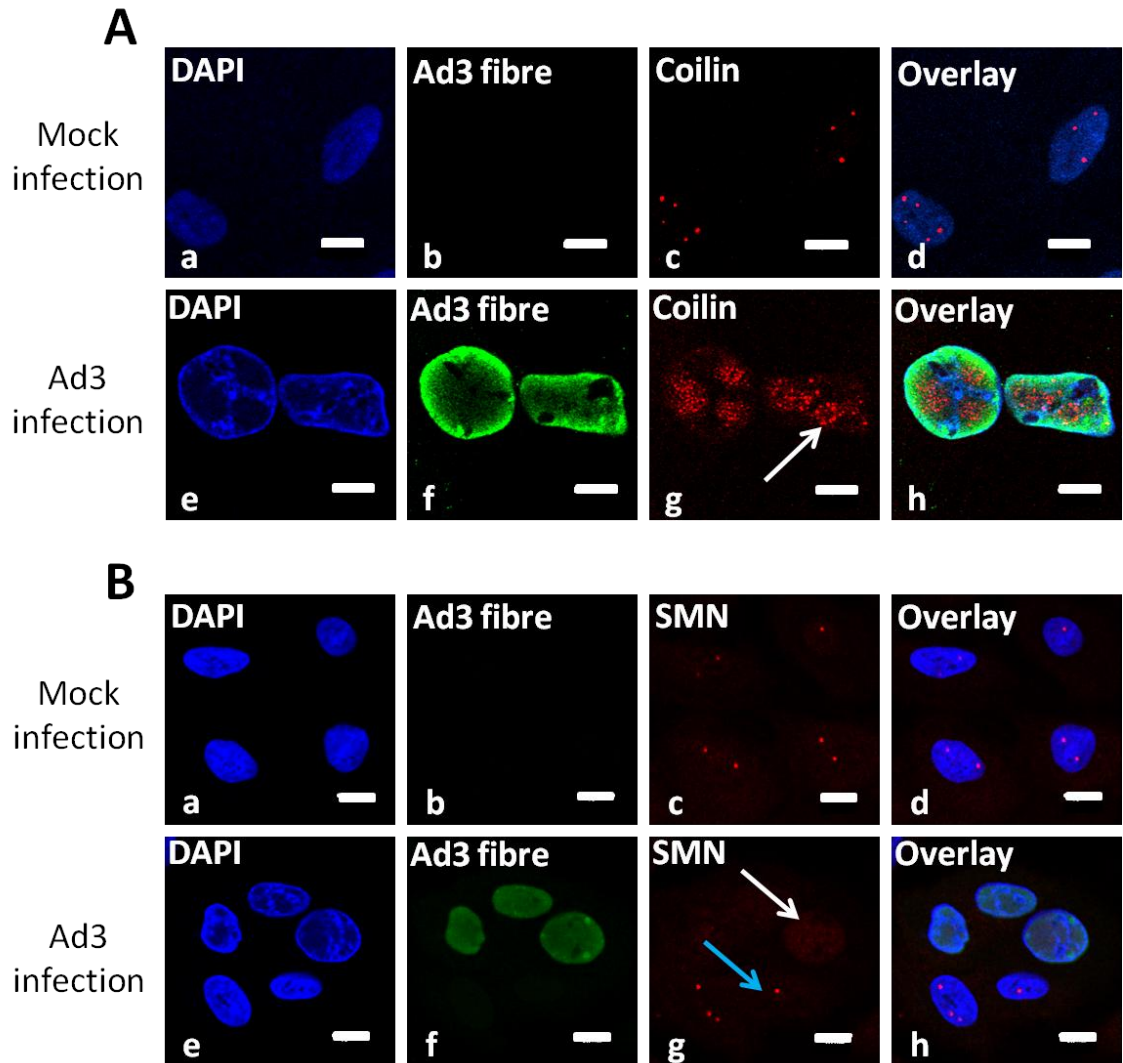
Figure 3-32. The redistribution of coilin and SMN following Ad3 infection of A549 cells.
A549 cells were mock or Ad3 infected at an MOI of 0.5 FFU/cell and incubated for 24 hours. Cells were fixed and subjected to indirect immunofluorescence. Cells were incubated with a rabbit anti-Ad3 fibre antibody along with a mouse anti-coilin or a mouse anti-SMN antibody followed by incubation with the appropriate fluorescent-labelled secondary antibodies. Nuclei were stained using DAPI. Confocal microscopy was performed using an inverted LSM510 confocal microscope coupled to LSM Image Browser. A. Redistribution of coilin following Ad3-infection of A549 cells. Mock-infected cells were negative for fibre expression (image b) and coilin was found in CBs (image c, arrow). Ad3-infected cells were positive for fibre (image f, green cells) and coilin was redistributed into nuclear microfoci (image g, arrow). B. Redistribution of SMN following Ad3-infection of A549 cells. Mock-infected cells were negative for fibre expression (image b) and SMN was found in CBs (image c, arrow). Ad3-infected cells were positive for fibre (image f, green cells); these cells exhibited a diffuse nucleoplasmic distribution of SMN (image g, white arrow) whereas in uninfected cells, SMN was located in CBs (image g, blue arrow). Bars = 10 μm (A) or 20 μm (B).

3.6 Analysis of CB redistribution during infection with Species A Ad12 and Species B Ad3 by immunofluorescence microscopy

To date, the redistribution of CBs has been characterised only in relation to infection with species C Ads (Rebelo *et al.*, 1996; Rodrigues *et al.*, 1996; James *et al.*, 2010). To investigate whether the redistribution of CB proteins was a conserved feature of infection by adenoviruses of other species, A549 cells were infected with Ad12 (Species A) or Ad3 (Species B) at an MOI of 5 or 0.5, respectively (Chapter 2.2.6.1). At 24 h.p.i, cells were subjected to indirect immunofluorescence (Chapter 2.2.7) using an anti-coilin or an anti-SMN antibody and an anti-Ad3 fibre or an anti-hexon antibody as markers of Ad3- and Ad12-infection, respectively.

As shown in Figure 3-31A, mock-infected cells were negative for hexon (image b) and coilin was found in CBs (image c, arrow) in these cells. Ad12-infected cells were positive for hexon (image f; green cells) and exhibited coilin microfoci in the nucleus (image g, white arrow) which appeared smaller in size than CBs found in uninfected cells (image g, blue arrow). These coilin microfoci did not form the regular, circular clusters seen in Ad5-infected cells (Figure 3-3), indicating that CB disassembly following Ad12 infection may differ to Ad5-infection.

Ad12-infected cells were also investigated for SMN redistribution (Figure 3-31B). Mock-infected cells were negative for hexon expression (image b) and SMN was located in CBs (image c, arrow) in these cells. Ad12-infected cells (image f, green cells) exhibited a diffuse distribution of SMN in the nucleus (image g, white arrow) and also strong SMN staining in the cytoplasm (image g, blue arrow). This contrasts with data in Ad5-infected cells, where SMN was redistributed into nuclear rod-shaped structures (Figure 3-6). However, these data with Ad12 were obtained using the rabbit anti-SMN antibody, which did not appear to stain the Ad5-induced rod-shaped structures as strongly as the mouse anti-SMN antibody (Figure 3-7).

The impact of Ad3 infection on the cellular localisation of coilin was investigated (Figure 3-32A). Mock-infected cells were negative for Ad3 fibre expression (image b) and coilin was located in punctate CBs in these cells (image c, arrow). Ad3 infection resulted in the expression of Ad3 fibre (image f, green cells) and the redistribution of coilin into rosettes (image g, arrow) which were very similar to those seen during Ad5 infection (Figure 3-3).

SMN distribution following Ad3 infection was also assessed (Figure 3-32B). Mock-infected cells were negative for Ad3 fibre (image b) and SMN was found within CBs in these cells (image c, arrow). Ad3-infected cells were positive for Ad3 fibre expression (image f, green cells) and exhibited a diffuse nucleoplasmic distribution of SMN (image g, white arrow). In contrast, the Ad3 fibre-negative cells (image f, blue arrow) exhibited CB distribution of SMN

(image g, blue arrow). These data showed that SMN was redistributed from CBs into the nucleoplasm during Ad3 infection. However, there was no evidence of increased cytoplasmic staining as seen with Ad12, nor were there concentrated regions of SMN in rod-shaped structures within the nucleus, as seen with Ad5.

Taken together, these data indicated that CB disassembly may be a conserved mechanism amongst adenoviruses, since infection with Ads from species A (Ad12), species B (Ad3) and species C (Ad5) all induced CB disassembly. However, the coilin microfoci formed during Ad12 infection appeared to differ from those formed during infection with Ad5 or Ad3, indicating that the interaction of Species A viruses with coilin may differ to that of Ads 3 and 5. Moreover, the redistribution of SMN from CBs appeared to differ in all three viruses: Ad5 induced rearrangement of SMN into nuclear rod-shaped structures, Ad3 infection resulted in diffuse nuclear SMN whilst Ad12 infection redistributed SMN diffusely within the nucleus and into the cytoplasm. This indicated that these viruses all interact with SMN in different ways.

3.7 Chapter 3 Discussion

The Cajal body (CB) is a multifunctional sub-nuclear body involved in the maturation and biogenesis of spliceosome components (reviewed in Morris, 2008). During Ad5 infection, the marker protein of CBs, p80 coilin, is redistributed into numerous microfoci (Rebelo *et al.*, 1996; Rodrigues *et al.*, 1996; James *et al.*, 2010). In order to begin an analysis of the function of coilin microfoci (termed 'rosettes'), the redistribution of coilin was investigated relative to known nuclear substructures by indirect immunofluorescence. Rosettes were not associated with PML-NBs or nucleoli, suggesting that rosettes are not involved in functions related to these nuclear bodies. Rosettes appeared to enclose viral DNA replication centres and were surrounded by sites of splicing, as reported previously (James *et al.*, 2010). It would be logical to consider that due to their close proximity to regions of splicing, rosettes may simply act as a local snRNP processing factory during Ad5 infection. However, unlike conventional CBs, rosettes do not contain snRNPs, indicating that rosettes do not function as sites for spliceosome subunit maturation (Bridge *et al.*, 1993a; Rebelo *et al.*, 1996). Taken together, these data indicated that rosettes may be providing a currently undefined function during Ad5 infection that is potentially distinct from normal CB function.

Interestingly, it has recently been shown that CB proteins are involved in diverse cellular processes aside from snRNP maturation. Coilin was suggested to play a role in DNA damage responses (Morency *et al.*, 2007; Gilder *et al.*, 2011). Ads have been shown to disrupt components of the DNA damage response pathway during infection; the E1B-55K/E4orf6 complex ubiquitinates and targets the MRN complex for degradation in order to prevent

concatemerisation of the Ad genome and the subsequent inhibition of DNA replication (Stracker *et al.*, 2002; Araujo *et al.*, 2005; Liu *et al.*, 2005). Therefore it is possible that CB disruption during Ad5 infection may be a mechanism to subvert coilin-mediated DNA damage responses. Indeed, analysis of coilin protein levels during Ad5 infection revealed that coilin levels are reduced by 48 h.p.i (Figures 3-1 and 3-2), indicating that coilin may be targeted for degradation during Ad5 infection. However, if coilin was a restrictive factor during Ad5 infection, coilin depletion might be expected to enhance Ad5 infection; previous data suggested that coilin depletion resulted in decreased production of Ad5 late proteins and reduced the virus titre (James *et al.*, 2010). This indicates that rather than being a restrictive factor, coilin may be required for a productive infection. Further work will be required to define the precise role of coilin during Ad5 infection and to clarify whether coilin is a target of the E1B-55K/E4orf6 ubiquitin ligase complex.

In contrast to coilin, spliceosomal snRNPs are redistributed into nucleoplasmic ring structures following Ad5 infection (Bridge *et al.*, 1993a; Rebelo *et al.*, 1996). This indicated that the trafficking of snRNPs to CBs was abrogated during Ad5 infection. However, the impact of Ad5 infection on the snRNP chaperone proteins SMN and WRAP53 was unknown. Immunofluorescence microscopy of Ad5-infected cells revealed that WRAP53 was redistributed into rosettes along with coilin (Figure 3-5). In striking contrast, SMN was redistributed from CBs into the nucleoplasm and nuclear rod-shaped structures (Figure 3-6). This indicated that SMN plays a different role to the CB proteins found in rosettes (coilin, fibrillarin and WRAP53) during Ad5 infection. Indeed, previous work has shown that protein components of other nuclear substructures (such as PML-NBs and nucleoli) are also redistributed to different nuclear domains during Ad infection in order to facilitate diverse functions (Puvion-Dutilleul and Christensen, 1993; Muller and Dejean, 1999; Matthews, 2001; Zhao *et al.*, 2003). For example, the nucleolar protein C23 (nucleolin) is redistributed into the cytoplasm, possibly to subvert the transcriptional-repressive properties of C23 (Matthews, 2001). In contrast, another nucleolar protein, B23, is sequestered into viral replication centres and appears to promote viral replication, possibly by aiding the assembly of viral chromatin or progeny virions (Okuwaki *et al.*, 2001; Lawrence *et al.*, 2006; Samad *et al.*, 2007; Samad *et al.*, 2012; Ugai *et al.*, 2012). Therefore different CB proteins may be redistributed to different subnuclear regions in order to promote distinct functions during a productive Ad5 infection.

In order to facilitate identification of the function of these novel SMN-containing domains, the redistribution of SMN was assessed relative to known nuclear domains. Immunofluorescence analysis of SMN redistribution in Ad5-infected cells revealed there was some overlap between redistributed SMN and sites of splicing (Figure 3-11). However, due to the nucleoplasmic

distribution of SMN and transcription/splicing factors during the later stages of Ad5 infection, it is possible that their partial colocalisation may simply be a result of their mutual nucleoplasmic distribution rather than a specific association. Interestingly, SMN has previously been reported to be involved in splicing regulation by both indirect and direct mechanisms (Pellizzoni *et al.*, 1998; Mourelatos *et al.*, 2001; Pellizzoni *et al.*, 2002; Zhang *et al.*, 2008; Makarov *et al.*, 2012). Further investigation is required to define a potential role of SMN in Ad splicing. It should be noted that snRNPs are not a definitive marker of active splicing since in uninfected cells under steady state conditions they are located diffusely within the cell and concentrate within CBs, which are not sites of active splicing (Bridge *et al.,* 1993a). Therefore, in order to more accurately identify an association between SMN and regions of active splicing during Ad5 infection, further immunofluorescence microscopic analyses using an antibody against an essential splicing factor such as SRSF2 is warranted.

In addition to partial colocalisation with regions of splicing, SMN also colocalised with regions of virus assembly (Figure 3-20). This indicated that SMN is involved in assembly of Ad virions. Intriguingly, the SMN complex has previously been implicated in virion assembly during infection with minute virus of mice (MVM) (Young *et al.,* 2002a, b; 2005). It is possible that the SMN complex is hijacked during Ad infection to facilitate assembly of progeny virions. Further work will be required to determine whether SMN plays a role in Ad virion assembly.

Identifying the stage of Ad infection at which a protein is redistributed may also aid with identification of its function. In this chapter, the redistribution of both coilin and SMN was prevented when DNA replication was inhibited (Figure 3-22 and Figure 3-23), suggesting that progression to the intermediate and late phase of infection is required for redistribution of coilin and SMN. CB redistribution was also prevented when Ad5-infected cells were treated with CHX during the late phase of infection (Figure 3-25 and Figure 3-26), indicating that protein synthesis in the late phase may be required for CB redistribution. Finally, the redistribution of both coilin and SMN appeared to occur after the expression of L4-33K (Figure 3-27 and Figure 3-28), indicating that CB disassembly occurs during the intermediate/late phase of Ad5 infection. These data indicated that both coilin and SMN may be targeted for redistribution by intermediate and/or late phase Ad protein(s), possibly to facilitate a currently undefined function during the later stages of the Ad lifecycle.

Although collectively these data give a strong argument for CB disassembly occurring during the intermediate/late phase, there were some limitations to these studies. CHX treatment resulted in a decreased accumulation of Ad DBP (Figure 3-24), an essential factor for Ad DNA replication. Furthermore, DNA replication centres appeared to have an altered morphology

following CHX treatment (Figure 3-25 and Figure 3-26). Indeed, CHX has been previously reported to directly inhibit Ad DNA replication (Sohn and Hearing, 2011). Therefore it should be noted that the observed inhibition of CB redistribution following CHX treatment may be due to DNA replication inhibition by CHX rather than inhibition of protein synthesis in the late phase. In addition, it was previously reported that treatment of HeLa cells with CHX induced the redistribution of CBs into microfoci (Rebelo *et al.*, 1996). The lack of CB fragmentation observed in the current experiment may be due to the removal of CHX-containing media at 18 h.p.i, allowing recovery of CB architecture by the time the cells were fixed (Rebelo *et al.*, 1996). Alternatively, the concentration of CHX used in this study (30 µg/ml) was lower than that used by Rebelo *et al* (100 µg/ml), therefore it is possible that CB reorganisation did not occur at this lower CHX concentration. Further work is required to address these suggestions.

CHX treatment was found to result in the partial co-localisation of coilin with Ad5 DBP in Ad DNA replication centres (Figure 3-25). This indicated that in the absence of late protein expression, coilin became associated with regions of Ad DNA replication. It is possible that the location of coilin in DNA replication domains is prevented during late phase infection by the interaction of coilin with a late Ad protein, resulting in redistribution of CB into rosettes rather than in replication centres. Further work will be required to determine whether coilin interacts with any Ad late phase proteins and/or early Ad proteins involved in DNA replication.

It was found in this study that disassembly of CBs occurred after the expression of L4-33K. This is in contrast to previous published data, which suggested that CB disassembly occurred prior to the L4-33K expression (James *et al.*, 2010). The discrepancy between these data and the published data may be due to differences in the virus titres used (an MOI of 1000 FFU/cell [James *et al.,*] versus MOI of 5 FFU/cell [in this study]) or the different cell lines used (HeLa [James *et al.,*] versus A549 [in this study]). In addition, the exposures used on the confocal microscope may have impacted on the results. Setting a too low exposure for L4-33K may result in cells expressing low levels of L4-33K to appear negative for L4-33K. This could result in some cells appearing to exhibit rosettes in the absence of L4-33K expression. The reciprocal may also occur; too low an exposure for coilin may not detect the rosette structures, which are generally much smaller than normal CBs. This could result in some cells appearing to be positive for L4-33K but negative for rosettes. However, the latter is less likely as these cells would appear to express no coilin at all, which would register as unusual. For the acquisition of these data, the exposures for both coilin and L4-33K were carefully adjusted by firstly optimising the exposures for L4-33K and coilin in the Ad5-infected cells, to ensure detection of coilin rosettes and cells expressing low-level L4-33K. The mock-infected cells were then used to check for over-exposure of coilin or non-specific background staining of L4-33K. The results

of this careful optimisation gave a strong argument for the rearrangement of coilin following expression of L4-33K. However, it should be noted that the anti-L4-33K antibody used may also detect L4-22K (Ostapchuk *et al.*, 2006), therefore the redistribution of CBs was likely shown relative to expression of L4-33K and/or L4-22K, rather than L4-33K alone.

To date, the redistribution of CB proteins has only been assessed in the cancer cell line HeLa (Rebelo *et al.*, 1996; Rodrigues *et al.*, 1996; James *et al.*, 2010). HeLa cells contain integrated HPV-18 DNA (Gey *et al.*, 1952); this is not ideal for the study of viral infection as expression of HPV-18 oncogenes in these cells may interfere with cellular processes. In this study, the impact of Ad5 infection on the subcellular distribution of CB proteins was assessed in the non-virally transformed cell line, A549. Coilin was redistributed following Ad5 infection of A549 cells in a manner very similar to results previously obtained in HeLa cells (Figure 3-3). Redistribution of coilin and SMN also occurred following Ad5-infection of primary human keratinocytes (Figure 3-30). This indicated that the observed effects on CB proteins following Ad5 infection of cancer cell lines are also applicable to Ad5 infection of primary cells.

Finally, the redistribution of CB proteins has previously only been assessed in cells infected with the species C Ads 2 and 5 (Rebelo *et al.*, 1996; Rodrigues *et al.*, 1996; James *et al.*, 2010). In this study, the redistribution of the CB proteins coilin and SMN was assessed following infection with the Species A virus Ad12 and the Species B virus Ad3. Coilin was redistributed into microfoci following infection with both Ad3 and Ad12. Although SMN was redistributed into the nucleoplasm following infection with Ad3 and Ad12, the nuclear rod-shaped accumulations of SMN observed during Ad5 infection were not evident during infection with Ad3 or Ad12. Furthermore, Ad12 infection resulted in increased cytoplasmic SMN staining. However, only one time point post-infection was observed (24 h.p.i) and it is possible that the kinetics of infection with these viruses may differ to that of Ad5. Therefore it is possible that the appearance of the nuclear-peripheral SMN structures may occur at a different time post-infection and so may have been missed in this study. Further work will be required to confirm this. Either way, these data indicated that the redistribution of CBs is a conserved event during Ad infection, suggesting that CB disassembly is an important process during the Ad lifecycle.

Interestingly, other viruses have also been shown to redistribute coilin from CBs into microfoci, including GRV, Influenza B virus (IBV) and HCMV (Kim *et al.,* 2007, Canetta *et al.,* 2008, Salsman *et al.,* 2008). However, the impact of infection with these viruses upon SMN distribution has not been established. It would be interesting to establish whether SMN is also redistributed into the nucleoplasm following infection with these viruses. It would also be tempting to identify the impact of virus infection on less well-characterised nuclear

substructures such as nSBs and cleavage bodies. As cleavage bodies have been shown to have a close association with CBs (Schul *et al.*, 1996; Schul *et al.*, 1999b; Li *et al.*, 2006b), establishing the impact of Ad infection on the cleavage body is particularly appealing.

In conclusion, the novel data from this investigation showed that during Ad5 infection, WRAP53 was redistributed from CBs into microfoci alongside coilin whilst SMN was redistributed to a novel nuclear domain. The redistribution of both coilin and SMN occurred during the intermediate/late phase of infection. Coilin microfoci did not co-localise with other well-characterised nuclear substructures or marker proteins. SMN partially colocalised with regions of splicing and virus assembly. The redistribution of CBs was conserved across Ad species A, B and C. Further work is now required to characterise the functions of SMN and the CB proteins redistributed to rosettes (coilin, WRAP53 and fibrillarin) during Ad infection.

Chapter 4 – Characterising the role of coilin during Ad5 infection

4.1 Introduction

In Chapter 3, the Ad5-induced rearrangement of the CB factors coilin, fibrillarin, WRAP53, snRNPs and SMN was characterised. It was found that coilin, fibrillarin and WRAP53 were redistributed into nuclear microfoci ('rosettes') during the intermediate/late phase of Ad5 infection. This indicated that these CB proteins may play important roles during the late phase of Ad infection. Moreover, previous data suggested a potential role for coilin in Ad late phase protein expression (James *et al.*, 2010). However, the mechanism by which coilin regulates Ad late protein expression is currently unknown. This chapter will focus on defining the role of coilin during Ad5 infection.

An effective, frequently used method of studying the role of a protein in a particular cellular process is to deplete the protein from the cell by treatment with small inhibitory RNA (siRNA). These RNAs are complementary in sequence to the target mRNA and have a distinct structure of double-stranded 21-23bp RNA with two nucleotide protrusions at the 3′ end (Elbashir *et al.*, 2001). When transfected into the cell, they associate in an ATP-dependent mechanism with a large multimeric complex known as the RNA-induced silencing complex (RISC) which functions to guide the siRNA to its complementary RNA target sequence (Nykanen *et al.*, 2001). The double-stranded molecule unwinds, the reverse complementary strand remains associated with the RISC and degradation of the target mRNA is stimulated by exo- and endonucleases (Martinez *et al.*, 2002). In this Chapter, depletion of cellular coilin was achieved by siRNA treatment and the impact on Ad virus titre, Ad protein levels and Ad mRNA levels was determined.

4.2 Analysis of coilin depletion using siRNA

The most appropriate time point after siRNA transfection at which to infect the cells with Ad5 was established. Transfection with coilin siRNA (siCoilin) or scrambled control siRNA (siControl) (Table 2-2) was performed in A549 cells (Chapter 2.2.5.1) and cells were incubated for 24 hours or 48 hours. By 48 h.p.i, the cells had reached 90-100% confluency; a further time point of 72 hours was not taken as the cells would have been over-confluent by this time and the viability of the cells may have been compromised as a result. Protein in whole cell lysates was separated by SDS-PAGE and analysed by Western blotting (Chapter 2.2.2).

As shown in Figure 4-1A, at 24 hours post-siRNA transfection the level of coilin protein in siCoilin-treated cells had decreased to around 60% of the level in siControl-treated cells. By 48 hours post-transfection, coilin levels in siCoilin-treated cells had further decreased to around 40% of the level in siControl-treated cells. From these data, it was decided that Ad5 infection would be carried out at 24 hours post-transfection, whereby a sufficient proportion of coilin
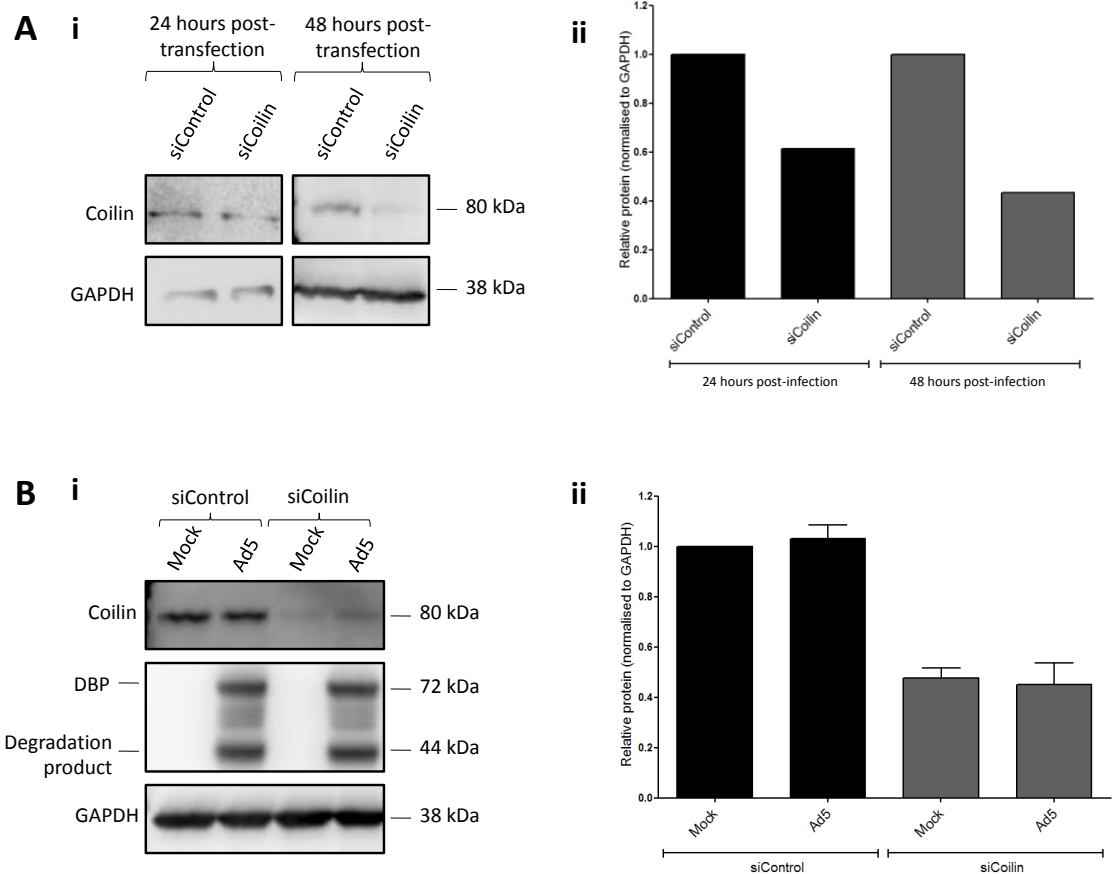
Figure 4-1. The depletion of coilin in A549 cells following siRNA treatment.

A. Coilin levels at 24 and 48 hours post-siRNA transfection. Cells were treated with siControl or siCoilin and incubated for 24 or 48 hours. Whole cell lysates were prepared and equal masses of protein (20 μg) from each sample were separated by SDS-PAGE and analysed by Western blotting. Bound antibody was detected using the ECL system and images were captured using a LAS 3000 Imager. Signal intensities from Western blots were calculated by densitometric analysis and were normalised to the signal intensity of the loading control, GAPDH. Results are displayed relative to the siControl-treated, mock-infected sample, which was set to a value of 1. i. Western blots of coilin levels. Compared with siControl-treated cells, coilin levels in siCoilin-treated cells were reduced at 24 hours post-transfection, with further reduction at 48 hours. ii. Densitometric analysis of coilin levels. Compared with siControl-treated cells, coilin levels in siCoilin-treated cells were decreased at 24 and 48 hours post-transfection by approximately 40% and 60%, respectively. B. Coilin levels at 48 hours post-siRNA transfection following Ad5 infection at 24 hours post-siRNA transfection. Cells were treated with siControl or siCoilin and incubated for 24 hours. Cells were mock or Ad5 infected at an MOI of 5 FFU/cell and incubated for 24 hours. Whole cell lysates were prepared and protein was analysed as described above. i. Western blots of coilin levels. Compared with siControl-treated cells, coilin levels were reduced in cells treated with siCoilin. Coilin levels were reduced to a similar extent in siCoilin-treated, mock-infected cells and in siCoilin-treated, Ad5-infected cells. ii. Densitometric analysis of coilin levels. Compared with siControl-treated, mock-infected cells, coilin levels were reduced in siCoilin-treated, mock-infected cells and siCoilin-treated, Ad5-infected cells by 53% and 55%, respectively.

would be depleted from cells (around a 40% decrease) and cells would be harvested at 48 hours post-transfection (24 h.p.i), when coilin levels had decreased by around 60% compared to siControl-treated cells.

The impact of Ad5 infection on the efficiency of coilin depletion was also assessed. Ad VA-RNAs have previously been shown to inhibit RNA silencing during the late phase of Ad infection by abrogating the functions of the RISC complex and Dicer, a endoribonuclease enzyme responsible for cleavage of double-stranded RNA (dsRNA) and pre-miRNA into siRNA (Andersson *et al.*, 2005). Therefore it was possible that Ad infection might affect the efficiency of coilin depletion by siRNA treatment. To investigate this possibility, siRNA transfection was performed in A549 cells using siControl or siCoilin (Chapter 2.2.5.1) and incubated for 24 hours. Cells were mock or Ad5 infected (Chapter 2.2.6.1) and incubated for a further 24 hours. Whole cell lysates were prepared, protein was separated by SDS-PAGE and analysed by Western blotting (Chapter 2.2.2).

As shown by the representative Western blots in Figure 4-1B, siCoilin treatment appeared to reduce protein levels of coilin by a similar factor in both mock- and Ad5-infected cells. This observation was confirmed by densitometric analysis of the protein band intensities; in comparison to siControl-treated, mock infection, siCoilin treatment reduced coilin levels in mock- and Ad5-infected cells to 47% and 45%, respectively (Figure 4-1B). There was no significant difference in the level of coilin depletion achieved in Ad5-infected cells compared to mock-infected cells. This indicates that Ad5 infection at 24 hours post-transfection does not alter the level of coilin depletion by 48 hours post-transfection.

4.3 Impact of coilin depletion on cell growth/viability using the MTT assay

Previously published data reported a significant reduction in proliferation in coilin-depleted HeLa cells, although cells still appeared to be viable (Lemm *et al.*, 2006). To assess the impact of coilin depletion on the viability and proliferation of A549 cells, the MTT assay was used as described in Chapter 2.2.9. The sensitivity of the MTT assay was assessed; serial dilution of A549 cells results in a linear, dilution-dependent decrease in the concentration of formazan detected (Appendix Figure 7). This indicated that the degree of change in formazan concentration directly correlates with the degree of change in the number/viability of the cells.

As analysis on a plate reader requires the experiment to be carried out in 96-well plates, where the wells are very small, it was more practical to perform the siRNA transfection in parallel with cell plating ('reverse siRNA transfection') rather than growing cells to the desired confluency on a small surface area (conventional siRNA transfection). In order to determine whether coilin
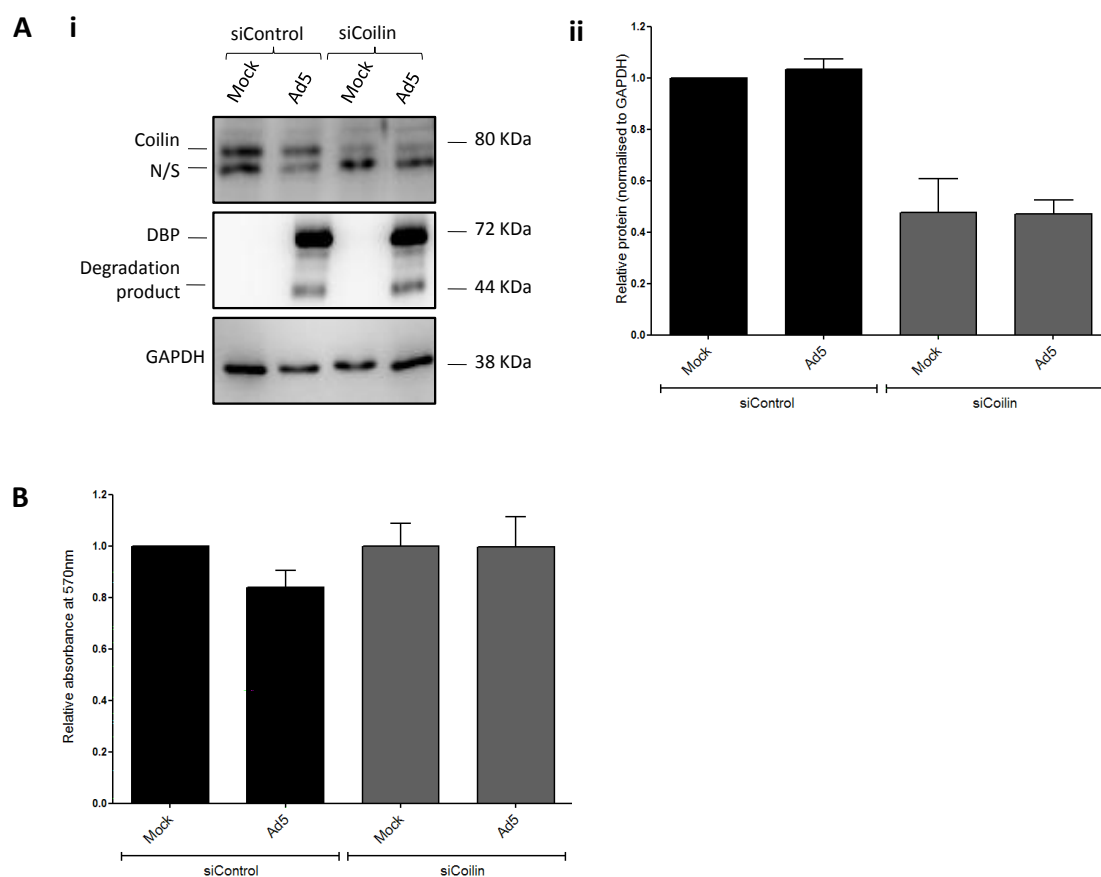
Figure 4-2. The impact of coilin depletion on the cell growth and/or viability of A549 cells.

A. 'Reverse' siRNA transfection and Ad5 infection of A549 cells. Cells were subjected to 'reverse' siRNA transfection using siControl or siCoilin and incubated for 24 hours. Cells were mock or Ad5 infected at an MOI of 5 FFU/cell and incubated for 24 hours. Whole cell lysates were prepared and equal masses of protein from each sample (20 μg) were separated by SDS-PAGE and analysed by Western blotting. Bound antibody was detected using the ECL system and images were captured using a Las 3000 Imager. Signal intensities from Western blotting were quantified by densitometric analysis and were normalised to the signal intensity of the loading control, GAPDH. Results are displayed as the mean fold change in protein level (± SEM) from three independent experiments. Results are displayed relative to the siControl-treated, mock-infected sample, which was set to a value of 1. Compared with siControl-treated cells, coilin levels were decreased to a similar extent in siCoilin-treated, mock-infected cells and siCoilin-treated, Ad5-infected cells. Quantification of coilin levels by densitometric analysis showed that compared with siControl-treated, mock-infected cells, coilin levels in siCoilin-treated, mock-infected cells and siCoilin-treated, Ad5 infected cells were reduced by 57% and 58%, respectively. n/s – non-specific cross-reacting protein species. B. MTT assay of A549 cells following coilin depletion and Ad5 infection. Results are displayed as the mean fold change in absorbance at 570 nm (± SEM) from three independent experiments. Data is displayed relative to the siControl-treated, mock-infected sample, which was set to a value of 1. Statistics were calculated using the paired 1-sample t-test. There was no significant change in absorbance at 570 nm in siCoilin-treated cells compared with siControl treated cells, indicating that siCoilin treatment does not affect the cell viability.

had been depleted to a similar level following 'reverse siRNA transfection' as compared to conventional siRNA transfection, 'reverse siRNA transfection' was carried out on A549 cells in 6-well plates (Chapter 2.2.5.2). Following a 24 hour incubation, cells were mock or Ad5 infected (Chapter 2.2.6.1). At 24 h.p.i, whole cell lysates were prepared, protein was separated by SDS-PAGE and analysed by Western blotting (Chapter 2.2.2). As shown in Figure 4-2Ai, 'reverse' siCoilin-treatment resulted in a decrease in coilin protein levels compared to siControl-treated cells. This decrease was calculated from densitometric analysis (Figure 4-2Bii) as 57% and 58% for mock- and Ad5-infected cells, respectively. This is very similar to the depletion of coilin achieved following the conventional siRNA transfection procedure (reductions of 53 and 55% respectively; Figure 4-1B). This indicates that the efficiency of depletion achieved is similar between these two methods.

Once the 'reverse siRNA transfection' procedure had been validated, 'reverse siRNA transfection' was performed on A549 cells in 96-well plates (Chapter 2.2.5.2). Following a 24 hour incubation, cells were mock or Ad5 infected (Chapter 2.2.6.1). At 24 h.p.i, cells were harvested and analysed by the MTT assay (Chapter 2.2.9). As shown in Figure 4-2Bii, the absorbance at 570 nm was not significantly altered compared to siControl treated, mock infected cells. This suggested that depletion of coilin to around 40% of siControl-treated cells did not affect either cell proliferation or viability.

4.4 The impact of coilin depletion on the cellular levels of other CB proteins

Coilin has been shown to interact with multiple protein partners including SMN, WRAP53 and SmB′, a component of the SMN complex (Hebert *et al.*, 2001; Mahmoudi *et al.*, 2010). It is possible that depletion of coilin may alter the levels of coilin-interacting proteins or proteins associated with the CB. If this is the case, any impact of coilin depletion on Ad5 infection could be indirectly due to alteration to the levels of a coilin-associated protein, rather than being a direct result of reduced coilin levels. To assess this possibility, the level of coilin-interacting or associated CB proteins (coilin, SMN, WRAP53, Sm and fibrillarin) following siRNA treatment (Chapter 2.2.5.1) and mock or Ad5 infection (Chapter 2.2.6.1) was assayed by SDS-PAGE and Western blotting (Chapter 2.2.2).

As shown by the Western blots in Figure 4-3A, depletion of coilin did not appear to significantly alter the levels of SMN, WRAP53, Sm or fibrillarin. This was confirmed by densitometric analysis of protein levels (Figure 4-3B). This indicated that coilin depletion did not significantly alter the cellular protein levels of SMN, WRAP53, fibrillarin or Sm.
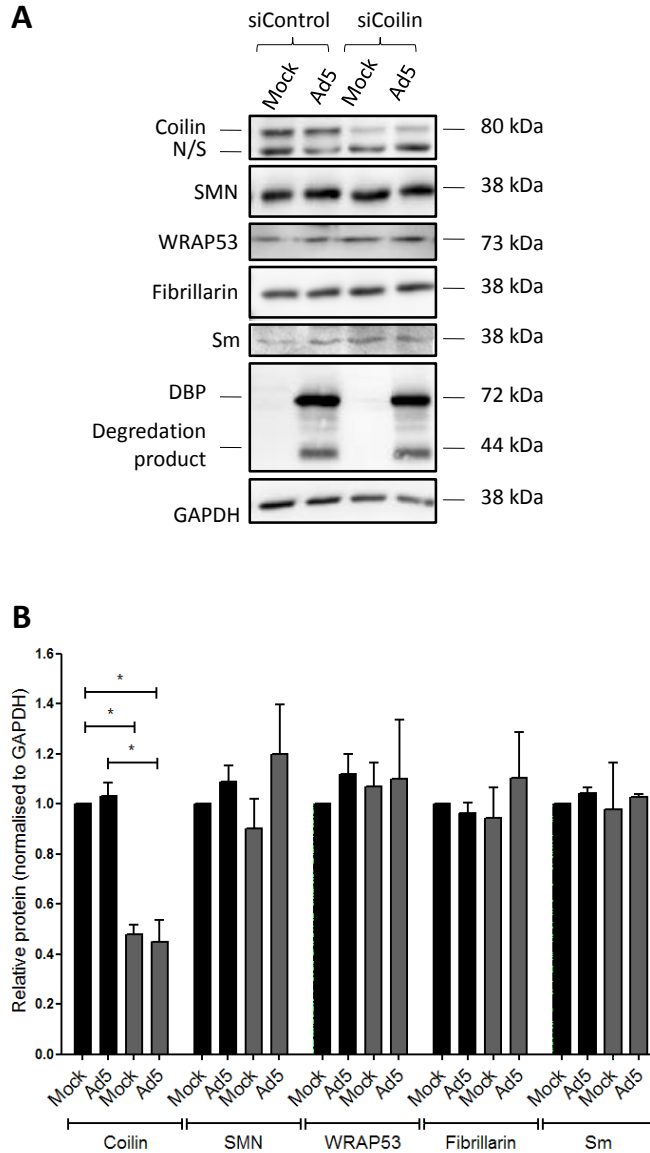
Figure 4-3. Western blot analysis of CB protein levels following coilin depletion and Ad5 infection.
A549 cells were treated with siControl or siCoilin and incubated for 24 hours. Cells were mock or Ad5 infected at an MOI of 5 FFU/cell and incubated for 24 hours. Whole cell lysates were prepared and equal masses of protein from each sample (20 μg) were separated by SDS-PAGE and analysed by Western blotting. Bound antibody was detected using the ECL system and images were captured using a LAS 3000 imaging system. Signal intensities were calculated by densitometric analysis and were normalised to the signal intensity of the internal loading control, GAPDH. A. Representative western blots of CB proteins. Compared with siControl-treated cells, levels of coilin were reduced in siCoilin-treated cells whilst levels of SMN, WRAP53, fibrillarin and Sm were not affected. N/S – non-specific cross-reacting protein species. B. Densitometric analyses of signal intensities from Western blotting. Results are the mean fold change in protein level (± SEM) from three independent experiments, displayed relative to the siControl-treated, mock-infected sample, which was set to a value of 1. Compared with siControl-treated cells, coilin levels were significantly reduced in siCoilin-treated cells whilst levels of SMN, WRAP53, fibrillarin and Sm were not affected. Black bars = siControl-treatment. Grey bars = siCoilin-treatment.
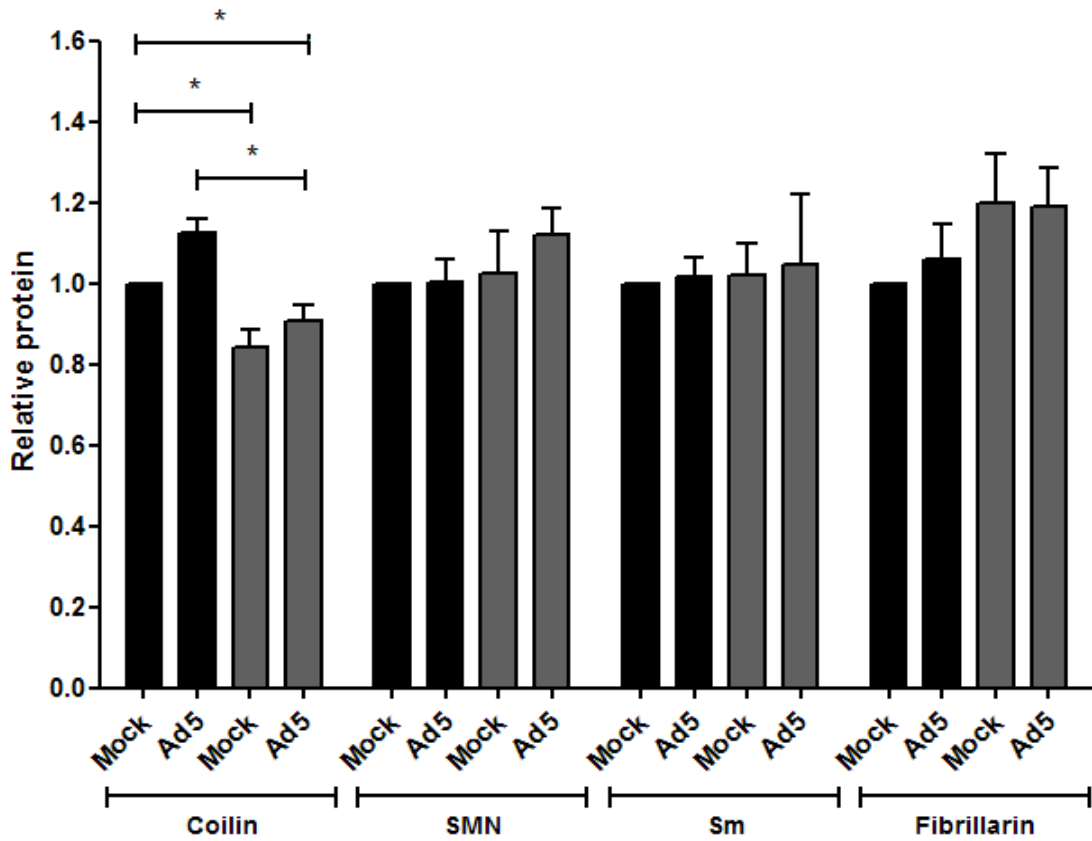
Figure 4-4. Flow cytometric analysis of CB proteins following coilin depletion and Ad5 infection.
A549 cells were transfected with siControl or siCoilin and incubated for 24 hours. Cells were mock or Ad5 infected and incubated for a further 24 hours. Cells were harvested and subjected to flow cytometric analysis. Results show the mean fold change in protein level ($\pm$ SEM) from at least three independent experiments performed in duplicate. Data is shown as relative to the siControl-treated, mock-infected sample, which was set to a value of 1. Statistics were calculated using a paired 1-sample t-test. Compared with siControl-treated cells, levels of coilin were significantly decreased in siCoilin-treated, mock-infected cells and siCoilin-treated, Ad5-infected cells. Levels of SMN, Sm and fibrillarin were not significantly affected by siCoilin treatment. Black bars = siControl-treated cells. Grey bars = siCoilin-treated cells. *$p<0.05$.

To support the Western blotting data, it was also decided to analyse the levels of CB proteins following coilin depletion by flow cytometry (Chapter 2.2.8). WRAP53 levels were not assayed by this method due to the strong non-specific cross reaction of the WRAP53 antibody with an unidentified 100 kDa protein (Figure 3-1); flow cytometric analysis of WRAP53 levels using this antibody could be compromised by variations in the level of this non-specific protein. Cellular levels of coilin, SMN, fibrillarin and Sm were assayed by flow cytometry (Chapter 2.2.8). As shown in Figure 4-4, flow cytometric analysis revealed there was no significant difference in expression levels of any of the CB proteins following siCoilin-treatment as compared to siControl-treated cells. This confirmed the Western blotting data that coilin depletion did not alter the levels of coilin-interacting proteins or associated CB proteins. Coilin depletion in the siCoilin-treated cells, although significant, appeared negligible by this method. However, from Western blotting analysis it was apparent that this antibody cross-reacted with a non-specific protein of around 65 kDa (Figure 4-3A), therefore the overall reduction in coilin levels will appear minimal by flow cytometric analysis due to non-specific binding of the antibody to the unidentified 65 kDa protein.

4.5 Impact of coilin depletion on the subcellular distribution of CB proteins

Coilin is required for CB integrity and recruitment of proteins to the CB (Tucker *et al.*, 2001; Mahmoudi *et al.*, 2010). Therefore it is possible that coilin depletion may alter the subcellular distribution of CB proteins. This could have a potential impact on Ad infection in an indirect manner by causing the redistribution of other CB proteins within the cell. To identify whether coilin depletion disrupted the subcellular distribution of WRAP53 or SMN, siRNA transfection was performed using siControl or siCoilin (Chapter 2.2.5.1) followed by mock or Ad5 infection (Chapter 2.2.6.1). Cells were then subjected to indirect immunofluorescence procedure (Chapter 2.2.7) using an anti-SMN or an anti-WRAP53 antibody alongside anti-coilin antibodies. A goat anti-Ad capsid antibody was used to identify Ad5-infected cells.

As shown in Figure 4-5, siControl-treated, mock-infected cells exhibited a punctate distribution of coilin in CBs (image b, arrow) and SMN was also located in CBs (image c, arrow); these proteins colocalised in CBs as shown by the yellow regions in the overlay (image q, arrow). Ad5 infection of siControl-treated cells resulted in the redistribution of coilin into rosettes (image f, arrow) and SMN into the nucleoplasm (image g, arrow), as previously described (Chapter 3.3). As shown in the overlay (image r), coilin microfoci (white arrow) did not co-localise with areas of SMN staining (blue arrow). These data indicated that siControl treatment did not disrupt CB structure or affect the redistribution of coilin or SMN following Ad5 infection.

siControl, mock infection   siControl, Ad5 infection

siCoilin, mock infection   siCoilin, Ad5 infection

142
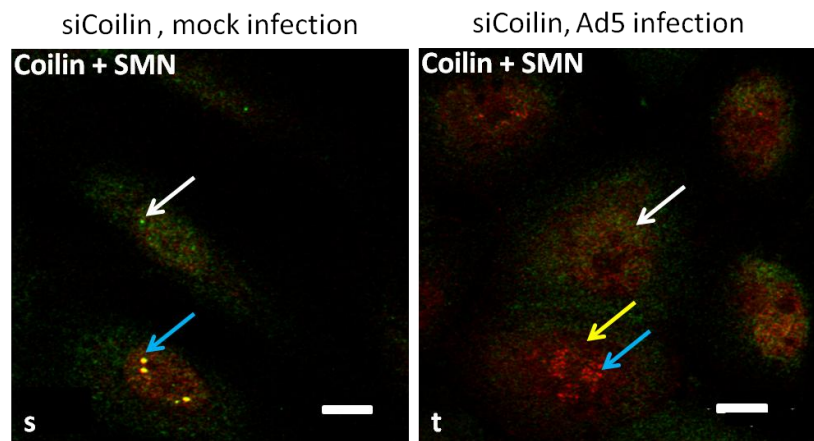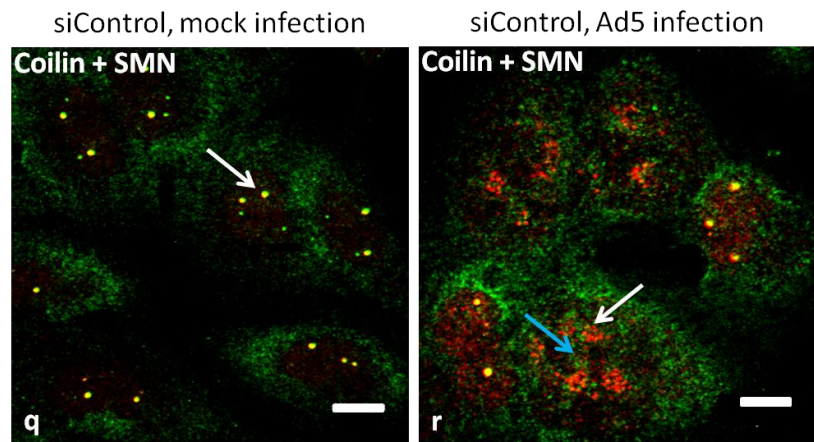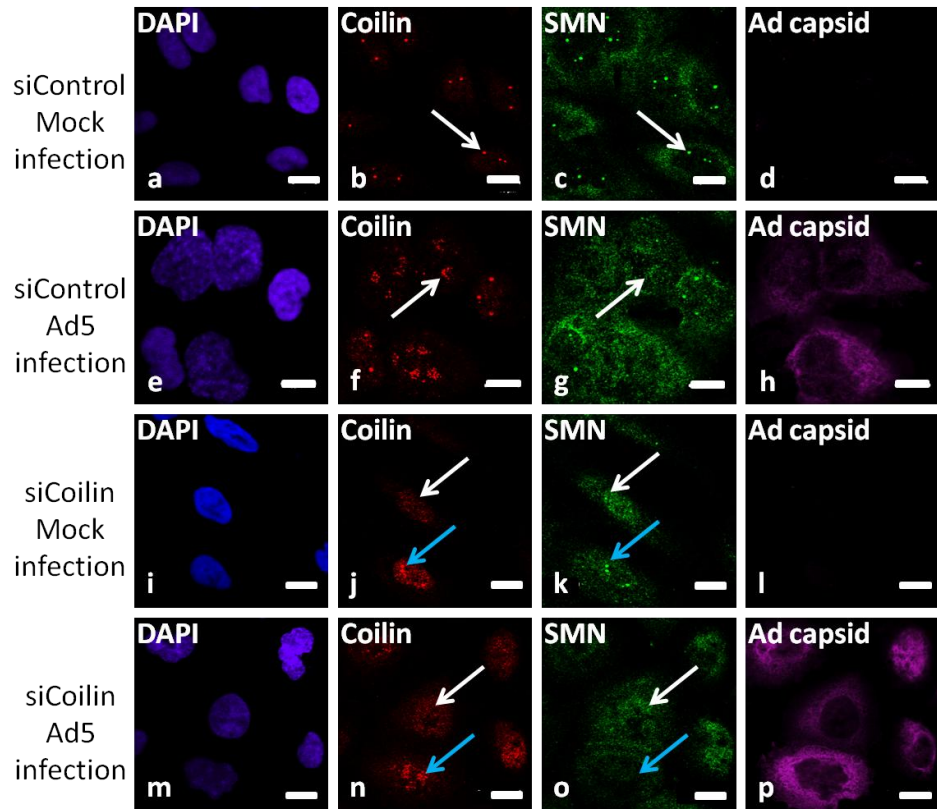
Figure 4-5. Redistribution of SMN following Ad5 infection of coilin-depleted A549 cells.

A549 cells were treated with siControl or siCoilin and incubated for 24 hours. Cells were mock or Ad5 infected at an MOI of 5 FFU/cell and incubated for 24 hours. Cells were fixed and subjected to indirect immunofluorescence. Cells were incubated with a mouse anti-SMN, a rabbit anti-coilin and a goat anti-Ad capsid followed by incubation with the appropriate fluorescent-labelled secondary antibodies. DAPI was used to stain nuclei. Confocal microscopy was performed using an inverted LSM510 confocal microscope coupled to LSM Image Browser. In siControl-treated, mock-infected cells, coilin was found in punctate CBs (image b, arrow) and SMN was also found in CBs (image c, arrow). Coilin and SMN co-localised in CBs, as shown by the yellow regions in the overlay (image q, arrow). In siControl treated, Ad5-infected cells, coilin was redistributed from CBs into microfoci (image f, arrow). SMN was redistributed from CBs into the nucleoplasm and within stronger staining, rod-shaped structures (image g, arrow). Ad shown in the overlay (image r), there was no colocalisation between redistributed SMN (blue arrow) and coilin microfoci (white arrow). In siCoilin-treated, mock-infected cells, coilin staining was reduced in the majority of cells (image j, white arrow); in these cells, SMN was found within punctate nuclear structures (image k, white arrow). Some cells were not depleted of coilin, and retained punctate CBs (image j, blue arrow). The punctate structures of SMN in coilin-depleted cells (image k, white arrow) appeared smaller in size than CBs seen in cells that were not depleted of coilin (image k, blue arrow). As shown by the yellow regions in the overlay (image s), cells that were not depleted of coilin exhibited strong colocalisation of SMN and coilin in CBs (blue arrow) whilst in cells depleted of coilin, SMN was retained in punctate nuclear structures in the absence of coilin (white arrow). In siCoilin-treated, Ad5-infected cells, coilin staining was reduced in the majority of cells, (image n, white arrow); SMN was redistributed into the nucleoplasm in these cells (image o, white arrow). Some cells were not depleted of coilin, and retained punctate CBs (image n, blue arrow). The redistribution of SMN into the nucleoplasm following Ad5-infection of coilin-depleted cells (image o, white arrow) appeared similar to SMN redistribution in cells that retained coilin expression (image o, blue arrow). As shown in the overlay (image t), in cells retaining coilin expression there was no colocalisation of coilin microfoci (blue arrow) with redistributed SMN (yellow arrow). In coilin-depleted cells, SMN was redistributed into the nucleoplasm in the absence of coilin (white arrow). Bars = 20 μm.

In siCoilin-treated, mock-infected cells, coilin staining was reduced in the majority of cells (image j, blue arrow), whilst some cells retained coilin expression (image j, white arrow). In cells depleted of coilin, SMN was located within residual punctate structures (image k, blue arrow), which appeared to be slightly smaller in size than conventional CBs seen in cells that were not depleted of coilin (image k, white arrow). This indicated that SMN was maintained within punctate nuclear domains following coilin depletion. As shown in the overlay (image s), in cells retaining coilin expression, coilin and SMN colocalised in CBs (blue arrow), whilst in coilin-depleted cells, SMN was found within punctate nuclear domains in the absence of coilin (white arrow). In siCoilin-treated, Ad5-infected cells, the majority of cells exhibited reduced coilin staining (image n, white arrow) whilst some cells retained coilin expression (image n, blue arrow). In cells depleted of coilin, SMN was redistributed into the nucleoplasm (image o, blue arrow), in a similar manner to that seen following Ad5 infection of cells that were not depleted of coilin (image o, white arrow). This indicated that coilin depletion did not alter the redistribution of SMN following Ad5 infection. As shown in the overlay (image t), in cells retaining coilin expression, coilin microfoci (blue arrow) did not colocalise with redistributed SMN (yellow arrow). In coilin-depleted cells, SMN was redistributed into the nucleoplasm in the absence of coilin (image t, white arrow).

The redistribution of WRAP53 by Ad5 in coilin-depleted cells was also assessed (Figure 4-6). In siControl-treated, mock-infected cells, WRAP53 was located in CBs (image b, arrow); coilin was also found in CBs (image c, arrow) and these two proteins colocalised in CBs as shown by the yellow regions in the overlay (image q, arrow). Ad5 infection of siControl-treated cells resulted in redistribution of coilin (image f, arrow) and WRAP53 (image g, arrow) into rosettes. These two proteins colocalised in rosettes, as shown by the yellow regions in the overlay (image r, arrow). In siCoilin-treated, mock-infected cells, the majority of cells exhibited a loss of coilin staining (image j, blue arrow), whilst a subset of cells retained coilin expression (image j, white arrow). In the coilin-depleted cells,, WRAP53 was located diffusely throughout the nucleoplasm and cytoplasm (image k, white arrow); this is in contrast to cells expressing coilin, in which WRAP53 is found concentrated within CBs along with coilin (image k, blue arrow). These data are consistent with previous studies indicating that coilin is required for maintenance of CB structure and for recruitment of WRAP53 to the CB (Mahmoudi *et al.*, 2010). This showed that there was substantial alteration to the subcellular distribution of WRAP53 when coilin was depleted from the cells.

In siCoilin-treated, Ad5-infected cells, the majority of cells exhibited a loss of coilin staining (image n, arrow). In these cells, WRAP53 was redistributed into nuclear microfoci (image o, arrow), indicating that Ad5 was able to redistribute WRAP53 in the absence of coilin. However,
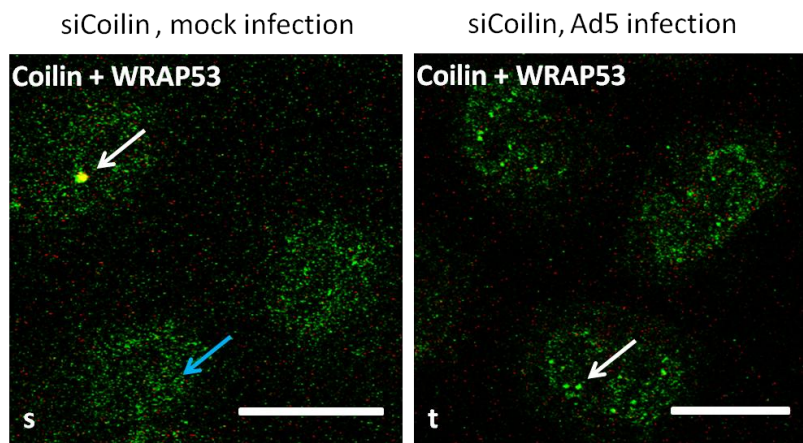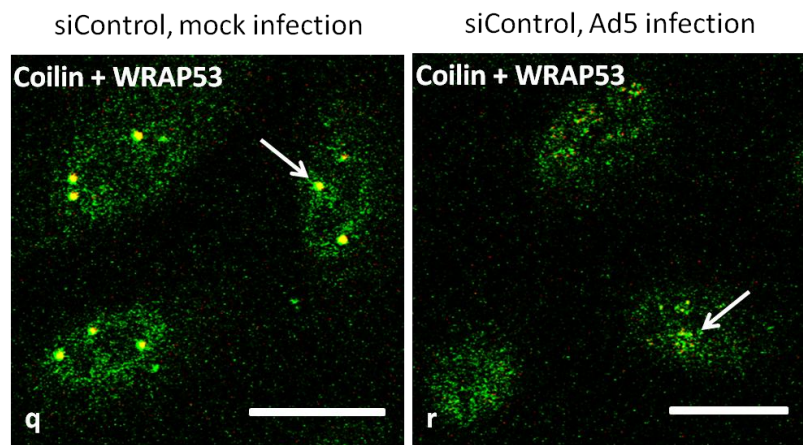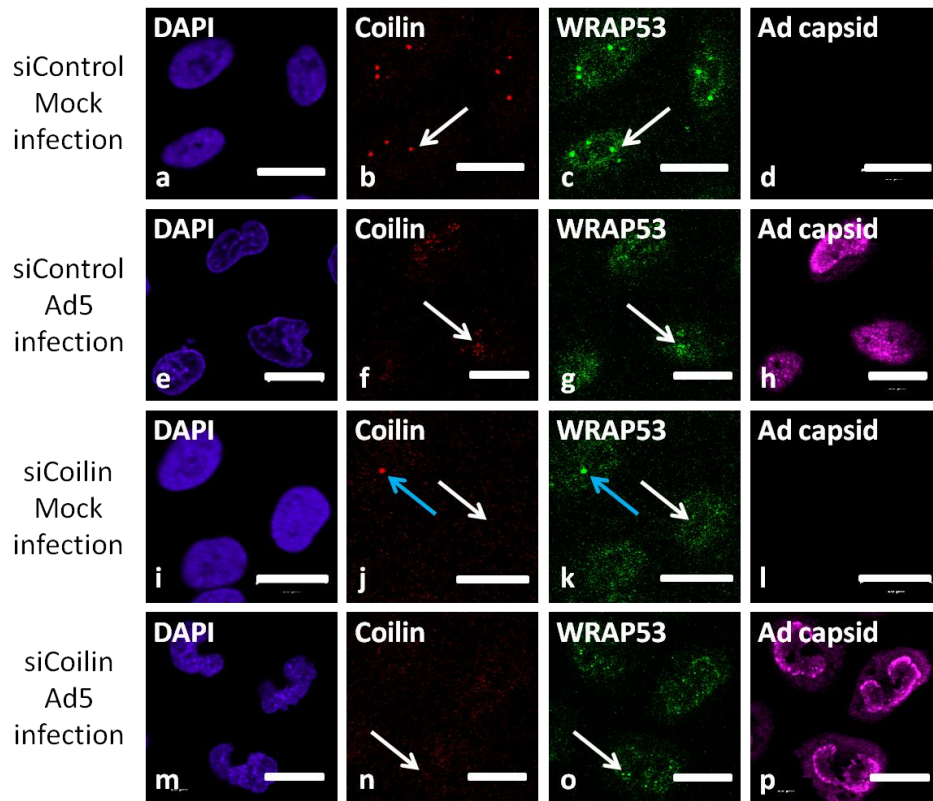
Figure 4-6. Redistribution of WRAP53 following Ad5 infection of coilin-depleted A549 cells.

A549 cells were treated with siControl or siCoilin and incubated for 24 hours. Cells were mock or Ad5 infected at an MOI of 5 FFU/cell and incubated for 24 hours. Cells were incubated with a rabbit anti-WRAP53, a mouse anti-coilin and a goat anti-Ad capsid antibody followed by incubation with the appropriate fluorescent-labelled secondary antibodies. DAPI was used to stain nuclei. Confocal microscopy was performed using an inverted LSM510 confocal microscope coupled to LSM Image Browser. . In siControl-treated, mock-infected cells, coilin was found in punctate CBs (image b, arrow) and WRAP53 was also found in CBs (image c, arrow). WRAP53 and coilin co-localised in CBs, as shown by the yellow regions in the overlay (image q, arrow). In siControl treated, Ad5-infected cells, coilin (image f, arrow) and WRAP53 (image g arrow) were redistributed into nuclear microfoci. As shown by the yellow regions in the overlay, there was partial colocalisation of WRAP53 and coilin in nuclear microfoci (image r, arrow). In siCoilin-treated, mock-infected cells, coilin was depleted in the majority of cells (image j, white arrow), whilst some cells were not depleted of coilin, and exhibited punctate CBs (image j, blue arrow). In cells depleted of coilin, WRAP53 was found diffusely in the nucleoplasm (image k, white arrow) whereas in cells expressing coilin, WRAP53 was found in CBs (image k, blue arrow). As shown by the yellow regions in the overlay (image s), cells that were not depleted of coilin exhibited strong colocalisation of WRAP53 and coilin in CBs (white arrow) whilst in cells depleted of coilin, WRAP53 was found diffusely in the cytoplasm (blue arrow). In siCoilin-treated, Ad5-infected cells, coilin expression was reduced in the majority of cells (image n, arrow) and WRAP53 was redistributed into nuclear microfoci (image o, arrow). These microfoci of WRAP53 did not form the regular clusters seen in siControl-treated, Ad5-infected cells (compare image g [arrow] with image n [arrow]). As shown in the overlay, coilin-depleted cells exhibited WRAP53 microfoci that did not contain coilin (image t, arrow). Bars = 20 μm.

the WRAP53 microfoci seen in siCoilin-treated, Ad5-infected cells did not appear to form the regular ring-shaped clusters characteristic of rosettes seen in siControl-treated, Ad5-infected cells (compare image o [arrow] with image g [arrow]). This indicated that in coilin-depleted cells, Ad5 was able to rearrange WRAP53 into microfoci. However, coilin was required for formation of rosette structures. Therefore, it should be noted that any observations on Ad5 infection following coilin depletion could be indirectly due to effects on the subcellular distribution of WRAP53, and the reduced capacity of Ad5 to rearrange WRAP53 into rosettes.

4.6 Impact of coilin depletion on Ad5 virus yield

To assess whether coilin depletion affected the production of infectious progeny viruses following infection, siRNA depletion using siControl or siCoilin was performed in A549 cells (Chapter 2.2.5.1). Following a 24 hour incubation, cells were mock or Ad5 infected (Chapter 2.2.6.1). At 24 h.p.i, cells were harvested and the cell lysate was used to infect fresh A549 cells (Chapter 2.2.6.2). Two methods were employed in order to assess the impact of Ad5 infection on virus yield: the plaque assay (Chapter 2.2.10) and the flow cytometry assay (Chapter 2.2.8) staining for the Ad late protein hexon. Two methods were employed to study virus yield as each method has advantages and disadvantages. An advantage of the plaque assay is that it is a direct measurement of virus infectivity; however there is a large margin for error since the plaques are counted manually. An advantage of the flow cytometry assay is that it is quantitative. However, it is not a direct measure of infectivity; it is a measurement of late protein expression (although this will be closely correlated with virion production). Therefore both techniques were employed to assess the impact of coilin depletion on Ad5 virus yield.

As shown in Figure 4-7A, plaque assay assessment of virus yield revealed that Ad5 infection of coilin-depleted A549 cells resulted in an 82% decrease in yield compared to Ad5 infection of siControl-treated cells. Similar results were obtained by flow cytometric analysis, where Ad5 infection of siCoilin-treated A549 cells significantly reduced levels of hexon expression by 65% compared to Ad5 infection of siControl-treated cells (Figure 4-7B). Taken together, these results strongly suggested that depletion of coilin significantly reduces the yield of Ad5.

4.7 The impact of coilin depletion on Ad5 protein expression

Previously published data from Ad5 infection of siCoilin-treated HeLa cells suggested a role for coilin in the expression of late but not early Ad proteins (James *et al.*, 2010). However, in the study by James *et al* only one early protein was assayed and the impact of coilin depletion on intermediate protein expression was not assessed. In order to gain a greater insight into the impact of coilin depletion on the expression of Ad5 proteins, the additional early protein E1A,
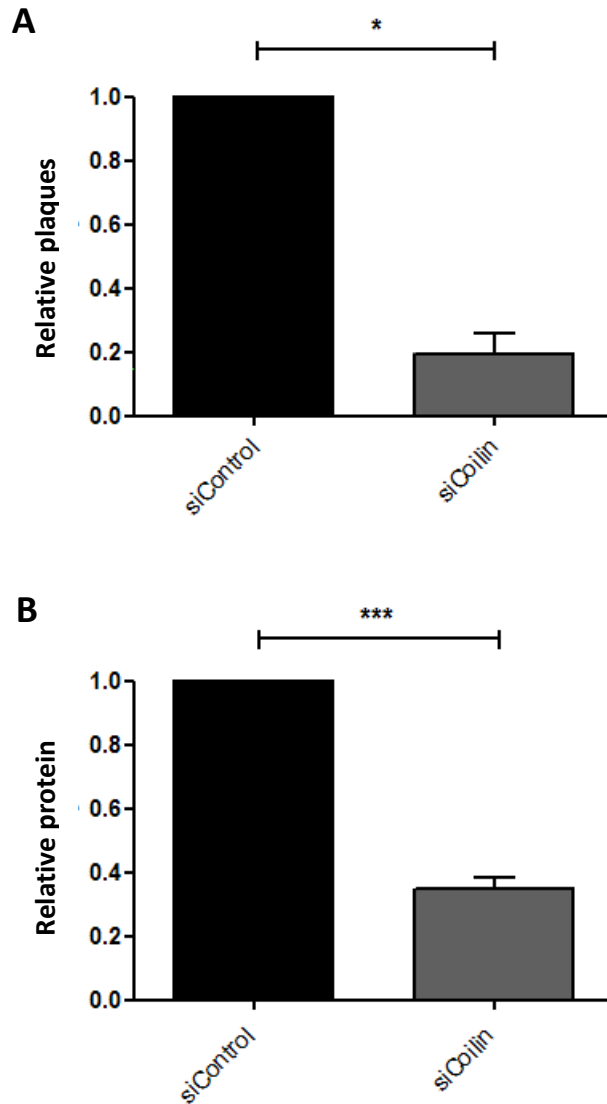
Figure 4-7. The impact of coilin depletion on Ad5 virus yield.

A549 cells were treated with siControl or siCoilin and incubated for 24 hours. Cells were mock or Ad5 infected at an MOI of 5 FFU/cell and incubated for 24 hours. Cells were harvested and ten-fold serial dilutions of cell lysate were used to infect fresh A549 cells. For analysis by plaque assay, cells were incubated for six days before plaques were counted. For the flow cytometric assay, cells were harvested at 48 h.p.i and subjected to flow cytometric analysis staining for the Ad5 late protein, hexon. Data are the mean fold change (± SEM) from at least three independent experiments performed in triplicate. Results are expressed as relative to the siControl-treated, Ad5-infected sample, which was set to a value of 1. Statistics were calculated using the paired 1-tailed t-test. A. Plaque assay analysis of Ad5 virus yield. The virus yield was reduced by 82% following Ad5 infection of siCoilin-treated cells compared with Ad5 infection of siControl-treated cells. The average virus titre following infection of A549 cells with cell lysate from siControl-treated, Ad5-infected cells was 1.5×10^8 plaque-forming units (PFU)/ml. B. Flow cytometric analysis of hexon expression. Levels of hexon were reduced by 65% following Ad5 infection of siCoilin-treated cells compared with Ad5 infection of siControl-treated cells. *p<0.05, ***p<0.001.

intermediate proteins IVa2 and pIX and the late protein L4-100K were included along with the previously characterised DBP, IIIa, hexon and fibre protein.

4.7.1 Western blotting analysis of Ad5 protein levels following Ad5 infection of coilin-depleted A549 cells

The impact of coilin depletion on Ad5 protein expression was initially analysed by Western blotting. Following siRNA treatment (Chapter 2.2.5.1) and mock or Ad5 infection (Chapter 2.2.6.1), whole cell lysates were prepared and subjected to analysis by SDS-PAGE and Western blotting (Chapter 2.2.2). Membranes were incubated with antibodies raised against the Ad E1A, DBP, IVa2, L4-100K, IIIa and fibre proteins. Hexon and pIX were not included in this analysis since the hexon antibody 2Hx2 is not suitable for Western blotting, whilst there was an insufficient amount available of the anti-pIX antibody to complete Western blotting analysis.

As shown by the Western blots in Figure 4.8A, Ad5 infection of coilin-depleted A549 cells resulted in a decrease in the levels of all Ad5 proteins as compared to siControl-treated cells. The decreases in Ad5 protein levels following coilin depletion were confirmed by densitometric analysis (Figure 4-8B). This indicated that depletion of coilin significantly reduces the expression levels of early, intermediate and late Ad proteins.

4.7.2 Flow cytometric analysis of Ad5 protein levels following Ad5 infection of coilin-depleted A549 cells

Following the Western blotting analysis described in the previous section, quantitative analysis of Ad5 protein levels following infection of coilin-depleted cells was determined by flow cytometry (Chapter 2.2.8). The early Ad proteins E1A and DBP were assayed along with intermediate proteins IVa2 and pIX and the late proteins L4-100K, IIIa, fibre and hexon.

Representative overlays from flow cytometric analysis of hexon expression are shown in Figure 4-9A. The FITC area (FITC-A) value for the negative control samples (mock-infected samples stained with mouse anti-hexon antibody and mock- and Ad5-infected samples treated with a mouse isotype antibody) are located in the range of $0-10^1$, i.e. negative for hexon staining. An increase in the expression level of the protein in question results in a shift of the population to more positive FITC-A values. Both Ad5-infected samples (siControl and siCoilin treated) exhibited a shift of a proportion of the cells to 10^4-10^5, reflecting the high hexon expression in these cells. Compared with siControl-treated, Ad5-infected cells, there was a slight shift of the cell population to the left in the siCoilin-treated, Ad5-infected cells, indicating reduced fluorescence levels in these cells. There also appeared to be fewer cells expressing hexon in the siCoilin-treated, Ad5-infected cell population compared with the siControl-treated, Ad5-
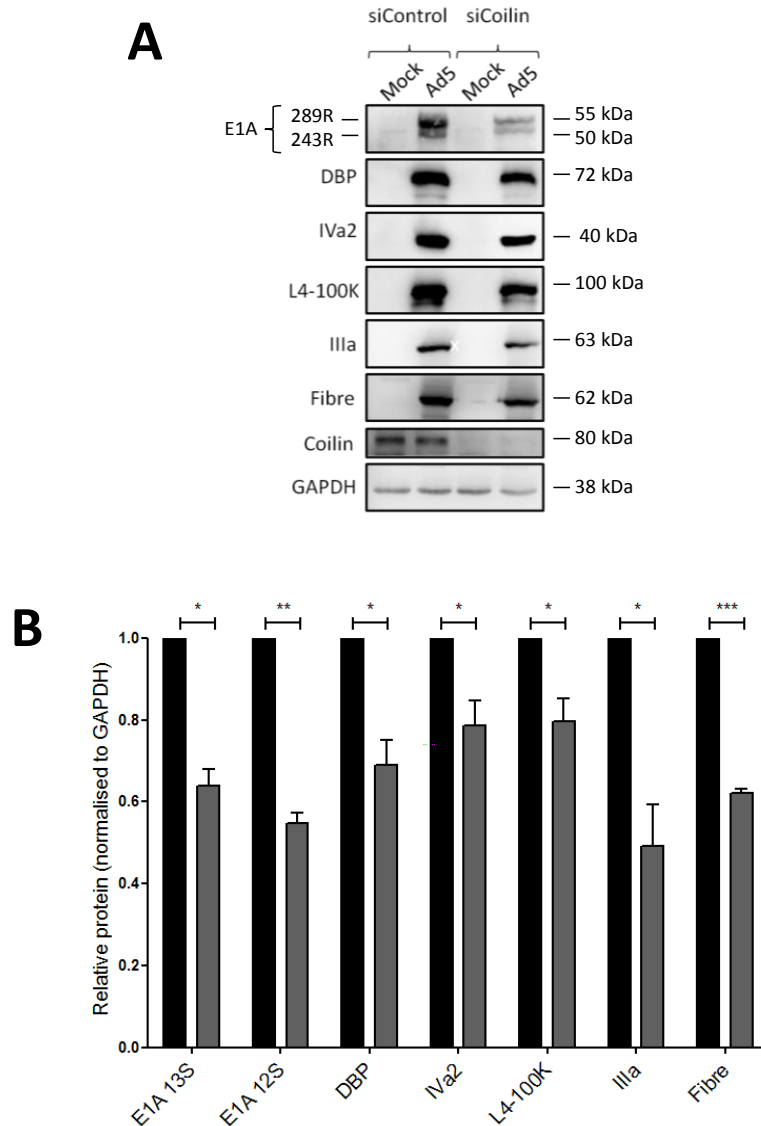
Figure 4-8. The expression of Ad5 proteins following infection of coilin-depleted A549 cells.

A549 cells were treated with siControl or siCoilin and incubated for 24 hours. Cells were mock or Ad5 infected at an MOI of 5 FFU/cell and incubated for 24 hours. Equal masses of protein (20 μg) from whole cell lysates were subjected to separation by SDS-PAGE and analysed by Western blotting. Bound antibody was detected using the ECL system on a Las 3000 Imager. Signal intensities were calculated by densitometric analysis, normalising to the signal intensity of the loading control, GAPDH. A. Representative Western blots of Ad5 protein levels following infection of coilin-depleted cells. Compared with siControl-treated, Ad5-infected cells, levels of all Ad proteins studied (E1A 12S, E1A 13S, DBP, IVa2, L4-100K, IIIa and fibre) were reduced in siCoilin-treated, Ad5-infected cells. B. Densitometric analysis of Western blots. Results are displayed as the mean fold change in protein level (± SEM) from at least three independent experiments. Results are displayed relative to the siControl-treated mock-infected sample, which was set to a value of 1. All statistics were calculated using the paired 1 sample t-test. Compared with Ad5 infection of siControl-treated cells, levels of all Ad proteins studied were significantly reduced following infection of siCoilin-treated cells. Black bars = siControl-treated cells. Grey bars = siCoilin-treated cells. *p<0.05, **p<0.01, ***p<0.001.
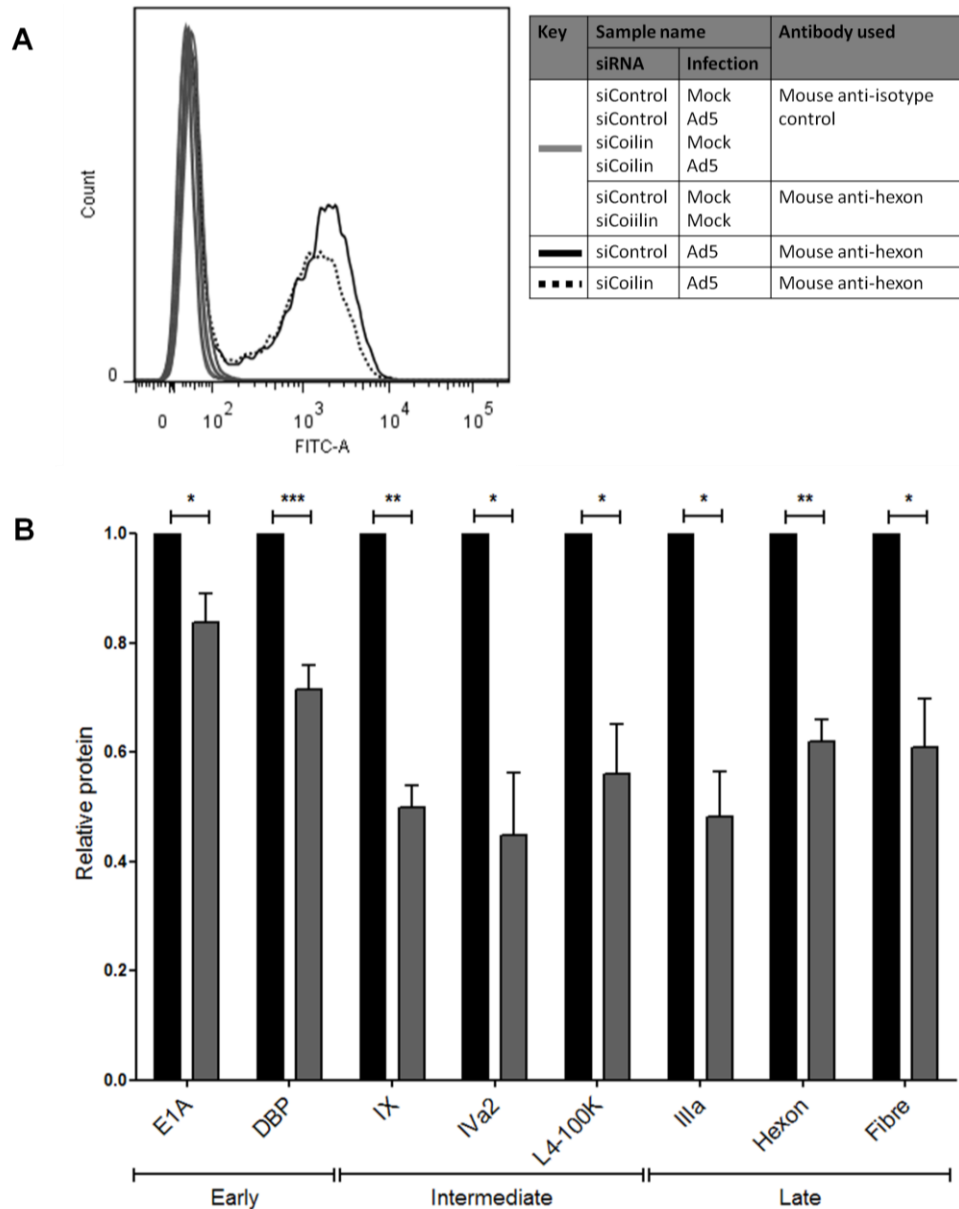
Figure 4-9. Flow cytometric analysis of Ad5 proteins following Ad5 infection of coilin-depleted cells. A549 cells were treated with siControl or siCoilin and incubated for 24 hours. Cells were mock- or Ad5-infected at an MOI of 5 FFU/cell and incubated for 24 hours. Cells were harvested and subject to flow cytometric analysis. A. Example overlay from flow cytometric analysis of Ad5 hexon. Compared with infection of siControl-treated cells, Ad5 infection of siCoilin-treated cells resulted in decreased overall hexon expression (as shown by a shift of the FITC curve to the left) and also resulted in a decrease in the number of hexon-positive cells. B. Flow cytometric analysis of Ad5 proteins following infection of coilin-depleted cells. Results are the mean fold change in protein level ($\pm$ SEM) from at least three independent experiments. Data are shown relative to the siControl-treated, Ad5-infected sample, which was set to a value of 1. Statistics were calculated using the paired 1 sample t-test. Compared with Ad5 infection of siControl-treated cells, infection of siCoilin-treated cells resulted in decreased expression of all Ad proteins studied (E1A, DBP, pIX, IVa2, L4-100K, IIIa, hexon and fibre). Black bars = siControl-treated cells. Grey bars = siCoilin-treated cells. *$p < 0.05$, **$p < 0.01$, ***$p < 0.001$.

infected cells. These data indicated that coilin depletion reduced the level of hexon expression in cells, and also reduced the number of cells expressing hexon.

The results of the complete flow cytometric analysis for all Ad proteins are displayed in Figure 4-9B. It was found that depletion of coilin resulted in a significant decrease in the levels of all the Ad5 proteins studied. This indicated that coilin is required for Ad early, intermediate and late phase protein expression.

4.7.3   The effect of varying the multiplicity of Ad infection in HeLa cells

Previous flow cytometric analysis of siRNA-mediated coilin depletion in Ad5-infected HeLa cells reported a significant decrease in levels of the late proteins hexon, IIIa and fibre whilst levels of the early protein DBP were unaffected (James *et al.*, 2010). This contrasts with the data in the previous sections (Chapter 4.7.1-4.7.2) where coilin depletion decreased the levels of Ad5 early, intermediate and late proteins. The discrepancy between these data and the published data by James *et al* may be due to differences in virus titre (an MOI of 1000 [James *et al*] vs. An MOI of 5 [in this study]) or the cell lines used (HeLa [James *et al*] vs. A549 [in this study]).

To address the potential role of the cell line used, siRNA treatment was performed in HeLa cells (Chapter 2.2.5.1) followed by mock or Ad5 infection at an MOI of 5 FFU/cell (Chapter 2.2.6.1). At 24 h.p.i, cells were subjected to flow cytometric analysis (Chapter 2.2.8). As the coilin depletion data presented by James *et al* included analysis of Ad5 DBP, IIIa, fibre and hexon, these were the proteins investigated in this comparative assay. As shown in Figure 4-10A, there was a significant reduction in the protein levels of Ad DBP, IIIa, hexon and fibre in siCoilin-treated, Ad5-infected cells as compared to siControl-treated, Ad5-infected cells. This is consistent with data obtained with A549 cells at this MOI (Chapter 4.7.2), indicating that the choice of cell line may not be the reason for the discrepancy between the results described here and those published by James *et al.*

The potential role of MOI was also addressed. HeLa cells were treated with siRNA (Chapter 2.2.5.1) prior to Ad5 infection at an MOI of 1000 (Chapter 2.2.6.1). Cells were harvested at 24 h.p.i and subjected to flow cytometric analysis (Chapter 2.2.8). As shown in Figure 4-10B, although there was a significant decrease in the level of fibre protein in the siCoilin-treated Ad5-infected cells compared to siControl-treated Ad5-infected cells, the levels of DBP, IIIa and hexon were not significantly affected. This indicates that at a higher MOI, Ad infection is less susceptible to the inhibitory effect of coilin depletion.
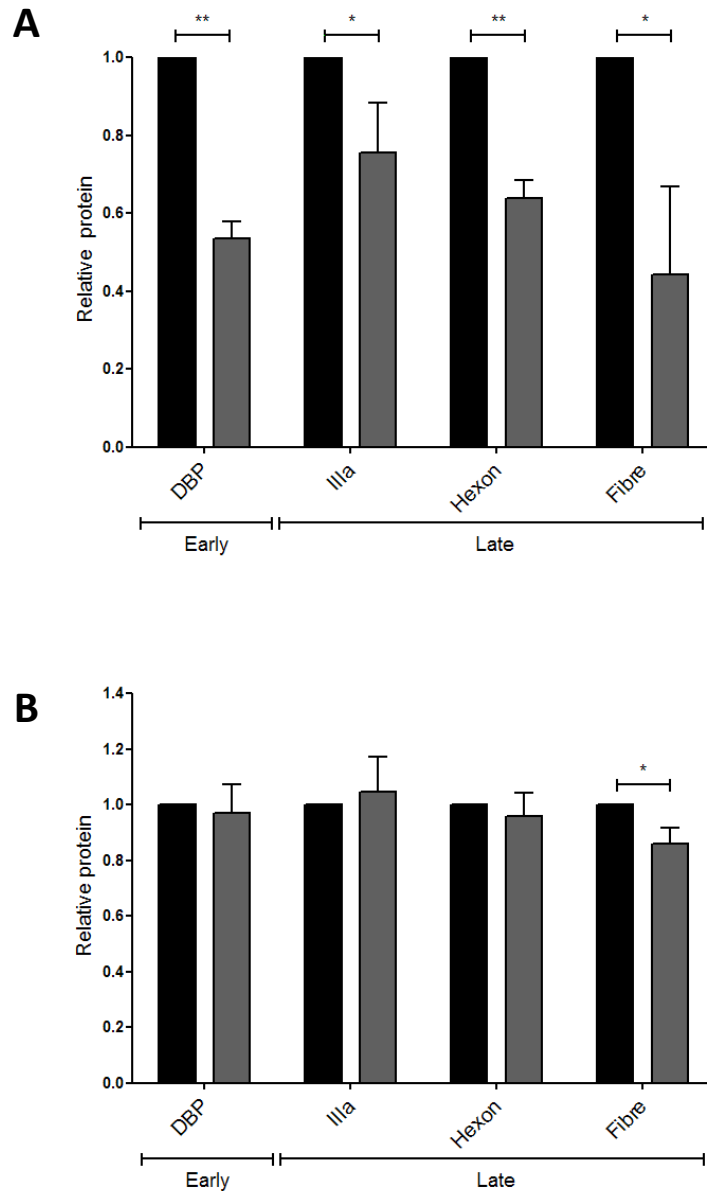
Figure 4-10. Flow cytometric analysis of Ad5 protein levels following infection of coilin-depleted HeLa cells.

HeLa cells were treated with siControl or siCoilin and incubated for 24 hours. Cells were mock or Ad5 infected at an MOI of 5 or 1000 FFU/cell and incubated for 24 hours. Cells were harvested and subjected to flow cytometric analysis. Results are the mean fold change in protein level (± SEM) from three independent experiments. Results are displayed relative to the siControl-treated, Ad5-infected sample, which was set to a value of 1. All statistics were calculated using the paired 1 tailed t-test. A. Ad5 protein levels in coilin-depleted HeLa cells following infection at an MOI of 5 FFU/cell. Compared with Ad5 infection of siControl-treated cells, levels of DBP, IIIa, hexon and fibre were significantly reduced following infection of siCoilin-treated cells. B. Ad5 protein levels in coilin-depleted HeLa cells following infection at an MOI of 1000 FFU/cell. Compared with Ad5 infection of siControl-treated cells, levels of DBP were significantly reduced following infection of siCoilin-treated cells, whilst levels of IIIa, hexon and fibre were not significantly affected. Black bars = siControl-treated cells. Grey bars = siCoilin-treated cells. *$p<0.05$, **$p<0.01$.

4.8 Impact of coilin depletion on Ad5 mRNA levels

The data from the previous section (Chapter 4.7) revealed that there was a significant reduction in Ad5 protein levels following infection of coilin-depleted cells compared to infection of siControl-treated cells. To establish whether the alterations in Ad5 protein levels were due to changes at the mRNA or the protein level, the levels of Ad5 mRNAs following coilin depletion was analysed. Exon-spanning primers were designed to amplify mature, spliced Ad5 mRNAs; E1A isoforms 13S, 12S, 11S, 10S, and 9S, DBP spliceoforms RT1 and RT2, L4-100K, IVa2, IIIa, hexon and fibre. Ad IX does not undergo splicing (Alestrom *et al.*, 1980), therefore primers for this mRNA were designed within the single exon of IX. All primers are listed in Table 2-1 and the design strategies for all primers are described in Appendix Figure 1-6. The specificity of the primers for their target mRNA was validated by semi-quantitative PCR (Chapter 2.2.4.3) and agarose gel electrophoresis (Chapter 2.2.4.5) as shown in Appendix Figure 8. Primer specificity was also verified by melting curve analysis.

4.8.1   Ad5 mRNA expression following Ad5 infection of coilin-depleted A549 cells

Since mRNA synthesis occurs prior to protein expression, if the alterations to Ad5 protein levels described in the previous section (Chapter 4.7) were due to changes at the mRNA level, these changes should occur earlier in the infectious cycle than the time point at which the effect on protein levels was observed. The decrease in Ad5 protein levels was observed at 24 h.p.i, therefore to ensure that any impact of coilin depletion on Ad5 mRNA levels would be observed, a time course of Ad5 hexon mRNA expression was carried out. Following siRNA treatment (Chapter 2.2.5.1), A549 cells were mock or Ad5 infected (Chapter 2.2.6.1). Cells were harvested at 18, 20, 22 and 24 h.p.i and total RNA was isolated by Trizol-chloroform extraction (Chapter 2.2.3.1). Total RNA was subjected to reverse transcription (Chapter 2.2.4.2) to produce cDNA from mRNA. Quantitative RT-PCR was performed (Chapter 2.2.4.4) using exon spanning primers specific for the mRNA target (Table 2-1).

As shown in Figure 4-11A, the time course of hexon mRNA expression following Ad5 infection of siCoilin-treated cells revealed no difference in the levels of hexon mRNA from 16 to 24 h.p.i as compared to Ad5 infection of siControl-treated cells. This indicated that coilin depletion did not impact the total cellular levels of Ad5 hexon mRNA.

4.8.2   Impact of coilin depletion on Ad5 mRNA expression at 20 hours post-infection

Following the qPCR analysis of hexon mRNA levels from 16-24 h.p.i, the qPCR analysis at 20 h.p.i was extended to include the spliced mRNA transcripts of E1A (9S, 10S, 11S, 12S, 13S), DBP (RT1 and RT2), L4-100K, IVa2, IIIa, hexon and fibre and the non-spliced mRNA
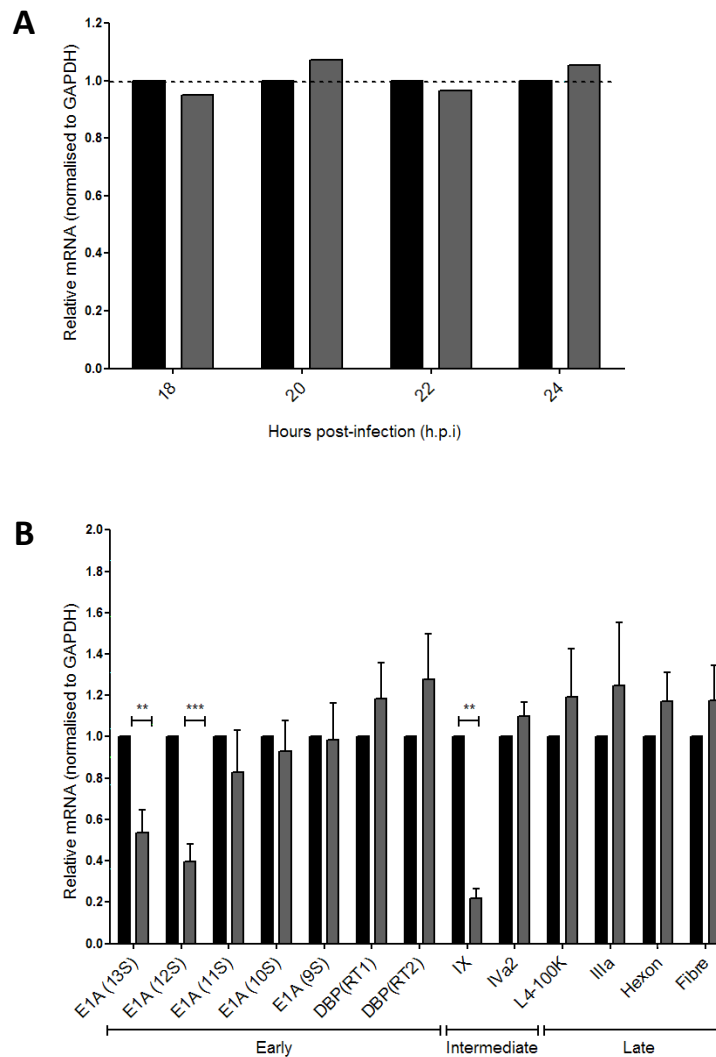
Figure 4-11. Ad5 mRNA levels following Ad5 infection of coilin-depleted A549 cells.

A549 cells were treated with siControl or siCoilin and incubated for 24 hours. Cells were mock or Ad5 infected at an MOI of 5 FFU/cell and incubated for 24 hours. Cells were harvested, total RNA was extracted by Trizol-chloroform extraction and cDNA was produced from RNA by reverse transcription. Quantitative PCR (qPCR) of cDNA was carried out using SYBR Green Taq PCR on a Rotorgene 6000 cycler. Delta Ct values were calculated using Rotorgene 6000 software and were normalised to the 'housekeeping' transcript, GAPDH. Results are shown as the mean fold change in mRNA level (±SEM) relative to the siControl-treated, Ad5-infected sample, which was set to a value of 1. Statistics were calculated using the paired one sample t-test. A. A time course of Ad5 hexon mRNA expression following coilin depletion. Hexon mRNA levels in siControl-treated, Ad5-infected cells were similar to those seen in Ad5-infected, siCoilin-treated cells from 18 to 24 h.p.i. B. Ad5 mRNA levels in siCoilin-treated, Ad5-infected A549 cells at 20 h.p.i. Compared with Ad5 infection of siControl-treated cells, levels of 13S E1A, 12S E1A and IX mRNAs were significantly reduced following Ad5-infection of siCoilin-treated cells. Levels of E1A 11S, E1A 10S, E1A 9S, DBP RT1, DBP RT2, IVa2, L4-100K, IIIa, hexon and fibre mRNAs were not significantly affected. Black bars = siControl-treated cells. Grey bars = siCoilin-treated cells. *p<0.05, **p<0.01, ***p<0.001.

155

transcript of IX. To ensure there was no non-specific amplification of Ad DNA, a control sample of total cellular RNA which had not been subject to reverse transcription was used in all experiments for each primer pair.

As shown in Figure 4-11B, the cellular levels of most Ad5 mRNA transcripts did not appear to be significantly altered following Ad5 infection of siCoilin-depleted cells compared to Ad5 infection of siControl-treated cells. This indicates that coilin depletion did not alter the cellular levels of the majority of Ad5 mRNA transcripts. However, a significant decrease was observed in the levels of E1A 12S, E1A 13S and IX mRNAs following coilin depletion. This indicates that coilin may be required for the expression, processing or stability of these transcripts.

4.8.3   Analysis of Ad5 pre-mRNA following depletion of coilin

Although the cellular levels of the majority of Ad5 transcripts did not appear to be affected by coilin depletion, the levels of the Ad immediate early transcripts 13S and 12S E1A and the intermediate transcript IX were significantly reduced. Considering the levels of E1A 9S, 10S and 11S spliceoforms were unaffected by coilin depletion, it seemed unlikely that coilin depletion would be affecting transcription of E1A, since the levels of all mature transcripts would be expected to decrease. Nevertheless, to clarify whether the reduction in 12S and 13S E1As following coilin depletion was due to effects on transcription or mRNA splicing/stability, qRT-PCR analysis of E1A pre-mRNA was performed (Chapter 2.2.4.4) using intron-exon spanning E1A primers (Table 2-1). If the levels of Ad E1A pre-mRNAs were also reduced, this might indicate that the reduction in the mature E1A transcripts was due to decreased production of pre-mRNA transcripts, i.e. at the level of primary transcription. If the levels of E1A pre-mRNAs were unaffected, this would suggest that the decrease seen in 13S and 12S transcripts is due to an effect at the level of mRNA splicing or stability. As IX mRNA is not subject to splicing, analysis of IX pre-mRNA was not possible by this method. To add strength to the investigation, the pre-mRNAs of IVa2, DBP and Ad late tripartite-leader (TPL)-containing mRNAs were also included in the analysis; the mature mRNAs of these transcripts were not altered following coilin depletion, therefore it would be expected that their corresponding pre-mRNAs would also be unaffected.

As shown in Figure 4-12, no significant difference was observed in the levels of E1A, DBP, IVa2 or TPL-containing pre-mRNA in siCoilin-treated cells compared to siControl-treated cells. This indicated that coilin depletion has no significant effect on Ad5 transcription. Therefore the observed decreases in levels of mature, spliced 13S and 12S E1As following coilin depletion may be due to altered stability or post-transcriptional processing of these transcripts following coilin depletion.
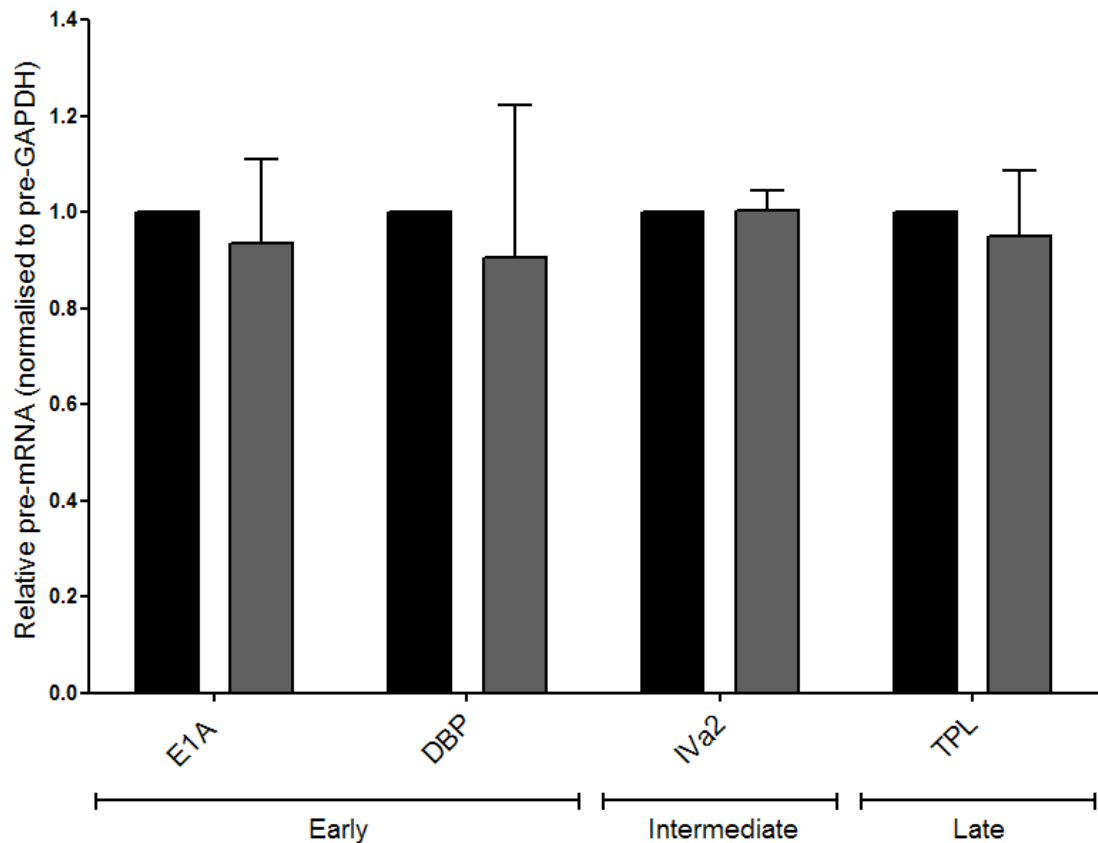
Figure 4-12. Expression levels of Ad5 pre-mRNAs following infection of coilin-depleted A549 cells.
A549 cells were treated with siControl or siCoilin and incubated for 24 hours. Cells were mock or Ad5 infected at an MOI of 5 FFU/cell and incubated for a further 24 hours. Cells were harvested and total RNA was extracted. Reverse transcription of total RNA was carried out to produce cDNA from RNA. QPCR analysis of cDNA was performed using exon-intron spanning primers specific for each pre-mRNA template. Delta Ct values were calculated using Rotorgene 6000 software and were normalised to the levels of the 'housekeeping' transcript, GAPDH. Results are displayed as the mean fold change in pre-mRNA level (±SEM) from at least three independent experiments performed in duplicate. Results are displayed relative to the siControl-treated, Ad5-infected sample, which was set to a value of 1. Compared with Ad5-infection of siControl-treated cells, levels of Ad pre-mRNAs were not significantly altered following Ad5-infection of siCoilin-treated cells. Black bars = siControl-treated cells. Grey bars = siCoilin-treated cells. TPL – tripartite leader-containing pre-mRNA.

4.8.4 Analysis of cytoplasmic and nuclear mRNA levels following depletion of coilin

From the results detailed in the previous section (Chapter 4.8.2 - 0), it was found that for the majority of Ad transcripts studied, there was no significant effect on production of mature Ad mRNAs following coilin depletion. However, coilin depletion resulted in a reduction in the levels of all Ad proteins (Chapter 4.7). This indicates that coilin may play a role at the post-transcriptional, post-splicing level, either in mRNA transport or mRNA translation. Considering that coilin is primarily a nuclear protein, it was decided to investigate a potential role for coilin in the export of Ad mRNAs from the nucleus into the cytoplasm.

To analyse the nuclear export of mRNA, cytoplasmic and nuclear RNA fractions can be isolated and, following standardisation of the mRNA levels to a 'housekeeping' transcript such as to GAPDH, the ratio of cytoplasmic to nuclear mRNA can be calculated. An increase in the cytoplasmic to nuclear mRNA ratio would indicate an increase in cytoplasmic levels compared to nuclear levels whereas a decrease would indicate reduced levels of cytoplasmic mRNA compared to nuclear mRNA levels. Therefore, a decrease in the cytoplasmic to nuclear mRNA ratio would suggest that less mRNA was reaching the cytoplasm, indicating a potential defect in mRNA transport.

The purity of the nuclear and cytoplasmic fractions following the subcellular fractionation procedure was assessed. As there are no mRNA markers for cytoplasmic or nuclear fractions, the purity of the fractions was assessed at the protein level. A549 cells were mock or Ad5 infected (Chapter 2.2.6.1) and either whole cell or cytoplasmic and nuclear fractions were isolated (Chapter 2.2.2.1-2.2.2.2). Protein from each fraction was separated by SDS-PAGE and analysed by Western blotting (Chapter 2.2.2). Histone H3 was used as a marker of the nuclear fraction and GAPDH as a marker of the cytoplasmic fraction. Ad5 penton base is found in both the nucleus and the cytoplasm of Ad-infected cells (Velicer and Ginsberg, 1968) and was used as a marker of Ad5 infection.

As shown in Figure 4-13A, the whole cell lysates contained both GAPDH and Histone H3 and the Ad5-infected samples were positive for penton base protein. The cytoplasmic fraction was positive for the cytoplasmic marker GAPDH, but contained very low levels of the nuclear marker Histone H3. This indicated that there was minimal nuclear contamination of the cytoplasmic fraction. Similarly, the nuclear fraction contained Histone H3 but was negative for GAPDH, indicating that there was minimal cytoplasmic contamination in the nuclear fraction. Taken together, this indicated that a good separation of the cytoplasmic and nuclear fractions had been achieved.
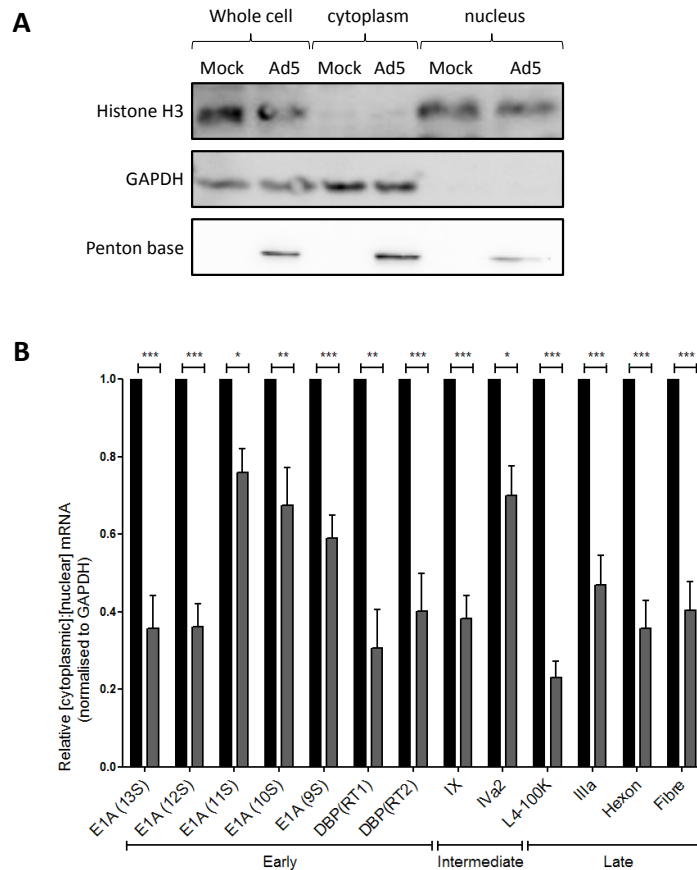
**Figure 4-13. Cytoplasmic: nuclear Ad5 mRNAs following infection of coilin-depleted A549 cells.**
A549 cells were treated with siControl or siCoilin and incubated for 24 hours. Cells were mock or Ad5 infected at an MOI of 5 FFU/cell and incubated for 24 hours. A. Subcellular fractionation of mock- and Ad5-infected cells. Whole cell, nuclear and cytoplasmic fractions were isolated. Equal masses of protein (20 μg) from each sample were separated by SDS-PAGE and analysed by Western blotting. Histone H3 was used as a nuclear marker, GAPDH as a cytoplasmic marker and Ad penton base as a marker of Ad5 infection. Whole cell fractions contained both histone H3 and GAPDH. Nuclear fractions contained histone H3 but were negative for GAPDH. Cytoplasmic fractions contained GAPDH but were negative for histone H3. Penton base was detected in whole cell, nuclear and cytoplasmic fractions of Ad5-infected cells. B. Nuclear: cytoplasmic ratio of Ad5 mRNAs following infection of coilin-depleted cells. Total RNA was extracted from nuclear and cytoplasmic cell fractions and was subjected to reverse transcription. Quantitative PCR analysis of target cDNA was performed using exon-spanning primers specific for the mRNA target. Rotorgene 6000 software was used to calculate delta Ct values. The 'housekeeping' transcript GAPDH was used to standardise transcript levels. Data are displayed as the mean fold change in cytoplasmic: nuclear mRNA (± SEM) relative to an siControl-treated Ad5-infected sample, which was set to a value of 1. Results are from at least three independent experiments performed in duplicate. Statistics were calculated using the paired 1 sample t-test. Compared with Ad5 infection of siControl-treated cells, the cytoplasmic: nuclear ratio of all Ad5 mRNAs studied was significantly reduced following infection of siCoilin-treated cells. Black bars = siControl-treated cells. Grey bars = siCoilin-treated cells. $*p < 0.05$, $**p < 0.01$, $***p < 0.001$.

The Ad mRNA levels in the nucleus and cytoplasm following coilin depletion and Ad5 infection was investigated. Coilin depletion was carried out by siRNA transfection (Chapter 2.2.5.1) and cells were incubated for 24 hours. Cells were mock or Ad5 infected (Chapter 2.2.6.1). At 20 h.p.i, total cytoplasmic and nuclear RNAs were extracted from cells (Chapter 2.2.3.2) and subject to reverse transcription (Chapter 2.2.4.2) to produce cDNA from mRNA. Target cDNAs were amplified by qPCR (Chapter 2.2.4.4) using exon-spanning primers specific for the cDNA target (Table 2-1). The levels of Ad cDNAs in the nuclear and cytoplasmic fractions were normalised to cDNA levels of the 'housekeeping' transcript GAPDH and the ratio of cytoplasmic to nuclear cDNA was subsequently calculated.

As shown in Figure 4-13B, the cytoplasmic to nuclear cDNA ratios in siCoilin-treated, Ad5-infected cells was significantly reduced compared to siControl-treated, Ad5-infected cells. This indicated that in coilin-depleted cells, Ad5 mRNA levels were decreased in the cytoplasm relative to the nucleus. As total mRNA levels for the majority of Ad mRNAs were unaffected following coilin depletion (Chapter 4.8.2), these data suggest that coilin depletion causes defective export of Ad mRNAs to the cytoplasm, resulting in accumulation of mature Ad mRNAs in the nucleus.

4.9 Location of coilin relative to mRNA export factors in Ad5-infected cells

In the previous section it was found that depletion of coilin reduced the transport of Ad mRNAs from the nucleus into the cytoplasm. A major pathway of mRNA transport into the cytoplasm involves the TREX complex, which is recruited to nascent mRNA in a transcription- and splicing-dependent manner (Fischer *et al.,* 2002; Strasser *et al.,* 2002; Abruzzi *et al.,* 2004; Masuda *et al.,* 2005; Cheng *et al.,* 2006). Therefore the potential association of coilin with the TREX complex in Ad5-infected cells was assessed by immunofluorescence microscopy using a rabbit anti-coilin antibody along with a mouse antibody raised against a sub-component of the TREX complex, Aly (Strasser *et al.*, 2002). A goat anti-Ad capsid antibody was used to identify Ad5-infected cells.

As shown in Figure 4-14, coilin was located in punctate CBs in mock-infected cells. Aly was located in separate nucleoplasmic speckles, with exclusion from large rounded structures within the nucleus which are likely to be nucleoli. In Ad5-infected cells, coilin was redistributed into rosettes and Aly was also redistributed into punctate nucleoplasmic foci. However, there did not appear to be any colocalisation between rosettes and the microfoci containing Aly. This indicated that rosettes are not associated with the TREX complex during Ad5 infection.
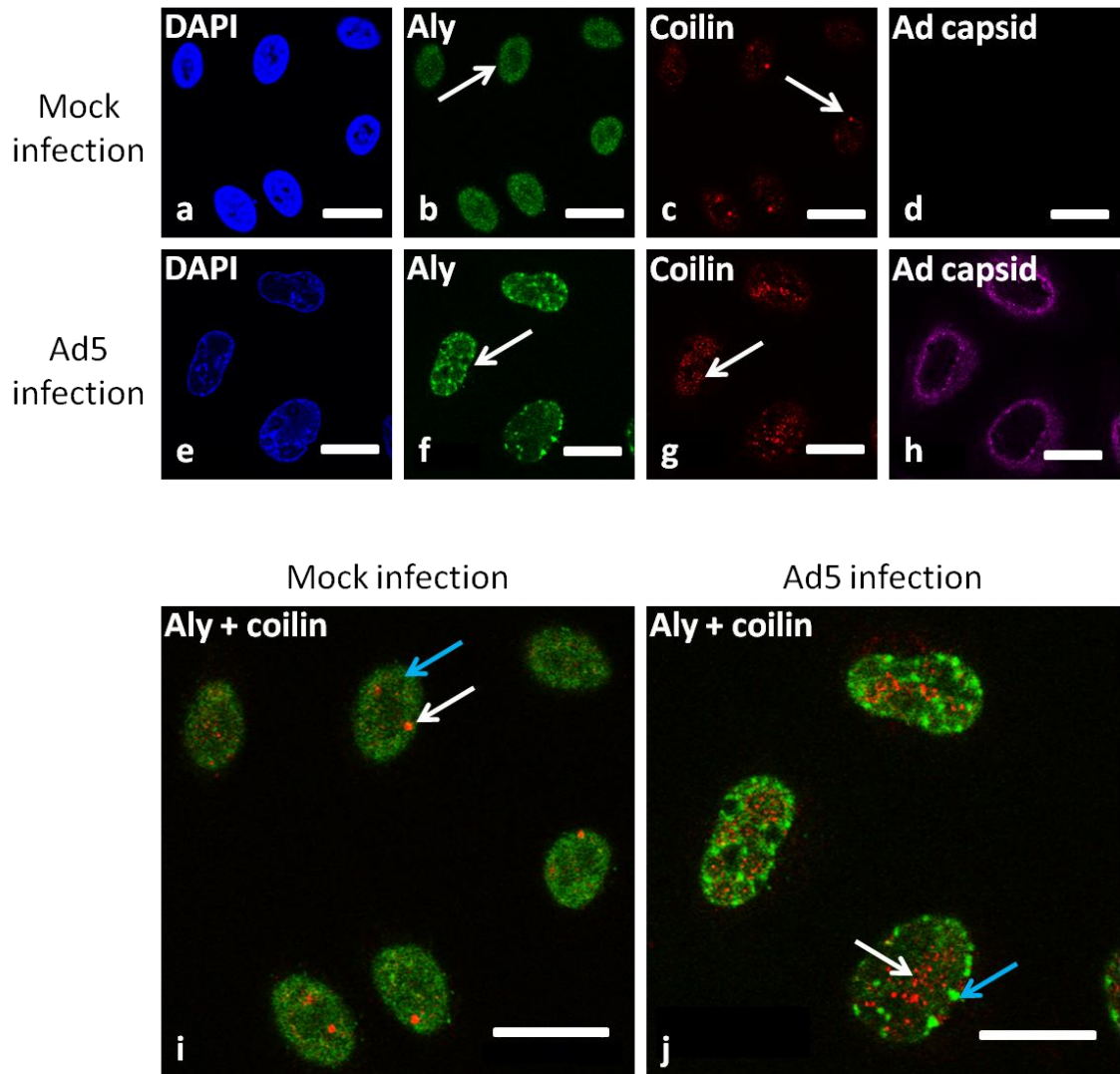
Figure 4-14. The redistribution of coilin following Ad5 infection relative to the cellular TREX-complex component, Aly.

A549 cells were mock or Ad5 infected at an MOI of 5 FFU/cell and incubated for 24 hours. Cells were fixed and subjected to indirect immunofluorescence. Cells were stained using a mouse anti-Aly and a rabbit anti-coilin antibody followed by incubation with the appropriate fluorescent-labelled secondary antibodies. Nuclei were stained using DAPI. Confocal microscopy was performed using an inverted LSM510 confocal microscope coupled to LSM Image Browser. In mock-infected cells, Aly was found diffusely within the nucleoplasm (image b, arrow) and coilin was located in punctate CBs (image c, arrow). As shown in the overlay (image i), there was no colocalisation between Aly (blue arrow) and coilin (white arrow). In Ad5-infected cells, Aly was rearranged into punctate foci that accumulated at the nuclear periphery (image f, arrow) and coilin was redistributed into rosettes (image g, arrow). As shown in the overlay (image j), there was no colocalisation between foci of Aly (blue arrow) and coilin foci (white arrow) in these cells. Bars = 20 μM.

161
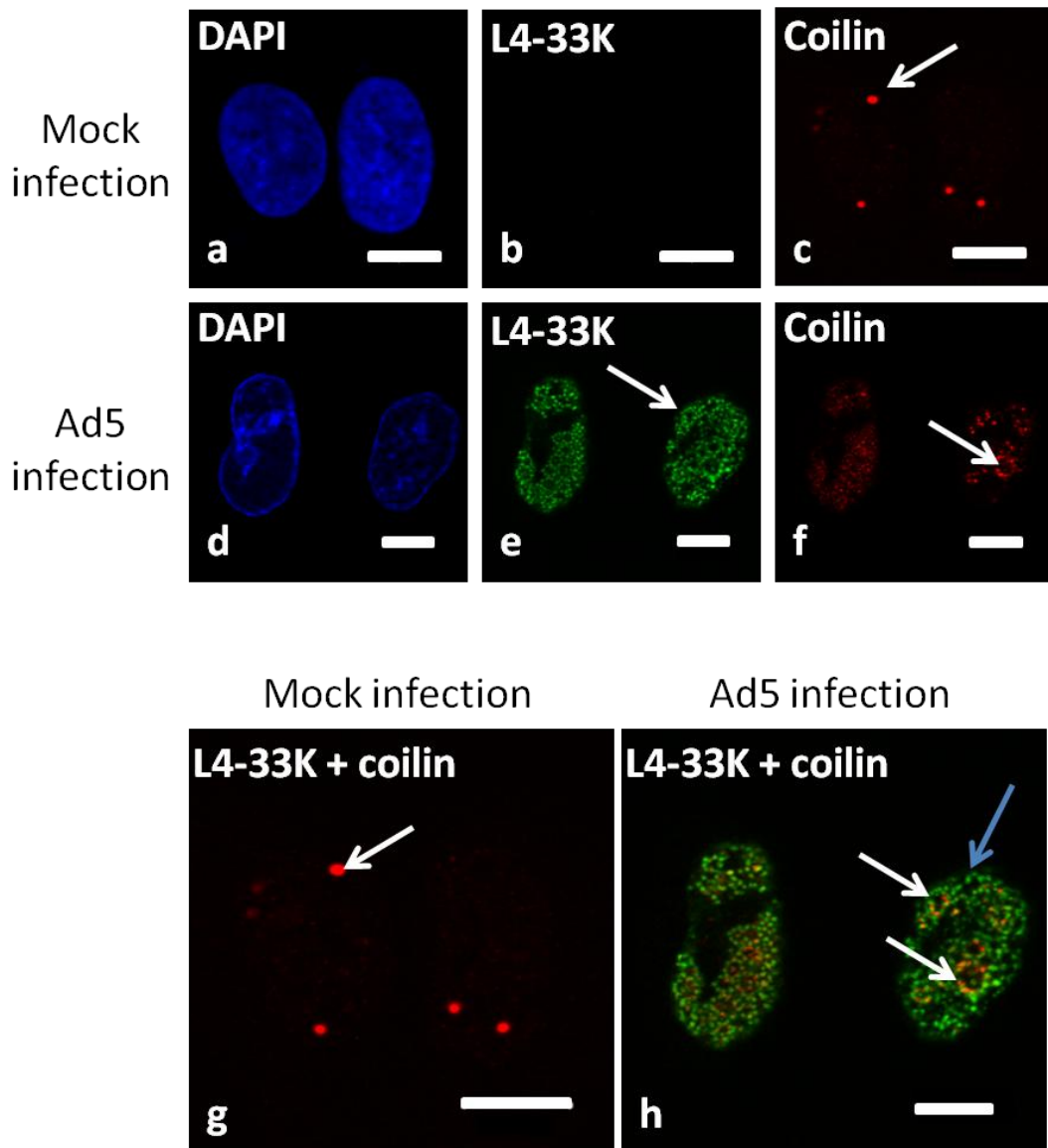
Figure 4-15. The redistribution of coilin following Ad5 infection relative to the Ad splicing factor, L4-33K.

A549 cells were mock or Ad5 infected at an MOI of 5 FFU/cell and incubated for 24 hours. Cells were fixed and subjected to indirect immunofluorescence. Cells were stained using a rabbit anti-L4-33K and a mouse anti-coilin antibody followed by incubation with the appropriate fluorescent-labelled secondary antibodies. Nuclei were stained using DAPI. Confocal microscopy was performed using an inverted LSM510 confocal microscope coupled to LSM Image Browser. Mock-infected cells were negative for L4-33K expression (image b) and coilin was located in punctate CBs (image c, arrow). In Ad5-infected cells, L4-33K was found in numerous nuclear foci arranged into clusters (image f, arrow). Coilin was redistributed into microfoci in Ad5-infected cells (image g, arrow). The coilin microfoci were less numerous than the L4-33K microfoci (compare image f, arrow with image g, arrow). As shown by the yellow regions in the overlay (image h, white arrows), there was partial colocalisation between coilin microfoci and L4-33K microfoci. However, some L4-33K microfoci did not colocalise with coilin (image h, blue arrow). Bars = 10 μM.

A key regulator of the switch from early to late splice site usage at the MLP is the Ad splicing factor, L4-33K. This protein is involved in the enhancement of IIIa splice site selection over that for 52/55K (Tormanen *et al.,* 2006). As completion of splicing is closely related to mRNA export, the location of coilin and L4-33K during Ad5 infection was investigated (Figure 4-15). Mock-infected cells did not express L4-33K (image b) and coilin was found in punctate CBs in these cells (image c, arrow). In Ad5-infected cells, L4-33K was located in numerous microfoci within the nucleus, which appeared to form circular clusters (image f, arrow). Coilin was also redistributed into microfoci in Ad5-infected cells (image g, arrow); however, the microfoci of coilin were larger and less numerous than the microfoci of L4-33K. As shown by the yellow regions in the overlay (image h, white arrow), coilin microfoci partially co-localised with microfoci of L4-33K. However, there were foci of L4-33K that did not contain coilin (image h, blue arrow). This indicated that some regions of L4-33K-dependent splicing may be associated with coilin foci during the later stages of Ad infection. However, as mentioned previously (Chapter 3.8), the antibody used to detect L4-33K may also detect L4-22K (Ostapchuk *et al.,* 2006). Therefore it is possible that the partial co-localisation of coilin with L4-33K could be colocalisation with L4-33K and/or L4-22K rather than L4-33K alone. Further studies are required to determine whether coilin partially co-localises with one or both of these proteins.

4.10   Chapter 4 Discussion

It was previously shown that during the late phase of Ad infection, CBs were disassembled from 1-6 punctate domains per cell into numerous microfoci (Rebelo *et al.,* 1996; Rodrigues *et al.,* 1996; James *et al.,* 2010). Furthermore, the marker protein of CB, p80 coilin, was suggested to play a role in the expression of Ad late phase proteins without altering the expression of an early protein (James *et al.,* 2010). However, the exact role of coilin in Ad late protein expression was unknown. In this Chapter, the role of coilin during Ad5 infection was investigated by depleting coilin in A549 cells by siRNA treatment. The impact of coilin depletion on Ad virus titre, Ad protein levels and Ad mRNA levels was then assessed. It was found that coilin depletion reduced the expression of early, intermediate and late phase Ad proteins. Although the majority of Ad mRNAs were not found to be significantly affected following coilin depletion, the export of Ad mRNAs from the nucleus to the cytoplasm was found to be greatly reduced. This indicated that the reduced expression of Ad proteins may be due to reduced export of Ad mRNAs into the cytoplasm. The yield of infectious virus was also found to be reduced following coilin depletion, indicating that reduced production of Ad late proteins results in reduced virus progeny. These are all novel findings which have not previously been shown.

Interestingly, the redistribution of coilin from CBs into microfoci has also been observed during infection with GRV, a highly unrelated plant virus. This was found to facilitate the trafficking of the GRV ORF3 protein to the nucleolus, allowing assembly of viral RNPs necessary for virus spread (Kim *et al.,* 2007, Canetta *et al.,* 2008). This indicates that CBs may be hijacked by different viruses to support diverse functions during infection. Other viruses shown to redistribute CBs include IBV and various herpesviruses (Fortes *et al.,* 1995; Salsman *et al.,* 2008). It would be interesting to establish the role of coilin and CBs during infection with these viruses to establish whether CB disassembly promotes functions similar to those reported during GRV and Ad infection or facilitates a novel role. As herpes viruses are DNA viruses requiring mRNA export from the nucleus, it would be of particular interest to determine whether, like Ad5, these viruses require coilin for mRNA export.

Late Ad mRNA export has been shown to require the ubiquitin ligase activity of the E1B-55K/E4orf6 complex, indicating that ubiquitination of a protein involved in mRNA export may be required for late Ad mRNA export (Woo and Berk, 2007; Blanchette *et al.*, 2008). In addition to marking proteins for degradation, ubiquitination is also a reversible posttranslational modification of protein activity (reviewed in Hunter, 2007). Therefore it is possible that ubiquitination of a currently undefined target protein involved in mRNA export by the E1B-55K/E4orf6 may either target that protein for degradation, or change the activity of the protein. To date, ubiquitination has not been shown to regulate coilin activity. Furthermore, the depletion of coilin appeared to reduce late Ad mRNA export, indicating that targeted ubiquitination and degradation of coilin by E1B-55K/E4orf6 would be unlikely to enhance mRNA export. However, as shown in Chapter 3.2, coilin appeared to be degraded at very late stages of Ad infection. It would therefore be interesting to investigate whether coilin is a target of E1B-55K/E4orf6 complex-dependent ubiquitination during the course of Ad5 infection.

The export of Ad early and intermediate mRNAs was recently shown to occur via the CRM1 export system (Schmid *et al.*, 2012) whilst Ad late mRNAs are exported via the Nxf1/TAP export complex (Yatherajam *et al.*, 2011). The Nxf1/TAP system is responsible for export of the majority of cellular mRNAs (Gruter *et al.*, 1998; Katahira *et al.*, 1999), whilst the CRM1 export system is primarily involved in the export of snRNAs and rRNAs (Fornerod *et al.*, 1997; Moy and Silver, 1999) and a subset of mRNAs corresponding to fast-acting response genes such as cytokine mRNAs (Kimura *et al.*, 2004). Whilst neither coilin nor the CB have been implicated in mRNA export in mammalian cells, CBs in larch microsporocytes were shown to accumulate poly(A) mRNA, suggesting a role for CBs in storage of mRNA prior to export (Kolowerzo *et al.,* 2009; Smolinski and Kolowerzo, 2012). Interestingly, it was recently suggested that trafficking via the CB was required for final maturation and export of snRNAs, which are

exported via the CRM1 pathway (Suzuki *et al.*, 2010). CBs are also known to be required for processing of histone mRNAs, which are exported via the Nxf1/TAP export system (Erkmann *et al.,* 2005). Therefore it appears that CBs may have links to both the CRM1 and Nxf1/TAP RNA export pathways. The apparent dependence of both early and late Ad mRNA export on coilin indicates a common role for coilin in both the CRM1 and Nxf1/TAP-mediated export pathways. Further work will be required to define the exact role of coilin in Ad mRNA export, and indeed a potential role in the export of cellular mRNAs. If coilin does have a role in cellular mRNA export, it is possible that levels of the cellular 'housekeeping' transcript GAPDH would be altered following coilin depletion. Normalisation of the levels of other transcripts to GAPDH transcript levels could then result in no apparent effect of coilin depletion on the cellular mRNA in question. Therefore, absolute quantification of cellular mRNA levels would be required to establish a potential role of coilin in cellular mRNA export (Bustin, 2000).

In addition to reducing Ad mRNA export, inhibition of CRM1 also appeared to compromise the stability of Ad early and intermediate mRNAs (Schmid *et al.*, 2012). In this Chapter, it was found for the majority of Ad mRNAs that coilin depletion did not cause a significant alteration to total mRNA levels (Figure 4-11). This indicated that for the majority of Ad mRNAs, coilin depletion does not alter their stability. This indicated that whereas CRM1 activity is required for both stability and export of Ad mRNAs, coilin is required only for export.

Whilst levels of the majority of Ad mRNAs were not found to be altered during Ad5 infection of siCoilin-treated cells as compared to siControl treated cells, E1A 13S and 12S and IX mRNAs were found to be significantly decreased (Figure 4-11). As Ad E1A mRNAs are spliced, it was possible to analyse pre-mRNAs and thus distinguish between a role for coilin in transcription or mRNA splicing/stability. It was found that coilin depletion did not affect pre-mRNA production, indicating that the transcription of E1A was not affected by coilin depletion (Figure 4-12). This suggested that the effect of coilin depletion alters either splicing or stability of 12S and 13S E1A mRNAs. As IX mRNA is not spliced, it was not possible to analyse IX pre-mRNA by this method. However, considering that coilin depletion did not appear to alter production of E1A, DBP, IVa2 or TPL-containing pre-mRNAs, this indicates that coilin is not involved in Ad transcription, and as a result, the decrease observed in IX mRNA levels following coilin depletion may be due to decreased stability. The mechanism by which coilin depletion alters the stability of some, but not all, Ad mRNAs requires further investigation.

The immediate early E1As 13S and 12S are required for the subsequent transcriptional activation of the other Ad transcriptional units (Berk *et al.*, 1979; Jones and Shenk, 1979; Nevins and Wilson, 1981; Morris *et al.*, 2010). Therefore it is surprising that a decrease in early

E1A transcripts, and subsequent decrease in E1A protein, did not impact on the production of the remaining early or major late transcripts. As E1A is produced in a greater excess than is required for saturation of cellular interaction partners (Barbeau *et al.*, 1992), it is possible that a threshold decrease in E1A protein levels is required before a negative effect is observed on the expression of the remaining Ad transcripts. Further work is required to clarify these suggestions.

The reduced early, intermediate and late phase protein expression following Ad5 infection of coilin-depleted cells reported in this Chapter contrasts with previously published data. James *et al.* (2010) reported that coilin depletion did not alter levels of DBP, whereas IIIa, hexon and fibre levels were significantly reduced. It was found that the discrepancies between the two sets of results were not due to the different cell lines used. However, Ad5 infection of coilin-depleted cells at an MOI of 1000 (the MOI used by James *et al.*) significantly reduced levels of fibre, whilst levels of DBP, IIIa and hexon were unaffected (Figure 4-10). Therefore these data at an MOI of 1000 partially explained the results obtained by James *et al*, as DBP was not affected following the depletion; however, levels of IIIa and hexon were not affected. It is possible that the depletion of coilin was greater in the study by James *et al,* resulting in an inhibitory effect on Ad5 protein production that was not observed in the current study. Nevertheless, the two separate studies do contribute to the idea that a greater virus input somehow overrides the inhibitory effect of coilin depletion on early protein expression, such that effects are only seen later in infection.

There are several points to consider when analysing the results from this Chapter. Coilin depletion was found to cause aberrant localisation of WRAP53 within the nucleus (Figure 4-6). Upon Ad5 infection of siCoilin-treated cells, WRAP53 was not redistributed within the nucleus in the same manner as in siControl-treated cells. Therefore the observed effects on the Ad lifecycle following coilin depletion could be due to mis-localisation of WRAP53 or other CB proteins that were not addressed in this study, rather than a direct effect due to reduced coilin levels. Further work will be required to investigate the roles of WRAP53 during Ad5 infection.

In this study, the siRNA depletion system used was not optimal as in siCoilin-treated cells infected with Ad5, early Ad proteins would have been expressed when the coilin level was around 60% the level of siControl-treated cells, whereas by the time of late protein expression, the coilin level will be further decreased to around 40% of siControl-treated cells (Figure 4-1A). Therefore any observed effects on the late phase of Ad infection may be more pronounced than effects on early phase. Furthermore, although the export of Ad mRNAs was significantly reduced following coilin depletion, export was not completely inhibited. As the depletion of coilin achieved in this investigation was around 60% (Figure 4-1), it is possible that low level

166

coilin expression was sufficient to support residual export of Ad mRNAs. Further studies are needed to establish whether coilin is absolutely required for Ad mRNA export by establishing the cytoplasmic: nuclear Ad mRNA ratio in coilin-knockout cell lines as compared to the parental cell line, or by the use of an inducible small hairpin RNA in A549 cells. It would also be of great interest to analyse the impact of coilin over-expression on Ad mRNA export to determine if this has the opposite effect to coilin depletion i.e. enhances Ad mRNA export. This could be achieved by using either stably-transformed coilin over-expressing cell lines or by transient transfection of cells with a coilin expression plasmid under the control of a constitutive promoter. However, considering that Ads do not appear to up-regulate coilin levels during infection (Figure 3-1), it is possible that existing steady-state cellular levels of coilin may be sufficient to support Ad mRNA export.

In summary, the novel results from this investigation uncovered a previously unknown role for coilin in the export of Ad5 mRNAs from the nucleus to the cytoplasm and a potential role for coilin in the post-transcriptional processing or stability of Ad5 13S, 12S and IX mRNAs. Depletion of coilin reduced the export of Ad5 mRNA, leading to reduced expression of Ad5 proteins and reduced virus titre. Further work is now required to determine the exact function of coilin in Ad5 mRNA export. Furthermore, investigation of a role for coilin in mRNA export with other viruses is also warranted.

Chapter 5 – Characterising the role of SMN during Ad5 infection

5.1 Introduction

In Chapter 3, it was shown that following Ad5 infection, the CB protein SMN is redistributed to a separate, as yet unidentified sub-nuclear domain to the CB proteins coilin, fibrillarin and WRAP53. Therefore SMN may play a different role to coilin, fibrillarin and WRAP53 during Ad5 infection. To date, there has been no reported involvement of SMN in Ad infection. In order to investigate the potential role of SMN during Ad5 infection, depletion of SMN was performed by siRNA treatment and the subsequent impact on Ad5 virus yield, protein levels and mRNA levels were assessed.

5.2 Western blot analysis of SMN depletion following siRNA transfection

In order to identify the most appropriate time point post-transfection to infect SMN-depleted cells with Ad5, siRNA treatment using scrambled control siRNA (siControl) or SMN siRNA (siSMN) (Table 2-2) was performed in A549 cells (Chapter 2.2.5.1) and incubated for 24 or 48 hours. At 48 hours post-transfection, cells were 90-100% confluent; therefore a further time point was not taken as it was reasoned that cell viability may be compromised in over-confluent cells. Whole cell lysates were prepared and protein was separated by SDS-PAGE and analysed by Western blotting (Chapter 2.2.2).

As shown in Figure 5-1A, at 24 hours post-transfection the level of SMN protein in siSMN-treated cells was decreased by around 40% compared to siControl-treated cells. By 48 hours post-transfection, the level of SMN in siSMN-treated cells was decreased by around 70% compared to siControl-treated cells. It was therefore decided to infect cells with Ad5 at 24 hours post-transfection when a substantial proportion of SMN protein was depleted. It was decided to harvest cells at 24 h.p.i (i.e. at 48 hours post-transfection) when SMN protein levels would be approaching 30% of the level of siControl-treated cells.

As mentioned in Chapter 4, the Ad VA-RNAs are known to interfere with the RNA silencing machinery (Andersson *et al.*, 2005). To test whether Ad5 infection altered the efficiency of SMN depletion, siRNA depletion was performed using siControl or siSMN (Chapter 2.2.5.1) and incubated for 24 hours. Cells were mock or Ad5 infected (Chapter 2.2.6.1). At 24 h.p.i, whole cell lysates were prepared and protein was separated by SDS-PAGE and analysed by Western blotting (Chapter 2.2.2). As shown in Figure 5-1B, compared to siControl mock-infected cells, the level of SMN in siSMN-treated, mock infected cells and siSMN-treated, Ad5-infected cells was 38% and 36%, respectively. This indicates that Ad5 infection of siSMN-treated cells did not affect the efficiency of SMN depletion. In addition, there was no difference in SMN protein levels between siControl-treated, mock-infected cells and siCoilin-treated, Ad5-infected cells (Figure 5.1B), showing that Ad5 infection does not alter SMN levels.
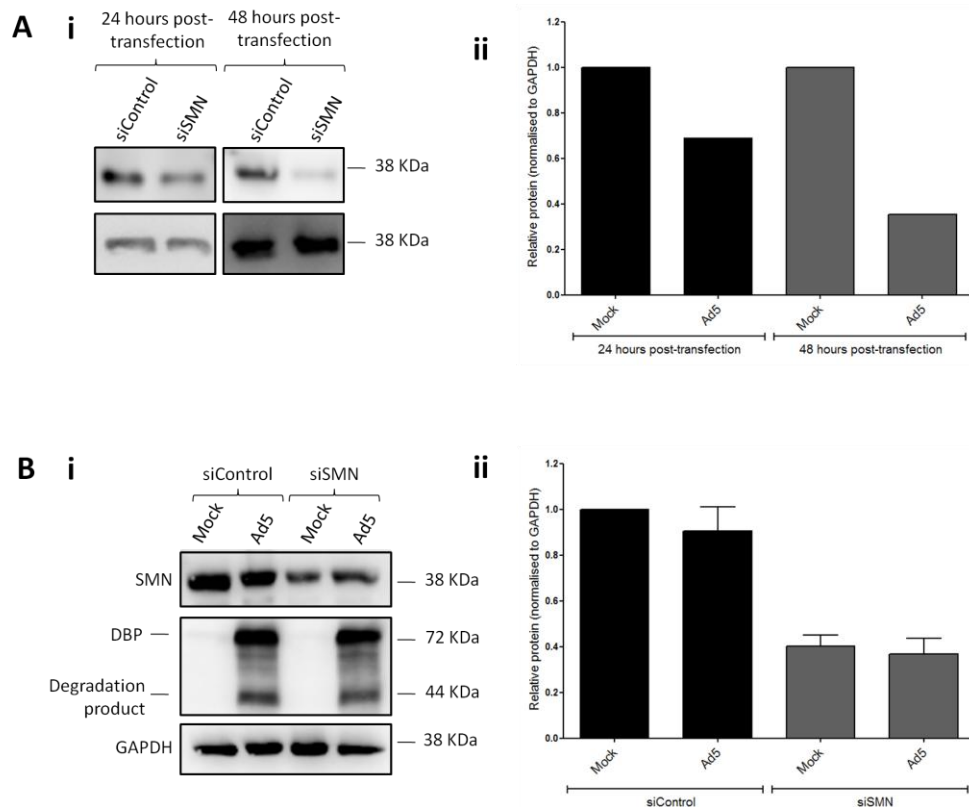
Figure 5-1. Depletion of SMN from A549 cells by siRNA transfection.

A549 cells were treated with siControl or siSMN and incubated for 24 hours. Cells were mock or Ad5 infected and incubated for 24 hours. Cells were harvested and equal amounts of protein from whole cell lysates (20 μg) was subjected to separation by SDS-PAGE and analysis by Western blotting. Bound antibody was detected using the ECL system and images were captured using a Las 3000 Imager. Signal intensities were calculated by densitometric analysis, normalising to the signal intensity of the loading control, GAPDH. Results are displayed relative to the siControl-treated, mock-infected sample, which was set to a value of 1. A. i. Analysis of SMN levels at 24 and 48 hours post-transfection by Western blot. Compared with siControl-treated cells, siSMN-treated cells exhibited decreased SMN levels at 24 hours post-transfection and at 48 hours post-transfection. ii. Densitometric analysis of SMN levels at 24 and 48 hours post-transfection. Compared with siControl-treated cells, SMN levels in siSMN-treated cells were reduced at 24 and 48 hours post-transfection by approximately 40% and 70%, respectively. B. i. Western blot analysis of SMN levels at 48 hours post-transfection, with mock or Ad5 infection performed at 24 hours post-transfection. Compared with siControl-treated cells, SMN levels were decreased in siSMN-treated, mock-infected cells and in siSMN-treated, Ad5-infected cells. ii. Densitometric analysis of SMN levels at 48 hours post-transfection, with mock or Ad5 infection performed at 24 hours post-transfection. Results are the mean fold change in protein level (± SEM) from at least three independent experiments. Results are displayed relative to the siControl-treated, mock-infected sample, which was set to a value of 1. Compared with siControl-treated, mock-infected cells, SMN levels were reduced in siSMN-treated, mock-infected cells and siSMN-treated, Ad5-infected cells by 62% and 64%, respectively.

170

5.3 The effect of SMN depletion on cell proliferation and/or viability using the MTT assay

SMN has previously been shown to be necessary for embryonic viability (Schrank *et al.*, 1997; Miguel-Aliaga *et al.*, 1999). Furthermore, SMN depletion in cultured cells appears to decrease cell proliferation and viability (Parker *et al.*, 2008; Grice and Liu, 2011). The MTT assay was therefore used to determine whether SMN depletion by approximately 70% resulted in decreased cell proliferation and/or viability of A549 cells. As with coilin depletion (Chapter 4), the MTT assay required the experiment to be performed in 96-well plates by 'reverse siRNA transfection'. In order to determine whether SMN is depleted to a similar level by the 'reverse transfection' procedure compared to conventional siRNA transfection, 'reverse transfection' using siControl or siSMN was carried out in 6 well plates (Chapter 2.2.5.2) and incubated for 24 hours. Cells were mock or Ad5 infected (Chapter 2.2.6.1) and incubated for a further 24 hours. Cell lysates were prepared and protein was separated by SDS-PAGE and analysed by Western blotting (Chapter 2.2.2). As shown in Figure 5-2A, when compared to mock-infected, siControl-treated cells, the level of SMN was substantially decreased in siSMN-treated mock-infected cells and siSMN-treated Ad5 infected cells, calculated from densitometric analysis as decreases of 61% and 63%, respectively (Figure 5-2B). This is comparable to the depletion achieved by conventional depletion (Figure 5-1B).

To assess whether cell proliferation and/or viability of A549 cells were altered following SMN depletion, 'reverse siRNA transfection' was carried out using siControl or siSMN in 96-well plates (Chapter 2.2.5.2) and incubated for 24 hours. Cells were mock or Ad5 infected (Chapter 2.2.6.1). At 24 h.p.i, cells were analysed by the MTT assay (Chapter 2.2.9). As shown in Figure 5-2C, siSMN-treated, mock-infected cells did not exhibit significantly altered absorbance at 570 nm compared to siControl-treated, mock-infected cells. This indicates that SMN depletion by 60-70% does not alter the cell viability or proliferation of A549 cells. As expected and as reported in Chapter 4, Ad5 infection of siControl-treated cells resulted in decreased viability compared to siControl-treated mock-infected cells, although this decrease was not significant. Cells treated with siSMN prior to Ad5 infection did not exhibit any significant change in the absorbance at 570 nm compared to siControl-treated, Ad5-infected cells or compared to siControl-treated, mock-infected cells. This indicates that depletion of SMN by 70% of siControl-treated cells did not alter the proliferation or viability of A549 cells infected with Ad5.
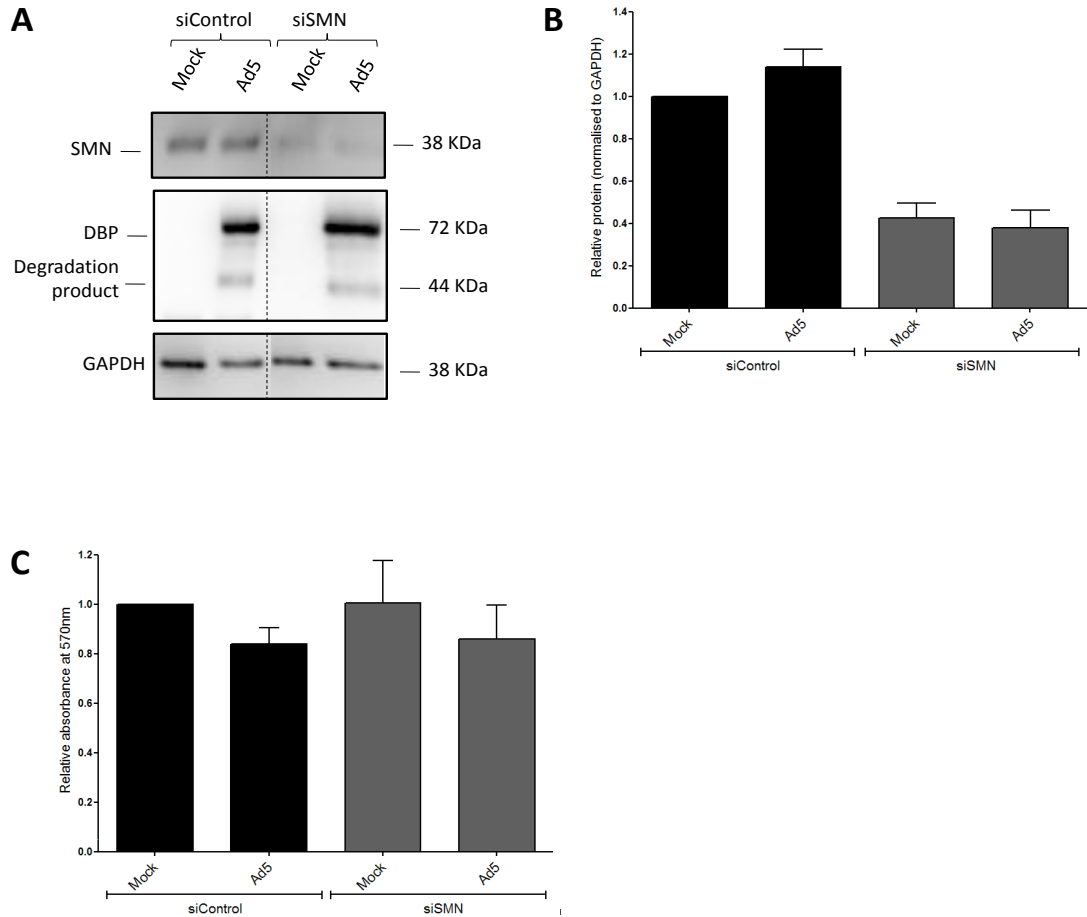
Figure 5-2. The impact of SMN depletion on the cell viability and proliferation of A549 cells.

A549 cells were treated with siControl or siSMN and incubated for 24 hours. Cells were mock or Ad5 infected and incubated for 24 hours before harvesting. A. Representative Western blots of A549 cells subjected to 'reverse siRNA transfection' followed by mock or Ad5 infection. Equal masses of protein from each sample (20 μg) were separated by SDS-PAGE and analysed by Western blotting. Bound antibody was visualised using the ECL system on a Las 3000 Imager. SMN levels were similar in siControl-treated, mock-infected cells and siControl-treated, Ad5-infected cells. Compared with siControl-treated cells, SMN levels were reduced in siSMN-treated, mock-infected cells and siSMN-treated, Ad5-infected cells by a similar degree. B. Densitometric analysis of Western blots from cells subjected to 'reverse' siRNA transfection followed by mock or Ad5 infection. Signal intensities were calculated by densitometric analysis, normalising to the signal intensity of the loading control, GAPDH. Results are the mean fold change in protein level (± SEM) from three independent experiments. SMN levels were similar in siControl-treated, mock-infected cells and siControl-treated, Ad5-infected cells. Compared with siControl-treated, mock-infected cells, SMN levels in siSMN-treated, mock-infected cells and siSMN-treated, Ad5-infected cells were reduced by 61% and 63%, respectively. C. Impact of SMN depletion on the viability of mock- and Ad5-infected A549 cells. Results are the mean fold change in absorbance at 570 nm (± SEM) from at least three independent experiments performed in triplicate. The absorbance at 570 nm was similar in siControl-treated, mock-infected cells and siControl-treated, Ad5-infected cells. Compared with siControl-treated, mock-infected cells, there was no significant difference in absorbance at 570 nm in siSMN-treated, mock-infected cells or in siSMN-treated, Ad5-infected cells.

5.4 The impact of SMN depletion on cellular levels of other CB proteins

SMN is known to interact with multiple cellular protein partners including the CB proteins coilin, WRAP53, Sm and the nucleolar protein fibrillarin (Liu *et al.*, 1997; Hebert *et al.*, 2001; Pellizzoni *et al.*, 2001a; Mahmoudi *et al.*, 2010). Therefore it is possible that SMN depletion may alter the levels of SMN-associated proteins. To address this, siRNA-mediated depletion of SMN was performed in A549 cells (Chapter 2.2.5.1) and incubated for 24 hours. Cells were mock or Ad5 infected (Chapter 2.2.6.1) and incubated for 24 hours. Whole cell lysates were prepared and protein was separated by SDS-PAGE and analysed by Western blotting (Chapter 2.2.2). As shown in the Western blots in Figure 5-3A, depletion of cellular SMN did not appear to alter the levels of coilin, Sm, WRAP53 or fibrillarin. This was confirmed by densitometric analysis (Figure 5-3B). This indicates that SMN depletion does not alter the cellular levels of SMN-interacting proteins or associated CB proteins.

To confirm the Western blotting data by a more quantitative method, levels of CB proteins following SMN depletion and Ad5 infection was also assayed by flow cytometry. As described in Chapter 4, WRAP53 were not assessed by this method as from Western blot analysis this antibody was found to exhibit non-specific binding to an unidentified protein of 65 kDa. SMN, fibrillarin, coilin and Sm were assayed by flow cytometry. As shown in Figure 5-4, siSMN-treated cells did not appear to alter the levels of coilin, Sm or fibrillarin compared to siControl-treated cells. Taken together, these data indicate that depletion of SMN does not significantly alter the cellular level of other CB proteins.

Interestingly, a significant increase was found in SMN levels following Ad5 infection of siControl-treated cells compared to mock-infection of siControl-treated cells (Figure 5-4). This suggested that SMN levels are increased by 24 h.p.i with Ad5. This contrasts with the flow cytometric data in Chapter 4.4, where no such increase in SMN levels was found following Ad5 infection. This inconsistency is likely due to fact that different SMN antibodies were used between these two sets of experiments; a mouse anti-SMN antibody was used in the flow cytometry experiments in Chapter 4.4, whereas a rabbit anti-SMN antibody was used in the experiments in this section.

5.5 The impact of SMN depletion on the subcellular distribution of other CB proteins

RNA interference of SMN has previously been shown to induce defects in CB formation, resulting in coilin become redistributed to multiple nuclear foci and also localising to the nucleolus (Girard *et al.*, 2006). However, contrasting results indicated that SMN is not required
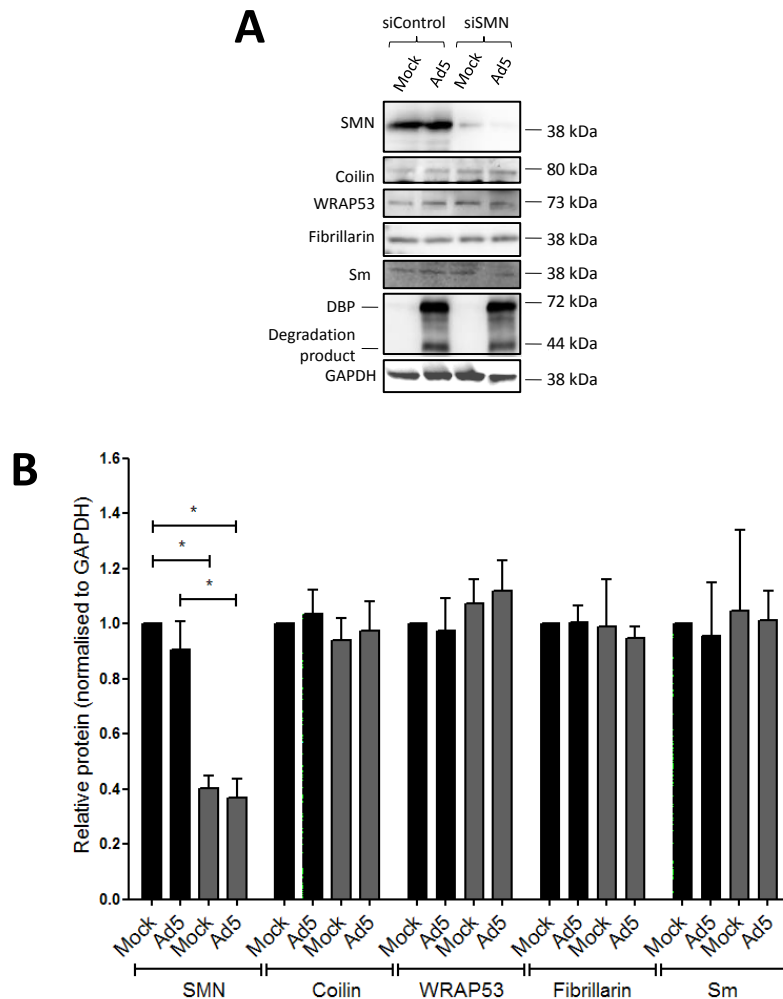
Figure 5-3. Western blot analysis of CB proteins following Ad5 infection of SMN-depleted cells.
A549 cells were treated with siControl or siSMN and incubated for 24 hours. Cells were mock or Ad5 infected and incubated for 24 hours. Cells were harvested, whole cell lysates were prepared and equal masses of protein (20 μg) was separated by SDS-PAGE and analysed by Western blotting. Bound antibody was detected using the ECL system and images were captured using a Las 3000 Imager. Signal intensities from Western blots were calculated by densitometric analysis and were normalised to the loading control, GAPDH. A. Representative Western blots of CB proteins following Ad5 infection of SMN-depleted cells. Levels SMN, coilin, WRAP53, fibrillarin and Sm were similar in siControl-treated, mock-infected cells and siControl-treated, Ad5-infected cells. SMN levels were decreased in siSMN-treated, mock-infected cells and in siSMN-treated, Ad5-infected cells by a similar degree, whilst levels of coilin, WRAP53, fibrillarin and Sm were not altered. B. Densitometric analysis of CB protein levels following Ad5 infection of SMN-depleted cells. Results are the mean fold change in protein level ($\pm$ SEM) from at least three independent repeats. Results are relative to the siControl-treated, mock-infected sample, which was set to a value of 1. Statistics were calculated using the paired one-tailed t-test. Levels of coilin, WRAP53, fibrillarin and Sm were similar in siControl-treated, mock-infected cells and siControl-treated, Ad5 infected cells. Compared with siControl-treated, mock-infected cells, levels of SMN in siSMN-treated, mock-infected cells and siSMN-treated, Ad5-infected cells were reduced by 61% and 64%, respectively. Black bars = siControl-treated cells. Grey bars = siSMN-treated cells. $*p<0.05$.
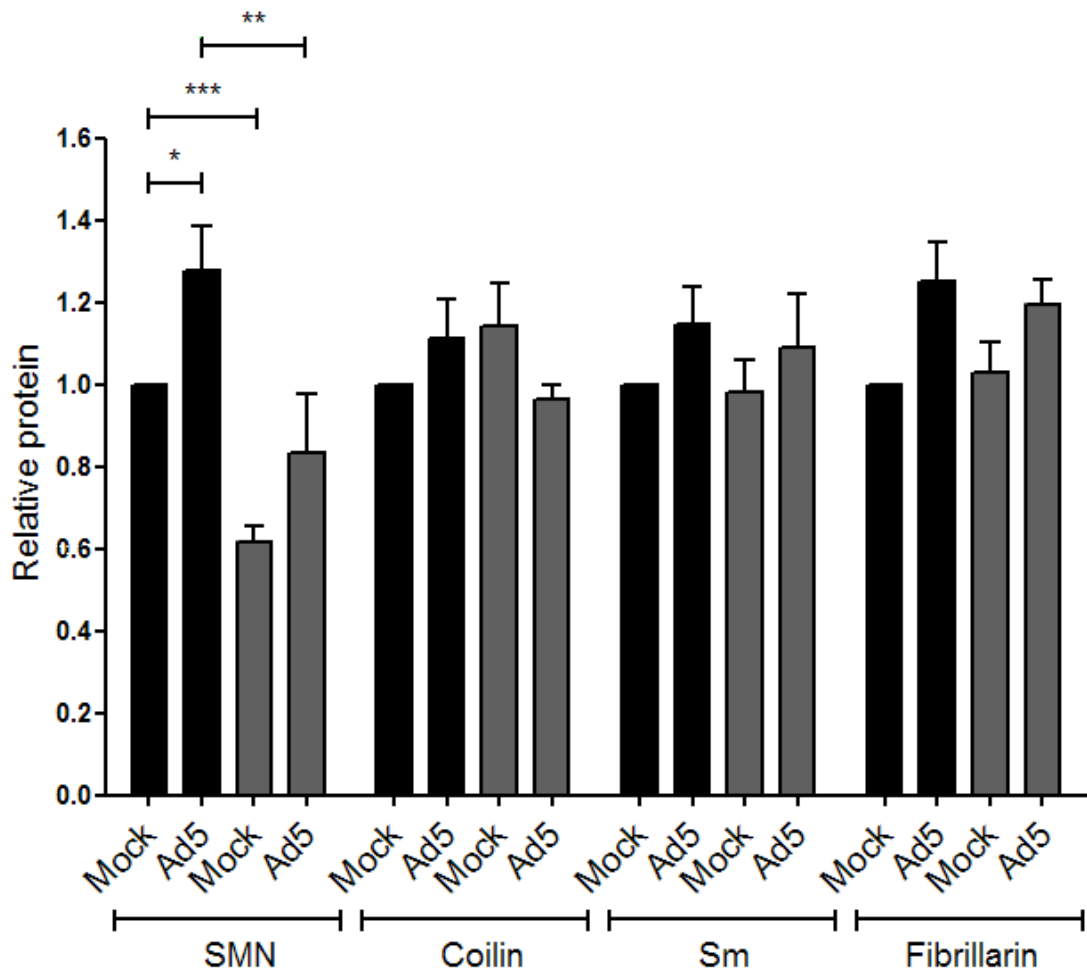
Figure 5-4. Flow cytometric analysis of CB proteins following Ad5 infection of SMN-depleted cells.
A549 cells were treated with siControl or siSMN and incubated for 24 hours. Cells were mock or A5 infected at an MOI of 5 FFU/cell and incubated for 24 hours. Cells were harvested and subjected to flow cytometric analysis. Results are the mean fold change in protein level (± SEM) from at least three independent experiments performed in duplicate. Results are displayed relative to the siControl-treated, mock-infected sample, which was set to a value of 1. Levels of coilin, Sm and fibrillarin were similar in siControl-treated, mock-infected cells and siControl-treated, Ad5-infected cells. A rabbit anti-SMN antibody was used in these experiments, and an increase in SMN levels was observed in siControl-treated, Ad5-infected cells compared with siControl-treated, mock-infected cells. Compared with siControl-treated, mock-infected cells, levels of SMN were reduced in siSMN-treated, mock-infected cells but were not significantly reduced in siSMN-treated, Ad5-infected cells. Compared with siControl-treated, Ad5-infected cells, SMN levels were reduced in siSMN-treated, Ad5-infected cells. Levels of coilin, Sm and fibrillarin were not significantly altered in siSMN-treated cells compared with siControl-treated cells. The Black bars = siControl-treated cells. Grey bars = siSMN-treated cells. * p<0.05, **p<0.01, ***p<0.001.

for the maintenance of CB structure (Lemm *et al.*, 2006). Therefore it is possible that depletion of cellular SMN may disrupt the subcellular distribution of other CB proteins. If this is the case, any effect of SMN depletion on Ad5 infection could be due to a secondary effect of SMN depletion on the subcellular distribution of an SMN-interacting protein. It was decided to identify whether SMN depletion disrupted the subcellular distribution of the CB proteins WRAP53 or coilin by immunofluorescence microscopy. A549 cells were subject to siRNA depletion using siControl or siSMN (Chapter 2.2.5.1) and were incubated for 24 hours. Cells were mock or Ad5 infected (Chapter 2.2.6.1). At 24 h.p.i, cells were harvested and subjected to indirect immunofluorescence (Chapter 2.2.7).

As shown in Figure 5-5, siControl-treated, mock-infected cells exhibited a punctate CB distribution of SMN (image b, arrow) and coilin (image c, arrow), with these two proteins colocalising in CBs, as shown by the yellow regions in the overlay (image q, arrow). Ad5 infection of siControl-treated cells resulted in redistribution of SMN into rod-shaped structures in the nucleus (image f, arrow) whilst coilin was redistributed into microfoci (image g, arrow). As shown in the overlay, there was no colocalisation between redistributed SMN (image r, blue arrow) and coilin microfoci (image r, white arrow). In siSMN-treated, mock-infected cells, SMN staining was reduced in the majority of cells (image j, white arrow) whilst some cells retained SMN expression (image j, blue arrow). In cells depleted of SMN, coilin was maintained in punctate CBs (image k, blue arrow), consistent with previous studies indicating that SMN is not required for CB integrity (Lemm *et al.*, 2006). These coilin foci in SMN-depleted cells (image k, blue arrow) appeared to be very similar in morphology to CBs in cells expressing SMN (image k, white arrow). As shown in the overlay (image s), in cells expressing SMN, coilin and SMN colocalised in CBs (blue arrow), whilst in cells depleted of SMN, coilin was found in CBs in the absence of SMN (white arrow). In siSMN-treated, Ad5-infected cells, SMN staining was reduced in the majority of cells (image n, white arrow) whilst some cells retained SMN expression (image n, blue arrow). In cells depleted of SMN, coilin appeared to be redistributed into rosettes (image o, white arrow) in a similar manner to coilin redistribution following Ad5 infection of SMN-expressing cells (image o, blue arrow). As shown in the overlay (image t), in cells retaining SMN expression, there was no colocalisation of coilin microfoci (yellow arrow) with SMN structures (blue arrow) and in cells lacking detectable SMN, coilin microfoci were present (white arrow). These date indicated that, in the absence of SMN, coilin distribution was minimally affected and coilin was still redistributed into rosettes following Ad5 infection.

The impact of SMN depletion on the subcellular distribution of WRAP53 was also assessed (Figure 5-6). In siControl-treated, mock-infected cells, SMN was found in CBs (image b,
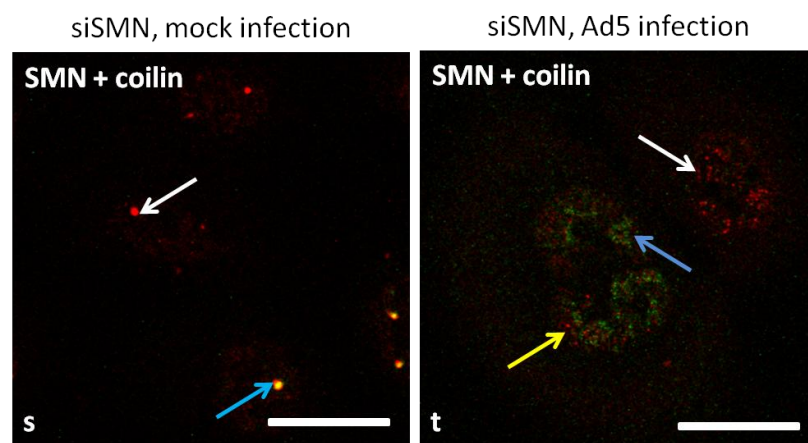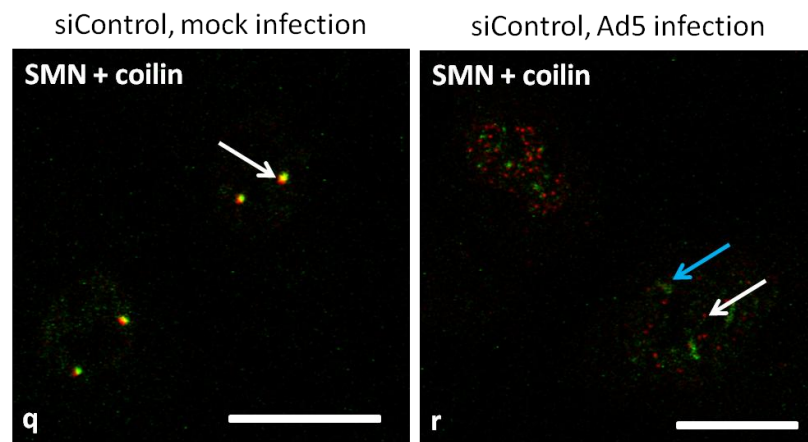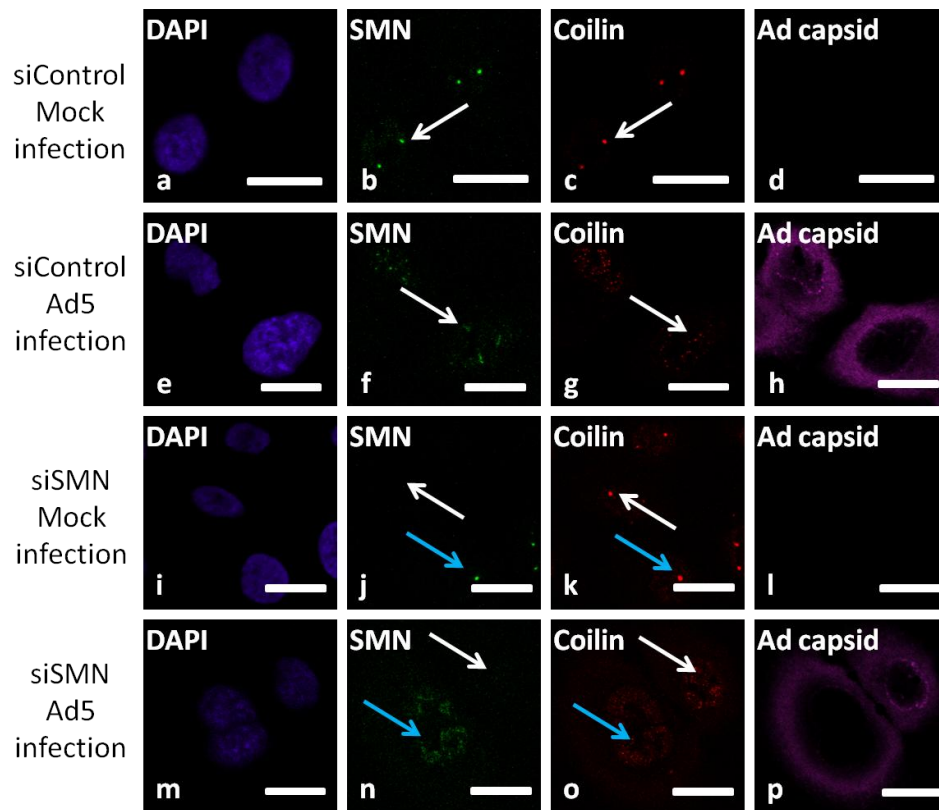
Figure 5-5. The subcellular localisation of coilin following Ad5 infection of SMN-depleted cells.
A549 cells were treated with siControl or siSMN and incubated for 24 hours. Cells were mock or Ad5 infected at an MOI of 5 FFU/cell and incubated for a further 24 hours. Cells were harvested and subjected to indirect immunofluorescence. Cells were incubated with a mouse anti-SMN, a rabbit anti-coilin and a goat anti-Ad capsid antibody followed by incubation with the appropriate fluorescent-labelled secondary antibodies. Nuclei were stained using DAPI. Confocal microscopy was performed using an inverted LSM510 confocal microscope coupled to LSM Image Browser. In siControl-treated, mock-infected cells, coilin was found in punctate CBs (image b, arrow); SMN was also found in punctate CBs (image c, arrow). As shown by the yellow regions in the overlay, coilin and SMN colocalised in CBs (image q, arrow). In siControl-treated, Ad5-infected cells, SMN was redistributed from CBs into the nucleoplasm, concentrated in rod-shaped structures (image f, arrow) whilst coilin was redistributed into microfoci (image g, arrow). As shown in the overlay (image r), redistributed SMN (blue arrow) did not colocalise with redistributed coilin (white arrow). In siSMN-treated, mock-infected cells, SMN staining was reduced in the nucleus in the majority of cells (image j, white arrow) whilst some cells retained SMN expression (image j, blue arrow). Cells depleted of SMN retained coilin staining in punctate CBs (image j, blue arrow) which appeared identical to CBs found in cells expressing SMN (image j, white arrow). As shown by the yellow regions in the overlay (image s), cells retaining SMN expression exhibited colocalisation of coilin and SMN in CBs (blue arrow) whilst CBs in cells depleted of SMN contained only coilin (white arrow). In siSMN-treated, Ad5-infected cells, SMN staining was reduced in the majority of cells (image n, blue arrow) whilst some cells retained SMN expression (image n, white arrow). Coilin was redistributed into microfoci in cells depleted of SMN (image o, blue arrow); these microfoci were similar to those seen following infection of cells expressing SMN (image o, white arrow). As shown in the overlay (image t), cells expressing SMN showed no colocalisation of SMN (blue arrow) with coilin microfoci (yellow arrow), whilst cells depleted of SMN exhibited only coilin microfoci (white arrow). Bars = 20 μm.
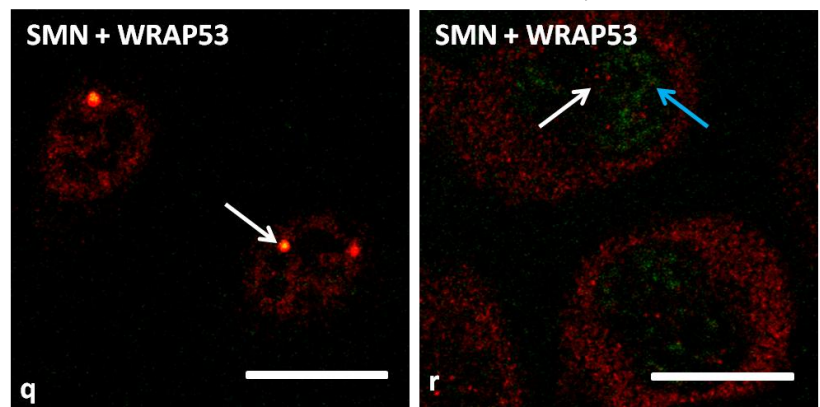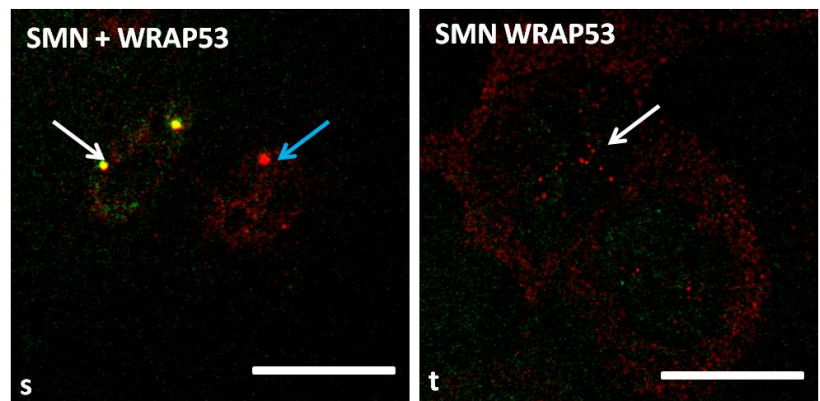
Figure 5-6. The subcellular localisation of WRAP53 following Ad5 infection of SMN-depleted cells.
A549 cells were treated with siControl or siSMN and incubated for 24 hours. Cells were mock or Ad5 infected at an MOI of 5 FFU/cell and incubated for a further 24 hours. Cells were harvested and subjected to indirect immunofluorescence. Cells were incubated with a mouse anti-SMN, a rabbit anti-WRAP53 and a goat anti-Ad capsid antibody followed by incubation with the appropriate fluorescent-labelled secondary antibodies. Nuclei were stained using DAPI. Confocal microscopy was performed using an inverted LSM510 confocal microscope coupled to LSM Image Browser. In siControl-treated, mock-infected cells, SMN was found in punctate CBs (image b, arrow) and WRAP53 was also found in CBs (image c, arrow). As shown by the yellow regions in the overlay, SMN and WRAP53 colocalised in CBs (image q, arrow). In siControl-treated, Ad5-infected cells, SMN was redistributed from CBs into rod-shaped structures in the nucleoplasm (image f, arrow). WRAP53 was redistributed into nuclear microfoci (image g, arrow). As shown in the overlay (image r), redistributed SMN (blue arrow) did not colocalise with microfoci of WRAP53 (white arrow). In siSMN-treated, mock-infected cells, there was reduced SMN staining in the majority of cells (image j, blue arrow) whilst some cells retained SMN expression (image j, white arrow). WRAP53 was retained in CBs in cells depleted of SMN (image k, blue arrow) which appeared similar to CBs seen in cells expressing SMN (image k, white arrow). As shown by the yellow regions in the overlay (image s), cells expressing SMN exhibited colocalisation of WRAP53 and SMN in CBs (white arrow) whilst cells depleted of SMN exhibited CBs containing only WRAP53 (blue arrow). In siSMN-treated, Ad5-infected cells, SMN staining was reduced in the majority of cells (image n, arrow). WRAP53 was redistributed into microfoci in these cells (image o, arrow). As shown in the overlay (image t), cells devoid of SMN exhibited microfoci of WRAP53 in the nucleus (white arrow). Bars = 20 μm.

arrow); WRAP53 was also located in CBs (image c, arrow). These two proteins colocalised in CBs, as shown by the yellow regions in the overlay (image q, arrow). In siControl-treated, Ad5 infected cells, SMN was redistributed into rod-shaped structures in the nucleoplasm (image f, arrow) and WRAP53 was redistributed into microfoci (image g, arrow). As shown in the overlay (image r), redistributed SMN (blue arrow) did not colocalise with WRAP53 foci (white arrow). In siSMN-treated, mock-infected cells, there was a loss of SMN staining in the majority of cells (image j, blue arrow) whilst some cells retained SMN expression (image j, white arrow). In SMN-depleted cells, WRAP53 was found in CBs (image k, blue arrow), which appeared analogous to WRAP53 staining in CBs in cells expressing SMN (image k, white arrow). This supports previously published data showing that whilst coilin and WRAP53 are integral for CB structure, SMN is not required (Lemm *et al.*, 2006; Mahmoudi *et al.*, 2010). As shown in the overlay (image s), WRAP53 and SMN colocalised in CBs in cells expressing SMN (white arrow), whilst in cells depleted of SMN, WRAP53 was found in CBs in the absence of SMN (blue arrow). In siSMN-treated, Ad5-infected cells, SMN staining was reduced in the majority of cells (image n, arrow) and WRAP53 was redistributed into microfoci (image o, arrow). These microfoci of WRAP53 appeared similar to WRAP53 microfoci seen in siControl-treated, Ad5-infected cells (image g, arrow). As shown in the overlay, in cells depleted of SMN, WRAP53 was found in nuclear microfoci (image t, arrow). These data indicated that there was no significant alteration to the subcellular distribution of WRAP53 following depletion of SMN, and, following Ad5 infection, WRAP53 was redistributed into rosettes in a similar manner to that seen in cells expressing SMN.

5.6 Impact of SMN depletion on Ad5 virus yield

To assess whether SMN depletion affected the production of infectious progeny viruses following Ad5 infection, A549 cells were subjected to siRNA transfection using siControl or siSMN (Chapter 2.2.5.1) and incubated for 24 hours. Cells were mock or Ad5 infected (Chapter 2.2.6.1) and incubated for 24 hours. Cell lysates were prepared and used to infect fresh A549 cells (Chapter 2.2.6.2). As with coilin depletion (Chapter 0), both plaque assays and flow cytometric assays were used to assess the impact of SMN depletion on virus yield.

As shown in Figure 5-7A, depletion of SMN resulted in a significant decrease in the production of Ad5 progeny virus as assessed by plaque assay. Similar results were obtained by flow cytometric analysis (Figure 5-7B), where SMN depletion significantly reduced the levels of hexon expression following re-infection. These results strongly suggest that depletion of SMN significantly impairs Ad replication. This indicates that, similar to coilin, SMN is required for a productive Ad5 infection.
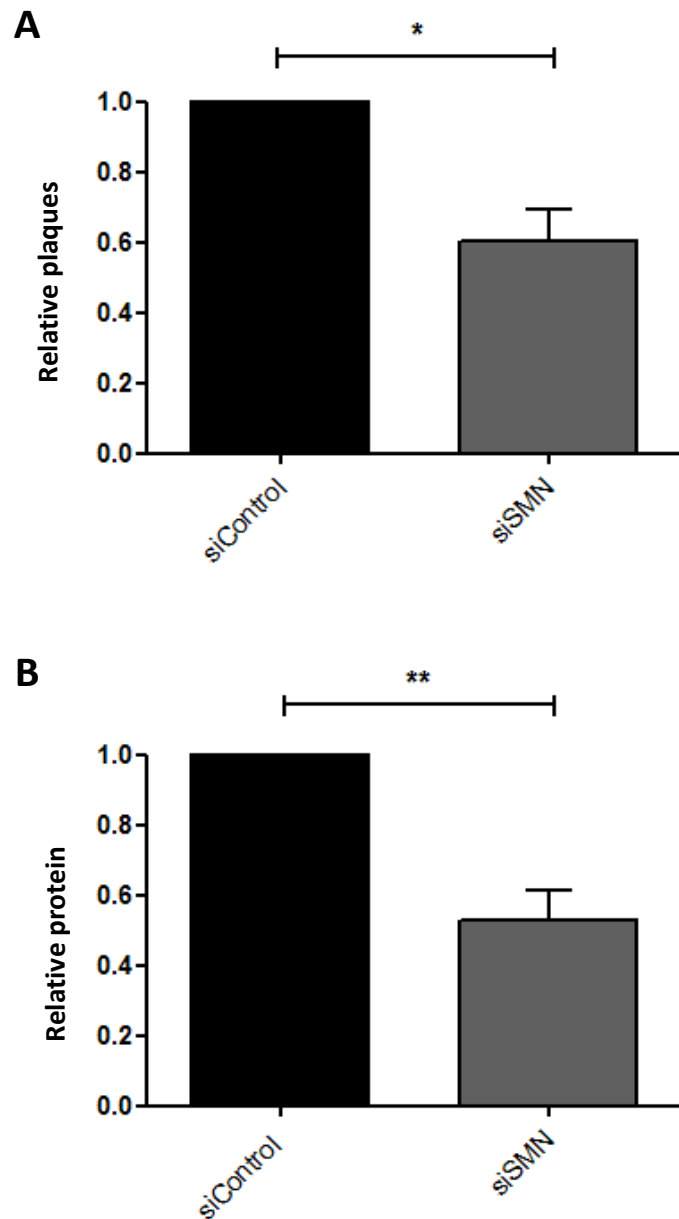
Figure 5-7. The impact of SMN depletion on Ad5 virus yield.

A549 cells were treated with siControl or siSMN and incubated for 24 hours. Cells were mock or Ad5 infected and incubated for a further 24 hours. Cells were harvested and whole cell lysates were prepared and used to infect fresh A549 cells. Cells were incubated for 48 hours for flow cytometric analysis or for six days for analysis by the plaque assay. Results are displayed as the mean fold change ($\pm$ SEM) from at least three independent repeats. Results are shown as relative to the siControl-treated, mock infected sample, which was set to a value of 1. All statistics were calculated using the paired 1 sample t-test. A. Plaque assay analysis. Compared with Ad5 infection of siControl-treated cells, the virus yield following infection of siSMN-treated cells was reduced by 62%. The average virus titre following infection of A549 cells with cell lysate from siControl-treated, Ad5-infected cells was 1.5×10^8 PFU/ml. B. Flow cytometric analysis of hexon expression. Compared with Ad5 infection of siControl-treated cells, hexon expression following infection of siSMN-treated cells was reduced by 48%. * $p<0.05$, **$p<0.01$.

5.7 The impact of SMN depletion on Ad5 protein expression

It was decided to investigate whether the observed decrease in virus yield following Ad5 infection of SMN-depleted cells was due to an effect on Ad protein levels. A549 cells were subjected to siRNA transfection using siControl or siSMN (Chapter 2.2.5.1). Following 24 hours incubation, cells were mock or Ad5 infected (Chapter 2.2.6.1). At 24 h.p.i, cells were harvested and analysed by either Western blotting (Chapter 2.2.2) or flow cytometry (Chapter 2.2.8).

5.7.1 Assay of Ad protein levels by Western blotting following infection of SMN-depleted A549 cells

The impact of SMN depletion on the expression of Ad5 proteins was analysed by Western blotting using antibodies raised against the Ad5 proteins E1A, DBP, IVa2, pIX, L4-100K, IIIa and fibre. As mentioned previously, the hexon antibody (2Hx2) cannot be used in Western blotting analysis, and there was an insufficient amount of the anti-IX antibody to perform Western blotting analysis.

As shown by the representative Western blots in Figure 5-8A, SMN depletion resulted in a decrease in the levels of the late proteins IIIa and fibre whilst the levels of DBP and IVa2 were not significantly altered. Interestingly, L4-100K was found to be slightly increased following Ad5 infection of SMN-depleted cells. Whilst the E1A 289R isoform appeared to be decreased following SMN depletion, the level of the 243R isoform appeared to be slightly increased. These observations were confirmed by densitometric analysis (Figure 5-8B). These data suggest that depletion of SMN significantly reduced the levels of the 289R E1A, IIIa and fibre proteins in Ad5-infected cells, did not affect the levels of DBP or IVa2 and increased the levels of 243R E1A and L4-100K.

5.7.2 Assay of protein levels by flow cytometry following SMN depletion in A549 cells

In order to obtain quantitative data on the impact of SMN depletion on Ad5 protein expression, the levels of the Ad5 early proteins E1A and DBP, intermediate proteins IVa2 and pIX and late proteins L4-100K, IIIa, fibre and hexon were assayed by flow cytometry following SMN depletion and Ad5 infection. Figure 5-9A shows representative overlays from flow cytometric analysis of (i) E1A and (ii) hexon. For Ad E1A expression, the isotype antibody controls are located in the region $0\text{-}10^1$ FITC-A. The mock-infected samples incubated with the anti-E1A antibody show a slight shift to the right toward more positive values, indicating there is some non-specific binding of the E1A antibody to cellular proteins. However, the peaks for siControl-treated, mock-infected cells and siSMN-treated, mock infected cells appeared to closely overlay, indicating that depletion of SMN does not alter the level of the non-specific protein(s).
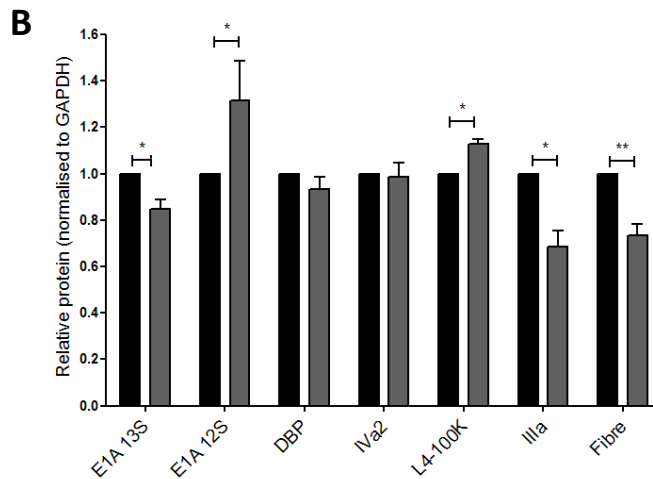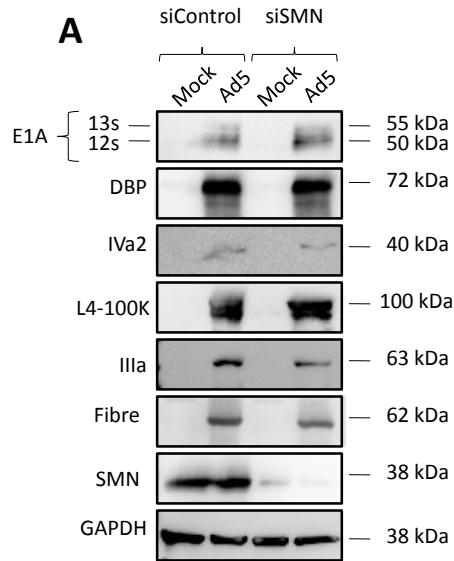
Figure 5-8. Western blot analysis of Ad5 proteins following infection of SMN-depleted A549 cells.
A549 cells were treated with siControl or siSMN and incubated for 24 hours. Cells were mock or Ad5 infected and incubated for 24 hours. Whole cell lysates were prepared and equal masses of protein from each sample (20 µg) was separated by SDS-PAGE and analysed by Western blotting. A. Representative Western blots of Ad5 proteins following Ad5 infection of SMN-depleted cells. Compared with infection of siControl-treated cells, Ad5 infection of siSMN-treated cells resulted in decreased levels of E1A 13S, IIIa and fibre whilst levels of E1A 12S and L4-100K were increased. Levels of DBP and IVa2 were not altered. B. Densitometric analysis of signal intensities from Western blots. Signal intensities were calculated by densitometric analysis and were normalised to the signal intensity of the loading control, GAPDH. Black bars represent the siControl-treated cells, grey bars represent the siSMN-treated cells. Results are the mean fold change in protein level ($\pm$ SEM) from at least three independent experiments. Results are displayed as relative to the siControl-treated, mock-infected sample, which was set to a value of 1. Statistics were calculated using the paired 1 sample t-test. Compared with infection of siControl-treated cells, Ad5 infection of siSMN-treated cells resulted in significant decreases to levels of E1A 13S, IIIa and fibre and significant increases in the levels of E1A 12S and L4-100K. Levels of DBP and IVa2 were not significantly affected. $*$ $p < 0.05$, $**$ $p < 0.01$.

184
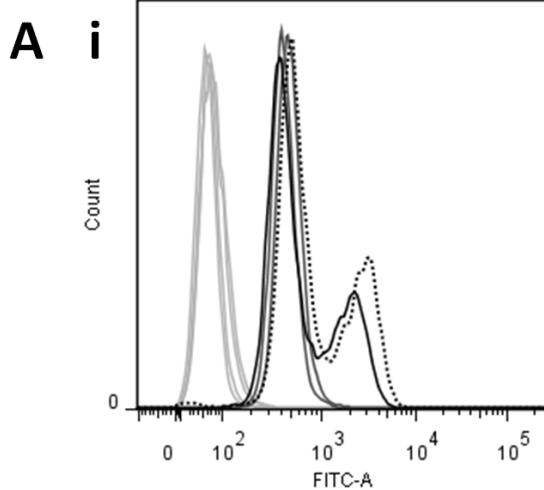
Key	Sample name		Antibody used
	siRNA	Infection	
(grey line)	siControl siControl siSMN siSMN	Mock Ad5 Mock Ad5	Mouse anti-isotype control
	siControl siSMN	Mock Mock	Mouse anti-hexon
(solid line)	siControl	Ad5	Mouse anti-hexon
(dotted line)	siSMN	Ad5	Mouse anti-hexon
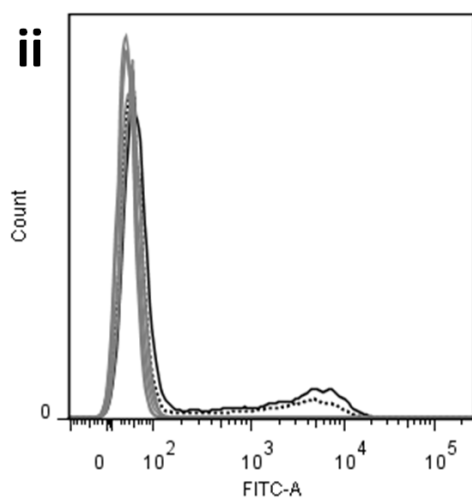
Key	Sample name		Antibody used
	siRNA	Infection	
(grey line)	siControl siControl siSMN siSMN	Mock Ad5 Mock Ad5	Rabbit anti-isotype control
	siControl siSMN	Mock Mock	Rabbit anti-E1A
(solid line)	siControl	Ad5	Rabbit anti-E1A
(dotted line)	siSMN	Ad5	Rabbit anti-E1A
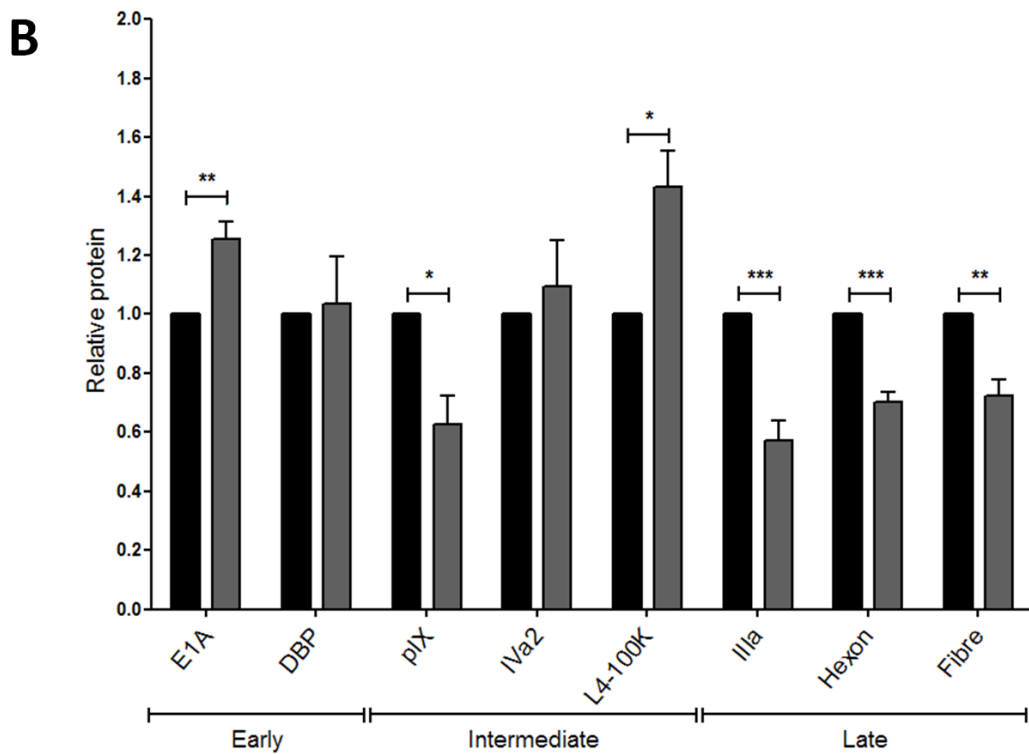
Figure 5-9. Flow cytometric analysis of Ad5 proteins following infection of SMN depleted cells.
A549 cells were treated with siControl or siSMN and incubated for 24 hours. Cells were mock- or Ad5-infected at an MOI of 5 FFU/cell and incubated for 24 hours. Cells were harvested and subject to flow cytometric analysis. A. Example overlays from flow cytometric analysis. (i) E1A. Compared with Ad5 infection of siControl-treated cells, infection of siSMN-treated cells resulted in increased overall E1A expression (as shown by a shift of the FITC curve to the right) and also resulted in an increase in the number of E1A-expressing cells. (ii) Hexon. Compared with infection of siControl-treated cells, Ad5 infection of siSMN-treated cells resulted in decreased overall hexon expression (as shown by a shift of the FITC curve to the left) and also resulted in a decrease in the number of hexon positive cells. B. Flow cytometric analysis of Ad5 proteins following infection of SMN-depleted cells. Black bars represent siControl-treated cells, grey bars represent siSMN-treated cells. Results are the mean fold change in protein level ($\pm$ SEM) from at least three independent experiments. Data are shown relative to the siControl-treated, Ad5-infected sample, which was set to a value of 1. Statistics were calculated using the paired 1 sample t-test. Compared with Ad5 infection of siControl-treated cells, infection of siSMN-treated cells resulted in decreased expression of pIX, IIIa, hexon and fibre, increased expression of E1A and L4-100K. Levels of DBP and IVa2 were not affected. *$p<0.05$, **$p<0.01$, ***$p<0.001$.

Therefore it seems that non-specific binding by this antibody does not vary when SMN is depleted, and as a result should not skew the results obtained for E1A. Both the Ad5-infected samples (siControl and siSMN-treated) exhibited large shifts in FITC-A to the right indicating high-level expression of E1A in these cells. Compared with the siControl-treated, Ad5-infected cells, the siSMN-treated, Ad5-infected sample revealed a greater shift of the positive cell population to the right. This indicated that SMN depletion increased the expression of E1A following Ad5 infection. In addition, a greater proportion of the cell population were fluorescent in the siSMN-treated, Ad5-infected cells compared with the siControl-treated, Ad5-infected cells, indicating that a greater proportion of the cell population were expressing E1A.

The flow cytometry overlay for hexon showed that the isotype antibody controls and mock-infected control samples located in the region $0-10^1$, i.e. were negative for hexon staining. Following Ad5 infection, there was a large shift of a proportion of the cell populations to the right, indicating a proportion of the cells were expressing hexon. Comparison of the siSMN-treated, Ad5-infected cells with the siControl-treated, Ad5-infected cells revealed that the population shift to the left was slightly less pronounced in the siSMN-treated cells, indicating that SMN depletion reduced the expression of Ad5 hexon. In addition, the number of fluorescent cells was also decreased in the siSMN-treated, Ad5 infected population compared with the siControl-treated, Ad5-infected population, suggesting that depletion of SMN reduced the proportion of cells that were expressing hexon.

Collated results from analysis of all Ad proteins are displayed in Figure 5-9B. Depletion of SMN resulted in a significant decrease in the levels of IIIa and fibre, consistent with the Western blotting analysis in the previous section (Chapter 5.7.1). Hexon and pIX were also found to be significantly decreased following SMN depletion. Levels of DBP and IVa2 were not significantly altered following SMN depletion, confirming the preliminary Western blotting analysis. Confirming the Western blotting results, L4-100K was found to be significantly increased following SMN depletion. Finally, levels of E1A were found to be significantly increased. As flow cytometric analysis cannot distinguish between protein isoforms, it is possible that the increase in the 289R E1A isoforms observed from Western blotting analysis is greater than the observed decrease in protein levels of the 243R isoform, resulting in an apparent small increase in total E1A levels by flow cytometric analysis.

5.8 Impact of SMN depletion on Ad mRNA levels

The data from the previous section (Chapter 5.7) revealed that following Ad5 infection of SMN-depleted A549 cells, there was a significant decrease in the levels of IIIa, hexon, fibre and pIX, an increase in E1A and L4-100K whilst DBP and IVa2 were not significantly affected. In order

to establish whether the alterations observed in Ad protein levels were due to changes at the mRNA level, QPCR was carried out using exon-spanning primers to amplify mature, spliced Ad5 E1A (13S, 12S, 11S, 10S, and 9S spliceoforms), DBP (RT1 and RT2 spliceoforms), L4-100K, IVa2, IIIa, hexon and fibre (Chapter 2.2.4.4). The unspliced Ad IX mRNA (Alestrom *et al.*, 1980) was also analysed.

5.8.1 The kinetics of Ad5 mRNA expression following SMN depletion

As the decrease in Ad5 protein levels following SMN depletion was observed at 24 h.p.i, a time course of Ad5 hexon mRNA expression was performed at 18, 20, 22 and 24 h.p.i to ensure that any impact of SMN depletion on Ad5 mRNA levels would be observed. A549 cells were subjected to siRNA treatment (Chapter 2.2.5.1) and incubated for 24 hours. Cells were mock or Ad5 infected (Chapter 2.2.6.1) and harvested at 18, 20, 22 and 24 h.p.i. Total cellular RNA was extracted from cells using Trizol-chloroform extraction (Chapter 2.2.3.1) prior to reverse transcription (Chapter 2.2.4.2) to produce cDNA from mRNA. QPCR was performed (Chapter 2.2.4.4) using exon-spanning hexon primers to specifically amplify mature, spliced hexon mRNA (Table 2-1).

As shown in Figure 5-10A, the time course of hexon mRNA expression following SMN depletion revealed a decrease in hexon mRNA levels from 18 to 22 h.p.i, with an increase to levels equivalent to siControl-treated by 24 h.p.i. This indicated that following Ad5 infection, SMN depletion may abrogate the expression of hexon mRNA. As 20 h.p.i was the time point at which the observed decrease in hexon mRNA was most pronounced, this was chosen as the time point at which to study Ad mRNA expression following SMN depletion.

5.8.2 Impact of SMN depletion on Ad5 mRNA expression

Following the identification of a suitable time point at which to study Ad5 mRNA expression following SMN depletion, the qPCR analysis at 20 h.p.i was extended to include all mRNA isoforms described in Table 2-1. As shown in Figure 5-10B, the depletion of SMN resulted in significant decreases in the levels of the following mature, spliced Ad transcripts: E1A 13S, E1A 9S, DBP (RT2), IX, IIIa, hexon and fibre. In contrast, the following transcripts were unaffected by SMN depletion: E1A 12S, E1A 11S, E1A 10S, DBP (RT1), IVa2 and L4-100K. No Ad transcripts were increased following SMN depletion. This suggested that SMN depletion caused a significant reduction in the levels of certain Ad mRNA transcripts.

Analysis of the unspliced Ad IX mRNA transcript was also performed. As shown in Figure 5-10B, SMN depletion significantly reduced the levels of IX mRNA. Therefore SMN depletion may affect transcription, post-transcriptional processing or mRNA stability of Ad pIX mRNA.
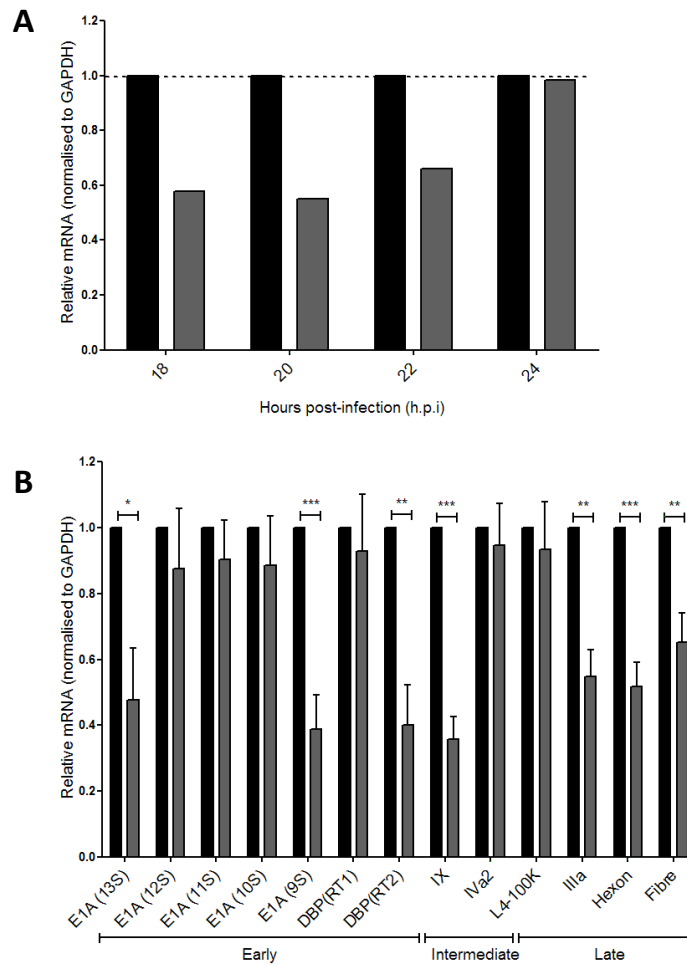
Figure 5-10. The expression of mature Ad5 mRNAs following infection of SMN-depleted A549 cells.
A549 cells were treated with siControl or siSMN incubated for 24 hours. Cells were infected with Ad5 at an MOI of 5 FFU/cell and harvested at 18, 20, 22 or 24 h.p.i. Total cellular RNA was extracted and subjected to reverse transcription to produce cDNA from RNA. QPCR was performed using cDNA and exon-spanning primers to amplify spliced Ad mRNAs. Intra-exon primers were used to amplify unspliced Ad pIX mRNA. Rotorgene 6000 software was used to calculate delta Ct values, which were standardised to levels of the 'housekeeping' transcript, GAPDH. Results are displayed relative to the siControl-treated, Ad5-infected sample, which was set to a value of 1. A. A time course of Ad5 hexon expression following infection of SMN-depleted cells. Compared with siControl-treated, Ad5-infected cells, levels of hexon were decreased at 18, 20 and 22 h.p.i in siSMN-treated, Ad5-infected cells. At 24 h.p.i, levels of hexon were similar in siControl-treated, Ad5-infected cells and siSMN-treated, Ad5-infected cells. B. Expression of spliced Ad5 mRNAs and non-spliced pIX mRNA at 20 h.p.i following infection of SMN-depleted cells. Results are the mean fold change in mRNA level (± SEM) from at least four independent experiments performed in duplicate. Statistics were calculated using the paired 1 sample t-test. Compared with Ad5 infection of siControl-treated cells, infection of siSMN-treated cells resulted in decreased levels of E1A 13S, E1A 9S, DBP RT2, IX, IIIa, hexon and fibre mRNAs whilst levels of E1A 12S, E1A 11S, E1A 10S, DBP RT1, IVa2 and L4-100K were not affected. Black bars = siControl-treated cells. Grey bars = siSMN-treated cells. *p<0.05, **p<0.01, ***p<0.001.

189
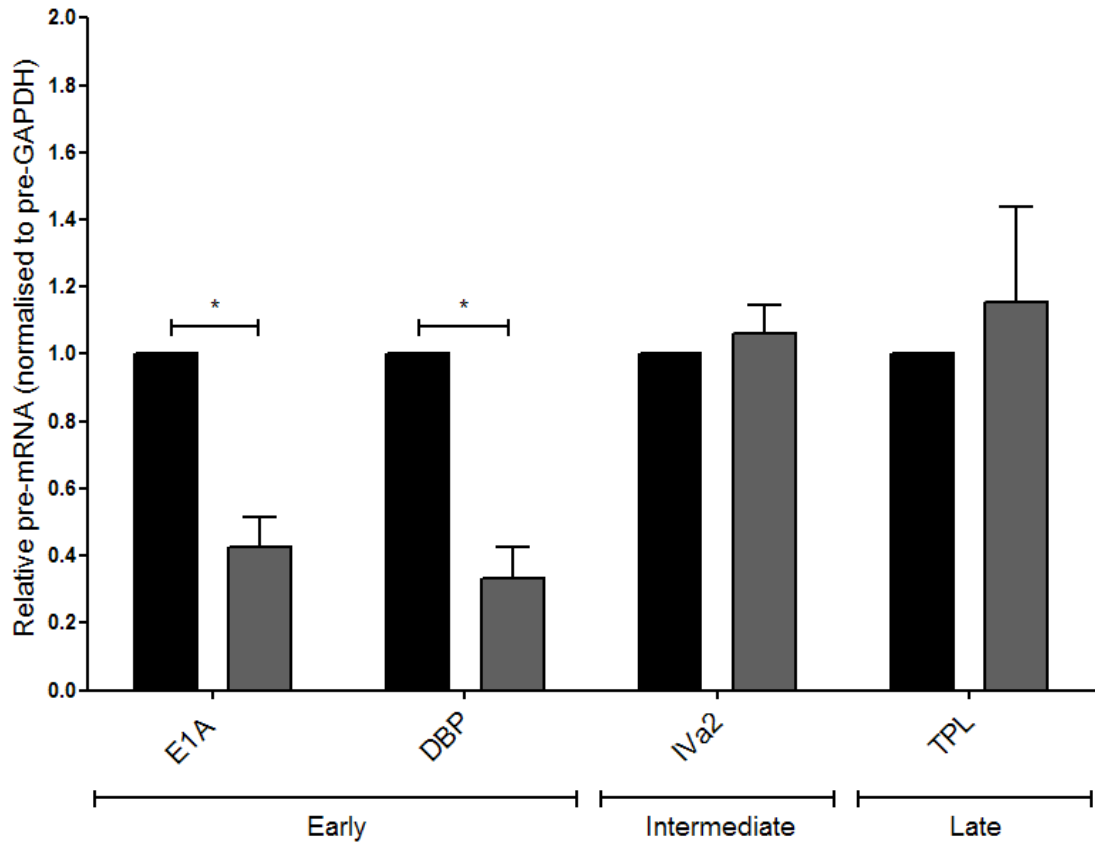
Figure 5-11. The expression of Ad5 pre-mRNAs following infection of SMN-depleted A549 cells.
A549 cells were treated with siControl or siSMN and incubated for 24 hours. Cells were mock or Ad infected at an MOI of 5 FFU/cell and incubated for 20 hours before harvesting. Total RNA was extracted from cells and subjected to reverse transcription to produce cDNA from RNA. QPCR was performed on cDNA using intron-exon spanning primers specific for E1A, DBP, IVa2 or tripartite-leader-containing (TPL) pre-mRNAs. Rotorgene 6000 software was used to calculate delta Ct values, which were standardised to levels of the 'housekeeping' transcript, GAPDH . Results are the mean fold change in pre-mRNA level ($\pm$ SEM) from at least three independent experiments performed in duplicate. Results are displayed as relative to the siControl-treated, Ad5-infected sample, which was set to a value of 1. All statistics were calculated using the paired 1 tailed t-test. Compared with siControl-treated, Ad5-infected cells, levels of E1A and DBP pre-mRNAs were significantly decreased in siSMN-treated, Ad5-infected cells whilst levels of IVa2 and TPL-containing pre-mRNAs were not significantly affected. Black bars = siControl-treated cells. Grey bars = siSMN-treated cells. $*p<0.05$.

5.8.3 Ad5 pre-mRNA expression following infection of SMN-depleted cells

As the production of certain Ad5 mRNAs appear to be reduced following SMN depletion, it was decided to investigate whether this was due to effects on transcription or splicing and/or mRNA stability. To distinguish potential effects on transcription, qPCR analysis of pre-mRNA transcripts was carried out using intron-exon spanning primers (Table 2-1).

As shown in Figure 5-11, no significant alteration was observed in the levels of IVa2 or late TPL-containing pre-mRNAs following Ad5 infection of siSMN-treated cells compared to siCoilin-treated cells. This indicated that transcription of IVa2 or late TPL-containing transcripts is not affected by SMN depletion. In contrast, E1A and DBP pre-mRNAs were found to be significantly reduced in SMN-depleted cells (Figure 5-11). This indicates that transcription of E1A and DBP are dependent on SMN. Therefore SMN may play a role in early Ad transcription but not in late phase transcription.

5.9 Depletion of SMN and coilin in A549 cells

In order to establish the impact of depleting both coilin and SMN on Ad5 infection, A549 cells were treated with siControl or siCoilin and siSMN and incubated for 24 hours. Cells were mock or Ad5 infected and incubated for a further 24 hours. Cells were harvested and equal masses of protein from whole cell lysates were separated by SDS-PAGE and analysed by Western blotting.

As shown in Figure 5-12Ai, siCoilin and siSMN treatment resulted in a marked reduction in the protein levels of SMN and coilin in both mock- and Ad5-infected cells. Densitometric analysis revealed that compared to siControl-treated, mock-infected cells, siCoilin and siSMN treatment reduced coilin levels by 56% and 58% in mock- and Ad5-infected cells, respectively (Figure 5-12Aii). This was similar to the level of coilin depletion achieved by siCoilin treatment alone (Chapter 4.1). Likewise, compared to siControl-treated, mock-infected cells, siSMN treatment reduced levels of SMN by 59% and 58% in mock- and Ad5-infected cells, respectively, similar to the level of SMN depletion as achieved by siSMN treatment alone (Chapter 5.1). Therefore it appeared that treatment of A549 cells with both siCoilin and siSMN achieves a similar level of depletion of coilin and SMN as single siRNA treatment.

To determine whether depletion of both coilin and SMN altered the viability of A549 cells, the cells were subjected to 'reverse siRNA transfection' (Chapter 2.2.5.2) and incubated for 24 hours. Cells were mock or Ad5 infected (Chapter 2.2.6.1) and incubated for 24 hours before analysis by the MTT assay (Chapter 2.2.9). As shown in Figure 5-12B, compared with siControl-treated, mock-infected cells, there was a significant decrease in the viability and/or
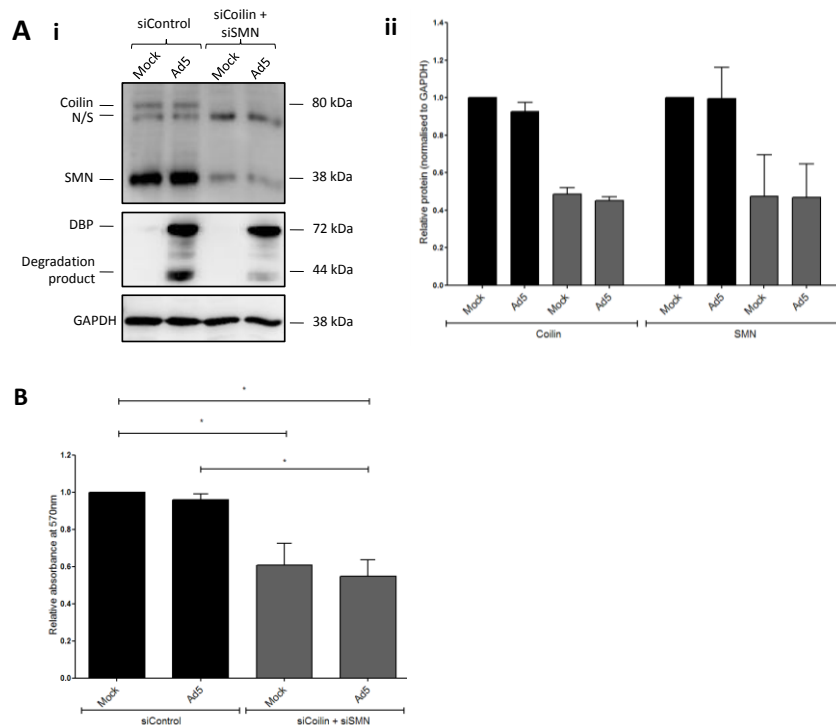
Figure 5-12. Impact of coilin and SMN depletion on the viability of mock- and Ad5-infected cells.
A549 cells were treated with siControl or siCoilin and siSMN. Following 24 hours incubation, cells were mock or Ad5 infected at an MOI of 5 FFU/cell. Cells were incubated for 24 hours before harvesting. A. Western blot analysis of coilin and SMN levels following depletion of coilin and SMN. Whole cell lysates were prepared and equal masses of protein (20 μg) from each sample were separated by SDS-PAGE and analysed by Western blotting. Bound antibody was detected using the ECL system and images were captured using a Las 3000 Imager. Signal intensities were calculated by densitometric analysis and were normalised to the signal intensity of the loading control, GAPDH. i. Western blots of coilin and SMN protein levels in coilin and SMN-depleted cells. Compared with siControl-treated cells, siCoilin/siSMN-treated cells showed reduced levels of coilin and SMN. N/S – non-specific cross-reacting protein species. ii. Densitometric analyses of coilin and SMN protein levels following depletion of coilin and SMN. Results are the mean fold change in protein (±SEM) from two independent repeats. Data are displayed as relative to the siControl-treated, mock-infected sample, which was set to a value of 1. Compared with siControl-treated, mock-infected cells, levels of coilin and SMN were reduced in siCoilin/siSMN-treated, mock-infected cells and siCoilin/siSMN-treated, Ad5-infected cells (coilin was reduced by 56% and 58%, respectively; SMN was reduced by 59% and 58%, respectively). B. Viability of coilin and SMN-depleted cells as analysed by the MTT assay. Results are the mean fold change in absorbance at 570 nm (±SEM) from at least three independent repeats performed in triplicate. Data are displayed relative to the siControl-treated, mock-infected sample, which was set to a value of 1. All statistics were calculated using the paired 1-sample t-test. Compared with siControl-treated, mock-infected cells, absorbance at 570 nm was significantly reduced in siCoilin/siSMN-treated, mock-infected cells and siControl/siSMN-treated, Ad5-infected cells. This indicated that the viability of the cells was reduced following depletion of both coilin and SMN. Black bars = siControl-treated cells. Grey bars = siCoilin/siSMN-treated cells.*p<0.05.

proliferation of siCoilin/siSMN-treated, mock-infected cells and siCoilin/siSMN-treated, Ad5-infected cells. There was also a significant reduction in the viability of siCoilin/SMN-treated, Ad5-infected cells compared with siControl-treated, Ad5-infected cells. This indicated that depletion of coilin and SMN significantly reduced the viability of the cells. As a result, the investigation of the impact of depletion of both coilin and SMN on Ad5 infection was not continued, as any results obtained from the double depletion could be indirectly due to the reduced viability and/or proliferation of the cells.

5.10   Chapter 5 Discussion

In Chapter 3, Ad5 infection was shown to redistribute SMN from CBs to a novel nuclear subdomain, which was distinct from the CB microfoci containing the CB proteins coilin, WRAP53 and fibrillarin (Figure 3-5). However, the role of SMN during Ad5 infection was unknown. In this chapter, the role of SMN during Ad5 infection was investigated. SMN was depleted in A549 cells by siRNA transfection and the impact on Ad5 virus titre, Ad protein expression and Ad mRNA expression was assessed. Expression of Ad5 proteins was shown to be altered following Ad5 infection of SMN-depleted cells, with significant decreases observed for Ad capsid proteins whilst early or late non-structural proteins were either increased or were unaffected by SMN depletion (Figure 5-8 and Figure 5-9). The virus yield was found to be significantly reduced (Figure 5-7), indicating that reduced production of Ad capsid proteins following SMN depletion resulted in decreased production of progeny virions. Analysis of mature, spliced mRNAs indicated that the production of IIIa, hexon and fibre was significantly reduced in Ad5-infected cells (Figure 5-10). This indicated that there was decreased production of certain late spliced mRNAs in SMN-depleted cells, resulting in decreased production of Ad capsid proteins. Analysis of pre-mRNA levels revealed that the level of tripartite leader-containing mRNAs was not altered following Ad5 infection of SMN-depleted cells (Figure 5-11). This indicates that transcription of late Ad genes from the MLP did not require SMN. Therefore the observed decrease in IIIa, hexon and fibre levels following SMN depletion may be due to altered mRNA splicing or mRNA stability. SMN has previously been shown to regulate pre-mRNA splicing (Pellizzoni *et al.*, 1998; Mourelatos *et al.*, 2001; Zhang *et al.*, 2008) and play a role in assembly of the spliceosome (Meister *et al.*, 2000; Makarov *et al.*, 2012). However, to date there has been no report of involvement of SMN in the splicing of viral transcripts. Therefore these data may be the first report of a potential role of SMN in viral mRNA splicing.

In contrast to IIIa, hexon and fibre, the level of L4-100K protein was significantly increased following Ad5 infection of SMN-depleted cells (Figure 5-3 and Figure 5-4); however, analysis

of L4-100K mRNA in SMN-depleted cells was not significantly altered (Figure 5-10). A possible explanation for these seemingly contradictory results is that during the late phase of Ad5 infection, there is enhanced translation of tripartite-leader-containing mRNAs (Cuesta *et al.*, 2000; Xi *et al.*, 2004, 2005). It is possible that in the absence of competition from other tripartite leader mRNAs such as IIIa, hexon and fibre (whose transcript levels are reduced following SMN depletion), there is increased translation of L4-100K transcripts resulting in an increase in L4-100K protein levels, despite there being no increase at the mRNA level. Alternatively, as Ad proteins and mRNAs were only analysed at one time point post-infection, it is possible that there is enhanced L4-100K at an earlier time point than 20 h.p.i and, as the half life of L4-100K protein is known to be greater than 3 hours (Hayes *et al.*, 1990), this may result in the accumulation of large amounts of L4-100K protein that persists even when high transcription levels are not maintained. A detailed analysis of Ad protein and mRNA levels at several points over the course of Ad infection would be required to clarify these matters.

The levels of the intermediate protein IVa2 was unaffected by SMN depletion (Figure 5-8 and Figure 5-9). There were no significant alterations to the levels of IVa2 mRNA or pre-mRNA following SMN depletion (Figure 5-10 and Figure 5-11), indicating that SMN is not required for transcription, RNA splicing or mRNA stability of IVa2. DBP mRNAs form two distinct species; the early expressed RT1, consisting of two short leader sequences and the main body of the mRNA and the delayed early RT2, consisting of a single short leader sequence and the main body (Kruijer et al., 1981). The DBP protein is encoded within the main body, producing the 72 kDa protein (Kruijer *et al.*, 1981). In this study, it was found that level of the RT1 spliceoform of DBP was unaffected following SMN depletion, whereas the level of the RT2 spliceoform was significantly decreased (Figure 5-10). Similar to the results obtained with the TPL-containing mRNAs, these results for DBP indicate a role for SMN in alternative splicing of DBP transcripts. However, despite the reduction in the RT2 transcript, no significant alteration was observed in the level of DBP protein (Figure 5-8 and Figure 5-9). As suggested for L4-100K, a more precise kinetic analysis of Ad5 protein and mRNA levels over a number of time points would establish the impact of SMN depletion on Ad5 protein and mRNA levels.

Interestingly, analysis of DBP pre-mRNA revealed that DBP pre-mRNA levels were also significantly reduced following SMN depletion (Figure 5-11). This indicated that SMN may be involved in DBP transcription. SMN has previously been implicated in transcription; SMN interacts with the transcriptional co-repressor mSin3A (Zou *et al.*, 2004), an RNA helicase (Campbell *et al.*, 2000) and RNA polymerase II (Pellizzoni *et al.*, 2001b). Moreover, SMN has been shown to play roles in transcription during virus infection; SMN acts as a transactivator of the BPV E2 promoter (Strasswimmer *et al.*, 1999) and also the EBV LMP1 promoter (Voss *et*

al., 2001). Therefore these data indicate that, in addition to BPV and EBV, SMN may also play a role in transactivation of the E2A promoter during Ad infection. Considering that the majority of Ad-splicing is believed to occur co-transcriptionally (Nevins *et al.*, 1979), it is possible that SMN may play a role in integrating transcription and splicing during Ad infection.

The levels of E1A proteins and mRNAs were also assessed following SMN depletion. There was an apparent decrease in the level of the 289R isoform of E1A with a concomitant increase in the levels of the 243R isoform as judged by Western blotting analysis (Figure 5-8). This indicated that there may be alterations to Ad mRNA splicing when SMN is depleted. Investigation of mature, spliced Ad mRNAs revealed that E1A 13S transcripts were significantly reduced following SMN depletion (Figure 5-10), which correlates with a resulting decreased production of 289R protein. Again, this indicates a role for SMN in Ad alternative splicing. Adding complexity is the apparent increase in protein levels of the 243R protein isoform, whilst levels of the mRNA encoding this isoform, 12S, did not appear to be affected. As suggested for L4-100K and DBP, it is possible that a more extensive analysis of Ad protein and mRNA levels over a number of time points during Ad5 infection may shed light on the regulation of E1A transcription and/or splicing.

Finally, levels of the 9S E1A transcript was found to be significantly decreased following SMN depletion whilst there appeared to be no effect on the levels of the 10S or 11S E1A transcripts (Figure 5-10), again implying a role for SMN in alternative splicing of Ad transcripts. However, as the E1A antibody used did not recognise the 217R, 171R or 55R E1A isoforms, the impact of SMN depletion on protein levels of these isoforms could not be assayed.

As with coilin, it was surprising that a decrease in the production of the early E1A transcript 13S did not affect the production of the DBP transcript RT1 or the major late transcript L4-100K, as the 289R protein is required for the subsequent transcriptional activation of the other Ad transcriptional units (Berk *et al.*, 1979; Jones and Shenk, 1979; Nevins and Wilson, 1981; Morris *et al.*, 2010). As suggested in Chapter 4.10, as the E1A proteins are produced in great excess (Barbeau *et al.*, 1992) it is possible that a threshold decrease in E1A protein levels is required before a negative effect is observed on the expression of the remaining Ad transcripts. Further investigation would be required to confirm this.

One consideration to be made when analysing these results is that at 24 hours post-transfection, SMN levels were around 60% of those in siControl-treated cells whilst at 48 hours post-transfection, SMN levels were decreased to around 30% of siControl-treated cells (Figure 5-1). This indicated that the level of SMN in the siSMN-treated cells was steadily decreasing as Ad5

infection progressed. Therefore, it is possible that effects of SMN depletion on late mRNA transcripts, which were expressed late in infection when SMN levels were very low, may be more pronounced than the effects observed on early expressed Ad transcripts, which were expressed when SMN levels were higher. Further work is required to determine the effect of SMN depletion on early expressed transcripts.

Although the expression of certain Ad transcripts was significantly decreased, SMN depletion did not completely abrogate the expression of these transcripts. This could be due to the fact that SMN levels were only depleted by 60-70% (Chapter 5, Figure 5-1), allowing a certain degree of splicing by low level SMN expression. Although it would be interesting to establish whether SMN is an absolute requirement for the splicing of certain Ad transcripts, unfortunately it is not possible to establish the ability of Ads to replicate in SMN-knockout cell lines as SMN is required for cell viability (Schrank *et al.*, 1997). It is possible that further optimisation of the depletion procedure using a mixture of siRNAs could be used to deplete SMN to a greater extent and establish an absolute requirement for SMN in the splicing of certain Ad transcripts. It would also be interesting to investigate the impact of SMN over-expression on Ad early gene transcription and Ad mRNA splicing, either by transient transfection of an SMN expression plasmid or by production of stably-transformed SMN over-expressing cell lines.

Taken together, the data from this Chapter indicate that SMN may play a role in the alternative splicing of Ad mRNA transcripts and may also facilitate early gene transcription. The alterations to Ad transcript levels resulted in abrogated late protein expression, leading to a decreased virus yield. Further work is now required to establish the mechanism by which SMN regulates early but not late Ad transcription, and to identify the precise role of SMN in Ad mRNA splicing. The role of SMN in splicing during infection with other viruses is also warranted.

Chapter 6 – General Discussion and Further Studies

6.1 General Discussion and Further Studies

Adenoviruses have long been known to hijack cellular proteins and compartments in order to efficiently complete their life cycles. One such compartment is Cajal body (CB), a sub-nuclear site involved in the metabolism of RNA. The disassembly of CBs during infection with Ad5 was first described over 15 years ago (Rebelo *et al.*, 1996; Rodrigues *et al.*, 1996), and until recently the function of this disassembly remained unknown. In 2010, it was suggested that CB disassembly promoted the expression of Ad late proteins (James *et al.*, 2010), however the mechanism remained unclear. The aim of this investigation was to investigate the role of coilin and other CB proteins during the life cycle of Ad5. The novel results obtained from this study are summarised in Table 6-1.

In this investigation, coilin depletion was found to abrogate the trafficking of Ad mRNA from the nucleus to the cytoplasm, resulting in decreased production of Ad proteins and a reduced virus titre. This indicated that coilin plays a role in the export of Ad mRNAs. Interestingly, it was recently shown that early and intermediate Ad mRNAs are exported by the CRM1 export system whereas late mRNAs are exported via TAP (Yatherajam *et al.*, 2011; Samad *et al.*, 2012). Given the apparent reliance of early, intermediate and late Ad mRNAs on coilin for export, this indicates that coilin may play a role in export of mRNAs through two separate export systems. Although CBs in mammalian cells do not appear to contain poly(A) RNA (Visa *et al.*, 1993; Huang *et al.*, 1994), CBs in larch microsporocytes were recently reported to contain poly(A) RNA and were suggested to function as storage site for mRNAs prior to export (Kolowerzo *et al.*, 2009; Smolinski and Kolowerzo, 2012). It is possible that coilin outside of the CB may mediate this function in mammalian cells. Interestingly, CBs have been implicated in the export of snRNAs, which are exported via CRM1 (Suzuki *et al.*, 2010) and also in the processing of histone mRNAs, which are exported via Nxf1/TAP (Erkmann *et al.,* 2005). It would be appealing to investigate the potential interaction of coilin with elements of the cellular TREX export complex, or with the Ad E1B-55K/E4orf6 complex, shown to be necessary for the export of Ad late mRNAs (Blanchette *et al.*, 2008; Woo and Berk, 2007). Potential interaction of coilin with these complexes would be investigated by co-immunoprecipitation and GST-coilin pull-down assays. In addition, as the ubiquitin ligase activity of the E1B-55K/E4orf6 complex is required for export of late mRNAs (Woo and Berk, 2007; Blanchette *et al.*, 2008), it would also be worth investigating if coilin is ubiquitinated by this complex. In addition to marking proteins for degradation, ubiquitin can also be used as a post-translational modification to change protein activity (reviewed in Hunter, 2007). Therefore it is possible that ubiquitination of coilin during Ad infection might facilitate a change in the activity of coilin, somehow resulting in the enhanced export of Ad mRNAs.

Table 6-1. Novel results obtained in this investigation.

*Previously documented in the literature (Rebelo *et al.,* 1996; Rodrigues *et al.,* 1996; James *et al.,* 2010). N/A – not applicable.

Protein	Subcellular location following Ad5 infection	Timepoint during infection at which redistribution occurs	Effect of siRNA-mediated knockdown of the protein on:				
			Ad5 virus titre	Ad5 protein levels	Ad mRNA levels	Ad pre-mRNA levels	Cytoplasmic: nuclear mRNA
Coilin	Nuclear microfoci*	After Ad DNA replication and intermediate protein expression	Decreased	Decreased	Decreased: 13S E1A, 12S E1A, IX No effect: 11S E1A, 10S E1A, DBP RT1, DBP RT2, IVa2, L4-100K, IIIa, hexon, fibre	No effect	Decreased
SMN	Nuclear rod-shaped structures	After Ad DNA replication and intermediate protein expression	Decreased	Decreased: pIX, IIIa, hexon, fibre Increased: E1A , L4-100K No effect: DBP, IVa2	Decreased: 13S E1A, 9S E1A, DBP RT2, IX, IIIa, hexon, fibre No effect: E1A 12S, E1A 11S, E1A 10S, DBP RT1, IVa2, L4-100K	Decreased: E1A, DBP No effect: IVa2, tripartite leader-containing pre-mRNAs	N/A

In recent years it has become apparent that RNA processing and export are inextricably linked, such that export factors become recruited to the pre-mRNA transcript before completion of processing (reviewed in Palazzo and Akef, 2012). Interestingly, coilin has been shown to possess RNA editing activity and is required for final processing of snRNAs (Broome and Hebert, 2012). Furthermore, during the late stage of Ad infection, coilin colocalised with the late Ad splicing factor L4-33K (Figure 4-15). This indicated that during Ad5 infection, there is a close association of coilin with regions of late mRNA processing, suggesting that coilin may be required for the final processing and/or release of RNAs for export. Therefore functional interactions between coilin and L4-33K and/or cellular splicing factors could be investigated by co-immunoprecipitation and GST-coilin pull-down assays. The potential RNA editing activity of coilin on Ad transcripts could also be investigated.

The role of coilin in the export of cellular mRNAs would also be worthy of further study. In this investigation, the housekeeping transcript GAPDH was used to normalise the Ad mRNA expression data, therefore it appears that the impact of coilin depletion upon Ad mRNA export supersedes the impact (if any) of coilin depletion on cellular mRNA export. Considering the mass synthesis of mRNA during Ad infection, this is not altogether surprising. Moreover, as the nuclear export of cellular mRNAs is inhibited during the late stages of Ad infection (Beltz and Flint, 1979; Babiss *et al.*, 1985; Pilder *et al.*, 1986), it is likely that depletion of coilin would not make any significant difference to the export of cellular mRNAs at late stages of Ad infection. Furthermore, as coilin appears to be non-essential for the viability of mammalian cells (Tucker *et al.*, 2001; Walker *et al.*, 2009), this indicates it is unlikely to be an essential factor for cellular mRNA export. Instead, coilin may simply act to accelerate export processes which would occur at a slower pace in its absence.

In stark contrast to coilin, SMN was found to be redistributed into rod-shaped structures in the nucleoplasm. This was the first indication that SMN may perform a function independent of coilin during Ad5 infection. It was subsequently found that SMN depletion resulted in altered transcription and splicing of Ad transcripts. Intriguingly, SMN depletion appeared to differentially impact on the expression levels of alternative transcripts from the same transcriptional unit; the level of the RT2 spliceoform of DBP was significantly reduced whilst DBP RT1 was unaffected, 9S and 13S E1As were significantly reduced whilst 10S, 11S and 12S were unaffected, and IIIa, hexon and fibre were significantly reduced whereas L4-100K was unaffected (Figure 5-10). This indicates that SMN may play a role in the alternative splicing of Ad transcripts, and that depletion of SMN results in the abrogated production of certain transcripts. Although SMN appears to play multiple roles in cellular splicing (Pellizzoni *et al.*, 1998; Pellizzoni *et al.*, 2001b; Boulisfane *et al.*, 2011; Makarov *et al.*, 2012), to date there

have been no reports of SMN playing a role in splicing of virus transcripts. Therefore this may be the first report of SMN being involved in the splicing of virus transcripts. Further investigation of the exact role of SMN in Ad mRNA splicing is warranted. To analyse the impact of SMN depletion on splicing separately from the possible effects of SMN on Ad transcription, the E1A, DBP, IVa2 and L1-5 coding regions would be cloned into an expression plasmid under the control of a constitutive promoter. These constructs could then be transfected into SMN-depleted cells and Ad transcript levels analysed by qPCR. This experiment could be repeated in SMN over-expressing cells (either cells transiently transfected with an SMN expression plasmid or stably-transformed SMN over-expressing cells) to determine whether SMN over-expression alters the production of differentially spliced transcripts.

In addition to splicing defects, the depletion of SMN also significantly reduced the abundance of E1A and DBP pre-mRNA transcripts, whilst IVa2 and tripartite leader-containing pre-mRNAs were unaffected (Figure 5-11). This indicated a role for SMN in early phase transcriptional activation. Interestingly, SMN has previously been shown to act as a transcriptional co-activator during infection with BPV and EBV (Strasswimmer *et al.*, 1999; Voss *et al.*, 2001). This suggests that SMN is hijacked during infection with multiple viruses in order to promote transcriptional activation. Further work is warranted to characterise the mechanism by which SMN induces Ad early transcriptional activation. To do this, expression plasmids containing the luciferase reporter gene under the control of Ad E1A, DBP, IVa2, IX and major late promoters would be constructed. These plasmids would be transfected into SMN-depleted or SMN over-expressing cells and the luciferase expression would be measured. Given that certain Ad proteins are also required as co-activators for certain Ad promoters (Berk *et al.*, 1979; Morris and Leppard, 2009; Morris *et al.*, 2010), this assay may also require co-transfection with plasmids encoding the Ad proteins required for transcriptional activation. It would also be interesting to establish an interaction of SMN with Ad promoters and cellular and viral transcription factors by chromatin immunoprecipitation from Ad5-infected cells.

Further investigations could also determine the impact of Ad infection upon protein-protein interactions between CB proteins. Coilin has been shown to interact with both SMN and WRAP53, whilst SMN and WRAP53 also mutually interact (Hebert *et al.*, 2001; Mahmoudi *et al.*, 2010). As SMN is redistributed to a separate compartment to coilin and WRAP53 following Ad5 infection (Figure 3-6), it would be interesting to determine whether this coincides with a loss of interaction between coilin and SMN and between WRAP53 and SMN. As coilin and WRAP53 remain colocalised in rosettes following Ad5 infection (Figure 3-5), it should also be determine whether the interaction between coilin and WRAP53 is maintained following Ad5 infection. Furthermore, as both WRAP53 and fibrillarin colocalised with coilin following Ad

infection (Chapter 3), the potential role of WRAP53 and/or fibrillarin in mRNA export could also be investigated.

The redistribution of coilin and SMN from CBs was found to occur during the late stages of infection, indicating that an intermediate or late phase Ad protein is likely to be responsible for the disassembly of CBs. Therefore further work could focus on identifying potential virus protein-interacting partners for both coilin and SMN. To this end, coilin and SMN could be immunoprecipitated from whole cell extracts and analysed by Western blotting, probing for the virus proteins of interest. As CB proteins have many interaction partners, any identified interaction from co-immunoprecipitation experiments would need to be further investigated to show if it was direct or indirect using GST-coilin and GST-SMN pull down assays.

A question that remains is how the disassembly of CB components relates to their function during Ad5 infection. An important fact to consider is that the bulk of SMN and coilin in the cell is located diffusely in the nucleoplasm outside of CBs (reviewed in Ogg and Lamond, 2002). Therefore it is possible that it is the nucleoplasmic fraction of the proteins which are responsible for the effects on Ad infection, rather than the CB-associated fraction. It is tempting to speculate that disruption of the CB following Ad5 infection may be a strategy to release more coilin or SMN into the nucleoplasm to enhance mRNA export and Ad transcription and/or splicing, respectively. Indeed, the massive up-regulation of mRNA synthesis during the late stages of infection (Flint and Sharp, 1976) may increase demand for free nucleoplasmic coilin and SMN within the cell, thus disruption of the CB may release these factors into the nucleoplasm to satisfy this demand. To investigate these suggestions, the potential shift of SMN and coilin from CBs into the nucleoplasm would be studied. CBs from mock- and Ad5-infected cells would be isolated by subcellular fractionation (Lam *et al.*, 2002) and the proportion of coilin and SMN protein located in CBs analysed compared to the nucleoplasmic fraction. The proportion of coilin and SMN in the nucleoplasm versus the CB could also be analysed by using time-lapse fluorescence microscopy in coilin-GFP-expressing cells over the course of Ad5 infection (Platani *et al.*, 2000).

The roles of coilin and SMN during Ad infection outlined in this report may also have implications for understanding the interaction of other viruses with the CB. The first characterised interaction of a virus with the CB was reported by Kim *et al*, who found that the plant virus GRV utilised CBs to traffic the GRV movement protein ORF3 to the nucleolus. This was found to facilitate the formation of viral snRNPs necessary for virus spread (Kim *et al.*, 2007b; Canetta *et al.*, 2008). From the data described in Chapter 4, it appears that coilin has a very different role during Ad infection as compared to infection with GRV. This is not

altogether surprising considering the lifecycle of an RNA virus is quite different to that of a DNA virus, with transcription and RNA processing generally occurring in the cytoplasm in RNA virus-infected cells. In addition to RNA viruses, other DNA viruses have also been shown to interact with CBs. Various herpes viruses have been shown to disrupt CBs as demarked by coilin staining in indirect immunofluorescence analysis (Salsman *et al.*, 2008). However, the reason for CB disassembly during infection with these viruses remains unknown. As herpes viruses also require the export of mRNA from the nucleus following synthesis, it is possible that herpes viruses may also redistribute coilin in order to facilitate mRNA export. It would be interesting to investigate the potential role of coilin in mRNA export with other DNA viruses to see whether this is a common mechanism during DNA virus infection. It would also be appealing to determine the role of other lesser-characterised nuclear bodies during infection with Ads and other viruses. It is completely unknown what the impact of Ad infection has on the subcellular distribution of PIKAs, OPT domains, nSBs or cleavage bodies. As cleavage bodies are believed to be functionally associated with CBs (Li *et al.*, 2006b), it would be interesting to determine whether components of cleavage bodies also play roles during Ad5 infection.

From a therapeutic point of view, it has become apparent that inhibition of essential cellular processes may be an effective mechanism of inhibiting virus infection. Indeed, the discovery of the dependence of HIV-1 on the nucleolus for mRNA trafficking led to the development of modified T-cell lines resistant to HIV-1 infection (Michienzi *et al.*, 2002; Paul *et al.*, 2003; Michienzi *et al.*, 2006). Therefore as mRNA export is a critical function during DNA virus infection, the inhibition of coilin function could potentially be a new anti-viral strategy. Furthermore, the non-essential role of coilin in normal cellular function indicates that inhibition of coilin activity might specifically impair virus replication without having a negative impact on normal cellular activity. Further investigation of the impact of coilin depletion during infection with other viruses is required.

The original aim of this work was to gain insight into the mechanisms controlling late gene expression for the benefit of replication-competent Ad vector development. As mentioned previously, E1-deleted Ad vectors appear to retain the ability to express residual late proteins, resulting in immune responses to the vector and reduced efficacy (Yang *et al.*, 1994b; Yang *et al.*, 1994c; Yang *et al.*, 1995). In this investigation neither SMN nor coilin appeared to play a role in the transcription of late Ad transcripts from the MLP (Figure 4-12 and Figure 5-11). Therefore further work is warranted to determine the mechanism by which E1-deleted Ad vectors express residual Ad late proteins. However, SMN depletion does appear to be required

for transcription of the E2 region gene DBP (Figure 5-11). Whether SMN is able to stimulate transcription of DBP in the absence of Ad E1 proteins would be worthy of future study.

This work may also have implications for Ad gene therapy vector development. This investigation revealed that Ads require both coilin and SMN for efficient expression of late virus proteins and for efficient virus replication, therefore it would seem that Ads may not replicate well in tissues expressing low levels of coilin and/or SMN. Although all tissues are believed to express both coilin and SMN, levels of these proteins appear to vary between tissues, for example there is very low level of SMN expressed in adult skeletal muscle compared to brain or lung tissue (Young *et al.*, 2000). Therefore it is possible that Ads may not be able to replicate efficiently in cell types expressing low levels of these proteins, which would reduce their efficacy as a therapy vector. In addition, not all tissues contain CBs, including smooth and cardiac muscle cells, dermal and epidermal skin cells and spleen parenchymal cells (Young *et al.*, 2000). It would therefore be of interest to establish whether Ads are able to infect cells which express coilin and SMN but do not form CBs.

Ads have previously been investigated as gene therapy vectors for SMA. These vectors were intended to increase SMN expression (DiDonato *et al.*, 2003; Geib and Hertel, 2009). As the data presented here indicated that E1A transcription may be dependent upon SMN, it is likely that Ad infection of cells from an SMA patient, which would be low in SMN, would result in low level expression of transgenes placed under the control of E1A promoter. However, to date all studies investigating the ability of Ads to restore SMN expression have used vectors where the E1A promoter has been replaced with a high expression promoter (e.g. rous sarcoma virus promoter) or an inducible expression promoter (e.g. tetracycline), thus bypassing this potential issue. However, the potential requirement of SMN for optimal E1A transcription may be noteworthy for the design of future Ad vectors for SMA gene therapy.

In summary, the data obtained from this investigation has highlighted the potential role of the CB protein SMN in Ad transcription and splicing, which is the first report of a role for SMN in splicing of virus transcripts. This study also uncovered a potential role of another CB protein, coilin, in Ad mRNA processing and export. This is the first suggestion for a role of the CB in mRNA export. This work highlights a potential new role for CB proteins in normal cellular function as well as during virus infection, and is thus of great interest for future virology and cellular biology research.

References

Abruzzi, K.C., Lacadie, S., and Rosbash, M. (2004). Biochemical analysis of TREX complex recruitment to intronless and intron-containing yeast genes. Embo Journal *23*, 2620-2631.

Ackrill, A.M., and Blair, G.E. (1988). Regulation of the major histocompatibility class-I gene-expression at the level of transcription in highly oncogenic adenovirus transformed rat cells. Oncogene *3*, 483-487.

Ackrill, A.M., Foster, G.R., Laxton, C.D., Flavell, D.M., Stark, G.R., and Kerr, I.M. (1991). Inhibition of the cellular response to interferons by the products of the adenovirus type 5 E1A oncogene. Nucleic Acids Research *19*, 4387-4393.

Adam, S.A., and Dreyfuss, G. (1987). Adenovirus proteins associated with messenger-RNA and hnRNA in infected HeLa cells. Journal of Virology *61*, 3276-3283.

Adamson, A.L., and Kenney, S. (2001). Epstein-Barr virus immediate-early protein BZLF1 is SUMO-1 modified and disrupts promyelocytic leukemia bodies. Journal of Virology *75*, 2388-2399.

Adler, M., Tavalai, N., Mueller, R., and Stamminger, T. (2011). Human cytomegalovirus immediate-early gene expression is restricted by the nuclear domain 10 component Sp100. Journal of General Virology *92*, 1532-1538.

Ahn, J.H., and Hayward, G.S. (1997). The major immediate-early proteins IE1 and IE2 of human cytomegalovirus colocalize with and disrupt PML-asscciated nuclear bodies at very early times in infected permissive cells. Journal of Virology *71*, 4599-4613.

Ahn, J.H., and Hayward, G.S. (2000). Disruption of PML-associated nuclear bodies by IE1 correlates with efficient early stages of viral gene expression and DNA replication in human cytomegalovirus infection. Virology *274*, 39-55.

Ahn, J.H., Jang, W.J., and Hayward, G.S. (1999). The human cytomegalovirus IE2 and UL112-113 proteins accumulate in viral DNA replication compartments that initiate from the periphery of promyelocytic leukemia protein-associated nuclear bodies (PODs or ND10). Journal of Virology *73*, 10458-10471.

Aittaleb, M., Rashid, R., Chen, Q., Palmer, J.R., Daniels, C.J., and Li, H. (2003). Structure and function of archaeal box C/D sRNP core proteins. Nature Structural Biology *10*, 256-263.

Akusjarvi, G. (2008). Temporal regulation of adenovirus major late alternative RNA splicing. Frontiers in Bioscience *13*, 5006-5015.

Akusjarvi, G., Alestrom, P., Pettersson, M., Lager, M., Jornvall, H., and Pettersson, U. (1984). The gene for the adenovirus 2 hexon polypeptide. Journal of Biological Chemistry *259*, 3976-3979.

Akusjarvi, G., and Pettersson, U. (1978). Sequence analysis od adenovirus DNA. 2. Nucleotide sequence at the junction between the coding region of the adenovirus 2 hexon messenger RNA and its leader sequence. Proc Natl Acad Sci U S A *75*, 5822-5826.

Akusjarvi, G., Zabielski, J., Perricaudet, M., and Pettersson, U. (1981). The sequence of the 3' non-coding region of the hexon messenger-RNA discloses a novel adenovirus gene. Nucleic Acids Research *9*, 1-17.

Alba, R., Bradshaw, A., Mestre-Francés, N., Verdier, J., ., Henaff, D., ., and Baker, A. (2012). Coagulation factor X mediates adenovirus type 5 liver gene transfer in non-human primates (Microcebus murinus). Gene Therapy *19*, 109-113.

Albrecht, J.C., Nicholas, J., Biller, D., Cameron, K.R., Biesinger, B., Newman, C., Wittmann, S., Craxton, M.A., Coleman, H., Fleckenstein, B*., et al.* (1992). Primary structure of the herpesvirus saimiri genome. Journal of Virology *66*, 5047-5058.

Alemany, R., and Curiel, D.T. (2001). CAR-binding ablation does not change biodistribution and toxicity of adenoviral vectors. Gene Therapy *8*, 1347-1353.

Alestrom, P., Akusjarvi, G., Lager, M., Liang, Y.K., and Pettersson, U. (1984). Genes encoding the core proteins of adenovirus type-2. Journal of Biological Chemistry *259*, 3980-3985.

Alestrom, P., Akusjarvi, G., Perricaudet, M., Mathews, M.B., Klessig, D.F., and Pettersson, U. (1980). Gene for polypeptide-IX of adenovirus type-2 and its un-spliced messenger-RNA. Cell *19*, 671-681.

Ali, H., Leroy, G., Bridge, G., and Flint, S.J. (2007). The adenovirus L4 33-kilodalton protein binds to intragenic sequences of the major late promoter required for late phase-specific stimulation of transcription. Journal of Virology *81*, 1327-1338.

Almstead, L.L., and Sarnow, P. (2007). Inhibition of U snRNP assembly by a virus-encoded proteinase. Genes & Development *21*, 1086-1097.

Amstutz, B., Gastaldelli, M., Kalin, S., Imelli, N., Boucke, K., Wandeler, E., Mercer, J., Hemmi, S., and Greber, U.F. (2008). Subversion of CtBP1-controlled macropinocytosis by human adenovirus serotype 3. Embo Journal *27*, 956-969.

Anderson, C.W. (1990). The proteinase polypeptide of adenovirus serotype-2 virions. Virology *177*, 259-272.

Anderson, C.W., Baum, P.R., and Gestelan.Rf (1973). Processing of adenovirus 2-induced proteins. Journal of Virology *12*, 241-252.

Anderson, C.W., Young, M.E., and Flint, S.J. (1989). Characterization of the adenovirus-2 virion protein, mu. Virology *172*, 506-512.

Andersson, M.G., Haasnoot, P.C.J., Xu, N., Berenjian, S., Berkhout, B., and Akusjarvi, G. (2005). Suppression of RNA interference by adenovirus virus-associated RNA. Journal of Virology *79*, 9556-9565.

Andrade, L.E.C., Tan, E.M., and Chan, E.K.L. (1993). Immunocytochemical analysis of the coiled body in the cell cycle and during cell-proliferation. Proc Natl Acad Sci U S A *90*, 1947-1951.

Angeletti, P.C., and Engler, J.A. (1998). Adenovirus preterminal protein binds to the CAD enzyme at active sites of viral DNA replication on the nuclear matrix. Journal of Virology *72*, 2896-2904.

Aoki, K., Ishiko, H., Konno, T., Shimada, Y., Hayashi, A., Kaneko, H., Ohguchi, T., Tagawa, Y., Ohno, S., and Yamazaki, S. (2008). Epidemic keratoconjunctivitis due to the novel hexon-chimeric-intermediate 22,37/H8 human adenovirus. Journal of Clinical Microbiology *46*, 3259-3269.

Arany, Z., Newsome, D., Oldread, E., Livingston, D.M., and Eckner, R. (1995). A family of transcriptional adaptor proteins targeted by the E1A oncoprotein. Nature *374*, 81-84.

Araujo, F.D., Stracker, T.H., Carson, C.T., Lee, D.V., and Weitzman, M.D. (2005). Adenovirus type 5 E4orf3 protein targets the Mre11 complex to cytoplasmic aggresomes. Journal of Virology *79*, 11382-11391.

Arcangeletti, M.C., Rodighiero, I., Mirandola, P., De Conto, F., Covan, S., Germini, D., Razin, S., Dettori, G., and Chezzi, C. (2011). Cell-Cycle-Dependent Localization of Human Cytomegalovirus UL83 Phosphoprotein in the Nucleolus and Modulation of Viral Gene Expression in Human Embryo Fibroblasts In Vitro. Journal of Cellular Biochemistry *112*, 307-317.

Armentano, D., Sookdeo, C.C., Hehir, K.M., Gregory, R.J., Stgeorge, J.A., Prince, G.A., Wadsworth, S.C., and Smith, A.E. (1995). Characterization of an adenovirus gene-transfer vector containing an E4 deletion. Human Gene Therapy *6*, 1343-1353.

Aspegren, A., Rabino, C., and Bridge, E. (1998). Organization of splicing factors in adenovirus-infected cells reflects changes in gene expression during the early to late phase transition. Experimental Cell Research *245*, 203-213.

Athappilly, F.K., Murali, R., Rux, J.J., Cai, Z.P., and Burnett, R.M. (1994). The refined crystal structure of hexon, the major coat protein of adenovirus type-2, at 2 center-dot-9 angstrom resolution. Journal of Molecular Biology *242*, 430-455.

Avantaggiati, M.L., Carbone, M., Graessmann, A., Nakatani, Y., Howard, B., and Levine, A.S. (1996). The SV40 large T antigen and adenovirus E1a oncoproteins interact with distinct isoforms of the transcriptional co-activator, p300. Embo Journal *15*, 2236-2248.

Babiss, L.E., Ginsberg, H.S., and Darnell, J.E. (1985). Adenovirus E1B proteins are required for accumulation of late viral messenger RNA and for effects on cellular messenger-RNA translation and transport. Molecular and Cellular Biology *5*, 2552-2558.

Bachand, F., Boisvert, F.M., Cote, J., Richard, S., and Autexier, C. (2002). The product of the Survival of Motor Neuron (SMN) gene is a human telomerase-associated protein. Molecular Biology of the Cell *13*, 3192-3202.

Baker, A., Rohleder, K.J., Hanakahi, L.A., and Ketner, G. (2007). Adenovirus E4 34k and E1b 55k oncoproteins target host DNA ligase IV for proteasomal degradation. Journal of Virology *81*, 7034-7040.

Baker, D.L., Youssef, O.A., Chastkofsky, M.I.R., Dy, D.A., Terns, R.M., and Terns, M.P. (2005). RNA-Guided RNA modification: functional organization of the archaeal H/ACA RNP. Genes & Development *19*, 1238-1248.

Barbeau, D., Marcellus, R.C., Bacchetti, S., Bayley, S.T., and Branton, P.E. (1992). Quantitative -analysis of regions of adenovirus E1A products involved in interactions with cellular proteins. Biochemistry and Cell Biology-Biochimie Et Biologie Cellulaire *70*, 1123-1134.

Barcaroli, D., Bongiorno-Borbone, L., Terrinoni, A., Hofmann, T.G., Rossi, M., Knight, R.A., Matera, A.G., Melino, G., and De Laurenzi, V. (2006a). FLASH is required for histone transcription and S-phase progression. Proc Natl Acad Sci U S A *103*, 14808-14812.

Barcaroli, D., Dinsdale, D., Neale, M.H., Bongiorno-Borbone, L., Ranalli, M., Munarriz, E., Sayan, A.E., McWilliam, J.M., Smith, T.M., Fava, E.*, et al.* (2006b). FLASH is an essential component of Cajal bodies. Proc Natl Acad Sci U S A *103*, 14802-14807.

Barouch, D.H., O'Brien, K.L., Simmons, N.L., King, S.L., Abbink, P., Maxfield, L.F., Sun, Y.-H., La Porte, A., Riggs, A.M., Lynch, D.M.*, et al.* (2010). Mosaic HIV-1 vaccines expand the breadth and depth of cellular immune responses in rhesus monkeys. Nature Medicine *16*, 319-U116.

Barth, S., Liss, M., Voss, M.D., Dobner, T., Fischer, U., Meister, G., and Grasser, F.A. (2003). Epstein-Barr virus nuclear antigen 2 binds via its methylated arginine-glycine repeat to the survival motor neuron protein. Journal of Virology *77*, 5008-5013.

Bass, B.L., and Weintraub, H. (1988). An unwinding activity that covalently modifies its double-stranded-RNA substrate. Cell *55*, 1089-1098.

Bauren, G., and Wieslander, L. (1994). Splicing of balbiani ring-1 gene premessenger RNA occurs simultaneously with transcription. Cell *76*, 183-192.

Bell, P., Lieberman, P.M., and Maul, G.G. (2000). Lytic but not latent replication of Epstein-Barr virus is associated with PML and induces sequential release of nuclear domain 10 proteins. Journal of Virology *74*, 11800-11810.

Beltz, G.A., and Flint, S.J. (1979). Inhibition of HeLa cell protein synthesis during adenovirus infection - restriction of cellular messenger RNA sequences to the nucleus. Journal of Molecular Biology *131*, 353-373.

Benko, M., and Harrach, B. (1998). A proposal for a new (third) genus within the family Adenoviridae. Archives of Virology *143*, 829-837.

Berezney, R., Dubey, D.D., and Huberman, J.A. (2000). Heterogeneity of eukaryotic replicons, replicon clusters, and replication foci. Chromosoma *108*, 471-484.

Bergelson, J.M., Cunningham, J.A., Droguett, G., KurtJones, E.A., Krithivas, A., Hong, J.S., Horwitz, M.S., Crowell, R.L., and Finberg, R.W. (1997). Isolation of a common receptor for coxsackie B viruses and adenoviruses 2 and 5. Science *275*, 1320-1323.

Berget, S.M., and Sharp, P.A. (1979). Structure of late adenovirus 2 heterogeneous nuclear RNA. Journal of Molecular Biology *129*, 547-565.

Berk, A.J. (2005). Recent lessons in gene expression, cell cycle control, and cell biology from adenovirus. Oncogene *24*, 7673-7685.

Berk, A.J. (2007). Adenoviridae: The Viruses and Their Replication. In Fields Virology, D.M. Knipe, P.M. Howley, D.E. Griffin, R.A. Lamb, and M.A. Martin, eds. (Philadelphia, Lippincott Williams and Wilkins), pp. 2355-2394.

Berk, A.J., Lee, F., Harrison, T., Williams, J., and Sharp, P.A. (1979). Pre-early adenovirus-5 gene-product regulates synthesis of early viral messenger RNAs. Cell *17*, 935-944.

Berk, A.J., and Sharp, P.A. (1978). Structure of adenovirus 2 early messenger-RNAs. Cell *14*, 695-711.

Bernard, D., Prasanth, K.V., Tripathi, V., Colasse, S., Nakamura, T., Xuan, Z., Zhang, M.Q., Sedel, F., Jourdren, L., Coulpier, F.*, et al.* (2010). A long nuclear-retained non-coding RNA regulates synaptogenesis by modulating gene expression. Embo Journal *29*, 3082-3093.

Bernardi, R., and Pandolfi, P.P. (2003). Role of PML and the PML-nuclear body in the control of programmed cell death. Oncogene *22*, 9048-9057.

Bernardi, R., and Pandolfi, P.P. (2007). Structure, dynamics and functions of promyelocytic leukaemia nuclear bodies. Nature Reviews Molecular Cell Biology *8*, 1006-1016.

Bernardi, R., Papa, A., and Pandolfi, P.P. (2008). Regulation of apoptosis by PML and the PML-NBs. Oncogene *27*, 6299-6312.

Bernardi, R., Scaglioni, P.P., Bergmann, S., Horn, H.F., Vousden, K.H., and Pandolfi, P.P. (2004). PML regulates p53 stability by sequestering Mdm2 to the nucleolus. Nature Cell Biology *6*, 665-672.

Bertrand, L., and Pearson, A. (2008). The conserved N-terminal domain of herpes simplex virus 1 UL24 protein is sufficient to induce the spatial redistribution of nucleolin. Journal of General Virology *89*, 1142-1151.

Besse, S., and Puvion-Dutilleul, F. (1995). Anchorage of adenoviral RNAs to clusters of interchromatin granules. Gene Expression *5*, 79-92.

Bessis, N., GarciaCozar, F.J., and Boissier, M.C. (2004). Immune responses to gene therapy vectors: influence on vector function and effector mechanisms. Gene Therapy *11*, S10-S17.

Bex, F., McDowall, A., Burny, A., and Gaynor, R. (1997). The human T-cell leukemia virus type 1 transactivator protein tax colocalizes in unique nuclear structures with NF-kappa B proteins. Journal of Virology *71*, 3484-3497.

Biamonti, G. (2004). Nuclear stress bodies: a heterochromatin affair? Nature Reviews Molecular Cell Biology *5*, 493-498.

Biggiogera, M., Burki, K., Kaufmann, S.H., Shaper, J.H., Gas, N., Amalric, F., and Fakan, S. (1990). Nucleolar distribution of proteins B23 and nucleolin in mouse preimplantation embryos as visulaized by immunoelectron microscopy. Development *110*, 1263-1270.

Bischof, O., Kim, S.H., Irving, J., Beresten, S., Ellis, N.A., and Campisi, J. (2001). Regulation and localization of the Bloom syndrome protein in response to DNA damage. Journal of Cell Biology *153*, 367-380.

Bischoff, J.R., Kim, D.H., Williams, A., Heise, C., Horn, S., Muna, M., Ng, L., Nye, J.A., SampsonJohannes, A., Fattaey, A.*, et al.* (1996). An adenovirus mutant that replicates selectively in p53-deficient human tumor cells. Science *274*, 373-376.

Black, B.C., and Center, M.S. (1979). DNA-binding properties of the major core protein of adenovirus-2. Nucleic Acids Research *6*, 2339-2353.

Blanchette, P., Cheng, C.Y., Yan, Q., Ketner, G., Ornelles, D.A., Dobner, T., Conaway, R.C., Conaway, J.W., and Branton, P.E. (2004). Both BC-Box motifs of adenovirus protein E4orf6 are required to efficiently assemble an E3 ligase complex that degrades p53. Molecular and Cellular Biology *24*, 9619-9629.

Blanchette, P., Kindsmueller, K., Groitl, P., Dallaire, F., Speiseder, T., Branton, P.E., and Dobner, T. (2008). Control of mRNA export by adenovirus E4orf6 and E1B55K proteins during productive infection requires E4orf6 ubiquitin ligase activity. Journal of Virology *82*, 2642-2651.

Bleoo, S., Sun, X.J., Hendzel, M.J., Rowe, J.M., Packer, M., and Godbout, R. (2001). Association of human DEAD box protein DDX1 with a cleavage stimulation factor involved in 3 '-end processing of pre-mRNA. Molecular Biology of the Cell *12*, 3046-3059.

Bodnar, A.G., Ouellette, M., Frolkis, M., Holt, S.E., Chiu, C.P., Morin, G.B., Harley, C.B., Shay, J.W., Lichtsteiner, S., and Wright, W.E. (1998). Extension of life-span by introduction of telomerase into normal human cells. Science *279*, 349-352.

Bodnar, J.W., and Pearson, G.D. (1980). Kinetics of adenovirus DNA-replication. 2. Initiation of adenovirus DNA replication. Virology *105*, 357-370.

Boe, S.O., Haave, M., Jul-Larsen, A., Grudic, A., Bjerkvig, R., and Lonning, P.E. (2006). Promyelocytic leukemia nuclear bodies are predetermined processing sites for damaged DNA. Journal of Cell Science *119*, 3284-3295.

Bohmann, K., Ferreira, J.A., and Lamond, A.I. (1995). Mutational analysis of p80 coilin indicates a functional interaction between coiled bodies and the nucleolus. Journal of Cell Biology *131*, 817-831.

Boisvert, F.-M., van Koningsbruggen, S., Navascues, J., and Lamond, A.I. (2007). The multifunctional nucleolus. Nature Reviews Molecular Cell Biology *8*, 574-585.

Boisvert, F.M., Hendzel, M.J., and Bazett-Jones, D.P. (2000). Promyelocytic leukemia (PML) nuclear bodies are protein structures that do not accumulate RNA. Journal of Cell Biology *148*, 283-292.

Bond, C.S., and Fox, A.H. (2009). Paraspeckles: nuclear bodies built on long noncoding RNA. Journal of Cell Biology *186*, 637-644.

Bondesson, M., Ohman, K., Mannervik, M., Fan, S., and Akusjarvi, G. (1996). Adenovirus E4 open reading frame 4 protein autoregulates E4 transcription by inhibiting E1A transactivation of the E4 promoter. Journal of Virology *70*, 3844-3851.

Bongiorno-Borbone, L., De Cola, A., Barcaroli, D., Knight, R.A., Di Ilio, C., Melino, G., and De Laurenzi, V. (2010). FLASH degradation in response to UV-C results in histone locus bodies disruption and cell-cycle arrest. Oncogene *29*, 802-810.

Bortolin, M.L., Bachellerie, J.P., and Clouet-d'Orval, B. (2003). In vitro RNP assembly and methylation guide activity of an unusual box C/D RNA, cis-acting archaeal pre-tRNA(Trp). Nucleic Acids Research *31*, 6524-6535.

Both, G.W. (2002). Identification of a unique family of F-box proteins in atadenoviruses. Virology *304*, 425-433.

Boudin, M.L., Dhalluin, J.C., Cousin, C., and Boulanger, P. (1980). Human adenovirus type-2 protein-IIIa. 2. Maturation and encapsidation. Virology *101*, 144-156.

Boudonck, K., Dolan, L., and Shaw, P.J. (1999). The movement of coiled bodies visualized in living plant cells by the green fluorescent protein. Molecular Biology of the Cell *10*, 2297-2307.

Boulanger, P., Lemay, P., Blair, G.E., and Russell, W.C. (1979). Characterization of adenovirus protein-IX. Journal of General Virology *44*, 783-800.

Boulanger, P.A., and Blair, G.E. (1991). Expression and interaction of human adenovirus oncoproteins. Biochemical Journal *275*, 281-299.

Boulisfane, N., Choleza, M., Rage, F., Neel, H., Soret, J., and Bordonne, R. (2011). Impaired minor tri-snRNP assembly generates differential splicing defects of U12-type introns in lymphoblasts derived from a type I SMA patient. Human Molecular Genetics *20*, 641-648.

Boulon, S., Westman, B.J., Hutten, S., Boisvert, F.-M., and Lamond, A.I. (2010). The Nucleolus under Stress. Molecular Cell *40*, 216-227.

Bourdin, M.L., D'Halluin, J.C., Cousin, C., and Boulanger, P. (1980). Human adenovirus type-2 protein IIIa. 2.Maturation and encapsidation. Virology *101*, 144-156.

Boutanaev, A.M., Kalmykova, A.I., Shevelyov, Y.Y., and Nurminsky, D.I. (2002). Large clusters of co-expressed genes in the Drosophila genome. Nature *420*, 666-669.

Boutell, C., Cuchet-Lourenco, D., Vanni, E., Orr, A., Glass, M., McFarlane, S., and Everett, R.D. (2011). A Viral Ubiquitin Ligase Has Substrate Preferential SUMO Targeted Ubiquitin Ligase Activity that Counteracts Intrinsic Antiviral Defence. Plos Pathogens *7*, e1002245.

Boyer, J., Rohleder, K., and Ketner, G. (1999a). Adenovirus E4 34k and E4 11k inhibit double strand break repair and are physically associated with the cellular DNA-dependent protein kinase. Virology *263*, 307-312.

Boyer, T.G., Martin, M.E.D., Lees, E., Ricciardi, R.P., and Berk, A.J. (1999b). Mammalian Srb Mediator complex is targeted by adenovirus E1A protein. Nature *399*, 276-279.

Boyne, J.R., and Whitehouse, A. (2006). Nucleolar trafficking is essential for nuclear export of intronless herpesvirus mRNA. Proc Natl Acad Sci U S A *103*, 15190-15195.

Bradshaw, A.C., Parker, A.L., Duffy, M.R., Coughlan, L., van Rooijen, N., Kahari, V.-M., Nicklin, S.A., and Baker, A.H. (2010). Requirements for Receptor Engagement during Infection by Adenovirus Complexed with Blood Coagulation Factor X. Plos Pathogens *6*, e1001142.

Braithwaite, A.W., Cheetham, B.F., Li, P., Parish, C.R., Waldronstevens, L.K., and Bellett, A.J.D. (1983). Adenovirus-induced alterations of the cell-growth cycle - a requirement for expression of E1A but not of E1B. Journal of Virology *45*, 192-199.

Brede, G., Solheim, J., and Prydz, H. (2002). PSKH1, a novel splice factor compartment-associated serine kinase. Nucleic Acids Research *30*, 5301-5309.

Bregman, D.B., Du, L., Vanderzee, S., and Warren, S.L. (1995). Transcription-dependent redistribution of the large subunit of RNA-polymerase-II to discrete nuclear domains. Journal of Cell Biology *129*, 287-298.

Brehm, A., Miska, E.A., McCance, D.J., Reid, J.L., Bannister, A.J., and Kouzarides, T. (1998). Retinoblastoma protein recruits histone deacetylase to repress transcription. Nature *391*, 597-601.

Bremner, K.H., Scherer, J., Yi, J.L., Vershinin, M., Gross, S.P., and Vallee, R.B. (2009). Adenovirus Transport via Direct Interaction of Cytoplasmic Dynein with the Viral Capsid Hexon Subunit. Cell Host Microbe *6*, 523-535.

Bridge, E., Carmo-Fonseca, M., Lamond, A., and Pettersson, U. (1993a). Nuclear organisation of splicing small nuclear ribonucleoproteins in adenovirus-infected cells. Journal of Virology *67*, 5792-5802.

Bridge, E., Carmo-Fonseca, M., Lamond, A., and Pettersson, U. (1993b). Nuclear organization of splicing small nuclear ribonucleoproteins in adenovirus-infected cells. Journal of Virology *67*, 5792-5802.

Bridge, E., Hemstrom, C., and Pettersson, U. (1991). Differential regulation of adenovirus late transcriptional units by the products of early region. Virology *183*, 260-266.

Bridge, E., and Ketner, G. (1990). Interaction of adenoviral E4 and E1B products in late gene expression. Virology *174*, 345-353.

Bridge, E., Mattsson, K., Aspegren, A., and Sengupta, A. (2003). Adenovirus early region 4 promotes the localization of splicing factors and viral RNA in late-phase interchromatin granule clusters. Virology *311*, 40-50.

Bridge, E., Riedel, K.U., Johansson, B.M., and Pettersson, U. (1996). Spliced exons of adenovirus late RNAs colocalize with snRNP in a specific nuclear domain. Journal of Cell Biology *135*, 303-314.

Bridge, E., Xia, D.X., Carmo-Fonseca, M., Cardinali, B., Lamond, A.I., and Pettersson, U. (1995). Dynamic organization of splicing factors in adenovirus-infected cells. Journal of Virology *69*, 281-290.

Broome, H.J., and Hebert, M.D. (2012). In Vitro RNase and Nucleic Acid Binding Activities Implicate Coilin in U snRNA Processing. Plos One *7*, e36300.

Brown, J.M., Green, J., das Neves, R.P., Wallace, H.A.C., Smith, A.J.H., Hughes, J., Gray, N., Taylor, S., Wood, W.G., Higgs, D.R.*, et al.* (2008). Association between active genes occurs at nuclear speckles and is modulated by chromatin environment. Journal of Cell Biology *182*, 1083-1097.

Brown, M.T., and Mangel, W.F. (2004). Interaction of actin and its 11-amino acid C-terminal peptide as cofactors with the adenovirus proteinase. FEBS Lett *563*(1-3), 213-218.

Brown, M.T., McBride, K.M., Baniecki, M.L., Reich, N.C., Marriotti, G., and Mangel, W.F. (2002). Actin can act as a cofactor for a viral proteinase in the cleavage of the cytoskeleton. Journal of Biological Chemistry *277*, 46298-46303.

Brunetti-Pierri, N., and Ng, P. (2008). Progress and prospects: gene therapy for genetic diseases with helper-dependent adenoviral vectors. Gene Therapy *15*, 553-560.

Bryant, H.E., Matthews, D.A., Wadd, S., Scott, J.E., Kean, J., Graham, S., Russell, W.C., and Clements, J.B. (2000). Interaction between herpes simplex virus type 1 IE63 protein and cellular protein p32. Journal of Virology *74*, 11322-11328.

Bryant, H.E., Wadd, S.E., Lamond, A.I., Silverstein, S.J., and Clements, J.B. (2001). Herpes simplex virus IE63 (ICP27) protein interacts with spliceosome-associated protein 145 and inhibits splicing prior to the first catalytic step. Journal of Virology *75*, 4376-4385.

Burch, B.D., Godfrey, A.C., Gasdaska, P.Y., Salzler, H.R., Duronio, R.J., Marzluff, W.F., and Dominski, Z. (2011). Interaction between FLASH and Lsm11 is essential for histone pre-mRNA processing in vivo in Drosophila. Rna-a Publication of the Rna Society *17*, 1132-1147.

Burckhardt, C.J., Suomalainen, M., Schoenenberger, P., Boucke, K., Hemmi, S., and Greber, U.F. (2011). Drifting Motions of the Adenovirus Receptor CAR and Immobile Integrins Initiate Virus Uncoating and Membrane Lytic Protein Exposure. Cell Host Microbe *10*, 105-117.

Burkham, J., Coen, D.M., Hwang, C.B.C., and Weller, S.K. (2001). Interactions of herpes simplex virus type 1 with ND10 and recruitment of PML to replication compartments. Journal of Virology *75*, 2353-2367.

Burkham, J., Coen, D.M., and Weller, S.K. (1998). ND10 protein PML is recruited to herpes simplex virus type 1 prereplicative sites and replication compartments in the presence of viral DNA polymerase. Journal of Virology *72*, 10100-10107.

Bustin, S.A. (2000). Absolute quantification of mRNA using real-time reverse transcription polymerase chain reaction assays. Journal of Molecular Endocrinology *25*, 169-193.

Caceres, J.F., Misteli, T., Screaton, G.R., Spector, D.L., and Krainer, A.R. (1997). Role of the modular domains of SR proteins in sub-nuclear localization and alternative splicing specificity. Journal of Cell Biology *138*, 225-238.

Cai, Q., Guo, Y., Xiao, B., Banerjee, S., Saha, A., Lu, J., Glisovic, T., and Robertson, E.S. (2011). Epstein-Barr Virus Nuclear Antigen 3C Stabilizes Gemin3 to Block p53-mediated Apoptosis. Plos Pathogens *7*, e1002418.

Cajal, S.R. (1903). New method for the colouration of neurofibrils. Comptes Rendus Des Seances De La Societe De Biologie Et De Ses Filiales *55*, 1565-1568.

Calle, A., Ugrinova, I., Epstein, A.L., Bouvet, P., Diaz, J.-J., and Greco, A. (2008a). Nucleolin is required for an efficient herpes simplex virus type 1 infection. Journal of Virology *82*, 4762-4773.

Calle, A., Ugrinova, I., Epstein, A.L., Bouvet, P., Diaz, J.J., and Greco, A. (2008b). Nucleolin is required for an efficient herpes simplex virus type 1 infection. Journal of Virology *82*, 4762-4773.

Campagna, M., Herranz, D., Garcia, M.A., Marcos-Villar, L., Gonzalez-Santamaria, J., Gallego, P., Gutierrez, S., Collado, M., Serrano, M., Esteban, M.*, et al.* (2011). SIRT1 stabilizes PML promoting its sumoylation. Cell Death and Differentiation *18*, 72-79.

Campbell, L., Hunter, K.M.D., Mohaghegh, P., Tinsley, J.M., Brasch, M.A., and Davies, K.E. (2000). Direct interaction of Smn with dp103, a putative RNA helicase: a role for Smn in transcription regulation? Human Molecular Genetics *9*, 1093-1100.

Cancio-Lonches, C., Yocupicio-Monroy, M., Sandoval-Jaime, C., Galvan-Mendoza, I., Urena, L., Vashist, S., Goodfellow, I., Salas-Benito, J., and Gutierrez-Escolano, A.L. (2011). Nucleolin Interacts with the Feline Calicivirus 3 ' Untranslated Region and the Protease-Polymerase NS6 and NS7 Proteins, Playing a Role in Virus Replication. Journal of Virology *85*, 8056-8068.

Canetta, E., Kim, S.H., Kalinina, N.O., Shaw, J., Adya, A.K., Gillespie, T., Brown, J.W.S., and Taliansky, M. (2008). A plant virus movement protein forms ringlike complexes with the major nucleolar protein, fibrillarin, in vitro. Journal of Molecular Biology *376*, 932-937.

Cantrell, S.R., and Bresnahan, W.A. (2006). Human cytomegalovirus (HCMV) UL82 gene product (pp71) relieves hDaxx-mediated repression of HCMV replication. Journal of Virology *80*, 6188-6191.

Caravokyri, C., and Leppard, K.N. (1996). Human adenovirus type 5 variants with sequence alterations flanking the E2A gene: Effects on E2 expression and DNA replication. Virus Genes *12*, 65-75.

Carbone, R., Pearson, M., Minucci, S., and Pelicci, P.G. (2002). PML NBs associate with the hMre11 complex and p53 at sites of irradiation induced DNA damage. Oncogene *21*, 1633-1640.

Cardoso, M.C., Leonhardt, H., and Nadalginard, B. (1993). Reversal of terminal differentiation and control of DNA-replication - cyclin-A and CDK2 specifically localise at sub-nuclear sites of DNA-replication. Cell *74*, 979-992.

Carmichael, J., Degraff, W.G., Gazdar, A.F., Minna, J.D., and Mitchell, J.B. (1987). Evaluation of a tetrazolium-based semiautomated colorimetric assay - assessment of chemosensitivity testing. Cancer Research *47*, 936-942.

Carmo-Fonseca, M., Ferreira, J., and Lamond, A.I. (1993). Assembly of snRNP-containing coiled bodies is regulated in interphase and mitosis - evidence that the coiled body is a kinetic nuclear structure. Journal of Cell Biology *120*, 841-852.

Carmo-Fonseca, M., Pepperkok, R., Carvalho, M.T., and Lamond, A.I. (1992). Transcription-dependent colocalisation of the U1, U2, U4/U6 and U5 snRNPs in coiled bodies. Journal of Cell Biology *117*, 1-14.

Caron, H., van Schaik, B., van der Mee, M., Baas, F., Riggins, G., van Sluis, P., Hermus, M.C., van Asperen, R., Boon, K., Voute, P.A.*, et al.* (2001). The human transcriptome map: Clustering of highly expressed genes in chromosomal domains. Science *291*, 1289-1292.

Carson, C.T., Schwartz, R.A., Stracker, T.H., Lilley, C.E., Lee, D.V., and Weitzman, M.D. (2003). The Mre11 complex is required for ATM activation and the G(2)/M checkpoint. Embo Journal *22*, 6610-6620.

Carvalho, T., Almeida, F., Calapez, A., Lafarga, M., Berciano, M.T., and Carmo-Fonseca, M. (1999). The spinal muscular atrophy disease gene product, SMN: A link between snRNP biogenesis and the Cajal (coiled) body. Journal of Cell Biology *147*, 715-727.

Carvalho, T., Seeler, J.S., Ohman, K., Jordan, P., Pettersson, U., Akusjarvi, G., Carmo-Fonseca, M., and Dejean, A. (1995). Targeting of adenovirus E1A and E4-ORF3 proteins to nuclear matrix-associated PML bodies. Journal of Cell Biology *131*, 45-56.

Caygill, R.L., Hodges, C.S., Holmes, J.L., Higson, S.P.J., Blair, G.E., and Millner, P.A. (2012). Novel impedimetric immunosensor for the detection and quantitation of Adenovirus using reduced antibody fragments immobilized onto a conducting copolymer surface. Biosensors & Bioelectronics *32*, 104-110.

Cepko, C.L., Changelian, P.S., and Sharp, P.A. (1981). Immunoprecipitation with two-dimensional pools as a hybridoma screening technique - production and characterisation of monoclonal antibodies against adenovirus-2 proteins. Virology *110*, 385-401.

Chang, K.S., Fan, Y.H., Andreeff, M., Liu, J.X., and Mu, Z.M. (1995). The PML gene encodes a phosphoprotein associated with the nuclear matrix. Blood *85*, 3646-3653.

Chang, L., Godinez, W.J., Kim, I.-H., Tektonidis, M., de Lanerolle, P., Eils, R., Rohr, K., and Knipe, D.M. (2011). Herpesviral replication compartments move and coalesce at nuclear speckles to enhance export of viral late mRNA. Proc Natl Acad Sci U S A *108*, E136-E144.

Chari, A., Paknia, E., and Fischer, U. (2009). The role of RNP biogenesis in spinal muscular atrophy. Current Opinion in Cell Biology *21*, 387-393.

Charpentier, B., Muller, S., and Branlant, C. (2005). Reconstitution of archaeal H/ACA small ribonucleoprotein complexes active in pseudouridylation. Nucleic Acids Research *33*, 3133-3144.

Chatterjee, P.K., Vayda, M.E., and Flint, S.J. (1985). Interactions amongst the 3 adenovirus core proteins. Journal of Virology *55*, 379-386.

Chatterjee, P.K., Vayda, M.E., Flint, S.E. Identification of proteins and protein domains that contact DNA within adenovirus nucleoprotein cores by ultraviolet light crosslinking of oligonucleotides P-32 labelled in vivo. Journal of Molecular Biology *188*, 23-37.

Chee, A.V., Lopez, P., Pandolfi, P.P., and Roizman, B. (2003). Promyelocytic leukemia protein mediates interferon-based anti-herpes simplex virus 1 effects. Journal of Virology *77*, 7101-7105.

Chellappan, S.P., Hiebert, S., Mudryj, M., Horowitz, J.M., and Nevins, J.R. (1991). The E2F transcription factor is a cellular target for the Rb protein. Cell *65*, 1053-1061.

Chen, E.C., Yagi, S., Kelly, K.R., Mendoza, S.P., Maninger, N., Rosenthal, A., Spinner, A., Bales, K.L., Schnurr, D.P., Lerche, N.W.*, et al.* (2011). Cross-Species Transmission of a Novel Adenovirus Associated with a Fulminant Pneumonia Outbreak in a New World Monkey Colony. Plos Pathogens *7*, e1002155.

Chen, J., Morral, N., and Engel, D.A. (2007). Transcription releases protein VII from adenovirus chromatin. Virology *369*, 411-422.

Chen, L.-L., and Carmichael, G.G. (2009). Altered Nuclear Retention of mRNAs Containing Inverted Repeats in Human Embryonic Stem Cells: Functional Role of a Nuclear Noncoding RNA. Molecular Cell *35*, 467-478.

Chen, L.L., and Carmichael, G.G. (2010). Decoding the function of nuclear long non-coding RNAs. Current Opinion in Cell Biology *22*, 357-364.

Chen, L.Y., and Chen, J.D. (2003). Daxx silencing sensitizes cells to multiple apoptotic pathways. Molecular and Cellular Biology *23*, 7108-7121.

Chen, M., Mermod, N., and Horwitz, M.S. (1990). Protein-protein interactions between adenovirus DNA-polymerase and Nuclear Factor I mediate formation of the DNA-replication preinitiation complex. Journal of Biological Chemistry *265*, 18634-18642.

Chen, P.H., Ornelles, D.A., and Shenk, T. (1993). The adenovirus L3 23-kilodalton proteinase cleaves the amino-terminal head domain from cytokeratin 18 and disrupts the cytokeratin network of HeLa cells. Journal of Virology *67*, 3507-3514.

Cheng, H., Dufu, K., Lee, C.-S., Hsu, J.L., Dias, A., and Reed, R. (2006). Human mRNA export machinery recruited to the 5 ' end of mRNA. Cell *127*, 1389-1400.

Chow, L.T., and Broker, T.R. (1978). Spliced structures of adenovirus 2 fiber message and other late messenger RNAs. Cell *15*, 497-510.

Chow, L.T., Broker, T.R., and Lewis, J.B. (1979). Complex splicing patterns of RNAs from the early regions of adenovirus-2. Journal of Molecular Biology *134*, 265-303.

Chroboczek, J., Viard, F., and Dhalluin, J.C. (1986). Human adenovirus-2 temperature-sensitive mutant-112 contains 3 mutations in the protein-IIIa gene. Gene *49*, 157-160.

Chuang, C.H., Carpenter, A.E., Fuchsova, B., Johnson, T., de Lanerolle, P., and Belmont, A.S. (2006). Long-range directional movement of an interphase chromosome site. Current Biology *16*, 825-831.

Cioce, M., and Lamond, A.I. (2005). Cajal bodies: A long history of discovery. In Annual Review of Cell and Developmental Biology, pp. 105-131.

Cleat, P.H., and Hay, R.T. (1989). Co-operative interactions between NFI and the adenovirus DNA-binding protein at the adenovirus origin of replication. Embo Journal *8*, 1841-1848.

Clemson, C.M., Hutchinson, J.N., Sara, S.A., Ensminger, A.W., Fox, A.H., Chess, A., and Lawrence, J.B. (2009). An Architectural Role for a Nuclear Noncoding RNA: NEAT1 RNA Is Essential for the Structure of Paraspeckles. Molecular Cell *33*, 717-726.

Cmarko, D., Verschure, P.J., Martin, T.E., Dahmus, M.E., Krause, S., Fu, X.D., van Driel, R., and Fakan, S. (1999). Ultrastructural analysis of transcription and splicing in the cell nucleus after bromo-UTP microinjection. Molecular Biology of the Cell *10*, 211-223.

Cochrane, A.W., Perkins, A., and Rosen, C.A. (1990). Identification of sequences important in the nucleolar localization of human immunodeficiency virus Rev - relevance of nucleolar localisation to function. Journal of Virology *64*, 881-885.

Cockell, M.M., and Gasser, S.M. (1999). The nucleolus: Nucleolar space for RENT. Current Biology *9*, R575-R576.

Cohen, S.B., Graham, M.E., Lovrecz, G.O., Bache, N., Robinson, P.J., and Reddel, R.R. (2007). Protein composition of catalytically active human telomerase from immortal cells. Science *315*, 1850-1853.

Colby, W.W., Shenk, T. (1981). Adenovirus type-5 virions can be assembled invivo in the absence of detectable polypeptide-IX. Journal of Virology *39*, 977-980.

Colwill, K., Pawson, T., Andrews, B., Prasad, J., Manley, J.L., Bell, J.C., and Duncan, P.I. (1996). The Clk/Sty protein kinase phosphorylates SR splicing factors and regulates their intranuclear distribution. Embo Journal *15*, 265-275.

Conlan, L.A., McNees, C.J., and Heierhorst, J. (2004). Proteasome-dependent dispersal of PML nuclear bodies in response to alkylating DNA damage. Oncogene *23*, 307-310.

Cook, P.R. (1999). Molecular biology - The organization of replication and transcription. Science *284*, 1790-1795.

Cook, P.R. (2010). A Model for all Genomes: The Role of Transcription Factories. Journal of Molecular Biology *395*, 1-10.

Copenhaver, G.P., Putnam, C.D., Denton, M.L., and Pikaard, C.S. (1994). The RNA-polymerase-I transcription factor UBF is a sequence-tolerant HMG-box protein that can recognize structured nucleic acids. Nucleic Acids Research *22*, 2651-2657.

Corjon, S., Gonzalez, G., Henning, P., Grichine, A., Lindholm, L., Boulanger, P., Fender, P., and Hong, S.-S. (2011). Cell Entry and Trafficking of Human Adenovirus Bound to Blood Factor X Is Determined by the Fiber Serotype and Not Hexon: Heparan Sulfate Interaction. Plos One *6*, e18205.

Counter, C.M., Avilion, A.A., Lefeuvre, C.E., Stewart, N.G., Greider, C.W., Harley, C.B., and Bacchetti, S. (1992). Telomere shortening associated with chromosome instability is arrested in immortal cells which express telomerase activity. Embo Journal *11*, 1921-1929.

Cuchet, D., Sykes, A., Nicolas, A., Orr, A., Murray, J., Sirma, H., Heeren, J., Bartelt, A., and Everett, R.D. (2011). PML isoforms I and II participate in PML-dependent restriction of HSV-1 replication. Journal of Cell Science *124*, 280-291.

Cuconati, A., Degenhardt, K., Sundararajan, R., Anschel, A., and White, E. (2002). Bak and Bax function to limit adenovirus replication through apoptosis induction. Journal of Virology *76*, 4547-4558.

Cuconati, A., Mukherjee, C., Perez, D., and White, E. (2003). DNA damage response and MCL-1 destruction initiate apoptosis in adenovirus-infected cells. Genes & Development *17*, 2922-2932.

Cuconati, A., and White, E. (2002). Viral homologs of BCL-2: role of apoptosis in the regulation of virus infection. Genes & Development *16*, 2465-2478.

Cuesta, R., Xi, Q.R., and Schneider, R.J. (2000). Adenovirus-specific translation by displacement of kinase Mnk1 from cap-initiation complex elF4F. Embo Journal *19*, 3465-3474.

D'Amours, D., and Jackson, S.P. (2002). The Mre11 complex: At the crossroads of DNA repair and checkpoint signalling. Nature Reviews Molecular Cell Biology *3*, 317-327.

Dales, S., and Chardonnet, Y. (1973). Early events in interaction of adenoviruses with HeLa cells. 4.Association with microtubules and nuclear-pore complex during vectorial movement of inoculum. Virology *56*, 465-483.

Daneshvar, K., Khan, A., and Goodliffe, J.M. (2011). Myc Localizes to Histone Locus Bodies during Replication in Drosophila. Plos One *6*, e23928.

Darzacq, X., Jady, B.E., Verheggen, C., Kiss, A.M., Bertrand, E., and Kiss, T. (2002). Cajal body-specific small nuclear RNAs: a novel class of 2 '-O-methylation and pseudouridylation guide RNAs. Embo Journal *21*, 2746-2756.

Davison, A.J., Benko, M., and Harrach, B. (2003). Genetic content and evolution of adenoviruses. Journal of General Virology *84*, 2895-2908.

De Clercq, E. (2003). Clinical potential of the acyclic nucleoside phosphonates cidofovir, adefovir, and tenofovir in treatment of DNA virus and retrovirus infections. Clinical Microbiology Reviews *16*, 569-596.

De Cola, A., Bongiorno-Borbone, L., Bianchi, E., Barcaroli, D., Carletti, E., Knight, R.A., Di Ilio, C., Melino, G., Sette, C., and De Laurenzi, V. (2012). FLASH is essential during early

embryogenesis and cooperates with p73 to regulate histone gene transcription. Oncogene *31*, 573-582.

de Jong, R.N., Meijer, L.A.T., and van der Vliet, P.C. (2003a). DNA binding properties of the adenovirus DNA replication priming protein pTP. Nucleic Acids Research *31*, 3274-3286.

de Jong, R.N., and van der Vliet, P.C. (1999). Mechanism of DNA replication in eukaryotic cells: cellular host factors stimulating adenovirus DNA replication. Gene *236*, 1-12.

De Jong, R.N., Van Der Vliet, P.C., and Brenkman, A.B. (2003b). Adenovirus DNA replication: Protein priming, jumping back and the role of the DNA binding protein DBP. Adenoviruses: Model and Vectors in Virus-Host Interactions *272*, 187-211.

de Stanchina, E., Querido, E., Narita, M., Davuluri, R.V., Pandolfi, P.P., Ferbeyre, G., and Lowe, S.W. (2004). PML is a direct p53 target that modulates p53 effector functions. Molecular Cell *13*, 523-535.

de Vrij, J., van den Hengel, S.K., Uil, T.G., Koppers-Lalic, D., Dautzenberg, I.J.C., Stassen, O.M.J.A., Barcena, M., Yamamoto, M., de Ridder, C.M.A., Kraaij, R.*, et al.* (2011). Enhanced transduction of CAR-negative cells by protein IX-gene deleted adenovirus 5 vectors. Virology *410*, 192-200.

Debbas, M., and White, E. (1993). Wild-type p53 mediates apoptosis by E1A, which is inhibited by E1B. Genes & Development *7*, 546-554.

Dekker, J., Kanellopoulos, P.N., Loonstra, A.K., vanOosterhout, J., Leonard, K., Tucker, P.A., and vanderVliet, P.C. (1997). Multimerization of the adenovirus DNA-binding protein is the driving force for ATP-independent DNA unwinding during strand displacement synthesis. Embo Journal *16*, 1455-1463.

Dellaire, G., and Bazett-Jones, D.P. (2004). PML nuclear bodies: dynamic sensors of DNA damage and cellular stress. Bioessays *26*, 963-977.

Dellaire, G., and Bazett-Jones, D.P. (2007). Beyond repair foci: Sub-nuclear domains and the cellular response to DNA damage. Cell Cycle *6*, 1864-1872.

Dellaire, G., Ching, R.W., Ahmed, K., Jalali, F., Tse, K.C.K., Bristow, R.G., and Bazett-Jones, D.P. (2006). Promyelocytic leukemia nuclear bodies behave as DNA damage sensors whose response to DNA double-strand breaks is regulated by NBS1 and the kinases ATM, Chk2, and ATR. Journal of Cell Biology *175*, 55-66.

Deryusheva, S., Choleza, M., Barbarossa, A., Gall, J.G., and Bordonne, R. (2012). Post-transcriptional modification of spliceosomal RNAs is normal in SMN-deficient cells. Rna-a Publication of the Rna Society *18*, 31-36.

Desterro, J.M.P., Keegan, L.R., Lafarga, M., Berciano, M.T., O'Connell, M., and Carmo-Fonseca, M. (2003). Dynamic association of RNA-editing enzymes with the nucleolus. Journal of Cell Science *116*, 1805-1818.

Dethe, H., Lavau, C., Marchio, A., Chomienne, C., Degos, L., and Dejean, A. (1991). The PML-RAR-alpha fusion messenger-RNA generated by the T(15-17) translocation in acute promyelocytic leukemia encodes a functionally altered RAR. Cell *66*, 675-684.

Di Bacco, A., Ouyang, J., Lee, H.Y., Catic, A., Ploegh, H., and Gill, G. (2006). The SUMO-specific protease SENP5 is required for cell division. Molecular and Cellular Biology *26*, 4489-4498.

Di Fruscio, M., Weiher, H., Vanderhyden, B.C., Imai, T., Shiomi, T., Hori, T.A., Jaenisch, R., and Gray, D.A. (1997). Proviral inactivation of the Npat gene of Mpv 20 mice results in early embryonic arrest. Molecular and Cellular Biology *17*, 4080-4086.

Dias, A.P., Dufu, K., Lei, H., and Reed, R. (2010). A role for TREX components in the release of spliced mRNA from nuclear speckle domains. Nature Communications *1*, 97.

Diaz-Cuervo, H., and Bueno, A. (2008). Cds1 controls the release of Cdc14-like phosphatase Flp1 from the nucleolus to drive full activation of the checkpoint response to replication stress in fission yeast. Molecular Biology of the Cell *19*, 2488-2499.

DiDonato, C.J., Parks, R.J., and Kothary, R. (2003). Development of a gene therapy strategy for the restoration of survival motor neuron protein expression: Implications for spinal muscular atrophy therapy. Human Gene Therapy *14*, 179-188.

Dolph, P.J., Huang, J., and Schneider, R.J. (1990). Translation by the adenovirus tripartite leader - elements which determine independence from cap-binding protein complex. Journal of Virology *64*, 2669-2677.

Dolph, P.J., Racaniello, V., Villamarin, A., Palladino, F., and Schneider, R.J. (1988). The adenovirus tripartite leader may eliminate the requirement for cap-binding protein complex during translation initiation. Journal of Virology *62*, 2059-2066.

Dominski, Z., Yang, X.C., and Marzluff, W.F. (2005). The polyadenylation factor CPSF-73 is involved in histone-pre-mRNA processing. Cell *123*, 37-48.

Dostie, J., Lejbkowicz, F., and Sonenberg, N. (2000). Nuclear eukaryotic initiation factor 4E (eIF4E) colocalizes with splicing factors in speckles. Journal of Cell Biology *148*, 239-245.

Doucas, V., Ishov, A.M., Romo, A., Juguilon, H., Weitzman, M.D., Evans, R.M., and Maul, G.G. (1996). Adenovirus replication is coupled with the dynamic properties of the PML nuclear structure. Genes & Development *10*, 196-207.

Draskovic, I., Arnoult, N., Steiner, V., Bacchetti, S., Lomonte, P., and Londono-Vallejo, A. (2009). Probing PML body function in ALT cells reveals spatiotemporal requirements for telomere recombination. Proc Natl Acad Sci U S A *106*, 15726-15731.

Duan, C.-G., Fang, Y.-Y., Zhou, B.-J., Zhao, J.-H., Hou, W.-N., Zhu, H., Ding, S.-W., and Guo, H.-S. (2012). Suppression of Arabidopsis ARGONAUTE1-Mediated Slicing, Transgene-Induced RNA Silencing, and DNA Methylation by Distinct Domains of the Cucumber mosaic virus 2b Protein. Plant Cell *24*, 259-274.

Dundr, M., Hebert, M.D., Karpova, T.S., Stanek, D., Xu, H.Z., Shpargel, K.B., Meier, U.T., Neugebauer, K.M., Matera, A.G., and Misteli, T. (2004). In vivo kinetics of Cajal body components. Journal of Cell Biology *164*, 831-842.

Dundr, M., and Misteli, T. (2002). Nucleolomics: An inventory of the nucleolus. Molecular Cell *9*, 5-7.

Dunn, A.R., Mathews, M.B., Chow, L.T., Sambrook, J., and Keller, W. (1978). Supplementary adenoviral leader sequence and its role in messenger translation. Cell *15*, 511-526.

Dyson, N. (1998). The regulation of E2F by pRB-family proteins. Genes & Development *12*, 2245-2262.

Dyson, N., Guida, P., Munger, K., and Harlow, E. (1992). Homologous sequences in adenovirus E1A and human papillomavirus E7 proteins mediate interaction with the same set of cellular proteins. Journal of Virology *66*, 6893-6902.

Eckner, R., Ewen, M.E., Newsome, D., Gerdes, M., Decaprio, J.A., Lawrence, J.B., and Livingston, D.M. (1994). Molecular cloning and functional analysis of the adenovirus E1A-associated 300KD protein (p300) reveals a protein with properties of a transcriptional adapter. Genes & Development *8*, 869-884.

El Mchichi, B., Regad, T., Maroui, M.A., Rodriguez, M.S., Aminev, A., Gerbaud, S., Escriou, N., Dianoux, L., and Chelbi-Alix, M.K. (2010). SUMOylation Promotes PML Degradation during Encephalomyocarditis Virus Infection. Journal of Virology *84*, 11634-11645.

Elbashir, S.M., Harborth, J., Lendeckel, W., Yalcin, A., Weber, K., and Tuschl, T. (2001). Duplexes of 21-nucleotide RNAs mediate RNA interference in cultured mammalian cells. Nature *411*, 494-498.

Enders, J.F., Bell, J.A., Dingle, J.H., Francis, T., Hilleman, M.R., Huebner, R.J., and Payne, A.M.M. (1956). Adenoviruses - Group name proposed for new respiratory-tract viruses. Science *124*, 119-120.

Engelhardt, J.F., Ye, X.H., Doranz, B., and Wilson, J.M. (1994). Ablation of E2A in recombinant adenoviruses improves transgene persistance and decreases inflammatory response in mouse liver. Proc Natl Acad Sci U S A *91*, 6196-6200.

Engelke, M.F., Burckhardt, C.J., Morf, M.K., and Greber, U.F. (2011). The Dynactin Complex Enhances the Speed of Microtubule-Dependent Motions of Adenovirus Both Towards and Away from the Nucleus. Viruses-Basel *3*, 233-253.

Enomoto, T., Lichy, J.H., Ikeda, J.E., and Hurwitz, J. (1981). Adenovirus DNA replication in vitro - purification of the terminal protein in a functional form. Proceedings of the National Academy of Sciences of the United States of America-Biological Sciences *78*, 6779-6783.

Ensinger, M.J., and Ginsberg, H.S. (1972). Selection and preliminary characterization of temperature-sensitive mutants of type-5 adenovirus. Journal of Virology *10*, 328-&.

Erkmann, JA; Sanchez, R; Treichel, N; Marzluff, WF; Kutay, U. (2005). Nuclear ==export== of metazoan replication-dependent ==histone== mRNAs is dependent on RNA length and is mediated by TAP. RNA - A publication of the RNA society. *11*, 45-58.

Evans, J.D., and Hearing, P. (2003). Distinct roles of the adenovirus E4 ORF3 protein in viral DNA replication and inhibition of genome concatenation. Journal of Virology *77*, 5295-5304.

Evans, J.D., and Hearing, P. (2005). Relocalization of the Mre11-Rad50-Nbs1 complex by the adenovirus E4 ORF3 protein is required for viral replication. Journal of Virology *79*, 6207-6215.

Everett, R.D., Freemont, P., Saitoh, H., Dasso, M., Orr, A., Kathoria, M., and Parkinson, J. (1998). The disruption of ND10 during herpes simplex virus infection correlates with the Vmw11O- and proteasome-dependent loss of several PML isoforms. Journal of Virology *72*, 6581-6591.

Everett, R.D., and Maul, G.G. (1994). HSV-1 IE protein VMW110 causes redistribution of PML. Embo Journal *13*, 5062-5069.

Everett, R.D., and Murray, J. (2005). ND10 components relocate to sites associated with herpes simplex virus type 1 nucleoprotein complexes during virus infection. Journal of Virology *79*, 5078-5089.

Everett, R.D., Murray, J., Orr, A., and Preston, C.M. (2007). Herpes simplex virus type 1 genomes are associated with ND10 nuclear substructures in quiescently infected human fibroblasts. Journal of Virology *81*, 10991-11004.

Everett, R.D., Parada, C., Gripon, P., Sirma, H., and Orr, A. (2008). Replication of ICP0-Null mutant herpes simplex virus type 1 is restricted by both PML and Sp100. Journal of Virology *82*, 2661-2672.

Everett, R.D., Rechter, S., Papior, P., Tavalai, N., Stamminger, T., and Orr, A. (2006). PML contributes to a cellular mechanism of repression of herpes simplex virus type 1 infection that is inactivated by ICP0. Journal of Virology *80*, 7995-8005.

Everett, R.S., Hodges, B.L., Ding, E.Y., Xu, F., Serra, D., and Amalfitano, A. (2003). Liver Toxicities typically induced by first-generation adenoviral vectors can be reduced by use of E1, E2b-deleted adenoviral vectors. Human Gene Therapy *14*, 1715-1726.

Everitt, E., Deluca, A., and Blixt, Y. (1992). Antibody-mediated uncoating of adenovirus in vitro. Fems Microbiology Letters *98*, 21-27.

Ewing, S.G., Byrd, S.A., Christensen, J.B., Tyler, R.E., and Imperiale, M.J. (2007). Ternary complex formation on the adenovirus packaging sequence by the IVa2 and L4 22-kilodalton proteins. Journal of Virology *81*, 12450-12457.

Excoffon, K., Gansemer, N.D., Mobily, M.E., Karp, P.H., Parekh, K.R., and Zabner, J. (2010). Isoform-Specific Regulation and Localization of the Coxsackie and Adenovirus Receptor in Human Airway Epithelia. Plos One *5*, e9909.

Fabry, C.M.S., Rosa-Calatrava, M., Moriscot, C., Ruigrok, R.W.H., Boulanger, P., and Schoehn, G. (2009). The C-Terminal Domains of Adenovirus Serotype 5 Protein IX Assemble into an Antiparallel Structure on the Facets of the Capsid. Journal of Virology *83*, 1135-1139.

Fakan, S., and Bernhard, W. (1971). Localisation of rapidly and slowly labelled nuclear RNA as visualized by high resolution autoradiography. Experimental Cell Research *67*, 129-141.

Fakan, S., and Nobis, P. (1978). Ultrastructural localization of transcription sites and of RNA distribution during cell cycle of synchronized CHO cells. Experimental Cell Research *113*, 327-337.

Fankhauser, C., Izaurralde, E., Adachi, Y., Wingfield, P., and Laemmli, U.K. (1991). Specific complex of Human- Immunodeficiency-Virus Type-1 Rev and nucleolar B23 proteins - Dissociation by the Rev response element. Molecular and Cellular Biology *11*, 2567-2575.

Farley, D.C., Brown, J.L., and Leppard, K.N. (2004). Activation of the early-late switch in adenovirus type 5 major late transcription unit expression by L4 gene products. Journal of Virology *78*, 1782-1791.

Faulkner, G.J., Kimura, Y., Daub, C.O., Wani, S., Plessy, C., Irvine, K.M., Schroder, K., Cloonan, N., Steptoe, A.L., Lassmann, T.*, et al.* (2009). The regulated retrotransposon transcriptome of mammalian cells. Nature Genetics *41*, 563-571.

Fechner, H., Haack, A., Wang, H., Wang, X., Eizema, K., Pauschinger, M., Schoemaker, R.G., van Veghel, R., Houtsmuller, A.B., Schultheiss, H.P.*, et al.* (1999). Expression of Coxsackie adenovirus receptor and alpha(v)-integrin does not correlate with adenovector targeting in vivo indicating anatomical vector barriers. Gene Therapy *6*, 1520-1535.

Feinberg, M.B., Jarrett, R.F., Aldovini, A., Gallo, R.C., and Wongstaal, F. (1986). HTLV-III expression and production involve complex regulation at the levels of splicing and translation of viral mRNA. Cell *46*, 807-817.

Fender, P., Hall, K., Schoehn, G., and Blair, G.E. (2012). Impact of Human Adenovirus Type 3 Dodecahedron on Host Cells and Its Potential Role in Viral Infection. Journal of Virology *86*, 5380-5385.

Fender, P., Ruigrok, R.W.H., Gout, E., Buffet, S., and Chroboczek, J. (1997). Adenovirus dodecahedron, a new vector for human gene transfer. Nature Biotechnology *15*, 52-56.

Feng, J.L., Funk, W.D., Wang, S.S., Weinrich, S.L., Avilion, A.A., Chiu, C.P., Adams, R.R., Chang, E., Allsopp, R.C., Yu, J.H.*, et al.* (1995). The RNA component of human telomerase. Science *269*, 1236-1241.

Fernandez, R., Pena, E., Navascues, J., Casafont, I., Lafarga, M., and Berciano, M.T. (2002). cAMP-dependent reorganization of the Cajal bodies and splicing machinery in cultured Schwann cells. Glia *40*, 378-388.

Ferreira, J.A., Carmo-Fonseca, M., and Lamond, A.I. (1994). Differential interaction of splicing snRNPs with coilied bodies and interchromatin granules duirng mitosis and assembly of daughter cell nuclei. Journal of Cell Biology *126*, 11-23.

Fessler, S.P., Delgado-Lopez, F., and Horwitz, M.S. (2004). Mechanisms of E3 modulation of immune and inflammatory responses. Adenoviruses: Model and Vectors in Virus-Host Interactions *273*, 113-135.

Fessler, S.P., and Young, C.S.H. (1999). The role of the L4 33K gene in adenovirus infection. Virology *263*, 507-516.

Fischer, T., Strasser, K., Racz, A., Rodriguez-Navarro, S., Oppizzi, M., Ihrig, P., Lechner, J., and Hurt, E. (2002). The mRNA export machinery requires the novel Sac3p-Thp1p complex to dock at the nucleoplasmic entrance of the nuclear pores. Embo Journal *21*, 5843-5852.

Flint, S.J., and Sharp, P.A. (1976). Adenovirus transcription. 5. Quantitation of viral RNA sequences in adenovirus 2-infected and transformed cells. Journal of Molecular Biology *106*, 749-771.

Flomenberg, P.R., Mei, C., Munk, G., and Horwitz, M.S. (1987). Molecular epidemiology of adenovirus type-35 infections in immunocompromised hosts. Journal of Infectious Diseases *155*, 1127-1134.

Florescu, D.F., Pergam, S.A., Neely, M.N., Qiu, F., Johnston, C., Way, S., Sande, J., Lewinsohn, D.A., Guzman-Cottrill, J.A., Graham, M.L., *et al.* (2012). Safety and Efficacy of CMX001 as Salvage Therapy for Severe Adenovirus Infections in Immunocompromised Patients. Biol Blood Marrow Transplant *18*, 731-738.

Ford, E., Nelson, K.E., and Warren, D. (1987). Epidemiology of epidemic keratoconjunctivitis. Epidemiologic Reviews *9*, 244-261.

Fornerod, M., Ohno, M., Yoshida, M., and Mattaj, I.W. (1997). CRM1 is an export receptor for leucine-rich nuclear export signals. Cell *90*, 1051-1060.

Forrester, N.A., Patel, R.N., Speiseder, T., Groitl, P., Sedgwick, G.G., Shimwell, N.J., Seed, R.I., Catnaigh, P.O., McCabe, C.J., Stewart, G.S., *et al.* (2012). Adenovirus E4orf3 Targets Transcriptional Intermediary Factor 1 gamma for Proteasome-Dependent Degradation during Infection. Journal of Virology *86*, 3167-3179.

Fortes, P., Lamond, A.I., and Ortin, J. (1995). Influenza-viurs NS1 protein alters the sub-nuclear localization of cellular splicing components. Journal of General Virology *76*, 1001-1007.

Fox, A.H., Lam, Y.W., Leung, A.K.L., Lyon, C.E., Andersen, J., Mann, M., and Lamond, A.I. (2002). Paraspeckles: A novel nuclear domain. Current Biology *12*, 13-25.

Franqueville, L., Henning, P., Magnusson, M., Vigne, E., Schoehn, G., Blair-Zajdel, M.E., Habib, N., Lindholm, L., Blair, G.E., Hong, S.S., *et al.* (2008). Protein Crystals in Adenovirus Type 5-Infected Cells: Requirements for Intranuclear Crystallogenesis, Structural and Functional Analysis. Plos One *3*, e2894.

Fraser, P., and Bickmore, W. (2007). Nuclear organization of the genome and the potential for gene regulation. Nature *447*, 413-417.

Frey, M.R., and Matera, A.G. (1995). Coiled bodies contain U7 small nuclear RNA and associate with specific DNA sequences in interphase human cells. Proc Natl Acad Sci U S A *92*, 5915-5919.

Frey, M.R., and Matera, A.G. (2001). RNA-mediated interaction of Cajal bodies and U2 snRNA genes. Journal of Cell Biology *154*, 499-509.

Frolov, M.V., and Dyson, N.J. (2004). Molecular mechanisms of E2F-dependent activation and pRB-mediated repression. Journal of Cell Science *117*, 2173-2181.

Fu, X.D. (1993). Specific commitment of different premessenger mRNAs to splicing by single SR proteins. Nature *365*, 82-85.

Fu, X.D. (1995). The superfamily of arginine serine-rich splicing factors. Rna-a Publication of the Rna Society *1*, 663-680.

Fu, X.D., and Maniatis, T. (1990). Factor required for mammalian spliceosome assembly is localized to discrete regions in the nucleus. Nature *343*, 437-441.

Furcinitti, P.S., Vanoostrum, J., and Burnett, R.M. (1989). Adenovirus polypeptide-IX revealed as capsid cement by difference images from electron-microscopy and crystallography. Embo Journal *8*, 3563-3570.

Fuschiotti, P., Schoehn, G., Fender, P., Fabry, C.M.S., Hewat, E.A., Chroboczek, J., Ruigrok, R.W.H., and Conway, J.F. (2006). Structure of the dodecahedral penton particle from human adenovirus type 3. Journal of Molecular Biology *356*, 510-520.

Gabanella, F., Butchbach, M.E.R., Saieva, L., Carissimi, C., Burghes, A.H.M., and Pellizzoni, L. (2007). Ribonucleoprotein Assembly Defects Correlate with Spinal Muscular Atrophy Severity and Preferentially Affect a Subset of Spliceosomal snRNPs. Plos One *2*, e921.

Gabitzsch, E.S., Xu, Y.N., Yoshida, L.H., Balint, J., Gayle, R.B., Amalfitano, A., and Jones, F.R. (2009). A preliminary and comparative evaluation of a novel Ad5 E1-, E2b- recombinant-based vaccine used to induce cell mediated immune responses. Immunology Letters *122*, 44-51.

Gabriela Thomas, M., Loschi, M., Andrea Desbats, M., and Lidia Boccaccio, G. (2011). RNA granules: The good, the bad and the ugly. Cellular Signalling *23*, 324-334.

Gaddy, C.E., Wong, D.S., Markowitz-Shulman, A., and Colberg-Poley, A.M. (2010). Regulation of the subcellular distribution of key cellular RNA-processing factors during permissive human cytomegalovirus infection. Journal of General Virology *91*, 1547-1559.

Galibert, F., Herisse, J., and Courtois, G. (1979). Nucleotide sequence of the EcoRI-F fragment of adenovirus-2 genome. Gene *6*, 1-22.

Gall, J.G. (2000). Cajal bodies: The first 100 years. Annual Review of Cell and Developmental Biology *16*, 273-300.

Gama-Carvalho, M., Condado, I., and Carmo-Fonseca, M. (2003a). Regulation of adenovirus alternative RNA splicing correlates with a reorganization of splicing factors in the nucleus. Experimental Cell Research *289*, 77-85.

Gama-Carvalho, M., Condado, I., and Carmo-Fonseca, M. (2003b). Regulation of adenovirus,alternative RNA splicing correlates with a reorganization of splicing factors in the nucleus. Experimental Cell Research *289*, 77-85.

Gama-Carvalho, M., Krauss, R.D., Chiang, L.J., Valcarcel, J., Green, M.R., and Carmo-Fonseca, M. (1997). Targeting of U2AF(65) to sites of active splicing in the nucleus. Journal of Cell Biology *137*, 975-987.

Gambke, C., and Deppert, W. (1981). Late non-structural 100,000-dalton and 33,000-dalton proteins of adenovirus type 2. 2.Immunological and protein chemical analysis. Journal of Virology *40*, 594-598.

Ganesh, S., Gonzalez-Edick, M., Gibbons, D., Waugh, J., Van Roey, M., and Jooss, K. (2009). Evaluation of Biodistribution of a Fiber-Chimeric, Conditionally Replication-Competent (Oncolytic) Adenovirus in CD46 Receptor Transgenic Mice. Human Gene Therapy *20*, 1201-1213.

Ganot, P., Bortolin, M.L., and Kiss, T. (1997a). Site-specific pseudouridine formation in preribosomal RNA is guided by small nucleolar RNAs. Cell *89*, 799-809.

Ganot, P., CaizerguesFerrer, M., and Kiss, T. (1997b). The family of box ACA small nucleolar RNAs is defined by an evolutionarily conserved secondary structure and ubiquitous sequence elements essential for RNA accumulation. Genes & Development *11*, 941-956.

Ganot, P., Jady, B.E., Bortolin, M.L., Darzacq, X., and Kiss, T. (1999). Nucleolar factors direct the 2 '-O-ribose methylation and pseudouridylation of U6 spliceosomal RNA. Molecular and Cellular Biology *19*, 6906-6917.

Gao, L.I., Frey, M.R., and Matera, A.G. (1997). Human genes encoding U3 snRNA associate with coiled bodies in interphase cells and are clustered on chromosome 17p11.2 in a complex inverted repeat structure. Nucleic Acids Research *25*, 4740-4747.

Garber, K. (2006). China approves world's first oncolytic virus therapy for cancer treatment. Journal of the National Cancer Institute *98*, 298-300.

Garcia-Mata, R., Gao, Y.S., and Sztul, E. (2002). Hassles with taking out the garbage: Aggravating aggresomes. Traffic *3*, 388-396.

Gastaldelli, M., Imelli, N., Boucke, K., Amstutz, B., Meier, O., and Greber, U.F. (2008). Infectious Adenovirus Type 2 Transport Through Early but not Late Endosomes. Traffic *9*, 2265-2278.

Gaynor, R.B., Tsukamoto, A., Montell, C., and Berk, A.J. (1982). Enhanced expression of adenovirus transforming proteins. Journal of Virology *44*, 276-285.

Gedge, L.J.E., Morrison, E.E., Blair, G.E., and Walker, J.H. (2005). Nuclear actin is partially associated with Cajal bodies in human cells in culture and relocates to the nuclear periphery after infection of cells by adenovirus 5. Experimental Cell Research *303*, 229-239.

Geib, T., and Hertel, K.J. (2009). Restoration of Full-Length SMN Promoted by Adenoviral Vectors Expressing RNA Antisense Oligonucleotides Embedded in U7 snRNAs. Plos One *4*.

Geoerger, B., Grill, J., Opolon, P., Morizet, J., Aubert, G., Lecluse, Y., van Beusechem, V.W., Gerritsen, W.R., Kirn, D.H., and Vassal, G. (2003). Potentiation of radiation therapy by the oncolytic adenovirus dl 1520 (ONYX-015) in human malignant glioma xenografts. British Journal of Cancer *89*, 577-584.

Georges, A., Benayoun, B.A., Marongiu, M., Dipietromaria, A., L'Hote, D., Todeschini, A.L., Auer, J., Crisponi, L., and Veitia, R.A. (2011). SUMOylation of the Forkhead Transcription Factor FOXL2 Promotes Its Stabilization/Activation through Transient Recruitment to PML Bodies. Plos One *6*.

Gerbi, S.A., Borovjagin, A.V., and Lange, T.S. (2003). The nucleolus: a site of ribonucleoprotein maturation. Current Opinion in Cell Biology *15*, 318-325.

Gey, G.O., Coffman, W.D., and Kubicek, M.T. (1952). Tissue culture studies of the proliferative capacity of cervical carcinoma and normal epithelium. Cancer Research *12*, 264-265.

Ghisolfi-Nieto, L., Joseph, G., Puvion-Dutilleul, F., Amalric, F., and Bouvet, P. (1996). Nucleolin is a sequence-specific RNA-binding protein: Characterization of targets on pre-ribosomal RNA. Journal of Molecular Biology *260*, 34-53.

Ghosh, M.K., and Harter, M.L. (2003). A viral mechanism for remodeling chromatin structure in G(0) cells. Molecular Cell *12*, 255-260.

Ghoshchoudhury, G., Hajahmad, Y., and Graham, F.L. (1987). Protein-IX, a minor component of the human adenovirus capsid, is essential for the packaging of full length genomes. Embo Journal *6*, 1733-1739.

Giard, D.J., Aaronson, S.A., Todaro, G.J., Arnstein, P., Kersey, J.H., Dosik, H., and Parks, W.P. (1973). In-vitro cultivation of human tumors - establishment of cell lines derived from a series of solid tumors. Journal of the National Cancer Institute *51*, 1417-1423.

Gilder, A.S., Do, P.M., Carrero, Z.I., Cosman, A.M., Broome, H.J., Velma, V., Martinez, L.A., and Hebert, M.D. (2011). Coilin participates in the suppression of RNA polymerase I in response to cisplatin-induced DNA damage. Molecular Biology of the Cell *22*, 1070-1079.

Gingeras, T.R., Sciaky, D., Gelinas, R.E., Bingdong, J., Yen, C.E., Kelly, M.M., Bullock, P.A., Parsons, B.L., Oneill, K.E., and Roberts, R.J. (1982). Nucleotide sequences from the adenovirus-2 genome. Journal of Biological Chemistry *257*, 3475-3491.

Girard, C., Neel, H., Bertrand, E., and Bordonne, R. (2006). Depletion of SMN by RNA interference in HeLa cells induces defects in Cajal body formation. Nucleic Acids Research *34*, 2925-2932.

Girard, C., Will, C.L., Peng, J., Makarov, E.M., Kastner, B., Lemm, I., Urlaub, H., Hartmuth, K., and Luhrmann, R. (2012). Post-transcriptional spliceosomes are retained in nuclear speckles until splicing completion. Nature Communications *3*, 994-994.

Gjerset, R.A. (2006). DNA damage, p14ARF, Nucleophosmin (NPM/B23), and cancer. Journal of Molecular Histology *37*, 239-251.

Glenn, G.M., and Ricciardi, R.P. (1988). Detailed kinetics of adenovirus type-5 steady-state transcripts during early infection. Virus Research *9*, 73-91.

Golembe, T.J., Yong, J.S., Battle, D.J., Feng, W.Q., Wan, L.L., and Dreyfuss, G. (2005). Lymphotropic Herpesvirus saimiri uses the SMN complex to assemble Sm cores on its small RNAs. Molecular and Cellular Biology *25*, 602-611.

Gong, L., and Yeh, E.T.H. (2006). Characterization of a family of nucleolar SUMO-specific proteases with preference for SUMO-2 or SUMO-3. Journal of Biological Chemistry *281*, 15869-15877.

Gooding, L.R., Ranheim, T.S., Tollefson, A.E., Aquino, L., Duerksenhughes, P., Horton, T.M., and Wold, W.S.M. (1991). The 10.400-dalton and 14,500-dalton proteins encoded by region E3 of adenovirus function together to protect many but not all mouse cell-lines against lysis by tumor-necrosis-factor. Journal of Virology *65*, 4114-4123.

Gorisch, S.M., Wachsmuth, M., Ittrich, C., Bacher, C.P., Rippe, K., and Lichter, P. (2004). Nuclear body movement is determined by chromatin accessibility and dynamics. Proc Natl Acad Sci U S A *101*, 13221-13226.

Gornemann, J., Kotovic, K.M., Hujer, K., and Neugebauer, K.M. (2005). Cotranscriptional spliceosome assembly occurs in a stepwise fashion and requires the cap binding complex. Molecular Cell *19*, 53-63.

Goto, K., Kobori, T., Kosaka, Y., Natsuaki, T., and Masuta, C. (2007). Characterization of silencing suppressor 2b of cucumber mosaic virus based on examination of its small RNA-Binding abilities. Plant and Cell Physiology *48*, 1050-1060.

Gounari, F., Defrancesco, R., Schmitt, J., Vandervliet, P.C., Cortese, R., and Stunnenberg, H. (1990). Amino-terminal domain of NF1 binds to DNA as a dimer and activates adenovirus DNA-replication. Embo Journal *9*, 559-566.

Grande, M.A., vanderKraan, I., vanSteensel, B., Schul, W., deThe, H., vanderVoort, H.T.M., deJong, L., and vanDriel, R. (1996). PML-containing nuclear bodies: Their spatial distribution in relation to other nuclear components. Journal of Cellular Biochemistry *63*, 280-291.

Gray, G.C., Goswami, P.R., Malasig, M.D., Hawksworth, A.W., Trump, D.H., Ryan, M.A., Schnurr, D.P., and Adenovirus Surveillance, G. (2000). Adult adenovirus infections: Loss of orphaned vaccines precipitates military respiratory disease epidemics. Clinical Infectious Diseases *31*, 663-670.

Greber, U.F., Suomalainen, M., Stidwill, R.P., Boucke, K., Ebersold, M.W., and Helenius, A. (1997). The role of the nuclear pore complex in adenovirus DNA entry. Embo Journal *16*, 5998-6007.

Greber, U.F., Willetts, M., Webster, P., and Helenius, A. (1993). Stepwise dismantling of adenovirus-2 during entry into cells. Cell *75*, 477-486.

Greco, A. (2009). Involvement of the nucleolus in replication of human viruses. Rev Med Virol *19*, 201-214.

Greco, A., Arata, L., Soler, E., Gaume, X., Coute, Y., Hacot, S., Calle, A., Monier, K., Epstein, A.L., Sanchez, J.-C.*, et al.* (2012). Nucleolin Interacts with US11 Protein of Herpes Simplex Virus 1 and Is Involved in Its Trafficking. Journal of Virology *86*, 1449-1457.

Green, M., Parsons, J.T., Pina, M., Fujinaga, K., Caffier, H., and Landgraf.I (1970). Transcription of adenovirus genes in productively infected and in transformed cells. Cold Spring Harbor Symp Quant Biol *35*, 803-818.

Greer, A.E., Hearing, P., and Ketner, G. (2011). The adenovirus E4 11 k protein binds and relocalizes the cytoplasmic P-body component Ddx6 to aggresomes. Virology *417*, 161-168.

Greig, J.A., Buckley, S.M.K., Waddington, S.N., Parker, A.L., Bhella, D., Pink, R., Rahim, A.A., Morita, T., Nicklin, S.A., McVey, J.H.*, et al.* (2009). Influence of Coagulation Factor X on In Vitro and In Vivo Gene Delivery by Adenovirus (Ad) 5, Ad35, and Chimeric Ad5/Ad35 Vectors. Molecular Therapy *17*, 1683-1691.

Grice, S.J., and Liu, J.-L. (2011). Survival Motor Neuron Protein Regulates Stem Cell Division, Proliferation, and Differentiation in Drosophila. PLoS Genetics *7*, e1002030.

Grotzinger, T., Sternsdorf, T., Jensen, K., and Will, H. (1996). Interferon-modulated expression of genes encoding the nuclear-dot-associated proteins Sp100 and promyelocytic leukemia protein (PML). European Journal of Biochemistry *238*, 554-560.

Gruter, P., Tabernero, C., von Kobbe, C., Schmitt, C., Saavedra, C., Bachi, A., Wilm, M., Felber, B.K., and Izaurralde, E. (1998). TAP, the human homolog of Mex67p, mediates CTE-dependent RNA export from the nucleus. Molecular Cell *1*, 649-659.

Guo, D.F., Shibata, R., Shinagawa, M., Sato, G., Aoki, K., and Sawada, H. (1988). Genomic comparison of adenovirus type-3 isolates from patients with acute conjunctivitis in Japan, Australia and the Phillipines. Microbiology and Immunology *32*, 833-842.

Gupta, S., Mangel, W.F., McGrath, W.J., Perek, J.L., Lee, D.W., Takamoto, K., and Chance, M.R. (2004). DNA binding provides a molecular strap activating the adenovirus proteinase. Molecular & Cellular Proteomics *3*, 950-959.

Guru, S.C., Olufemi, S.E., Manickam, P., Cummings, C., Gieser, L.M., Pike, B.L., Bittner, M.L., Jiang, Y., Chinault, A.C., Nowak, N.J.*, et al.* (1997). A 2.8-Mb clone contig of the multiple endocrine neoplasia type 1 (MEN1) region at 11q13. Genomics *42*, 436-445.

Gutch, M.J., and Reich, N.C. (1991). Repression of the interferon signal transduction pathway by the adenovirus E1A oncogene. Proc Natl Acad Sci U S A *88*, 7913-7917.

Hagiwara, M., and Nojima, T. (2007). Cross-talks between transcription and post-transcriptional events within a 'mRNA factory'. Journal of Biochemistry *142*, 11-15.

Hale, G.A., Heslop, H.E., Krance, R.A., Brenner, M.A., Jayawardene, D., Srivastava, D.K., and Patrick, C.C. (1999). Adenovirus infection after pediatric bone marrow transplantation. Bone Marrow Transplantation *23*, 277-282.

Hall, K., Zajdel, M.E.B., and Blair, G.E. (2010). Unity and diversity in the human adenoviruses: exploiting alternative entry pathways for gene therapy. Biochemical Journal *431*, 321-336.

Hamamoto, S., Nishitsuji, H., Amagasa, T., Kannagi, M., and Masuda, T. (2006). Identification of a novel human immunodeficiency virus type 1 integrase interactor, Gemin2, that facilitates efficient viral cDNA synthesis in vivo. Journal of Virology *80*, 5670-5677.

Hamera, S., Song, X.G., Su, L., Chen, X.Y., and Fang, R.X. (2012). Cucumber mosaic virus suppressor 2b binds to AGO4-related small RNAs and impairs AGO4 activities. Plant J *69*, 104-115.

Han, J.H., Xiong, J., Wang, D., and Fu, X.D. (2011). Pre-mRNA splicing: where and when in the nucleus. Trends in Cell Biology *21*, 336-343.

Harada, J.N., and Berk, A.J. (1999). p53-independent and -dependent requirements for E1B-55K in adenovirus type 5 replication. Journal of Virology *73*, 5333-5344.

Harada, J.N., Shevchenko, A., Pallas, D.C., and Berk, A.J. (2002). Analysis of the adenovirus E1B-55K-anchored proteome reveals its link to ubiquitination machinery. Journal of Virology *76*, 9194-9206.

Hardin, J.H., Spicer, S.S., and Greene, W.B. (1969). Paranucleolar structure, accessory body of Cajal, sex chromatin, and related structures in nuclei of rat trigeminal neurons - a cytochemical and ultrastructural study. Anatomical Record *164*, 403-431.

Harley, C.B., Futcher, A.B., and Greider, C.W. (1990). Telomeres shorten during ageing of human fibroblasts. Nature *345*, 458-460.

Harrigan, J.A., Belotserkovskaya, R., Coates, J., Dimitrova, D.S., Polo, S.E., Bradshaw, C.R., Fraser, P., and Jackson, S.P. (2011). Replication stress induces 53BP1-containing OPT domains in G1 cells. Journal of Cell Biology *193*, 97-108.

Haruki, H., Okuwaki, M., Miyagishi, M., Taira, K., and Nagata, K. (2006). Involvement of template-activating factor I/SET in transcription of adenovirus early genes as a positive-acting factor. Journal of Virology *80*, 794-801.

Hayes, B.W., Telling, G.C., Myat, M.M., Williams, J.F., and Flint, S.J. (1990). The adenovirus L4 100-Kilodalton protein is necessary for efficient translation of viral late messenger-RNA species. Journal of Virology *64*, 2732-2742.

Hearing, P., and Shenk, T. (1983). The adenovirus type-5 E1A transcriptional control region contains a duplicated enhancer element. Cell *33*, 695-703.

Hebert, M.D., Szymczyk, P.W., Shpargel, K.B., and Matera, A.G. (2001). Coilin forms the bridge between Cajal bodies and SMN, the spinal muscular atrophy protein. Genes & Development *15*, 2720-2729.

Hemmerich, P., Schmiedeberg, L., and Diekmann, S. (2011). Dynamic as well as stable protein interactions contribute to genome function and maintenance. Chromosome Research *19*, 131-151.

Herisse, J., Courtois, G., and Galibert, F. (1980). Nucleotide sequence of the EcoRI D fragment of adenovirus-2 genome. Nucleic Acids Research *8*, 2173-2192.

Herisse, J., Rigolet, M., Dedinechin, S.D., and Galibert, F. (1981). Nucleotide sequence of adenovirus-2 DNA fragment encoding for the carboxylic region of the fiber protein and entire E4 region. Nucleic Acids Research *9*, 4023-4042.

Herrmann, C.H., and Mancini, M.A. (2001). The Cdk9 and cyclin T subunits of TAK/P-TEFb localize to splicing factor-rich nuclear speckle regions. Journal of Cell Science *114*, 1491-1503.

Hierholzer, J.C. (1992). Adenoviruses in the immunocompromised host. Clinical Microbiology Reviews *5*, 262-274.

Hilleman, M.R., Stallones, R.A., Gauld, R.L., Warfield, M.S., and Anderson, S.A. (1956). Prevention of acute respiratory illness in recruits by adenovirus (RI-APC-ARD) vaccine. Proceedings of the Society for Experimental Biology and Medicine *92*, 377-383.

Hilleman, M.R., and Werner, J.H. (1954). Recovery of new agent from patients with acute respiratory illness. Proceedings of the Society for Experimental Biology and Medicine *85*, 183-188.

Hindley, C.E., Lawrence, F.J., and Matthews, D.A. (2007). A role for transportin in the nuclear import of adenovirus core proteins and DNA. Traffic *8*, 1313-1322.

Hiraga, S.I., Hagihara-Hayashi, A., Ohya, T., and Sugino, A. (2005). DNA polymerases alpha, delta, and epsilon localize and function together at replication forks in Saccharomyces cerevisiae. Genes to Cells *10*, 297-309.

Hiscox, J.A. (2007). RNA viruses: hijacking the dynamic nucleolus. Nature Reviews Microbiology *5*, 119-127.

Hiscox, J.A., Whitehouse, A., and Matthews, D.A. (2010). Nucleolar proteomics and viral infection. Proteomics *10*, 4077-4086.

Hock, R., Wilde, F., Scheer, U., and Bustin, M. (1998). Dynamic relocation of chromosomal protein HMG-17 in the nucleus is dependent on transcriptional activity. Embo Journal *17*, 6992-7001.

Hofmann, H., Sindre, H., and Stamminger, T. (2002a). Functional interaction between the pp71 protein of human cytomegalovirus and the PML-interacting protein human Daxx. Journal of Virology *76*, 5769-5783.

Hofmann, T.G., Moller, A., Sirma, H., Zentgraf, H., Taya, Y., Droge, W., Will, H., and Schmitz, M.L. (2002b). Regulation of p53 activity by its interaction with homeodomain-interacting protein kinase-2. Nature Cell Biology *4*, 1-10.

Hofmann, W.A., Stojiljkovic, L., Fuchsova, B., Vargas, G.M., Mavrommatis, E., Philimonenko, V., Kysela, K., Goodrich, J.A., Lessard, J.L., Hope, T.J.*, et al.* (2004). Actin is part of pre-initiation complexes and is necessary for transcription by RNA polymerase II. Nature Cell Biology *6*, 1094-U18.

Hong, J.S., and Engler, J.A. (1996). Domains required for assembly of adenovirus type 2 fiber trimers. Journal of Virology *70*, 7071-7078.

Hong, S.S., Szolajska, E., Schoehn, G., Franqueville, L., Myhre, S., Lindholm, L., Ruigrok, R.W.H., Boulanger, P., and Chroboczek, J. (2005). The 100K-chaperone protein from adenovirus serotype 2 (subgroup C) assists in trimerization and nuclear localization of hexons from subgroups C and B adenoviruses. Journal of Molecular Biology *352*, 125-138.

Hoppe, A., Beech, S.J., Dimmock, J., and Leppard, K.N. (2006). Interaction of the adenovirus type 5 E4 Orf3 protein with promyelocytic leukemia protein isoform II is required for ND10 disruption. Journal of Virology *80*, 3042-3049.

Horwitz, M.S. (2004). Function of adenovirus E-3 proteins and their interactions with immunoregulatory cell proteins. J Gene Med *6*, S172-S183.

Horwitz, M.S., Brayton, C., and Baum, S.G. (1973). Synthesis of type-2 adenovirus DNA in presence of cyclohexamide. Journal of Virology *11*, 544-551.

Howe, J.A., Mymryk, J.S., Egan, C., Branton, P.E., and Bayley, S.T. (1990). Retinoblastoma growth suppressor and a 300KDa protein appear to regulate cellular DNA-synthesis. Proc Natl Acad Sci U S A *87*, 5883-5887.

Hozak, P., Cook, P.R., Schofer, C., Mosgoller, W., and Wachtler, F. (1994). Site of transcription of ribosomal RNA and intranucleolar structure in HeLa cells. Journal of Cell Science *107*, 639-648.

Huang, J., and Schneider, R.J. (1991). Adenovirus inhibition of cellular protein synthesis involves inactivation of cap-binding protein. Cell *65*, 271-280.

Huang, L., Xu, G.-l., Zhang, J.-q., Tian, L., Xue, J.-l., Chen, J.-z., and Jia, W. (2008). Daxx interacts with HIV-1 integrase and inhibits lentiviral gene expression. Biochemical and Biophysical Research Communications *373*, 241-245.

Huang, S., Deerinck, T.J., Ellisman, M.H., and Spector, D.L. (1994). In-vivo analysis of the stability and transport of nuclear poly(A)+ mRNA. Journal of Cell Biology *126*, 877-899.

Huang, S., and Spector, D.L. (1996). Intron-dependent recruitment of Pre-mRNA splicing factors to sites of transcription. Journal of Cell Biology *133*, 719-732.

Huang, W., and Flint, S.J. (1998). The tripartite leader sequence of subgroup C adenovirus major late mRNAs can increase the efficiency of mRNA export. Journal of Virology *72*, 225-235.

Huang, W.Y., Kiefer, J., Whalen, D., and Flint, S.J. (2003). DNA synthesis-dependent relief of repression of transcription from the adenovirus type 2 IVa(2) promoter by a cellular protein. Virology *314*, 394-402.

Huber, J., Cronshagen, U., Kadokura, M., Marshallsay, C., Wada, T., Sekine, M., and Luhrmann, R. (1998). Snurportin1, an m(3)G-cap-specific nuclear import receptor with a novel domain structure. Embo Journal *17*, 4114-4126.

Hunter, T. (2007). The age of crosstalk: Phosphorylation, ubiquitination, and beyond. Molecular Cell *28*, 730-738.

Hutchinson, J.N., Ensminger, A.W., Clemson, C.M., Lynch, C.R., Lawrence, J.B., and Chess, A. (2007). A screen for nuclear transcripts identifies two linked noncoding RNAs associated with SC35 splicing domains. BMC Genomics *8*, 39.

Hwang, W.W., and Madhani, H.D. (2009). Nonredundant requirement for multiple histone modifications for the early anaphase release of the mitotic exit regulator Cdc14 from nucleolar chromatin. PLoS Genetics *5*, e1000588.

Iborra, F.J., Pombo, A., Jackson, D.A., and Cook, P.R. (1996). Active RNA polymerases are localized within discrete transcription 'factories' in human nuclei. Journal of Cell Science *109*, 1427-1436.

Iftode, C., and Flint, S.J. (2004). Viral DNA synthesis-dependent titration of a cellular repressor activates transcription of the human adenovirus type 2 IVa(2) gene. Proc Natl Acad Sci U S A *101*, 17831-17836.

Isaac, C., Yang, Y.F., and Meier, U.T. (1998). Nopp140 functions as a molecular link between the nucleolus and the coiled bodies. Journal of Cell Biology *142*, 319-329.

Ishiko, H., Shimada, Y., Konno, T., Hayashi, A., Ohguchi, T., Tagawa, Y., Aoki, K., Ohno, S., and Yamazaki, S. (2008). Novel human adenovirus causing nosocomial epidemic keratoconjunctivitis. Journal of Clinical Microbiology *46*, 2002-2008.

Ishov, A.M., Sotnikov, A.G., Negorev, D., Vladimirova, O.V., Neff, N., Kamitani, T., Yeh, E.T.H., Strauss, J.F., and Maul, G.G. (1999). PML is critical for ND10 formation and recruits the PML-interacting protein Daxx to this nuclear structure when modified by SUMO-1. Journal of Cell Biology *147*, 221-233.

Itahana, K., Bhat, K.P., Jin, A.W., Itahana, Y., Hawke, D., Kobayashi, R., and Zhang, Y.P. (2003). Tumor suppressor ARF degrades B23, a nucleolar protein involved in ribosome biogenesis and cell proliferation. Molecular Cell *12*, 1151-1164.

Iwamoto, S., Eggerding, F., Falckpederson, E., and Darnell, J.E. (1986). Transcription unit mapping in adenovrius - regions of termination. Journal of Virology *59*, 112-119.

Jackson, D.A. (1995). Nuclear organization - uniting replication foci, chromatin domains and chromosome structure. Bioessays *17*, 587-591.

Jackson, D.A., Hassan, A.B., Errington, R.J., and Cook, P.R. (1993). Visualization of focal sites of transcription within human nuclei. Embo Journal *12*, 1059-1065.

Jackson, D.A., Iborra, F.J., Manders, E.M.M., and Cook, P.R. (1998). Numbers and organization of RNA polymerases, nascent transcripts, and transcription units in HeLa nuclei. Molecular Biology of the Cell *9*, 1523-1536.

Jacobs, E.Y., Frey, M.R., Wu, W., Ingledue, T.C., Gebuhr, T.C., Gao, L.M., Marzluff, W.F., and Matera, A.G. (1999). Coiled bodies preferentially associate with U4, U11, and U12 small nuclear RNA genes in interphase HeLa cells but not with U6 and U7 genes. Molecular Biology of the Cell *10*, 1653-1663.

Jacobson, M.R., Cao, L.G., Taneja, K., Singer, R.H., Wang, Y.L., and Pederson, T. (1997). Nuclear domains of the RNA subunit of RNase P. Journal of Cell Science *110*, 829-837.

Jacobson, M.R., and Pederson, T. (1998). Localization of signal recognition particle RNA in the nucleolus of mammalian cells. Proc Natl Acad Sci U S A *95*, 7981-7986.

Jacobson, M.R., Rhoadhouse, M., and Pederson, T. (1993). U2 small nuclear RNA 3' end formation is directed by a critical internal structure distinct from the processing site. Molecular and Cellular Biology *13*, 1119-1129.

Jady, B.E., Bertrand, E., and Kiss, T. (2004). Human telomerase RNA and box H/ACA scaRNAs share a common Cajal body-specific localization signal. Journal of Cell Biology *164*, 647-652.

Jady, B.E., Darzacq, X., Tucker, K.E., Matera, A.G., Bertrand, E., and Kiss, T. (2003). Modification of Sm small nuclear RNAs occurs in the nucleoplasmic Cajal body following import from the cytoplasm. Embo Journal *22*, 1878-1888.

Jady, B.E., Richard, P., Bertrand, E., and Kiss, T. (2006). Cell cycle-dependent recruitment of telomerase RNA and Cajal bodies to human telomeres. Molecular Biology of the Cell *17*, 944-954.

James, M.J., and Zomerdijk, J. (2004). Phosphatidylinositol 3-kinase and mTOR signaling pathways regulate RNA polymerase I transcription in response to IGF-1 and nutrients. Journal of Biological Chemistry *279*, 8911-8918.

James, N.J., Howell, G.J., Walker, J.H., and Blair, G.E. (2010). The role of Cajal bodies in the expression of late phase adenovirus proteins. Virology *399*, 299-311.

Jeyapalan, J.N., Mendez-Bermudez, A., Zaffaroni, N., Dubrova, Y.E., and Royle, N.J. (2008). Evidence for alternative lengthening of telomeres in liposarcomas in the absence of ALT-associated PML bodies. International Journal of Cancer *122*, 2414-2421.

Jiang, H., White, E.J., Gomez-Manzano, C., and Fueyo, J. (2008). Adenovirus's last trick: You say lysis, we say autophagy. Autophagy *4*, 118-120.

Jiang, M.X., Entezami, P., Gamez, M., Stamminger, T., and Imperiale, M.J. (2011a). Functional Reorganization of Promyelocytic Leukemia Nuclear Bodies during BK Virus Infection. mBio *2*, e00281-10.

Jiang, W.Q., Nguyen, A., Cao, Y., Chang, A.C.M., and Reddel, R.R. (2011b). HP1-Mediated Formation of Alternative Lengthening of Telomeres-Associated PML Bodies Requires HIRA but Not ASF1a. Plos One *6*, e17036.

Jimenez-Garcia, L.F., and Spector, D.L. (1993). In vivo evidence that transcription and splicing are co-ordinated by a recruiting mechanism. Cell *73*, 47-59.

Johnson, C., Primorac, D., McKinstry, M., McNeil, J., Rowe, D., and Lawrence, J.B. (2000). Tracking COL1A1 RNA in osteogenesis imperfecta: Splice-defective transcripts initiate transport from the gene but are retained within the SC35 domain. Journal of Cell Biology *150*, 417-431.

Johnson, E.S., and Blobel, G. (1997). Ubc9p is the conjugating enzyme for the ubiquitin-like protein Smt3p. Journal of Biological Chemistry *272*, 26799-26802.

Johnson, E.S., Schwienhorst, I., Dohmen, R.J., and Blobel, G. (1997). The ubiquitin-like protein Smt3p is activated for conjugation to other proteins by an Aos1p/Uba2p heterodimer. Embo Journal *16*, 5509-5519.

Jones, M.S., Harrach, B., Ganac, R.D., Gozum, M.M.A., dela Cruz, W.P., Riedel, B., Pan, C., Delwart, E.L., and Schnurr, D.P. (2007). New adenovirus species found in a patient presenting with gastroenteritis. Journal of Virology *81*, 5978-5984.

Jones, N., and Shenk, T. (1979). Isolation of adenovirus type-5 host range mutants defective for transformation of rat embryo cells. Cell *17*, 683-689.

Jordan, P., Cunha, C., and CarmoFonseca, M. (1997). The cdk7 cyclin H MAT1 complex associated with TFIIH is localized in coiled bodies. Molecular Biology of the Cell *8*, 1207-1217.

Kaelin, S., Amstutz, B., Gastaldelli, M., Wolfrum, N., Boucke, K., Havenga, M., DiGennaro, F., Liska, N., Hemmi, S., and Greber, U.F. (2010). Macropinocytotic Uptake and Infection of Human Epithelial Cells with Species B2 Adenovirus Type 35. Journal of Virology *84*, 5336-5350.

Kakizuka, A., Miller, W.H., Umesono, K., Warrell, R.P., Frankel, S.R., Murty, V., Dmitrovsky, E., and Evans, R.M. (1991). Chromosomal translocation T(15-17) in human acute promyelocytic leukemia fuses RAR-alpha with a novel putative transcription factor, PML. Cell *66*, 663-674.

Kalyuzhniy, O., Di Paolo, N.C., Silvestry, M., Hofherr, S.E., Barry, M.A., Stewart, P.L., and Shayakhmetov, D.M. (2008). Adenovirus serotype 5 hexon is critical for virus infection of heptocytes in vivo. Proc Natl Acad Sci U S A *105*, 5483-5488.

Kaneko, H., Aoki, K., Ishida, S., Ohno, S., Kitaichi, N., Ishiko, H., Fujimoto, T., Ikeda, Y., Nakamura, M., Gonzalez, G.*, et al.* (2011a). Recombination analysis of intermediate human adenovirus type 53 in Japan by complete genome sequence. Journal of General Virology *92*, 1251-1259.

Kaneko, H., Aoki, K., Ohno, S., Ishiko, H., Fujimoto, T., Kikuchi, M., Harada, S., Gonzalez, G., Koyanagi, K.O., Watanabe, H.*, et al.* (2011b). Complete Genome Analysis of a Novel Intertypic Recombinant Human Adenovirus Causing Epidemic Keratoconjunctivitis in Japan. Journal of Clinical Microbiology *49*, 484-490.

Kaneko, H., Suzutani, T., Aoki, K., Kitaichi, N., Ishida, S., Ishiko, H., Ohashi, T., Okamoto, S., Nakagawa, H., Hinokuma, R.*, et al.* (2011c). Epidemiological and virological features of epidemic keratoconjunctivitis due to new human adenovirus type 54 in Japan. British Journal of Ophthalmology *95*, 32-36.

Kanopka, A., Muhlemann, O., and Akusjarvi, G. (1996). Inhibition by SR proteins of splicing of a regulated adenovirus pre-mRNA. Nature *381*, 535-538.

Kanopka, A., Muhlemann, O., Petersen-Mahrt, S., Estmer, C., Ohrmalm, C., and Akusjarvi, G. (1998). Regulation of adenovirus alternative RNA splicing by dephosphorylation of SR proteins. Nature *393*, 185-187.

Karayan, L., Gay, B., Gerfaux, J., and Boulanger, P.A. (1994). Oligomerization of recombinant penton base of adenovirus type 2 and its assembly with fiber in baculovirus-infected cells. Virology *202*, 782-795.

Karen, K.A., and Hearing, P. (2011). Adenovirus Core Protein VII Protects the Viral Genome from a DNA Damage Response at Early Times after Infection. Journal of Virology *85*, 4135-4142.

Katahira, J., Strasser, K., Podtelejnikov, A., Mann, M., Jung, J.U., and Hurt, E. (1999). The Mex67p-mediated nuclear mRNA export pathway is conserved from yeast to human. Embo Journal *18*, 2593-2609.

Kato, J., Matsushime, H., Hiebert, S.W., Ewen, M.E., and Sherr, C.J. (1993). Direct binding of cyclin-D to the retinoblastoma gene-product (pRB) and pRb phosphorylation by the cyclin D-dependent kinase CDK4. Genes & Development *7*, 331-342.

Kauffman, R.S., and Ginsberg, H.S. (1976). Characterisation of a temperature sensitive, hexon transport mutant of type-5 adenovirus. Journal of Virology *19*, 643-658.

Kawase, H., Okuwaki, M., Miyaji, M., Ohba, R., Handa, H., Ishimi, Y., FujiiNakata, T., Kikuchi, A., and Nagata, K. (1996). NAP-I is a functional homologue of TAP-I that is required

for replication and transcription of the adenovirus genome in a chromatin-like structure. Genes to Cells *1*, 1045-1056.

Kelkar, S., De, B.P., Gao, G.P., Wilson, J.M., Crystal, R.G., and Leopold, P.L. (2006). A common mechanism for cytoplasmic dynein-dependent microtubule binding shared among adeno-associated virus and adenovirus serotypes. Journal of Virology *80*, 7781-7785.

Khuri, F.R., Nemunaitis, J., Ganly, I., Arseneau, J., Tannock, I.F., Romel, L., Gore, M., Ironside, J., MacDougall, R.H., Heise, C.*, et al.* (2000). A controlled trial of intratumoral ONYX-015, a selectively-replicating adenovirus, in combination with cisplatin and 5-fluorouracil in patients with recurrent head and neck cancer. Nature Medicine *6*, 879-885.

Khurts, S., Masutomi, K., Delgermaa, L., Arai, K., Oishi, N., Mizuno, H., Hayashi, N., Hahn, W.C., and Murakami, S. (2004). Nucleolin interacts with telomerase. Journal of Biological Chemistry *279*, 51508-51515.

Kidd, A.H., Chroboczek, J., Cusack, S., and Ruigrok, R.W.H. (1993). Adenovirus type-40 virions contain 2 distinct fibers. Virology *192*, 73-84.

Kiesslich, A., von Mikecz, A., and Hemmerich, P. (2002). Cell cycle-dependent association of PML bodies with sites of active transcription in nuclei of mammalian cells. Journal of Structural Biology *140*, 167-179.

Kim, N.W., Piatyszek, M.A., Prowse, K.R., Harley, C.B., West, M.D., Ho, P.L.C., Coviello, G.M., Wright, W.E., Weinrich, S.L., and Shay, J.W. (1994). Specific association of human telomerase activity with immortla cells and cancer. Science *266*, 2011-2015.

Kim, S.H., MacFarlane, S., Kalinina, N.O., Rakitina, D.V., Ryabov, E.V., Gillespie, T., Haupt, S., Brown, J.W.S., and Taliansky, M. (2007a). Interaction of a plant virus-encoded protein with the major nucleolar protein fibrillarin is required for systemic virus infection. Proc Natl Acad Sci U S A *104*, 11115-11120.

Kim, S.H., Ryabov, E.V., Kalinina, N.O., Rakitina, D.V., Gillespie, T., MacFarlane, S., Haupt, S., Brown, J.W.S., and Taliansky, M. (2007b). Cajal bodies and the nucleolus are required for a plant virus systemic infection. Embo Journal *26*, 2169-2179.

Kim, Y.-E., Lee, J.-H., Kim, E.T., Shin, H.J., Gu, S.Y., Seol, H.S., Ling, P.D., Lee, C.H., and Ahn, J.-H. (2011). Human Cytomegalovirus Infection Causes Degradation of Sp100 Proteins That Suppress Viral Gene Expression. Journal of Virology *85*, 11928-11937.

Kimura, H., Tao, Y., Roeder, R.G., and Cook, P.R. (1999). Quantitation of RNA polymerase II and its transcription factors in an HeLa cell: Little soluble holoenzyme but significant amounts of polymerases attached to the nuclear substructure. Molecular and Cellular Biology *19*, 5383-5392.

Kimura, T., Hashimoto, I., Nagase, T., and Fujisawa, J.I. (2004). CRM1-dependent, but not ARE-mediated, nuclear export of IFN-alpha l mRNA. Journal of Cell Science *117*, 2259-2270.

King, A.J., Teertstra, W.R., and vanderVliet, P.C. (1997). Dissociation of the protein primer and DNA polymerase after initiation of adenovirus DNA replication. Journal of Biological Chemistry *272*, 24617-24623.

Kiss, T. (2002). Small nucleolar RNAs: An abundant group of noncoding RNAs with diverse cellular functions. Cell *109*, 145-148.

KissLaszlo, Z., Henry, Y., Bachellerie, J.P., CaizerguesFerrer, M., and Kiss, T. (1996). Site-specific ribose methylation of preribosomal RNA: A novel function for small nucleolar RNAs. Cell *85*, 1077-1088.

Kitamura, E., Blow, J.J., and Tanaka, T.U. (2006). Live-cell imaging reveals replication of individual replicons in eukaryotic replication factories. Cell *125*, 1297-1308.

Kleinberger, T., and Shenk, T. (1993). Adenovirus E4ORF4 binds to protein phosphatase-2A, and the complex down-regulates E1A-enhanced JUNB transcription. Journal of Virology *67*, 7556-7560.

Ko, T.K., Kelly, E., and Pines, J. (2001). CrkRS: a novel conserved Cdc2-related protein kinase that colocalises with SC35 speckles. Journal of Cell Science *114*, 2591-2603.

Kojima, T., Zama, T., Wada, K., Onogi, H., and Hagiwara, M. (2001). Cloning of human PRP4 reveals interaction with Clk1. Journal of Biological Chemistry *276*, 32247-32256.

Kolb, S.J., Battle, D.J., and Dreyfuss, G. (2007). Molecular functions of the SMN complex. Journal of Child Neurology *22*, 990-994.

Kolev, N.G., and Steitz, J.A. (2005). Symplekin and multiple other polyadenylation factors participate in 3 '-end maturation of histone mRNAs. Genes & Development *19*, 2583-2592.

Kolev, N.G., Yario, T.A., Benson, E., and Steitz, J.A. (2008). Conserved motifs in both CPSF73 and CPSF100 are required to assemble the active endonuclease for histone mRNA 3 '-end maturation. Embo Reports *9*, 1013-1018.

Kolowerzo, A., Smolinski, D.J., and Bednarska, E. (2009). Poly(A) RNA a new component of Cajal bodies. Protoplasma *236*, 13-19.

Kopito, R.R. (2000). Aggresomes, inclusion bodies and protein aggregation. Trends in Cell Biology *10*, 524-530.

Korgaonkar, C., Hagen, J., Tompkins, V., Frazier, A.A., Allamargot, C., Quelle, F.W., and Quelle, D.E. (2005). Nucleophosmin (B23) targets ARF to nucleoli and inhibits its function. Molecular and Cellular Biology *25*, 1258-1271.

Kotoglou, P., Kalaitzakis, A., Vezyraki, P., Tzavaras, T., Michalis, L.K., Dantzer, F., Jung, J.U., and Angelidis, C. (2009). Hsp70 translocates to the nuclei and nucleoli, binds to XRCC1 and PARP-1, and protects HeLa cells from single-strand DNA breaks. Cell Stress Chaperones *14*, 391-406.

Koup, R.A., Roederer, M., Lamoreaux, L., Fischer, J., Novik, L., Nason, M.C., Larkin, B.D., Enama, M.E., Ledgerwood, J.E., Bailer, R.T.*, et al.* (2010). Priming Immunization with DNA Augments Immunogenicity of Recombinant Adenoviral Vectors for Both HIV-1 Specific Antibody and T-Cell Responses. Plos One *5*, e9015.

Kovacs, G.M., LaPatra, S.E., D'Halluin, J.C., and Benko, M. (2003). Phylogenetic analysis of the hexon and protease genes of a fish adenovirus isolated from white sturgeon (Acipenser transmontanus) supports the proposal for a new adenovirus genus. Virus Research *98*, 27-34.

Krauer, K.G., Buck, M., Belzer, D.K., Flanagan, J., Chojnowski, G.M., and Sculley, T.B. (2004). The Epstein-Barr virus nuclear antigen-6 protein co-localizes with EBNA-3 and survival of motor neurons protein. Virology *318*, 280-294.

Kreivi, J.P., Zerivitz, K., and Akusjarvi, G. (1991). Sequences involved in the control of adenovirus L1 alternative RNA splicing. Nucleic Acids Research *19*, 2379-2386.

Kruhlak, M., Crouch, E.E., Orlov, M., Montano, C., Gorski, S.A., Nussenzweig, A., Misteli, T., Phair, R.D., and Casellas, R. (2007). The ATM repair pathway inhibits RNA polymerase I transcription in response to chromosome breaks. Nature *447*, 730-U16.

Kruhlak, M.J., Lever, M.A., Fischle, W., Verdin, E., Bazett-Jones, D.P., and Hendzel, M.J. (2000). Reduced mobility of the alternate splicing factor (ASF) through the nucleoplasm and steady state speckle compartments. Journal of Cell Biology *150*, 41-51.

Kruijer, W., Vanschaik, F.M.A., and Sussenbach, J.S. (1981). Structure and organization of the gene coding for the DNA-binding protein of adenovirus type-5. Nucleic Acids Research *9*, 4439-4457.

Kruijer, W., Vanschaik, F.M.A., and Sussenbach, J.S. (1982). Nucleotide sequence of the gene encoding adenovirus type-2 DNA-binding protein. Nucleic Acids Research *10*, 4493-4500.

Kumar, P.P., Bischof, O., Purbey, P.K., Notani, D., Urlaub, H., Dejean, A., and Galande, S. (2007). Functional interaction between PML and SATB1 regulates chromatin-loop architecture and transcription of the MHC class I locus. Nature Cell Biology *9*, 45-U57.

Kurki, S., Latonen, L., and Laiho, M. (2003). Cellular stress and DNA damage invoke temporally distinct Mdm2, p53 and PML complexes and damage-specific nuclear relocalization. Journal of Cell Science *116*, 3917-3925.

Lacadie, S.A., and Rosbash, M. (2005). Cotranscriptional spliceosome assembly dynamics and the role of U1 snRNA : 5 ' ss base pairing in yeast. Molecular Cell *19*, 65-75.

Lafarga, M., Hervas, J.P., Santacruz, M.C., Villegas, J., and Crespo, D. (1983). The accessory body of Cajal in the neuronal nucleus - a light and electron-microscopic approach. Anatomy and Embryology *166*, 19-30.

Lai, M.C., Lin, R.I., and Tarn, W.Y. (2001). Transportin-SR2 mediates nuclear import of phosphorylated SR proteins. Proc Natl Acad Sci U S A *98*, 10154-10159.

Lai, M.C., Teh, B.H., and Tarn, W.Y. (1999). A human papillomavirus E2 transcriptional activator - The interactions with cellular splicing factors and potential function in pre-mRNA processing. Journal of Biological Chemistry *274*, 11832-11841.

Lam, Y.W., Evans, V.C., Heesom, K.J., Lamond, A.I., and Matthews, D.A. (2010). Proteomics Analysis of the Nucleolus in Adenovirus-infected Cells. Molecular & Cellular Proteomics *9*, 117-130.

Lam, Y.W., Lyon, C.E., and Lamond, A.I. (2002). Large-scale isolation of Cajal bodies from HeLa cells. Molecular Biology of the Cell *13*, 2461-2473.

Lamond, A.I., and Spector, D.L. (2003). Nuclear speckles: A model for nuclear organelles. Nature Reviews Molecular Cell Biology *4*, 605-612.

Lanctot, C., Cheutin, T., Cremer, M., Cavalli, G., and Cremer, T. (2007). Dynamic genome architecture in the nuclear space: regulation of gene expression in three dimensions. Nature Reviews Genetics *8*, 104-115.

Larkin, J.D., Cook, P.R., and Papantonis, A. (2012). Dynamic Reconfiguration of Long Human Genes during One Transcription Cycle. Molecular and Cellular Biology *32*, 2738-2747.

Larsson, S., Svensson, C., and Akusjarvi, G. (1992). Control of adenovirus major late gene expression at multiple levels. Journal of Molecular Biology *225*, 287-298.

Larsson, S.H., Charlieu, J.P., Miyagawa, K., Engelkamp, D., Rassoulzadegan, M., Ross, A., Cuzin, F., Vanheyningen, V., and Hastie, N.D. (1995). Sub-nuclear localization of WT1 in splicing or transcription factor domains is regulated by alternative splicing. Cell *81*, 391-401.

Lawrence, F.J., McStay, B., and Matthews, D.A. (2006). Nucleolar protein upstream binding factor is sequestered into adenovirus DNA replication centres during infection without affecting RNA polymerase I location or ablating rRNA synthesis. Journal of Cell Science *119*, 2621-2631.

Lee, S.Y., Park, J.H., Kim, S., Park, E.J., Yun, Y.D., and Kwon, J. (2005). A proteomics approach for the identification of nucleophosmin and heterogeneous nuclear ribonucleoprotein C1/C2 as chromatin-binding proteins in response to DNA double-strand breaks. Biochemical Journal *388*, 7-15.

Lee, T.W.R., Blair, G.E., and Matthews, D.A. (2003). Adenovirus core protein VII contains distinct sequences that mediate targeting to the nucleus and nucleolus, and colocalization with human chromosomes. Journal of General Virology *84*, 3423-3428.

Lee, T.W.R., Lawrence, F.J., Dauksaite, V., Akusjarvi, G., Blair, G.E., and Matthews, D.A. (2004). Precursor of human adenovirus core polypeptide Mu targets the nucleolus and modulates the expression of E2 proteins. Journal of General Virology *85*, 185-196.

Lee, Y.-R., Yuan, W.-C., Ho, H.-C., Chen, C.-H., Shih, H.-M., and Chen, R.-H. (2010). The Cullin 3 substrate adaptor KLHL20 mediates DAPK ubiquitination to control interferon responses. Embo Journal *29*, 1748-1761.

Leegwater, P.A.J., Vandriel, W., and Vandervliet, P.C. (1985). Recognition site of nuclear factor-I, a sequence specific DNA-binding protein from HeLa cells that stimulates adenovirus DNA replication. Embo Journal *4*, 1515-1521.

Lefebvre, S., Burglen, L., Reboullet, S., Clermont, O., Burlet, P., Viollet, L., Benichou, B., Cruaud, C., Millasseau, P., Zeviani, M.*, et al.* (1995). Identification and characterization of a spinal muscular atrophy-determining gene. Cell *80*, 155-165.

Lefebvre, S., Burlet, P., Viollet, L., Bertrandy, S., Huber, C., Belser, C., and Munnich, A. (2002). A novel association of the SMN protein with two major non-ribosomal nucleolar proteins and its implication in spinal muscular atrophy. Human Molecular Genetics *11*, 1017-1027.

Lemay, P., Boudin, M.L., Milleville, M., and Boulanger, P. (1980). Human adenovirus type-2 protein-IIIa. 1.Purification and characterization. Virology *101*, 131-143.

Lemm, I., Girard, C., Kuhn, A.N., Watkins, N.J., Schneider, M., Bordonne, R., and Luehrmann, R. (2006). Ongoing U snRNP biogenesis is required for the integrity of Cajal bodies. Molecular Biology of the Cell *17*, 3221-3231.

Lenman, A., Mueller, S., Nygren, M.I., Fraengsmyr, L., Stehle, T., and Arnberg, N. (2011). Coagulation Factor IX Mediates Serotype-Specific Binding of Species A Adenoviruses to Host Cells. Journal of Virology *85*, 13420-13431.

Leonard, G.T., and Sen, G.C. (1997). Restoration of interferon responses of adenovirus E1A-expressing HT1080 cell lines by overexpression of p48 protein. Journal of Virology *71*, 5095-5101.

Leonhardt, H., Rahn, H.P., Weinzierl, P., Sporbert, A., Cremer, T., Zink, D., and Cardoso, M.C. (2000). Dynamics of DNA replication factories in living cells. Journal of Cell Biology *149*, 271-279.

Leopold, P.L., Kreitzer, G., Miyazawa, N., Rempel, S., Pfister, K.K., Rodriguez-Boulan, E., and Crystal, R.G. (2000). Dynein- and microtubule-mediated translocation of adenovirus serotype 5 occurs after endosomal lysis. Human Gene Therapy *11*, 151-165.

Leppard, K.N., Emmott, E., Cortese, M.S., and Rich, T. (2009). Adenovirus type 5 E4 Orf3 protein targets promyelocytic leukaemia (PML) protein nuclear domains for disruption via a sequence in PML isoform II that is predicted as a protein interaction site by bioinformatic analysis. Journal of General Virology *90*, 95-104.

Leppard, K.N., and Everett, R.D. (1999). The adenovirus type 5 E1b 55K and E4 Orf3 proteins associate in infected cells and affect ND10 components. Journal of General Virology *80*, 997-1008.

Leser, G.P., Fakan, S., and Martin, T.E. (1989). Ultrastructural distribution of ribonucleoprotein complexes during mitosis - snRNP antigens are contained in mitotic granule clusters. European Journal of Cell Biology *50*, 376-389.

Lethbridge, K.J., Scott, G.E., and Leppard, K.N. (2003). Nuclear matrix localization and SUMO-1 modification of adenovirus type 5 E1b 55K protein are controlled by E4 Orf6 protein. Journal of General Virology *84*, 259-268.

Li, C.F., Pontes, O., El-Shami, M., Henderson, I.R., Bernatavichute, Y.V., Chan, S.W.L., Lagrange, T., Pikaard, C.S., and Jacobsen, S.E. (2006a). An ARGONAUTE4-containing

nuclear processing center colocalized with Cajal bodies in Arabidopsis thaliana. Cell *126*, 93-106.

Li, E., Stupack, D., Bokoch, G.M., and Nemerow, G.R. (1998a). Adenovirus endocytosis requires actin cytoskeleton reorganization mediated by Rho family GTPases. Journal of Virology *72*, 8806-8812.

Li, E.G., Stupack, D., Klemke, R., Cheresh, D.A., and Nemerow, G.R. (1998b). Adenovirus endocytosis via alpha(v) integrins requires phosphoinositide-3-OH kinase. Journal of Virology *72*, 2055-2061.

Li, L., Roy, K., Katyal, S., Sun, X.J., Bleoo, S., and Godbout, R. (2006b). Dynamic nature of cleavage bodies and their spatial relationship to DDX1 bodies, Cajal bodies, and gems. Molecular Biology of the Cell *17*, 1126-1140.

Li, Z.-H., Tomlinson, R.L., Terns, R.M., and Terns, M.P. (2010). Telomerase trafficking and assembly in Xenopus oocytes. Journal of Cell Science *123*, 2464-2472.

Lichter, P., Cremer, T., Borden, J., Manuelidis, L., and Ward, D.C. (1988). Delineation of individual human-chromosomes in metaphase and interphase cells by insitu suppression hybridization using recombinant DNA libraries. Hum Genet *80*, 224-234.

Lichy, J.H., Field, J., Horwitz, M.S., and Hurwitz, J. (1982). Separation of the adenovirus terminal protein precursor from its associated DNA polymerase - role of both proteins in the initiation of adenovirus DNA replication. Proceedings of the National Academy of Sciences of the United States of America-Biological Sciences *79*, 5225-5229.

Lichy, J.H., Horwitz, M.S., and Hurwitz, J. (1981). Formation of a covalent complex between the 80,000-dalton adenovirus terminal protein and 5'-DCMP in vitro. Proceedings of the National Academy of Sciences of the United States of America-Biological Sciences *78*, 2678-2682.

Lieber, A., He, C.Y., Meuse, L., Schowalter, D., Kirillova, I., Winther, B., and Kay, M.A. (1997). The role of Kupffer cell activation and viral gene expression in early liver toxicity after infusion of recombinant adenovirus vectors. Journal of Virology *71*, 8798-8807.

Lin, S.R., Xiao, R., Sun, P.Q., Xu, X.D., and Fu, X.D. (2005). Dephosphorylation-dependent sorting of SR splicing factors during mRNP maturation. Molecular Cell *20*, 413-425.

Lindberg, A., Gama-Carvalho, M., Carmo-Fonseca, M., and Kreivi, J.P. (2004). A single RNA recognition motif in splicing factor ASF/SF2 directs it to nuclear sites of adenovirus transcription. Journal of General Virology *85*, 603-608.

Lindenbaum, J.O., Field, J., and Hurwitz, J. (1986). The adenovirus DNA-binding protein and adenovirus DNA polymerase interact to catalyse elongation of primed DNA templates. Journal of Biological Chemistry *261*, 218-227.

Listerman, I., Sapra, A.K., and Neugebauer, K.M. (2006). Cotranscriptional coupling of splicing factor recruitment and precursor messenger RNA splicing in mammalian cells. Nat Struct Mol Biol *13*, 815-822.

Liu, F., and Green, M.R. (1994). Promoter targeting by adenovirus-E1A through interaction with different cellular DNA-binding domains. Nature *368*, 520-525.

Liu, G.Q., Babiss, L.E., Volkert, F.C., Young, C.S.H., and Ginsberg, H.S. (1985). A thermolaible mutant of adenovirus-5 resulting from a substitution in the protein-VIII gene. Journal of Virology *53*, 920-925.

Liu, H., Naismith, J.H., and Hay, R.T. (2003). Adenovirus DNA replication. Adenoviruses: Model and Vectors in Virus-Host Interactions *272*, 131-164.

Liu, H.R., Jin, L., Koh, S.B.S., Atanasov, I., Schein, S., Wu, L., and Zhou, Z.H. (2010). Atomic Structure of Human Adenovirus by Cryo-EM Reveals Interactions Among Protein Networks. Science *329*, 1038-1043.

Liu, J.L., Murphy, C., Buszczak, M., Clatterbuck, S., Goodman, R., and Gall, J.G. (2006). The Drosophila melanogaster Cajal body. Journal of Cell Biology *172*, 875-884.

Liu, Q., Fischer, U., Wang, F., and Dreyfuss, G. (1997). The spinal muscular atrophy disease gene product, SMN, and its associated protein SIP1 are in a complex with spliceosomal snRNP proteins. Cell *90*, 1013-1021.

Liu, Y., Colosimo, A.L., Yang, X.J., and Liao, D.Q. (2000). Adenovirus E1B 55-kilodalton oncoprotein inhibits p53 acetylation by PCAF. Molecular and Cellular Biology *20*, 5540-5553.

Liu, Y., Shevchenko, A., and Berk, A.J. (2005). Adenovirus exploits the cellular aggresome response to accelerate inactivation of the MRN complex. Journal of Virology *79*, 14004-14016.

Logan, J., and Shenk, T. (1984). Adenovirus tripartite leader sequence enhances translation of messenger RNAs late after infection. Proceedings of the National Academy of Sciences of the United States of America-Biological Sciences *81*, 3655-3659.

Look, D.C., Roswit, W.T., Frick, A.G., Gris-Alevy, Y., Dickhaus, D.M., Walter, M.J., and Holtzman, M.J. (1998). Direct suppression of Stat1 function during adenoviral infection. Immunity *9*, 871-880.

Louis, N., Fender, P., Barge, A., Kitts, P., and Chroboczek, J. (1994). Cell-binding domain of adenovirus serotype-2 fiber. Journal of Virology *68*, 4104-4106.

Lowe, S.W., and Ruley, H.E. (1993). Stabilization of the p53 tumor suppressor is induced by adenovirus-E1A and accompanies apoptosis. Genes & Development *7*, 535-545.

Luciani, J.J., Depetris, D., Usson, Y., Metzler-Guillemain, C., Mignon-Ravix, C., Mitchell, M.J., Megarbane, A., Sarda, P., Sirma, H., Moncla, A.*, et al.* (2006). PML nuclear bodies are highly organised DNA-protein structures with a function in heterochromatin remodelling at the G2 phase. Journal of Cell Science *119*, 2518-2531.

Luco, R.F., and Misteli, T. (2011). More than a splicing code: integrating the role of RNA, chromatin and non-coding RNA in alternative splicing regulation. Current Opinion in Genetics & Development *21*, 366-372.

Lukas, C., Bartek, J., and Lukas, J. (2005). Imaging of protein movement induced by chromosomal breakage: tiny 'local' lesions pose great 'global' challenges. Chromosoma *114*, 146-154.

Lundblad, J.R., Kwok, R.P.S., Laurance, M.E., Harter, M.L., and Goodman, R.H. (1995). Adenoviral E1A-associated protein p300 as a functional homolog of the transcriptional co-activator CBP. Nature *374*, 85-88.

Lutschg, V., Boucke, K., Hemmi, S., and Greber, U.F. (2011). Chemotactic antiviral cytokines promote infectious apical entry of human adenovirus into polarized epithelial cells. Nature Communications *2,* 391.

Lutz, P., and Kedinger, C. (1996). Properties of the adenovirus IVa2 gene product, an effector of late-phase-dependent activation of the major late promoter. Journal of Virology *70*, 1396-1405.

Lutz, P., Puvion-Dutilleul, F., Lutz, Y., and Kedinger, C. (1996). Nucleoplasmic and nucleolar distribution of the adenovirus IVa2 gene product. Journal of Virology *70*, 3449-3460.

Lutz, P., RosaCalatrava, M., and Kedinger, C. (1997). The product of the adenovirus intermediate gene IX is a transcriptional activator. Journal of Virology *71*, 5102-5109.

Lygerou, Z., Pluk, H., vanVenrooij, W.J., and Seraphin, B. (1996). hPop1: An autoantigenic protein subunit shared by the human RNase P and RNase MRP ribonucleoproteins. Embo Journal *15*, 5936-5948.

Lymberopoulos, M.H., Bourget, A., Ben Abdeljelil, N., and Pearson, A. (2011). Involvement of the UL24 protein in herpes simplex virus 1-induced dispersal of B23 and in nuclear egress. Virology *412*, 341-348.

Lymberopoulos, M.H., and Pearson, A. (2007). Involvement of UL24 in herpes-simplex-virus-1-induced dispersal of nucleolin. Virology *363*, 397-409.

Lymberopoulos, M.H., and Pearson, A. (2010). Relocalization of Upstream Binding Factor to Viral Replication Compartments Is UL24 Independent and Follows the Onset of Herpes Simplex Virus 1 DNA Synthesis. Journal of Virology *84*, 4810-4815.

Ma, H.-C., and Hearing, P. (2011). Adenovirus Structural Protein IIIa Is Involved in the Serotype Specificity of Viral DNA Packaging. Journal of Virology *85*, 7849-7855.

Ma, T.L., Van Tine, B.A., Wei, Y., Garrett, M.D., Nelson, D., Adams, P.D., Wang, J., Qin, J., Chow, L.T., and Harper, J.W. (2000). Cell cycle-regulated phosphorylation of p220(NPAT) by cyclin E/Cdk2 in Cajal bodies promotes histone gene transcription. Genes & Development *14*, 2298-2313.

Mabit, H., Nakano, M.Y., Prank, U., Sam, B., Dohner, K., Sodeik, B., and Greber, U.F. (2002). Intact microtubules support adenovirus and herpes simplex virus infections. Journal of Virology *76*, 9962-9971.

Mahmoudi, S., Henriksson, S., Weibrecht, I., Smith, S., Soderberg, O., Stromblad, S., Wiman, K.G., and Farnebo, M. (2010). WRAP53 Is Essential for Cajal Body Formation and for Targeting the Survival of Motor Neuron Complex to Cajal Bodies. Plos Biology *8*, e1000521.

Maier, O., Galan, D.L., Wodrich, H., and Wiethoff, C.M. (2010). An N-terminal domain of adenovirus protein VI fragments membranes by inducing positive membrane curvature. Virology *402*, 11-19.

Maier, O., and Wiethoff, C.M. (2010). N-terminal alpha-helix-independent membrane interactions facilitate adenovirus protein VI induction of membrane tubule formation. Virology *408*, 31-38.

Mais, C., Wright, J.E., Prieto, J.L., Raggett, S.L., and McStay, B. (2005). UBF-binding site arrays form pseudo-NORs and sequester the RNA polymerase I transcription machinery. Genes & Development *19*, 50-64.

Maizel, J.V., White, D.O., and Scharff, M.D. (1968). Polypeptides of adenovirus .1. Evidence for multiple protein components in virion and a comparison of types 2, 7A and 12. Virology *36*, 115-125.

Majerciak, V., Yamanegi, K., Allemand, E., Kruhlak, M., Krainer, A.R., and Zheng, Z.M. (2008). Kaposi's sarcoma-associated herpesvirus ORF57 functions as a viral splicing factor and promotes expression of intron-containing viral lytic genes in spliceosome-mediated RNA splicing. Journal of Virology *82*, 2792-2801.

Makarov, E.M., Owen, N., Bottrill, A., and Makarova, O.V. (2012). Functional mammalian spliceosomal complex E contains SMN complex proteins in addition to U1 and U2 snRNPs. Nucleic Acids Research *40*, 2639-2652.

Malatesta, M., Zancanaro, C., Martin, T.E., Chan, E.K.L., Amalric, F., Luhrmann, R., Vogel, P., and Fakan, S. (1994). Is the coiled body involved in nucleolar functions. Experimental Cell Research *211*, 415-419.

Malmstrom, P.U., Loskog, A.S.I., Lindqvist, C.A., Mangsbo, S.M., Fransson, M., Wanders, A., Gardmark, T., and Totterman, T.H. (2010). AdCD40L Immunogene Therapy for Bladder Carcinoma-The First Phase I/IIa Trial. Clinical Cancer Research *16*, 3279-3287.

Mangel, W.F., Baniecki, M.L., and McGrath, W.J. (2003). Specific interactions of the adenovirus proteinase with the viral DNA, an 11-amino-acid viral peptide, and the cellular protein actin. Cell Mol Life Sci *60*, 2347-2355.

Mangel, W.F., McGrath, W.J., Toledo, D.L., and Anderson, C.W. (1993). Viral-DNA and a viral peptide can act as cofactors of adenovirus virion proteinase activity. Nature *361*, 274-275.

Maniatis, T., and Reed, R. (2002). An extensive network of coupling among gene expression machines. Nature *416*, 499-506.

Manley, J.L., Fire, A., Cano, A., Sharp, P.A., and Gefter, M.L. (1980). DNA-dependent transcription of adenovirus genes in a soluble whole-cell extract. Proceedings of the National Academy of Sciences of the United States of America-Biological Sciences *77*, 3855-3859.

Mannervik, M., Fan, S., Strom, A.C., Helin, K., and Akusjarvi, G. (1999). Adenovirus E4 open reading frame 4-induced dephosphorylation inhibits E1A activation of the E2 promoter and E2F-1-mediated transactivation independently of the retinoblastoma tumor suppressor protein. Virology *256*, 313-321.

Margueron, R., and Reinberg, D. (2011). The Polycomb complex PRC2 and its mark in life. Nature *469*, 343-349.

Martin, K., Brie, A., Saulnier, P., Perricaudet, M., Yeh, P., and Vigne, E. (2003). Simultaneous CAR- and alpha(V) integrin-binding ablation fails to reduce Ad5 liver tropism. Molecular Therapy *8*, 485-494.

Martin, M.E.D., and Berk, A.J. (1998). Adenovirus E1B 55K represses p53 activation in vitro. Journal of Virology *72*, 3146-3154.

Martin, M.E.D., and Berk, A.J. (1999). Corepressor required for adenovirus E1B 55,000-molecular-weight protein repression of basal transcription. Molecular and Cellular Biology *19*, 3403-3414.

Martinez, J., Patkaniowska, A., Urlaub, H., Luhrmann, R., and Tuschl, T. (2002). Single-stranded antisense siRNAs guide target RNA cleavage in RNAi. Cell *110*, 563-574.

Marttila, M., Persson, D., Gustafsson, D., Liszewski, M.K., Atkinson, J.P., Wadell, G., and Arnberg, N. (2005). CD46 is a cellular receptor for all species B adenoviruses except types 3 and 7. Journal of Virology *79*, 14429-14436.

Marzluff, W.F., Wagner, E.J., and Duronio, R.J. (2008). Metabolism and regulation of canonical histone mRNAs: life without a poly(A) tail. Nature Reviews Genetics *9*, 843-854.

Mastrocola, A.S., and Heinen, C.D. (2010). Nuclear reorganization of DNA mismatch repair proteins in response to DNA damage. DNA Repair *9*, 120-133.

Masuda, S., Das, R., Cheng, H., Hurt, E., Dorman, N., and Reed, R. (2005). Recruitment of the human TREX complex to mRNA during splicing. Genes & Development *19*, 1512-1517.

Matera, A.G., Terns, R.M., and Terns, M.P. (2007). Non-coding RNAs: lessons from the small nuclear and small nucleolar RNAs. Nature Reviews Molecular Cell Biology *8*, 209-220.

Matera, A.G., and Ward, D.C. (1993). Nucleoplasmic organization of small nuclear ribonucleoproteins in cultured human cells. Journal of Cell Biology *121*, 715-727.

Mathews, M.B. (1975). Genes for VA-RNA in adenovirus 2. Cell *6*, 223-229.

Mathias, P., Wickham, T., Moore, M., and Nemerow, G. (1994). Multiple adenovirus serotypes use alpha-v integrins for infection. Journal of Virology *68*, 6811-6814.

Matsui, T., Murayama, M., and Mita, T. (1986). Adenovirus-2 peptide-IX gene is expressed only on replicated DNA molecules. Molecular and Cellular Biology *6*, 4149-4154.

Mattaj, I.W. (1986). Cap trimethylation of U-snRNA is cytoplasmic and dependent on U-snRNP protein binding. Cell *46*, 905-911.

Matthews, D.A. (2001). Adenovirus protein V induces redistribution of nucleolin and B23 from nucleolus to cytoplasm. Journal of Virology *75*, 1031-1038.

Matthews, D.A., and Russell, W.C. (1994). Adenovirus protein-protein interactions - hexon and protein-VI. Journal of General Virology *75*, 3365-3374.

Matthews, D.A., and Russell, W.C. (1995). Adenovirus protein-protein interactions - molecular parameters governing the binding of protein-VI to hexon and the activation of the adenovirus 23K protease. Journal of General Virology *76*, 1959-1969.

Matthews, D.A., and Russell, W.C. (1998a). Adenovirus core protein V interacts with p32 - a protein which is associated with both the mitochondria and the nucleus. Journal of General Virology *79*, 1677-1685.

Matthews, D.A., and Russell, W.C. (1998b). Adenovirus core protein V is delivered by the invading virus to the nucleus of the infected cell and later in infection is associated with nucleoli. Journal of General Virology *79*, 1671-1675.

Maul, G.G., Guldner, H.H., and Spivack, J.G. (1993). Modification of discrete nuclear domains induced by herpes simplex virus type 1 early gene 1 product (ICP0). Journal of General Virology *74*, 2679-2690.

Maul, G.G., Yu, E., Ishov, A.M., and Epstein, A.L. (1995). Nuclear domain 10 (ND10) associated proteins are also present in nuclear bodies and redistribute to hundreds of nuclear sites after stress. Journal of Cellular Biochemistry *59*, 498-513.

Mayer, C., Bierhoff, H., and Grummt, I. (2005). The nucleolus as a stress sensor: JNK2 inactivates the transcription factor TIF-IA and down-regulates rRNA synthesis. Genes & Development *19*, 933-941.

McGrath, W.J., Ding, J.Z., Didwania, A., Sweet, R.M., and Mangel, W.F. (2003). Crystallographic structure at 1.6-angstrom resolution of the human adenovirus proteinase in a covalent complex with its 11-amino-acid peptide cofactor: insights on a new fold. Biochimica Et Biophysica Acta-Proteins and Proteomics *1648*, 1-11.

McSharry, B.P., Burgert, H.-G., Owen, D.P., Stanton, R.J., Prod'homme, V., Sester, M., Koebernick, K., Groh, V., Spies, T., Cox, S.*, et al.* (2008). Adenovirus E3/19K promotes evasion of NK cell recognition by intracellular sequestration of the NKG2D ligands, major histocompatibility complex class I chain-related proteins A and B. Journal of Virology *82*, 4585-4594.

Meier, O., Boucke, K., Hammer, S.V., Keller, S., Stidwill, R.P., Hemmi, S., and Greber, U.F. (2002). Adenovirus triggers macropinocytosis and endosomal leakage together with its clathrin-mediated uptake. Journal of Cell Biology *158*, 1119-1131.

Meier, U.T., and Blobel, G. (1992). Nopp140 shuttles on tracks between nucleolus and cytoplasm. Cell *70*, 127-138.

Meinecke, I., Cinski, A., Baier, A., Peters, M.A., Dankbar, B., Wille, A., Drynda, A., Mendoza, H., Gay, R.E., Hay, R.T.*, et al.* (2007). Modification of nuclear PML protein by SUMO-1 regulates Fas-induced apoptosis in rheumatoid arthritis synovial fibroblasts. Proc Natl Acad Sci U S A *104*, 5073-5078.

Meister, G., Buhler, D., Laggerbauer, B., Zobawa, M., Lottspeich, F., and Fischer, U. (2000). Characterization of a nuclear 20S complex containing the survival of motor neurons (SMN) protein and a specific subset of spliceosomal Sm proteins. Human Molecular Genetics *9*, 1977-1986.

Meister, P., Taddei, A., Ponti, A., Baldacci, G., and Gasser, S.M. (2007). Replication foci dynamics: replication patterns are modulated by S-phase checkpoint kinases in fission yeast. Embo Journal *26*, 1315-1326.

Meister, P., Taddei, A., Vernis, L., Poidevin, M., Gasser, S.M., and Baldacci, G. (2005). Temporal separation of replication and recombination requires the intra-S checkpoint. Journal of Cell Biology *168*, 537-544.

Melcak, I., Cermanova, S., Jirsova, K., Koberna, K., Malinsky, J., and Raska, I. (2000). Nuclear pre-mRNA compartmentalization: Trafficking of released transcripts to splicing factor reservoirs. Molecular Biology of the Cell *11*, 497-510.

Melnik, S., Deng, B., Papantonis, A., Baboo, S., Carr, I.M., and Cook, P.R. (2011). The proteomes of transcription factories containing RNA polymerases I, II or III. Nature Methods *8*, 963-968.

Mermoud, J.E., Cohen, P.T.W., and Lamond, A.I. (1994). Regulation of mammalian spliceosome assembly by a protein-phosphorylation mechanism. Embo Journal *13*, 5679-5688.

Michienzi, A., Cagnon, L., Bahner, I., and Rossi, J.J. (2000). Ribozyme-mediated inhibition of HIV 1 suggests nucleolar trafficking of HIV-1 RNA. Proc Natl Acad Sci U S A *97*, 8955-8960.

Michienzi, A., De Angelis, F.G., Bozzoni, I., and Rossi, J.J. (2006). A nucleolar localizing Rev binding element inhibits HIV replication. AIDS research and therapy *3*, 13.

Michienzi, A., Li, S., Zaia, J.A., and Rossi, J.J. (2002). A nucleolar TAR decoy inhibitor of HIV-1 replication. Proc Natl Acad Sci U S A *99*, 14047-14052.

Miele, A., Braastad, C.D., Holmes, W.F., Mitra, P., Medina, R., Xie, R.L., Zaidi, S.K., Ye, X., Wei, Y., Harper, J.W.*, et al.* (2005). HiNF-P directly links the cyclin E/CDK2/p220(NPAT) pathway to histone H4 gene regulation at the G(1)/S phase cell cycle transition. Molecular and Cellular Biology *25*, 6140-6153.

Miguel-Aliaga, I., Culetto, E., Walker, D.S., Baylis, H.A., Sattelle, D.B., and Davies, K.E. (1999). The Caenorhabditis elegans orthologue of the human gene responsible for spinal muscular atrophy is a maternal product critical for germline maturation and embryonic viability. Human Molecular Genetics *8*, 2133-2143.

Miller, M.S., Pelka, P., Fonseca, G.J., Cohen, M.J., Kelly, J.N., Barr, S.D., Grand, R.J.A., Turnell, A.S., Whyte, P., and Mymryk, J.S. (2012). Characterization of the 55-Residue Protein Encoded by the 9S E1A mRNA of Species C Adenovirus. Journal of Virology *86*, 4222-4233.

Milovic-Holm, K., Krieghoff, E., Jensen, K., Will, H., and Hofmann, T.G. (2007). FLASH links the CD95 signaling pathway to the cell nucleus and nuclear bodies. Embo Journal *26*, 391-401.

Mintz, P.J., Patterson, S.D., Neuwald, A.F., Spahr, C.S., and Spector, D.L. (1999). Purification and biochemical characterization of interchromatin granule clusters. Embo Journal *18*, 4308-4320.

Mintzer, M.A., and Simanek, E.E. (2009). Nonviral Vectors for Gene Delivery. Chemical Reviews *109*, 259-302.

Miron, M.J., Gallouzi, I.E., Lavoie, J.N., and Branton, P.E. (2004). Nuclear localization of the adenovirus E4orf4 protein is mediated through an arginine-rich motif and correlates with cell death. Oncogene *23*, 7458-7468.

Misteli, T., Caceres, J.F., Clement, J.Q., Krainer, A.R., Wilkinson, M.F., and Spector, D.L. (1998). Serine phosphorylation of SR proteins is required for their recruitment to sites of transcription in vivo. Journal of Cell Biology *143*, 297-307.

Misteli, T., Caceres, J.F., and Spector, D.L. (1997). The dynamics of a pre-mRNA splicing factor in living cells. Nature *387*, 523-527.

Misteli, T., and Spector, D.L. (1997). Protein phosphorylation and the nuclear organization of pre-mRNA splicing. Trends in Cell Biology *7*, 135-138.

Mitchell, J.R., Wood, E., and Collins, K. (1999). A telomerase component is defective in the human disease dyskeratosis congenita. Nature *402*, 551-555.

Miyazawa, N., Crystal, R.G., and Leopold, P.L. (2001). Adenovirus serotype 7 retention in a late endosomal compartment prior to cytosol escape is modulated by fiber protein. Journal of Virology *75*, 1387-1400.

Moen, P.T., Johnson, C.V., Byron, M., Shopland, L.S., de la Serna, I.L., Imbalzano, A.N., and Lawrence, J.B. (2004). Repositioning of muscle-specific genes relative to the periphery of SC-35 domains during skeletal myogenesis. Molecular Biology of the Cell *15*, 197-206.

Monneron, A., and Bernhard, W. (1969). Fine structural organization of interphase nucleus in some mammalian cells. Journal of Ultrastructure Research *27*, 266-288.

Montes, M., Cloutier, A., Sanchez-Hernandez, N., Michelle, L., Lemieux, B., Blanchette, M., Hernandez-Munain, C., Chabot, B., and Sune, C. (2012). TCERG1 Regulates Alternative Splicing of the Bcl-x Gene by Modulating the Rate of RNA Polymerase II Transcription. Molecular and Cellular Biology *32*, 751-762.

Morency, E., Sabra, M., Catez, F., Texier, P., and Lomonte, P. (2007). A novel cell response triggered by interphase centromere structural instability. Journal of Cell Biology *177*, 757-768.

Morris, G.E. (2008). The Cajal body. Biochimica Et Biophysica Acta-Molecular Cell Research *1783*, 2108-2115.

Morris, S.J., and Leppard, K.N. (2009). Adenovirus Serotype 5 L4-22K and L4-33K Proteins Have Distinct Functions in Regulating Late Gene Expression. Journal of Virology *83*, 3049-3058.

Morris, S.J., Scott, G.E., and Leppard, K.N. (2010). Adenovirus Late-Phase Infection Is Controlled by a Novel L4 Promoter. Journal of Virology *84*, 7096-7104.

Mortillaro, M.J., Blencowe, B.J., Wei, X.Y., Nakayasu, H., Du, L., Warren, S.L., Sharp, P.A., and Berezney, R. (1996). A hyperphosphorylated form of the large subunit of RNA polymerase II is associated with splicing complexes and the nuclear matrix. Proc Natl Acad Sci U S A *93*, 8253-8257.

Mourelatos, Z., Abel, L., Yong, J.S., Kataoka, N., and Dreyfuss, G. (2001). SMN interacts with a novel family of hnRNP and spliceosomal proteins. Embo Journal *20*, 5443-5452.

Mowry, K.L., and Steitz, J.A. (1987). Identification of the human snRNP as one of several factors involved in the 3' end maturation of histone pre-messenger RNAs. Science *238*, 1682-1687.

Moy, T.I., and Silver, P.A. (1999). Nuclear export of the small ribosomal subunit requires the Ran-GTPase cycle and certain nucleoporins. Genes & Development *13*, 2118-2133.

Moyer, C.L., Wiethoff, C.M., Maier, O., Smith, J.G., and Nemerow, G.R. (2011). Functional Genetic and Biophysical Analyses of Membrane Disruption by Human Adenovirus. Journal of Virology *85*, 2631-2641.

Mui, M.Z., Roopchand, D.E., Gentry, M.S., Hallberg, R.L., Vogel, J., and Branton, P.E. (2010). Adenovirus Protein E4orf4 Induces Premature APC(Cdc20) Activation in Saccharomyces cerevisiae by a Protein Phosphatase 2A-Dependent Mechanism. Journal of Virology *84*, 4798-4809.

Mul, Y.M., Verrijzer, C.P., and Vandervliet, P.C. (1990). Transcription factors NFI and NFIII/OCT-1 function independently, employing different mechanisms to enhance adenovirus DNA-replication. Journal of Virology *64*, 5510-5518.

Muller, D., Schreiner, S., Schmid, M., Groitl, P., Winkler, M., and Dobner, T. (2012). Functional Cooperation between Human Adenovirus Type 5 Early Region 4, Open Reading Frame 6 Protein, and Cellular Homeobox Protein HoxB7. Journal of Virology *86*, 8296-8308.

Muller, S., and Dejean, A. (1999). Viral immediate-early proteins abrogate the modification by SUMO-1 of PML and Sp100 proteins, correlating with nuclear body disruption. Journal of Virology *73*, 5137-5143.

Muller, S., Matunis, M.J., and Dejean, A. (1998). Conjugation with the ubiquitin-related modifier SUMO-1 regulates the partitioning of PML within the nucleus. Embo Journal *17*, 61-70.

Mulvihlll, S., Warren, R., Venook, A., Adler, A., Randlev, B., Heise, C., and Kirn, D. (2001). Safety and feasibility of injection with an E1B-55 kDa gene-deleted, replication-selective adenovirus (ONYX-015) into primary carcinomas of the pancreas: a phase I trial. Gene Therapy *8*, 308-315.

Muntoni, A., and Reddel, R.R. (2005). The first molecular details of ALT in human tumor cells. Human Molecular Genetics *14*, R191-R196.

Muratani, M., Gerlich, D., Janicki, S.M., Gebhard, M., Eils, R., and Spector, D.L. (2002). Metabolic-energy-dependent movement of PML bodies within the mammalian cell nucleus. Nature Cell Biology *4*, 106-110.

Murphy, J.T., Burgess, R.R., Dahlberg, J.E., and Lund, E. (1982). Transcription of a gene for human U1 small nuclear RNA. Cell *29*, 265-274.

Mysiak, M.E., Bleijenberg, M.H., Wyman, C., Holthuizen, P.E., and van der Vliet, P.C. (2004a). Bending of adenovirus origin DNA by nuclear factor I as shown by scanning force microscopy is required for optimal DNA replication. Journal of Virology *78*, 1928-1935.

Mysiak, M.E., Holthuizen, P.E., and van der Vliet, P.C. (2004b). Adenovirus priming protein pTP contributes to the kinetics of initiation of DNA replication. Nucleic Acids Research *32*, 3913-3920.

Mysiak, M.E., Wyman, C., Holthuizen, P.E., and van der Vliet, P.C. (2004c). NFI and Oct-1 bend the Ad5 origin in the same direction leading to optimal DNA replication. Nucleic Acids Research *32*, 6218-6225.

Nagata, K., Guggenheimer, R.A., Enomoto, T., Lichy, J.H., and Hurwitz, J. (1982). Adenovirus DNA replication in vitro - Identification of a host factor that stimulates synthesis of the pre-terminal protein-dCMP complex. Proceedings of the National Academy of Sciences of the United States of America-Biological Sciences *79*, 6438-6442.

Nagata, K., Guggenheimer, R.A., and Hurwitz, J. (1983). Specific binding of a cellular DNA-replication protein to the origin of replication of adenovirus. Proceedings of the National Academy of Sciences of the United States of America-Biological Sciences *80*, 6177-6181.

Nakagawa, S., Naganuma, T., Shioi, G., and Hirose, T. (2011). Paraspeckles are subpopulation-specific nuclear bodies that are not essential in mice. Journal of Cell Biology *193*, 31-39.

Nakamura, H., Morita, T., and Sato, C. (1986). Structural organisations of replicon domains during DNA synthetic phase in the mammalian nucleus. Experimental Cell Research *165*, 291-297.

Nakamura, T.M., Morin, G.B., Chapman, K.B., Weinrich, S.L., Andrews, W.H., Lingner, J., Harley, C.B., and Cech, T.R. (1997). Telomerase catalytic subunit homologs from fission yeast and human. Science *277*, 955-959.

Nakayasu, H., and Berezney, R. (1989). Mapping replication sites in thee eukaryotic neuclus. Journal of Cell Biology *108*, 1-11.

Narayanan, U., Achsel, T., Luhrmann, R., and Matera, A.G. (2004). Coupled in vitro import of U snRNPs and SMN, the spinal muscular atrophy protein. Molecular Cell *16*, 223-234.

Narita, M., Nunez, S., Heard, E., Lin, A.W., Hearn, S.A., Spector, D.L., Hannon, G.J., and Lowe, S.W. (2003). Rb-mediated heterochromatin formation and silencing of E2F target genes during cellular senescence. Cell *113*, 703-716.

Natarajan, V., Madden, M.J., and Salzman, N.P. (1984). Proximal and distal domains that control invotro transcription of the adenovirus IVa2 gene. Proceedings of the National Academy of Sciences of the United States of America-Biological Sciences *81*, 6290-6294.

Natsume, T., Tsutsui, Y., Sutani, T., Dunleavy, E.M., Pidoux, A.L., Iwasaki, H., Shirahige, K., Allshire, R.C., and Yamao, F. (2008). A DNA Polymerase alpha Accessory Protein, Mcl1, Is Required for Propagation of Centromere Structures in Fission Yeast. Plos One *3,* e2221.

Navascues, J., Berciano, M.T., Tucker, K.E., Lafarga, M., and Matera, A.G. (2004). Targeting SMN to Cajal bodies and nuclear gems during neuritogenesis. Chromosoma *112*, 398-409.

Neale, G.A.M., and Kitchingman, G.R. (1989). Biochemical analysis of adenovirus type-5 DNA binding protein mutants. Journal of Biological Chemistry *264*, 3153-3159.

Negorev, D.G., Vladimirova, O.V., and Maul, G.G. (2009). Differential Functions of Interferon-Upregulated Sp100 Isoforms: Herpes Simplex Virus Type 1 Promoter-Based Immediate-Early Gene Suppression and PML Protection from ICP0-Mediated Degradation. Journal of Virology *83*, 5168-5180.

Nemerow, G.R., and Stewart, P.L. (1999). Role of alpha(v) integrins in adenovirus cell entry and gene delivery. Microbiology and Molecular Biology Reviews *63*, 725-734.

Nemunaitis, J., Khuri, F., Ganly, I., Arseneau, J., Posner, M., Vokes, E., Kuhn, J., McCarty, T., Landers, S., Blackburn, A.*, et al.* (2001). Phase II trial of intratumoral administration of ONYX-015, a replication-selective adenovirus, in patients with refractory head and neck cancer. Journal of Clinical Oncology *19*, 289-298.

Nesic, D., Tanackovic, G., and Kramer, A. (2004). A role for Cajal bodies in the final steps of U2 snRNP biogenesis. Journal of Cell Science *117*, 4423-4433.

Nevins, J.R. (1992). E2F - A link between the Rb tumor suppressor protein and viral oncoproteins. Science *258*, 424-429.

Nevins, J.R. (2001). The Rb/E2F pathway and cancer. Human Molecular Genetics *10*, 699-703.

Nevins, J.R., DeGregori, J., Jakoi, L., and Leone, G. (1997). Functional analysis of E2F transcription factor. Cell Cycle Control *283*, 205-219.

Nevins, J.R., Ginsberg, H.S., Blanchard, J.M., Wilson, M.C., and Darnell, J.E. (1979). Regulation of the primary expression of the early adenovirus transcription units. Journal of Virology *32*, 727-733.

Nevins, J.R., and Wilson, M.C. (1981). Regulation of adenovirus 2 gene expression at the level of transcriptional termination and RNA processing. Nature *290*, 113-118.

Nilsen, T.W. (2003). The spliceosome: the most complex macromolecular machine in the cell? Bioessays *25*, 1147-1149.

Nilsson, C.E., Petersen-Mahrt, S., Durot, C., Shtrichman, R., Krainer, A.R., Kleinberger, T., and Akusjarvi, G. (2001). The adenovirus E4-ORF4 splicing enhancer protein interacts with a subset of phosphorylated SR proteins. Embo Journal *20*, 864-871.

Novotny, I., Blazikova, M., Stanek, D., Herman, P., and Malinsky, J. (2011). In vivo kinetics of U4/U6.U5 tri-snRNP formation in Cajal bodies. Molecular Biology of the Cell *22*, 513-523.

Nowock, J., Borgmeyer, U., Puschel, A.W., Rupp, R.A.W., and Sippel, A.E. (1985). The TGGCA protein binds to the MMTV-LTR, the adenvirus oringin of replication, and the BK virus enhancer. Nucleic Acids Research *13*, 2045-2061.

Nykanen, A., Haley, B., and Zamore, P.D. (2001). ATP requirements and small interfering RNA structure in the RNA interference pathway. Cell *107*, 309-321.

O'Donnell, B., Bell, E., Payne, S.B., Mautner, V., and Desselberger, U. (1986). Genome analysis of species-3 adenoviruses isolated during summer outbreaks of conjunctivitis and pharyngoconjunctival fever in the Glasgow and London areas in 1981. Journal of Medical Virology *18*, 213-227.

Obert, S., Oconnor, R.J., Schmid, S., and Hearing, P. (1994). The adenovirus E4-6/7 protein transactivates the E2 promoter by inducing dimerization of a heteromeric E2F complex. Molecular and Cellular Biology *14*, 1333-1346.

Ogg, S.C., and Lamond, A.I. (2002). Cajal bodies and coilin - moving towards function. Journal of Cell Biology *159*, 17-21.

Ohno, M., Segref, A., Bachi, A., Wilm, M., and Mattaj, I.W. (2000). PHAX, a mediator of U snRNA nuclear export whose activity is regulated by phosphorylation. Cell *101*, 187-198.

Okuwaki, M., Iwamatsu, A., Tsujimoto, M., and Nagata, K. (2001). Identification of nucleophosmin/B23, an acidic nucleolar protein, as a stimulatory factor for in vitro replication of adenovirus DNA complexed with viral basic core proteins. Journal of Molecular Biology *311*, 41-55.

Omer, A.D., Ziesche, S., Ebhardt, H., and Dennis, P.P. (2002). In vitro reconstitution and activity of a C/D box methylation guide ribonucleoprotein complex. Proc Natl Acad Sci U S A *99*, 5289-5294.

Osborne, C.S., Chakalova, L., Brown, K.E., Carter, D., Horton, A., Debrand, E., Goyenechea, B., Mitchell, J.A., Lopes, S., Reik, W.*, et al.* (2004). Active genes dynamically colocalize to shared sites of ongoing transcription. Nature Genetics *36*, 1065-1071.

Osborne, C.S., Chakalova, L., Mitchell, J.A., Horton, A., Wood, A.L., Bolland, D.J., Corcoran, A.E., and Fraser, P. (2007). Myc dynamically and preferentially relocates to a transcription factory occupied by Igh. Plos Biology *5*, 1763-1772.

Ostapchuk, P., Almond, M., and Hearing, P. (2011). Characterization of Empty Adenovirus Particles Assembled in the Absence of a Functional Adenovirus IVa2 Protein. Journal of Virology *85*, 5524-5531.

Ostapchuk, P., Anderson, M.E., Chandrasekhar, S., and Hearing, P. (2006). The L4 22-kilodalton protein plays a role in packaging of the adenovirus. Journal of Virology *80*, 6973-6981.

Ostapchuk, P., and Hearing, P. (2003). Minimal cis-acting elements required for adenovirus genome packaging. Journal of Virology *77*, 5127-5135.

Ostapchuk, P., and Hearing, P. (2005). Control of adenovirus packaging. Journal of Cellular Biochemistry *96*, 25-35.

Ostapchuk, P., and Hearing, P. (2008). Adenovirus IVa2 Protein Binds ATP. Journal of Virology *82*, 10290-10294.

Ostapchuk, P., Yang, J.H., Auffarth, E., and Hearing, P. (2005). Functional interaction of the adenovirus IVa2 protein with adenovirus type 5 packaging sequences. Journal of Virology *79*, 2831-2838.

Pacheco, A., de Quinto, S.L., Ramajo, J., Fernandez, N., and Martinez-Salas, E. (2009). A novel role for Gemin5 in mRNA translation. Nucleic Acids Research *37*, 582-590.

Palazzo, A.F., and Akef, A. (2012). Nuclear export as a key arbiter of "mRNA identity" in eukaryotes. Biochim Biophys Acta-Gene Regul Mech *1819*, 566-577.

Pandit, S., Wang, D., and Fu, X.-D. (2008). Functional integration of transcriptional and RNA processing machineries. Current Opinion in Cell Biology *20*, 260-265.

Pandya-Jones, A., and Black, D.L. (2009). Co-transcriptional splicing of constitutive and alternative exons. Rna-a Publication of the Rna Society *15*, 1896-1908.

Papantonis, A., Larkin, J.D., Wada, Y., Ohta, Y., Ihara, S., Kodama, T., and Cook, P.R. (2010). Active RNA Polymerases: Mobile or Immobile Molecular Machines? Plos Biology *8,* e1000419.

Park, S.W., Hu, X.L., Gupta, P., Lin, Y.P., Ha, S.G., and Wei, L.N. (2007). SUMOylation of Tr2 orphan receptor involves Pml and fine-tunes Oct4 expression in stem cells. Nat Struct Mol Biol *14*, 68-75.

Parker, A.L., McVey, J.H., Doctor, J.H., Lopez-Franco, O., Waddington, S.N., Havenga, M.J.E., Nicklin, S.A., and Baker, A.H. (2007). Influence of coagulation factor zymogens on the

infectivity of adenoviruses pseudotyped with fibers from subgroup D. Journal of Virology *81*, 3627-3631.

Parker, A.L., Waddington, S.N., Nicol, C.G., Shayakhmetov, D.M., Buckley, S.M., Denby, L., Kemball-Cook, G., Ni, S.H., Lieber, A., McVey, J.H.*, et al.* (2006). Multiple vitamin K-dependent coagulation zymogens promote adenovirus-mediated gene delivery to hepatocytes. Blood *108*, 2554-2561.

Parker, G.C., Li, X., Anguelov, R.A., Toth, G., Cristescu, A., and Acsadi, G. (2008). Survival motor neuron protein regulates apoptosis in an in vitro model of spinal muscular atrophy. Neurotoxicity Research *13*, 39-48.

Patel, S.B., and Bellini, M. (2008). The assembly of a spliceosomal small nuclear ribonucleoprotein particle. Nucleic Acids Research *36*, 6482-6493.

Paul, C.P., Good, P.D., Li, S.X.L., Kleihauer, A., Rossi, J.J., and Engelke, D.R. (2003). Localized expression of small RNA inhibitors in human cells. Molecular Therapy *7*, 237-247.

Pellizzoni, L., Baccon, J., Charroux, B., and Dreyfuss, G. (2001a). The survival of motor neurons (SMN) protein interacts with the snoRNP proteins fibrillarin and GAR1. Current Biology *11*, 1079-1088.

Pellizzoni, L., Charroux, B., Rappsilber, J., Mann, M., and Dreyfuss, G. (2001b). A functional interaction between the survival motor neuron complex and RNA polymerase II. Journal of Cell Biology *152*, 75-85.

Pellizzoni, L., Kataoka, N., Charroux, B., and Dreyfuss, G. (1998). A novel function for SMN, the spinal muscular atrophy disease gene product, in pre-mRNA splicing. Cell *95*, 615-624.

Pellizzoni, L., Yong, J., and Dreyfuss, G. (2002). Essential role for the SMN complex in the specificity of snRNP assembly. Science *298*, 1775-1779.

Pendergrast, P.S., Wang, C., Hernandez, N., and Huang, S. (2002). FBI-1 can stimulate HIV-1 Tat activity and is targeted to a novel sub-nuclear domain that includes the Tat-P-TEFb-containing nuclear speckles. Molecular Biology of the Cell *13*, 915-929.

Pennella, M.A., Liu, Y., Woo, J.L., Kim, C.A., and Berk, A.J. (2010). Adenovirus E1B 55-Kilodalton Protein Is a p53-SUMO1 E3 Ligase That Represses p53 and Stimulates Its Nuclear Export through Interactions with Promyelocytic Leukemia Nuclear Bodies. Journal of Virology *84*, 12210-12225.

Perez-Romero, P., Tyler, R.E., Abend, J.R., Dus, M., and Imperiale, M.J. (2005). Analysis of the interaction of the adenovirus L1 52/55-kilodalton and IVa2 proteins with the packaging sequence in vivo and in vitro. Journal of Virology *79*, 2366-2374.

Perlaky, L., Valdez, B.C., and Busch, H. (1997). Effects of cytotoxic drugs on translocation of nucleolar RNA helicase RH-II/Gu. Experimental Cell Research *235*, 413-420.

Perraud, M., Gioud, M., and Monier, J.C. (1979). Intranuclear structures of monkey kidney cells recognized by immunofluorescence and immunoelectron microscopy using anti-ribonucleoprotein antibodies. Annales D Immunologie *C130*, 635-647.

Perricaudet, M., Akusjarvi, G., Virtanen, A., and Pettersson, U. (1979). Structure of 2 spliced messenger RNAs from the transforming region of human subgroup C adenoviruses. Nature *281*, 694-696.

Persson, H.T., Aksaas, A.K., Kvissel, A.K., Punga, T., Engstrom, A., Skalhegg, B.S., and Akusjarvi, G. (2012). Two Cellular Protein Kinases, DNA-PK and PKA, Phosphorylate the Adenoviral L4-33K Protein and Have Opposite Effects on L1 Alternative RNA Splicing. Plos One *7,* e31871.

Pesonen, S., Diaconu, I., Kangasniemi, L., Ranki, T., Kanerva, A., Pesonen, S.K., Gerdemann, U., Leen, A.M., Kairemo, K., Oksanen, M.*, et al.* (2012). Oncolytic Immunotherapy of

Advanced Solid Tumors with a CD40L-Expressing Replicating Adenovirus: Assessment of Safety and Immunologic Responses in Patients. Cancer Research *72*, 1621-1631.

Pessler, F., Pendergrast, P.S., and Hernandez, N. (1997). Purification and characterization of FBI-1, a cellular factor that binds to the human immunodeficiency virus type 1 inducer of short transcripts. Molecular and Cellular Biology *17*, 3786-3798.

Petrini, J.H.J., and Stracker, T.H. (2003). The cellular response to DNA double-strand breaks: defining the sensors and mediators. Trends in Cell Biology *13*, 458-462.

Pettersson, U., and Hoglund, S. (1969). Structural proteins of adenoviruses. 3. Purification and characterization of adenovirus type-2 penton antigen. Virology *39*, 90-106.

Pettersson, U., Philipson.L, and Hoglund, S. (1968). Structural proteins of adenoviruses. 2.Purification and characterization of adenovirus type 2 fiber antigen. Virology *35*, 204-215.

Phair, R.D., and Misteli, T. (2000). High mobility of proteins in the mammalian cell nucleus. Nature *404*, 604-609.

Phelan, A., Carmo-Fonseca, M., McLauchlan, J., Lamond, A.I., and Clements, J.B. (1993). A herpes simplex virus type-1 immediate early gene product, IE63, regulates small nuclear ribonucleoprotein distribution. Proc Natl Acad Sci U S A *90*, 9056-9060.

Philipson, L., Lonbergh.K, and Petterss.U (1968). Virus-receptor interaction in an adenovirus system. Journal of Virology *2*, 1064-1075.

Philipson, L., and Pettersson, R.F. (2004). The coxsackie-adenovirus receptor - A new receptor in the immunoglobulin family involved in cell adhesion. Adenoviruses: Model and Vectors in Virus-Host Interactions *273*, 87-111.

Pilder, S., Moore, M., Logan, J., and Shenk, T. (1986). The adenovirus E1B-55K transforming polypeptide modulates transport or cytoplasmic stabilization of viral and host-cell messenger RNAs. Molecular and Cellular Biology *6*, 470-476.

Platani, M., Goldberg, I., Lamond, A.I., and Swedlow, J.R. (2002). Cajal Body dynamics and association with chromatin are ATP-dependent. Nature Cell Biology *4*, 502-508.

Platani, M., Goldberg, I., Swedlow, J.R., and Lamond, A.I. (2000). In vivo analysis of Cajal body movement, separation, and joining in live human cells. Journal of Cell Biology *151*, 1561-1574.

Politz, J.C.R., Zhang, F., and Pederson, T. (2006). MicroRNA-206 colocalizes with ribosome-rich regions in both the nucleolus and cytoplasm of rat myogenic cells. Proc Natl Acad Sci U S A *103*, 18957-18962.

Pombo, A., Cuello, P., Schul, W., Yoon, J.B., Roeder, R.G., Cook, P.R., and Murphy, S. (1998). Regional and temporal specialization in the nucleus: a transcriptionally-active nuclear domain rich in PTF, Oct1 and PIKA antigens associates with specific chromosomes early in the cell cycle. Embo Journal *17*, 1768-1778.

Pombo, A., Ferreira, J., Bridge, E., and Carmo-Fonseca, M. (1994). Adenovirus replication and transcription sites are spatially seperated in the nucleus of infected cells. Embo Journal *13*, 5075-5085.

Pombo, A., Jackson, D.A., Hollinshead, M., Wang, Z.X., Roeder, R.G., and Cook, P.R. (1999). Regional specialization in human nuclei: visualization of discrete sites of transcription by RNA polymerase III. Embo Journal *18*, 2241-2253.

Pontes, O., Li, C.F., Nunes, P.C., Haag, J., Ream, T., Vitins, A., Jacobsen, S.E., and Pikaard, C.S. (2006). The Arabidopsis chromatin-modifying nuclear siRNA pathway involves a nucleolar RNA processing center. Cell *126*, 79-92.

Prasanth, K.V., Prasanth, S.G., Xuan, Z.Y., Hearn, S., Freier, S.M., Bennett, C.F., Zhang, M.Q., and Spector, D.L. (2005). Regulating gene expression through RNA nuclear retention. Cell *123*, 249-263.

Prasanth, K.V., Sacco-Bubulya, P.A., Prasanth, S.G., and Spector, D.L. (2003). Sequential entry of components of gene expression machinery into daughter nuclei. Molecular Biology of the Cell *14*, 1043-1057.

Price, D.H. (2000). P-TEFb, a cyclin-dependent kinase controlling elongation by RNA polymerase II. Molecular and Cellular Biology *20*, 2629-2634.

Prieto, J.-L., and McStay, B. (2007). Recruitment of factors linking transcription and processing of pre-rRNA to NOR chromatin is UBF-dependent and occurs independent of transcription in human cells. Genes & Development *21*, 2041-2054.

Punga, T., and Akusjarvi, G. (2000). The adenovirus-2 E1B-55K protein interacts with a mSin3A/histone deacetylase 1 complex. FEBS Lett *476*, 248-252.

Puvion-Dutilleul, F., Bachellerie, J.P., Visa, N., and Puvion, E. (1994). Rearrangements of intranuclear structures involved in RNA processing in response to adenovirus infection. Journal of Cell Science *107*, 1457-1468.

Puvion-Dutilleul, F., Chelbialix, M.K., Koken, M., Quignon, F., Puvion, E., and Dethe, H. (1995). Adenovirus infection induces rearrangements in the intranuclear distribution of the nuclear body-associated PML protein. Experimental Cell Research *218*, 9-16.

Puvion-Dutilleul, F., and Christensen, M.E. (1993). Alterations of fibrillarin distribution and nucleolar ultrastructure induced by adenovirus infection. European Journal of Cell Biology *61*, 168-176.

Querido, E., Marcellus, R.C., Lai, A., Charbonneau, R., Teodoro, J.G., Ketner, G., and Branton, P.E. (1997). Regulation of p53 levels by the E1B 55-kilodalton protein and E40rf6 in adenovirus-infected cells. Journal of Virology *71*, 3788-3798.

Querido, E., Morison, M.R., Chu-Pham-Dang, H., Thirlwell, S.W.L., Boivin, D., and Branton, P.E. (2001). Identification of three functions of the adenovirus E4orf6 protein that mediate p53 degradation by the E4orf6-E1B55K complex. Journal of Virology *75*, 699-709.

Quimby, B.B., Yong-Gonzalez, V., Anan, T., Strunnikov, A.V., and Dasso, M. (2006). The promyelocytic leukemia protein stimulates SUMO conjugation in yeast. Oncogene *25*, 2999-3005.

Rao, L., Debbas, M., Sabbatini, P., Hockenbery, D., Korsmeyer, S., and White, E. (1992). The adenovirus E1A proteins induce apoptosis, which is inhibited by the E1B 19-KDa and Bcl-2 proteins. Proc Natl Acad Sci U S A *89*, 7742-7746.

Raper, S.E., Chirmule, N., Lee, F.S., Wivel, N.A., Bagg, A., Gao, G.P., Wilson, J.M., and Batshaw, M.L. (2003). Fatal systemic inflammatory response syndrome in a ornithine transcarbamylase deficient patient following adenoviral gene transfer. Molecular Genetics and Metabolism *80*, 148-158.

Rashid, R., Aittaleb, M., Chen, Q., Spiegel, K., Demeler, B., and Li, H. (2003). Functional requirement for symmetric assembly of archaeal box C/D small ribonucleoprotein particles. Journal of Molecular Biology *333*, 295-306.

Raska, I. (1995). Nuclear ultrastructures associated with the RNA synthesis and processing. Journal of Cellular Biochemistry *59*, 11-26.

Raska, I., Ochs, R.L., Andrade, L.E.C., Chan, E.K.L., Burlingame, R., Peebles, C., Gruol, D., and Tan, E.M. (1990). Association between the nucleolus and the coiled body. Journal of Structural Biology *104*, 120-127.

Razin, S.V., Gavrilov, A.A., Pichugin, A., Lipinski, M., Iarovaia, O.V., and Vassetzky, Y.S. (2011). Transcription factories in the context of the nuclear and genome organization. Nucleic Acids Research *39*, 9085-9092.

Rebelo, L., Almeida, F., Ramos, C., Bohmann, K., Lamond, A.I., and Carmo-Fonseca, M. (1996). The dynamics of coiled bodies in the nucleus of adenovirus-infected cells. Molecular Biology of the Cell *7*, 1137-1151.

Reddy, V.S., Natchiar, S.K., Stewart, P.L., and Nemerow, G.R. (2010). Crystal Structure of Human Adenovirus at 3.5 angstrom Resolution. Science *329*, 1071-1075.

Regad, T., Bellodi, C., Nicotera, P., and Salomoni, P. (2009). The tumor suppressor Pml regulates cell fate in the developing neocortex. Nature Neuroscience *12*, 132-140.

Reich, N.C., Sarnow, P., Duprey, E., and Levine, A.J. (1983). Monoclonal antibodies which recognize native and denatured forms of the adenovirus DNA-binding protein. Virology *128*, 480-484.

Reichelt, M., Wang, L., Sommer, M., Perrino, J., Nour, A.M., Sen, N., Baiker, A., Zerboni, L., and Arvin, A.M. (2011). Entrapment of Viral Capsids in Nuclear PML Cages Is an Intrinsic Antiviral Host Defense against Varicella-Zoster Virus. Plos Pathogens *7,* e1001266.

Rekosh, D.M.K., Russell, W.C., Bellet, A.J.D., and Robinson, A.J. (1977). Identification of a protein linked to ends of adenovirus DNA. Cell *11*, 283-295.

Reuter, R., Appel, B., Rinke, J., and Luhrmann, R. (1985). Localization and structure of snRNPs during mitosis - immunofluorescent and biochemical studies. Experimental Cell Research *159*, 63-79.

Rivera, S., Wellehan, J.F.X., Jr., McManamon, R., Innis, C.J., Garner, M.M., Raphael, B.L., Gregory, C.R., Latimer, K.S., Rodriguez, C.E., Diaz-Figueroa, O.*, et al.* (2009). Systemic adenovirus infection in Sulawesi tortoises (Indotestudo forsteni) caused by a novel siadenovirus. Journal of Veterinary Diagnostic Investigation *21*, 415-426.

Roberts, M.M., White, J.L., Grutter, M.G., and Burnett, R.M. (1986). 3-dimensional structure of the adenovirus major coat protein hexon. Science *232*, 1148-1151.

Roberts, R.J., Oneill, K.E., and Yen, C.T. (1984). DNA-sequences from the adenovirus-2 genome. Journal of Biological Chemistry *259*, 3968-3975.

Robinson, C.M., Singh, G., Henquell, C., Walsh, M.P., Peigue-Lafeuille, H., Seto, D., Jones, M.S., Dyer, D.W., and Chodosh, J. (2011). Computational analysis and identification of an emergent human adenovirus pathogen implicated in a respiratory fatality. Virology *409*, 141-147.

Rodrigues, S.H., Silva, N.P., Delicio, L.R., Granato, C., and Andrade, L.E.C. (1996). The behavior of the coiled body in cells infected with adenovirus in vitro. Molecular Biology Reports *23*, 183-189.

Roelvink, P.W., Lizonova, A., Lee, J.G.M., Li, Y., Bergelson, J.M., Finberg, R.W., Brough, D.E., Kovesdi, I., and Wickham, T.J. (1998). The coxsackievirus-adenovirus receptor protein can function as a cellular attachment protein for adenovirus serotypes from subgroups A, C, D, E, and F. Journal of Virology *72*, 7909-7915.

Rogee, S., Grellier, E., Bernard, C., Jouy, N., Loyens, A., Beauvillain, J.C., Fender, P., Corjon, S., Hong, S.S., Boulanger, P.*, et al.* (2010). Influence of chimeric human-bovine fibers on adenoviral uptake by liver cells and the antiviral immune response. Gene Therapy *17*, 880-891.

Rosa-Calatrava, M., Grave, L., Puvion-Dutilleul, F., Chatton, B., and Kedinger, C. (2001). Functional analysis of adenovirus protein IX identifies domains involved in capsid stability, transcriptional activity, and nuclear reorganization. Journal of Virology *75*, 7131-7141.

Rosa-Calatrava, M., Puvion-Dutilleul, F., Lutz, P., Dreyer, D., De The, H., Chatton, B., and Kedinger, C. (2003). Adenovirus protein IX sequesters host-cell promyelocytic leukaemia protein and contributes to efficient viral proliferation. Embo Reports *4*, 969-975.

Roussel, P., Andre, C., Comai, L., and HernandezVerdun, D. (1996). The rDNA transcription machinery is assembled during mitosis in active NORs and absent in inactive NORs. Journal of Cell Biology *133*, 235-246.

Rowe, D.T., Branton, P.E., and Graham, F.L. (1984). The kinetics of synthesis of early viral proteins in KB cells infected with wild-type and transformation-defective host-range mutants of human adenovirus type-5. Journal of General Virology *65*, 585-597.

Rowe, W.P., Huebner, R.J., Hartley, J.W., Ward, T.G., and Parrott, R.H. (1955). Studies of the adenoidal-pharyngeal-conjunctival (APC) group of viruses American Journal of Hygiene *61*, 197-218.

Rubbi, C.P., and Milner, J. (2003). Disruption of the nucleolus mediates stabilization of p53 in response to DNA damage and other stresses. Embo Journal *22*, 6068-6077.

Saban, S.D., Silvestry, M., Nemerow, G.R., and Stewart, P.L. (2006). Visualization of alpha-helices in a 6-angstrom resolution cryoelectron microscopy structure of adenovirus allows refinement of capsid protein assignments. Journal of Virology *80*, 12049-12059.

Sacco-Bubulya, P., and Spector, D.L. (2002). Disassembly of interchromatin granule clusters alters the coordination of transcription and pre-mRNA splicing. Journal of Cell Biology *156*, 425-436.

Sadoni, N., Cardoso, M.C., Stelzer, E.H.K., Leonhardt, H., and Zink, D. (2004). Stable chromosomal units determine the spatial and temporal organization of DNA replication. Journal of Cell Science *117*, 5353-5365.

Saffert, R.T., and Kalejta, R.F. (2006). Inactivating a cellular intrinsic immune defense mediated by Daxx is the mechanism through which the human cytomegalovirus pp71 protein stimulates viral immediate-early gene expression. Journal of Virology *80*, 3863-3871.

Sagou, K., Uema, M., and Kawaguchi, Y. (2010). Nucleolin Is Required for Efficient Nuclear Egress of Herpes Simplex Virus Type 1 Nucleocapsids. Journal of Virology *84*, 2110-2121.

Saitoh, N., Spahr, C.S., Patterson, S.D., Bubulya, P., Neuwald, A.F., and Spector, D.L. (2004). Proteomic analysis of interchromatin granule clusters. Molecular Biology of the Cell *15*, 3876-3890.

Saitoh, N., Uchimura, Y., Tachibana, T., Sugahara, S., Saitoh, H., and Nakao, M. (2006). In situ SUMOylation analysis reveals a modulatory role of RanBP2 in the nuclear rim and PML bodies. Experimental Cell Research *312*, 1418-1430.

Sakurai, F., Nakamura, S.I., Akitomo, K., Shibata, H., Terao, K., Kawabata, K., Hayakawa, T., and Mizuguchi, H. (2008). Transduction properties of adenovirus serotype 35 vectors after intravenous administration into nonhuman primates. Molecular Therapy *16*, 726-733.

Salomoni, P., Bernardi, R., Bergmann, S., Changou, A., Tuttle, S., and Pandolfi, P.P. (2005). The promyelocytic leukemia protein PML regulates c-Jun function in response to DNA damage. Blood *105*, 3686-3690.

Salsman, J., Wang, X., and Frappier, L. (2011). Nuclear body formation and PML body remodeling by the human cytomegalovirus protein UL35. Virology *414*, 119-129.

Salsman, J., Zimmerman, N., Chen, T., Domagala, M., and Frappier, L. (2008). Genome-wide screen of three herpesviruses for protein subcellular localization and alteration of PML nuclear bodies. Plos Pathogens *4,* e1000100.

Samad, M.A., Komatsu, T., Okuwaki, M., and Nagata, K. (2012). B23/nucleophosmin is involved in regulation of adenovirus chromatin structure at late infection stages, but not in virus replication and transcription. The Journal of General Virology *93*, 1328-38.

Samad, M.A., Okuwaki, M., Haruki, H., and Nagata, K. (2007). Physical and functional interaction between a nucleolar protein nucleophosmin/B23 and adenovirus basic core proteins. FEBS Lett *581*, 3283-3288.

San Martin, C., Glasgow, J.N., Borovjagin, A., Beatty, M.S., Kashentseva, E.A., Curiel, D.T., Marabini, R., and Dmitriev, I.P. (2008). Localization of the N-Terminus of Minor Coat Protein IIIa in the Adenovirus Capsid. Journal of Molecular Biology *383*, 923-934.

Sanchez-Alvarez, M., Goldstrohm, A.C., Garcia-Blanco, M.A., and Sune, C. (2006). Human transcription elongation factor CA150 localizes to splicing factor-rich nuclear speckles and assembles transcription and splicing components into complexes through its amino and carboxyl regions. Molecular and Cellular Biology *26*, 4998-5014.

SandriGoldin, R.M., and Hibbard, M.K. (1996). The herpes simplex virus type 1 regulatory protein ICP27 coimmunoprecipitates with anti-sm antiserum, and the C terminus appears to be required for this interaction. Journal of Virology *70*, 108-118.

Sandrigoldin, R.M., Hibbard, M.K., and Hardwicke, M.A. (1995). The C-TERMINAL repressor region of herpes-simplex virus type-1 ICP27 is required for the redistribution of small nuclear ribonucleoprotein particles and splicing factor SC35 -however these alterations are not sufficient to inhibit host cell splicing. Journal of Virology *69*, 6063-6076.

Saphire, A.C.S., Guan, T.L., Schirmer, E.C., Nemerow, G.R., and Gerace, L. (2000). Nuclear import adenovirus DNA in vitro involves the nuclear protein import pathway and hsc70. Journal of Biological Chemistry *275*, 4298-4304.

Sarnow, P., Hearing, P., Anderson, C.W., Halbert, D.N., Shenk, T., and Levine, A.J. (1984). Adenovirus early region-1B 58,000-dalton tumor antigen is physically associated with an early region-4 25,000-dalton protein in productively infected cells. Journal of Virology *49*, 692-700.

Sarnow, P., Sullivan, C.A., and Levine, A.J. (1982). A monoclonal-antibody detecting the adenovirus type-5 E1B-58KD tumor antigen - characterization of the E1B-58KD tumor antigen in adenovirus-infected and adenovirus-transformed cells. Virology *120*, 510-517.

Sasaki, Y.T.F., Ideue, T., Sano, M., Mituyama, T., and Hirose, T. (2009). MEN epsilon/beta noncoding RNAs are essential for structural integrity of nuclear paraspeckles. Proc Natl Acad Sci U S A *106*, 2525-2530.

Saunders, W.S., Cooke, C.A., and Earnshaw, W.C. (1991). Compartmentalisation within the nucleus - discovery of a novel sub-nuclear region. Journal of Cell Biology *115*, 919-931.

Savelyeva, I., and Dobbelstein, M. (2011). Infection with E1B-mutant adenovirus stabilizes p53 but blocks p53 acetylation and activity through E1A. Oncogene *30*, 865-875.

Schaffert, N., Hossbach, M., Heintzmann, R., Achsel, T., and Luhrmann, R. (2004). RNAi knockdown of hPrp31 leads to an accumulation of U4/U6 di-snRNPs in Cajal bodies. Embo Journal *23*, 3000-3009.

Schaley, J., O'Connor, R.J., Taylor, L.J., Bar-Sagi, D., and Hearing, P. (2000). Induction of the cellular E2F-1 promoter by the adenovirus E4-6/7 protein. Journal of Virology *74*, 2084-2093.

Scheer, U., and Hock, R. (1999). Structure and function of the nucleolus. Current Opinion in Cell Biology *11*, 385-390.

Schiedner, G., Morral, N., Parks, R.J., Wu, Y., Koopmans, S.C., Langston, C., Graham, F.L., Beaudet, A.L., and Kochanek, S. (1998). Genomic DNA transfer with a high-capacity adenovirus vector results in improved in vivo gene expression and decreased toxicity. Nature Genetics *18*, 180-183.

Schmid, M., Gonzalez, R.A., and Dobner, T. (2012). CRM1-Dependent Transport Supports Cytoplasmic Accumulation of Adenoviral Early Transcripts. Journal of Virology *86*, 2282-2292.

Schmitz, H., Wigand, R., and Heinrich, W. (1983). Worldwide epidemiology of human adenovirus infections. Am J Epidemiol *117*, 455-466.

Schneider-Brachert, W., Tchikov, V., Merkel, O., Jakob, M., Hallas, C., Kruse, M.-L., Groitl, P., Lehn, A., Hildt, E., Held-Feindt, J*., et al.* (2006). Inhibition of TNF receptor 1 internalization by adenovirus 14.7K as a novel immune escape mechanism. Journal of Clinical Investigation *116*, 2901-2913.

Schneider, J., Dauber, B., Melen, K., Julkunen, I., and Wolff, T. (2009). Analysis of Influenza B Virus NS1 Protein Trafficking Reveals a Novel Interaction with Nuclear Speckle Domains. Journal of Virology *83*, 701-711.

Schoenfelder, S., Sexton, T., Chakalova, L., Cope, N.F., Horton, A., Andrews, S., Kurukuti, S., Mitchell, J.A., Umlauf, D., Dimitrova, D.S*., et al.* (2010). Preferential associations between co-regulated genes reveal a transcriptional interactome in erythroid cells. Nature Genetics *42*, 53-U71.

Schrank, B., Gotz, R., Gunnersen, J.M., Ure, J.M., Toyka, K.V., Smith, A.G., and Sendtner, M. (1997). Inactivation of the survival motor neuron gene, a candidate gene for human spinal muscular atrophy, leads to massive cell death in early mouse embryos. Proc Natl Acad Sci U S A *94*, 9920-9925.

Schreiner, S., Martinez, R., Groitl, P., Rayne, F., Vaillant, R., Wimmer, P., Bossis, G., Sternsdorf, T., Marcinowski, L., Ruzsics, Z*., et al.* (2012). Transcriptional Activation of the Adenoviral Genome Is Mediated by Capsid Protein VI. Plos Pathogens *8,* e1002549.

Schreiner, S., Wimmer, P., Groitl, P., Chen, S.Y., Blanchette, P., Branton, P.E., and Dobner, T. (2011). Adenovirus Type 5 Early Region 1B 55K Oncoprotein-Dependent Degradation of Cellular Factor Daxx Is Required for Efficient Transformation of Primary Rodent Cells. Journal of Virology *85*, 8752-8765.

Schreiner, S., Wimmer, P., Sirma, H., Everett, R.D., Blanchette, P., Groitl, P., and Dobner, T. (2010). Proteasome-Dependent Degradation of Daxx by the Viral E1B-55K Protein in Human Adenovirus-Infected Cells. Journal of Virology *84*, 7029-7038.

Schul, W., Adelaar, B., van Driel, R., and de Jong, L. (1999a). Coiled bodies are predisposed to a spatial association with genes that contain snoRNA sequences in their introns. Journal of Cellular Biochemistry *75*, 393-403.

Schul, W., Groenhout, B., Koberna, K., Takagaki, Y., Jenny, A., Manders, E.M.M., Raska, I., vanDriel, R., and deJong, L. (1996). The RNA 3' cleavage factors CstF 64 kDa and CPSF 100 kDa are concentrated in nuclear domains closely associated with coiled bodies and newly synthesized RNA. Embo Journal *15*, 2883-2892.

Schul, W., van der Kraan, I., Matera, A.G., van Driel, R., and de Jong, L. (1999b). Nuclear domains enriched in RNA 3 '-processing factors associate with coiled bodies and histone genes in a cell cycle-dependent manner. Molecular Biology of the Cell *10*, 3815-3824.

Schul, W., van Driel, R., and de Jong, L. (1998a). Coiled bodies and U2 snRNA genes adjacent to coiled bodies are enriched in factors required for snRNA transcription. Molecular Biology of the Cell *9*, 1025-1036.

Schul, W., van Driel, R., and de Jong, L. (1998b). A subset of poly(A) polymerase is concentrated at sites of RNA synthesis and is associated with domains enriched in splicing factors and poly(A) RNA. Experimental Cell Research *238*, 1-12.

Schwarz, S.E., Matuschewski, K., Liakopoulos, D., Scheffner, M., and Jentsch, S. (1998). The ubiquitin-like proteins SMT3 and SUMO-1 are conjugated by the UBC9 E2 enzyme. Proc Natl Acad Sci U S A *95*, 560-564.

Sciabica, K.S., Dai, Q.J., and Sandri-Goldin, R.M. (2003). ICP27 interacts with SRPK1 to mediate HSV splicing inhibition by altering SR protein phosphorylation. Embo Journal *22*, 1608-1619.

Seeler, J.S., and Dejean, A. (2003). Nuclear and unclear functions of SUMO. Nature Reviews Molecular Cell Biology *4*, 690-699.

Segerman, A., Arnberg, N., Erikson, A., Lindman, K., and Wadell, G. (2003). There are two different species B adenovirus receptors: sBAR, common to species B1 and B2 adenoviruses, and sB2AR, exclusively used by species B2 adenoviruses. Journal of Virology *77*, 1157-1162.

Seiradake, E., and Cusack, S. (2005). Crystal structure of enteric adenovirus serotype 41 short fiber head. Journal of Virology *79*, 14088-14094.

Semashko, M.A., Gonzalez, I., Shaw, J., Leonova, O.G., Popenko, V.I., Taliansky, M.E., Canto, T., and Kalinina, N.O. (2012a). The extreme N-terminal domain of a hordeivirus TGB1 movement protein mediates its localization to the nucleolus and interaction with fibrillarin. Biochimie *94*, 1180-1188.

Semashko, M.A., Rakitina, D.V., Gonzalez, I., Canto, T., Kalinina, N.O., and Taliansky, M.E. (2012b). Movement protein of hordeivirus interacts in vitro and in vivo with coilin, a major structural protein of Cajal bodies. Doklady Biochemistry and Biophysics *442*, 57-60.

Semmes, O.J., and Jeang, K.T. (1996). Localization of human T-cell leukemia virus type 1 Tax to sub-nuclear compartments that overlap with interchromatin speckles. Journal of Virology *70*, 6347-6357.

Seto, D., Chodosh, J., Brister, J.R., Jones, M.S., and Adenovirus Res, C. (2011). Using the Whole-Genome Sequence To Characterize and Name Human Adenoviruses. Journal of Virology *85*, 5701-5702.

Sexton, T., Umlauf, D., Kurukuti, S., and Fraser, P. (2007). The role of transcription factories in large-scale structure and dynamics of interphase chromatin. Semin Cell Dev Biol *18*, 691-697.

Sharma, A., Takata, H., Shibahara, K.-i., Bubulya, A., and Bubulya, P.A. (2010). Son Is Essential for Nuclear Speckle Organization and Cell Cycle Progression. Molecular Biology of the Cell *21*, 650-663.

Sharp, P.A., Gallimore, P.H., and Flint, S.J. (1974). Mapping of adenovirus 2 sequences in lytically infected cells and transformed cell lines. Cold Spring Harbor Symp Quant Biol *39*, 457-474.

Shaw, A.R., and Ziff, E.B. (1980). Transcripts from the adenovirus 2 major late promoter yield a single early family of 3' coterminal messenger RNAs and 5 late families. Cell *22*, 905-916.

Shay, J.W., and Bacchetti, S. (1997). A survey of telomerase activity in human cancer. European Journal of Cancer *33*, 787-791.

Shayakhmetov, D.M., Li, Z.Y., Ni, S.H., and Lieber, A. (2004). Analysis of adenovirus sequestration in the liver, transduction of hepatic cells, and innate toxicity after injection of fiber-modified vectors. Journal of Virology *78*, 5368-5381.

Shayakhmetov, D.M., Li, Z.Y., Ternovoi, V., Gaggar, A., Gharwan, H., and Lieber, A. (2003). The interaction between the fiber knob domain and the cellular attachment receptor determines the intracellular trafficking route of adenoviruses. Journal of Virology *77*, 3712-3723.

Shen, T.H., Lin, H.-K., Scaglioni, P.P., Yung, T.M., and Pandolfi, P.P. (2006). The mechanisms of PML-nuclear body formation. Molecular Cell *24*, 331-339.

Shen, Y., and Post, L. (2007). Viral Vectors and Their Applications. In Fields Virology, D.M. Knipe, P.M. Howley, D.E. Griffin, R.A. Lamb, M.A. Martin, B. Roizman, and S.E. Straus, eds. (Philadelphia, Lippincott Williams and Wilkins), pp. 539-564.

Shepard, R.N., and Ornelles, D.A. (2004). Diverse roles for E4orf3 at late times of infection revealed in an E1B 55-kilodalton protein mutant background. Journal of Virology *78*, 9924-9935.

Shevtsov, S.P., and Dundr, M. (2011). Nucleation of nuclear bodies by RNA. Nature Cell Biology *13*, 167-U134.

Shiels, C., Islam, S.A., Vatcheva, R., Sasieni, P., Sternberg, M.J.E., Freemont, P.S., and Sheer, D. (2001). PML bodies associate specifically with the MHC gene cluster in interphase nuclei. Journal of Cell Science *114*, 3705-3716.

Shisler, J., Yang, C., Walter, B., Ware, C.F., and Gooding, L.R. (1997). The adenovirus E3-10.4K/14.5K complex mediates loss of cell surface Fas (CD95) and resistance to fas-induced apoptosis. Journal of Virology *71*, 8299-8306.

Shopland, L.S., Byron, M., Stein, J.L., Lian, J.B., Stein, G.S., and Lawrence, J.B. (2001). Replication-dependent histone gene expression is related to Cajal body (CB) association but does not require sustained CB contact. Molecular Biology of the Cell *12*, 565-576.

Shopland, L.S., Johnson, C.V., Byron, M., McNeil, J., and Lawrence, J.B. (2003). Clustering of multiple specific genes and gene-rich R-bands around SC-35 domains: evidence for local euchromatic neighborhoods. Journal of Cell Biology *162*, 981-990.

Silvestry, M., Lindert, S., Smith, J.G., Maier, O., Wiethoff, C.M., Nemerow, G.R., and Stewart, P.L. (2009). Cryo-Electron Microscopy Structure of Adenovirus Type 2 Temperature-Sensitive Mutant 1 Reveals Insight into the Cell Entry Defect. Journal of Virology *83*, 7375-7383.

Singh, G., Robinson, C.M., Dehghan, S., Schmidt, T., Seto, D., Jones, M.S., Dyer, D.W., and Chodosh, J. (2012). Overreliance on the hexon gene, leading to misclassification of human adenoviruses. Journal of Virology *86*, 4693-4695.

Singh, J., and Padgett, R.A. (2009). Rates of in situ transcription and splicing in large human genes. Nat Struct Mol Biol *16*, 1128-U1.

Sirri, V., Urcuqui-Inchima, S., Roussel, P., and Hernandez-Verdun, D. (2008). Nucleolus: the fascinating nuclear body. Histochemistry and Cell Biology *129*, 13-31.

Sivachandran, N., Cao, J.Y., and Frappier, L. (2010). Epstein-Barr Virus Nuclear Antigen 1 Hijacks the Host Kinase CK2 To Disrupt PML Nuclear Bodies. Journal of Virology *84*, 11113-11123.

Sleeman, J.E., Ajuh, P., and Lamond, A.I. (2001). snRNP protein expression enhances the formation of Cajal bodies containing p80-coilin and SMN. Journal of Cell Science *114*, 4407-4419.

Sleeman, J.E., Trinkle-Mulcahy, L., Prescott, A.R., Ogg, S.C., and Lamond, A.I. (2003). Cajal body proteins SMN and coilin show differential dynamic behaviour in vivo. Journal of Cell Science *116*, 2039-2050.

Smith, K.P., Carter, K.C., Johnson, C.V., and Lawrence, J.B. (1995). U2 and U1 snRNA gene loci associate with coiled bodies. Journal of Cellular Biochemistry *59*, 473-485.

Smith, K.P., Moen, P.T., Wydner, K.L., Coleman, J.R., and Lawrence, J.B. (1999). Processing of endogenous pre-mRNAs in association with SC-35 domains is gene specific. Journal of Cell Biology *144*, 617-629.

Smolinski, D.J., and Kolowerzo, A. (2012). mRNA accumulation in the Cajal bodies of the diplotene larch microsporocyte. Chromosoma *121*, 37-48.

Sohn, S.-Y., and Hearing, P. (2011). Adenovirus Sequesters Phosphorylated STAT1 at Viral Replication Centers and Inhibits STAT Dephosphorylation. Journal of Virology *85*, 7555-7562.

Somanathan, S., Suchyna, T.M., Siegel, A.J., and Berezney, R. (2001). Targeting of PCNA to sites of DNA replication in the mammalian cell nucleus. Journal of Cellular Biochemistry *81*, 56-67.

Somasundaram, K., and El-Deiry, W.S. (1997). Inhibition of p53-mediated transactivation and cell cycle arrest by E1A through its p300/CBP-interacting region. Oncogene *14*, 1047-1057.

Song, M.S., Salmena, L., Carracedo, A., Egia, A., Lo-Coco, F., Teruya-Feldstein, J., and Pandolfi, P.P. (2008). The deubiquitinylation and localization of PTEN are regulated by a HAUSP-PML network. Nature *455*, 813-U11.

Sonntag, F., Schmidt, K., and Kleinschmidt, J.A. (2010). A viral assembly factor promotes AAV2 capsid formation in the nucleolus. Proc Natl Acad Sci U S A *107*, 10220-10225.

Soria, C., Estermann, F.E., Espantman, K.C., and O'Shea, C.C. (2010). Heterochromatin silencing of p53 target genes by a small viral protein. Nature *466*, 1076-U85.

Souquere, S., Beauclair, G., Harper, F., Fox, A., and Pierron, G. (2010). Highly Ordered Spatial Organization of the Structural Long Noncoding NEAT1 RNAs within Paraspeckle Nuclear Bodies. Molecular Biology of the Cell *21*, 4020-4027.

Sourvinos, G., and Everett, R.D. (2002). Visualization of parental HSV-1 genomes and replication compartments in association with ND10 in live infected cells. Embo Journal *21*, 4989-4997.

Spector, D.L. (1993). Nuclear organization of pre-mRNA processing. Current Opinion in Cell Biology *5*, 442-447.

Spector, D.L., Fu, X.D., and Maniatis, T. (1991). Associations between distinct pre-messenger RNA splicing components and the cell nucleus. Embo Journal *10*, 3467-3481.

Spector, D.L., and Lamond, A.I. (2011). Nuclear Speckles. Cold Spring Harbor Perspectives in Biology *3*, a000646.

Spector, D.L., Schrier, W.H., and Busch, H. (1983). Immunoelectron microscopic localization of snRNPs. Biology of the Cell *49*, 1-10.

Spector, D.L., and Smith, H.C. (1986). Redistribution of U snRNPs during mitosis. Experimental Cell Research *163*, 87-94.

Spellman, P.T., and Rubin, G.M. (2002). Evidence for large domains of similarly expressed genes in the Drosophila genome. Journal of biology *1*, 5-5.

Spindler, K.R., Rosser, D.S.E., Berk, A.J. (1984). Analysis of adenovirus transforming proteins from early region-1A and region-1B with antisera to inducible fusion antigens produced in eschericia-coli. Journal of Virology *49*, 132-141.

Spindler, K.R., Eng, C.Y., and Berk, A.J. (1985). An adenovirus early region-1A protein is required for maximal viral-DNA replication in growth arrested human cells. Journal of Virology *53*, 742-750.

Sporbert, A., Gahl, A., Ankerhold, R., Leonhardt, H., and Cardoso, M.C. (2002). DNA polymerase clamp shows little turnover at established replication sites but sequential de novo assembly at adjacent origin clusters. Molecular Cell *10*, 1355-1365.

Stanek, D., and Neugebauer, K.M. (2004). Detection of snRNP assembly intermediates in Cajal bodies by fluorescence resonance energy transfer. Journal of Cell Biology *166*, 1015-1025.

Stanek, D., and Neugebauer, K.M. (2006). The Cajal body: a meeting place for spliceosomal snRNPs in the nuclear maze. Chromosoma *115*, 343-354.

Stanek, D., Pridalova-Hnilicova, J., Novotny, I., Huranova, M., Blazikova, M., Wen, X., Sapra, A.K., and Neugebauer, K.M. (2008). Spliceosomal small nuclear ribonucleoprotein particles repeatedly cycle through Cajal bodies. Molecular Biology of the Cell *19*, 2534-2543.

Stein, G.H., Beeson, M., and Gordon, L. (1990). Failure to phosphorylate the retinoblastoma gene-product in senescent human fibroblasts. Science *249*, 666-669.

Stephens, C., and Harlow, E. (1987). Differential splicing yields novel adenovirus 5-E1A messenger-RNAS that encode 30-KD and 35-KD proteins. Embo Journal *6*, 2027-2035.

Stern, J.L., Zyner, K.G., Pickett, H.A., Cohen, S.B., and Bryan, T.M. (2012). Telomerase Recruitment Requires both TCAB1 and Cajal Bodies Independently. Molecular and Cellular Biology *32*, 2384-2395.

Sternsdorf, T., Jensen, K., and Will, H. (1997). Evidence for covalent modification of the nuclear dot-associated proteins PML and Sp100 by PIC1/SUMO-1. Journal of Cell Biology *139*, 1621-1634.

Stevens, D.A., Schaeffe.M, Fox, J.P., Brandt, C.D., and Romano, M. (1967). Standardization and certification of reference antigens and antisera for 30 human adenovirus serotypes. Am J Epidemiol *86*, 617-633.

Stevens, J.L., Cantin, G.T., Wang, G., Shevchenko, A., and Berk, A.J. (2002). Transcription control by E1A and MAP kinase pathway via Sur2 mediator subunit. Science *296*, 755-758.

Stewart, P.L., Fuller, S.D., and Burnett, R.M. (1993). Difference imaging of adenovirus - bridging the resolution gap between X-ray crystallograpgy and electron-microscopy. Embo Journal *12*, 2589-2599.

Stow, N.D., Evans, V.C., and Matthews, D.A. (2009). Upstream-binding factor is sequestered into herpes simplex virus type 1 replication compartments. Journal of General Virology *90*, 69-73.

Stracker, T.H., Carson, C.T., and Weitzman, M.D. (2002). Adenovirus oncoproteins inactivate the Mre11-Rad50-NBS1 DNA repair complex. Nature *418*, 348-352.

Strang, B.L., Boulant, S., and Coen, D.M. (2010). Nucleolin Associates with the Human Cytomegalovirus DNA Polymerase Accessory Subunit UL44 and Is Necessary for Efficient Viral Replication. Journal of Virology *84*, 1771-1784.

Strang, B.L., Boulant, S., Kirchhausen, T., and Coen, D.M. (2012). Host cell nucleolin is required to maintain the architecture of human cytomegalovirus replication compartments. mBio *3,* e00301-11.

Strasser, K., Masuda, S., Mason, P., Pfannstiel, J., Oppizzi, M., Rodriguez-Navarro, S., Rondon, A.G., Aguilera, A., Struhl, K., Reed, R.*, et al.* (2002). TREX is a conserved complex coupling transcription with messenger RNA export. Nature *417*, 304-308.

Strasswimmer, J., Lorson, C.L., Breiding, D.E., Chen, J.J., Le, T., Burghes, A.H.M., and Androphy, E.J. (1999). Identification of survival motor neuron as a transcriptional activator-binding protein. Human Molecular Genetics *8*, 1219-1226.

Strunze, S., Engelke, M.F., Wang, I.H., Puntener, D., Boucke, K., Schleich, S., Way, M., Schoenenberger, P., Burckhardt, C.J., and Greber, U.F. (2011). Kinesin-1-Mediated Capsid Disassembly and Disruption of the Nuclear Pore Complex Promote Virus Infection. Cell Host Microbe *10*, 210-223.

Strunze, S., Trotman, L.C., Boucke, K., and Greber, U.F. (2005). Nuclear targeting of adenovirus type 2 requires CRM1-mediated nuclear export. Molecular Biology of the Cell *16*, 2999-3009.

Sullivan, K.D., Steiniger, M., and Marzluff, W.F. (2009). A Core Complex of CPSF73, CPSF100, and Symplekin May Form Two Different Cleavage Factors for Processing of Poly(A) and Histone mRNAs. Molecular Cell *34*, 322-332.

Sun, J., Xu, H.Z., Subramony, S.H., and Hebert, M.D. (2005). Interactions between Coilin and PIASy partially link Cajal bodies to PML bodies. Journal of Cell Science *118*, 4995-5003.

Sun, Y.J., Durrin, L.K., and Krontiris, T.G. (2003). Specific interaction of PML bodies with the TP53 locus in Jurkat interphase nuclei. Genomics *82*, 250-252.

Sung, M.T., Cao, T.M., Coleman, R.T., and Budelier, K.A. (1983a). Gene and protein sequences of adenovirus protein-VII, a hybrid basic chromosomal protein. Proceedings of the National Academy of Sciences of the United States of America-Biological Sciences *80*, 2902-2906.

Sung, M.T., Cao, T.M., Lischwe, M.A., and Coleman, R.T. (1983b). Molecular processing of adenovirus proteins. Journal of Biological Chemistry *258*, 8266-8272.

Sunwoo, H., Dinger, M.E., Wilusz, J.E., Amaral, P.P., Mattick, J.S., and Spector, D.L. (2009). MEN epsilon/beta nuclear-retained non-coding RNAs are up-regulated upon muscle differentiation and are essential components of paraspeckles. Genome Research *19*, 347-359.

Suomalainen, M., Nakano, M.Y., Boucke, K., Keller, S., and Greber, U.F. (2001). Adenovirus-activated PKA and p38/MAPK pathways boost microtubule-mediated nuclear targeting of virus. Embo Journal *20*, 1310-1319.

Suomalainen, M., Nakano, M.Y., Keller, S., Boucke, K., Stidwill, R.P., and Geber, U.F. (1999). Microtubule-dependent plus- and minus end-directed motilities are competing processes for nuclear targeting of adenovirus. Journal of Cell Biology *144*, 657-672.

Suzuki, T., Izumi, H., and Ohno, M. (2010). Cajal body surveillance of U snRNA export complex assembly. Journal of Cell Biology *190*, 603-612.

Takahashi, Y., Lallemand-Breitenbach, V., Zhu, J., and de The, H. (2004). PML nuclear bodies and apoptosis. Oncogene *23*, 2819-2824.

Tanaka, Y., Okamoto, K., Teye, K., Umata, T., Yamagiwa, N., Suto, Y., Zhang, Y., and Tsuneoka, M. (2010). JmjC enzyme KDM2A is a regulator of rRNA transcription in response to starvation. Embo Journal *29*, 1510-1522.

Tang, Q.Y., Li, L.G., Ishov, A.M., Revol, V., Epstein, A.L., and Maul, G.G. (2003). Determination of minimum herpes simplex virus type 1 components necessary to localize transcriptionally active DNA to ND10. Journal of Virology *77*, 5821-5828.

Tavalai, N., and Stamminger, T. (2008). New insights into the role of the sub-nuclear structure ND10 for viral infection. Biochimica Et Biophysica Acta-Molecular Cell Research *1783*, 2207-2221.

Teodoro, J.G., and Branton, P.E. (1997). Regulation of p53-dependent apoptosis, transcriptional repression, and cell transformation by phosphorylation of the 55-kilodalton E1B protein of human adenovirus type 5. Journal of Virology *71*, 3620-3627.

Terada, Y., and Yasuda, Y. (2006). Human immunodeficiency virus type 1 Vpr induces G(2) checkpoint activation by interacting with the splicing factor SAP145. Molecular and Cellular Biology *26*, 8149-8158.

Terwilliger, E., Sodroski, J.G., Rosen, C.A., and Haseltine, W.A. (1986). Effects of mutations within the 3' ORF open reading frame region of human T-cell lymphotrophic virus (HTLV-III/LAV) on replication and cytopathogenicity. Journal of Virology *60*, 754-760.

Thiry, M. (1995). Behaviour of interchromatin granules during the cell-cycle. European Journal of Cell Biology *68*, 14-24.

Tibbetts, C., Petterss.U, Johansso.K, and Philpson, L. (1974). Relationship of messenger-RNA from productively infected cells to complementary strands of adenovirus type 2 DNA. Journal of Virology *13*, 370-377.

Tollefson, A.E., Hermiston, T.W., and Wold, W.S.M. (1999). Preparation and titration of CsCl-banded adenovirus stock, Vol 21.

Tollefson, A.E., Ryerse, J.S., Scaria, A., Hermiston, T.W., and Wold, W.S.M. (1996a). The E3-11.6-kDa adenovirus death protein (ADP) is required for efficient cell death: Characterization of cells infected with adp mutants. Virology *220*, 152-162.

Tollefson, A.E., Scaria, A., Hermiston, T., Ryerse, J.S., Wold, L.J., and Wold, W.S.M. (1996b). The adenovirus death protein (E3-11.6K) is required at very late stages of infection for efficient cell lysis and release of adenovirus from infected cells. Journal of Virology *70*, 2296-2306.

Tollefson, A.E., Toth, K., Doronin, K., Kuppuswamy, M., Doronina, O.A., Lichtenstein, D.L., Hermiston, T.W., Smith, C.A., and Wold, W.S.M. (2001). Inhibition of TRAIL-induced apoptosis and forced internalization of TRAIL receptor 1 by adenovirus proteins. Journal of Virology *75*, 8875-8887.

Tomlinson, R.L., Li, J., Culp, B.R., Terns, R.M., and Terns, M.P. (2010). A Cajal body-independent pathway for telomerase trafficking in mice. Experimental Cell Research *316*, 2797-2809.

Torii, S., Egan, D.A., Evans, R.A., and Reed, J.C. (1999). Human Daxx regulates Fas-induced apoptosis from nuclear PML oncogenic domains (PODs). Embo Journal *18*, 6037-6049.

Tormanen, H., Backstrom, E., Carlsson, A., and Akusjarvi, G. (2006). L4-33K, an adenovirus-encoded alternative RNA splicing factor. Journal of Biological Chemistry *281*, 36510-36517.

Toyota, C.G., Davis, M.D., Cosman, A.M., and Hebert, M.D. (2010). Coilin phosphorylation mediates interaction with SMN and SmB'. Chromosoma *119*, 205-215.

Tran, E.J., Zhang, X.X., and Maxwell, E.S. (2003). Efficient RNA 2 '-O-methylation requires juxtaposed and symmetrically assembled archaeal box C/D and C '/D ' RNPs. Embo Journal *22*, 3930-3940.

Tremblay, M.L., Dery, C.V., Talbot, B.G., and Weber, J. (1983). Invitro cleavage specificity of the adenovirus type-2 proteinase. Biochimica Et Biophysica Acta *743*, 239-245.

Tribouley, C., Lutz, P., Staub, A., and Kedinger, C. (1994). Product of the adenovirus intermediate gene IVa2 is a transcriptional activator of the major late promoter. Journal of Virology *68*, 4450-4457.

Trimarchi, J.M., Fairchild, B., Wen, J., and Lees, J.A. (2001). The E2F6 transcription factor is a component of the mammalian Bmi1-containing polycomb complex. Proc Natl Acad Sci U S A *98*, 1519-1524.

Trinkle-Mulcahy, L., Ajuh, P., Prescott, A., Claverie-Martin, F., Cohen, S., Lamond, A.I., and Cohen, P. (1999). Nuclear organisation of NIPP1, a regulatory subunit of protein phosphatase 1 that associates with pre-mRNA splicing factors. Journal of Cell Science *112*, 157-168.

Trinkle-Mulcahy, L., Andersen, J., Lam, Y.W., Moorhead, G., Mann, M., and Lamond, A.I. (2006). Repo-Man recruits PP1 gamma to chromatin and is essential for cell viability. Journal of Cell Biology *172*, 679-692.

Trinkle-Mulcahy, L., Sleeman, J.E., and Lamond, A.I. (2001). Dynamic targeting of protein phosphatase 1 within the nuclei of living mammalian cells. Journal of Cell Science *114*, 4219-4228.

Tripathi, V., Ellis, J.D., Shen, Z., Song, D.Y., Pan, Q., Watt, A.T., Freier, S.M., Bennett, C.F., Sharma, A., Bubulya, P.A.*, et al.* (2010). The Nuclear-Retained Noncoding RNA MALAT1 Regulates Alternative Splicing by Modulating SR Splicing Factor Phosphorylation. Molecular Cell *39*, 925-938.

Trotman, L.C., Alimonti, A., Scaglioni, P.P., Koutcher, J.A., Cordon-Cardo, C., and Pandolfi, P.P. (2006). Identification of a tumour suppressor network opposing nuclear Akt function. Nature *441*, 523-527.

Trotman, L.C., Mosberger, N., Fornerod, M., Stidwill, R.P., and Greber, U.F. (2001). Import of adenovirus DNA involves the nuclear pore complex receptor CAN/Nup214 and histone H1. Nature Cell Biology *3*, 1092-1100.

Tsai, K., Thikmyanova, N., Wojcechowskyj, J.A., Delecluse, H.-J., and Lieberman, P.M. (2011). EBV Tegument Protein BNRF1 Disrupts DAXX-ATRX to Activate Viral Early Gene Transcription. Plos Pathogens *7,* e1002376.

Tucker, K.E., Berciano, M.T., Jacobs, E.Y., LePage, D.F., Shpargel, K.B., Rossire, J.J., Chan, E.K.L., Lafarga, M., Conlon, R.A., and Matera, A.G. (2001). Residual Cajal bodies in coilin knockout mice fail to recruit Sm snRNPs and SMN, the spinal muscular atrophy gene product. Journal of Cell Biology *154*, 293-307.

Tuve, S., Wang, H.J., Ware, C., Liu, Y., Gaggar, A., Bernt, K., Shayakhmetov, D., Li, Z.Y., Strauss, R., Stone, D*., et al.* (2006). A new group B adenovirus receptor is expressed at high levels on human stem and tumor cells. Journal of Virology *80*, 12109-12120.

Tycowski, K.T., Shu, M.-D., Kukoyi, A., and Steitz, J.A. (2009). A Conserved WD40 Protein Binds the Cajal Body Localization Signal of scaRNP Particles. Molecular Cell *34*, 47-57.

Tyler, R.E., Ewing, S.G., and Imperiale, M.J. (2007). Formation of a multiple protein complex on the adenovirus packaging sequence by the IVa2 protein. Journal of Virology *81*, 3447-3454.

Ugai, H., Dobbins, G.C., Wang, M., Le, L.P., Matthews, D.A., and Curiel, D.T. (2012). Adenoviral protein V promotes a process of viral assembly through nucleophosmin 1. Virology *432*, 283-95.

Ulfendahl, P.J., Kreivi, J.P., and Akusjarvi, G. (1989). Role of the branch site 3'-splice site region in adenovirus-2 E1A pre-messenger RNA alternative splicing - Evidence for 5'-splice and 3'-splice site co-operation. Nucleic Acids Research *17*, 925-938.

Ulfendahl, P.J., Linder, S., Kreivi, J.P., Nordqvist, K., Sevensson, C., Hultberg, H., and Akusjarvi, G. (1987). A novel adenovirus-2 E1A messenger-RNA encoding a protein with transcription activation properties. Embo Journal *6*, 2037-2044.

Ullman, A.J., and Hearing, P. (2008). Cellular proteins PML and Daxx mediate an innate antiviral defense antagonized by the adenovirus E4 ORF3 protein. Journal of Virology *82*, 7325-7335.

Ullman, A.J., Reich, N.C., and Hearing, P. (2007). Adenovirus E4 ORF3 protein inhibits the interferon-mediated antiviral response. Journal of Virology *81*, 4744-4752.

Vagnarelli, P., Hudson, D.F., Ribeiro, S.A., Trinkle-Mulcahy, L., Spence, J.M., Lai, F., Farr, C.J., Lamond, A.I., and Earnshaw, W.C. (2006). Condensin and Repo-Man-PP1 co-operate in the regulation of chromosome architecture during mitosis. Nature Cell Biology *8*, 1133-U161.

Vales, L.D., and Darnell, J.E. (1989). Promoter occlusion prevents transcription of adenovirus polypeptide IX messenger RNA until after DNA replication. Genes & Development *3*, 49-59.

Valgardsdottir, R., Chiodi, F., Giordano, M., Cobianchi, F., Riva, S., and Biamonti, G. (2005). Structural and functional characterization of noncoding repetitive RNAs transcribed in stressed human cells. Molecular Biology of the Cell *16*, 2597-2604.

Van Beveren, C.P., Maat, J., Dekker, B.M.M., and Vanormondt, H. (1981). The nucleotide sequence of the gene for protein IVa2 and of the 5' leader segment of the major late messenger mRNAs of adenovirus serotype 5. Gene *16*, 179-189.

Van Damme, E., Laukens, K., Dang, T.H., and Van Ostade, X. (2010). A manually curated network of the PML nuclear body interactome reveals an important role for PML-NBs in SUMOylation dynamics. International Journal of Biological Sciences *6*, 51-67.

van den Bosch, M., Bree, R.T., and Lowndes, N.F. (2003). The MRN complex: coordinating and mediating the response to broken chromosomes. Embo Reports *4*, 844-849.

Van Oostrum, J., and Burnett, R.M. (1985). Molecular composition of the adenovirus type-2 virion. Journal of Virology *56*, 439-448.

Van Oostrum, J., Smith, P.R., Mohraz, M., and Burnett, R.M. (1987). The structure of the adenovirus capsid. 3. Hexon packaging determined from electron-micrographs of capsid fragments. Journal of Molecular Biology *198*, 73-89.

Vargas, D.Y., Shah, K., Batish, M., Levandoski, M., Sinha, S., Marras, S.A.E., Schedl, P., and Tyagi, S. (2011). Single-Molecule Imaging of Transcriptionally Coupled and Uncoupled Splicing. Cell *147*, 1054-1065.

Varnavski, A.N., Calcedo, R., Bove, M., Gao, G., and Wilson, J.M. (2005). Evaluation of toxicity from high-dose systemic administration of recombinant adenovirus vector in vector-naive and pre-immunized mice. Gene Therapy *12*, 427-436.

Vayda, M.E., and Flint, S.J. (1987). Isolation and characterization of adenovirus core nucleoprotein subunits. Journal of Virology *61*, 3335-3339.

Vayda, M.E., Rogers, A.E., and Flint, S.J. (1983). The structure of nucleoprotein cores released from adenovirus. Nucleic Acids Research *11*, 441-460.

Velicer, L.F., and Ginsberg, H.S. (1968). Cytoplasmic synthesis of type 5 adenovirus capsid proteins. Proc Natl Acad Sci U S A *61*, 1264-1271.

Vellinga, J., Van der Heijdt, S., and Hoeben, R.C. (2005). The adenovirus capsid: major progress in minor proteins. Journal of General Virology *86*, 1581-1588.

Venteicher, A.S., Abreu, E.B., Meng, Z., McCann, K.E., Terns, R.M., Veenstra, T.D., Terns, M.P., and Artandi, S.E. (2009). A Human Telomerase Holoenzyme Protein Required for Cajal Body Localization and Telomere Synthesis. Science *323*, 644-648.

Verheijen, R., Kuijpers, H., Vooijs, P., Vanvenrooij, W., and Ramaekers, F. (1986). Distribution of the 70K-U1 RNA-associated protein during interphase and mitosis - correlation with other U-RNP particles and proteins of the nuclear matrix. Journal of Cell Science *86*, 173-190.

Vernier, M., Bourdeau, V., Gaumont-Leclerc, M.-F., Moiseeva, O., Begin, V., Saad, F., Mes-Masson, A.-M., and Ferbeyre, G. (2011). Regulation of E2Fs and senescence by PML nuclear bodies. Genes & Development *25*, 41-50.

Virtanen, A., and Pettersson, U. (1983). The molecular structure of the 9 S messenger-RNA from early region-1A of adenovirus serotype-2. Journal of Molecular Biology *165*, 496-499.

Visa, N., Puvion-Dutilleul, F., Harper, F., Bachellerie, J.P., and Puvion, E. (1993). Intranulcear distribution of poly(A) RNA determined by electron microscope in situ hybridization. Experimental Cell Research *208*, 19-34.

Vitali, P., Basyuk, E., Le Meur, E., Bertrand, E., Muscatelli, F., Cavaille, J., and Huttenhofer, A. (2005). ADAR2-mediated editing of RNA substrates in the nucleolus is inhibited by C/D small nucleolar RNAs. Journal of Cell Biology *169*, 745-753.

Voit, R., and Grummt, I. (2001). Phosphorylation of UBF at serine 388 is required for interaction with RNA polymerase I and activation of rDNA transcription. Proc Natl Acad Sci U S A *98*, 13631-13636.

Voss, M.D., Hille, A., Barth, S., Spurk, A., Hennrich, F., Holzer, D., Mueller-Lantzsch, N., Kremmer, E., and Grasser, F.A. (2001). Functional cooperation of Epstein-Barr virus nuclear antigen 2 and the survival motor neuron protein in transactivation of the viral LMP1 promoter. Journal of Virology *75*, 11781-11790.

Wadd, S., Bryant, H., Filhol, O., Scott, J.E., Hsieh, T.Y., Everett, R.D., and Clements, J.B. (1999). The multifunctional herpes simplex virus IE63 protein interacts with heterogeneous ribonucleoprotein K and with casein kinase 2. Journal of Biological Chemistry *274*, 28991-28998.

Waddington, S.N., McVey, J.H., Bhella, D., Parker, A.L., Barker, K., Atoda, H., Pink, R., Buckley, S.M.K., Greig, J.A., Denby, L.*, et al.* (2008). Adenovirus serotype 5 hexon mediates liver gene transfer. Cell *132*, 397-409.

Waddington, S.N., Parker, A.L., Havenga, M., Nicklin, S.A., Buckley, S.M.K., McVey, J.H., and Baker, A.H. (2007). Targeting of adenovirus serotype 5 (Ad5) and 5/47 pseudotyped vectors in vivo: Fundamental involvement of coagulation factors and redundancy of CAR binding by Ad5. Journal of Virology *81*, 9568-9571.

Wadell, G. (1984). Molecular epidemiology of human adenoviruses. Current Topics in Microbiology and Immunology *110*, 191-220.

Wadell, G., Allard, A., Evander, M., and Li, Q.G. (1986). Genetic-variability and evolution of adenoviruses. Chemica Scripta *26B*, 325-335.

Wadell, G., and Norrby, E. (1969). Immunological and other biological characteristics of pentons of human adenoviruses. Journal of Virology *4*, 671-680.

Wagner, E.J., Burch, B.D., Godfrey, A.C., Salzler, H.R., Duronio, R.J., and Marzluff, W.F. (2007). A genome-wide RNA interference screen reveals that variant histones, are necessary for replication-dependent histone pre-mRNA processing. Molecular Cell *28*, 692-699.

Wagner, R.W., Smith, J.E., Cooperman, B.S., and Nishikura, K. (1989). A double-stranded-RNA unwinding activity introduces structural alterations by means of adenosine to inosine conversions in mammalian cells and xenopus eggs. Proc Natl Acad Sci U S A *86*, 2647-2651.

Wahl, M.C., Will, C.L., and Luehrmann, R. (2009). The Spliceosome: Design Principles of a Dynamic RNP Machine. Cell *136*, 701-718.

Walker, M.P., Tian, L., and Matera, A.G. (2009). Reduced Viability, Fertility and Fecundity in Mice Lacking the Cajal Body Marker Protein, Coilin. Plos One *4,* e6171.

Walsh, M.P., Chintakuntlawar, A., Robinson, C.M., Madisch, I., Harrach, B., Hudson, N.R., Schnurr, D., Heim, A., Chodosh, J., Seto, D.*, et al.* (2009). Evidence of Molecular Evolution Driven by Recombination Events Influencing Tropism in a Novel Human Adenovirus that Causes Epidemic Keratoconjunctivitis. Plos One *4,* e5635.

Walsh, M.P., Seto, J., Jones, M.S., Chodosh, J., Xu, W.B., and Seto, D. (2010). Computational Analysis Identifies Human Adenovirus Type 55 as a Re-Emergent Acute Respiratory Disease Pathogen. Journal of Clinical Microbiology *48*, 991-993.

Walters, R.W., Freimuth, P., Moninger, T.O., Ganske, I., Zabner, J., and Welsh, M.J. (2002). Adenovirus fiber disrupts CAR-mediated intercellular adhesion allowing virus escape. Cell *110*, 789-799.

Walton, T.H., Moen, P.T., Fox, E., and Bodnar, J.W. (1989). Interactions of minute virus of mice and adenovirus with host nucleoli. Journal of Virology *63*, 3651-3660.

Wang, H., Li, Z.-Y., Liu, Y., Persson, J., Beyer, I., Moller, T., Koyuncu, D., Drescher, M.R., Strauss, R., Zhang, X.-B.*, et al.* (2010). Desmoglein 2 is a receptor for adenovirus serotypes 3, 7, 11 and 14. Nat Med *17*, 96-104.

Wang, J., Shiels, C., Sasieni, P., Wu, P.J., Islam, S.A., Freemont, P.S., and Sheer, D. (2004). Promyelocytic leukemia nuclear bodies associate with transcriptionally active genomic regions. Journal of Cell Biology *164*, 515-526.

Wang, K.N., Huang, S., Kapoor-Munshi, A., and Nemerow, G. (1998). Adenovirus internalization and infection require dynamin. Journal of Virology *72*, 3455-3458.

Wang, L., Oliver, S.L., Sommer, M., Rajamani, J., Reichelt, M., and Arvin, A.M. (2011). Disruption of PML Nuclear Bodies Is Mediated by ORF61 SUMO-Interacting Motifs and Required for Varicella-Zoster Virus Pathogenesis in Skin. Plos Pathogens *7,* e1002157.

Weber, J. (1976). Genetic analysis of adenovirus type-2. 3. Temperature sensitivity of processing of viral proteins. Journal of Virology *17*, 462-471.

Webster, A., Hay, R.T., and Kemp, G. (1993). The adenovirus proteinase is activated by a virus-coded disulfide-linked peptide. Cell *72*, 97-104.

Webster, A., Leith, I.R., Nicholson, J., Hounsell, J., and Hay, R.T. (1997). Role of preterminal protein processing in adenovirus replication. Journal of Virology *71*, 6381-6389.

Webster, L.C., and Ricciardi, R.P. (1991). Transdominant mutants of E1A provide genetic evidence that the zinc finger of the trans-activating domain binds a transcription factor. Molecular and Cellular Biology *11*, 4287-4296.

Wei, X.Y., Samarabandu, J., Devdhar, R.S., Siegel, A.J., Acharya, R., and Berezney, R. (1998). Segregation of transcription and replication sites into higher order domains. Science *281*, 1502-1505.

Weiden, M.D., and Ginsberg, H.S. (1994). Deletion of the E4 region of the genome produces adenovrius DNA concateners. Proc Natl Acad Sci U S A *91*, 153-157.

Weigel, S., and Dobbelstein, M. (2000). The nuclear export signal within the E4orf6 protein of adenovirus type 5 supports virus replication and cytoplasmic accumulation of viral mRNA. Journal of Virology *74*, 764-772.

Welting, T.J.M., Kikkert, B.J., van Venrooij, W.J., and Pruijn, G.J.M. (2006). Differential association of protein subunits with the human RNase MRP and RNase P complexes. Rna-a Publication of the Rna Society *12*, 1373-1382.

White, L., and Blair, G.E. (2012). Adenoviruses and Gene Therapy: The Role of the Immune System. In Small DNA Tumour Viruses, K. Gaston, ed. (Bristol, UK, Caister Academic Press).

Wickham, T.J., Filardo, E.J., Cheresh, D.A., and Nemerow, G.R. (1994). Integrin alpha-v-beta-5 selectively promotes adenovirus-mediated cell-membrane permeabilization. Journal of Cell Biology *127*, 257-264.

Wickham, T.J., Mathias, P., Cheresh, D.A., and Nemerow, G.R. (1993). Integrin alpha-v-beta-3 and integrin alpha-v-beta-5 promote adenovirus internalization but not virus attachment. Cell *73*, 309-319.

Wiethoff, C.M., Wodrich, H., Gerace, L., and Nemerow, G.R. (2005). Adenovirus protein VI mediates membrane disruption following capsid disassembly. Journal of Virology *79*, 1992-2000.

Wigand, R., and Kumel, G. (1977). Kinetics of adenovirus infection and spread in cell cultures infected with low multiplicity. Archives of Virology *54*, 177-187.

Wilkinson, G.W.G., Kelly, C., Sinclair, J.H., and Rickards, C. (1998). Disruption of PML-associated nuclear bodies mediated by the human cytomegalovirus major immediate early gene product. Journal of General Virology *79*, 1233-1245.

Will, C.L., and Luhrmann, R. (2005). Splicing of a rare class of introns by the U12-dependent spliceosome. Biological Chemistry *386*, 713-724.

Wilusz, J.E., Sunwoo, H., and Spector, D.L. (2009). Long noncoding RNAs: functional surprises from the RNA world. Genes & Development *23*, 1494-1504.

Wimmer, P., Schreiner, S., Everett, R.D., Sirma, H., Groitl, P., and Dobner, T. (2010). SUMO modification of E1B-55K oncoprotein regulates isoform-specific binding to the tumour suppressor protein PML. Oncogene *29*, 5511-5522.

Winter, N., and Dhalluin, J.C. (1991). Regulation of the biosynthesis of subgroup-C adenovirus protein IVa2. Journal of Virology *65*, 5250-5259.

Wodrich, H., Cassany, A., D'Angelo, M.A., Guan, T., Nemerow, G., and Gerace, L. (2006). Adenovirus core protein pVII is translocated into the nucleus by multiple import receptor pathways. Journal of Virology *80*, 9608-9618.

Wodrich, H., Guan, T.L., Cingolani, G., Von Seggern, D., Nemerow, G., and Gerace, L. (2003). Switch from capsid protein import to adenovirus assembly by cleavage of nuclear transport signals. Embo Journal *22*, 6245-6255.

Wodrich, H., Henaff, D., Jammart, B., Segura-Morales, C., Seelmeir, S., Coux, O., Ruzsics, Z., Wiethoff, C.M., and Kremer, E.J. (2010). A Capsid-Encoded PPxY-Motif Facilitates Adenovirus Entry. Plos Pathogens *6*, e1000808.

Wohlfart, C., and Everitt, E. (1985). Human adenovirus-2 as immunogen in rabbits yields antisera with high titers of antibodies against the nonstructural 72K DNA-binding protein. Virus Research *3*, 77-85.

Wong, J.M.Y., Kusdra, L., and Collins, K. (2002). Sub-nuclear shuttling of human telomerase induced by transformation and DNA damage. Nature Cell Biology *4*, 731-U5.

Woo, J.L., and Berk, A.J. (2007). Adenovirus ubiquitin-protein ligase stimulates viral late mRNA nuclear export. Journal of Virology *81*, 575-587.

Wsierska-Gadek, J., and Horky, M. (2003). How the nucleolar sequestration of p53 protein or its interplayers contributes to its (re)-activation. Annals of the New York Academy of Sciences *1010*, 266-72.

Wu, C.H.H., and Gall, J.G. (1993). U7 small nuclear RNA in c-snurposomes of the xenopus germinal vesicle. Proc Natl Acad Sci U S A *90*, 6257-6259.

Xi, Q.R., Cuesta, R., and Schneider, R.J. (2004). Tethering of eIF4G to adenoviral mRNAs by viral 100k protein drives ribosome shunting. Genes & Development *18*, 1997-2009.

Xi, Q.R., Cuesta, R., and Schneider, R.J. (2005). Regulation of translation by ribosome shunting through phosphotyrosine-dependent coupling of adenovirus protein 100k to viral mRNAs. Journal of Virology *79*, 5676-5683.

Xia, D., Henry, L.J., Gerard, R.D., and Deisenhofer, J. (1994). Crystal structure of the receptor binding domain of adenovirus type-5 fiber protein at 1.7-angstrom resolution. Structure *2*, 1259-1270.

Xiao, S.H., and Manley, J.L. (1997). Phosphorylation of the ASE/SF2 RS domain affects both protein-protein and protein-RNA interactions and is necessary for splicing. Genes & Development *11*, 334-344.

Xie, R., Medina, R., Zhang, Y., Hussain, S., Colby, J., Ghule, P., Sundararajan, S., Keeler, M., Liu, L.-J., van der Deen, M.*, et al.* (2009). The histone gene activator HINFP is a nonredundant cyclin E/CDK2 effector during early embryonic cell cycles. Proc Natl Acad Sci U S A *106*, 12359-12364.

Xie, S.Q., and Pombo, A. (2006). Distribution of different phosphorylated forms of RNA polymerase II in relation to Cajal and PML bodies in human cells: an ultrastructural study. Histochemistry and Cell Biology *125*, 21-31.

Xie, W.B., Ling, T., Zhou, Y.G., Feng, W.J., Zhu, Q.Y., Stunnenberg, H.G., Grummt, I., and Tao, W. (2012). The chromatin remodeling complex NuRD establishes the poised state of rRNA genes characterized by bivalent histone modifications and altered nucleosome positions. Proc Natl Acad Sci U S A *109*, 8161-8166.

Xing, Y.G., Johnson, C.V., Dobner, P.R., and Lawrence, J.B. (1993). Higher level organization of individual gene transcription and RNA splicing. Science *259*, 1326-1330.

Xing, Y.G., Johnson, C.V., Moen, P.T., McNeil, J.A., and Lawrence, J.B. (1995). Nonrandom gene organization: Structural arrangements of specific pre-mRNA transcription and splicing with SC-35 domains. Journal of Cell Biology *131*, 1635-1647.

Xu, M., and Cook, P.R. (2008). Similar active genes cluster in specialized transcription factories. Journal of Cell Biology *181*, 615-623.

Xu, Y.X., Ahn, J.H., Cheng, M.F., Ap Rhys, C.M., Chiou, C.J., Zong, J.H., Matunis, M.J., and Hayward, G.S. (2001). Proteasome-independent disruption of PML oncogenic domains (PODs), but not covalent modification by SUMO-1, is required for human cytomegalovirus immediate-early protein IE1 to inhibit PML-mediated transcriptional repression. Journal of Virology *75*, 10683-10695.

Xu, Z.K., Anderson, R., and Hobman, T.C. (2011). The Capsid-Binding Nucleolar Helicase DDX56 Is Important for Infectivity of West Nile Virus. Journal of Virology *85*, 5571-5580.

Yager, T.D., Dempsey, A.A., Tang, H., Stamatiou, D., Chao, S., Marshall, K.W., and Liew, C.C. (2004). First comprehensive mapping of cartilage transcripts to the human genome. Genomics *84*, 524-535.

Yageta, M., Tsunoda, H., Yamanaka, T., Nakajima, T., Tomooka, Y., Tsuchida, N., and Oda, K. (1999). The adenovirus E1A domains required for induction of DNA rereplication in G(2)/M arrested cells coincide with those required for apoptosis. Oncogene *18*, 4767-4776.

Yan, H., and Newport, J. (1995). FFA-1, a protein that promotes the formation of replication centres within nuclei. Science *269*, 1883-1885.

Yang, S., Jeong, J.-H., Brown, A.L., Lee, C.-H., Pandolfi, P.P., Chung, J.H., and Kim, M.K. (2006). Promyelocytic leukemia activates Chk2 by mediating Chk2 autophosphorylation. Journal of Biological Chemistry *281*, 26645-26654.

Yang, S.T., Kuo, C., Bisi, J.E., and Kim, M.K. (2002). PML-dependent apoptosis after DNA damage is regulated by the checkpoint kinase hCds1/Chk2. Nature Cell Biology *4*, 865-870.

Yang, T.-C., and Maluf, N.K. (2012). Cooperative Heteroassembly of the Adenoviral L4-22K and IVa2 Proteins onto the Viral Packaging Sequence DNA. Biochemistry *51*, 1357-1368.

Yang, T.H., Tsai, W.H., Lee, Y.M., Lei, H.Y., Lai, M.Y., Chen, D.S., Yeh, N.H., and Lee, S.C. (1994a). Purification and characterisation of nucleolin an its identification as a transcription repressor. Molecular and Cellular Biology *14*, 6068-6074.

Yang, X.-c., Burch, B.D., Yan, Y., Marzluff, W.F., and Dominski, Z. (2009). FLASH, a Proapoptotic Protein Involved in Activation of Caspase-8, Is Essential for 3 ' End Processing of Histone Pre-mRNAs. Molecular Cell *36*, 267-278.

Yang, X.J., Ogryzko, V.V., Nishikawa, J., Howard, B.H., and Nakatani, Y. (1996). A p300/CBP-associated factor that competes with the adenoviral oncoprotein E1A. Nature *382*, 319-324.

Yang, Y.P., Li, Q., Ertl, H.C.J., and Wilson, J.M. (1995). Cellular and humoral immune-responses to viral-antigens create barriers to lung-directed gene-therapy with recombinant adenoviruses. Journal of Virology *69*, 2004-2015.

Yang, Y.P., Nunes, F.A., Berencsi, K., Furth, E.E., Gonczol, E., and Wilson, J.M. (1994b). Cellular-immunity to viral-antigens limits E1-deleted adenoviruses for gene therapy. Proc Natl Acad Sci U S A *91*, 4407-4411.

Yang, Y.P., Nunes, F.A., Berencsi, K., Gonczol, E., Engelhardt, J.F., and Wilson, J.M. (1994c). Inactivation of E2A in recombinant adenoviruses improves the prospect for gene-therapy in cystic-fibrosis. Nature Genetics *7*, 362-369.

Yatherajam, G., Huang, W., and Flint, S.J. (2011). Export of Adenoviral Late mRNA from the Nucleus Requires the Nxf1/Tap Export Receptor. Journal of Virology *85*, 1429-1438.

Ye, X., Zerlanko, B., Zhang, R., Somaiah, N., Lipinski, M., Salomoni, P., and Adams, P.D. (2007). Definition of pRB- and p53-dependent and -independent steps in HIRA/ASF1a-mediated formation of senescence-associated heterochromatin foci. Molecular and Cellular Biology *27*, 2452-2465.

Yew, P.R., and Berk, A.J. (1992). Inhibition of p53 transactivation required for transformation by adenovirus early 1B protein Nature *357*, 82-85.

Yew, P.R., Liu, X., and Berk, A.J. (1994). Adenovirus E1B oncoprotein tethers a transcriptional repression domain to p53. Genes & Development *8*, 190-202.

Ying, B.L., and Wold, W.S.M. (2003). Adenovirus ADP protein (E3-11.6K), which is required for efficient cell lysis and virus release, interacts with human MAD2B. Virology *313*, 224-234.

Yondola, M.A., and Hearing, P. (2007). The adenovirus E4 ORF3 protein binds and reorganizes the TRIM family member transcriptional intermediary factor 1 alpha. Journal of Virology *81*, 4264-4271.

Young, P.J., Jensen, K.T., Burger, L.R., Pintel, D.J., and Lorson, C.L. (2002a). Minute virus of mice NS1 interacts with the SMN protein, and they colocalize in novel nuclear bodies induced by parvovirus infection. Journal of Virology *76*, 3892-3904.

Young, P.J., Jensen, K.T., Burger, L.R., Pintel, D.J., and Lorson, C.L. (2002b). Minute virus of mice small nonstructural protein NS2 interacts and colocalizes with the Smn protein. Journal of Virology *76*, 6364-6369.

Young, P.J., Le, T.T., Man, N.T., Burghes, A.H.M., and Morris, G.E. (2000). The relationship between SMN, the spinal muscular atrophy protein, and nuclear coiled bodies in differentiated tissues and cultured cells. Experimental Cell Research *256*, 365-374.

Young, P.J., Newman, A., Jensen, K.T., Burger, L.R., Pintel, D.J., and Lorson, C.L. (2005). Minute virus of mice small non-structural protein NS2 localizes within, but is not required for the formation of, Smn-associated autonomous parvovirus-associated replication bodies. Journal of General Virology *86*, 1009-1014.

Yousef, A.F., Fonseca, G.J., Pelka, P., Ablack, J.N.G., Walsh, C., Dick, F.A., Bazett-Jones, D.P., Shaw, G.S., and Mymryk, J.S. (2010). Identification of a molecular recognition feature in the E1A oncoprotein that binds the SUMO conjugase UBC9 and likely interferes with polySUMOylation. Oncogene *29*, 4693-4704.

Yueh, A., and Schneider, R.J. (1996). Selective translation initiation by ribosome jumping in adenovirus-infected and heat-shocked cells. Genes & Development *10*, 1557-1567.

Yueh, A., and Schneider, R.J. (2000). Translation by ribosome shunting on adenovirus and hsp70 mRNAs facilitated by complementarity to 18S rRNA. Genes & Development *14*, 414-421.

Yung, B.Y.M., Busch, H., and Chan, P.K. (1985). Translocation of nucleolar phosphoprotein B23 (37KDA PI5.1) induced by selective inhibitors of ribosome synthesis. Biochimica Et Biophysica Acta *826*, 167-173.

Zakaryan, H., and Stamminger, T. (2011). Nuclear remodelling during viral infections. Cell Microbiol *13*, 806-813.

Zantema, A., Schrier, P.I., Davisolivier, A., Vanlaar, T., Vaessen, R., and Vandereb, A.J. (1985). Adenovirus serotype determines association and localization of the large E1B tumor antigen with cellular tumor antigen p53 in transformed cells. Molecular and Cellular Biology *5*, 3084-3091.

Zeng, C.Q., Kim, E., Warren, S.L., and Berget, S.M. (1997). Dynamic relocation of transcription and splicing factors dependent upon transcriptional activity. Embo Journal *16*, 1401-1412.

Zerler, B., Roberts, R.J., Mathews, M.B., and Moran, E. (1987). Different functional domains of the adenovirus E1A gene are involved in regulation of host cell-cyle products. Molecular and Cellular Biology *7*, 821-829.

Zhang, G.H., Taneja, K.L., Singer, R.H., and Green, M.R. (1994). Localization of pre-messenger RNA splicing in mammalian nuclei. Nature *372*, 809-812.

Zhang, R.G., Poustovoitov, M.V., Ye, X.F., Santos, H.A., Chen, W., Daganzo, S.M., Erzberger, J.P., Serebriiskii, I.G., Canutescu, A.A., Dunbrack, R.L., *et al.* (2005). Formation of MacroH2A-containing senescence-associated heterochromatin foci and senescence driven by ASF1a and HIRA. Developmental Cell *8*, 19-30.

Zhang, W., and Arcos, R. (2005). Interaction of the adenovirus major core protein precursor, pVII, with the viral DNA packaging machinery. Virology *334*, 194-202.

Zhang, W., and Imperiale, M.J. (2000). Interaction of the adenovirus IVa2 protein with viral packaging sequences. Journal of Virology *74*, 2687-2693.

Zhang, W., and Imperiale, M.J. (2003). Requirement of the adenovirus IVa2 protein for virus assembly. Journal of Virology *77*, 3586-3594.

Zhang, W., Low, J.A., Christensen, J.B., and Imperiale, M.J. (2001). Role for the adenovirus 1Va2 protein in packaging of viral DNA. Journal of Virology *75*, 10446-10454.

Zhang, X., Turnell, A.S., Gorbea, C., Mymryk, J.S., Gallimore, P.H., and Grand, R.J.A. (2004). The targeting of the proteasomal regulatory subunit S2 by adenovirus E1A causes inhibition of proteasomal activity and increased p53 expression. Journal of Biological Chemistry *279*, 25122-25133.

Zhang, X., Yuan, Y.-R., Pei, Y., Lin, S.-S., Tuschl, T., Patel, D.J., and Chua, N.-H. (2006). Cucumber mosaic virus-encoded 2b suppressor inhibits Arabidopsis Argonaute1 cleavage activity to counter plant defense. Genes & Development *20*, 3255-3268.

Zhang, Y.M., and Bergelson, J.M. (2005). Adenovirus receptors. Journal of Virology *79*, 12125-12131.

Zhang, Z., Lotti, F., Dittmar, K., Younis, I., Wan, L., Kasim, M., and Dreyfuss, G. (2008). SMN deficiency causes tissue-specific perturbations in the repertoire of snRNAs and widespread defects in splicing. Cell *133*, 585-600.

Zhao, J.Y., Dynlacht, B., Imai, T., Hori, T., and Harlow, E. (1998). Expression of NPAT, a novel substrate of cyclin E-CDK2, promotes S-phase entry. Genes & Development *12*, 456-461.

Zhao, J.Y., Kennedy, B.K., Lawrence, B.D., Barbie, D.A., Matera, A.G., Fletcher, J.A., and Harlow, E. (2000). NPAT links cyclin E-Cdk2 to the regulation of replication-dependent histone gene transcription. Genes & Development *14*, 2283-2297.

Zhao, L.Y., Colosimo, A.L., Liu, Y., Wan, Y.P., and Liao, D.Q. (2003). Adenovirus E1B 55-kilodalton oncoprotein binds to Daxx and eliminates enhancement of p53-dependent transcription by Daxx. Journal of Virology *77*, 11809-11821.

Zhong, F., Savage, S.A., Shkreli, M., Giri, N., Jessop, L., Myers, T., Chen, R., Alter, B.P., and Artandi, S.E. (2011). Disruption of telomerase trafficking by TCAB1 mutation causes dyskeratosis congenita. Genes & Development *25*, 11-16.

Zhong, S., Hu, P., Ye, T.-Z., Stan, R., Ellis, N.A., and Pandolfi, P.P. (1999). A role for PML and the nuclear body in genomic stability. Oncogene *18*, 7941-7947.

Zhong, S., Muller, S., Ronchetti, S., Freemont, P.S., Dejean, A., and Pandolfi, P.P. (2000a). Role of SUMO-1-modified PML in nuclear body formation. Blood *95*, 2748-2753.

Zhong, S., Salomoni, P., Ronchetti, S., Guo, A., Ruggero, D., and Pandolfi, P.P. (2000b). Promyelocytic leukemia protein (PML) and Daxx participate in a novel nuclear pathway for apoptosis. Journal of Experimental Medicine *191*, 631-639.

Zhou, G.L., Xin, L., Song, W., Di, L.J., Liu, G.A., Wu, X.S., Liu, D.P., and Liang, C.C. (2006). Active chromatin hub of the mouse alpha-globin locus forms in a transcription factory of clustered housekeeping genes. Molecular and Cellular Biology *26*, 5096-5105.

Zhu, J.G., Huang, X.P., Yang, Y.P. (2007). Innate immune response to adenoviral vectors is mediated by both Toll-like receptor-dependent and -independent pathways. Journal of Virology 81, 3170-3180.

Zhu, Y.S., Tomlinson, R.L., Lukowiak, A.A., Terns, R.M., and Terns, M.P. (2004). Telomerase RNA accumulates in Cajal bodies in human cancer cells. Molecular Biology of the Cell *15*, 81-90.

Ziff, E.B., and Evans, R.M. (1978). Coincidence of the promoter and capped 5' terminus of RNA from the adenovirus 2 major late transcription unit. Cell *15*, 1463-1475.

Zou, J.H., Barahmand-pour, F., Blackburn, M.L., Matsui, Y., Chansky, H.A., and Yang, L. (2004). Survival motor neuron (SMN) protein interacts with transcription corepressor mSin3A. Journal of Biological Chemistry *279*, 14922-14928.

Zsivanovits, P., Monks, D.J., Forbes, N.A., Ursu, K., Raue, R., and Benko, M. (2006). Presumptive identification of a novel adenovirus in a Harris hawk (Parabuteo unicinctus), a Bengal eagle owl (Bubo bengalensis), and a Verreaux's eagle owl (Bubo lacteus). Journal of Avian Medicine and Surgery *20*, 105-112.

Appendix
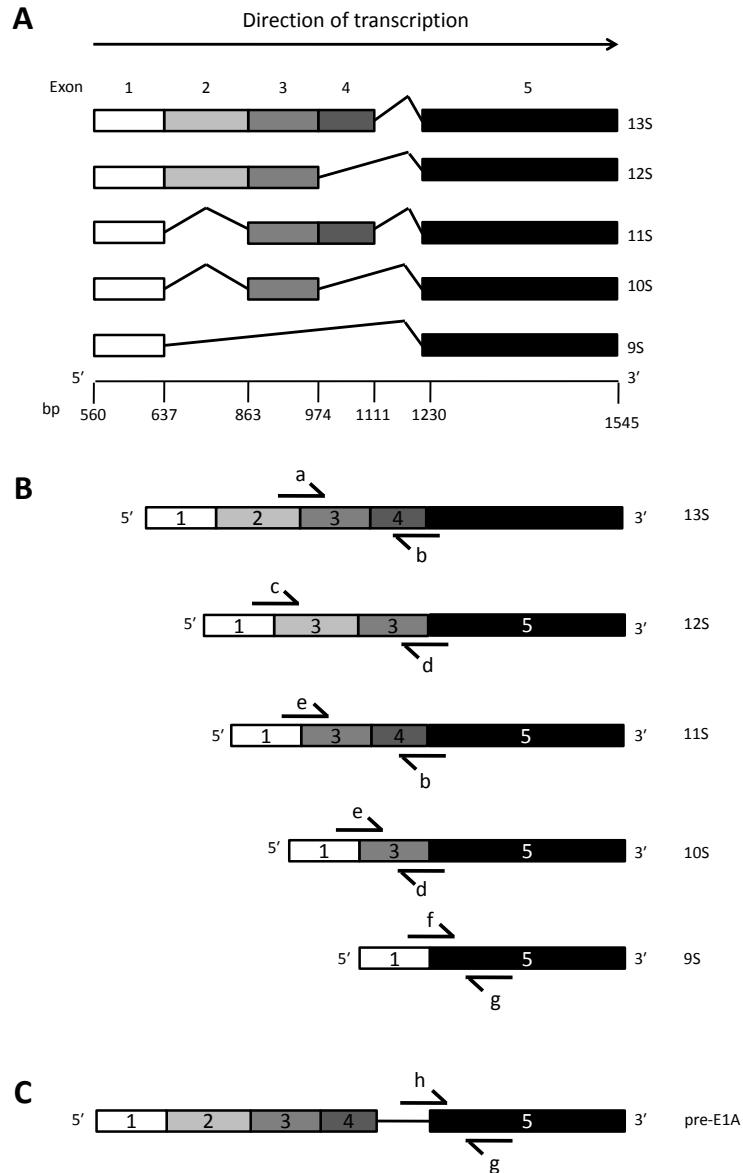
Appendix Figure 1. Primer design for PCR amplification of Ad5 E1A mRNAs and pre-mRNA.

A. A schematic representation of the Ad5 E1A spliceoforms. There are 5 E1A spliceoforms (13S, 12S, 11S, 10S and 9S). Boxes represent exons and thin lines represent introns. Nucleotide positions of the splice donor and acceptor sites are shown in base pairs (bp) on the Ad5 genome (not to scale). B. Positions of exon-spanning primers on the mature Ad5 E1A mRNAs. a – E1A 13S Forward primer; b – E1A 13S and 11S Reverse primer; c – E1A 12S Forward primer; d – E1A 12S and 10s Reverse primer; e – E1A 11S and 10s Forward primer; f – E1A 9S Forward primer; g – E1A 9S Reverse primer. C. Position of intron-exon spanning E1A primers for amplification of pre-E1A mRNA. h - pre-E1A Forward primer; g - E1A 9S Reverse primer. Sequence information was obtained from NCBI Nucleotide. Splice site information was obtained from Perricaudet *et al.*, 1979; Virtanen and Pettersson, 1983; Stephens and Harlow, 1987; Ulfendahl *et al.*, 1987a; Ulfendahl *et al.*, 1989.
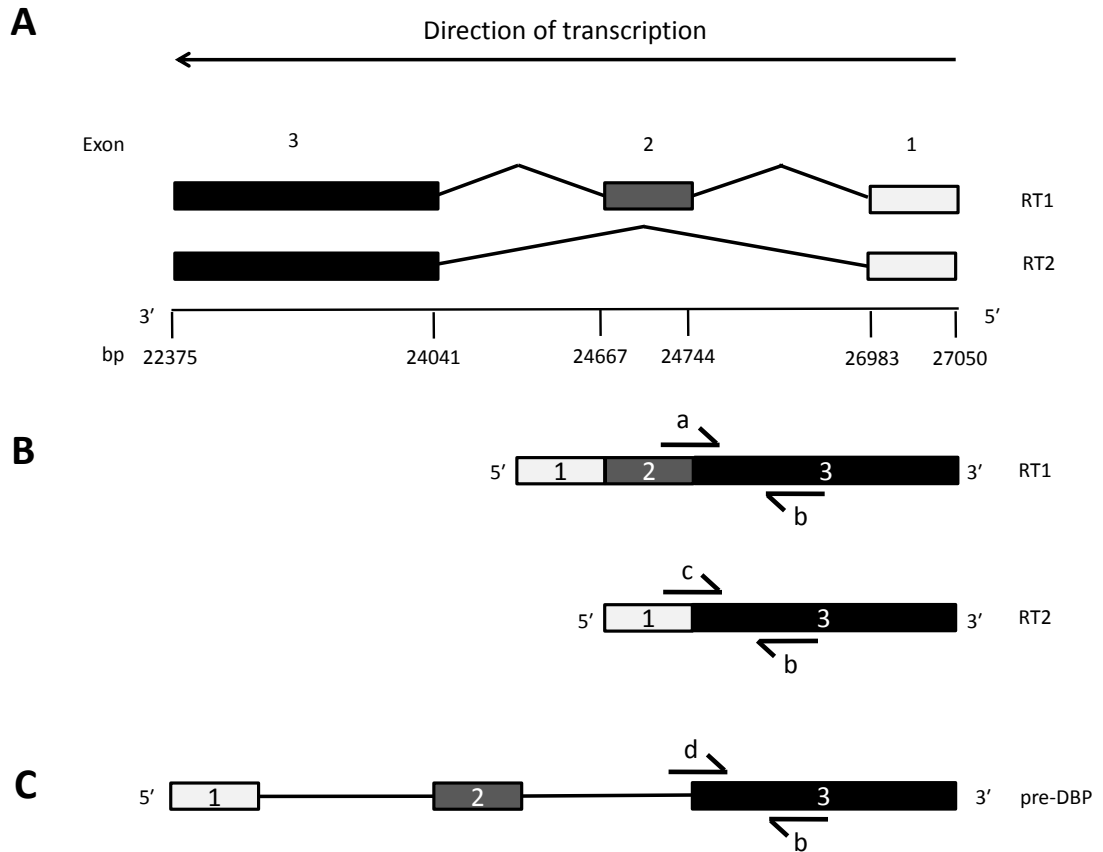
Appendix Figure 2. Primer design for PCR amplification of Ad5 DBP mRNAs and pre-mRNA.
A. A schematic representation of the Ad5 DBP spliceoforms. There are 2 spliceoforms (RT1 and RT2), encoded on the leftward-reading strand of the Ad5 genome. Boxes represent exons and thin lines represent introns. Nucleotide positions of the splice donor and acceptor sites are shown in base pairs (bp) (genome not to scale). B. Positions of exon-spanning primers on the mature Ad5 DBP mRNAs. a – DBP RT1 Forward primer; b - DBP reverse primer; c - DBP RT2 Forward primer. C. Position of intron-exon spanning DBP primers for amplification of pre-DBP mRNA. D - pre-DBP Forward primer; b - DBP Reverse primer. Sequence information was obtained from NCBI Nucleotide. Splice site information was obtained from Kruijer *et al.*, 1981; Caravokyri and Leppard, 1996.
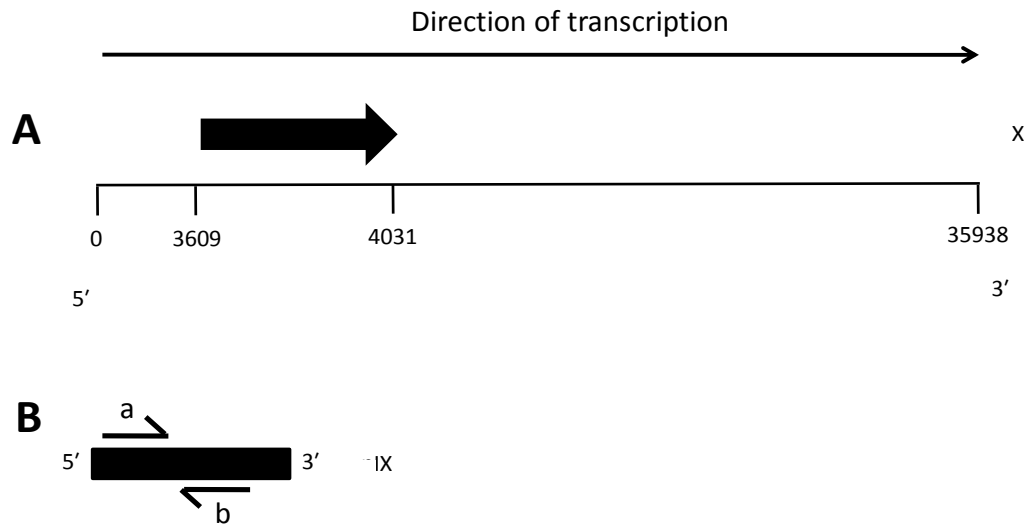
Appendix Figure 3. Primer design for PCR amplification of IX mRNA.

A. The transcription pathway for IX on the rightward-reading strand of the Ad5 genome. Boxes represent exons. Nucleotide positions of the transcription start sites are shown in base pairs (bp) on the Ad5 genome (genome not to scale). B. Primer design for IX primers. Primers were designed to span a region within the single intron of IX. a – IX Forward primer; b – IX Reverse primer. Sequence information was obtained from NCBI Nucleotide.
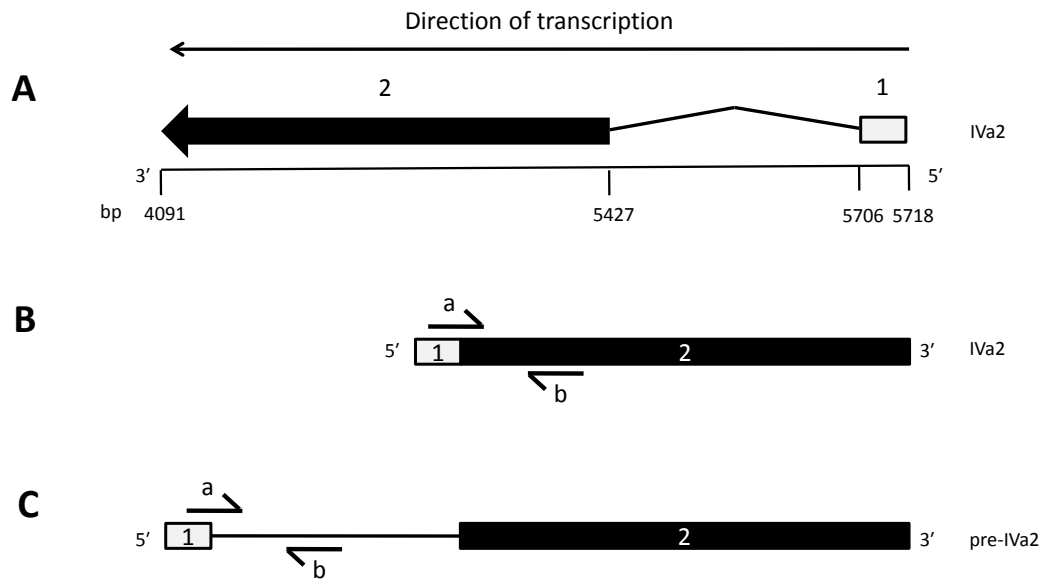
Appendix Figure 4. Primer design for PCR amplification of Ad5 IVa2 mRNA and pre-mRNA.

A. A schematic representation of the Ad5 IVa2 splicing pathway. Boxes represent exons and thin lines represent introns. Nucleotide positions of the splice donor and acceptor sites are shown in base pairs (bp) on the Ad5 genome. B. Positions of exon-spanning primers on the mature Ad5 IVa2 mRNA. a - IVa2 Forward primer; b - IVa2 reverse primer. C. Position of intron-exon spanning IVa2 primers for amplification of pre-IVa2 mRNA. A - pre-IVa2 Forward primer; b - pre-IVa2 Reverse primer. Sequence information was obtained from NCBI Nucleotide. Splice site information was obtained from Van Beveren *et al.*, 1981.
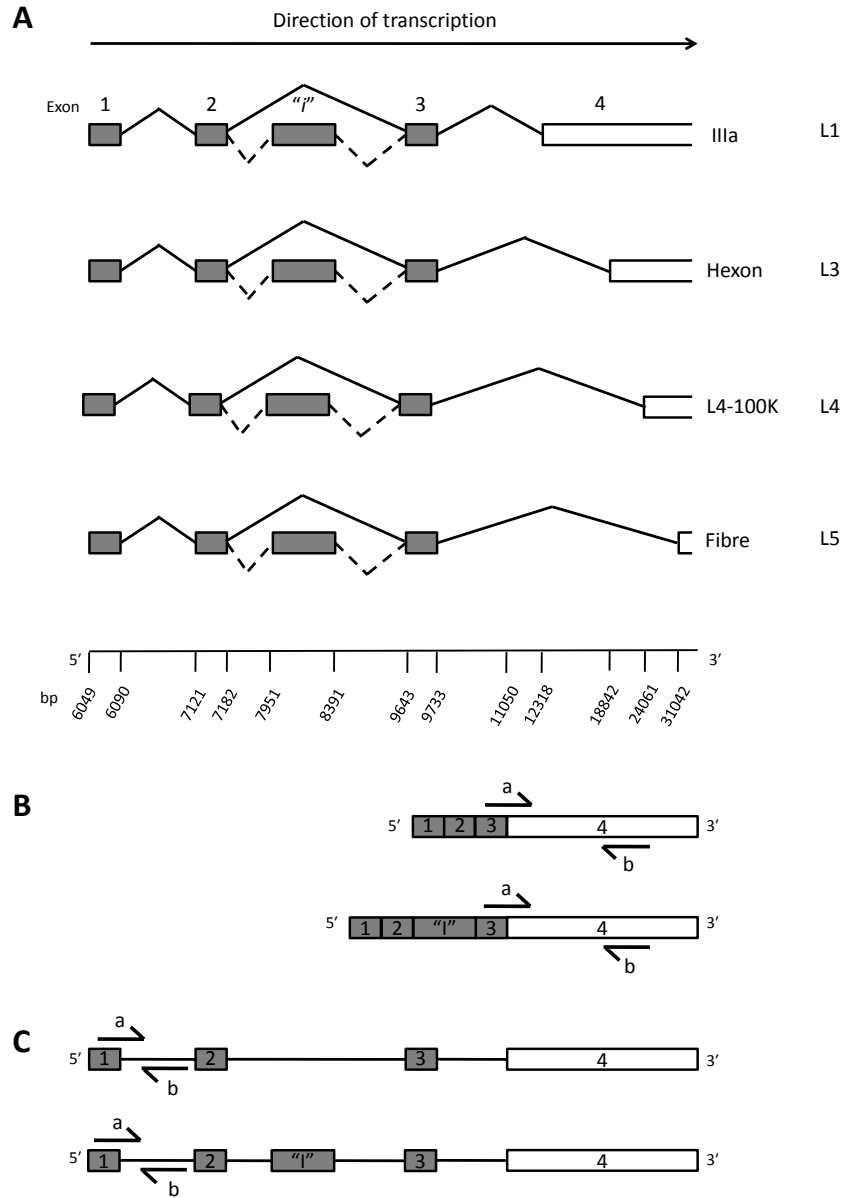
Appendix Figure 5. Primer design for PCR amplification of the Ad5 major late mRNAs.

A. A schematic representation of the Ad5 mRNAs expressed from the major late transcription unit. The mRNAs each contain a common set of 5′ -leaders (1, 2, *i* and 3) and are split into 5 families (L1-L5, L1, L3, L4 and L5 depicted above). The inclusion of the *i*-leader occurs only in a small proportion of the late mRNAs and this minor splicing pathway is represented as dashed lines. Boxes represent exons and thin lines represent introns. Nucleotide positions of the splice donor and acceptor sites are shown in base pairs (bp) on the Ad5 genome (not to scale). B. Positions of exon-spanning primers on the mature Ad5 late mRNAs. a – IIIa/hexon/L4-100K/Fibre Forward primer; b - IIIa/hexon/L4-100K/Fibre Reverse primer. C. Position of intron-exon spanning primers for amplification of Ad major late pre-mRNAs. A – Tripartite Leader Forward primer b) Tripartite Leader Reverse primer. Sequence information was obtained from NCBI Nucleotide. Splice site information was obtained from Gingeras *et al.*, 1982; Kreivi *et al.*, 1991. Figure is adapted from Kreivi *et a*l, 1991.
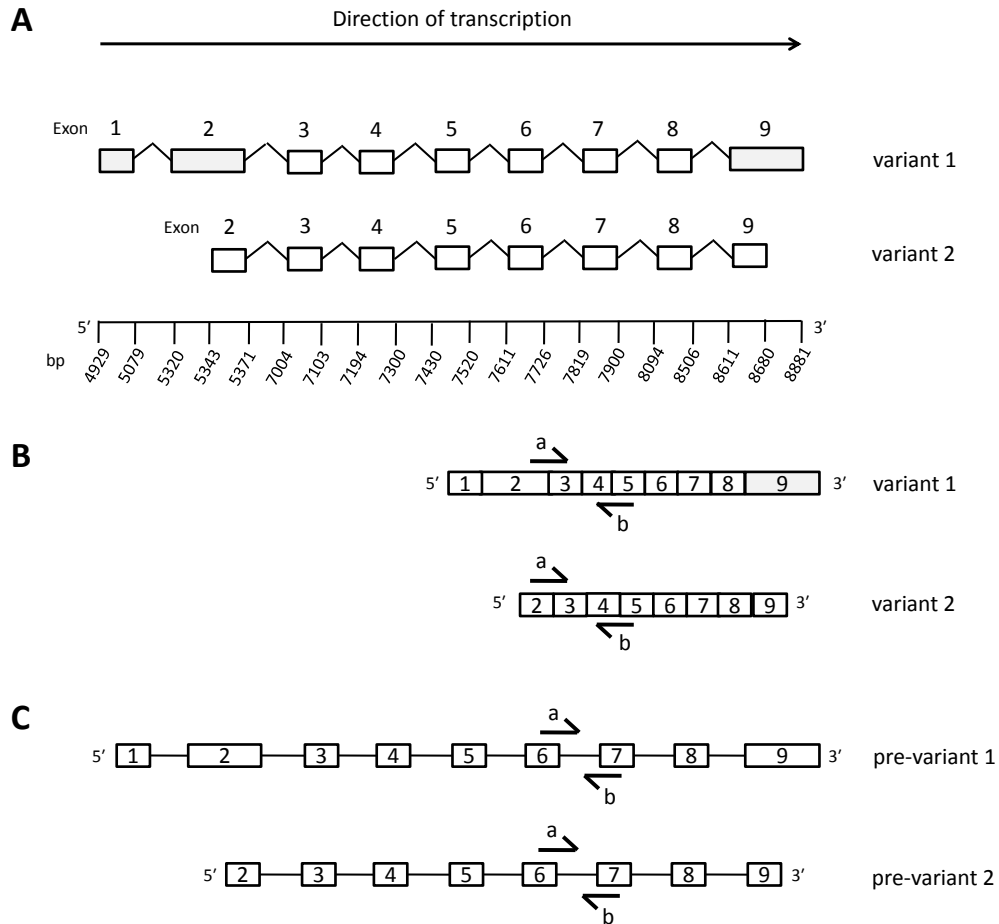
Appendix Figure 6. Primer design for PCR amplification of human GAPDH mRNAs.

A. A schematic representation of the GAPDH mRNA transcription pathway. Boxes represent exons and thin lines represent introns. Nucleotide positions of the splice donor and acceptor sites on chromosome 12 are shown in base pairs (bp) (not to scale). B. Positions of exon-spanning primers on the mature GAPDH mRNAs. a – GAPDH Forward primer; b – GAPDH Reverse primer. C. Position of intron-exon spanning primers for amplification of GAPDH pre-mRNAs. a - pre-GAPDH Forward primer; b - pre-GAPDH Reverse primer. Nucleotide sequences and location of splice sites were obtained from NCBI Nucleotide.
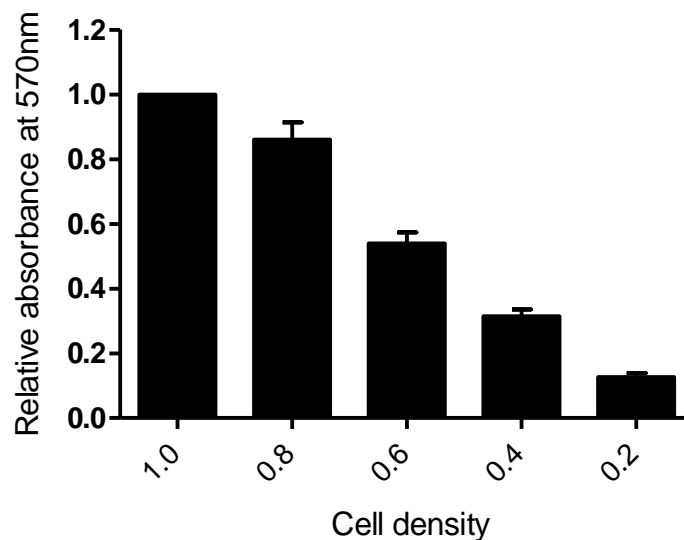
Appendix Figure 7. Dilution dependent decrease in absorbance by the MTT assay.

A549 cells were serially diluted, seeded in 96-well plates and incubated for 24 hours. Cells were harvested and subjected to analysis by the MTT assay. Results are the mean fold change in absorbance at 570 nm (± SEM) from two independent repeats performed in duplicate. Data is shown as relative to the highest cell concentration, which was set to a value of 1. It was found that the relative absorbance at 570 nm directly correlated with the cell density.
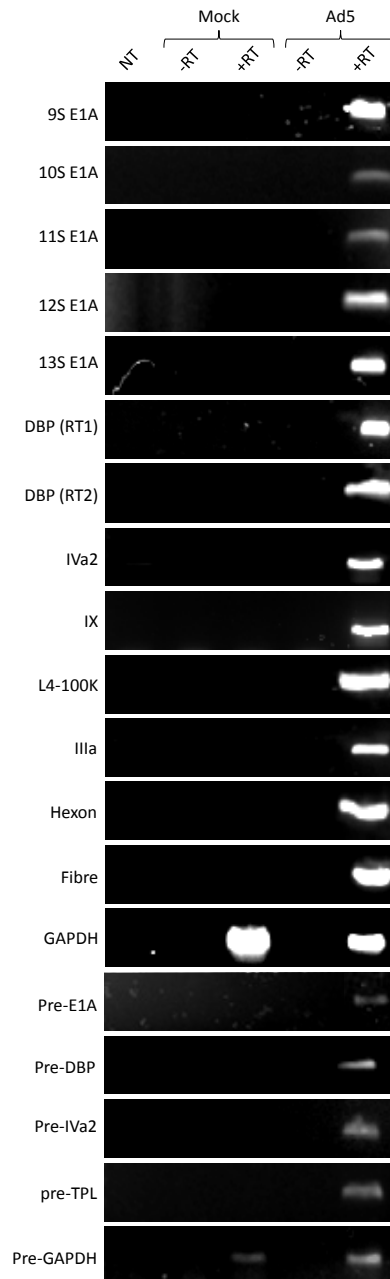
Appendix Figure 8. Validation of primer specificity by semi-quantitative PCR.

A549 cells were mock or Ad5 infected at an MOI of 5 and incubated for 24 hours. Cells were harvested and total RNA was extracted followed by DNAse treatment to remove contaminant DNA. Reverse transcription was carried out on total RNA to produce cDNA from mRNA. A non-template control (NT) was included to ensure amplified product was specific to the template. Control reactions which did not contain reverse transcriptase (RT) were also included to verify that specific cDNA sequences were being amplified. Target cDNA was amplified in PCR reaction using exon-spanning or intro-exon spanning primers. PCR products were separated on a 2% agarose gel by electrophoresis. Images were captured using a Las 3000 Imager. For all primer pairs, the NT control and no RT control were negative for PCR product. For all primer pairs specific for Ad mRNA sequences, no product was detected in the mock-infected samples.